CONTAMINATED SOILS, SEDIMENTS, AND WATER
Volume 13

CONTAMINATED SOILS, SEDIMENTS, AND WATER
Volume 13

Analysis
Bioremediation
Brownfields
Chemical Oxidation
Environmental Fate
Environmental Forensics
Ethics in Environmental Practice
Heavy Metals
Modeling
Regulatory
Remediation
Risk Assessment
Sediments

Edited by

Paul T. Kostecki
Edward Calabrese
James Dragun

ISBN-10: 0-9787640-2-1 ISBN-13: 978-0-9787640-2-1

Annual International Conference on Soil, Sediments and Water
Environmental Health Sciences Department
School of Public Health and Health Sciences
N 344 Morrill Science Center
University of Massachusetts
Amherst, MA 01003 USA

Contents

PART VII: ETHICS IN ENVIRONMENTAL PRACTICE: RESPONSIBILITIES, BENEFITS, AND CASE EXAMPLES

PART VIII: HEAVY METALS

PART IX: MODELING

PART X: REGULATORY

PART XI: REMEDIATION

Foreword

For the biosphere to sustain human life ecosystem components must function collectively to provide the physical, chemical, and biological services on which we depend. Energy flux, matter cycling, temperature amelioration, gas exchange, water provision, and pH constraints are among the large-scale processes on which life depends. For these and the infinitely intricate web of interactions at lower levels of the biogeochemical hierarchy to continue, each ecosystem structure and function must operate within individual limits that allow the aggregated holistic enterprise to prosper.

In the middle decades of the past century, medical researcher Hans Selye postulated and documented a General Adaptation Syndrome of consistent physiological responses of organisms to diverse challenges. His original vision of G.A. Syndrome has needed some tweaking to accommodate subsequent findings regarding the importance of nonspecific inflammatory response and the pathogenic nature of gastrointestinal ulcers. But Selye's elucidation of changes in structures and functions of an organism fighting for homeostasis under threat provided a useful framework for understanding relationships between stress and health.

Stresses beyond the individual level in the ecosystem engender homeostatic resistance (for example, fecundity drops in some populations when trophic resources are limited) and potential for permanent alteration when pushed beyond response thresholds. By analogy, ecosystem "stresses" can be characterized diagnostically and treated when long-term consequences are anticipated.

The "good earth" of the ecosystem—soils and sediments—is the source of many of the biogeochemical responses to environmental stress, and a critically important component that, when "broken"—impaired at substantive levels—must be "repaired"—restored—for the system as a whole to function effectively. Stewardship of soils and sediments for sustainability requires that we diagnose impairments, reduce or eliminate impairments by remediation, and assist whole-system recovery by restoration. The papers gathered in this volume provide a rich source of resources for evaluating, remediating, and restoring stressed soils and sediments. The authors are practitioners at the cutting edge of the field of environmental management. Their contributions published here represent reports from the front lines on the state-of-the-science of analysis, assessment, management policy, remediation technology, and regulation. The compendium you hold in your hands is a source of information to help you keep up-to-date and a challenge to you to build out the next steps in soil and sediment assessment and management. We look forward to working with you to maintain and enhance the health of the biosphere for our children and their children.

David F. Ludwig, Scientist

ARCADIS

Contributing Authors

Mohamed S. Abdel-Rahman, UMDNJ, 2690 Ballard Ave., Orlando, FL 32833
Halim Md. Abdul, Kyushu University, Department of Urban and Environmental Engineering, Graduate School of Engineering, 6-10-1 Hakozaki, Higashi-ku, Fukuoka 812-8581, Japan
Razzak Abdur, Kyushu University, Department of Urban and Environmental Engineering, Graduate School of Engineering, 6-10-1 Hakozaki, Higashi-ku, Fukuoka 812-8581, Japan
George R. Alther, Biomin, Inc., PO Box 22028, Ferndale, MI 48220
Joseph A. Amari, Bechtel Savannah River Co.
Norman Anderson, American Lung Association of Maine, 122 State Street, Augusta, ME 04330
Gianni Andreottola, University of Trento, Department of Civil and Environmental Engineering, Via Mesiano 77, 38050 Trento (TN), Italy
Violina R. Angelova, Agricultural University, Dept. of Chemistry, Mendeleev street 12, Plovdiv, 4000, Bulgaria
Blanca Antizar-Ladislao, Universidad de Cantabria -Campus de Torrelavega, Dpto. de Ciencias y Técnicas del Agua y del Medio Ambiente, Bulevard Ronda Rufino Peón, 254 – Tanos, 39316 Torrelavega, Cantabria Spain
Il-Sang Bae, Seoul Metropolitan Govern Research Institute of Public, Health and Environment, 202-3 Yangjae-Dong Seocho-Gu, Seoul, 137-130Korea
Michael Berger, Simmons College, 300 The Fenway, Boston, MA 02115
David A. Binstock, RTI International, P.O. Box 12194, Research Triangle Park, NC 27709
Robert Blundy, Washington Savannah River Company, Savannah River Site, , , , Aiken, SC 29808
Richard C. Bost, Environmental Resources Management, 15810 Park Ten Place, , , , Houston, Texas 77084
Lorenzo Reyes Bozo, Pontificia Universidad Católica de Chile, Department of Chemical Engineering and Bioprocesses, Vic. Mackenna 4860, , , Macul, Santago Chile
Dean Brammer, Weston Solutions, Inc., 1 Wall Street, Manchester, NH 03101
Rosemary Carroll, Desert Research Institute, Division of Hydrologic Sciences, 2215 Raggio Parkway, Reno, NV 89512
Liliana Cecan, McLane Environmental, LLC, 707 Alexander Road, Suite 206, Princeton, NJ 08540
E. Cervantes-González, Escuela Nacional de Ciencias Biológicas, Depto. de Microbiología, Casco de Sto. Tomas, Mexico City, 11340 México
Douglas J. Covert, Hazardous Substance & Waste Management Research, 2976 Wellington Circle West, Tallahassee, FL 32309
R. Cruz-Camarillo, Escuela Nacional de Ciencias Biológicas, Depto. de Microbiología, Casco de Sto. Tomas, Mexico City, 11340México
Ahmed H. A. Dabwan, Mie Industry and Enterprise, Support Center, Shima, Ugata, Mie 517-0501, Japan
Paul A. Eisenstat, Bechtel Savannah River Co.

Seok-Won Eom, Seoul Metropolitan Government Research Institute of Public Health and Environment, 202-3 Yangjae-dong Sucho-Gu, Seoul 137-130, Korea
Lonnie Fallin, Jacobs Engineering, 6 Otis Park Drive, Bourne, MA 02532
Mark E. Farrar, Savannah River National Laboratory
Elisa Ferrarese, University of Trento, Department of Civil and Environmental Engineering, Via Mesiano 77, 38050 Trento (TN), Italy
Bob Frye, GEC Environmental Contracting Corp, 13880 Berlin Turnpike, Lovettsville, VA 20180
Satya Ganti, Sarva Bio Remed, LLC, 36 South Broad Street, Trenton, NJ 08608
J. García-Mena, Cinvestav- Unidad Zacatenco, Depto. de Genética y Biología Molecular, Av. IPN 2508, Mexico City, 07360México
Alex Godoy-Faúndez, Universidad Andrés Bello, Ave Repulbica 200, , , , Santiago Centro, Santago Chile
William F. Gutknecht, RTI International, P.O. Box 12194, Research Triangle Park, NC 27709
Amy Hanna, Case Western Reserve University, Department of Civil Engineering, Cleveland, OH 44106-7201
Anna Marie M. Herb, Savannah River National Laboratory
Brad Horn, Redux Technology, P.O. Box 331, Newfane, VT 05345
Daizo Imai, Mie Industry and Enterprise, Support Center, Shima, Ugata, Mie 517-0501, Japan
Krasimir I. Ivanov, Agricultural University, Dept. of Chemistry, Mendeleev street 12, Plovdiv, 4000, Bulgaria
Aaron A. Jennings, Case Western Reserve University, Department of Civil Engineering, Cleveland, OH 44106-7201
Barry L. Johnson, Assistant Surgeon General (ret.), 2618 Riverglenn Circle, Dunwoody, GA 30338
Satoshi Kaneco, Mie University, Department of Chemistry for Materials, Faculty of Engineering, Tsu, , Mie 514-8507, Japan
Ludvík Kašpar, DIAMO, s. p., o. z. TUU, 471 27 Straz pod Ralskem, Czech Republic
Tadaya Kato, Mie Industry and Enterprise, Support Center, Tsu, Mie 514-0056, Japan
Hideyuki Katumata, Mie University, Department of Chemistry for Materials, Faculty of Engineering, Tsu, Mie 514-8507, Japan
Oda Keita, Kyushu University, Department of Urban and Environmental Engineering, Graduate School of Engineering, 6-10-1 Hakozaki, Higashi-ku, Fukuoka 812-8581, Japan
Jinno Kenji, Kyushu University, Department of Urban and Environmental Engineering, Graduate School of Engineering, 6-10-1 Hakozaki, Higashi-ku, Fukuoka 812-8581, Japan
Majeda Khraisheh, University College London, Department of Civil and Environmental Engineering, Gower street, London WC1E 6BT, UK
Terry P. Killeen, Washington Savannah River Co.
Donald N. Kirkland, GZA GeoEnvironmental, Inc, 380 Harvey Road, Manchester, NH 03103
Hidetoshi Kohashi, Public Works Research Institute, 1-6 Minamihara, Tsukuba City, Ibaraki Prefecture 305-8516Japan
Robert Kondelin, Environmental Alliance, Inc., 1812 Newport Gap Pike, Wilmington, DE 19808
Srikant Kothur, Hazardous Substance & Waste Management Research, 2976 Wellington Circle West, Tallahassee, FL 32309
Stefan V. Krustev, Agricultural University, Dept. of Chemistry, Mendeleev street 12, Plovdiv, 4000, Bulgaria
Steven R. Lamb, GZA GeoEnvironmental, Inc, 380 Harvey Road, Manchester, NH 03103
Valerie Lane, GeoTrans, Inc., One Monarch Drive, Suite 101, Littleton, MA 01460
Jae-Seung Lee, Seoul Metropolitan Govern Research Institute of Public, Health and Environment, 202-3 Yangjae-Dong Seocho-Gu, Seoul, 137-130Korea

Aiduan Li, University College London, Department of Civil and Environmental Engineering, Gower Street, London WC1E 6BT, UK
Annamarie MacMurray, Savannah River National Laboratory, Aiken, SC 29808
Steve Markesic, Redox Technology, LLC, 1441 Branding Lane, Suite 100, Downers Grove, IL 60515
Yugo Masuya, Public Works Research Institute, 1-6 Minamihara, Tsukuba City, Ibaraki Prefecture 305-8516Japan
Andrea C. McWilliams, RTI International, P.O. Box 12194, Research Triangle Park, NC 27709
Michael R. Morgenstern, Bechtel Savannah River Co.
Michael W. Morris, Jacobs Engineering, 6 Otis Park Drive, Bourne, MA 02532
Jiří Mužák, DIAMO, s. p., o. z. TUU, Machova 201, 471 27 Straz pod Ralskem, Czech Republic
César Sáez Navarrete, Pontificia Universidad Católica de Chile, Department of Chemical Engineering and Bioprocesses, Vic. Mackenna 4860, Macul, Santago Chile
Bette Nowack, Weston Solutions, Inc., 1 Wall Street, Manchester, NH 03101
Kiyohisa Ohta, Mie University, Department of Chemistry for Materials, Faculty of Engineering, Tsu, Mie 514-8507, Japan
Paul Ollila, MassDEP, 627 Main Street, Worcester, MA 01608
Robert G. Perry, Environmental Resources Management, 15810 Park Ten Place, Houston, Texas 77084
Bernd W. Rehm, ReSolution Partners, LLC, P.O. Box 44181, Madison, WI 53744-4181
Gary Richards, Redux Technology, 1317 Pennsridge Court, Downingtown, PA 19335
N.G. Rojas-Avelizapa, Centro de Investigación en Ciencia Aplicada y Tecnología Avanzada – IPN, Cerro Blanco 141, Col. Colinas del Cimatario, , , Querétaro, Qro 76090México
L.I. Rojas-Avelizapa, Escuela Nacional de Ciencias Biológicas, Depto. de Microbiología, Casco de Sto. Tomas, Mexico City, 11340México
I. Richard Schaffner, Jr., GZA GeoEnvironmental, Inc, 380 Harvey Road, Manchester, NH 03103
Robert Schleicher, Thermo Fisher Scientific, 900 Middlesex Turnpike, Building 8, Billerica, MA 01821
Robert A. Schneiker, Environmental Software Consultants, Inc., P.O. Box 2622, Madison, WI 53701-2622
Henry J. Schuver, U.S. EPA – OSW, Ariel Rios Bldg (MC-5303W), 1200 Pennsylvania Ave. NW, Washington, DC 20460
Elizabeth A. Shaffer, Malcolm Pirnie Inc, 1300 E 8th Ave, Tampa, FL 33607
Gerald K. Sims, USDA Agricultural Research Service, 1102 S. Goodwin Ave, Urbana, IL 61801
Rajiv Kumar Singh, Central Pollution Control Board, M/o Envt.& Forests; Govt.of Ind, PIC-UP Building (GF), Gomtinagar, Lucknow-10, Uttar Pradesh, India
Gloria A. Skowronski, UMDNJ, New Jersey Medical School, Pharmacology and Physiology Dept., 185 South Orange Avenue, Newark, NJ 07101
James S. Smith, Trillium, Inc., 8 Grace's Drive, Coatesville, PA 19320-1206
Jim Soukup, Weston Solutions, Inc., 1 Wall Street, Manchester, NH 03101
Laura Stupi, Thermo Fisher Scientific, 900 Middlesex Turnpike, Building 8, Billerica, MA 01821
Tohru Suzuki, Mie University, Environmental Preservation Center, Tsu, Mie 514-8507, Japan
Isamu Takahashi, Public Works Research Institute, 1-6 Minamihara, Tsukuba City, Ibaraki Prefecture 305-8516Japan
Hitoshi Taninaka, Public Works Research Institute, 1-6 Minamihara, Tsukuba City, Ibaraki Prefecture 305-8516Japan
Christopher Teaf, Florida State University, Center for Biomedical & Toxicological Research and Waste Management, 2035 East Dirac Drive, Suite 226 HMB, , , Tallahassee, FL 32310-3700USA
Janis Tsang, USEPA, Region I, One Congress Street, Suite 1100, Boston, MA 02114
Rita M. Turkall, UMDNJ, Newark, NJ
John J. Warwick, Desert Research Institute, Division of Hydrologic Sciences, 2215 Raggio Parkway, Reno, NV 89512

Hiroshiro Yoshinari, Kyushu University, Department of Urban and Environmental Engineering, Graduate School of Engineering, 6-10-1 Hakozaki, Higashi-ku, Fukuoka 812-8581, Japan

Acknowledgments

We wish to thank all agencies, organizations and companies that sponsored the conference. Without their generosity and assistance, the conference and this book would not have been possible.

Benefactors

American Petroleum Institute
ENSR Corporation

Sponsors

Arcadis US, Inc.
Geovation Technologies, Inc
Kerfoot Technologies, Inc.
International Tungsten Industry Association (ITIA)
Northeast Analytical
Regenesis Bioremediation Products
MA DEP
Shaw Group

Supporters

3M
Adventus Americas
Alpha Analytical Labs
Environmental Remediation and Financial Services, LLC
LSPA
New York DEC
The Dragun Corporation

In addition, we express out deepest appreciation to the members of the Scientific Advisory Boards. The tremendous success of the conference has been the result of the dedication and hard work of our board members.

General Advisory Board

Ralph S. Baker	*TerraTherm, Inc.*
Bruce Bauman	*American Petroleum Institute*
Mark Begley	*Environmental Management Commission*

Scott R. Blaha	*GE*
Carol de Groot Bois	*Bois Consulting Company*
Clifford J. Bruell	*University of Massachusetts Lowell*
Barbara Callahan	*University Research*
Robert H. Clemens	*AMEC Earth & Environmental, Inc.*
Andrew Coleman	*Electric Power Research Institute*
Janine Commerford	*MA Department of Environmental Protection*
Kathy Creighton	*Shaw Group*
James Dragun	*The Dragun Corporation*
John W. Duggan	*Wentworth Institute of Technology*
Mohamed Elnabarawy	
Kevin T. Finneran	*University of Illinois at Urbana/Champaign*
John Fitzgerald	*MA DEP*
Millie Garcia-Serrano	*MA DEP*
Eric Hince	*Geovation Technologies, Inc.*
Robert Kelley	*Regenesis Bioremediation Products*
William B. Kerfoot	*Kerfoot Technologies, Inc.*
Stephen S. Koenigsberg	*Environmental Strategies Consulting*
Fayaz Lakhawala	*Adventus Group*
David Ludwig	*ARCADIS BBL*
Rick McCullough	*MA Turnpike Authority*
Chris Mitchell	*ENSR Corporation*
Ellen Moyer	*Greenvironment, LLC*
Jim Mueller	*Adventus Group*
Willard Murray	
Lee Newman	*University of South Carolina*
Eric Nichols	*LFR/Levine-Fricke*
Dawn Oliveira	*EFI Global, Inc.*
Om Parkash	*University of Massachusetts Amherst*
Gopal Pathak	*Birla Institute of Technology*
Frank Peduto	*Spectra Environmental Group*
Ioana G. Petrisor	*Haley & Aldrich, Inc.*
Paul Rakowski	*Booz | Allen | Hamilton*
Julia Sechen	*MA DEP*
Frank Sweet	*ENSR Corporation*
Christopher Teaf	*Florida State University*
James C. Todaro	*Alpha Woods Hole Labs*
Mark Vigneri	*Environmental Remediation and Financial Services, LLC*
Robert Wagner	*Northeast Analytical*
A. Dallas Wait	*Gradient Corporation*
Richard Waterman	*EA Engineering, Science, and Technology, Inc.*
Jason White	*The Connecticut Agricultural Experiment Station, New Haven, CT*
Paul A. White	*Health Canada*
Katie Winogroszki	*3M*
Peter Woodman	*Risk Management Incorporated*

Federal Advisory Board

John Cullinane	*US Army Engineer Waterways Exp. Sta.*
John Glaser	*US EPAgency*

Douglas W. Grosse	*USEPA*
Leslie Karr	*Naval Facilities Engineering Service*
Mike Reynolds	*USA - Cold Regions Research and Engineering Laboratory*
Alex Sherrin	*US EPA*
Henry H. Tabak	*US EPA*

About the Editors

Paul T. Kostecki, Vice Provost for Research Affairs, University of Massachusetts at Amherst and Associate Director, Northeast Regional Environmental Public Health Center, School of Public Health, University of Massachusetts at Amherst, received his Ph.D. from the School of Natural Resources at the University of Michigan in 1980. He has been involved with human and ecological risk assessment and risk management research for the last 13 years. Dr. Kostecki has co-authored and co-edited over 50 articles and 16 books on environmental assessment and cleanup including: Remedial Technologies for Leaking Underground Storage Tanks; Soils Contaminated by Petroleum Products; Petroleum Contaminated Soils, Vols. 1, 2, and 3; Hydrocarbon Contaminated Soils and Groundwater, Vols. 1, 2, 3 and 4; Hydrocarbon Contaminated Soils, Vols. 1, 2, 3, 4 and 5; Principles ad Practices for Petroleum Contaminated Soils; Principles and Practices for Diesel Contaminated Soils, Vols. 1, 2, 3, 4 and 5; SESOIL in Environmental Fate and Risk modeling; Contaminated Soils, Vol. 1; and Risk Assessment and Environmental Fate Methodologies. Dr. Kostecki also serves as Associate Editor for the Journal of Soil Contamination, Chairman of the Scientific Advisory Board for Soil and Groundwater Cleanup Magazine, as well as an editorial board member for the journal Human and Ecological Risk Assessment.

Edward J. Calabrese is a board certified toxicologist and professor of toxicology at the University of Massachusetts School of Public Health at Amherst. Dr. Calabrese has researched extensively in the area of host factors affecting susceptibility to pollutants and has authored more than 300 papers in scholarly journals, as well as 24 books, including: Principles of Animal Extrapolation; Nutrition and Environmental Health, Vols. 1 and 2; Ecogenetic: Safe Drinking Water Act: Amendments. Regulations, and Standards; Soils Contaminated by Petroleum: Environmental and Public Health Effects; Petroleum Contaminated Soils, Vols. 1, 2 and 3; Ozone Risk Communication and Management; Hydrocarbon Contaminated Soils, Vols. 1, 2, 3, 4 and 5; Hydrocarbon Contaminated Soils and Groundwater, Vols. 1, 2, 3, and 4; Multiple Chemical Interactions; Air Toxics and Risk Assessment; Alcohol Interactions with Drugs and Chemicals; Regulating Drinking Water Quality; Biological Effects of Low Level Exposures to Chemicals and Radiation; Contaminated Soils; Diesel Fuel Contamination; Risk Assessment and Environmental Fate Methodologies; Principles and Practices for Petroleum Contaminated Soils, Vols. 1, 2, 3, 4, and 5; Contaminated Soils, Vol. 1; and Performing Ecological Risk Assessments. He has been a member of the U.S. National Academy of Sciences and NATO Countries Safe Drinking Water Committees, and the Board of Scientific Counselors for the Agency for Toxic Substances and Disease Registry (ATSDR). Dr. Calabrese also serves as Director of the Northeast Regional Environmental Public Health Center at the University of Massachusetts, Chairman of the BELLE Advisory Committee and Director of the International Hormesis Society.

James Dragun, Ph.D., is a soil chemist with extensive experience dealing with soil remediation. He has addressed the extent, danger, and/or cleanup of chemicals at sites of national and international concern such as the oil lakes caused by the 1991 Persian Gulf War (Kuwait), VX chemical warfare agent for the U.N. Weapons Inspection Program (Iraq), malfunction of the Three Mile Island Nuclear Power Plant USA), and dioxin in Missouri (USA). Twenty-four nations including Japan, Canada, the United Kingdom, Australia, Germany, Switzerland, Italy, France, Spain, Scandinavia, and the Netherlands have utilized his expertise.

He founded and built an environmental engineering-science consulting company. For 18 years, he has led a team of specialists in chemical engineering, civil engineering, environmental engineering, geotechnical engineering, mechanical engineering, physics, plant engineering, environmental science, geology, hydrogeology, chemistry, biochemistry, toxicology, and biology. Dr. Dragun and his associates have solved environmental issues for major companies and governments in six continents (Africa, Asia, Australia, Europe, North America, and South America).

Dr. Dragun is a full Professor at the University of Massachusetts and at Wayne State University, Detroit, MI. He has authored two college textbooks and co-authored/edited eight technical books. Also, Dr. Dragun has been the Editor-in-Chief of the International Journal of Soil and Sediment Contamination for over 15 years.

PART I: Analysis

Chapter 1

ANALYSIS OF SULFUR IN THE COPPER BASIN AND MUDDY RIVER SITES USING PORTABLE XRF INSTRUMENTATION

Michael Berger[1§] Ling Zou[1] and Robert Schleicher[2]
[1] *Simmons College, Department of Chemistry 300 The Fenway, Boston, Massachusetts, USA,* [2] *NITON Analyzers, Thermo Fisher Scientific, 900 Middlesex Turnpike, Billerica, Massachusetts, USA*

ABSTRACT

The feasibility of using a portable analytical instrument, the Niton XRF XLt 500He, was tested as a technique for sulfur analysis of wet sediment or soil samples in the field. The effect of sample preparation on the precision and accuracy of sulfur determination was specifically evaluated. The Niton XRF XLt 500He uses X-ray fluorescence to detect different elements. This unit employs a helium purge to allow the analysis of elements lighter than potassium. Samples with sulfur varying from 0.3 to 2.0% were successfully measured with the instrument. The precision of the unit is excellent and the limit of detection can be extremely low with careful attention to sample preparation. The quantitation limit was estimated as 237 ppm sulfur.

Keywords: x-ray fluorescence, sulfur, sediment

1. PURPOSE OF THE STUDY

Experiments were conducted to determine to what accuracy and how precisely could sulfur be determined in sediments and soils using a portable Niton XRF Model XLt 500He. This unit has been modified by NITON Analyzers (Niton) to allow a flow of helium to displace the ambient air present in the instrument, especially in the areas of the sample and detector. Portable field analyzers using X-ray fluorescence are normally limited to the quantitative analysis of elements heavier than potassium, because air and moisture effectively scatter the weaker fluorescence from the lighter elements. Since helium does not appreciably scatter or absorb

§ Corresponding Author: Michael Berger, Simmons College, 300 The Fenway, Boston, MA, 02115, Tel: 617-521-2722, Email: bergerm@simmons.edu

sulfur x-ray fluorescence, it was hoped that the helium purge method would allow better limits of detection and quantitation of sulfur in a portable analyzer.

2. INTRODUCTION

The presence of sulfur in soil can present potential risks of harm to human health and the environment. The Copper Basin, located near the junction of Tennessee, Georgia, and North Carolina and the Muddy River in Boston, Massachusetts both present significant levels of sulfur (S) in soils and sediments. The Copper Basin was once an active mining site and the elevated sulfur presence there is a result of pollution from mining activities. These elevated levels of sulfur can create high levels of acidity in water runoff, causing detrimental effects on the natural habitat and environment. The first step in the remediation of this site is a determination of the spatial extent of soils with greater than 2% sulfur, soils which are thought to have the greatest potential for acid mine drainage. XRF was used for the analysis of sulfur in the Copper Basin tailings. The Muddy River is the backbone of the Emerald Necklace, a historic landscape surrounding Boston, Massachusetts. Over the years, the Muddy River has accumulated large quantities of sediment consisting of decaying vegetation, sand from stormwater drains, and riverbank erosion. These sediments are contaminated with high levels of metals and petroleum hydrocarbons. The concentration of total sulfur in the sediment varies with location – roughly from 0.2% to 2%. Depending on the availability of oxygen in the sediments, sulfur can be generated as hydrogen sulfide under anoxic conditions, which is toxic to fish and when volatilized unpleasant to humans at extremely low concentrations in the air. Dredging of the river is planned for the near future and may release harmful levels of hydrogen sulfide into the air and water. The selection of a remediation strategy for the river that minimizes sulfur volatile emissions during sediment dredging operations could be guided by a sulfur analysis of Muddy River sediments. Portable XRF represents a convenient analytical option. Our study evaluates the suitability of the Niton XRF XLt 500He as a portable handheld instrument for sulfur quantitation.

Earlier studies conducted by A. Richter in 2005 (Richter, 2005) of tailings from the Copper Basin analyzed sulfur content with a portable XRF unit without a helium purge and showed promising results. Moist silty samples containing from 1 to 6% sulfur were analyzed with the aid of a special filter optimized for light elements. Calibration of the device was shown to be possible by taking into account the iron content of the sample, and a complex calibration was found to work with a number of different samples. However, the signal/noise was low, and the device offered the best performance for samples with high levels of sulfur. Improvements in the technology and the inclusion of a helium purge increased the signal/noise by a significant amount and promised analysis of samples with lower amounts of sulfur, such as sediments.

There are several well established methods for the analysis of total sulfur in soil, including combustion in an oxygen bomb (Parr, Bailey and Gehring, 1961) followed by analysis of the sulfate produced or alkaline oxidation followed by X-ray fluorescence (Tabatabai and Bremmer, 1970 and Perrott et al, 1991). However, XRF for sulfur analysis normally requires high vacuum pumps to eliminate the scattering effects of the air. These devices are not suited for portable use

due to the size of the instruments and the supporting operational requirements, such as power and vacuum pumps.

In this study, we compared the sulfur analyses obtained by the Niton XRF XLt 500He with the analyses of similar samples using the oxygen bomb method followed by sulfate analysis. Samples with certified sulfur concentrations were used for calibration. Sediment samples were run with and without the helium purge in the Niton XRF Model 500He in order to determine the degree of improvement in the signal detection attributable to helium's elimination of scattering by atmospheric gases.

The theory of X-ray fluorescence has been described previously (Jenkins, 1999). The X-ray sulfur fluorescence occurs from 2.2 to 2.4 keV and is relatively free from intereference attributable to fluorescence from other elements or to excitation lines from the source.

Figure 1. The Niton XLt 500 He system with sample stand, analyzer, and Helium purge.

The Thermo Fisher Scientific Niton XLt 500He system uses the helium purge technique in a portable, handheld format. The analyzer has a sealed measurement head which is purged at 150 mL/min with pure helium to remove air from the X-ray analysis path. This allows the light element X-rays to pass through and reach the X-ray detector. The analyzer has factory calibration for various common applications using certified reference material. The factory calibration can be modified, if necessary, by the user to improve the accuracy for a particular type of material being analyzed. The analyzer uses a 40 Kev miniaturized X-ray tube and can determine, using K shell radiation, elements Mg to Ba and L shell radiation for elements Cs to U.

The XRF signal can be significantly influenced by the preparative technique (Pasmore et al, 2005 and Shefsky, 1997). For the most precise work, drying the sample to eliminate water followed by grinding and sieving to 120 mesh is recommended (Niton). The advantages of this

procedure are: representativeness of the sample is excellent since homogeneity is achieved, intimate contact and flatness of the sample will produce the highest and most reproducible fluorescence, and the sample concentration reported will not diluted by water content, which must be separately determined. Our study evaluated the effect of water on the sulfur analysis, since it is not always convenient to dry the sample in the field. We studied whether water content presented additional unique analytical problems in the analysis of the lighter elements with the Niton XRF Model 500He compared to the analysis of the heavier elements.

Elements heavier than potassium are excited by x-rays in the 5 to 40 keV range. One can estimate the penetration distance, $x = 46000/\mu*\rho$, where x is the distance traveled for 99% absorption , μ is the mass absorption coefficient and ρ is the density. The X-ray excitation of heavier elements penetrates a couple of mm into the sample, and the fluorescence readily passes back through a thickness of the sample before being detected. However X-rays used to excite the lighter elements, like sulfur, are only 5 keV and thus will only pass only a few microns into the sample. The resulting X-ray fluorescence will also emerge from only the top few microns of the sample. In recognition of the "weak" penetration of x-rays involved in the analysis of lighter elements, sediment samples were prepared with a thinner sample covering – 4 micron thick clear polypropylene cover. This thin cover protects the source and detector from the sediment sample. The cover also is used in the preparation of the sample "cup" which provides a clear "window" covering for the soil. In comparison a clear 6 micron Mylar cover is recommended (Niton) for analysis of the heavier elements.

Several experiments were conducted to determine what factors influence the accuracy of the sulfur analysis using the portable XRF XLt 500He. Certified soil and sediment standards containing a range of total sulfur content (0.3% to 2%) typically found in sediments were analyzed. Indeed, sediment samples collected from two different locations in the Muddy River were found to have sulfur at the extremes of the calibration range.

2.1 The Effect of Water Content on Sulfur Determination

Experiments were conducted to determine the effects of water content in soil and sample preparative techniques on the determination sulfur in soil and sediment samples. The effect of significant water content in sediment samples and the effect of particle size homogeneity were studied. Four sample preparative methods were studied to determine the effect on the resulting analytical results. Table 1 summarizes the different Sediment Methods described above.

Table 1. Summary of Sediment Sample Preparation

Summary of Sediment Sample Preparation

	Dried?	Ground?	Water
Method 1	Yes	yes	Added to dry sample
Method 2	Yes	No	Added to dry sample
Method 3	No	No	Dried to differing degrees
Method 4	No	No	Excess water blotted

2.2 The Effect of Water Content on Other Elements

Samples prepared by the methods shown in Table 1 were also analyzed for other "light" elements as well as for iron, a typical "heavier" element found in sediments to determine if the conclusions based on Sulfur data could be generalized to other elements.

2.3 The Benefit of Helium for Sulfur Analysis

Samples were analyzed for sulfur with and without helium flow in order to determine the benefit (i.e., an expected increase in signal to noise) based on the reduction of fluorescence scatter from air due to the use of a helium "purge".

2.4 Accuracy of Sulfur Analysis

In order to determine the accuracy of the sulfur analysis, identical samples were analyzed using an alternate method for the determination of total sulfur to compare to the results obtained with XRF. Thus the "oxygen bomb" method (described as modified below) is relatively inexpensive and has been used for many years for the successful determination of sulfur in a variety of materials. One of the goals of this paper is the comparison of the accuracy and precision of sulfur concentrations in soils determined by the two methods.

2.5 Calibration of the Niton XRF XLt 500He

Standard sediments samples, with known and certified composition were used for calibration of the Niton XRF XLt 500He. Data for all experiments consisted of counts (of X-ray fluorescence) detected per second. Additional experiments were conducted to quantify the signal to noise ratio (S/N) as a function of total signal acquisition time. For the Studies (A) – (C), total acquisition times were kept constant nominally at 240 seconds for Sulfur and other "light" elements, and 60 seconds for the "heavier" elements. Filtration and x-ray tube operating conditions are set up in the instrument to individually optimize excitation of the light and heavy elements in order to maximize the signal to noise ratio. Different sediment and soil "standards" containing certified leves of sulfur were used to calibrate the Niton XRF XLt 500He. Table 2 shows the fluorescence level in counts per second (cps) for different concentrations of sulfur. These data were used to create calibration curves. Different calibration curves were used to best match the actual sulfur concentration present in the sediments tested. The two ranges of sulfur found in the sediments best matched the calibration curves in the range of 0 to 0.3% (low) or 0 to 3.0% (high) as shown in Figures 2 and 3.

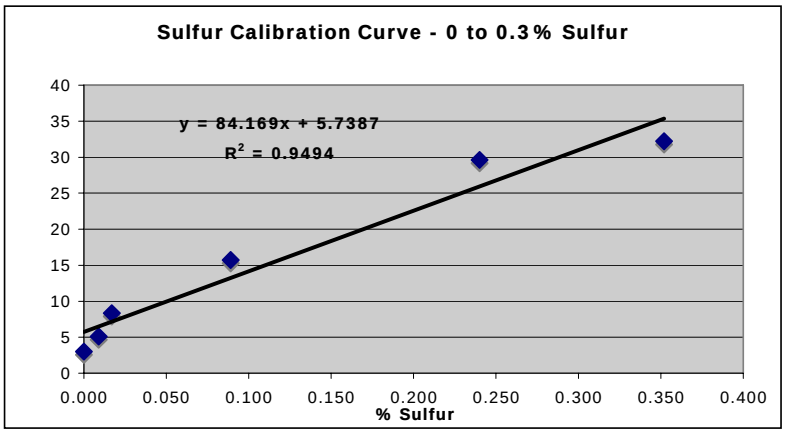

Figure 2. XRF calibration at low sulfur concentrations

Table 2. Certified Standards used for Calibration of XRF

Sample	S cert. %	S cps
99.999% Silica	0.00	2.99
NCS DC73308	0.01	5.09
NCS DC73309	0.02	8.33
NIST2709	0.09	15.71
NIST2710	0.24	29.59
NIST 1646a	0.35	32.23
NIST 2684b	3.08	484.78

2.6 The Effect of Sampling Time on Signal/Noise

As predicted by statistical considerations, the standard deviation of the sulfur signal decreases as the sampling time is increased. Figure 4 shows the expected relationship between the standard deviation and the inverse square root of the sampling time. (It is assumed that the total sample excitation is directly proportional to the sampling time for constant excitation power.

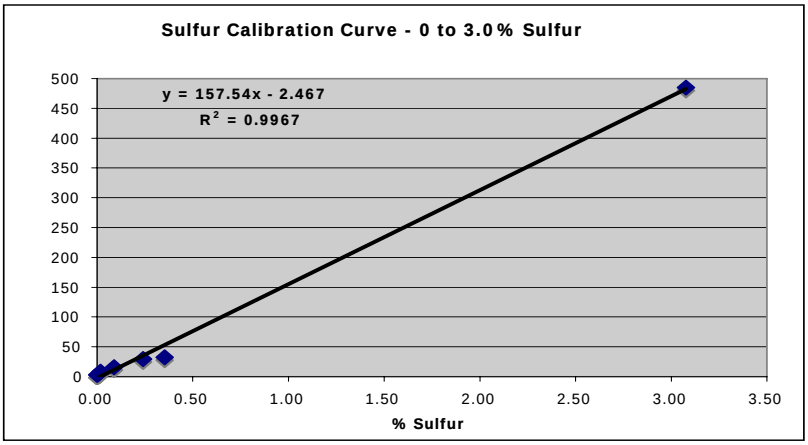

Figure 3. XRF calibration at high sulfur concentrations

The non-zero intercept indicates that there is a significant contribution to the standard deviation of the sulfur signal that does not arise from stochastic events involved in excitation of or fluorescence from sulfur in the sample. While data collection for longer times does improve the signal to noise ratio, a significant component of noise remains even at longer measurement times. The portability of the XRF XLt 500He permits data collection in the field. In field situations, measurements at shorter times allow a large area to be screened in a relatively short period of time. In this case, it may be more important to have data from many samples with a larger standard deviation, than data from fewer samples that have a smaller standard deviation. In general, we found that collecting fluorescence data with the XRF XLt 500He for a period of four minutes improves the S/N by a factor of two over data measured for only 30 seconds. Only additional slight improvement in S/N can be realized by data measurements longer than 4 or five minutes.

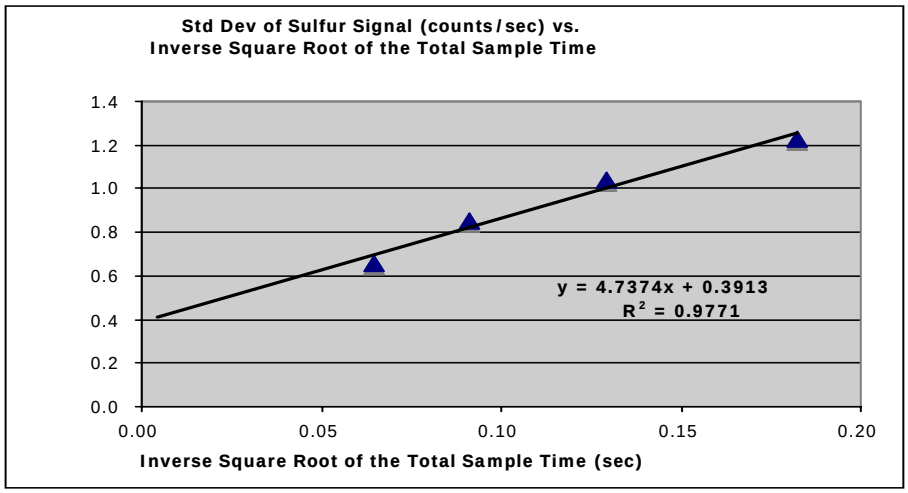

Figure 4. Standard deviation of sulfur fluorescence as a function of the inverse square root of the total sample time

3. RESULTS

3.1 The Effect of Water Content on Sulfur Determination

3.1.1 Sediment Method 1

Sediment samples were placed in an oven overnight at 60°C to dry completely, then ground with a mortar and pestle and passed through a 120 mesh screen. The effect of water on the analysis was studied by adding organic-free water to the dried sample and then thoroughly mixing the dried sediment and water. Sediment samples were prepared with water varying from 0 to 50% w/w. Figure 5 was based on XRF data of shallow sediments in a portion of the Muddy

River with approximately 0.30% sulfur. A linear trend of decrease in sulfur x-ray fluorescence with increase in water concentration is consistent with a simple dilution of the sediment with added water; the sulfur fluorescence is practically halved (44% decrease) as the sample is diluted to about 50% with added water.

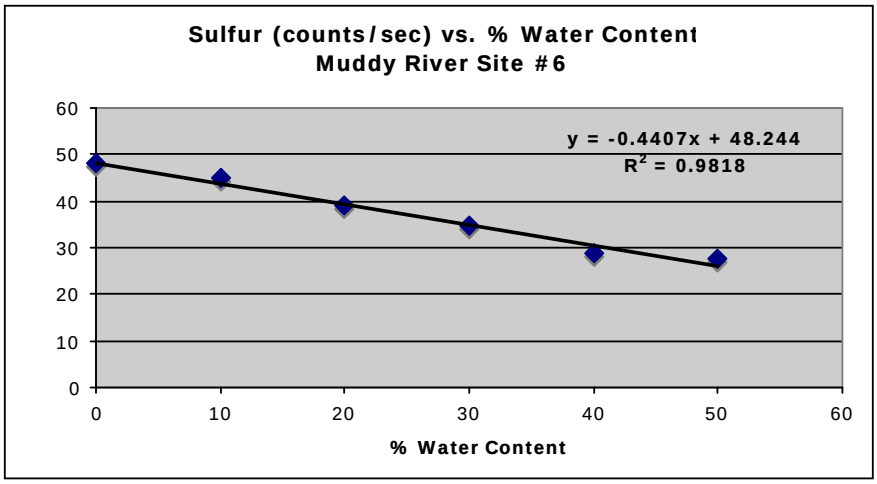

Figure 5. Sulfur (cps) versus water content for Method 1

3.1.2 Sediment Method 2

Sediment samples were placed in oven at 60°C overnight to dry completely, and then they were simply forced through a coarse screen (approximately 60 mesh) in order to remove stones, sticks, and leaf fragments. The effect of water on the analysis was studied by adding organic-free water to the dried sample. Comparison of the results from Method 1 and Method 2 show how important particle size and homogeneity is for sulfur analysis of

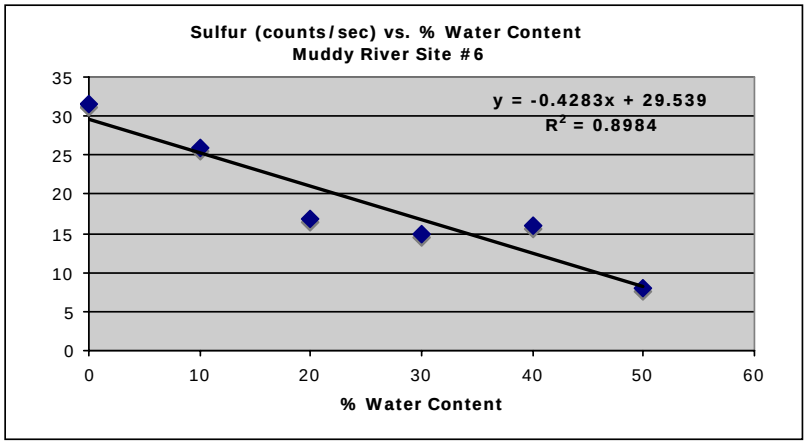

Figure 6. Sulfur (cps) versus water content for Method 2

sediment samples. While both methods show a dilution effect as water is added to the dried sediment, the effect is much larger for the coarsely sieved sediment; the sulfur fluorescence has decreased 76% with the addition of 50% water by weight in Method 2, much more than with Method 1. Note in **Figure 6** that R^2 for Method 2 is significantly poorer than for Method 1, probably due the greater homogeneity of the samples created with Method 2. In addition, the number of counts decreased overall for the sample created with Method 2. The coarseness and irregularity of the front surface of the Method 2 sample creates greater scattering at angles not captured by the fluorescence detector.

3.1.3 Sediment Method 3

Wet sediment samples were passed through a coarse screen (approximately 60 mesh) to remove bulky particles, then put in an oven at 60◦C for different lengths of time to obtain samples of different water content. In this case, no water was added to the analyzed

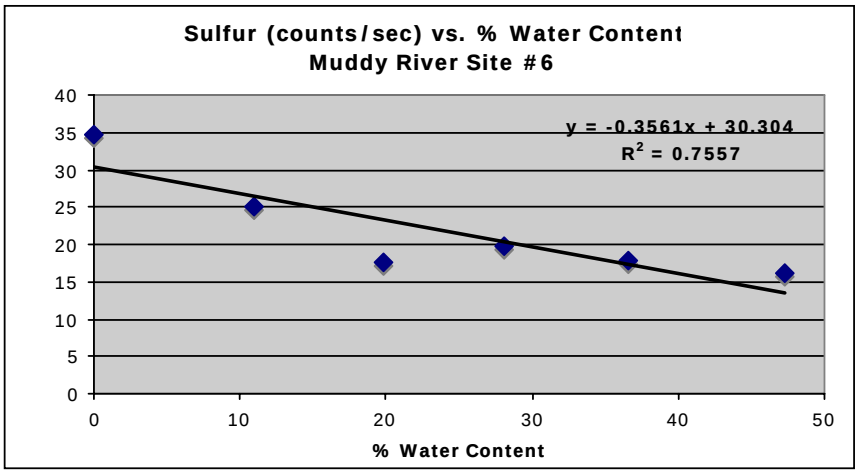

Figure 7. Sulfur (cps) versus water content for Method 3

sediment as was the case for Methods 1 and 2. Method 3 is a closer representation of natural samples. Figure 7 shows that the linear regression for Method 3 fits the data less well than in Method 1 or Method 2. Method 3 produces samples that are possibly more heterogeneous than the previous methods that may be the cause of greater scatter in the graph. The overall quantitation extrapolated to zero % water content is similar to that of Method 2 – only 60% of the "dry" quantitation extrapolation using Method 1.

Methods 1 – 3 were also used to evaluate the sediment in a different section of the Muddy River. While Site #6 sediment could be characterized as sandy with low levels of organic matter, Site #3 sediment appeared to contain high levels organic matter and petroleum compounds (approximately 1,700 ppm extractable petroleum hydrocarbons). Upon analysis, Site #3 had approximately 2% sulfur – considerably higher sulfur than at Site #6. However, the conclusions about the effect of water content on sulfur analysis were the same for either Site.

Figure 8 shows the effect of sample preparation for the different methods on the precision and accuracy for Muddy River Site #3.

3.1.4 Sediment Method 4

This method for sample preparation and analysis was a simulation of a very simple procedure that potentially could be used in the field. Wet sediment samples were passed through a coarse screen (approximately 60 mesh) to remove bulky particles, then simply blotted for about 30 seconds with a paper towel to remove water as much water as possible. Each sample was then assembled in a measurement cup with the sediment still in contact with the paper towel. Five replicate samples were prepared and sulfur counts/sec (cps) recorded normally with the Niton XLt 500He (Filter 2 for 240 seconds). The mean sulfur cps was 109.1 with a standard deviation of 7.8 cps. This sulfur content is only 53% of the sulfur content of the "dry" sample determined by Method 1. The results of this test indicate that Method 4 can give reproducible sulfur content based on wet weight, but will naturally report a sulfur content lower than that of a thoroughly dried sample.

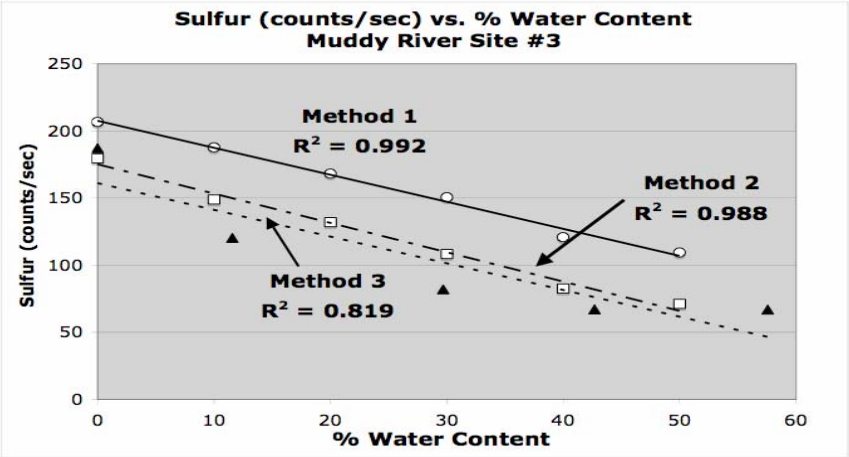

Figure 8. Effect of sample preparation on precision and accuracy – Site #3

3.2 The Effect of Water Content on Other Elements

The effect of water content in the sediment on the counts was studied for a number of different elements. Figure 10 shows the ratio of the counts per second on a sample with a certain water content compared to a thoroughly dried sample using Method 1. The "dilution" effect of water on the dry (maximum) signal varied with the element. While the X-ray fluorescence from iron only decreased 23% when the sample contained 50% water, aluminum, silicon, and phosphorus and sulfur X-ray fluorescence decreased approximately 50% with a dilution of 50% by water. The background fluorescence for all elements was assumed to be zero for each element, but in reality, there are background counts/sec that must be subtracted for each

element for the most accurate work. The different background levels may account for the apparent differences in the effect of water. For the most accurate research, it is important to characterize the background and the "dilution" effect of water content for the samples of each element.

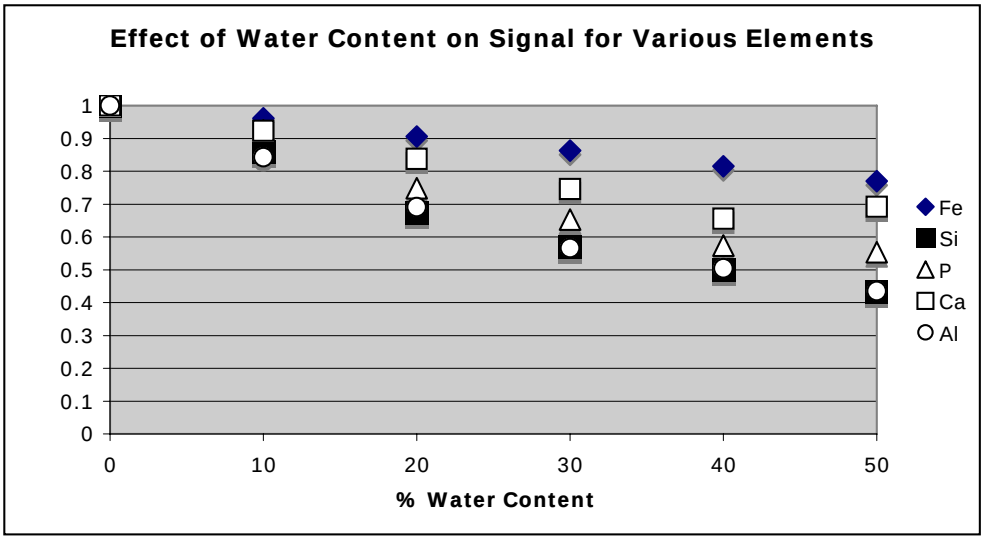

Figure 9. Effect of water content on x-ray fluorescence for elements other than sulfur

3.3 The Benefit of Helium for Sulfur Analysis

The effect of the helium on S/N was determined by calculating the relative standard deviation (RSD in parts per thousand, ppt) for a sediment standard with a low concentration of sulfur, NIST 1646a with 0.35% Sulfur. The RSD for the sample with helium was 19.9 ppt, compared to an RSD of 28.3 ppt when the helium was not used, a 30% improvement in RSD that is attributable to the helium purge.

3.4 Accuracy of Sulfur Analysis

There are several methods to analyze sulfur and sulfate resulting from the oxidation of sulfur (Eaton and Franson, 2005). The sulfur analytical methods used in this investigation are described in this section. In order to determine the accuracy of the portable XRF device, sulfur determinations using the Niton XLt 500He (X-Ray fluorescence) were compared to results using the "oxygen bomb" method. While the XRF method reports the concentration of sulfur directly to the user in a single step, the oxygen bomb method first requires combustion of the sample and subsequent analysis of the combustion residue as described below in order to determine the sulfur concentration in the original sediment sample.

An oxygen bomb (Model 1108 Oxygen Combustion Bomb, Parr Instrument Company, 211 Fifty-Third Street, Moline, Illinois 61265 USA) was used to oxidize the sediment samples and the combustion methodology described (Parr Instrument Company) was followed closely, except

as noted below. In this method, one gram of the sediment was exactly weighed and finely ground to make a pellet with a compression press (Model 2811 Parr Pellet Press). The pellet was reweighed before placing it in contact with a wire fuse and then placed into the stainless steel bomb. One to five milliliters of organic-free water was added to the bomb before final assembly in order to provide a "sink" for the conversion of oxidized sulfur as SO_2 into sulfate as sulfuric acid. After assembly, pure oxygen was admitted up to a pressure of 30 atmospheres in order to provide sufficient oxygen for complete combustion of the pellet. The fuse was ignited with the application of an electric current that in turn initiates the combustion of the pellet. The sulfur is then oxidized to sulfate, which is recovered quantitatively by washing the residue from the spent bomb. Depending on the concentration of sulfur in the sample, 250 mL to 500 mL of organic-free water was used for rinsing the stainless steel bomb after combustion. The washings containing the sulfate were analyzed using both the turbidity method (Hach, 2004) to quantitate sulfur, or using ICP - AES. The ICP - AES analysis was performed by VHG labs, Inc., 276 Abby Road, Manchester, New Hampshire.

Initial tests with calibration sediment sample 1646a in pelletized form showed evidence of incomplete combustion. Since the calibration sediment standard had a low percentage of organic content, it was thought that the bomb did not completely ignite due to insufficient heat. Upon the recommendation of Parr, Inc., a couple of drops of mineral oil were added to the pellet before ignition. However, based on observations of the pellet after combustion, and based on the recorded temperature rise in the calorimeter, mineral oil was rejected as an ignition aid. Instead, naphthalene was selected as an ignition aid for two reasons. Naphthalene has a high heat of combustion, 9.62 kcal/gram (Atkins, 2006), which can be obtained with high purity, and it contributes no sulfur to the residue and washings. Blanks consisting of approximately 0.9 gram of naphthalene with no sediment were combusted in the oxygen bomb and analyzed for sulfur; the blanks yielded no detectable sulfate as analyzed by the turbidity method. However, a small and variable amount of sulfur was detected with the combustion of the naphthalene blank in the washings when analyzed by ICP-AES; this blank was used to correct the sulfur values for the baseline tests summarized in Table 2, below. It was found that consistent combustion based on a consistent increase in the calorimeter temperature and by visual observations of the residue was achieved with one gram sample pellets prepared from a mixture of sediment and naphthalene in a 2:1 w/w ratio. Based on these results, naphthalene was selected as a combustion aide and added to all standard and sediment samples for oxygen bomb combustion.

The sulfur concentration in the original sediment sample was calculated based on the sulfate concentration of the washings from the oxygen bomb combustion. The procedure for sulfate determination from bomb washings described by Parr Instrument Company was modified. Parr's procedure specifies boiling the residue and washings from the spent oxygen bomb in a platinum crucible with hydrochloric acid before analysis of the sulfate. While this step was not performed, satisfactory results were obtained based on the results from calibration standards. Upon combustion in oxygen, it is assumed that one mole of sulfur produces one mole of sulfate, and one mg of sulfur produces three mg of sulfate. Two methods were used to determine the sulfate concentration in the bomb washings.

The turbidity method for sulfate (Eaton and Franson, 2005) is based on the decrease in light transmission due to the formation of a fine dispersion of a precipitate of barium sulfate when a test sample containing sulfate is added to barium chloride. The turbidity determination is usually

regarded as semi-quantitative, since the amount of the decrease in light transmission due to light scattering from the barium sulfate precipitate is sensitive to several factors: other constituents in the unknown solution, the specific conditions of precipitation – such as agitation and temperature, and the elapsed time between the beginning of the analysis and the final light transmission reading. Turbidity measurements were performed using the Hach DR/890 Colorimeter following the procedures described for the Sulfa Ver 4 Method (Procedures Manual. 2005, Ed.7). Best results were achieved using the "user calibration mode" calibrating between 10 and 50 mg/L sulfate. Samples with concentrations greater than 50 mg/L sulfate were diluted so that the resulting concentrations fell within the calibrated range of concentrations. Hach reports the precision of the sulfate turbidity test as +/- 3 mg/L. The user calibration curve prepared with 8 standard sulfate solutions gave a R2 goodness of fit value of 0.946. It was essential to prepare a new calibration curve for each lot of barium chloride ampules used in the Hach turbidity analytical method.

Samples of bomb washings were also analyzed by ICP - AES (Inductively Coupled Plasma – Atomic Emission Spectroscopy). Table 2 compares the results of sulfur determinations in the washings for five replicate bomb combustion experiments comparing the results from the turbidity and the ICP - AES methods for sulfate (and thus sulfur). The original sample was a certified sediment standard "1646a" with 0.352% +/- 0.004% sulfur. Based on this test of five samples, the standard deviation of the turbidity method is 0.0074%, while the standard deviation of the ICP - AES is smaller, at 0.0046%. The turbidity method is biased 18% low, while the ICP - AES method is biased 15% low. Both methods appear to be biased low. Possibilities for this bias may be due to the modification and simplification of the oxygen bomb procedure used for this work. The residue digestion described (Parr) with concentrated hydrochloric acid in a platinum crucible was not conducted for our experiments. The turbidity method may have an additional negative bias due to settling or agglomeration of the barium sulfate produced in the method.

Table 2. Comparison of % S for Turbidity Method and ICP – AES with Modified Oxygen Bomb Method

	Turbidity	ICP
	0.2923	0.306
	0.2959	0.299
	0.2966	0.304
	0.2818	0.297
	0.2818	0.295
	0.2897	0.300
Std Deviation	**0.0074**	**0.0047**
Bias	**-18%**	**-15%**

Table 3 compares the sulfur analyses carried out by different methods. The known % for sulfur is given (if known). Two XRF results are given in the Table: "low S" based on a calibration with standards from 0 to 0.35% sulfur and "high S" based on calibration with standards from 0 to 3.076% sulfur. The analysis based on the oxygen bomb method use the ICP analysis of the bomb combustion products to determine the sulfur %. Sample 1646a is a standard sample with a certified sulfur percentage of 0.352%. The Sediment samples (Sed#3

and Sed#6) have unknown true sulfur values, and the bomb and XRF analyses were conducted on dried and ground samples. Sediment #3 was analyzed to have a sulfur concentration of 1.85%, while the XRF analyses varied from 2.56% to 1.41% based on which calibration graph was used. The "high S" calibration was more appropriate, since Sediment #3 had a concentration of sulfur of 1.85%. On the other hand, the "low S" calibration graph was used for Sediment #6 since it had a sulfur concentration of 0.415% as determined with the oxygen bomb method.

Table 3.

Comparison of Sulfur Analyses (w/w%)

Sample	True Value	XRF *low S*	XRF *high S*	Bomb*
1646a	0.352	0.315	0.22	0.327
Sed #3	unknown	2.56	1.41	1.85
Sed #6	unknown	0.504	0.322	0.415

**Sulfur based on ICP analysis of bomb combustion produc*

4. DISCUSSION AND CONCLUSIONS

The effect of water on the analysis of sulfur with the Niton XRF XLt 500He appears to be linear; that is, the sulfur XRF signal decreases linearly with the water content, apparently due to simple dilution of the sample with water. Highest precision and the best accuracy is achieved by the sample preparative technique recommended by Niton: the sample should be dried and ground to pass through a 120 mesh sieve. An increase in water content leads to a decrease in the detected sulfur fluorescence signal (a dilution effect resulting in decreased accuracy) and an increase in the variance of the fluorescence (decreased precision). The coarse screening (greater than 60 mesh) of the dried or wet sample results in a decrease of about one-third of the sulfur fluorescence even with dried samples. Table 4 summarizes the results of the experiments with samples of different % water content.

Table 4.

Effect of Water Content on S (cps) and Regression

	Site #3 1.8 % S		Site #6 0.4% S	
	R^2	S (cps)	R^2	S (cps)
Method 1	0.992	221.4	0.982	48.2
Method 2	0.989	175.0	0.898	29.5
Method 3	0.818	152.2	0.786	30.3

The effect of dilution by water for other elements showed the same qualitative linear decrease in fluorescence with increase in water content; however, the slope of the regression varied with the element.

Helium increased the S/N by 30% for sulfur, leading to greater sensitivity. The limit of detection is a measure of the sensitivity of the analytic method and its determination has been described (Harris, 2007). The limit of detection is defined as the three times the standard deviation of a blank sample divided by the slope of a calibration curve for that sample. For this determination a silica standard certified as 99.999% pure was used as the blank. In the case of XRF analysis of sulfur, the limit of detection is 0.0071% or 71 ppm. The quantitation limit is defined as ten times the standard deviation of a blank sample divided by the slope of a calibration curve, or 0.0237% or 237 ppm. Since many sediments contain 0.20% to 2.0% sulfur, the sensitivity of the portable XRF method is adequate for most investigations. It should be noted that the detection limits used samples that were dried and sieved to pass 120 mesh. The limits of detection for sulfur in samples without the most careful preparation will be higher.

For the most accurate and precise work, it is essential that samples are dried, ground, and sieved (as recommended) to achieve a fine degree of homogeneity. In addition, if the highest accuracy is required for sulfur determination, a calibration curve must be constructed with a number of different standards with sulfur content approximately that of the unknown.

The Niton XRF XLt 500He can be used for semiquantitative sulfur analysis (+/- 20%) portably in the field with wet sediment samples. It is recommended that one remove as much water from the samples as possible in the field before taking measurements, and then correcting for the water content in the samples, which can be determined at a later time. A handheld XRF device has been shown to be a versatile and easy to use analytical method for a number of metals and non-metals. Use of the helium purge extends the utility of the device by permitting the analysis not only of the heavy metals but also of elements that could not previously be analyzed in the field with a hand-held unit. The precision of the unit is excellent, and the limit of detection can be quite low with proper sample preparation.

5. REFERENCES

Analytical Methods for Oxygen Bombs; Parr Instrument; http://www.parrinst.com/doc_library/members/207m.pdf (accessed Oct. 9, 2007).

Atkins, P.; Paula, J. *Physical Chemistry,* 8th ed.; Freeman: NY, **2006**; p994.

Bailey, J. and Gehring, D.; Determination of Traces of Sulfur, Fluorine, and Boron in Organic Materials by Oxygen Bomb Combustion, *Analytical Chemistry,* Vol 33, No 12. November **1961** pp1760-1762.

DR/890 Cataloging Colorimeter Handbook, 6th ed.; Hach Co, **2004**; pp 563-569.

Eaton, A.; Franson, M. *Standard Methods for the Examination of Water & Wastewater*, 21st ed., Centennial ed.; American Publisher Health Association: DC, 2005; pp188-189.

Harris, D., *Quantitative Chemical Analysis,* 7th Edition, W. H. Freeman and Company, **2007**, pp 53-96.

Jenkins, R. *X-Ray Fluorescence Spectrometry*, 2nd ed.; John Wiley and Sons: NY, 1999.

NITON Environmental Analyzer User's Guide, Version 4.2

Operating Instructions for the 1108 Oxygen Combustion Bomb; Parr Instrument; http://www.parrinst.com/doc_library/members/205M.pdf (accessed October 9, 2007.)

Perrott, K.; Kerr, B.; Kear, M.; Sutton, M. Determination of Total Sulphur in Soil Using Inductively Coupled Plasma-Atomic Emission Spectrometry; *Commn. Soil Sci. Plant Anal.* **1991**, 22(13&14), 1477-1487.

Pasmore, J.; Anderson, T.; Shein, J. Portable Tools Pack Plenty of Analyzing Power. *Inspection trends*. [Online] 2005, 8, http://www.niton.com/documents/Literature/
inspectiontrendsarticle0104.pdf (accessed October 10, 2007.)

Richter, A. *Determination of Sulfur in Soil*; Thermo Electron Corporation Internal publication.

Shefsky, S., Comparing Field Portable X-Ray Fluorescence To Laboratory Analysis Of Heavy Metals in Soil; Presented at the International Symposium of Field Screening Methods for Hazardous Wastes and Toxic Chemicals. Las Vegas, Nevada, USA. January 1997. http://www.niton.com/shef02.html (accessed October 9, 2007).

Tabatabai, M. and Bremner, J., Comparison of Some Methods for Determination of Total Sulfur in Soils, *Soil Sci. Soc. Amer. Proc*., **1970,** 34.

Chapter 2

LEAD IN SOIL BY FIELD PORTABLE X-RAY FLUORESCENCE SPECTROMETRY— AN EXAMINATION OF PAIRED IN-SITU AND LABORATORY ICP-AES RESULTS

D.A. Binstock[§], W.F. Gutknecht, A.C. McWilliams
RTI International, P.O. Box 12194, Research Triangle Park, NC 27709

ABSTRACT

A major aspect of lead hazard control is the evaluation of soil lead hazards around housing coated with lead-based paint. The use of field-portable X-ray fluorescence (FPXRF) to do detailed surveying, with limited laboratory confirmation, can provide lead measurements in soil (especially for planning abatement activities) in a far more cost-efficient and timely manner than laboratory analysis. To date, one obstacle to the acceptance of FPXRF as an approved method of measuring lead in soil has been a lack of correspondence between field and laboratory results. In order to minimize the differences between field and laboratory results, RTI International (RTI) has developed a new protocol for field drying and sieving of collected samples for field measurement by FPXRF. To evaluate this new protocol, composite samples were collected in the field following both HUD Guidelines and American Society for Testing and Materials (ASTM) protocols, measured after drying by FPXRF, and returned to the laboratory for confirmatory inductively coupled plasma atomic emission spectroscopy (ICP-AES) analysis. Evaluation of study data from several diverse sites revealed no statistical difference between paired FPXRF and ICP-AES measurements using the new method.

Keywords: lead, soil, XRF, ICP-AES, HUD, field

1. INTRODUCTION

Two major aspects of lead hazard control are the evaluation and mitigation of soil lead hazards around housing that is coated in part with lead-based paint or that exhibits lead contamination from other sources. Major sources of lead in soil include lead-based paint on

[§] Corresponding author: Dr. David A. Binstock, RTI International, P.O. Box 12194, Research Triangle Park, NC; phone: 919-541-6896; fax: 919-541-7215; e-mail: binnie@rti.org.

exterior surfaces that have deteriorated, allowing the lead from the paint to leach into the drip line soil, or organo-lead from automobile exhaust that has been deposited as ultra-fine metal halide aerosols directly onto the soil or onto other surfaces and then leached into the soil. Lead-containing soil may be ingested by children when they play outdoors. It may also be tracked into the house and collect as dust on floors, window sills, toys, utensils, etc., and be ingested through hand-to-mouth activities or inhaled as dust (Mielke and Reagan, 1998). Lead, even at low levels, can cause central nervous system impairment, mental retardation, and behavioral disorders (Needleman et al., 1990).

Recent advances in analytical measurement and sampling design for lead in soil offer significant opportunities for improving soil testing methodology. Using FPXRF to do detailed surveying, with limited laboratory confirmation, can provide more cost-efficient and timely lead measurements in soil (especially for planning abatement activities) than laboratory analysis can. U.S. Environmental Protection Agency (USEPA) Method 6200 provides an approved FPXRF screening method for 26 analytes (including lead) in soil and sediment (USEPA, 1998).

Several groups have reported on the successful use of FPXRF for soil-lead measurement. A pilot study of sources of lead exposure in residential settings was conducted in a mining and smelting district in northern Armenia. A multi-element XRF analyzer was used to test for lead in soil. The highest lead levels were found in loose exterior dust samples, and lead concentrations in yard soil were higher than those in garden soil (Petrosyan et al., 2004). In another study, lead in soil adjacent to an urban highway was measured using FPXRF. Lead content in soil samples collected 15 feet from the highway was determined to be greater than 2,000 ppm. Soil lead decreased as the perpendicular distance from the highway increased (Bachofer, 2004). Lead in soil was tested at 11 San Francisco area houses. FPXRF readings were significantly correlated ($p<0.0005$) with laboratory results and met the study criteria for an acceptable screening method (Reames and Lance, 2002). Although this study and others have shown a correlation between field and laboratory results, the lack of a 1:1 correspondence has essentially hindered the practical application of field XRF measurements.

Several previous studies have indicated that if you provide a field sample similar in particle size and dryness to the prepared laboratory confirmatory sample, a near 1:1 correspondence can be obtained when comparing FPXRF to ICP-AES (Maxfield, 2000). In a study comparing field FPXRF values measured in situ on soils in Poland, geometric mean soil lead concentrations were 200 ppm with the portable XRF and 190 ppm using atomic absorption, with excellent correlation for samples sieved to less than 250µ ($p=0.0001$) (Clark et al., 1999). Another study concluded that "the best results were achieved when the soil samples were prepared prior to their FPXRF analysis" (Boyle and Fitzgerald, 2004). Previous work conducted by RTI has shown a near 1:1 correlation between prepared (dried, ground, sieved) samples measured by both FPXRF and ICP-AES (Binstock and Gutknecht, 2002). Ideally, each field sample would be dried and sieved for FPXRF measurement. The question is how to accomplish this in the field in a cost-efficient manner.

RTI has developed a new protocol for field drying and sieving of collected samples for measurement by FPXRF. This protocol follows traditional HUD and ASTM sampling protocols for housing, with field measurement by FPXRF of the collected samples. In order to evaluate this protocol, composite samples were collected following both HUD Guidelines and ASTM

protocols, measured after drying and sieving by FPXRF, and returned to the laboratory for confirmatory ICP-AES analysis.

2. MATERIAL AND METHODS

Soil sampling and measurement of soil lead in residential yards was performed in six cities across the United States. Site locations ranged from Charlotte, NC, to Minneapolis, MN (Table 1). At several potential sites in each city, FPXRF screening analysis was performed in situ, and the two most suitable sites (based on lead levels, accessibility, and size of drip line) were chosen for the study. Screening analysis involved taking several 30-second surface XRF readings at locations along the drip line and from any bare play areas around the dwelling to gain an estimate of soil lead levels. The instrument used was a Niton XL-309 equipped with a 10mCi Cd-109 source.

Table 1. Site Locations for FPXRF Sampling

Site Location	ID	Year Built
Greensboro, NC	NCG-1	1931
	NCG-2	1922
Rochester, NY	NY-1	1925
	NY-2	1920
Knoxville, TN	TN-1	1945
	TN-2	1947
Charlotte, NC	NCC-1	1922
	NCC-2	1929
Petersburg, VA	VA-1	1940
	VA-2	1917
Minneapolis, MN	MN-1	1900
	MN-2	1900

Following HUD Guidelines protocol for soil sampling, at least two composite samples were collected from each drip line area (HUD, 1995). Each composite was composed of five individual 0.5-inch cores; each core was taken from an area at least 2 feet from another core and 2 feet from the dwelling foundation. All cores were collected using a 10-gram Terra Core® single-use device sampler (En Novative Technologies, Inc., Green Bay, WI). In addition, at least two composites were collected from the same area following the ASTM standard practice for field collection of soil samples for lead determination (ASTM, 2000). Each composite was composed of three individual 0.5-inch deep cores collected from an area 2 feet from the dwelling foundation; one of the cores was collected at the center of this area, and two more cores from within a 1-foot diameter circle around this initial core.

All composite soil samples were placed in a 5-inch hexagonal weigh boat (VWR 25433-104), lightly pulverized with a glass rod to facilitate mixing, and dried. Average sample size was

approximately 75 grams. Depending on their moisture condition, samples were dried either by air (if slightly wet) or by a 700-watt microwave oven (GE JES738WJ) connected to a car battery using an inverter (Xantrex 1200 plus). If residential power was available, the microwave oven was connected directly to the house current. Drying typically required one 3-minute cycle at full microwave power. After being dried, the entire sample was placed on a 3-inch diameter stacked sieve composed of a 2mm screen atop a 250µ screen, and shaken vigorously for 2 minutes. A stiff nylon bristle brush was used to clean the screens between samples (VWR 17210-008). Screened material of less than 250µ was put into an XRF sample cup (Chemplex Industries No. 1330, Palm City, FL) and analyzed in duplicate by FPXRF using a 30-second exposure time (Niton XL-309 instrument).

Dried and sieved samples were shipped to the laboratory for acid digestion and ICP-AES analysis (Binstock et al., 1997). In the laboratory, a 0.2g portion of the sieved sample was removed from each XRF cup and placed into a 50mL centrifuge tube (BD Falcon 352098). Five mL of 25% HNO3 was added and the centrifuge tubes immersed in an ultrasonic bath (Branson, model 5510) for 30 minutes. Upon removal of the tubes from the bath, deionized water was added to the 50mL mark. The samples were then shaken for 30 seconds and centrifuged for 20 minutes at 2,000 rpm. ICP-AES analysis was done using a Leeman Labs Prodigy high-dispersion ICP.

3. RESULTS

Table 2 presents mean FPXRF and mean ICP-AES results for all 12 sites. Statistical tests (sign test, Wilcoxon signed rank test, and paired t-test) on 11 of the 12 sites show no statistical difference between mean FPXRF and ICP-AES soil lead using HUD and ASTM sampling methods. The VA-1 site did not pass equivalency for the signed rank test.

Table 2. Results of FPXRF and ICP-AES Measurement of Soil Lead by Site

Site	Number of Composite Samples*	Mean XRF (mg Pb/Kg)	Mean ICP-AES (mg Pb/Kg)	R^2
NCG-1	4	2,660	2,800	0.92
NCG-2	8	1,620	1,690	0.99
NY-1	4	743	778	0.99
NY-2	4	960	974	1.00
TN-1	5	162	152	0.99
TN-2	6	291	298	0.98
NCC-1	6	3,180	3,070	0.98
NCC-2	6	399	337	1.00
VA-1	8	1,380	1,410	1.00
VA-2	8	828	845	1.00
MN-1	6	1,140	1,130	0.99
MN-2	7	3,490	3,590	0.99

*Collected using HUD and ASTM protocols

Regression analysis by sampling method over all sites similarly shows a near 1:1 correspondence between mean FPXRF and ICP-AES soil lead measurements with a slope of 1.02 for the HUD sampling method and a slope of 1.06 for the ASTM sampling method (Figures 1 and 2). Additionally, statistical tests (sign test, Wilcoxon signed rank test, and paired t-test) by sampling method over all sites shows no statistical difference between mean FPXRF and ICP-AES soil lead measurements.

Figure 1. FPXRF Pb of Dried, Sieved Soil vs. ICP-AES Pb of Acid-Digested Soil, HUD Sampling Method (N=35)

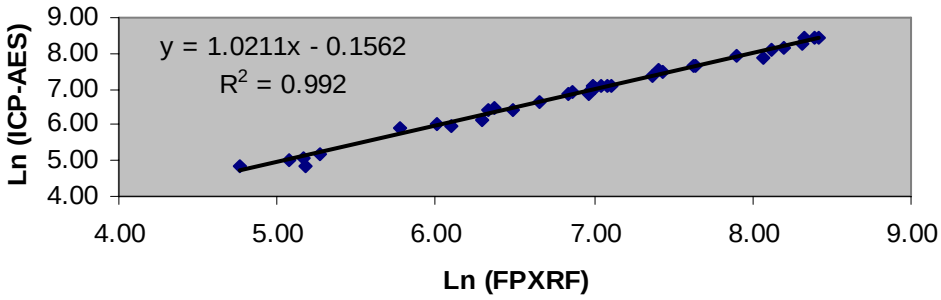

Figure 2. FPXRF Pb of Dried, Sieved Soil vs. ICP-AES Pb of Acid-Digested Soil, ASTM Sampling Method (N=37)

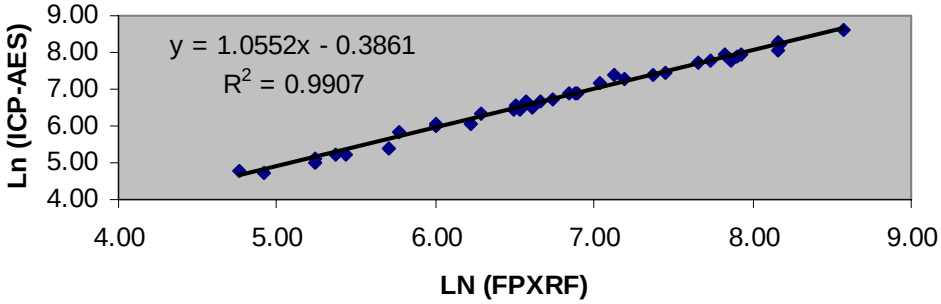

4. DISCUSSION/CONCLUSIONS

Examination of the data clearly shows a statistical equivalence for mean soil lead values of paired samples collected following HUD Guidelines and ASTM protocols and measured by FPXRF and laboratory ICP-AES values. The data is fairly extensive, comprising a total of 72 paired samples collected from 12 residential sites in 6 U.S. cities. A variety of soil types ranging from dry loam to sandy is represented. Each site presents a similar statistical equivalence between in situ FPXRF soil lead values and laboratory ICP-AES soil lead values.

The current approved methods of collecting residential soil samples used by lead inspectors and risk assessors—either HUD Guidelines, ASTM E1727-99 sampling protocol, or similar methods based on these, followed by shipment of the samples to an accredited laboratory for analysis—are fairly time consuming. In some cases, turnaround time for lab results can be as much as 2 weeks. In contrast, collecting, drying, sieving, and measuring composite samples in the field following current sampling protocol with FPXRF measurement can be done in less than 2 hours.

This research presents a strong case for the use of FPXRF methodology as a significant improvement over current protocols for sampling and analyzing lead in residential soils. With proper sample preparation, one can obtain results in the field that are not only statistically equivalent to those obtained in the laboratory, but also more timely and cost-efficient.

5. REFERENCES

ASTM (American Society for Testing and Materials). 2000. ASTM E 1727-99. Standard Practice for Field Collection of Soil Samples for Lead Determination by Atomic Spectrometry Techniques. West Conshohocken, PA.

Bachofer, S.J. 2004. Field Sampling with a FP-XRF: A Real-World Lab Experience. Spectros Lett 37(2), 115–128.

Binstock, D.A., Hodson, L.L., and Gutknecht, W.F. 1997. Standard Operating Procedure for Extraction of Lead-in-Paint, Bulk Dust and Soil by Ultrasonic Acid Digestion and Atomic Absorption or Inductively Coupled Plasma Emission Spectrometry. RTI No. EG-8476-111.

Binstock, D.A., and Gutknecht, W.F. 2002. Final Report for Research to Develop a Cost-Effective Approach to Residential Soil-Lead Risk Assessment. HUD Cooperative Agreement NCLH R0055-99.

Boyle, T.J., and Fitzgerald, J. 2004. A Comparison of FPXRF Data with ICP/AA Data. The Annual International Conference on Soils, Sediments and Water. Amherst, MA.

Clark, S., Menrath, W., Chen, M., Roda, S., and Succop, P. 1999. Use of a Field Portable X-ray Fluorescence Analyzer to Determine the Concentration of Lead and Other Metals in Soil Samples. Ann Agric Environ Med 6(1), 27–32.

HUD (U.S. Department of Housing and Urban Development). 1995. Guidelines for the Evaluation and Control of Lead-Based Paint Hazards in Housing. Washington, DC.

Maxfield, R. 2000. A Community Based Environmental Lead Assessment and Remediation Program. Presented at the 2000 National Lead Grantee Conference. Atlanta, GA.

Mielke, H.W., and Reagan, P.L. 1998. Soil is an important pathway of human lead exposure. Environ Health Perspect 106, 217–229.

Needleman, H.L., Schell, A., Bellinger, D., Leviton, A., and Allred, E.N. 1990. The long-term effects of exposure to low doses of lead in childhood. An 11-year follow-up report. N Engl J Med 322, 83–88.

Petrosyan, V., Orlova, A., Dunlap, C.E., Babayan, E., Farfel, M., and Von Braun, M. 2004. Lead in residential soil and dust in a mining and smelting district in Northern Armenia: a pilot study. Environ Res 94(3), 297–308.

Reames, G., and Lance, L.L. 2002. Childhood lead poisoning investigators: Evaluating a portable instrument for testing soil lead. J Environ Health 64(8), 9–13.

USEPA (U.S. Environmental Protection Agency). 1998. Method 6200: Field Portable X-Ray Fluorescence Spectrometry for the Determination of Elemental Concentrations in Soil and Sediment. Washington, DC.

PART II: Bioremediation

Chapter 3

BIOREMEDIATION OF TOCS PRESENT IN FUEL-CONTAMINATED DESERT MINING SOIL AND SAWDUST IN THE ATACAMA DESERT (CHILE)

Alex Godoy-Faúndez[1§], Lorenzo Reyes-Bozo[1], Blanca Antizar-Lalislao[2] and César Sáez-Navarrete[1]

[1]*Department of Chemical Engineering and Bioprocesses, Pontificia Universidad Católica de Chile, Vic. Mackenna 4860, Macul, Santiago, CHILE.*

[2] *Department of Water and Environment Science and Technology, University of Cantabria, 39316 Tanos, Cantabria, SPAIN.*

ABSTRACT

Repetitive spills of fuels and lubricants during reparation and maintenance of machinery within Chilean mining industry constitute an unseen pollution of current environmental concern. These spills had subsequently been adsorbed by desert soils and sawdust used as cheap sorbent materials are considered hazardous wastes (Chilean legislation) and must be contained and disposed on a hazardous waste landfill. Alternative accepted treatments to landfilling consist in biological treatments such as bioremediation, a cost-effective opportunity for Chile. Nevertheless, it remains unknown if bioremediation of fuel-contaminated wastes is feasible under in desert mining soils. In this study we determined the feasibility of bioremediation by aerated in-vessel composting of an aged fuel-contaminated desert mining soil and sawdust. We investigated the removal of total organic compounds (TOCs) in a composting process at laboratory scale under controlled conditions of temperature, humidity and ventilation at five soil to sawdust ratios (S:SD, 1:0, 3:1, 1:1, 1:3, 0:1). Terminal-restriction fragment length polymorphism (TRFLP) tests were conducted in order to determinate the Richness and Diversity of Operational Taxonomic Units through treatment (O.T.U.). We relate removal curves to changes in the diversity of microbial communities determinate molecular tools. Different TOC removal curves were obtained and observed after 56 days of treatment. The highest (50%) and the lowest (35%) removal rate were found in reactor S: SD-0:1 and S: SD-1:0, respectively. Interaction between presence of sawdust and time factors, both as source of variation, was statistically significative on removal curves. No trends were found among changes in richness and diversity as well as in correlation between them and removal curves. However, higher levels of sawdust corresponded with an incremental number of O.T.U., diversity and higher removal's rate. Our results shown that removal TOCs are feasible desert soil at every ratio S: SD but with differential goal achievements and molecular profiles obtained are not a predictive tool related to abatement of pollution in this treatment.

§ Corresponding Author: Alex Godoy-Faúndez, Department of Chemical Engineering and Bioprocesses, Pontificia Universidad Católica de Chile, Vic. Mackenna 4860, Macul, Santiago, CHILE, Email: agodoy@ing.puc.cl

Keywords: Bioremediation, desert mining soils, TOC, Atacama Desert.

1. INTRODUCTION

Continuous fuel spills within the Chilean mining industry at Atacama Desert (Chile) and necessity of abatement pollution attempts have allowed using soils and sawdust as a low-cost locally available sorbent material, resulting in large amounts of fuel-contaminated materials disposed in landfills by hazardous wastes. Chilean legislation treats this fuel-contaminated material as hazardous waste and therefore, it should be contained or treated (Ministerio de Salud, Chile, 2004). These materials are accumulated on hazardous waste landfills over time and need to be cleaned-up. This research investigated the application of in-vessel composting of a fuel-contaminated desert-mining soil and sawdust in the Atacama Desert as a bioremediation treatment technology monitored by molecular tools.

2. MATERIALS AND METHODS

30 cylindrical poly-vinyl-chloride aerated composting reactors were set-up at laboratory-scale and operated continuously during 56 days at constant ventilation (16 L min^{-1}) by introduction of atmospheric air previously warmed at 60ºC for maintain internal a mesophilic temperature range (30 ± 2ºC at the top surface of the composting mixture in contact with the head space, and 40 ± 2ºC at the bottom). Moisture content was adjusted at 50%. Composting reactors were operated using 2000gr of five soil to sawdust ratios (S: SD, 1:0, 3:1, 1:1, 1:3, 0:1, on a dry weight basis) in triplicate previously mixed, homogenized and air-dried. Total organic carbon (TOC) concentrations were monitored according to Standard Methods (USEPA, 2005). Terminal-restriction fragment length polymorphism (TRFLP) was performed by isolation communitarian microbial DNA (DNA isolation kit, MOBIO), and used as the template for the polymerase chain reaction (PCR) using primer pairs 8F labeled by NED fluorochrome (5´ AGA GTT TGA TCC TGG CTC AG 3´) and 1392R (5´ ACG GGC GGT GTG TAC 3´) both designed for the 16S eubacterial rDNA sequences. PCR product was digested with the enzyme HhaI and restriction fragments. Restriction fragments were separated (capillary electrophoresis) and detected in Perkin Elmer ABI Prism 310 sequencer. For each microbial community, richness and diversity were also determined. Richness (S) was defined as the number of phylotypes (O.T.U.) and the Diversity expressed as Shannon-Wiener index (H´) (Kowalchuk et al., 2004). Abiotic controls comprised the same ratios previously radiated with three doses of Gamma rays at 25 kGy. Two-factor ANOVA test (factor 1, treatment (sawdust percentage); factor 2, time) was applied for each removal curves to determinate their contribution as variation sources in removal fuel.

3. RESULTS

For study the feasibility of applying composting as a bioremediation treatment, bioreactors at lab scale were used (Godoy-Faúndez et al., 2007). Different removal curves were obtained. Highest TOC removals rates were observed in all reactors after 28 days of treatment (Fig.1). The highest removal rate was found in the reactor with 100% sawdust (56, 8%) and the lowest in

reactor with 100% soil (34, 6%). Reactors with ratios S: SD, 3:1, 1:1 and 1:3 had removal rates among 39 and 44% (data not shown). These results support the idea that microbial communities need turning on or lag phase before to activate their degradative metabolic activities. No changes were observed in abiotic controls displaying that mainly the removal TOCs could be due to biological degradation and not by mass transfer phenomenon.

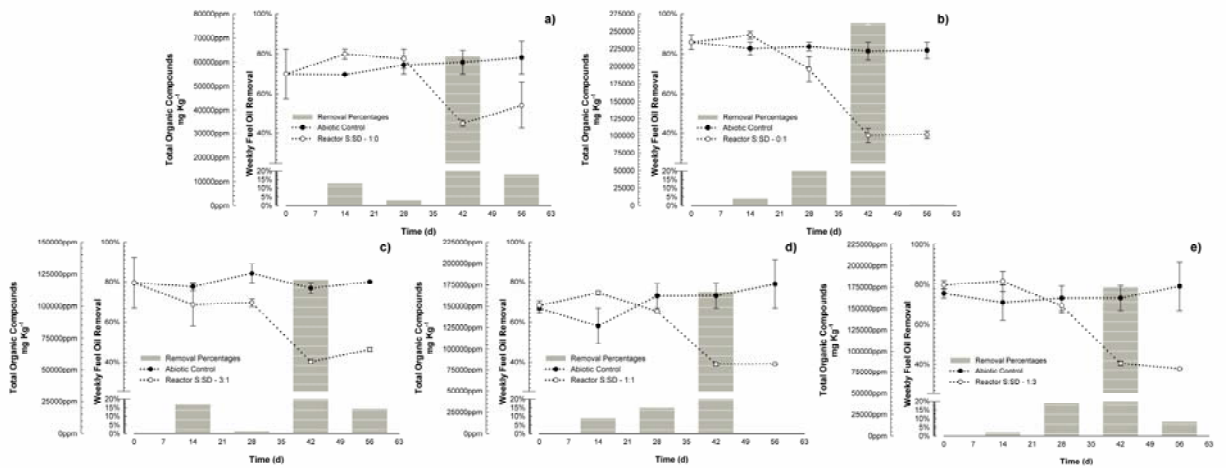

Figure 1. The figure show removal curves and weekly fuel oil removal percentages calculated as the remotion percentage among two consecutive measurements for every ratio Soil: Sawdust (S:SD) by week: a) Reactor with 100% soil; b) Reactor with 100% Sawdust; c) Reactor with Ratio S:SD-3:1; c) Reactor with Ratio S:SD-1:1; c) Reactor with Ratio S:SD-1:3.

For determining the influence of factors (presence of sawdust and time of treatment) on removal curves, Two-Way ANOVA was performed. In our experiment was not feasible separate both effects due to significant interaction between both parameters ($p<0.0001$) (Fig. 2). In abiotic controls, variations in removal curves could be due mainly to uncertainness associated on standard errors in detection's techniques. However, presence of sawdust and time of treatment are having a relevant effect on treatment.

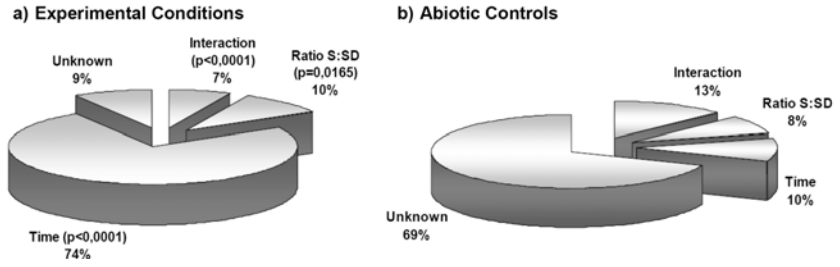

Figure 2. The figures show the effect of Time, Ratios S:SD and Interaction among factors as variation sources percentages on removal curves (changes and differences among removal curves, respectively) by Two-Way Repeated Measures ANOVA.

For determining if changes in molecular profiles can be used as bioindicator of process, community indexes such as Richness and Diversity were obtained by T-RFLP. Low number of O.T.U.s (fragments detected) were found in all reactor expressed as Richness index (Fig.3) perhaps due to a poor isolation of DNA or low abundance of microorganism in ratios S:SD. Nevertheless, higher levels of sawdust corresponded with an incremental number of O.T.U. coupled to higher diversities in microbial communities. Diversities changed throughout the treatment, but without correlations with the removal curves or removal rates per week (data not shown).

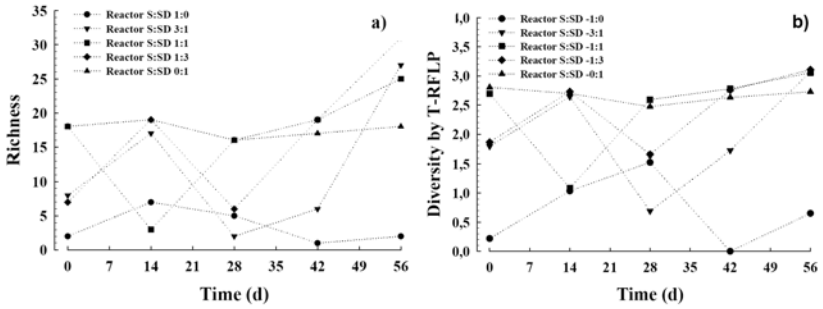

Figure 3. The figures show changes related to Richness and Diversity. a) Changes associated to Richness along of treatment. b) Changes associated to Diversity along of treatment

4. DISCUSSION AND CONCLUSIONS

Our results indicate that bioremediation of desert mining soils and sawdust contaminated with fuel-oil is feasible to be applied. Different TOC removal curves were obtained after 56 days of treatment. All obtained curves have a lag phase with a huge decreasing in final times. These results are supported by large removal percentages after middle times. Aforementioned, is not correlated to number of fragments detected by molecular profiles found it. In our results, at higher levels of sawdust, Richness and Diversity was higher at compare with other ratios S: SD. Changes in profiling have not correlations with the removal curves. Higher removal rates were found in reactors with S: SD ratios 1:3 and 100% sawdust. These removal rates perhaps were feasible due to higher presence of sawdust as bulking agent (porous media) that could allow desorption processes as well as biodegradation supported by metabolism present in alochtonous microorganisms. No changes were found in abiotic controls suggesting that TOC removals in the treated reactors were mainly due to biodegradation mechanisms.

5. REFERENCES

Godoy-Faúndez A., Antizar-Ladislao B., Reyes-Bozo L., Camaño A. and Sáez-Navarrete C. 2007. Bioremediation of contaminated mixtures of desert mining soil and sawdust with fuel oil by aerated in-vessel composting in the Atacama Region (Chile). Journal of Hazardous Materials. 2008 Vol 151/2-3 pp 649-657.

Kowalchuk, G., de Bruijn, F., Head, I., Akkermans, A. and van Elsas, J. 2004. Molecular Microbial Ecology Manual, Second Edition Volume 1.11, pp 149-158 and 3.15, pp 789-808. Kluwer Academic.

MS, Ministerio de Salud (Ministry of Health). Decreto Supremo No. 148: Reglamento Sanitario Sobre Manejo de Residuos Peligrosos (Sanitary normative on handling hazardous wastes), Santiago, República de Chile, 2004.

USEPA (U.S. Environmental Protection Agency). 2005. Methods for evaluating solid wastes physical/chemical methods. 8000 Series: Method 8260 B-Method 8270. Web site visited, March 2007. <http://www.epa.gov/epaoswer/hazwaste/test/8_series.htm>.

Chapter 4

USE OF DEGRADABLE, NON-OXIDIZING BIOCIDES AND BIODISPERSANTS FOR THE MAINTENANCE OF CAPACITY IN NUTRIENT INJECTION WELLS

Brad Horn, PE[1§], Gary Richards[2]
[1] *Redux Technology, P.O. Box 331, Newfane, Vermont* [2] *Redux Technology, 1317 Pennsridge Court, Downingtown, PA*

ABSTRACT

Fouling of water supply wells is a common problem dating from the time humans started using groundwater resources for water supply. In the groundwater remediation field, fouling of recovery and treatment systems has been a similarly common operating problem. Thus, it is not surprising, with the increased use of in-situ remedial methods, that fouling of in-situ treatment units is becoming a major design concern. In-situ treatment units include recovery wells, injection wells, recirculating wells, flow-through treatment cells, and in some cases, geologic formations themselves. The very effectiveness of these units depends greatly upon retention of permeability or hydraulic capacity. Capacity can be dramatically reduced due to fouling by naturally occurring inorganic precipitates or by microbial deposits.

One of the least surprising instances of fouling of an in-situ treatment unit involves various bioenhancement techniques, where nutrients are injected with the intention of enhancing certain types of bioactivity and subsequent biodegradation of contamination. The data presented in this paper are derived from experience at remedial sites where bioenhancement activities have been self-defeating by causing a loss of permeability in injection wells, surrounding geological formations, or down-gradient recovery or recirculation wells. In these cases, non-oxidizing biocides, bio-dispersants, saponification agents or other additives have been applied to retain permeability in the hydraulic "bottlenecks" of these systems, such as injection wells and surrounding formations. Data collected from such applications shows that proper characterization of fouling mechanisms and subsequent application of well-designed deposit control programs can eliminate operational problems associated with fouling arising from bioenhancement.

This paper introduces the key concepts in deposit control practices as they apply to fouling of in-situ treatment units. It provides an overview of the various agents and techniques used in

§ Corresponding Author: Brad Horn, Redux Technology, P.O. Box 331, Newfane, Vermont 05345, Tel: 802-365-7200, Fax: 802-365-4652, email: bhorn@reduxtech.com

such deposit control programs. Regulatory and design issues are discussed, and subsequently illustrated by a series of brief case studies.

1. INTRODUCTION

Fouling of water treatment equipment by inorganic and microbial deposition is a common and widespread operating and maintenance challenge. The annual expense incurred in controlling fouling of drinking water systems, boilers, cooling water systems, irrigation systems and wastewater systems exceeds billions of dollars worldwide. In the groundwater remediation market in the United States, the vast majority of expenditures go to operations and maintenance costs, with control of fouling being a major maintenance cost at many sites (API, 1990). The authors of this paper have specialized exclusively in solving fouling problems in groundwater remediation systems, with a combined experience of about forty years in this area. According to their experience, fouling occurs at a minority of sites where groundwater is treated, but at those sites where it is occurring, controlling fouling is always a significant portion of operations costs.

Inorganic deposition or microbial growth comprises all fouling in groundwater remediation systems. Inorganic deposition usually consists of iron-related deposits or hardness scales. Iron-related deposits typically involve both iron and manganese, naturally occurring, which are soluble in the reducing conditions found in most aquifers, but which easily oxidize and thus precipitate when the oxidation-reduction potential of groundwater increases due to certain ex-situ or in-situ treatments. The oxidation of iron and manganese may be a simple chemical oxidation or it may be microbially mediated, yielding energy for certain iron-related bacterial species. Thus it is not uncommon to find a significant microbial component in iron-related deposition. Hardness deposition consists primarily of naturally occurring calcium and manganese carbonates, which are dissolved to saturation (or equilibrium) in groundwater at some ambient pH in-situ, but which precipitate due to changes in pH which may occur upon treatment. Microbial deposition is rarely associated with hardness deposits.

While microorganisms are widely known to be pervasive in groundwater, the formation of concentrations of microbial consortia associated with troublesome fouling usually involves the exposure of naturally occurring microbial species to a sudden increase in substrate or growth-limiting nutrient. Examples of this phenomenon would be conditions in an oil-water separator, resulting from aeration and mixing occurring during pumping, or those occurring around a nutrient injection well during in-situ biostimulation.

Biofouling problems in environmental systems tend to be due to 1) slime forming bacteria, 2) iron-related bacteria or 3) biologically stabilized emulsions. Biofouling problems may manifest themselves in remedial systems in many ways. Examples include:

- Slime that blinds bag filters and reduces service life
- Emulsions that clog coalescing plate oil-water separators
- Deposits that plug the surface of activated carbon filters
- Slime and encrustation of well screens and subsequent loss of capacity
- Deposits in pumps, conveyance pipes, and transfer equipment
- Flow restrictions in treated water reinjection systems

This paper provides an overview of methods used to control biofouling in the groundwater remediation field. It includes a description of common characteristics of biofouling in these applications, chemicals and techniques that have been applied for control, and provides several case studies for illustration.

2. BASIC MICROBIOLOGY RELEVANT TO SITE REMEDIATION

Both bacteria and fungi can achieve biodegradation of organic materials in natural environments. These two types of organisms utilize different chemical pathways for degradation and thrive in slightly different environmental conditions. While fungi and bacteria commonly coexist in natural environments, the optimum pH for fungal growth is lower than that for bacteria. While bacteria are certainly the dominant biodegraders in conditions found at remedial sites, both types of organisms can contribute to biofouling.

Bacteria that cause biofouling in remedial systems tend to be indigenous, except in cases of bio-augmentation, which involves the introduction of cultured or "manufactured" contaminant-targeted microbial species. Unlike certain fungi, all bacteria are single-celled organisms. They range in size from approximately one to five microns. Bacteria reproduce by binary fission, in which a mature cell splits into two new cells. For many species found at remedial sites, the time required for a cell to divide, or generation time, is as short as thirty minutes. At this rate a single organism can become ten million cells within 12 hours. This exponential growth can produce huge amounts of biomass in a short amount of time.

Bacteria require an energy source and nutrients (primarily carbon-based molecules) to grow, and are thus classified based upon their energy source and nutritive requirements. Bacteria which derive energy from light are termed phototrophs, and those that derive energy from either organic or inorganic molecules in their environment are called chemotrophs. Those which obtain carbon from carbon dioxide are autotrophs, and those which obtain carbon from organic molecules are called heterotrophs. Combining these terms allows the classification of all bacteria into four categories, as illustrated in Table I (adapted from Baker and Herson, 1994).

Table 1. Classification of Micro-organisms

Classification	Energy Source	Carbon Source
Photoautotroph	Light	Carbon dioxide
Photoheterotroph	Light	Organic carbon
Chemoautotroph	Inorganic chemical	Carbon dioxide
Chemoheterotroph	Organic carbon	Organic carbon

The most important class of bacteria, in terms of bioremediation, is clearly the chemoheterotrophs, which use organic compounds as both an energy and carbon source for cell synthesis. In terms of biofouling, however, both types of chemotrophs are important, and in rare cases where treatment units are exposed to light (as in above-grade translucent treatment units) photoheterotrophs and algae can become important contributors to fouling problems.

Finally, in considering the impact of chemoheterotrophs, in terms of bioremedial and biofouling considerations, one must understand the various metabolic modes used by these organisms. Bacteria degrade organic molecules through a series of microbially mediated reduction-oxidation (redox) reactions, in which one compound is reduced (gains electrons) and another is oxidized (loses electrons), and in the process, energy is liberated. Bacteria produce enzymes which catalyze these reactions in order to harvest energy from the degradation process, and utilize adenosine triphosphate (ATP) to gather the energy, and release it later when needed elsewhere for cellular activity. The metabolic processes used by various bacteria to degrade organic molecules are categorized by the type of compound which initially is oxidized (electron donor) and the compound which is finally reduced, referred to as the terminal electron acceptor. Table 2 (adapted from Baker and Herson, 1994) shows this categorization.

Table 2. Classification of Metabolic Sequences

Type of Metabolism	Electron Donor	Terminal Electron Acceptor
Respiration	Organic or Inorganic Compound	Inorganic Compound
Aerobic		Oxygen (O_2)
Anaerobic		Fe^{+3}, SO_4^{-2}, CO_2, NO_3^-,
Fermentation	Organic Compound	Organic Compound

While fermentation has been shown to play an insignificant role in bioremediation, respiratory metabolism Is a very important process in terms of both bioremediation and biofouling. The type of respiration that occurs at remedial sites is a function of the available oxygen, among other factors. A lack of oxygen favors bacteria that use pathways involving anaerobic respiration and, if inorganic compounds are also absent, fermentation. Bacteria utilizing aerobic respiration metabolize more organic mass than those using anaerobic processes, and so, for purposes of degradation of organic contaminants at remedial sites, aerobic processes are most important and much more commonly employed. Research over the past ten years, however, shows that anaerobic processes may be more capable of degrading certain halogenated (highly oxidized) compounds, as well as nitroaromatic and aminoaromatic compounds, which include certain pesticides and energetic compounds (Liss and Baker, 1994).

Availability of oxygen in groundwater is related to a characteristic of aqueous environments called the redox potential, denoted Eh. This parameter expresses the activity of electrons in a solution, just as pH

expresses the activity of protons. Eh can be measured as the potential for a redox reaction in relation to a standard hydrogen electrode, and is expressed in millivolt units. While oxygen is available as O2 when redox potential is high (>800 mV at pH 8), it is reduced to O-2 (as in H2O) at lower Eh, thus forcing microbial consortia to utilize a variety of other inorganic compounds as terminal electron acceptor. For example, at Eh of 770 millivolts, ferric iron, or iron III, can serve as terminal electron acceptor thus being reduced to ferrous iron, or iron II (Deutsch, 1997). The oxidized and reduced inorganic species involved in a redox reaction (such as ferrous and ferric iron) are also referred to as a redox pair. Table 3 (adapted from Liss and Baker, 1994) shows the relationship between various redox pairs, associated respiratory processes, and redox conditions.

While anaerobic respiratory processes may not be important in most bioremediation applications, certain anaerobic microbial processes are important in terms of biofouling. Redox pairs shown in Table 3 are by nature sensitive to redox potential. Of note, in terms of fouling, is that for some redox pairs, solubility of the two species involved are different. For example, ferric iron salts are relatively insoluble while ferrous iron salts are quite soluble. Also, sulfate salts are generally soluble, while hydrogen sulfide is a gas with limited solubility. Thus microbial activity of certain types can create insoluble inorganic deposits (or gases) that can be problematic.

Table 3. Redox Conditions Versus Favored Respiratory Processes

Redox Pair	Respiratory Process	Redox Conditions
O_2, / H_2O	Aerobic Respiration	Oxidized
Fe^{+3} / Fe^{+2}	Iron Reduction	↓
NO_3^- / N_2	Denitrification	
NO_3^- / NO_2^-	Nitrate Reduction	
SO_4^{-2} / H_2S	Sulfate Reduction	
CO_2 / CH_3COO^-	Methanogenesis/Fermentation	
CO_2 / CH_4	Methanogenesis	Highly Reduced

FOULING ASSOCIATED WITH BIOREMEDIATION APPLICATIONS

Fouling in bioremediation systems can involve precipitation of naturally occurring inorganic compounds or excess growth of microbial masses. In some cases inorganic precipitation is associated with microbial growth as is the case with bacterial consortia associated with high iron or sulfate concentrations in groundwater.

Inorganic precipitation usually involves precipitation of iron oxyhydroxides or hardness salts. Iron deposition occurs due to the oxidation of iron from the ferrous to the ferric state, with the resulting formation of insoluble iron (III) hydroxide. Newly formed iron (III) hydroxide can remain mobile as submicron colloidal particulate, but usually agglomerates in time, and subsequently precipitates in above grade treatment vessels, or sorbs on soil surfaces in-situ. Hardness salts usually precipitate as a result of pH changes which are common in above-grade treatment systems involving aeration, which also desorbs carbon dioxide, typically increasing pH about 1 unit. Such pH changes are unusual in in-situ bioremediation projects. While the authors have studied hundreds of remedial sites with inorganic fouling in ex-situ treatment equipment, they have received few reports of such precipitation in-situ, where oxidizing agents have been added. This may be that precipitation is so distributed that its impact on permeability is rarely observed.

Biofouling, both in-situ and ex-situ, generally involves the development of a biofilm which is detected due to its effect on permeability or hydraulic capacity of the aquifer, injection/recovery well or treatment equipment. Bacteria in water systems are either free-floating, also called planktonic bacteria, or attach themselves to surfaces, and are then termed sessile bacteria. Sessile bacteria have appendages which allow them to adhere surfaces. Most of the organisms important in bioremedial applications are sessile (This is why most biotreatability studies are typically done using soil samples rather than groundwater samples, as the latter would contain mostly planktonic organisms). A thin layer of sessile bacteria forms the basis for development of a thicker biofilm, usually composed of a consortium of many different species.

Within a biofilm, bacteria secrete complex sugars known as polysaccharides during their metabolism process. These polysaccharides have a high affinity to adsorb water into their matrix. The polysaccharide and water complex (or biopolymer) can exceed the mass of the bacterial cells by more than 100 times. This biopolymer provides a protective environment that promotes rapid growth of bacteria. Chemically, the polysaccharide also has an affinity for divalent metals. Dissolved calcium, magnesium, and iron react with carboxyl groups on the biopolymer. Eventually, a thick film consisting of bacteria, bacterial by-products, and entrapped minerals accumulates. This accumulated mass is known as biofilm. Depending on ambient water conditions, the surface of the biofilm can support aerobic bacterial activity, while the lower layer of the biofilm is typically deprived of oxygen, and supports development of anaerobic bacteria. These anaerobic bacteria produce troublesome metabolism by-products, including organic intermediates, sulfur compounds, organic acids, and sulfuric acid.

Biofouling in bioremediation projects is often the unavoidable consequence of an effort to stimulate the growth of degrading organisms, and the difficulty in focusing this stimulation on the preferred organisms. The distinction between successful biostimulation and biofouling lies in the extent of operations impediment posed by the biomass generated. When biofilms grow to the extent that flow required to deliver substrate, nutrients or oxidizing/reducing agents is hindered, further biostimulation becomes impossible and self-defeating.

In the authors' experience, the most common point of biofouling at in-situ remediation projects is in the well pack and aquifer surrounding reagent injection wells. Such biofouling is particularly acute when injection is continuous or regular, with little time between injections. Depending on the redox conditions of the injected fluids, changes in redox conditions in the aquifer around an injection point can also contribute to the deposition of redox sensitive inorganic species, particularly iron.

Another common location for both microbial and inorganic deposition, at sites that involve groundwater recovery, is the well pack and well screen of recovery wells. If recovery pumps utilize a control system where pumps cycle on and off at different elevations, oxygenation of the aquifer occurs near the well, causing oxidation of iron, if present. Lower pressure upon groundwater, as it approaches the cone of groundwater table depression formed at a recovery well, can result in the release of carbon dioxide, and associated pH change and precipitation of hardness salts. Exposure of groundwater to air in and around the well bore can stimulate the growth of aerobic organisms, generating biofilms. Finally, iron-related bacteria are prevalent, near recovery wells where redox conditions favor microbially-induced oxidation of iron. Iron bacteria are filamentous organisms that oxidize inorganic ferrous iron as a source of energy and deposit oxidized iron ($Fe(OH)_3$) in their bacterial sheath. *Leptothrix, Crenothrix, and Gallionella* are fairly common species of iron bacteria encountered in groundwater treatment systems. The basic reaction of these bacteria is given below:

$$Fe^{++}\,(\text{ferrous}) + \text{oxygen} \;>\; Fe^{+++}\,(\text{ferric}) + 1\,e^{-}$$

$$Fe^{+++} + 3\,H_2O \;>\; Fe\,(OH)_3 + 3\,H^{+}$$

The electron released in this process is utilized by the bacterium for energy production. Ferric hydroxide is adsorbed into the bacterial sheath. The evolution of hydrogen further depresses pH, which in turn increases the dissolution rate of minerals.

The various types of fouling discussed in this section can be detected by visual inspection (among other methods) in ex-situ applications, but fouling in-situ can only be detected by regular measurement of groundwater flow and specific capacities of recovery and injection wells. In addition, measurement of various parameters pertaining to groundwater chemistry, at sample locations upgradient (or upstream) and downgradient (or downstream) of locations where fouling is occurring can provide valuable clues as to the mechanisms causing deposition.

3. METHODS OF CONTROL OF BIOFOULING

Various chemical methods for controlling inorganic fouling in remedial systems have been successfully applied since 1990. Blended deposit control agents, formulated specifically for groundwater remediation applications, have been applied at hundreds of sites by the authors. However, methods for successfully controlling biofouling are less common in the literature relating to groundwater remediation, and in the experience of the authors. A small number of applications, including those case studies discussed below are instructive.

Many of the commonly employed methods for biofouling control in remediation wells are derived from methods historically used with water supply wells. While some of these methods may be useful in remedial applications, groundwater remediation systems are prone to different, and more severe, biological problems than those encountered in water supply wells. This is due to the fact that contaminated groundwater has more complex chemistry and microbiology than drinking water sources. In addition, chemicals used in rehabilitation of water supply wells (in the US) must be certified for drinking water use (compliant with Standard 60 written by the National Sanitation Foundation, or NSF). This requirement does not apply to remedial well

applications, allowing the use of much more effective products. There are many such agents available that have very favorable toxicological profiles, but for a variety of reasons, do not carry NSF certifications. For the reasons described above, many of the well rehabilitation and deposit control techniques that have been widely applied to municipal water supply systems are ineffective or inappropriate in remedial applications.

Two notable examples are the use of oxidizing biocides and polyphosphate-based sequestering agents, both widely used in rehabilitation of water supply wells. Oxidizing biocides, which include sodium hypochlorite (bleach) and chlorine dioxide may be effective, if properly applied, in temporarily eliminating biomass. However, their use in remedial applications, where high concentrations of redox sensitive depositing species are present, is problematic. For example, where ferrous iron is present in groundwater, these biocide products will necessarily result in deposition of all iron present, solving one problem (biofouling) but creating another (deposition of iron). Polyphosphate-based sequestering agents are widely used to dissolve inorganic deposits. While these products do aid in sequestering iron and hardness deposits, they can enhance ongoing biofouling, because they degrade to orthophosphate, a limiting nutrient in many groundwaters. In remedial applications, more challenging and complex water chemistry, and the potential to use products that are not NSF-approved, combine to allow the use of much higher performance deposit control chemicals.

Well rehabilitation techniques currently used in the remedial field are also derived from those developed in the water supply market. They involve a significant effort in aggressive physical swabbing and surging using large, expensive equipment. Such efforts are necessitated due to the use of relatively ineffective chemical agents, which are limited to those that are NSF-approved. The choice of high performance cleaning and preventative agents, which are not NSF-approved, and not necessary in remedial applications, obviates the need for expensive and aggressive physical cleaning methods, thereby reducing overall costs.

High performance chemicals which have been recently and successfully applied for rehabilitation of fouled wells at remedial sites include non-oxidizing biocides, bio-dispersants, chelating acids and saponification agents. Most of these products are available in proprietary blends that have been developed for site-specific applications, based upon the operating characteristics and nature of fouling at a particular site. Biocides are certainly the most effective way of eliminating biofouling, but the application of biocides in-situ involves regulatory hurdles that vary from state to state. Biocides must be registered federally, and in any state in which they are used, according to the Federal Insecticide, Fungicide and Rodenticide Act (FIFRA). Bio-dispersants, chelating acids and saponification agents are less burdensome to apply, from a regulatory perspective, as they are not subject to the FIFRA requirements.

Non-oxidizing biocides have been used by the authors to control biofouling at hundreds of remedial applications since 1990. These biocides are chosen for their effectiveness on a broad range of microbial species, favorable toxicological profile, rapid degradation characteristics, chemical characteristics which make them non-reactive with organic contaminants commonly present, and safe to operations personnel and treatment equipment. The most effective biocide products are blended with non-biocide ingredients which enhance penetration of dense biofilms, and help disperse non-living biomass. Biocides are typically applied in periodic high-dose ("slug") applications, rather than continuously at lower doses. This avoids adaptation of the microbial consortia, which involves the death of the most sensitive species, yielding resources which enhance growth of more resistant species, resulting, over time, in a biomass resistant to

the treatment. It also results in significant cost savings compared to continuous dosing. Alteration of the biocide used is also a common technique employed to avoid this adaptation process.

Bio-dispersants are non-biocidal surface-active agents which break up biofilms and cause them to "slough off" of surfaces to which they attach. They can be continuously applied or periodically "slug-dosed". Since these products effectively mobilize solids, they can cause clogging in downstream and down-gradient locations, and this potential must be taken into account when designing proper application.

Chelating acids and other sequestering agents reduce biomass in two ways. First, they can be applied in a slug dose to create a low pH shock. Second, their ability to react with inorganics can help to mobilize inorganic components in biofilms, and prevent their "bio-availabilty". Specifically, the authors' have used iron sequestrants, under the right conditions, to control iron bacteria by reducing the presence of free ferrous iron.

Saponfication agents are caustic chemicals which react with bio-organic molecules to enhance their solubility, thus dispersing the polysaccharide slime constituting the majority of biomass. Saponification is the reaction by which soaps are made, creating molecules that are non-polar organic (and therefore water insoluble) on one end, but polar (water soluble) on the other end.

The chemical agents described above have been used to control biofouling of injection and recovery wells, as well as biofouling of ex-situ treatment systems. They have been used individually or in combination, depending upon the application, and have been applied in a variety of ways. At any particular site, the final long-term deposit control program has typically been derived by a series of adjustments in dose rate and feed points, with subsequent monitoring of pressure drops due to re-establishment of biofilm. In all cases involving deposition, treatment must be ongoing to retain hydraulic capacity of treatment units. At sites where well rehabilitation was performed, periodic rehabilitation is required. In other cases, a preventative program of regular chemical dosing can be developed. Case studies described below illustrate how biofouling control programs are site-specific

4. CASE STUDIES

Three brief cases studies are described below, each involving in-situ biofouling at NPL listed Superfund sites. Additional information about these and other applications is available for interested readers.

4.1 Case Study 1: East Coast DOD Site

This site involves a large US Department of Defense installation that includes several locations where remedial activities are ongoing. The subject location had been contaminated with various chlorinated solvents. A major national consulting firm was hired to conduct a pilot test demonstrating in-situ reductive dechlorination, using a recirculating well, screened at two

isolated elevations. While analytical data from the pilot test showed favorable degradation results, water levels in the injection zone began to increase precipitously within two weeks of operation, ultimately resulting in termination of the pilot test work. Figure 1 below gives water levels in the injection and extraction zones during this work. It was subsequently determined that microbiological fouling of the well pack and formation around the recirculation well had caused the permeability loss.

Figure 1
Water Level (Initial operation w/ no bioicide)

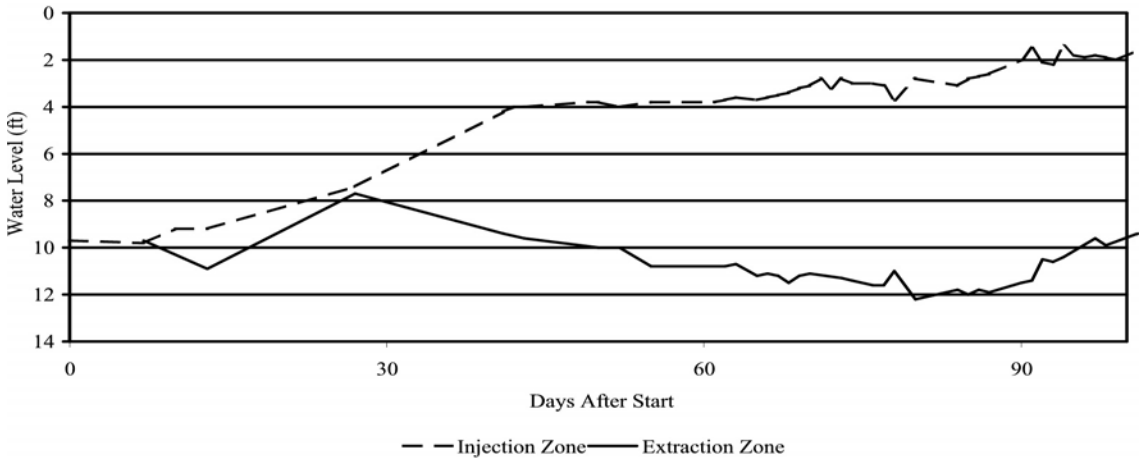

A second phase of pilot testing was planned, after initial investigations into alternative biofouling control methods. Redux B-T20, a non-oxidizing biocide was utilized to redevelop the well, and subsequent operation involved regular injections of B-T20. Subsequent data collection documented the effects of these injections. Of note was the fact that biocidal activity in the aquifer was limited to a certain radius around the well, with intended biodegradation occurring outside this zone, resulting in the maintenance of injection zone permeability, without deleterious effect to overall remedial goals. Figure 2 illustrates water levels in the second phase.

Figure 2
Water Level (Restart with biocide)

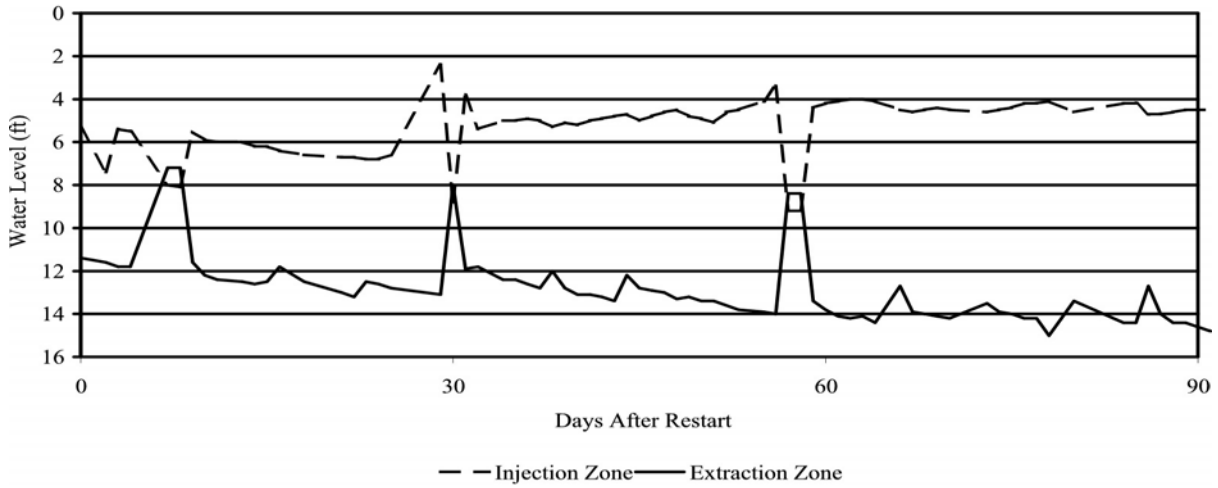

System operation after the restart of the pilot study involved monthly biocide soak of the recirculation well and well pack. The biocide feed was inadvertently lost about 26 days after the restart, after which a loss of permeability occurred, illustrating the bacteriostatic effects of the biofouling control program. A full-scale system has been in successful operation for several years now using regular B-T20 dosing.

4.2 Case Study 2: Long Island Superfund Site

This site involves a historic release of chlorinated solvents from an industrial facility. As is typical of Long Island geology, a sandy permeable aquifer lies under the site, and a public water supply well is located approximately 9,000 feet down-gradient. Three recirculating wells were installed to intercept groundwater, utilizing the UVB design, which involves groundwater recovery at a certain elevation, in-well induced air stripping for removal of VOC's, and recirculation to a different aquifer elevation. These ten-inch wells are nearly 400 feet in total depth, with the water table at about 55 feet below grade. Each well treats about 70 gallons per minute. One of the three wells went on-line in advance of the other two, but within a few weeks, fouling with iron and iron bacteria became evident. Video inspections of well screen showed orange filamentous growths characteristic of iron bacteria. Though iron levels are relatively low (100 to 500 ug/l), they are high enough, in conjunction with other groundwater quality parameters, to result in a significant iron bacteria problem.

Site operators and regulators initially opted to apply an iron deposit control chemical that contains only NSF Standard 60 certified ingredients, in this case a polyphosphate-based sequestering agent. As discussed earlier in this paper, limiting chemical choices to those with NSF certification limits possible ingredients to only a few moderately performing products, and thus results in a severe performance limitation. Application of this deposit control agent was not effective, and well fouling became worse over time, requiring shutdown due to low flows within several months after start-up.

At this time, a thorough well redevelopment was performed and the well was restarted using Redux 601, a blended bio-dispersant comprised of a chelating acid and a polymeric dispersant. The chelating acid reacts with ferrous iron to reduce its bio-availability, and the dispersing polymer reduces the ability of biomass to adhere to well and soil surfaces. As of late 2007, all three wells have been operating successfully for nearly two years without downtime.

4.3 Case Study 3: New Jersey Superfund Site

This major New Jersey superfund site has the highest operating costs of any superfund site, approaching four million dollars annually. Various fouling problems plague the site's multiple recovery wells, which recover groundwater contaminated with chlorinated VOC's and certain heavy metals. Like many sites, fouling by iron and iron-related bacteria did not become serious until an initial operating period of about two years. On many sites, well fouling is not aggressively monitored, and gradual well fouling goes unnoticed, until target recovery rates

simply are not achievable. Upon recognition that well fouling was occurring, extraction well redevelopment and pipeline cleaning has been required at least twice yearly.

Redux Technology became involved in 2005 and has since been developing well-specific deposit control programs for each well, in stepwise fashion. Initial efforts focused on improving well development procedures so that maximum specific capacities could be recovered in the regular redevelopment program. A multi-step well redevelopment procedure has shown the best results. The procedure developed to date includes the following steps:

- Physically remove accumulated debris via "hydroblast" or brush
- Acidify well with Redux 510, low corrosivity acid, for sixteen to twenty-four hours. This step dissolves the mineral portion of the biomass
- Surge well with surge block for two to four hours
- Airlift resulting debris
- Apply alkaline saponification treatment, for sixteen to twenty-four hours. This step removes residual polysaccharide "bioslime" deposits.
- Surge well with surge block for two to four hours
- Airlift any residual debris

In addition to an improved well redevelopment program, Redux has instituted preventative chemical additions for certain wells, eliminating the need for regular well redevelopment. For most wells, this has involved down-hole application of a small continuous dose of Redux 333, a high performance agent which contains an iron sequestering agent and a bio-dispersant. Project managers recently decided to expand the application of the preventative program to additional recovery wells.

5. CONCLUSIONS

Important issues discussed in this paper which should be re-iterated include:

- The exponential growth of bacteria can produce huge amounts of biomass in a short amount of time. This can result in sudden and surprising changes in the operating characteristics at sites with biofouling.
- Biofilm is the term for an accumulated mass comprised of bacteria, polysaccharide secretions, and inorganic particulates deposited within.
- Aerobic and anaerobic respiratory bacterial processes are the most important contributors to biofilm production.
- Certain types of microbial activity can create insoluble inorganic deposits that contribute to biofouling.
- Non-oxidizing biocides have been used to control biofouling at numerous remediation sites since 1990.
- Various non-biocidal methods of controlling biofouling have been successfully applied on a limited number of sites in the US recently.
- Dosing techniques play an important role in overall biofouling control program effectiveness and costs.

The pervasiveness of fouling of ex-situ treatment units in the groundwater remediation field is now well recognized by system designers. While there has been continued technology

advances and increased popularity of innovative in-situ treatment methods in recent years, fouling in these application often goes unrecognized. This often results in increased operations costs as retrofit deposit control programs become required. A wider recognition of the potential for fouling and its operating complications is required, since design forethought can often greatly ameliorate the operating impact of these common operating problems. Along with the recent developments in the application of in-situ treatment programs, new chemicals and techniques have been developed which apply to fouling in this type of application. These new chemical products provide increased performance, and present lower toxicological impact than previously available alternatives. While applications data is not widely available in the literature, the number of in-situ applications with integral deposit control programs continue to grow.

6. REFERENCES

American Petroleum Institute. A Compilation of Field Collected Cost and Treatment Effectiveness Data for the Removal of Dissolved Gasoline Components from Groundwater. API Publication 4525, 1990.

Benefield, L. and Randall C. Biological Process Design for Wastewater Treatment. Englewood Cliffs, NJ: Prentice Hall, 1980.

Baker, K. and Herson, D. Microbiology and Biodegradation. In: Bioremediation (Baker, K. and Herson, D, Eds.). New York, NY: McGraw-Hill, 1994.

Deutsch, W. Groundwater Geochemistry: Fundamentals and Applications to Contamination. New York: Lewis Publishers, 1997.

Frayne, C. Cooling Water Treatment: Principles and Practice. New York: Chemical Publishing Company, 1999.

Horn, B. Fouling in Remediation Equipment: Effectively Confronting the Most Common Operating Impediment. Proceedings of 2004 Petroleum Hydrocarbons and Organic Chemicals in Groundwater, National Groundwater Association, 2004.

Johnson, G. and Raven, P. Biology. Austin, Texas: Holt, Rinehart and Winston, 2004.

Liss, S. and Baker, K. Anoxic/Anaerobic Bioremediation. In: Bioremediation (Baker, K. and Herson, D, Eds.). New York, NY: McGraw-Hill, 1994.

Chapter 5

SPILL CLEANUP OF FUEL CONTAMINATED SOILS AFTER ROADWAY ACCIDENTS USING IN SITU BIOREMEDIATION

Satya Ganti[1§] and Bob Frye[2]
[1]Sarva Bio Remed, LLC, NJ; [2]GEC Environmental Contracting Corp., VA

ABSTRACT

Release of fuel oils during transportation or during roadside accidents is very common. According to the figures available, number of incidents involving hazmat accidents has increased from 7,297 in 1990 to 14,443 in 1999. In most cases the standard cleanup protocol is followed but in some cases it is not possible to follow the protocol because of the accident locations. It is particularly difficult to excavate surface soil where utility lines are very near to the surface and services of utility agencies are not immediately available. In such situations, it is considered safe to use effective bioremediation solution for on-site cleanup. In these situations, AgroRemed has been employed with successful results. Two case studies are presented in this paper. One case demonstrates revitalization of roadside vegetation through bioremediation after a spill of motor oil and another case describes application of AgroRemed to sites affected by diesel spill with underlying utility cables. The TPH of the soil after bioremediation was reduced by more than 95% from 65,000 ppm in the first case, while in the second case the TPH was found to be below the detectable values from the initial value of 47,000 ppm. VaporRemed was employed for fumes originating from the spilled site and where the spill had affected the fertility of soil, AgroRemed was used. Both these products are available in a ready to use liquid form and are known to effectively bioremediate the contaminated soils and fumes in a very short period of time. The advantage of these products is that they de-toxify the contaminated soils and facilitate growth of vegetation.

The Virginia Department of Transportation was actively involved in the cleanup operations, and although the Virginia DEQ was not directly involved, the department reviewed the data to confirm that the values of TPH were below the accepted levels.

§ Corresponding Author: Satya Ganti, Sarva Bio Remed, LLC, 36 South Broad Street, Trenton, NJ 08608, Tel: 609-695-4922, Fax: 419-710-5831, Email: sales@sarvabioremed.com

1. INTRODUCTION

1.1 Fuel Oil Spills in first 3 months of 2007

An oil delivery truck overturned on the morning of Jan. 16, 2007 at the intersection of Old Pawling and Nanny Hill roads in New York State. It spilled 4,200 gallons of heating oil onto the road and surrounding properties, including a regulated wetland and a stream that flows into the Ten Mile River. Another spill occurred thirty days later on February 15, 2007 in Massachusetts releasing 2000 gallons of home heating oil coincidentally near Ten Mile River. Road accidents involving fuel oil spills are common and both the state environment agencies and cleanup contractors are busy most of the year attending to these spills. Route 117 in Warwick, MA was closed after truck carrying heating oil flipped over morning of 20th March, 2007 and leaked the fuel into the road.

Spills on roadways due to transportation accidents are not uncommon resulting into release of fuels on the road and embankment and destroying the vegetation in the impacted zone. The first task of the cleanup crew is to remove the free product from the impacted surface and then excavate the area and transport the contaminated soils to the landfill site for disposal and replace the area with sanitized soil or crushed gravel followed by restoration of vegetation. Excavation of contaminated soils and replacement with sanitized soil may not be very difficult, but rejuvenation and restoration of the impacted soil is more difficult as the toxicity of the hydrocarbons is more lasting.

Road transportation services are employed for shipments of oils and fuels in the USA and other countries because of easy accessibility of gas stations and terminals. Bulk transportation of fuels is still carried out by rail roads and Kirton & Beaulieu (2005) have reported their experiences on bioremediation of spill in a rail yard in Massachusetts. Both highways and rail road services are prone to accidental spills and are critical for the emergency response bodies. However, it is road transport that is used for supplying fuel oils to distant places and is more critical from the point of view of seriousness of accidents as it affects local populations and damage to the vegetation along the edge of the road.

The cause of such accidents may be many including the age of these tankers as even today some of the tankers on the road may be more than 20 years old and may be structurally weak (Anonymous, 2003). Complete statistical information of roadways spills of fuel oil are not available in the USA but a recent report (Weyls, 2003) indicates that the number of incidents involving roadway spills has doubled from 7,297 in 1990 to 14,443 in 1999 in just 10 years. A similar study was carried out in the UK identifying the types of releases in England and Wales by Lee & Fitzsimons (2005) who reported that soil receives the greatest impact of these spills as seen from their data. Spills of diesel also affect the structure of asphalt pavement (Balwin et al, 2005)

This paper describes results of two case studies on the use of AgroRemed a bioremediation product for cleanup of diesel oil spills along the roadside in Virginia. In both these cases application of bioremediation products was carried out with the approval from State Department of Transportations and also with the concurrence from the State Department of Environment.

Results show that use of AgroRemed not only reduced the costs of cleanup but also rejuvenated the soil for healthy growth of vegetation through detoxifying the effects of hydrocarbons.

1.1.1 Case Study 1. Restoration of Vegetation Affected By Diesel Spill

A tractor/trailer was involved in a highway accident, resulting in the release of approximately 100 gallons of diesel fuel from a ruptured saddle tank and ten gallons of motor oil from the truck engine. The wreckage ended at the bottom of the embankment, immediately adjacent the opening of the subsurface storm piping. Diesel fuel, released from the truck, flowed into soil immediate the wreckage and the open ditch. Several hundred feet of guardrail was destroyed in the accident, causing engine oil to disperse over approximately 100 feet of vegetation at the pavement edge. GEC Environmental Contracting Corp. (GEC) was contacted to provide clean up of the release. The wreckage and the site are seen in Figure 1.

Figure 1. The accident site and the wreckage of the truck.

Discussions were held with representatives of the Virginia Department of Transportation (VDOT) and implications of soil removal in this area were reviewed. The spill site was on a slope and it would be difficult to use mechanized cleanup vehicles for the cleanup. Excavation of the soil was not considered as an option for the cleanup.

It was agreed that this site is suitable for evaluation of on-site (in situ) bioremediation cleanup of highway spills. AgroRemed manufactured by Sarva Bio Remed, LLC was selected for direct application to the release point and affected soil and vegetation. AgroRemed has a track record for successful cleanup of contaminated soils after spills of diesel or heating oil both in residential and industrial facilities. AgroRemed has shown reduction in TPH values by 90% in

three weeks in a pilot study. In one case the TPH of the impacted soil was reduced from 25,000 ppm to 93 ppm. Advantages of AgroRemed and benefits of bioremediation are listed below.

- Treats the spill at the source and rejuvenates the soil
- Reduces the fumes produced by the spill almost instantly
- Available in easily spray able liquid form
- Easy to apply and environmentally safe
- Generally a one time application under favorable conditions
- Fast remediation time and reduces the TPH by more than 95% in 3 weeks time
- AgroRemed is a complete solution
- No waste for disposal

The conditions essential are the availability of moisture and easy permeability in soil. AgroRemed has cleaned up petroleum contaminated soils even with a history of contaminant more than 10 years. Under availability of moist soil conditions, the bacteria in the product continue to consume hydrocarbons as long as the source of hydrocarbon is available. Minimum supervision is required after application to the soil and does not need periodical additions of nutrients or products. Addition of these microbes and natural attenuation would provide a practical and cost effective method with little or no post-restoration efforts. The diesel fuel release and surface staining caused by engine oil would both be addressed in this manor. Multiple applications were anticipated for significant decrease of petroleum content in the saturated area.

Figure 2. Application of AgroRemed to impacted soils

A soil sample was collected from the center of the diesel staining, approximately 2" below the surface. It showed a concentration of 65,000 parts per million (ppm). Impacted soil saturated with diesel was manually turned/ tilled to allow natural oxygenation before application of AgroRemed as seen in Figure 2.

A soil sample was collected after 20 days of application from this location and analyzed for TPH/DRO values and the results of hydrocarbon range C-5 to C-30 showed a value of 26,000

ppm or more than 40% reduction in the value. Application of AgroRemed was continued at regular intervals; it was noticed that the TPH/DRO was reduced from 26,000 ppm to 11,800 ppm because of drought conditions, and the soil was very dry. The conditions became favorable in September before the final application, and this time soil was sprayed with water from a tanker immediately before application of AgroRemed. In addition to the wetting, the surface of the soil was also covered with straw mulch to prevent excessive evaporation. The TPH of the soil was examined after 15 days and the levels of TPH were reduced to 650 ppm with no signs of tainting of the grass and interestingly no diesel odor. Further, the area was found to support healthy growth of grass and other vegetation indicating no residual toxicity and restoration of the soil to its condition before the spill. The DEQ agreed that there was no further action required. The total time required for the cleanup was a total of 103 days for reaching the accepted levels of contaminant.

1.1.2 Case Study 2: Diesel Fuel Release after a Vehicle Accident

A tractor/trailer was involved in a highway accident, resulting in the release of approximately 75 gallons of diesel fuel from a ruptured saddle tank. Free petroleum product flowed into the gravel road shoulder and adjacent embankment. The site is a single lane, north/south highway of typical asphalt paved construction (Figure 3). Road shoulders are intermittent gravel, grass, and embankments. Potential receptors are humans, wildlife, and groundwater. Multiple major underground communication utilities lines were present in the accident area making it difficult to excavate.

Figure 3. Accident site showing the asphalted road affected by spill.

Diesel fuel had released on the pavement edge and gravel shoulder causing surface staining. Debris on the pavement was pushed to the gravel to allow normal traffic patterns for evening hours. Petroleum-absorbent booms were placed along the down-gradient edges of the spill area to prevent further migration during anticipated storm events. Anti-slip absorbent media was

applied to the impacted pavement and scrubbed to remove residual phase petroleum. As this material was spent, it was removed, and the process repeated until practical recovery was achieved. An additional application was then made as a slip preventative measure for traffic.

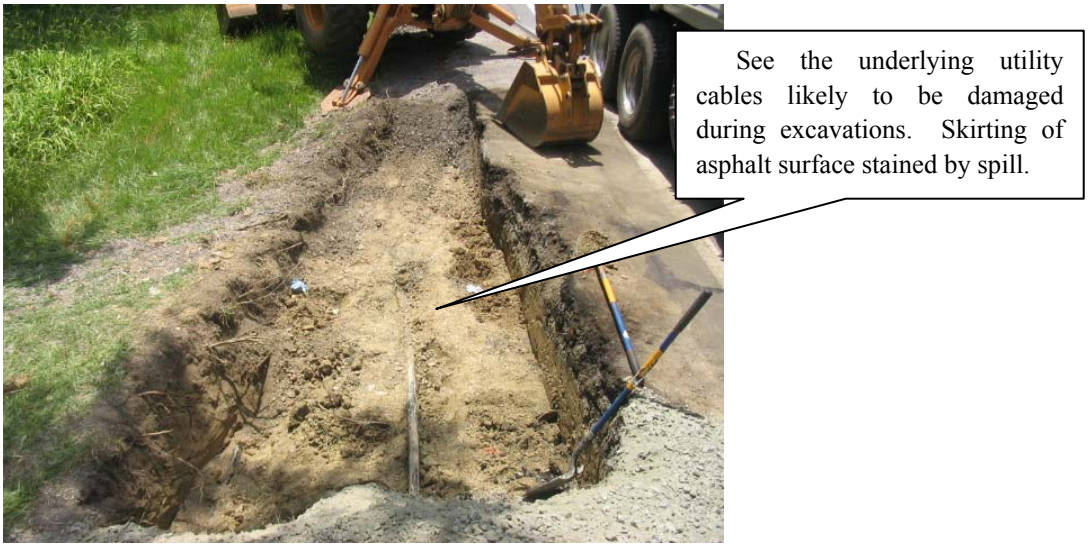

Figure 4. Showing underlying cables and stained skirting of pavement.

Soil excavation/disposal would be conducted in the petroleum stained areas under the supervision of the state environment protection agency. The West Virginia Department of Environmental Protection (DEP) supervised the cleanup. Several ground communication pedestals were present both north and south of the incident site, indicating buried utilities in the area; the cleanup had to be coordinated with the concerned utility agencies. A soil sample was collected from the center of the surface staining to provide waste characterization and analysis of the petroleum concentrations showed TPH at 47,000 parts per million (ppm).

As the excavation continued along the embankment towards the open side ditch, depth was increased once equipment progressed beyond the exposed cable (Figure 4). At the east side of the excavation, a depth of 48" was achieved when a third unknown communication cable was damaged by the backhoe. Awaiting repair technicians, it was determined further soil removal is not practical or even possible by conventional means due to the position of buried cables. With cables significantly reducing the area of excavation accessibility and time constraints of two-way traffic closure, the decision to apply petroleum degrading microbes was made.

In situ bioremediation using AgroRemed was considered a less disruptive and safe method for cleanup. Repair technicians had not arrived at this time, and AgroRemed was readily available on site. Areas of the excavation bottom and depths were measured for sampling locations. Four locations were determined necessary to observe soil conditions. These locations

were monitored several times in the future to observe microbial activity and decrease of petroleum concentrations during bioremediation. Two pine trees located along the east bank of the right-of-way were identified as bench marks for future sampling events. Soil samples were collected from these two west locations at the pit bottom showed 2,500 ppm and 4,000 ppm respectively after 20 days of treatment.

Individual tests of the soil samples did not indicate vapor levels above background readings of 2.3 for Photo-ionization Detector (PID). Laboratory results for soil samples collected on July 26th showed the results as follows; Sample 1 showed values below laboratory detection limits of 50 ppm, Sample 2 showed 570 ppm, Sample 3 showed 830 ppm, and Sample 4 showed 290 ppm. These results indicated an aggressive degradation of petroleum hydrocarbons within seven days of the previous application. An additional application was conducted after these samples were collected. Application of bioremediation product under such situation was justified. As seen from the results, total remediation of diesel fuel was completed in 35 days and no further action (NFA) was decided by the state DEP and the project was closed.

2. CONCLUSIONS

The average amount of fuel spilled in a saddle tank release is 104 gallons while the average cost to clean it up is $9,200 nationwide. Costs for on-site cleanup using AgroRemed for similar size of spill are considerably less, and for less than $ 2,000.00 the soil is cleaned and rejuvenated, supporting healthy vegetation. In fact, reuse of the same soil also reduces costs of transportation with minimum disturbance to the local ecosystems.

The two case studies indicate that application of AgroRemed remediated the adverse effects of diesel oil in a very short time. Advantage of bioremediation is evident in both the cases. It has been seen that the immediate effect of AgroRemed is to detoxify the toxic nature of the hydrocarbon and then consume the contaminant in a shortest period of time provided all the conditions favoring the growth of bacteria are available. Restoration of the fertility of the soil was noticed by the regular growth of grass and weeds in the denuded area near the accident site. The time for bioremediation was longer in the first test case due to severe drought conditions coupled with high summer temperatures that did not allow growth of bacteria. In the second test case since the moisture was available in plenty, the complete bioremediation was achieved in 35 days with minimum supervision.

Accidents on the highways are often away from city, so it is difficult to monitor these situations. Excavation of soil though is considered a preferred method for cleanup, it is not always convenient or feasible and AgroRemed delivers a clean and efficient cleanup solution. Application of AgroRemed to the accident site immediately after a spill will reduce the damage to the asphalt surface and also reduce the damage to the roadside vegetation. It is a solution that is safe, easy to use, and a non-invasive, and it should form an important part a of spill cleanup kit for the emergency response operations.

3. ACKNOWLEDGEMENTS

Authors wish to acknowledge thanks to Jeff Boyer and Brett Waller of Virginia Department of Transportation (VDOT) for their support and encouragement in implementing for the first time a bioremediation solution for cleanup of highway oil spills.

4. REFERENCES

Anonymous (2003) "Ageing tank fleet raises concerns", Bulk Transporter http://bulktransporter.com/mag/transportation_aging_tank_fleet/

Weyls, R (2003) "Hazardous Materials: Being Safe on the Highway"

Balwin B, Carmod, O and Collins, T (2005) "Degradation of asphalt due to diesel spill" Road systems and engineering technology forum.

Kirton, TD and Beaulieu, PG (2005) "Bioremediation of rail road spill in Palmer, MA" Contaminated soils, water and sediments, Springer Verlag, USA ISBN 978-0-387-23036-8

Lee, P and Fitzsimons, D (2005) "An analysis of inland oil, fuel incidents in England and Wales"

Chapter 6

FEATHER WASTE AS PETROLEUM SORBENT: A STUDY OF ITS STRUCTURAL BIODEGRADATION

Cervantes-González, E[1,3], Rojas-Avelizapa, L.I[1], Cruz-Camarillo, R[1], Rojas-Avelizapa, N.G[2§], García-Mena, J[3].

[1]Departamento. de Microbiología, Escuela Nacional de Ciencias Biológicas IPN, Carpio y Plan de Ayala s/n Casco de Sto. Tomas, 11340. México D.F., México.[2]Departamento de Investigación y Posgrado, Centro de Investigación en Ciencia Aplicada y Tecnología Avanzada IPN, Cerro Blanco 141 Col. Colinas del Cimatario, 76090. Santiago de Querétaro Qro. México.[3]Departamento de Genética y Biología Molecular, Cinvestav-IPN, Unidad Zacatenco, Av. IPN 2508, Col. San Pedro Zacatenco, 07360. México D.F. México.

ABSTRACT

Using scanning electron microscopy (SEM), the present study evaluated the biodegradation of chicken feathers during a petroleum hydrocarbon removal process by a defined-mixed culture that pose the simultaneous abilities to remove petroleum hydrocarbons and produce keratinases in liquid culture. Biodegradation treatments were performed in Erlenmeyer flasks containing mineral media, 6% w/v of chicken feathers and 64,800 mg l^{-1} of petroleum hydrocarbons. Flasks were inoculated with the keratinolytic-mixed culture, which was previously obtained from a petroleum-polluted site, and then incubated at 28ºC, 180 rpm during 21 days. Every 7th day, a sample was collected and fractioned; one fraction was processed to be analyzed by SEM while the residual petroleum-hydrocarbons were extracted from the other fraction and quantified by gas chromatography. Controls without inocula were processed under same conditions. The photomicrographs illustrated the different stages of the feathers' biodegradation; they are first found intact without degradation while the microorganisms from the mixed culture appear only in the supernatants. After the 7th day a remarkable colonization of the feathers begins to be observed, along with a considerable degradation observed after the 14th day of incubation.

Keywords: chicken feathers, electron microscopy, sorbent, keratinases.

1. INTRODUCTION

In the Southeast of Mexico, it is common to encounter hydrocarbon-polluted sites located in areas of difficult access such as swamps, marshes, and mangles. This situation represents a challenge to any remediation effort due to the complicated entrance of appropriate machinery

§ Corresponding author: Dr. N.G. Rojas Avelizapa, Departamento de Investigación y Posgrado, Centro de Investigación en Ciencia Aplicada y Tecnología Avanzada IPN. Cerro Blanco 141 Col. Colinas del Cimatario, 76090. Santiago de Querétaro Qro, México, Tel. 52+ 5557296000 ext. 81031, Email: nrojasa@ipn.mx

and personal activities. One of the strategies that have been implemented to clean up these sites includes the use of sorbents to recover pollutants and afterwards dispose of them. Synthetic compounds are the most used sorbents among them; polypropylene, polyurethane, polyethylene-tereftalate and teflon are the materials commonly employed (Ro et al., 1998). Despite the effectiveness of this strategy, the disposal of contaminated materials implies a complicated operation process. The cost related to the confinement and incineration of these polluted materials is high, without mention that the last alternative might cause even more environmental contamination, contributing to climate changes (Inagaki et al., 2002). Therefore the use of biodegradable sorbents to remove pollutants could be an "earth-friendly" and attractive alternative to eliminate definitively pollutants at these site conditions.

Different sorbents have been used for inorganic and organic contaminants, such as the wheat bran used for the removal of cadmium from wastewater (Singh et al., 2006). Choi and Cloud (1992) showed the high capacity of milkweed fiber (*Asclepias*) and cotton fiber to retain crude oil, and also the excellent oil sorption capacity and hydrophobic–oleophilic characteristics of the agricultural product, kapok (*Ceiba pentandra*) have been evaluated (Lim and Huang, 2007). The use of sorbents has been also appointed to enhance oil biodegradation (Biswas et al., 2005; Setti, et al., 1999).

As it was mentioned previously, different types of sorbents and other organic residues have been used both to remove pollutants in water, soil and sediments and to improve the remediation of polluted sites; however, there is scarce information about the effective degradation of these organic materials. Thus, although they are considered as biodegradable, it is necessary to determine if native microorganisms pose the abilities to degrade them at a great extent, in such a manner that their presence in the environment does not represent an additional pollution source. Then, the aim of the present work was to monitor the biodegradation of chicken feathers during a petroleum hydrocarbon removal process by a keratinolytic and petroleum-degrading mixed culture.

2. MATERIAL AND METHODS

2.1 Feather waste

Chicken feathers (CF) were used as feather waste and they were obtained from a poultry processing plant located in the neighborhood of Ecatepec, in the State of México. Previously to use, feathers were immersed overnight in a neutral detergent solution, then washed and rinsed thoroughly with tap water to remove the detergent. The sun-dried CF were ground in a Willey mill (A.H. Thomas, Philadelphia USA) using a 20 mesh sieve.

2.2 Treatment preparation

Treatments were carried out in batch format using Erlenmeyer flasks, containing 25 ml of liquid mineral media (MM), containing (g l^{-1}): KNO_3, 1; $FeCl_3$, 0.02; $MgSO_4$, 0.2; $CaCl_2$, 0.1 and

K_2HPO_4, 1, at pH 6.8; 6% w/v of chicken feathers and 64,800 mg l^{-1} of petroleum hydrocarbons. Flasks were inoculated with the keratinolytic-mixed culture obtained from a petroleum-polluted site (Cervantes et al., 2007), and incubated at 28ºC, 180 rpm during 21 days. Every 7th day, samples were collected and processed to be analyzed by SEM and residual petroleum-hydrocarbons were extracted and quantified by gas chromatography. Controls without inocula were processed at the same conditions.

2.3 Residual petroleum-hydrocarbons

The residual petroleum-hydrocarbons in culture media were extracted from eight successive additions (20 ml) of dichloromethane and then concentrated. One µl of each organic extract was analyzed by gas chromatography (Agilent Technologies, GC-FID system) with a HP capillary column (30 m x 320 µm x 0.25 µm), as follows: initial temperature 30°C; 30-100°C at 15°C min^{-1}; 100-200°C at 7°C min^{-1}; 200-250°C at 6°C min^{-1}. Injector and detector temperatures were 250 and 280°C, respectively. Helium was used as the carrier gas (1.5 ml min^{-1}). The petroleum-hydrocarbons concentration, expressed as total petroleum hydrocarbons (TPH), was calculated interpolating the total area in a calibration curve prepared with crude oil at concentrations of 0-300 mg l^{-1}. The petroleum-hydrocarbons absorbed into the waste were extracted in a Soxhlet apparatus during 8 h using dichloromethane as solvent. The content was concentrated and quantified as indicated above. This value was subtracted from the corresponding treatment, and then petroleum hydrocarbon removal is reported as a net loss value.

2.4 Scanning electron microscope (SEM) analysis

The samples of residual feather waste from each 7th day of the treatment and the inoculum added at initial time of the treatment were processed to be analyzed by SEM. The first processing step was an exhaustive wash with Luria-Bertoni (LB) broth, each sample was in a 1.5 ml polypropylene tube containing 1 ml of broth. It was agitated by inverting the tube and it was left to rest 15 min to sediment the sample. This procedure was repeated at least 6 more times. As soon as the sample was washed, the fixation process with glutaraldehyde at 25% (in LB broth, pH 6.8) was performed during 1.5 h by inversion agitation at room temperature and later it was incubated on ice during 1.5 h more. Afterwards, each sample was washed three times as mentioned previously with broth LB and then post-fixed adding 500 µl of OsO4 at 2% (in broth LB) during 1 h at 25°C in agitation by inversion in the dark. After this treatment, three washes were realized with broth LB in the same way and the tubes were kept overnight in refrigeration; later on, the sample was dehydrated using increasing concentrations of ethanol as follows. The first wash was with ethanol at 60% during 15 min, later another wash with ethanol at 70% during 15 min, the last wash was made using absolute ethanol and it was repeated three times. It is necessary to mention that in all washes the sample was mixed by inversion. Later the samples were dried out to critical point using a SAMDRI-780 TO dryer (Tousimis Research Corporation) and finally the samples were coated with gold using the Desk II (Denton vacuum) gold evaporator. Samples were visualized using a JSM 35C scanning electronic microscope (JEOL LTD, Tokyo, Japan).

3. RESULTS

The use of feather waste as petroleum sorbent has been reported by some authors (Breitenbeck and Grace, 1998). However none of these studies have shown the biodegradation of feathers during a hydrocarbon removal process. The present study analyzes by SEM the biodegradation of feathers during the process of petroleum removal. The Figure 1 shows the residual TPH content in the treatment during the incubation period, it illustrates that the petroleum removal presented maximum consumption (almost 60,000 mg l-1) until 9th day. This value was almost 90% of the initial petroleum-hydrocarbon content (64,800 mg l-1).

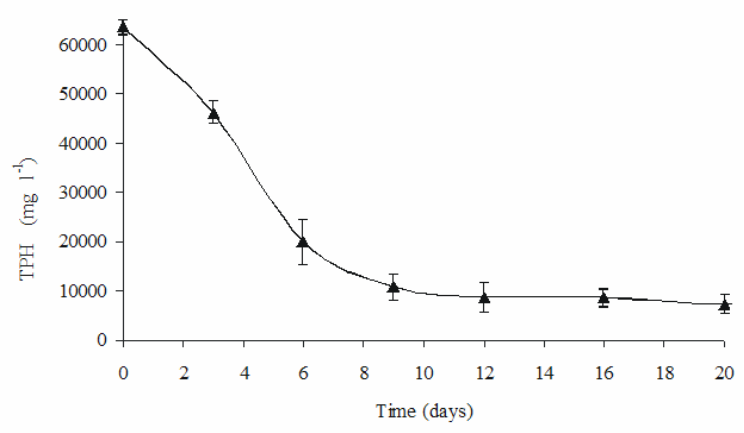

Figure 1. TPH consumption in the presence of chicken feathers by a keratinolytic and petroleum-degrading mixed culture.

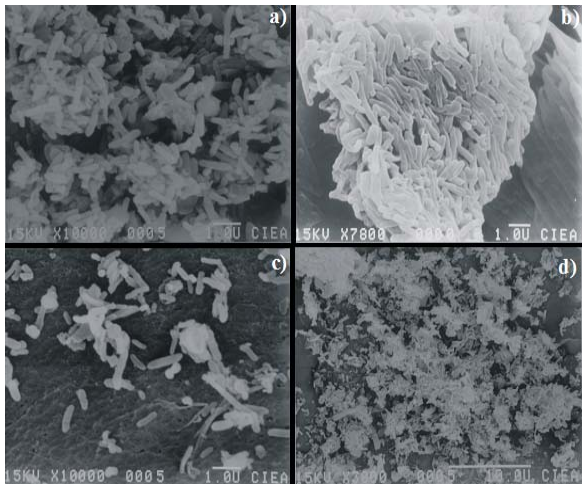

Figure 2. Representative SEM images of the inoculum used in the petroleum removal process. a) and c) 10,000X magnification, Bar 1.0 µm; b) 7,800X magnification, Bar 1.0 µm and c) 3,000X magnification, Bar 10.0 µm.

The micrographs corresponding to a sample of the inoculum added to the system are shown in Figure 2. The observed richness of the inoculum is the result of the presence of the eleven previously isolated bacteria (Cervantes et al., 2007) which exhibited capacity to degrade hydrocarbons and keratin. Each SEM image corresponds to a different area of the sample.

The monitoring of feather waste biodegradation was made every 7 days during the 21 days of treatment. The first sample corresponded to day 0 at the initial time of incubation; Figure 3 shows the keratin fibers from chicken feathers at this time.

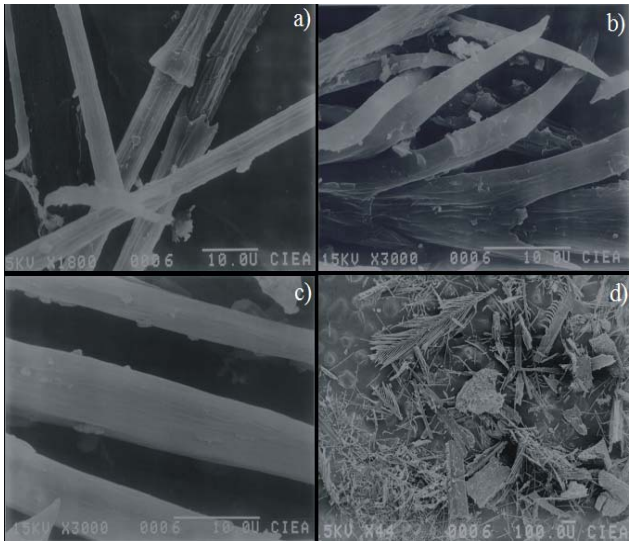

Figure 3. Scanning electron micrographs of feather waste at initial time of treatment. a) 1,800X magnification, Bar 10.0 μm; b) and c) 3,000X magnification, Bar 10.0 μm and c) 44X magnification, Bar 100.0 μm.

The degradation of the feather's structure was initially detected in the micrographs corresponding to the 7th day of incubation (Figure 4); the bacteria began to adhere on the feather's surface, and an apparent sporulation process of some bacillar structures could also be observed.

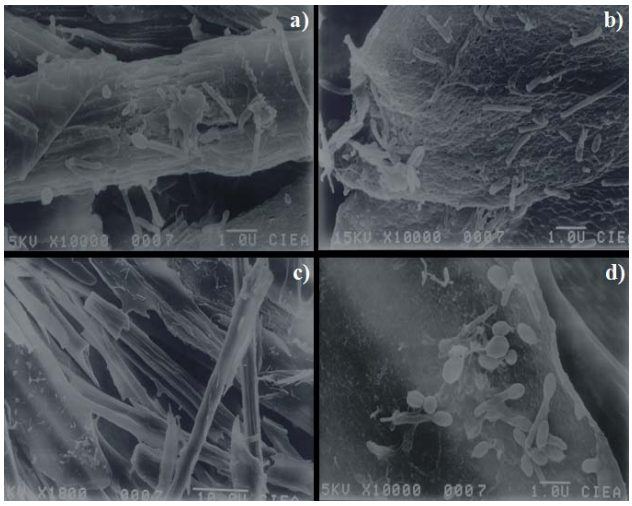

Figure 4. SEM images of feathers degradation by the mixed culture after a seven days period of petroleum removal. a), b) and d) 10,000X magnification, Bar 1.0 μm and c) 1,800X magnification, Bar 10.0 μm.

During the subsequent days of incubation, the adherence of microorganisms on the surface of chicken feathers continued (Figure 5). The bacterial colonization increased remarkably, and the sample corresponding to 14th day showed a massive growth in the majority of the fibers.

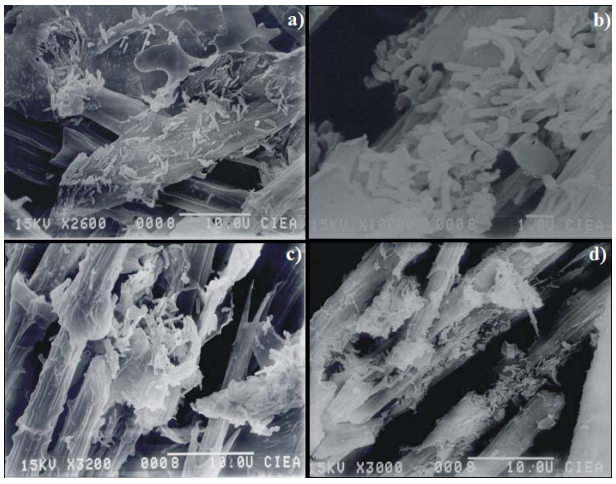

Figure 5. Scanning electron micrographs of feathers degradation by mixed culture at 14th day of petroleum removal. a) 2,600X magnification, Bar 10.0 μm b), e) and f) 10,000X magnification, Bar 1.0 μm; c) 3200X magnification, Bar 10.0 μm and d) 3,000X magnification, Bar 10.0 μm.

During the last 7 days of incubation, the scanning electron micrographs showed a total colonization on the keratin fibers which were attacked and in some zones the fiber was reduced to debris (Figure 6). However, there were some fibers which were not colonized and remained intact. It probably was due to the roughness of the same keratin fibers; however, there is not an exact description of this phenomenon.

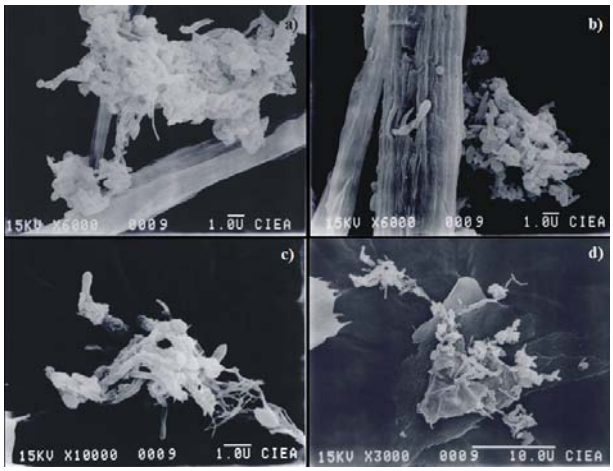

Figure 6. SEM images of feathers degradation by mixed culture at the 21th day of petroleum removal. a) and b) 6,000X magnification, Bar 1.0 μm; c) 10,000X magnification, Bar 1.0 μm and d) 3,000X magnification, Bar 10.0 μm.

4. DISCUSSION

The structural biodegradation of feather waste was studied using Scanning Electron Microscope analysis. According to the results it was possible to evidence the heterogeneous size of feathers at the initial time in spite of their milling. Additionally, it was possible to see apparent particles of different composition, which probably are originated in the rachis of feathers. These particles were in a minor proportion the most abundant the keratin fibers (Figure 2). The colonization on residual feathers was detected at day 7th (Figure 3), these micrographs showed that bacteria grew closely to the surface of keratin fibers and the fibers began to break down.

The surface of the residual keratin fibers were more severely attacked at day 14 of the incubation period; at this time the colonization was very evident and the keratin structure was significantly damaged. However, no bacterial cells were found attacking the rachis, suggesting that these particles were less biodegradable. Rammani et al., (2005) studied the structural and biochemical mechanism of feather degradation by Bacillus licheniformis strain RG1 and discovered a lack of bacterial cells on the rachis; but their structural studies reported that the bacteria closely adhere to the barbules, which produce keratinases that diffuse laterally, degrading the rachis and barbules. This phenomenon was not observed in the present work because the rachis of feathers was not degraded.

According to the gravimetrical quantification of the chicken feathers' degradation in the same treatment, the high degradation of this residue occurred during the first twelve days of treatment (Cervantes et al., 2007); however, according to the micrographs, the colonization was detected after the 7th day, which indicates two possible options.

First, the analysis by SEM was realized in residual feathers; therefore the chicken feathers degraded during the first 7 days of treatment were not evidenced by SEM, and it is not possible to assure that they were not colonized. Most likely, the feathers degraded during this period were

totally colonized and removed and therefore were not observed. This hypothesis can be sustained because the colonization was not homogeneous and only the particles colonized were removed.

On the other hand, in this treatment where the enhancement of petroleum removal was evidenced by the presence of chicken feathers, some interesting correlations were determined. During the first twelve days of treatment the exponential growth phase of bacteria and the simultaneous degradation of feathers and the petroleum were evident (Cervantes, et al., 2007); also the highest removal of TPH was detected (Figure 1). These events suggest the highest metabolism of involved bacteria during this period, and it is very important in the treatment. The enhancement of petroleum removal due to the presence of feathers could be attributed to the adherence of bacteria on the surface of keratin fibers because it could increase the contact between petroleum and bacteria.

However, the second option must also be considered: during the 12 first days of treatment the adherence of bacteria on keratin fibers was not very strong due to the petroleum sorbed into the fibers, and the biodegradation of chicken feathers may be attributable to extracellular enzymes released to the liquid media without contact between the bacteria and the surface of keratin, which could cause the visible colonization on keratin fibers after the petroleum removal process. At day 21, it was possible to evidence the total colonization of some keratin fibers but it was not possible to see the entire structure of these keratin fibers.

There are some SEM reports that shown the biodegradation of chicken feathers and it is correlated with keratinolytic activity, production of sulfhydryl groups and mid-exponential growth phase (Nam et al., 2002). The detection of colonization in the present study was not correlated with the loss of waste due to the complexity of treatment; however, the visual degradation of keratin fibers by the keratinolytic mixed culture was evident.

5. CONCLUSIONS

Scanning electron microscopy (SEM) showed the biodegradation of chicken feathers during a petroleum hydrocarbon removal process by a defined-mixed culture. Photomicrographs showed the different stages of feathers' biodegradation and also the colonization of bacteria on the surface of keratin fibers. However, additional studies are needed to evidence that chicken feathers increase the contact hydrocarbon-bacteria and then hydrocarbon removal.

6. ACKNOWLEDGEMENTS

The present work was financed by Cinvestav-IPN and by COFAA-IPN. We thank the help of Q. F. B. Sirenia González Pozos from the Electronic Microscopy Unit, Cinvestav-IPN, Zacatenco. N.G. Rojas, L.I. Rojas and R. Cruz C are recipients of CONACYT, COFAA and EDI fellowships.

7. REFERENCES

Biswas, S., Chaudhari, S.K., and Mukherji, S. 2005. Microbial uptake of diesel oil sorbed on soil and oil spill clean-up sorbents. J. Chem. Technol. Biotechnol. 80, 587-593.

Breitenbeck, G.A., and Grace, B.L. 1998. Use of ammoniated cellulosic materials for remediation of oil-contaminated wetlands. Louisiana Applied Oil SIPI Research and Development Program, OSRADP Technical Report Series 97-003.

Cervantes-González, E., Rojas-Avelizapa, N.G., Cruz-Camarillo R., García-Mena, J., and Rojas-Avelizapa, L.I. 2007. Oil-removal enhancement in media with keratinous or chitinous wastes by hydrocarbon-degrading bacteria isolated from oil-polluted soils. Environ. Technol. Accepted.

Choi, H.H., and Cloud, R. M. 1992. Natural Sorbents in Oil Spill Cleanup. Environ. Sci. Technol. 26, 772-776.

Inagaki, M., Kawahara, A., Aizawa, J., and Konno, H. 2002. Sorption and recovery of heavy oils using carbonized fir fibers and recycling. Carbon. 40, 105-111.

Lim, T.T., and Huang, X.F. 2007. Evaluation of kapok (Ceiba pentandra (L.) Gaertn.) as a natural hollow hydrophobic-oleophilic fibrous sorbent for oil spill cleanup. Chemosphere. 66, 955-963.

Nam, G. W., Lee, D.W., Lee, H. S., Lee, N.J., Kim, B. C., Choe, E, A., Hwang, J. K., Maggy, T., Suhartono, and Pyun, Y. R. 2002. Native-feather degradation by Fervidobacterium islandicum AW-1, a newly isolated keratinase-producing thermophilic anaerobe. Arch. Microbiol. 178, 538–547.

Ramnani, P., Singh, R., and Gupta, R. 2005. Keratinolytic potential of Bacillus licheniformis RG1: structural and biochemical mechanism of feather degradation. Can. J. Microbiol. 51, 191-196.

Ro K. S., Breitenbeck G. A., and Ghalambor A. 1998. Composting technology for practical and safe remediation or oil spill residuals. Louisiana Oil Spill Coordinator´s Office/Office of governor, Louisiana Applied Oil Spill Research and Development Program, Baton Rouge, Louisiana. Technical Report Series 97-009.

Setti, L., Mazzieri, S., and Giorgio, P. P. 1999. Enhanced degradation of heavy oil in an aqueous system by a Pseudomonas sp. in the presence of natural and synthetic sorbents. Biores. Technol. 67, 191-199.

Singh, K. K., Singh, A. K., and Hasan, S.H. 2006. Low cost bio-sorbent (wheat bran) for the removal of cadmium from wastewater: Kinetic and equilibrium studies. Biores. Technol. 97, 994–1001.

Chapter 7

ENHANCED BIOREMEDIATION PILOT STUDY OF A CR(VI)-IMPACTED OVERBURDEN GROUNDWATER SYSTEM IN KANPUR, UTTAR PRADESH, INDIA

I. Richard Schaffner, Jr., P.G., C.G.W.P.[1§], Rajiv Kumar Singh, Ph.D.[2], Steven R. Lamb, P.G., C.G.W.P.[3], Donald N. Kirkland, P.E.[4]

[1]GZA GeoEnvironmental, Inc, 380 Harvey Road, Manchester, NH 03103, Tel: 603-623-3600, Fax: 603-624-9463, Email: rschaffner@gza.com, [2] Central Pollution Control Board, M/o Envt.& Forests; Govt.of India, PIC-UP Building (GF),Gomtinagar, Lucknow-10, Uttar Pradesh, India, Tel: 91-522-2721915, Fax: 91-522-2721891, Email: rsingh1962@rediffmail.com, rksingh.cpcb@nic.in, [3]GZA GeoEnvironmental, Inc, 4 Free Street, Portland, ME 04101, Tel: 207-879-9190, Fax: 207-879-0099, Email: slamb@gza.com, [4]GZA GeoEnvironmental, Inc, 380 Harvey Road, Manchester, NH 03103 , Tel: 603-623-3600, Fax: 603-624-9463, Email: dkirkland@gza.com

ABSTRACT

Pilot-scale electron donor injection enhances hexavalent chromium, Cr(VI), biochemical reduction to trivalent chromium, Cr(III), in an overburden groundwater system impacted by Cr(VI) disposal in Kanpur, Uttar Pradesh, India . The study area is located in the Indo-Gangetic alluvial plain, and is characterized by overburden stratigraphy consisting of up to about 50 meters of generally fine to medium sand interbedded with silty clay, which is underlain by about 100 meters of laterally continuous clay. The clay is underlain by interbedded fine to medium sand and clay to a depth of about 500 meters, which overlies granitic bedrock. Cr(VI) has been detected for about 20 years at concentration up to 16 milligrams per liter in groundwater samples collected from the shallower fine to medium sand unit. The source is believed to be indiscriminate dumping of wastes resulting from production of Basic Chrome Sulfate ($Cr(OH)_2SO_4$, BCS) and other reagents used by local leather tanneries. Approximately 540 kilograms of a carbohydrate-based remedial additive were injected into two wells screened in the fine to medium sand unit using about 40,000 liters of groundwater. Treatment solution make-up water was obtained from a downgradient extraction well located within the Cr(VI) plume, amended with remedial additive, and then injected into the upgradient wells to establish hydraulic control on the injection and minimize dilution. Performance monitoring included five rounds of groundwater sampling for Cr(VI), total chromium, and certain indicator parameters, including total organic carbon (TOC) as an electron donor surrogate. Pilot study results suggest that remedial additive amendment resulted in an up to 99.9% reduction in Cr(VI) concentration; an up to 97% reduction in total chromium; and up to an order of magnitude increase in TOC concentration over the four month study.

§ Corresponding Author: I. Richard Schaffner, Jr., P.G., C.G.W.P., GZA GeoEnvironmental, Inc, 380 Harvey Road, Manchester, NH 03103, Tel: 603-623-3600, Fax: 603-624-9463, Email: rschaffner@gza.com

1. BACKGROUND

Appreciating the gravity of the alarming status of contaminated groundwater resources on the Indian subcontinent and the local reliance upon these resources for potable water, the Government of India is developing a concerted effort to preserve and protect India's groundwater. In light of the technological advancements in the field of groundwater remediation, India has sought to employ an innovative remedial approach to address a Cr(VI) contaminant condition in overburden groundwater in Kanpur, Uttar Pradesh. In fact, the work reported herein was carried out in 2006 and represents, to the author's knowledge, the first reported field-scale groundwater remediation project on the Indian subcontinent.

Kanpur, a major industrial city in north Indian state of Uttar Pradesh (U.P), where the study was undertaken, includes a municipal area of about 260 square kilometers (KMC, 2006). Bordered in the north by river Ganga and in the south by the river Pandu, the city lies between latitudes of about 26021‘0‘‘ and 26030‘0‘‘ north and longitudes of about 80010‘0‘‘ and 80030‘0‘‘ east, included in the Survey of India topographic Sheet Nos. 63B/3 and B/7. Previous studies have indicated that the process of urbanization in the city is associated with higher concentration of heavy metals in river sediments (Singh et al, 1999), low lying lands, and groundwater. The chromium concentration in groundwater and the pattern of land use in the city are interrelated (CPCB, 1997).

Groundwater samples collected from potable water supply wells in Nauriakhera, the present area of the investigation, contain Cr(VI) at concentrations ranging from about 0.008 to 16.00 milligrams per liter (mg/l), owing to indiscriminate disposal practices of waste sludge (5-10% Cr2O3 by weight) generated from industrial production of BCS, an important reagent used by local tanneries. Such industries, existing in the general vicinity of the Study Area up to about the late 1980s, have been either closed or moved to more rural areas.

Cr(VI) in the waste sludge is leachable and has ultimately reached overburden groundwater. The Cr(VI) plume has impacted sensitive receptors such as shallow drinking water wells.

The Study Area is part of Indo-Gangetic alluvial plane, exhibiting more or less flat topographic relief, with the major slope running from northwest to southeast and subsurface stratigraphy predominated by medium sand and gravel inter-bedded with silty clay (CGWB, 2000). The micaceous sandy horizons have Himalayan provenance (Singh and Bajpai, 1989). Based on borehole data (CGWB, 2000), granitic bedrock underlies overburden soils at a depth of about 500 meters in the general Study Area.

2. METHODS

To evaluate an in-situ bioremediation approach for addressing the Cr(VI) contamination in overburden groundwater, the following work was completed:

- Macro-level investigation of groundwater quality, in a quasi grid of 40 productive water supply wells screened in the shallow groundwater system, was carried out to assess the spatial distribution of Cr(VI) and other associated ions and also to locate highest Cr(IV)

impacted area in which to carry out the remedial pilot study. Please refer to the Pilot Study Location Plan for the approximate location of the pilot study within the Study Area.

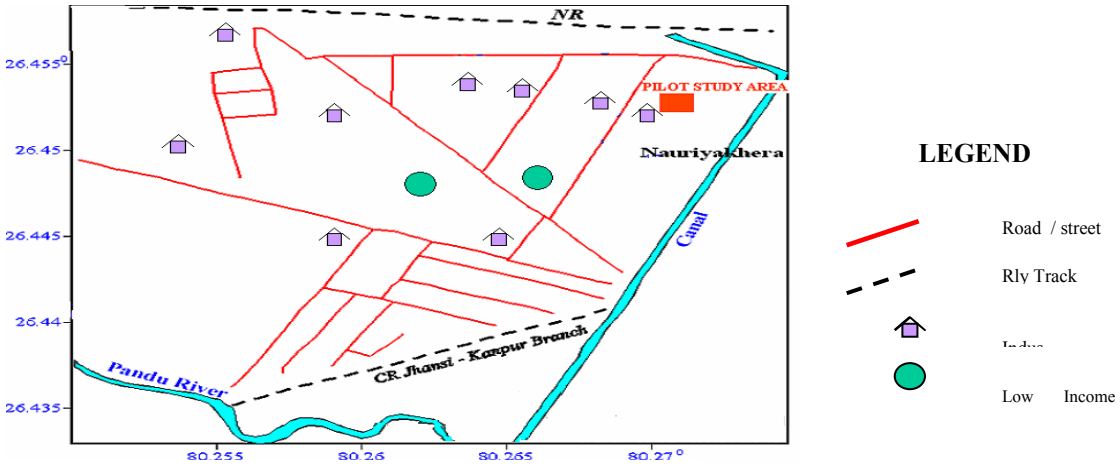

Pilot Study Location Plan

- Installation of a well field comprised of four new injection/monitoring wells (IW, SMW, DW-1, DW-2) as well as an existing piezometer (PM), with well screens intersecting the same laterally-continuous Cr(VI)-impacted hydrostratigraphic unit consisting of sand lenses, inter-layered between clay and/or clayey caliche. The drilling program was carried out using water rotary drilling technique to advance each borehole to its termination depth of about 47.2 meters below ground surface (bgs). Refer to the Well Field Location Plan for exploration locations relative to the general direction of groundwater flow.

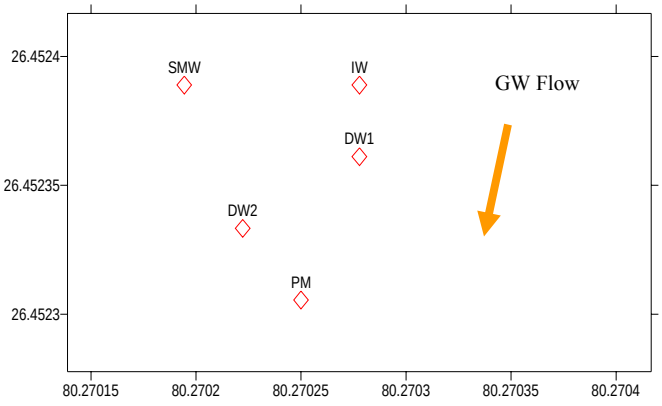

Legend: IW: Injection Well; itoring Wells, PM: Piezometer

Well Field Location Plan

- The baseline monitoring program was executed using a modified low-flow sampling technique. The purpose was to establish baseline groundwater quality conditions for the pilot study from which performance could be evaluated. The scope of baseline

monitoring included 10 metals and 7 indicator parameters. Results are appended in the Data Summary Table.

- The remedial additive injection program, using a groundwater recirculation approach, was executed by achieving steady state pumping conditions, with a recirculation rate of about 22 liter per minute (LPM) through split injection into two wells (IW & SMW).

- Remedial additive injection into the IW and SMW was carried out for about 43.5 hours at about 15 LPM mean flow rate (4 to 21 LPM range), for a total injection load of about 540 kilograms of EDC-M (Electron Donor Compound-Metals, manufactured by EcoCycle Corporation of Toyama, Japan) dissolved in about 40,000 liters of re-circulated groundwater. Note that EDC-M is formulated with two components, EDC-M1 and EDC-M2, each of which is packaged separately and injected sequentially (*i.e.*, EDC-M1 before EDC-M2). For the pilot study injection, about 210 kilograms of EDC-M1 were injected first, diluted in about 12,000 liters of re-circulated groundwater, followed by about 330 kilograms of EDC-M2, diluted in about 28,000 liters of groundwater, in consideration of the manufacturer's recommendations. Refer to the Remedial Pilot Study Process Diagram for additional information on the recirculation/injection program.

- Five rounds of (post-injection) performance monitoring were performed (same wells and parameters) using similar sampling technique, as for baseline sampling. Post-injection groundwater sampling results are also summarized in the Data Summary table.

3. RESULTS

3.1 Hydrostratigraphy

Based on the results of the drilling program carried out to install the pilot test well field as well as those of previous work performed in the Study Area, the overburden hydrostratigraphy includes two notable groundwater flow systems, each of which can be classified as an overburden aquifer given is used for water supply:

- A deep regional flow system occurring in stratified sand at a depth greater than about 300 meters bgs; and
- Local/intermediate flow systems occurring in sand lenses at shallower depth intervals.

The regional flow system within the deep overburden is hydraulically confined and characterized by an approximately 100-meter thick laterally continuous and generally transmissive stratified sand unit overlying granitic bedrock likely of the Archaean-age Bundelkhand complex. The regional flow system occurs at a depth of about 300 to 500 meters bgs.

The subordinate local and intermediate flow systems in the shallow overburden are generally at least partially hydraulically confined and characterized, at least at the scale of the pilot study, by relatively continuous transmissive sand lenses, interlayered clay and/or clayey caliche, to a depth of up to about 300 meters bgs.

Water supply wells are installed in both the shallow local/intermediate groundwater flow systems serving residential or small community users and the deep regional flow system serving industrial, municipal, or large community users in the Study Area, and both represent potential sensitive receptors owing to the current Cr(VI) condition.

3.2 Spatial Impact of Cr(VI)

With respect to Cr(VI) contamination in Study Area overburden groundwater, the highest detected concentrations are typically for samples collected from the local and intermediate groundwater flow systems in the shallow overburden at depths ranging from about 20 to 50 meters bgs. While the deep regional groundwater flow system has reportedly not yet been impacted by Cr(VI) contamination from the shallow flow systems, there is the potential for downward advection of Cr(VI), driven by downward vertical hydraulic gradients, to deleteriously impact groundwater quality of the deep flow system. Therefore, it is imperative that Cr(VI) contamination in the shallow groundwater flow systems be addressed before it impacts the deep flow system, notwithstanding the current unacceptable risk Cr(VI) poses to identified sensitive receptors of shallow overburden groundwater in the Study Area.

3.3 Remedial Pilot Study Performance Data

Baseline and post-injection performance monitoring results for the parameters identified in the Remedial Pilot Study are summarized in the attached Data Summary Table. Specific observations regarding Chromium, the critical parameters of interest, are summarized below.

3.3.1 Hexavalent Chromium, Cr(VI)

As shown on the Data Summary Table, baseline Cr(VI) concentrations ranged from 8.16 mg/L to 12.55 mg/L (arithmetic mean: 10.74 mg/L1) for groundwater samples collected from all five wells, whereas post-injection concentrations for the same well locations ranged from non-detectable above the analytical reporting limit (RL) of 0.03 mg/L to 4.17 mg/L (geometric mean: 0.71 mg/L) over the pilot study duration, which is consistent with an overall 93 percent reduction (%Reduction) in Cr(VI) concentration. The magnitude of the overall %Reduction is consistent with the biochemical transformation of Cr(VI) to Cr(III), driven by electron donor amendment.

Post-injection Cr(VI) results are summarized below on a round-specific basis:

- For the first post-injection sampling round, detected Cr(VI) concentrations ranged from 0.23 to 4.17 mg/L, reflecting an up to two orders of magnitude decrease in Cr(VI) concentrations within about 2 weeks of the injection program;

[1] Our statistical approach for estimating means as well as or percent reductions assumes a value of 0.01 mg/L for non detects above the analytical RL of 0.03 mg/L.

- For the second post-injection round, Cr(VI) concentrations ranged from non-detectable above analytical RLs to 0.32 mg/L Cr(VI), reflecting an up to three orders of magnitude decrease in Cr(VI) concentrations within about 4 weeks of the injection program;
- For the third post-injection sampling round, Cr(VI) concentrations were non-detectable above analytical RLs, reflecting a three orders of magnitude decrease in Cr(VI) concentrations within about 10 weeks of the injection program;
- For the fourth post-injection sampling round, Cr(VI) concentrations were non-detectable above analytical RLs, reflecting a three orders of magnitude decrease in Cr(VI) concentrations within about 13 weeks of the injection program; and
- For the fifth post-injection round, Cr(VI) concentrations ranged from non-detectable above analytical RLs to 0.67 mg/L Cr(VI), reflecting an up to three orders of magnitude decrease in Cr(VI) concentrations within about 17 weeks of the injection program.

A notable rebound in the Cr(VI) concentration for the groundwater sample collected from DW-2, the well with the highest baseline Cr(VI) concentration, was detected during the fifth post-injection sampling round. This apparent rebound may either represent analytical variability or possibly Cr(VI) advection to the well DW-2 location, and not to chemical oxidation of Cr(III) to Cr(VI) given there was no significant (order of magnitude or greater) increase in total chromium concentration for this well location that would be consistent with that transformation pathway as discussed in the following section.

3.3.2 Total Chromium, T-Cr

Based on the Data Summary Table, baseline T-Cr concentrations ranged from 12.88 to 19.49 mg/L (arithmetic mean: 15.80 mg/L) for groundwater samples collected from all five wells, whereas post-injection concentrations for the same well locations ranged from 0.4 mg/L to 10.66 mg/L (geometric mean: 1.21 mg/L), which is consistent with an overall $92\%_{Reduction}$ in T-Cr concentration. The magnitude of this overall $\%_{Reduction}$ is the same as the overall reduction observed for Cr(VI), and is consistent with the biochemical transformation of more mobile Cr(VI) to immobile Cr(III), driven by electron donor amendment.

T-Cr results on a round-specific basis are summarized as follows for the five rounds of post-injection monitoring:

- For the first post-injection sampling round, detected T-Cr concentrations ranged from 9.09 to 10.66 mg/L (arithmetic mean: 9.97 mg/L), reflecting a 37% decrease in mean T-Cr concentrations within about 2 weeks of the injection program;
- For the second post-injection sampling round, T-Cr concentrations ranged from 0.46 to 7.79 mg/L Total Cr (geometric mean: 2.02 mg/L), reflecting an 87% decrease in T-Cr concentrations within about 4 weeks of the injection program;
- For the third post-injection sampling round, T-Cr concentrations ranged from 0.19 to 7.78 mg/L (geometric mean: 1.27 mg/L), reflecting a 92% decrease in T-Cr concentration within about 10 weeks of the injection program;
- For the fourth post-injection sampling round, T-Cr concentrations ranged from 0.08 to 2.71 mg/L (geometric mean: 0.84 mg/L), reflecting a 95% decrease in T-Cr concentrations within about 13 weeks of the injection program; and

- For the fifth post-injection sampling round, T-Cr concentrations ranged from 0.12 to 2.87 mg/L (geometric mean: 0.41 mg/L), reflecting a 97% decrease in T-Cr concentrations within about 17 weeks of the injection program.

3.3.3 Biological transformation Indicator Parameters

To evaluate the sequential development of anaerobic, chemically reducing conditions stimulated by electron donor amendment, seven criteria parameters including dissolved oxygen (DO), Redox Potential (Eh), sulfate, nitrate, dissolved iron, dissolved manganese, and TOC were identified. The trend of these parameters as depicted in Data Summary table is consistent with the biologically-mediated transformation of Cr(VI) to Cr(III).

4. DISCUSSIONS

4.1 Groundwater Quality

- Based on the Data Summary Table, the indicator parameters each exhibited a decreasing trend with time, relative to baseline conditions, over the pilot study duration (*i.e.,* DO, up to 77% reduction; ORP, up to 271% reduction; sulfate, up to 74% reduction; and nitrate, up to 83% reduction). This trend is directly consistent with the development of anaerobic, chemically reducing conditions stimulated by electron donor amendment. The reduction in DO, sulfate, and nitrate concentrations are respectively consistent with the microbial metabolic processes of aerobic mineralization, sulfate reduction, and nitrate reduction, respectively. The reduction in ORP values with time is consistent with the development of chemically reducing conditions owing to electron donor amendment perturbing the groundwater system by scavenging terminal electron acceptors DO, nitrate, oxidized metals, and sulfate;
- The indicator parameter, sulfide, was also analyzed as part of performance monitoring. Sulfide was not detected above analytical RLs during baseline groundwater sampling, but was detected at concentrations ranging from 0.5 mg/L to 34.2 mg/l during post-injection sampling. The increased sulfide concentration with time, in response to electron donor amendment, represents a secondary line of evidence that sulfate reduction was stimulated by electron donor amendment, and is consistent with the generally depressed sulfate concentrations, in response to the pilot study injection, as discussed above;
- The indicator parameters dissolved iron, dissolved manganese, and TOC exhibited a generally increasing trend over the pilot study duration consistent with the typical response of groundwater systems to electron donor amendment. With respect to these metals, the increased dissolved iron concentration is consistent with the enhanced biochemical reduction of insoluble ferric iron (III) to soluble ferrous iron (II), mediated by iron-reducing bacteria. The increased dissolved manganese concentration is consistent with the enhanced biochemical reduction of insoluble manganese (IV) to soluble manganese (II), mediated by manganese-reducing bacteria. In the case of both iron and manganese oxide reduction, transformation was stimulated by electron donor amendment, which provided the organic carbon driving biochemical reduction;

- The liberated ferrous iron (II) and manganese (II) are expected to be respectively oxidized to ferric iron (III) and manganese (IV), and then re-sorbed onto the formation matrix once they migrate beyond the anaerobic, chemically reducing treatment zone effected by electron donor amendment into the initially aerobic, chemically oxidizing shallow overburden groundwater system (Brömssen, M.V., 1999). With respect to TOC, the increased concentration is consistent with EDC-M amendment, as TOC is a suitable surrogate measurement for that remedial additive;
- pH values, in standard log units, for baseline groundwater samples ranged from about 6.7 (IW) to 7.0 (DW-1 and DW-2), whereas values for post-injection samples ranged from about 4.6 (IW) to 7.5 (existing Piezometer). Post-injection values for groundwater samples collected from wells IW, SMW, DW-1, and DW-2 were typically lower than the baseline values approaching neutrality for these same locations, likely reflecting organic acid fermentation products of the remedial additive as well as biogenic production of carbon dioxide from remedial additive mineralization to yield carbonic acid. Despite the general post-injection decrease in pH for the groundwater samples collected from these wells, the values generally remained within the pH range considered conducive for microbial activity and did not appear to become inhibitory. Subsurface soils in the site vicinity are believed to contain significant bulk fraction of calcium carbonate, which serves as a natural buffering agent to maintain pH near baseline values. The baseline pH value for the groundwater sample collected from the existing piezometer was generally similar to the post-injection pH values for the same well, likely reflecting its respective location within the well field (*i.e.,* the most downgradient well); and
- Specific conductivity values, in microsiemens per centimeter (*u*s/cm), for baseline groundwater samples ranged from about 865 (IW) to 1,450 (existing piezometer) *u*s/cm, whereas values for post-injection samples ranged from about 962 (SMW) to 10,160 (IW) *u*s/cm. Post-injection specific conductivity values for groundwater samples collected from the IW, SMW, DW-1, and DW-2 were typically lower than baseline values, likely reflecting the total dissolved solid contribution to groundwater from remedial additive amendment. The baseline specific conductivity value for the groundwater sample collected from the existing piezometer was generally similar to the post-injection specific conductivity values for the same well, likely reflecting its respective location within the well field (*i.e.,* the most downgradient well).

4.2 Groundwater Elevation Data

As depicted in Baseline and Post-Injection Groundwater Elevation Contour Plans included below, baseline groundwater flow was generally toward the south to southwest, trending roughly parallel with the canal to the east. As shown in the Post-Injection Groundwater Elevation Contour Plans, the groundwater flow net initially reflected a groundwater depression in the general vicinity of the extraction well (DW-2), owing to groundwater pumping during re-circulation, followed by variable flow directions that ultimately, resulted in a general flow reversal from the baseline direction of south to southwest, to the final apparent post-injection direction of north to northeast. Groundwater flow nets, following remedial injection programs, typically equilibrate to baseline conditions within a few weeks based on our experience. Therefore, the baseline and post-injection groundwater elevation contour plan sets are more consistent with conditions unrelated to the Remedial Pilot Study, such as the pumping of nearby shallow wells to meet potable/process water demand, irrigation associated with local agriculture, or variation in canal or other surface water stage.

Pre-Injection Groundwater Elevation Contour Scenario

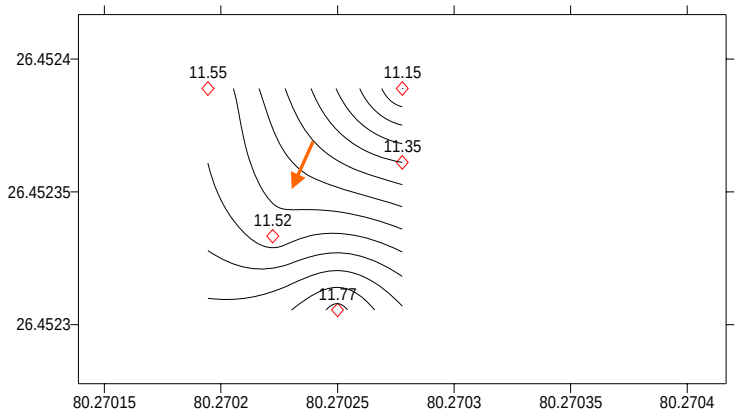

Post-Injection Groundwater Elevation Contour Scenario

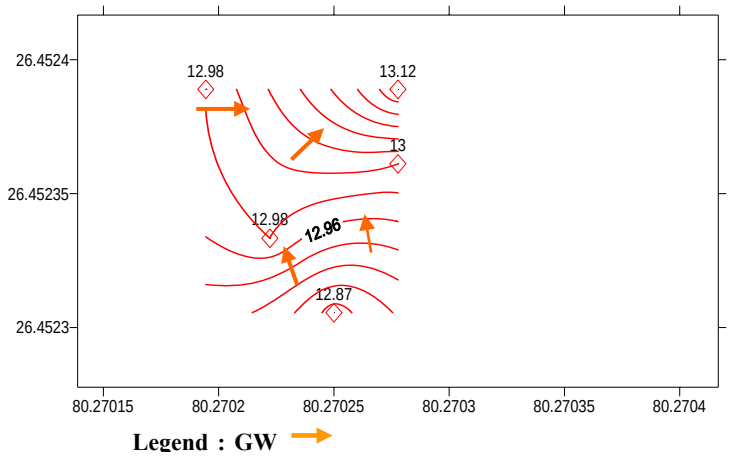

Note : Contours plotted using depth to groundwater level (DWL) in meters below ground surface (bgs)

5. CONCLUSIONS

The pertinent conclusions of the Remedial Pilot Study are as follows:

- Cr(VI) contamination in the local and intermediate groundwater flow systems poses unacceptable risk to:

  - Potential sensitive receptors for shallow overburden groundwater owing to its presence at concentrations exceeding the Indian Standard for Drinking Water Quality, and
  - The deep, regional groundwater flow system owing to potential for vertical migration from the shallow Cr(VI)-impacted groundwater flow system driven by the generally downward hydraulic gradient;
- Electron donor amendment stimulated the biologically-mediated transformation of up to about 99.9% of mobile and toxic Cr(VI) mass to immobile and nontoxic Cr(III) during the 17-week pilot study. In fact, laboratory analysis (Clesceri, *et al* 2005) of groundwater samples collected from four of five well field locations during the last post-injection sampling round did not detect Cr(VI) at concentrations exceeding Indian Standard for Drinking Water Quality. Indicator parameter data were consistent with Cr(VI) transformation to Cr(III) owing to microbially-mediated processes in accordance with the Remedial Pilot Study technical approach; and
- Based on the range of pH and Eh values for overburden groundwater in the Study Area, it is unlikely that the Cr(III) can undergo reversal to Cr(VI) following treatment. Even so, given the shallow groundwater system is used as a drinking water source in the Study Area, long term groundwater monitoring would be prudent to protect sensitive receptors.

Based on the positive results of the Remedial Pilot Study and the preliminary Conceptual Site Model developed as part of this work, the authors recommend implementing a full-scale remedial program in the Study Area including a data gap investigation as expeditiously as practical to advance it toward closure.

6. REFERENCES

Central Pollution Control Board, India, 1997, Report, Groundwater quality in Kanpur, status sources and control measures no. GWQS/8/1996-97, vol.-I pp 4,5

Brömssen, M.V., 1999, Genesis of high arsenic groundwater in the Bengal Delta Plains, West-Bengal and Bangladesh, in Thesis, Division of Land and Water Resources, Department of Civil and Environmental Engineering, Royal Institute of Technology, Stockholm, Sweden, 49 p

Kanpur Municipal Corporation, Kanpur, 2006, Detailed Feasibility Report on Jawahar Lal Nehru Urban Renewal Mission.

Groundwater Department, Uttar Pradesh, 1994, Report on Technical Feasibility of Groundwater Development in various blocks of District Kanpur, India, pp 2-4

Central Ground Water Board, (CGWB), Lucknow, 2000, Groundwater Pollution Studies in Unnao-Kanpur Industrial Areas, Uttar Pradesh, pp 21

Clesceri, L.S., Greenberg , Arnold E., Trussel, R.R., Standard Methods for the examination of water and wastewater, 1989, 17th edition, APHA-AWWA-WPCF, American Public Health Association, Washington D.C. 2005.

Singh, I.B. and Bajpai, V.N., 1989, Significance of syn-depositional tectonics in facies development, Gangetic alluvium near Kanpur, Uttar Pradesh. Jour. Geol. Soc. Ind. Vol 34, pp 61-66.

Ansari, A.A.. Singh, I.B., and Tobschall, 1999, Status of anthropogenically induced metal pollution in the Kanpur Unnao industrial region of the Ganga plain, India. . Environmental Geology V. 38 (1) pp 25-33.

DATA SUMMARY TABLE

Location : Injection Well (IW)

Date	SWL	PH	DO	Eh	Cond	S2-	SO4 2-	NO3	TOC	Cr +6	T-Cr	Fe	Mn	Ni	Cu	Co	Zn	Hg	As
26.01	11.2	6.91	4.1	118	865	ND	139	3.52	34.46	10.01	12.9	0.17	0.06	0	0.01	0	0.08	ND	ND
9.02	11.8	Sampling was not possible due to excessive foaming																	
24.02	12	4.6	0.9	-25	10160	**	270	**	34.22	**	6.42	351.7	71	0.34	0.53	0.5	2.13	**	**
10.04	12	6.96	1.7	-	3870	5.96	35.18	0.92	420.2	ND	0.19	40.45	15.1	ND	1.58	ND	1.16	0.04	ND
28.04	12.4	6.71	1.6		2290	24.2	28.04	0.25	72.89	ND	0.08	9.04	2.98	ND	0.15	ND	0.06	ND	0.06
26.05	13.1	6.45	1	-110	1140	3.3	61	0.23	82.39	ND	0.12	7.16	1.9	ND	0.06	ND	0.03	ND	0.08

Location : Side Gradient Monitoring Well (SMW)

Date	SWL	pH	DO	Eh	Cond	S2-	SO4	NO3	TOC	Cr	T-	Fe	Mn	Ni	Cu	Co	Zn	Hg	As
26.01	11.6	6.94	4.8	115	1014	ND	263	5.45	52.14	8.16	16.4	0.31	0.06	0	0.03	0	0.07	ND	ND
9.02	11.9	Sampling was not possible due to excessive foaming																	
24.02	12.6	6.06	1.8	-93	3290	1	140	1.73	46.23	0.56	0.86	67.95	11.1	0.05	0.2	0	0.14	**	**
10.04	12	6.55	1	-70	1535	3.73	60.41	1.03	211.7	ND	0.47	14.68	2.91	ND	0.94	ND	0.17	0.06	ND
28.04	12.6	6.74	1.8		1019	1.2	77.28	0.55	20.28	ND	0.87	7.02	2.22	ND	0.08	ND	0.22	ND	0.05
26.05	13	6.62	1.4	-234	962	6.2	161	1.4	39.23	ND	0.57	5.03	0.74	ND	0.05	ND	0.03	ND	0.04

Location : Down-gradient Well No. 1 (DW-1)

Date	SWL	pH	DO	Eh	Cond	S2-	SO4	NO3	TOC	Cr	T-	Fe	Mn	Ni	Cu	Co	Zn	Hg	As
26.01	11.4	7.04	4.6	105	1120	ND	214	2.2	52.02	11.2	15.3	0.27	0.03	0.02	0.4	0	0.23	ND	ND
9.02	12.2	5.83	3.7	-18	2250	2.24	337	1.46	51.35	0.34	10.2	37.13	11.8	0.05	0.08	0	0.28	ND	ND
24.02	12.4	6.39	2.9	-49	1657	0.6	142	1.05	51.64	0.06	1.68	19.78	7.95	0	0.04	0	0.25	0.05	ND
10.04	12.2	6.44	0.8	-70	2380	10.2	58.57	0.52	446.8	ND	7.78	100.6	11	ND	0.6	ND	0.22	0.08	ND
28.04	12.8	6.52	1.3		1309	6.8	31.32	0.52	128.4	ND	0.4	17.94	3.83	ND	0.12	ND	0.32	ND	0.08
26.05	13	6.24	1.2	-128	1216	92	76	1.3	98.3	ND	0.2	13.71	2.51	ND	ND	ND	0.19	ND	0.1

Location : Down-gradient Well No. 2 (DW-2)

Date	SWL	pH	DO	Eh	Cond	S2-	SO4	NO3	TOC	Cr	T-Cr	Fe	Mn	Ni	Cu	Co	Zn	Hg	As
26.01	11.5	7.02	4.9	112	1256	ND	289	4.89	46.04	12.55	19.5	5.2	0.3	0.01	0.07	0	0.19	ND	ND
9.02	12.1	6.15	3.4	-15	1838	12.2	352	2.09	47.33	0.23	9.09	16.82	8.82	0.01	0.03	0	0.18	ND	ND
24.02	12.4	6.42	2.7	-24	2080	0.5	236	1.33	50.28	ND	7.79	24.45	7	0.03	0.01	0	0.09	0.06	ND
10.04	12	6.58	0.8	-43	1454	4.26	92.98	1.4	225.9	ND	3.3	17.17	4.26	ND	0.09	ND	0.19	0.09	ND
28.04	12.5	6.78	1.2	-	968	8.24	96.09	1.27	41.6	ND	2.71	5.99	1.71	ND	0.08	ND	1.09	ND	0.05
26.05	13	6.48	0.8	-1	1039	ND	93	2.15	61.6	0.67	2.87	4.03	0.87	ND	0.02	ND	0.02	ND	0.07

Location : Piezometer (PM)

Date	SWL	pH	DO	Eh	Cond	S2-	SO4 2-	NO3	TOC	Cr +6	T-Cr	Fe	Mn	Ni	Cu	Co	Zn	Hg	As
26.01	11.8	6.73	3.2	105	1450	ND	394	9.79	37.57	11.8	14.9	0.66	0.15	0.04	0.08	0	0.12	ND	ND
9.02	10.8	6.74	3.8	-12	1330	0.85	183	6.09	38.21	4.17	10.7	28.36	2.42	0.11	1.8	0	1.01	ND	ND
24.02	11.8	7.16	3	13	1563	ND	235	1.34	39.2	0.32	0.46	4.7	1.68	0.04	0.1	0	0.11	0.01	ND
10.04	11.9	6.75	0.8	-36	1376	3.98	95.33	1.31	208.2	ND	1.44	6.7	2.63	ND	0.87	ND	0.23	0.02	ND
28.04	12.2	7.51	1.3	-88	1438	7.7	148.9	1.73	56.92	ND	0.9	54.27	4.91	ND	0.84	ND	0.65	ND	0.1
26.05	12.9	7.4	1.5	-156	1372	2.7	55	0.35	66.86	ND	0.28	27.12	2.36	0.05	1.06	ND	0.29	ND	0.05

Notes:

1. Results for heavy metals, except Cr(VI), are reported as total dissolved metals, analyzed using atomic absorption spectroscopy in the flame mode.
2. SWL: Static water level in meters below ground surface (bgs).
3. Eh in mV.
4. Conductivity in µS /cm.
5. All others except pH in mg/l. pH is in standard units.
6. ND: Not detectable above analytical reporting limits.
7. ** : could not be completed due to excessive turbidity.
8. Date of Injection: February 8, 2006.
9. Dates are in day/month format. Note that 26.01 refers to a baseline sampling round; other dates refer to Post Injection sampling rounds.

PART III: Brownfields

Chapter 8

DATABASE ANALYSIS OF STATE SURFACE SOIL REGULATORY GUIDANCE VALUES

Aaron A. Jennings[§], Ph.D., P.E.[1] and Amy Hanna[2]
[1]*Professor, Department of Civil Engineering, Case Western Reserve University, 10900 Euclid Ave, Cleveland, OH 44106-7201 (aaj2@case.edu) (Fax: 216-368-5229)* [2]*Associate Civil Engineer, MHW, 1300 East 9th St. Suite 1100, Cleveland, OH 44113*

ABSTRACT

A 2001 study of Cleveland, Ohio brownfield surface soil contamination led to the examination of state regulatory guidance values for soils. Surface soils were of particular interest since these generally pose the greatest risk to human health at brownfield sites. This investigation initially focused on heavy metals, common contaminants at Cleveland brownfields. However, the observation of significant variability in guidance values applied to Cd, Cr, Cu, Pb, Ni, and Zn led to questions about other state-regulated components and ultimately to research examining the origins, magnitudes, and explanations for regulatory guidance value variability.

The results presented here are based on the compilation of an 18,776 state surface soil database assembled from regulatory guidance for organic, inorganic, and element contaminants. All values were captured electronically from internet sources. The structure of each guidance value dataset was then standardized in a database-compatible format. Chemical Abstract Service (CAS) registry numbers were added to each record if they were not already provided. Identification of all records by CAS number resolves the problem of chemical synonyms. All value datasets were then assembled into the ACCESS database S^3GVD (State Surface Soil Guidance Value Database)

Statistical analysis is presented to characterize the nature and extent of variability in state surface soil guidance values. The organics, inorganics, and elements most and least commonly regulated and the range of guidance values are discussed. Log-scale Ordered Column Diagrams (LOCDs) are used to explore the nature of individual chemical guidance value distributions.

Keywords: surface soil contamination, regulatory guidance values, database analysis

[§] Corresponding Author: Aaron A. Jennings, Case Western Reserve University, Department of Civil Engineering, Cleveland, OH 44106-7201, Tel: 216-368-4998, Email: aqaj2@case.edu

1. INTRODUCTION

This manuscript describes the development and application of a database titled S3GVD (State Surface Soil Guidance Value Database) that contains data on current state regulatory guidance values used to determine significant levels of surface soil contamination. The database was assembled to help identify the extent of regulated contaminants and to explore the variability of the guidance "mass burden" values being applied. In this context, "current" means regulatory guidance that was available online via regulatory agency portals after January, 2006. The term "mass burden" refers to contamination levels specified in units of mg/kg. Measures in these units are sometimes referred to as "concentrations," but we prefer to reserve the term "concentration" for contaminants defined as mass of solute per volume of liquid solvent. There are subtleties in the differences between the two that have implications for guidance values. For example, it is possible for a concentration to exceed 1,000,000 mg/l. This would be the case for a pure organic liquid with a density greater than water. However, it is not possible for a mass burden to exceed 1,000,000 mg/kg. No matter what it is made of, 1 kg is still 1,000,000 mg. If the chemical is a soil contaminant, mass burdens must be substantially less than this. This imposes a physical constraint of guidance values that is not always respected in regulation.

This manuscript describes how state guidance value datasets were identified, standardized, assembled, and vetted, and illustrates how S3GVD may be applied to examine the state of practice in regulatory surface soil contamination guidance.

This effort originated in a 2001 field survey of surface soil heavy metal contamination and implied health risks of brownfield soils of Cleveland, OH (Jennings et al. 2002a). Reconnaissance analysis indicated that many of these sites had high levels of Cd, Cr, Cu, Ni, Pb, and Zn. However, risk assessment was complicated by the fact that the State of Ohio was shifting from "background" guidance (values set at estimates of the naturally-occurring levels in uncontaminated soils) to health-based guidance (values set at estimates of the maximum contaminant mass burdens believed to maintain human health risk below a specified level in a predetermined exposure scenario). Ohio's 1999 background standards for Cd, Cr, Ni, Pb, and Zn were 1.25, 22, 37, 33, and 90 mg/kg respectively (OEPA, 1999). Ohio's 2002 health-based "Generic Remediation Standards (OEPA, 2002) raised these values to 35,120,000/230 (CrIII/CrT), 1,500, 400, and 23,000 mg/kg respectively (increased of up to 55,000%). This led to obvious questions about the applicability of the new standards, and to comparison between these and the guidance values used in other Midwestern states. The result was that, with the exception of Pb guidance, heavy metal regulatory guidance was found to differ by orders of magnitude, and these differences yielded significant changes in the implied risks (Petersen et al., 2006). Expansions of the basis of comparison ultimately led to an analysis of the heavy metal surface soil guidance available in all of the state, province, commonwealth, and territory environmental jurisdictions of North America (Jennings and Petersen 2006; Jennings and Ma 2006) and to a preliminary effort to examine the guidance for common organic pollutants (benzene, ethylbenzene, pentachlorophenol, phenol, naphthalene, tertachloroethylene, toluene, trichloroethylene, and xylenes) (Jennings, 2005). Results indicated that guidance value variability ranged from 4 to 6 orders of magnitude, but that organic compounds were difficult to compare because of differences in the way they were identified.

The analysis presented here was conducted to provide a more comprehensive assessment of the scope and variability in the U.S. regulatory guidance being applied to surface soil contamination. Database analysis was required to help manage the huge amount of data involved.

2. MATERIALS AND METHODS

2.1 Dataset Identification

Regulatory Guidance Value Datasets (GVDs) were identified by internet search. Many states provide more than one set of values because individual agencies or regulatory programs promulgate application-specific guidance. For example, Ohio provides guidance under both its Remedial Response and Voluntary Action programs. Delaware allows users to apply either "default" background standards or risk-based standards. Vermont allows users to apply alternatives such as guidance provided by EPA regions III, VI, or IX. Several states also list previous, current, and proposed GVDs and stage in changes over several years. Internet searches identified 80 GVDs. It is certainly possible that datasets were overlooked or that sets have been added or revised, but these 80 datasets provide a large sample of currently-available surface soil mass burden guidance.

Table 1 identifies the 80 regulatory guidance datasets identified. Detailed references (100+ web citations) are available for each (see Hanna, 2007), but have not been included here because of length restrictions. States are identified by their postal code abbreviation. The Guidance Value Designation column identifies the jurisdiction's name for its guidance values. These vary from demonstrative designations such as "Soil Remediation Standards", "Predetermined Soil Remediation Levels", or "Soil Cleanup Value Standards" to less explicit identities such as "Soil Level", "Remediation Objectives" or "Suggested Generic Soil Cleanup Levels", but they all serve the same purpose. They identify contamination levels that are high enough to be of environmental or human health concern to warrant additional analysis. Many states provide guidance for a variety of site conditions (proximity to surface water bodies or potable groundwater), site uses (parks, residential, commercial, light industrial, heavy industrial), exposure types (ingestion, inhalation, dermal exposure) or exposure objects (child, indoor adult worker, outdoor adult worker, construction worker). The values selected were either generic values that apply to all sites, or residential, commercial, and industrial values that apply to surface soils where risk is dominated by inhalation, ingestion, or dermal contact. The final three columns of Table 1 summarize the number of guidance values found for organic, inorganic, and element contamination. Guidance values are characterized as element values if they specified mass burden for an element or elemental ion (e.g. Cr+3, Cr+6, Na+, Cl-, F-).

Table 1. Surface Soil RGD Identification, Type and Size Summary

RGD	State	Guidance Value Designation	O	I	E
1	Alabama (AL)	Preliminary Screening Values	165	9	22
2	Alaska (AK)	Cleanup Levels	108	2	15
3	Arizona (AZ)	Soil Remediation Standards, Soil Remediation Level (SRL)	492	41	26
4	Arizona (AZ)	Predetermined Soil Remediation Levels	519	19	30
5	Arkansas(AR)	Human Health Medium-Specific Screening Levels	388	44	28
6	California (CA)	Soil Level	34	3	19
7	California (CA)	Environmental Screening Levels	98	2	20
8	Colorado (CO)	Soil Cleanup Value Standards	19	0	6
9	Connecticut (CT)	Standards for Soil Remediation	151	3	22
10	Delaware (DE)	Default Background Remediation Standards	27	0	20
11	Delaware (DE)	Uniform Risk-Based Remediation Standards	363	37	30
12	Florida (FL)	Soil Cleanup Target Levels	373	11	28
13	Georgia (GA)	Risk Reduction Standards	394	143	19
14	Hawaii (HI)	Tier 1 Action Levels	17	0	2
15	Hawaii (HI)	Tier 1 Environmental Action Levels (EALs)	96	2	21
16	Idaho (ID)	Initial Default Target Levels	161	6	18
17	Illinois (IL)	Remediation Objectives	104	3	21
18	Indiana (IN)	Residential Closure Levels	122	3	14
19	Iowa (IA)	Statewide Standard for Soil	198	11	23
20	Kansas (KS)	Risk-Based Standards	157	4	15
21	Kentucky (KY)	Preliminary Remediation Goals	519	21	30
22	Louisiana (LA)	Screening Standards for Soil	124	5	16
23	Maine (ME)	Remedial Action Guidelines	40	1	13
24	Maryland (MD)	Uniform Numeric Risk-Based Standards Generic Numeric Cleanup Standards	122	2	20
25	Massachusetts (MA)	MCP Numerical Standards	99	2	16
26	Massachusetts (MA)	MCP Numerical Standards	95	1	16
27	Massachusetts (MA)	MCP Numerical Standards	95	1	16
28	Michigan (MI)	Risk-Based Screening Levels, Generic Cleanup Criteria and Screening Levels	227	3	29
29	Minnesota (MN)	Soil Reference Value	128	5	26
30	Mississippi (MS)	Target Remediation Goals	441	47	30
31	Missouri (MO)	Soil Target Concentrations	202	4	20
32	Montana (MT)	Preliminary Remediation Goals (Adjusted)	519	19	30
33	Montana (MT)	Risk-based Screening Level	25	0	0
34	Nebraska (NE)	Voluntary Cleanup Program Remediation Goals	521	28	30
35	Nevada (NV)	Interim Action Level	2	0	0
36	New Hampshire (NH)	Soil Standards	131	2	15

Table 1. Continued

RGD	State	Guidance Value Designation	O[(1)]	I[(2)]	E[(3)]
37	New Hampshire (NH)	Soil Standards	131	2	16
38	New Jersey (NJ)	Soil Cleanup Criteria	92	1	16
39	New Jersey (NJ)	Generic Soil Remediation Standards	117	2	17
40	New Mexico (NM)	Soil Screening Levels	175	8	24
41	New York (NY)	Recommended Soil Cleanup Objectives	95	1	23
42	New York (NY)	Recommended soil cleanup objectives for Gasoline and Fuel Oil Contaminated Soils	29	0	0
43	New York (NY)	Soil Cleanup Objectives	70	2	14
44	North Carolina (NC)	Soil Remediation Goals	248	6	17
45	North Dakota (ND)	Cleanup Action Level	1	0	0
46	Ohio (OH)	Generic Numerical Standards	105	2	18
47	Ohio (OH)	Residential Generic Cleanup Numbers (GNCs)	166	6	20
48	Oklahoma (OK)	Risk-Based Cleanup Levels	3	0	0
49	Oklahoma (OK)	Generic SSLs for Residential Scenario	92	2	15
50	Oklahoma (OK)	Medium Specific Screening Levels	388	41	28
51	Oregon (OR)	Soil Cleanup Level	64	1	11
52	Oregon (OR)	Residential Maximum Allowable Soil Concentration	64	1	11
53	Oregon (OR)	Preliminary Remediation Goals	520	18	30
54	Pennsylvania (PA)	Medium Specific Concentrations (MSC)	317	4	22
55.	Rhode Island (RI)	Direct Exposure Criteria	77	1	17
56.	South Carolina (SC)	Risk Based Screening Levels	77	1	17
57.	South Dakota (SD)	Action Level	6	0	0
58.	South Dakota (SD)	Look-up Table (sites without a water ingestion pathway)	6	0	0
59.	Tennessee (TN)	Preliminary Remediation Goals	519	19	30
60.	Texas (TX)	Protective Concentration Levels (PCLs)	590	12	30
61.	Texas (TX)	Surface/Air and Ingestion Standard (SAI)	588	10	30
62.	Texas (TX)	Risk-Based Screening Values (RBSVs)	588	10	30
63.	Utah (UT)	Risk-Based Corrective Action Screening Levels (SL)	9	0	0
64.	Utah (UT)	Recommended Cleanup Levels (RCLs)	9	0	1
65.	Vermont (VT)	Risk Based Concentration	293	25	27
67.	Vermont (VT)	Preliminary Remediation Goals	519	21	30
67.	Virginia (VA)	Risk Based Concentration	288	24	24
68.	Virginia (VA)	Soil Screening Level (SSL)	162	4	19
69.	Virginia (VA)	Risk-Based Concentration (RBC)	161	4	19
70.	Virginia (VA)	VRP Tier II Screening Concentration	163	4	19
71.	Washington (WA)	Soil Cleanup Levels	18	0	6
72.	Washington (WA)	Cleanup Levels	493	45	25
73.	West Virginia (WV)	De Minimis Standards for Soil	353	20	25

Table 1. Continued

RGD	State	Guidance Value Designation	O(1)	I(2)	E(3)
74.	West Virginia (WV)	Uniform Standards for Soil	495	42	0
75.	West Virginia (WV)	Natural Background	0	0	34
76.	Wisconsin (WI)	Suggested Generic Soil Cleanup Levels	18	0	0
77.	Wisconsin (WI)	Soil Cleanup Standards	7	0	5
78.	Wisconsin (WI)	Soil Screening Levels	8	0	0
79.	Wisconsin (WI)	Soil Screening Levels, Soil Screening Guidance	529	49	28
80.	Wyoming (WY)	Soil Cleanup Levels	522	19	30

Table Notes: RGD – Regulatory Guidance Database ; O – Number of Organic Guidance Values
I – Number of Inorganic Guidance Values; E – Number of Element Guidance Values

2.2 Guidance Value Database Standardization

All GVDs were edited into a standard format for incorporation into **S^{3}GVD.** This required resolving several format issues including the issue of chemical name. Regulatory guidance almost always identifies contaminants by name. This poses a significant challenge to database analysis because there is little consistency in the way chemicals are named. Many organics are identified by their chemical structure, abbreviation, common name, or manufacturer's designation. This leads to three major data base analysis challenges.

2.2.1 Nomenclature versus common names

Organics such as toluene (C7H8) may be identified by the common name "toluene" or by the more descriptive nomenclature names of methylbenzene, monomethyl benzene, or phenylmetane. This is significant because a database search using any one of these names would yield incomplete results. Name variations also cause problems if guidance values are listed under multiple names. This inflates the apparent number of organics for which guidance is provided.

2.2.2 Name syntax

There are syntax variations by which nomenclature names may be listed. For example, the 1,1,1 version of the C2H3Cl3 may be identified as (ethane, 1,1,1,-trichloro-), (1,1,1-trichloroethane), (trichloro-1,1,1-ethane), or (□-trichloroethane) and the number of possible variations grows rapidly with structure complexity. Any of these name variations could be incorrectly interpreted as a unique chemical by database software.

2.2.3 Product Names

Organics such as Fluorene (C13H10; 2,2'-methylenebiphenyl), Lindane (C6H6Cl6; 1,2,3,4,5,6-hexachlorocyclohexane), or Endosuflan (C9H6Cl6O3S; 6,7,8,9,10,10-hexachloro-1,5,5a,6,9,9a-hexahydro,3-oxide) are often identified by a product name. The National Institute of Standards and Technology (NIST) records data for each of these under their product name rather than their chemical nomenclature.

To illustrate the potential magnitude of these problems, consider that NIST lists 86 synonyms for the common lawn and garden insecticide Dimpylate (C12H21N2O3PS) which is regulated in 31 states. Table 2 lists the 23 chemical nomenclature name variations listed in the NIST directory. Table 3 completes this list with 63 product names also listed by NIST. Considering the variations that can be created by capitalization and punctuation, there is a nearly unlimited number of name variations under which Dimpylate could be regulated.

One solution for the chemical name problem is to replace the names used by regulatory jurisdictions with a standard name for each contaminant. This was not done. There is no universal authority for determining "standard" names. Even in the NIST registry, chemicals are not consistently identified by nomenclature names and the punctuation used in nomenclature designations is not always consistent. Furthermore, even if names were standardized, database users might not recognize the contaminant by its standard name.

Table 2. Nomenclature Name Variation for Dimpylate, CAS No 333-41-5 (NIST, 2007)

No.	Nomenclature Name Variation
1	Phosphorothioic acid, O,O-diethyl O-[6-methyl-2-(1-methylethyl)-4-pyrimidinyl] ester
2	Phosphorothioic acid, O,O-diethyl O-(2-isopropyl-6-methyl-4-pyrimidinyl) ester
3	O,O-Diethyl-O-(2-isopropyl-4-methylpyrimidyl)thiophosphate
4	Diethyl 4-(2-isopropyl-6-methylpyrimidinyl)phosphorothionate
5	Isopropylmethylpyrimidyl diethyl thiophosphate
6	O-2-Isopropyl-4-methylpyrimidyl-O,O-diethyl phosphorothioate
7	O,O-Diaethyl-O-(2-isopropyl-4-methyl-pyrinidin-6-yl)-monothiophosphat
8	O,O-Diethyl O-(2-isopropyl-4-methyl-6-pyrimidinyl) phosphorothioate
9	O,O-Diethyl O-(2-isopropyl-4-methyl-6-pyrimidyl) phosphorothioate
10	O,O-Diethyl O-(2-isopropyl-4-methyl-6-pyrimidyl) thionophosphate
11	O,O-Diethyl O-(2-isopropyl-6-methyl-4-primidinyl)phosphorothioate
12	O,O-Diethyl O-(2-isopropyl-6-methyl-4-pyrimidinyl) phosphorothioate
13	O,O-Diethyl O-6-methyl-2-isopropyl-4-pyrimidinyl phosphorothioate
14	O,O-Diethyl 2-isopropyl-4-methylpyrimidyl-6-thiophosphate
15	O,O-Diethyl-O-(2-isopropyl-4-methyl-pyrimidin-6-yl)-monothiofosfaat
16	Phosphorothioate, O,O-diethyl O-6-(2-isopropyl-4-methylpyrimidyl)
17	Thiophosphate de O,O-diethyle et de O-2-isopropyl-4-methyl-6-pyrimidyle
18	4-Pyrimidinol, 2-isopropyl-6-methyl-, O-ester with O,O-diethyl phosphorothioate
19	O,O-Diethyl 2-isopropyl-6-methyl-4-pyrimidinylphosphorothioate
20	Diethyl 2-isopropyl-4-methyl-6-pyrimidinyl phosphorothionate
21	Phosphorothioic acid, O,O-diethyl 2-isopropyl-6-methyl-4-pyrimidinyl ester
22	o,o-Diethyl-O-(6-methyl-2-(1-methylethyl)-4-pyrimidinyl)phosophorothioate
23	o,o-Diethyl o-(2-isopropyl-6-methyl-4-pyrimidinyl) thiophosphate

Rather than standardize chemical names, a record was added (where it did not already exist) to identify each chemical by its Chemical Abstract Service registry number (CAS number). CAS numbers are unique numbers containing up to 9 digits that identify every substance that has been registered with the American Chemical Society. The CAS registry contains information on more than 31 million substances and is believed to be the most comprehensive database of this type in the world (ACS, 2005). The CAS numbers themselves have no chemical significance, but each is unique and the final digit in the sequence may be used in a validity test of the number. CAS numbers should be written with a hyphen in front of the third-from-last and last number in the digit sequence. For example, the CAS No. for Lindane is 58-89-9. Several states use CAS numbers, but some omit hyphens. Omitted hyphens were replaced. This avoided problems such as 58899 and 58-89-9 being identified as different classifications by database software. CAS numbers were added to all records in each guidance value dataset that did not already contain them. Several resources were used for this. The NIST web site (NIST, 2007) is very helpful, but requires that one know the CAS number to find a chemical. Several other resources were used to identify CAS numbers for chemicals regulated only by name. ***Chemexper*** (2006), proved to be most helpful. This provides information on most chemicals currently being manufactured. ***PubChem*** (NCBE 2006) maintained by the National Center for Biotechnology Information and the ***Substance Registry System*** (USEPA, 2006) maintained by the Environmental Protection Agency were also used to identify CAS numbers for chemicals not listed in ***Chemexper***.

Table 3. Product Name Variation for Dimpylate, CAS No. 333-41-5, (NIST, 2007)

No.	Name	No.	Name	No	Name e
24	Diazinone	45	AG-500	66	Bassadinon
25	Antigal	46	Basudin 10 G	67	Disonex
26	Basudin	47	Bazuden	68	Agridin 60
27	Bazudin	48	Dazzel	69	Antlak
28	Ciazinon	49	Diazajet	70	Diagran
29	Dacutox	50	Diazide	71	Diazinon AG 500
30	Dassitox	51	Diazitol	72	Diaterr-fos
31	Dianon	52	Diazol	73	Diazinon liquid
32	Dicid	53	Dipofene	74	Diethyl dimpylatum
33	Dimpylat	54	Ektoband	75	Diziktol
34	Exodin	55	Geigy 24480	76	Dizinon
35	ENT 19,507	56	Nedcidol	77	Drawizon
36	Flytrol	57	Neocidol (oil)	78	Dyzol
37	G 301	58	Nucidol	79	Fezudin
38	G-24480	59	NCI-C08673	80	Kayazinon
39	Galesan	60	Oleodiazinon	81	Kayazol
40	Garden Tox	61	Nemacur	82	Knox Out 2FM
41	Neocidol	62	Basudin 5G	83	Neocidol veterinary powder
42	Sarolex	63	Nipsan	84	Spectracide 25EC
43	Spectracide	64	Knox-out	85	Root guard
44	Alfa-Tox	65	Meodinon	86	Diazinon

In addition to adding CAS numbers, records were added to identify the data source, the dates of origin and electronic capture, and a code to distinguish organic, inorganic, and element guidance. Records were also reordered into a consistent format, but efforts were made to maintain the format and precision of all numerical information. In some instances, this led to questions about the true value of the guidance. Some states compute values from formula and coefficients stored in on-line spreadsheets. The results are displayed using a format set in the spreadsheet, but the actual values are stored to much higher precision. When these values are copied, the whole computation (to many significant figures) is preserved, so it can be displayed to any desired precision. For this analysis, the displayed precision was assumed to be the intended accuracy.

2.3 Database Verification

Once GVDs were standardized, each was imported into S3GVD. This resulted in a database of 18,776 guidance value records. A series of verification protocols were then applied to detect and help resolve inconsistencies.

One method of checking for consistencies was to sort all database records by CAS number and then examine the names associated with all identical CAS numbers. When names appeared that were not synonyms, the original state documentation was consulted. If discrepancies existed between state-supplied names and CAS numbers, the name was assumed to be correct.

Inconsistencies were also sought by sorting the database by chemical name and verifying that each unique name was associated with the appropriate CAS number. Because of the use of synonyms, this resulted in more name groups than CAS numbers, but helped identify name/number associations that were not consistent.

As a final check, an inverse CAS registry was used to identify chemical structure and verify CAS numbers for each unique contaminant name group.

The verification test sequence yielded a diminishing number of inconsistencies. Most of these were typographical or syntax errors in chemical names or CAS numbers. In the final verification test, only 3 inconsistencies were detected out of 18,776 records (an error rate of 0.016%), but it is possible that errors remain. It is also likely that states have added new contaminants or updated existing values since the dataset was captured. S3GVD should be updated frequently to accommodate the evolution of regulatory guidance.

2.4 Log Ordered Column Diagrams

Jennings and Petersen 2006 applied Log Ordered Column Diagrams (LOCDs) to illustrate the variability of regulatory guidance values for residential soils. Jennings, and Ma (2007) extended this method to include the use of the fuzzy mode ($\tilde{M}$) to help identify "common" ranges in guidance value distributions. These approaches will be applied here. Furthermore, to help serve as a basis of comparison for the whole value distribution, consider the following:

Let x be a lognormally distributed random variable that has a probability of 0.998 of falling within the number range [1 – 100,000]. This random variable would have a mean (μ_L) of 2.50 and a standard deviation (σ_L) of 0.809.

Generate 50 random samples of x, (50 xi realizations) by using a normal random number generator to generate values of log(x). Order these realizations from highest to lowest.

Repeat "ii" several (N) times and average the results.

Plot the results as a LOCD.

The results of this process are illustrated in Fig. 1. Given a sufficiently large value of N, what will emerge is a column diagram approximation of the cumulative distribution function (CDF) of x. The results of Fig. 1 were calculated from 10 realizations. This is an easily anticipated result, but is noteworthy because of a few of its properties. Note that the arithmetic mean (in this case 1,568) is substantially higher than 10^{μ_L} (102.564=366) and the median. Also note that there is no mode. However, one should also note that the "nice" version of Fig. 1 only emerges in the average after realizations are averaged. Figure 2 illustrates a LOCD of one single realization. In Fig. 2 the parent distribution is not as easily detected.

Finally, consider that it is possible (but unlikely) to randomly generate a number set with a non-trivial mode. In the example of Fig.3, a mode was created by rounding off values in the neighborhood of 300 to one significant figure. This can be extended to a "fuzzy mode" by extending the range by some percent of the mode. Jennings and Ma (2007) found that 10% was a reasonable extension based on the way regulatory guidance values are calculated and rounded.

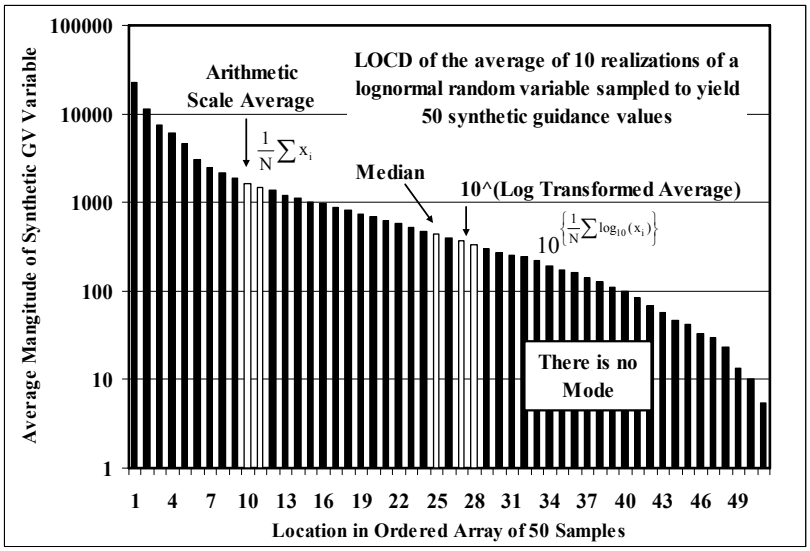

Figure 1. LOCD of the Average of 10 Realizations Each of 50 Ranked, Lognormal Random Numbers

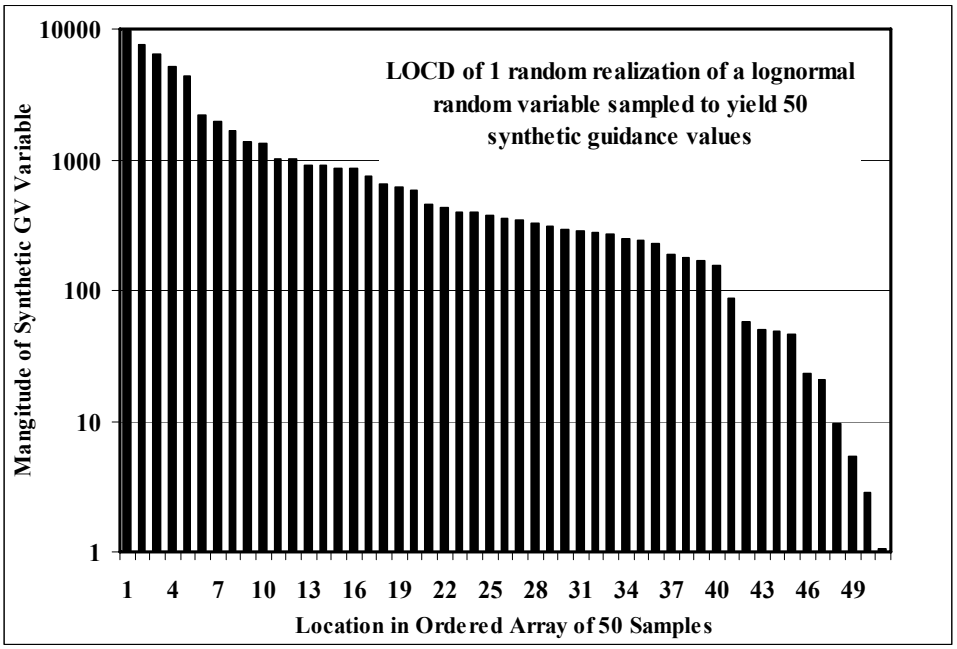

Figure 2. LOCD of 1 Realization of 50 Ranked Lognormal Random Numbers

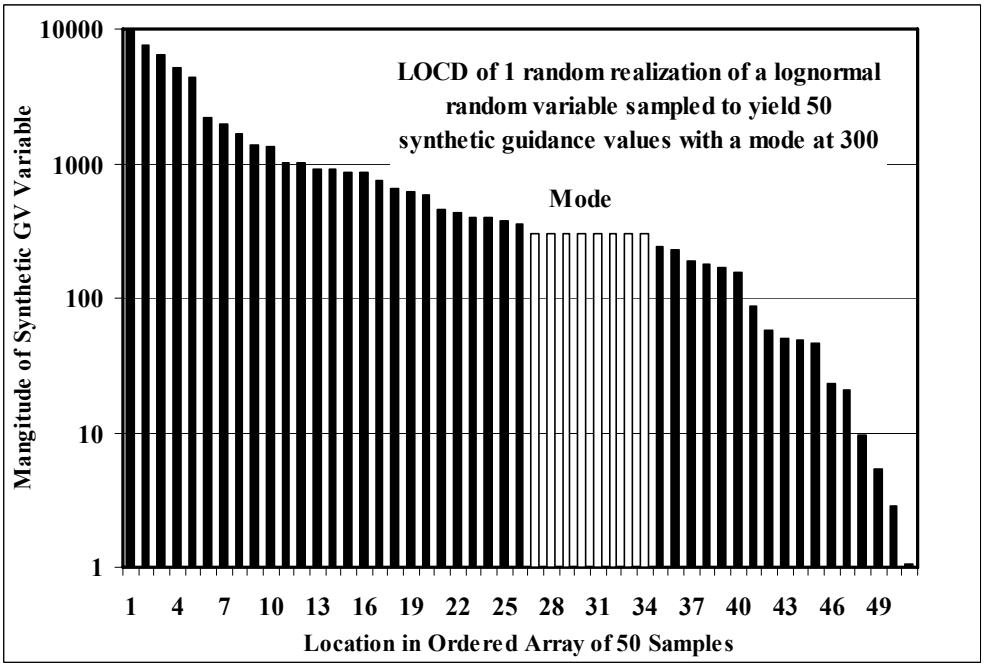

Figure 3. LOCD of 1 Realization of 50 Lognormally Random Numbers with a Synthetic Mode

Fig. 3 provides a useful (but not particularly complementary) basis by which to compare the value distributions of regulatory guidance values.

Figure 5 presents a histogram of the data of Fig. 4 using an interval size of approximately $\sigma/4$. The number of values in national superfund or by EPA region guidance have been indicated. It seems likely (but not apparent) that these numbers have influenced the size of state GVDs.

One obvious question one might ask is which state has the most (or least) conservative guidance. This is easy to answer for any one compound, but more difficult to characterize across the whole array of regulated compounds. One method of approaching the question is to examine the extremes of the guidance values for each compound, and to count the number of times a state's guidance falls at a compound extreme. The resulting counts are summarized in Table 5.

Note that counts have been provided for the number of times a state's guidance value is at the compound extreme, and the number of times this occurs for compounds with 10 or more guidance values. This second statistic was selected because some states provide guidance for unusual chemicals. When there is only 1 guidance value, the state's value is both a maximum and a minimum. When there are a few values, this need not be true, but the probability of a state's guidance value being at the compound extreme is still high. Furthermore, one must attempt to normalize these counts by the number of guidance values actually provided. States that provide few values will have few set at compound extremes even if they are all at extremes. Therefore, Table 5 presents the number of extreme values as a percentage of the state's total number of values.

By the measures of Table 5, one might suggest that MI, WA, TX, IN, and WV have the least conservative guidance values because more than 10% of their values are set at compound maxima. One might also suggest that AZ, WA, MI, IA, WV, and OR have the most conservative values because more than 10% of their values are set at compound minima. Clearly, both of these suggestions are imperfect because WA and MI appear on both lists, and either could correct if limited to a subset of regulated chemicals.

Rather than pursue additional general analysis, it seems more appropriate to explore the nature of the guidance provided for classes of compounds or for individual contaminants.

Table 4. Summary of ***S^{3}GVD*** Attributes for Residential Surface Soils

Measure	Value
Total Number of Guidance Values (GVs)	18,776
Total Number of GVs for Organics	16,451
Total Number of GVs for Inorganics	891
Total Number of GVs for Elements	1,434
Total Number of States Represented	50
Maximum Number of Total State GVs (TX)	1888
Minimum Number of State Total GVs (ND)	1
Maximum Number of State Organics GVs (TX)	1766
Minimum Number of State Organics GVs (ND)	1
Maximum Number of State Inorganics GVs (GA)	143
Minimum Number of State Inorganics GVs (CO,ND,NV,SD,UT)	0
Maximum Number of State Element GVs (TX)	90
Minimum Number of StateElement GVs (ND,NV,SD)	0
Average Number of GVs per state	376
Average Number of Organic GVs per state	329
Average Number of Inorganic GVs per state	18
Average Number of Element GVs per state	29
Total Number of Unique CAS Numbers	1221
Total Number of Unique Organic CAS Numbers	994
Total Number of Unique Inorganic CAS Numbers	178
Total Number of Unique Element CAS Numbers	49
Total Number of Distinct Elements	43
Average Number of Unique CAS GVs per State	291
Maximum Number of Unique CAS GVs per State	632
Minimum Number of Unique CAS GVs per Sate	1
Average Number of Unique Organic CAS GVs per State	291
Average Number of Unique Inorganic CAS GVs per State	178
Average Number of Unique Element CAS GVs per State	43

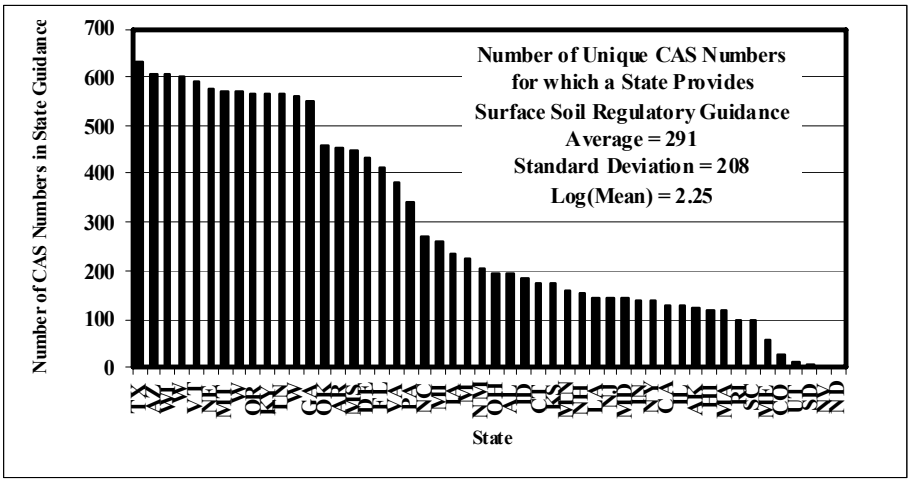

Figure 4. OCD of the Total Number of Unique CAS Numbers for which States Provide Surface Soil Regulatory Guidance Values

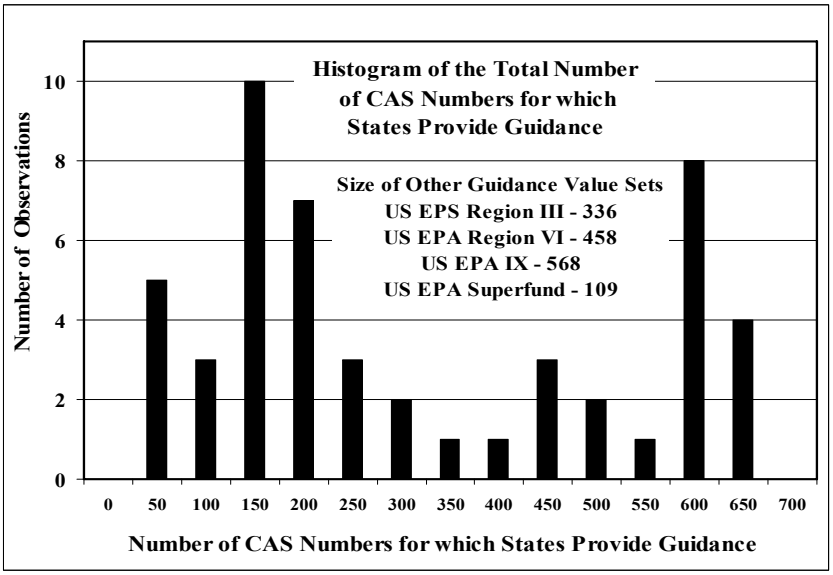

Figure 5. Histogram of the Total Number of CAS Numbers for which States Provide Guidance

2.5 Guidance Values for Organic Compounds *S*^{3}*GVD*

Guidance Values for Organic Compounds *S*^{3}*GVD* contains data on state regulatory guidance for 329 unique organic compound CAS designations. Selected data for the 100 most frequently regulated of these is presented in Table 5.

One useful statistic is the log10 order of variation (LOV) computed as Log10 {(maximum guidance value)/(minimum guidance value)}. The average LOV of all 100 compounds is 4.44 (a factor of 27,500). The LOV of all 100 chemicals has a standard deviation of 1.11.

Figure 6 illustrates this average as a function of location in the ranked array of compounds. Note that variation is even higher for the most commonly regulated compounds. One possible explanation for this is that 4 of the 5 most commonly regulated compounds are the BTEX association (benzene, toluene, ethylbenzene, and xylenes) if dimethylbenzene is assumed to represent all (1,2- 1,3- and 1,4-dimethylbenzene). It seems likely that the range of values for these has been impacted by the differences between generic soil remediation regulation and underground storage tank programs.

Jennings and Hanna (2007) illustrated LOCD's for the top 10 organics of Table 6. Here, we will present LODC of other compounds that illustrate the same basic features.

Figure 7 illustrates a LOCD of the residential surface soil guidance values for methylene chloride (CAS 75-09-2), the 12th most commonly regulated organic compound. Note that this has a LOV of more than 5 orders of magnitude. The fuzzy mode encompass 14 of the 64 regulatory values (22%), but appears quite far to the right in the distribution. There seem to be additional groups of similar values, but these appear closer than they are because of the log scale.

Figure 8 – 11 present LOCDs for 1,2-dichloroethane (CAS 107-06-2), 1,1,1-trichloroethane (CAS 71-55-6), Anthracene (CAS 120-12-7) and acetone (CAS 67-64-1) which are #13, #14, #17, and # 36 respectively on the list of the most regulated organics. Not that all of these are characterized by a high degree of variation (LOV>5). The fuzzy mode approach captures "typical" ranges with mixed success. The range captured for 1,2-dichloroethane only spans 8 of the 64 values (12.5%) and appears far to the right in the distribution. The range captured for Anthracene contains 21 of the 65 values (33%) but appears uncomfortably left (i.e. less conservative values) in the distribution.

Figure 12 presents a final example LOCD for heazchlorobenzene. This was selected as an example of an organic for which there appears to be more universal agreement on guidance value numbers. Note that hexachlorobenzene (#42 in Table 6) has a LOV of 2.35. The guidance value distribution of hexachlorozene also appears to be bi-fuzzy-modal. There is a fuzzy mode in the neighborhood of 0.3 mg/kg that captures 16 of the guidance values. There is also a fuzzy mode in the neighborhood of 0.4 that captures 14 guidance values. The ranges of these two modes do not overlap, but they are quite close. It the degree of fuzziness is expanded a bit, the modes would merge and capture 55% of the guidance values.

Table 5. Frequency of State Guidance Values at Compound Guidance Extremes

State	NGVUB	NGVUB>9	ΣGVs	% >9	State	NGVLB	NGVLB>9	ΣGV	%>9
TX	339	125	632	19.8	TX	240	29	632	4.6
WA	191	170	569	29.9	MT	213	199	569	35.0
GA	187	25	549	4.6	GA	202	34	549	6.2
MI	130	106	259	40.9	WI	124	93	608	15.3
WV	70	60	603	10.0	VA	108	49	382	12.8
AZ	46	36	608	5.9	ID	81	78	184	42.4
MS	40	8	450	1.8	DE	34	26	432	6.0
IA	32	23	232	9.9	NY	32	28	137	20.4
FL	31	25	412	6.1	MI	24	0	259	0.0
WI	29	7	608	1.2	OR	21	18	566	3.2
OR	20	16	566	2.8	CA	19	13	130	10.0
VA	19	18	382	4.7	AZ	16	5	608	0.8
IN	18	18	138	13.0	NC	15	2	271	0.7
VT	18	13	593	2.2	WA	14	1	569	0.2
MA	17	2	117	1.7	NH	12	2	154	1.3
NH	10	2	154	1.3	NE	10	8	574	1.4
OH	10	7	196	3.6	FL	9	0	412	0.0
KS	9	8	174	4.6	MS	9	1	450	0.2
NE	9	7	574	1.2	OK	8	3	460	0.7
KY	8	4	564	0.7	WY	8	7	562	1.2
TN	8	4	563	0.7	MA	8	4	117	3.4
MD	7	3	143	2.1	IA	7	1	232	0.4
OK	6	5	460	1.1	AL	7	6	192	3.1
AR	5	4	455	0.9	AR	5	1	455	0.2
CT	5	1	174	0.6	KS	5	4	174	2.3
ME	5	5	54	9.3	OH	4	3	196	1.5
CA	4	0	130	0.0	CT	4	2	174	1.1
DE	4	0	432	0.0	WV	4	0	603	0.0
MO	4	3	226	1.3	RI	3	3	95	3.2
NC	3	1	271	0.4	SC	3	3	95	3.2
NJ	3	3	144	2.1	NM	3	3	204	1.5
NM	3	3	204	1.5	VT	3	3	593	0.5
AL	1	0	192	0.0	KY	2	2	564	0.4
IL	1	1	128	0.8	MO	2	2	226	0.9
NY	1	0	137	0.0	CO	1	1	25	4.0
WY	1	1	562	0.2	MD	1	0	143	0.0
					ME	1	1	54	1.9
					TN	1	1	563	0.2
					ND	1	0	1	0.0
					NJ	1	1	144	0.7
					NV	1	0	2	0.0
					IN	1	1	138	0.7
					MD	1	0	143	0.0

NGVUB – No. of guidance values at upper bound

NGVUB>9 – No. of guidance values at upper bound for CAS numbers with 10 or more values

□GV – Total number of state guidance values

%>9 - % of guidance values at the indicated bound for CAS numbers with 10 or more values

"LB" – lower bound

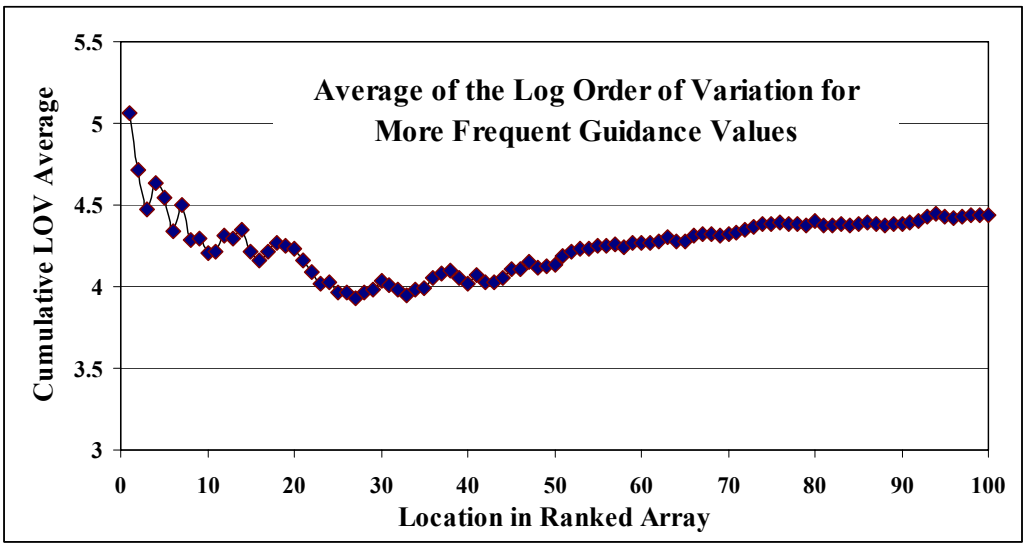

Figure 6. Average LOV as a Function of Position In the Ranked Array of The Most Frequently Regulated Organic Compounds

Table 6. Top 100 Organic Compounds for which Residential Surface Soil Guidance (mg/kg) is Provided

Rank	Freq.	CAS No.	Formulae	Name	Min	Max	LOV
1	76	91-20-3	$C_{10}H_8$	Naphthalene	0.138	16000	5.06
2	74	108-88-3	C_7H_8	Toluene	0.7	16000	4.36
3	74	71-43-2	C_6H_6	Benzene	0.0178	180	4.00
4	73	1330-20-7	C_8H_{10}	Dimethylbenzene	1.2	160000	5.12
5	72	100-41-4	C_8H_{10}	Ethylbenzene	1	15000	4.18
6	69	50-32-8	$C_{20}H_{12}$	Benzo[a]pyrene	0.00875	17.7	3.31
7	67	79-01-6	C_2HCl_3	Trichloroethylene	0.00159	500	5.50
8	67	75-01-4	C_2H_3Cl	Chloroethene	0.0067	3.8	2.75
9	67	127-18-4	C_2Cl_4	Tetrachloroethylene	0.0302	780	4.41
10	66	206-44-0	$C_{16}H_{10}$	Fluoranthene	20	46000	3.36
11	66	83-32-9	$C_{12}H_{10}$	Acenaphthene	2.2	41000	4.27
12	65	75-09-2	CH_2Cl_2	Methylene chloride	0.0169	5010	5.47
13	65	107-06-2	$C_2H_4Cl_2$	1,2-dichlorethane	0.00771	91	4.07
14	65	71-55-6	$C_2H_3Cl_3$	1,1,1-trichloroethane	0.68	72000	5.02
15	65	56-55-3	$C_{18}H_{12}$	Benz[a]anthracene	0.0875	20	2.36
16	65	129-00-0	$C_{16}H_{10}$	Pyrene	13	29000	3.35
17	65	120-12-7	$C_{14}H_{10}$	Anthracene	1.93	230000	5.08
18	64	67-66-3	$CHCl_3$	Chloroform	0.00783	1200	5.19
19	64	56-23-5	CCl_4	Carbon tetrachloride	0.012	96	3.90
20	64	108-90-7	C_6H_5Cl	Chlorobenzene	0.618	5000	3.91
21	64	53-70-3	$C_{22}H_{14}$	Dibenz[a,h]anthracene	0.00875	5	2.76
22	64	193-39-5	$C_{22}H_{12}$	o-phenylenepyrene	0.0875	32.8	2.57
23	64	205-99-2	$C_{20}H_{12}$	Benz[e]acephenanthrylene	0.0875	20	2.36
24	64	218-01-9	$C_{18}H_{12}$	Chrysene	0.1	2000	4.30
25	64	50-29-3	$C_{14}H_9Cl_5$	1,1'(2,2,2-trichloroethylidene) bis[4-chlorobenzene]	0.188	57	2.48
26	64	86-73-7	$C_{13}H_{10}$	Fluorene	3.71	27000	3.86
27	63	87-86-5	C_6HCl_5O	Pentachlorophenol	0.073	90	3.09
28	63	58-89-9	$C_6H_6Cl_6$	Lindane	0.000896	80	4.95
29	63	156-60-5	$C_2H_2Cl_2$	1,2-dichloroethene	0.19	5000	4.42
30	63	75-35-4	$C_2H_2Cl_2$	1,1-dichloroethene	0.01	3910	5.59
31	63	207-08-9	$C_{20}H_{12}$	Benzo[k]fluoranthene	0.1	200	3.30
32	63	60-57-1	$C_{12}H_8Cl_6O$	1,2,3,4,10,10-Hexachloro-6,7-epoxy-1,4,4a,5,6,7,8,8a-octahydro-1,4-endo-exo-5,8-dimethanonaphthalene	0.001	1.1	3.04
33	62	117-81-7	$C_{24}H_{38}O_4$	Bis(2-ethylhexyl)phthalate	4	2800	2.85
34	62	72-20-8	$C_{12}H_8Cl_6O$	Endrin	0.00065	80	5.09
35	62	76-44-8	$C_{10}H_5Cl_7$	Heptachlor	0.0002	5.6	4.45
36	61	67-64-1	C_3H_6O	Acetone	0.05	70400	6.15
37	61	75-34-3	$C_2H_4Cl_2$	1,1-dichloroethane	0.2	15600	4.89
38	61	79-00-5	$C_2H_3Cl_3$	1,1,2-trichloroethane	0.0141	1000	4.85
39	61	72-55-9	$C_{14}H_8Cl_4$	P,p'-dde	0.188	45	2.38

Table 6. Continued

Rank	Freq.	CAS No.	Formulae	Name	Min	Max	LOV
40	61	72-54-8	$C_{14}H_{10}Cl_4$	1,1-dichloro-2,2-bis(4 chlorophenyl)-ethane	0.266	95	2.55
41	60	108-95-2	C_6H_6O	Phenol	0.03	48000	6.20
42	60	118-74-1	C_6Cl_6	Hexachlorobenzene	0.0399	8.9	2.35
43	60	95-50-1	$C_6H_4Cl_2$	1,2-dichlorobenzene	1.1	7200	3.82
44	59	106-46-7	$C6H_4Cl_2$	1,4-dichlorobenzene	0.046	11000	5.38
45	59	124-48-1	$CHBr_2Cl$	Dibromochloroemthane	0.00202	5000	6.39
46	59	156-59-2	$C_2H_2Cl_2$	2,4-dichloroethene	0.193	3000	4.19
47	59	1634-04-4	$C_5H_{12}O$	2-methoxy-2-methyl-propane	0.00667	8760	6.12
48	59	309-00-2	$C_{12}H_8Cl_6$	Aldrin	0.00376	1	2.42
49	59	75-25-2	$CHBr_3$	Tribromomethane	0.0292	1100	4.58
50	59	75-27-4	$CHBrCl_2$	Bromodichloromethane	0.00268	110	4.61
51	59	78-93-3	C_4H_8O	1-butanone	0.00486	48000	6.99
52	59	88-06-2	$C_6H_3Cl_3O$	2,4,6-trichlorophenol	0.00436	1000	5.36
53	59	95-95-4	$C_6H_3Cl_3O$	2,4,5-trichlorophenol	0.1	23000	5.36
54	58	100-42-5	C_8H_8	Styrene	1.83	16000	3.94
55	58	111-44-4	$C_4H_8Cl_2O$	Beta,beta'-dichloroethyl ether	4.06E-05	13	5.51
56	58	120-82-1	$C_6H_3Cl_3$	1,2,4-trichlorobenzene	0.11	1800	4.21
57	58	120-83-2	$C_6H_4Cl_2O$	2,4-dichlorophenol	0.0217	660	4.48
58	58	67-72-1	C_2Cl_6	Hexachloroethane	0.138	300	3.34
59	58	74-83-9	CH_3Br	Methyl bromide	0.000359	400	6.05
60	58	91-94-1	$C_{12}H_{10}Cl_2N_2$	3,3'-dichloro-[1,1'-Biphenyl]-4,4' diamine	0.00183	25	4.14
61	57	1024-57-3	$C_{10}H_5Cl_7O$	Heptachlor epoxide	0.0003	4.39	4.17
62	57	105-67-9	$C_8H_{10}O$	2,4-dimethylphenol	0.174	11000	4.80
63	57	115-29-7	$C_9H_6Cl_6O_3S$	Encosulfan	0.0006	1400	6.37
64	57	72-43-5	$C_{16}H_{15}Cl_3O_2$	Methoxychlor	8.8	1900	2.33
65	57	78-87-5	$C_3H_6Cl_2$	1,2-dichloropropane	0.00933	140	4.18
66	57	84-66-2	$C_{12}H_{14}O_4$	Diethyl phthalate	0.035	150000	6.63
67	56	79-34-5	$C_2H_2Cl_4$	1,1,2,2-tetrachloroethane	0.000704	53	4.88
68	56	8001-35-2	$C_{10}H_{15}Cl$	Toxaphene	0.00042	20	4.68
69	56	87-68-3	C_4Cl_6	1,1,2,3,4,4-hexachloro-1,3-Butadiene	0.0318	100	3.50
70	55	95-57-8	C_6H_5ClO	2-chlorophenol	0.0146	1400	4.98
71	54	106-93-4	$C_2H_4Br_2$	1,2-dibromoethane	1.9E-05	1.6	4.93
72	54	121-14-2	$C_7H_6N_2O_4$	1-methyl-2,4-dinitrobenzene	0.00029	160	5.74
73	54	51-28-5	$C_6H_4N_2O_5$	2,4-dinitrophenol	0.00146	370	5.40
74	54	541-73-1	$C_6H_4Cl_2$	1,3-dichlorobenzene	0.0188	7000	5.57
75	53	106-47-8	C_6H_6ClN	p-Chloroaniline	0.0119	730	4.79
76	53	630-20-6	$C_2H_2Cl_4$	1,1,2,2-tetrachloroethane	0.0158	2300	5.16

Table 6. Continued

Rank	Freq.	CAS No.	Formulae	Name	Min	Max	LOV
77	52	1746-01-6	$C_{12}H_4Cl_4O_2$	2,3,7,8-Tetrachlorodibenzo-p-dioxin	4.26E-07	0.001	3.37
78	52	319-84-6	$C_6H_6Cl_6$	a-Lindane	0.00021	2.6	4.09
79	52	542-75-6	$C_3H_4Cl_2$	1,3-dichloro-1-Propene	0.0023	26	4.05
80	52	75-00-3	C_2H_5Cl	Ethyl chloride	0.0191	31000	6.21
81	51	1336-36-3	(varies)	Polychlorinated biphenyls	0.07	14	2.30
82	50	108-10-1	$C_6H_{12}O$	Methyl isobutyl ketone	0.207	13000	4.80
83	50	95-48-7	C_7H_8O	2-methylphenol	0.1	7700	4.89
84	50	98-82-8	C_9H_{12}	(1-methylethyl)-benzene	1.95	8000	3.61
85	49	108-60-1	$C_6H_{12}C_{l2}O$	2,2'-oxybis[1-chloro-propane	0.00908	3100	5.53
86	49	78-59-1	$C_9H_{14}O$	3,5,5-trimethyl-2-cyclohexen-1-one	0.14	16000	5.06
87	49	84-74-2	$C_{16}H_{22}O_4$	Dibutyl phthalate	8.1	18000	3.35
88	48	319-85-7	$C_6H_6Cl_6$	1,2,3,4,5,6-hexachloro (1a,2ß,3a,4ß,5a,6ß) -cyclohexane	0.000751	5.4	3.86
89	48	77-47-4	C_5Cl_6	1,2,3,4,5,5-hexachloro-1,3-cyclopentadiene	0.0117	1100	4.97
90	48	86-30-6	$C_{12}H_{10}N_2O$	N-nitroso-N-phenyl-benzenamine	0.088	2200	4.40
91	48	98-95-3	$C_6H_5NO_2$	Nitrobenzene	0.000347	100	5.46
92	47	106-44-5	C_7H_8O	4-methylphenol	0.021	910	4.64
93	47	131-11-3	$C_{10}H_{10}O_4$	Dimethyl phthalate	0.035	1000000	7.46
94	47	606-20-2	$C_7H_6N_2O_4$	2-methyl-1,3-dinitro-benzene	0.000212	80	5.58
95	47	85-68-7	$C_{19}H_{20}O_4$	Benzyl butyl ester phthalic acid	50	37000	2.87
96	46	96-12-8	$C_3H_5Br_2Cl$	1,2-dibromo-3-chloro-propane	0.000975	4.1	3.62
97	45	117-84-0	$C_{24}H_{38}O_4$	Di-n-octyl phthalate	0.3	151000	5.70
98	45	621-64-7	$C_6H_{14}N_2O$	n-nitroso-n-propyl-1-Propanamine	1.81E-05	1.71	4.98
99	45	75-69-4	CCl_3F	Trichloromonofluoro-methane	0.41	24000	4.77
100	45	94-75-7	$C_8H_6Cl_2O_3$	(2,4 Dichlorophenoxy) acetic acid	0.3	3000	4.00

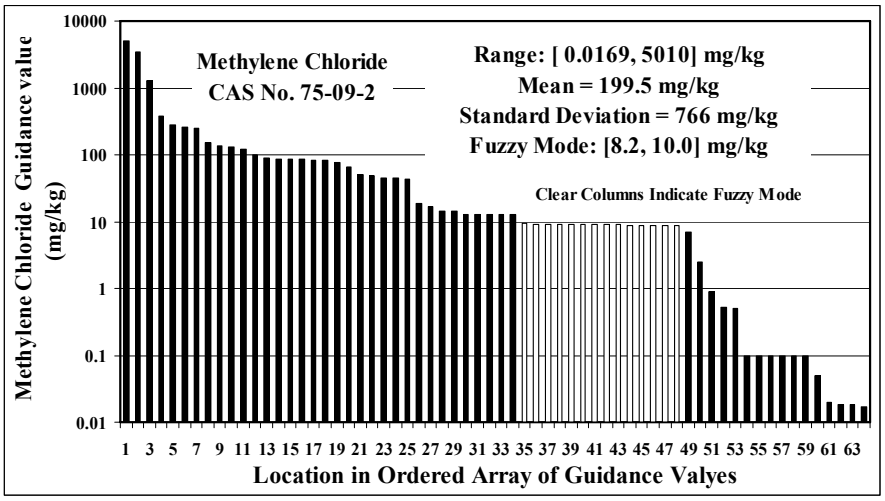

Figure 7. LOCD of Residential Surface Soil Regulatory Guidance Values for Methylene Chloride

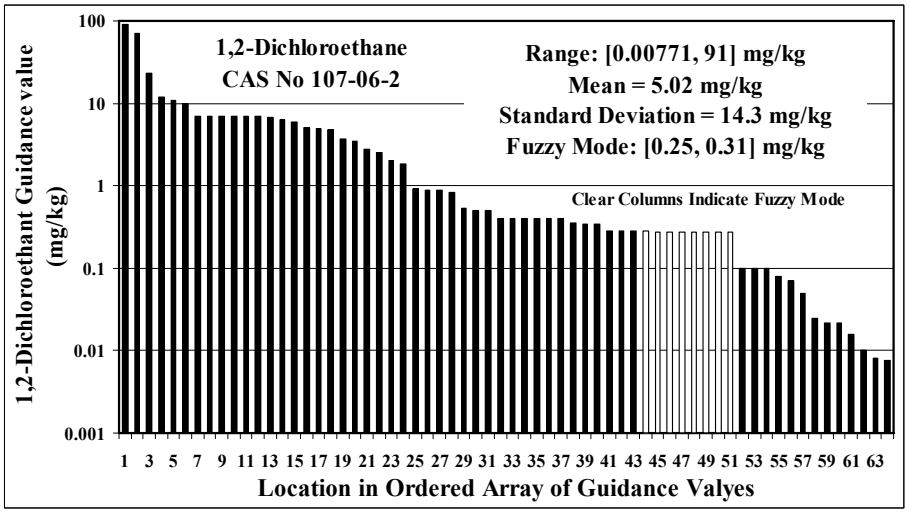

Figure 8. LOCD of Residential Surface Soil Regulatory Guidance Values for 1,2-Dichloroethane

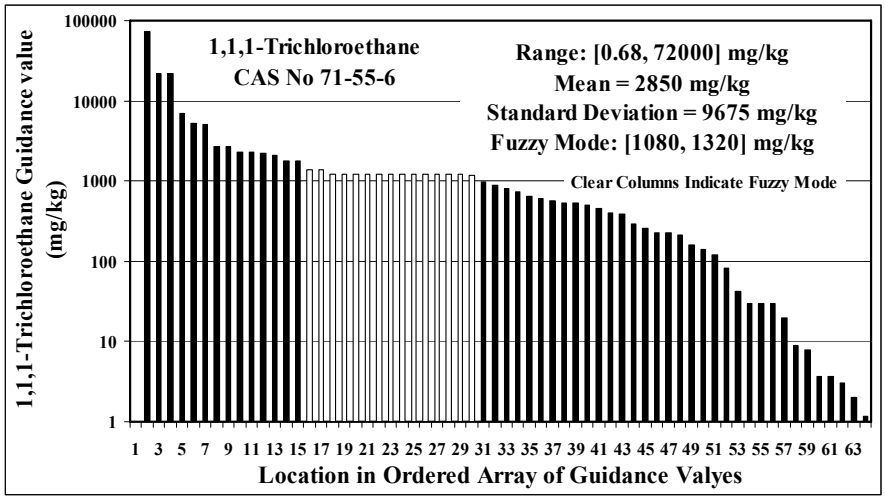

Figure 9. LOCD of Residential Surface Soil Regulatory Guidance Values for 1,1,1-Trichloroethane

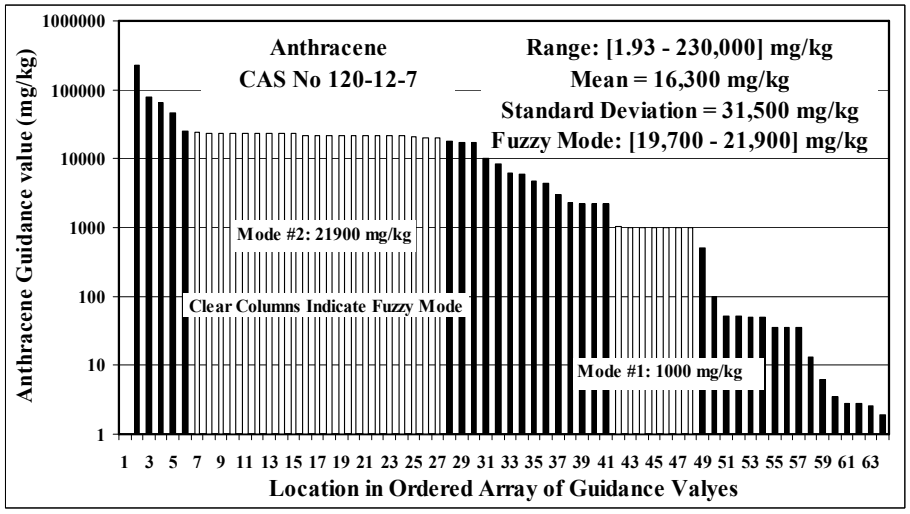

Figure 10. LOCD of Residential Surface Soil Regulatory Guidance Values for Anthracene

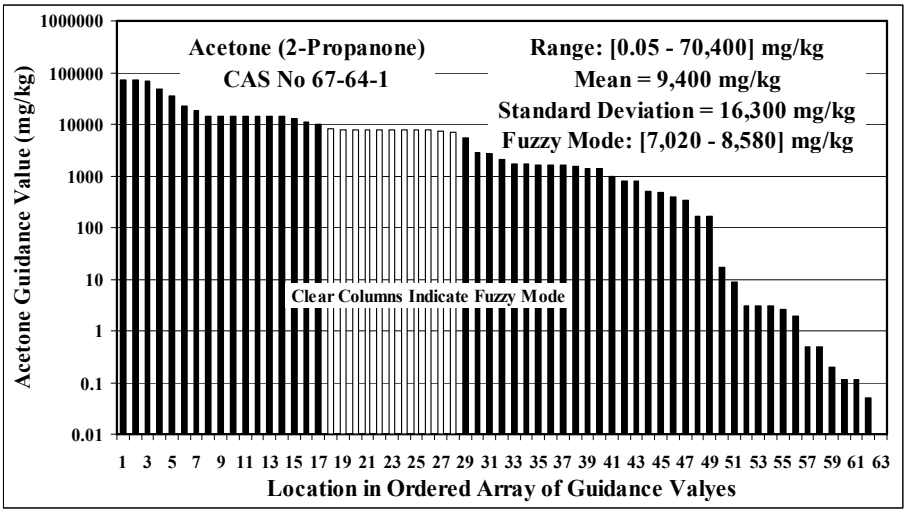

Figure 11. LOCD of Residential Surface Soil Regulatory Guidance Values for Acetone

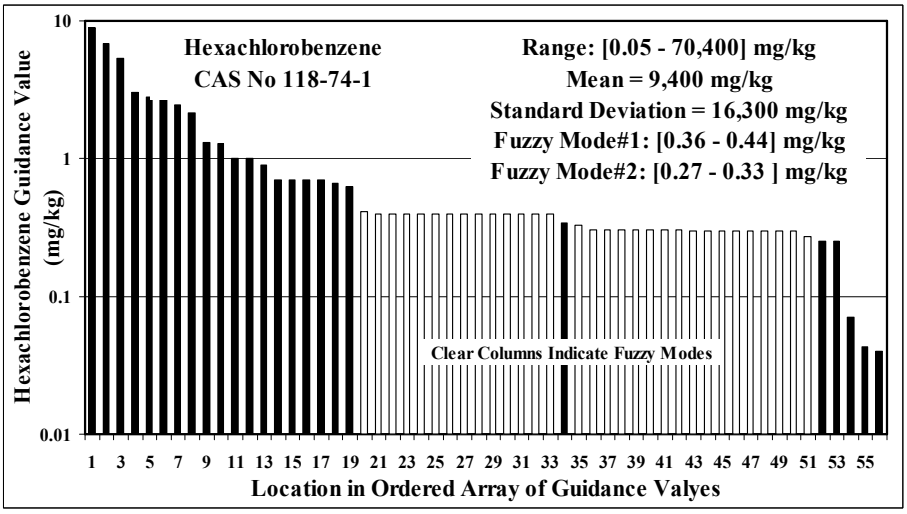

Figure 12. LOCD of Residential Surface Soil Regulatory Guidance Values for Hexachlorobenzene

All of the LOCDs of Fig. 7-12 seem to have strong similarities with the "small sample" synthetic log-normally distributed LOCD of Fig. 3.

2.6 Guidance Values for Inorganic Compounds - *S³GVD*

Guidance Values for Inorganic Compounds S³GVD contains regulatory guidance on 178 unique inorganic chemical CAS number designations, but only 60 of these have more than 1 guidance value, and only 38 have 10 or more guidance values. Information on the 20 most frequently regulated inorganics is summarized in Table 7, which lists the minimum and maximum residential value for each compound. The 158 inorganics not listed in Table 7, include:

23 sulfates – (e.g. dithalluim sulfate, Tl_2SO_4, CAS No. 7446-18-6)
22 chlorides (e.g. mercury dichloride, $HgCl_2$, CAS No.7487-94-7)
15 oxides (e.g. vanadium oxide, V_2O_5, CAS No.1314-62-1)
11 cyanides (e.g. sodium cyanide, NaCN, CAS No.143-33-9)
10 nitrates or nitrites (e.g. mercury nitrate $Hg_2N_2O_6$, CAS No.7782-86-7)
10 arsenates or arsenites (e.g. lead hydrogen arsenate, $PbAsHO_4$, CAS No.7784-40-9),
8 chromates (e.g. sodium chromate, $CrNa_2O_4$, CAS No.7775-11-3) and
7 fluorides (e.g. zinc difluoride, ZnF_2, CAS No.7783-49-5).

Table 7. Top 20 Inorganics for which Residential Surface Soil Guidance (mg/kg) is Provided

Rank	Frequency	CAS NO.	Formulae	Name	Min	Max	LOV
1	59	57-12-5	CN^-	Cyanide anion	0.0036	6900	6.28
2	49	75-15-0	CS_2	Carbon disulfide	0.152	8000	4.72
3	32	74-90-8	CHN	Hydrogen cyanide	1.08	1600	3.17
4	30	7803-51-2	H_3P	Phosphine	1.83	59	1.51
5	29	7487-94-7	Hg Cl_2	Mercury dichloride	0.011	383000	7.54
6	25	460-19-5	C_2N_2	Cyanogen	0.43	3200	3.87
7	23	7601-90-3	$HClO_4$	Perchloric acid	0.1	871000	6.94
8	22	506-77-4	CClN	Cyanogen chloride	10	4000	2.60
9	20	7783-00-8	H_2O_3Se	Selenious acid	30.6	400	1.12
10	21	10599-90-3	H_2ClN	Chloramide	610	8000	1.12
11	20	1314-84-7	P_2Zn_3	Zinc(II) diphosphide	2	26	1.11
12	20	506-68-3	CBrN	Cyanogen bromide	10	7200	2.86
13	19	14797-55-8	NO_3^-	NO_3 anion	18.4	410000	4.35
14	18	14797-65-0	NO_2^-	Nitrogen oxide anion	1.84	130000	4.85
15	16	7773-06-0	$H_3NO_3S{\cdot}H_3N$	Ammonium sulfamate	1220	16000	1.12
16	15	1309-64-4	O_3Sb_2	Antimony trioxide	3	32	1.03
17	15	20859-73-8	AlP	Aluminum monophosphide	3.13	35	1.05
18	15	302-04-5	SCN^-	Thiocyanate	1.5	6110	3.61
19	14	7791-12-0	ClTl	Thalium monochloride	0.6	20	1.52
20	14	13718-26-8	NaO_3V	Sodium vanadium(V) trioxide	6.11	80	1.12

On average, there is a variation of 3 orders of magnitude in the range of the 20 most commonly regulated inorganics. This falls to LOV=2 for the 60 CAS number designations with more than one guidance value if phosphoric acid (CAS No. 7664-38-2) is omitted. The guidance set for 7664-38-2 contains a value of 6.39×10^{33} mg/kg which is a physical impossibility and is believed to be an error in MS documentation. Readers should note, however, that physically impossible values (i.e. >1,000,000 mg/kg) are intentionally specified by some jurisdictions.

Figure 13 illustrates a LOCD of the guidance values for the most regulated inorganic compound (cyanide anion). The guidance values for cyanide anion vary over 6 orders of magnitude, but all but 2 values are contained within 3 orders of magnitude. If these guidance values are assumed to be log-normally distributed, then one would probably conclude that the lowest value is unlikely to belong to this population of numbers. The probability of observing a value as low as 0.368 mg/kg (the second lowest value) is about 0.003. One should observe a random value this low about once every 350 values. However the probability of observing a value of 0.0036 mg/kg (the lowest value) is approximately 1.7×10^{-6} (i.e. about once every 585,000 values). The fuzzy mode of the guidance value distribution spans 14 of the 59 guidance values, but is located near the high end of the distribution.

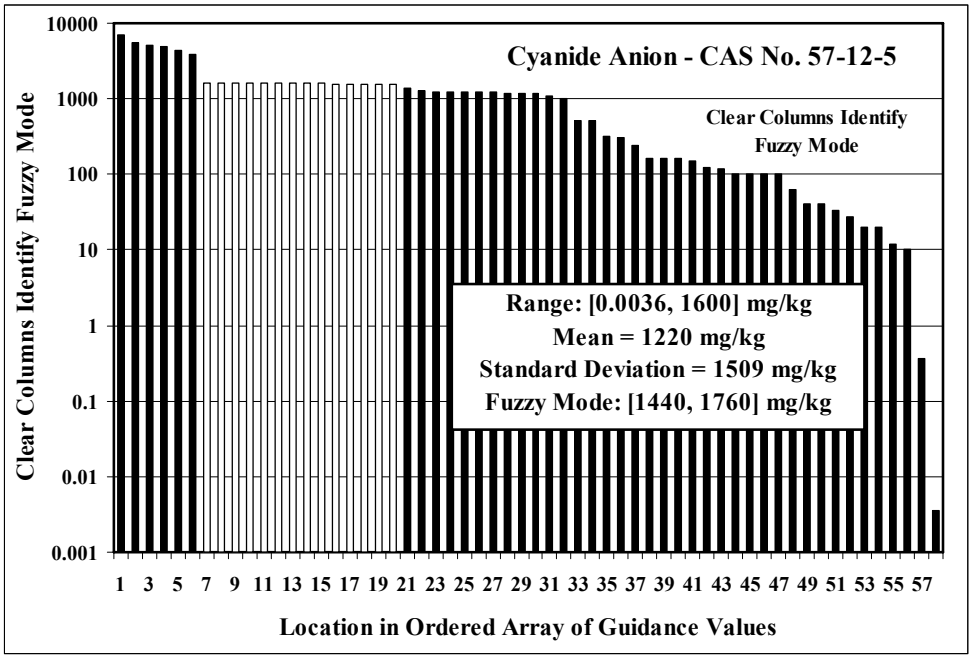

Figure 13. LOCD of Residential Surface Soil Regulatory Guidance Values for Cyanide Anion

Figure 14 illustrates a LOCD of the guidance for carbon disulfide (CS_2, CAS No. 75-15-0), the second most commonly regulated inorganic. The carbon disulfide guidance values are more evenly distributed (compared to Fig. 13) over 5 orders of magnitude. Although the fuzzy

mode spans a smaller percentage of the guidance values (9 of 49) it does appear to be more central in the value range.

Beyond cyanide and carbon disulfide, the numbers of and variability in guidance values is substantially lower than the numbers for organic compounds or elements. The LOV results for mercury dichloride ($HgCl_2$, CAS No. 7487-94-7) and perchloric acid ($HClO_4$, CAS No. 7601-90-3) are exceptions that are influenced by one unusual value. For mercury dichloride, no guidance value exceeds 100 mg/kg except for the extreme value of 383,000 mg/kg in the VA guidance. For perchloric acid, no value exceeds 55 mg/kg except for the extreme value of 871,000 mg/kg. Both of these values were based on an inhalation hazard, and both are substantially lower in alternative VA guidance value sets.

As a final example of the distributions of inorganic contaminant guidance values, Fig. 15 presents an arithmetic scale OCD for the residential soil guidance values of selenious acid (CAS No. 7783-00-8) for which there is only 1 order of magnitude in guidance value variation. For this case, the fuzzy mode captures 11 of the 20 guidance values.

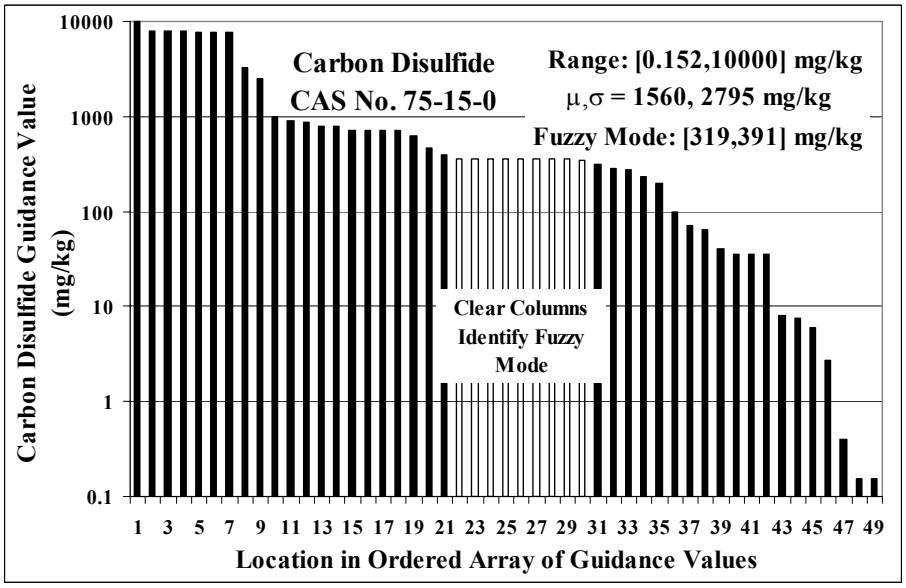

Figure 14. LOCD of Residential Surface Soil Regulatory Guidance Values for Carbon Disulfide

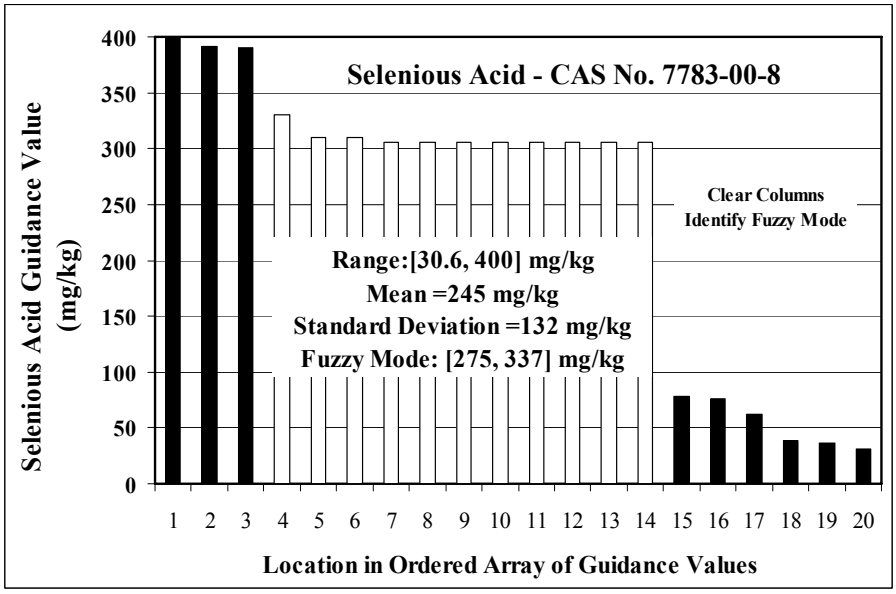

Figure 15. LOCD of Residential Surface Soil Regulatory Guidance Values for Selenious Acid

2.7 Guidance Values for Elements - *S³GVD*

Guidance Values for Elements - *S³GVD* also contains values for 49 element designations, but this total includes four different specifications for chromium (as Cr^{+3}, Cr^{+6}, Cr(total) and Cr(total as 1:6 Cr^{+6}:Cr^{+3}), and two specifications each for chlorine (Cl and Cl^{-}), fluorine (F and F^{-}), and sodium (Na and Na^{+}). If valance state differences are ignored, there are guidance values for 43 elements. The most common 32 of these are listed in Table 8. The remainder are made up of 3 guidance values each for magnesium and bismuth, 2 values each for calcium and potassium, and 1 value each for lanthanum, niobium, scandium, cerium, gallium, ytterbium, yttrium and zirconium. For the elements with 10 or more residential guidance values, there is an average LOV of 3.

A detailed analysis of the statistical properties of Cd, Cr, Cu, Pb, Ni, and Zn guidance values of North America may be found in Jennings and Petersen (2006) and Jennings and Ma (2007). Figures 16-21 complete the analysis of the top ten regulated elements (As, Be, Ag, Ba, Se, Sb).

Table 8. Top 30 Elements for which Residential Surface Soil Guidance (mg/kg) is Provided

Rank	Frequency	CAS No.	Element	Element	Min	Max	LOV
1	69	7440-38-2	As	Arsenic	0.004	30	3.88
2	68	7440-43-9	Cd	Cadmium	0.5	550	3.04
3	65	7440-02-0	Ni	Nickel	10	40000	3.60
4	64	7440-41-7	Be	Beryllium	0.002	680	5.53
5	63	7440-22-4	Ag	Silver	0.189	2500	4.12
6	63	7440-39-3	Ba	Barium	100	63000	2.80
7	62	7439-92-1	Pb	Lead	2	500	2.40
8	62	7440-66-6	Zn	Zinc	20	170000	3.93
9	62	7782-49-2	Se	Selenium	1	2600	3.41
10	60	7440-36-0	Sb	Antimony	3	180	1.78
11	57	7440-50-8	Cu	Copper	25	20000	2.90
12	56	7440-62-2	V	Vanadium	7.4	1500	2.31
13	55	18540-29-9	Cr(VI)	Chromium (VI)	1.8	2500	3.14
------	53	16065-83-1	Cr(III)	Chromium (III)	36	790000	4.34
14	52	7439-97-6	Hg	Mercury	0.00509	100000	7.29
15	52	7440-28-0	Tl	Thallium	0.516	35	1.83
16	49	7439-96-5	Mn	Manganese	9.5	30000	3.50
17	41	7440-48-4	Co	Cobalt	10	15000	3.18
18	37	7782-41-4 (1)	F- or F	Fluorine anion	7.36	15000	3.31
------	34	7440-47-3 (2)	Cr (Total)	Total Chromium	10	59000	3.77
19	34	7429-90-5	Al	Aluminum	7600	150000	1.30
20	34	7440-42-8	B	Boron	1.6	51000	4.50
21	30	7439-98-7	Mo	Molybdenum	39	2600	1.82
22	29	7439-89-6	Fe	Iron	5.76	160000	4.44
23	29	7440-24-6	Sr	Strontium	4690	330000	1.85
24	29	7440-31-5	Sn	Tin	2000	93000	1.67
25	26	7723-14-0	P	Phosphorous	0.156	1000000	6.81
26	24	7439-93-2	Li	Lithium	136	5100	1.57
27	21	7440-61-1	U	Uranium	1.56	760	2.69
28	13	7782-50-5	Cl or Cl^-	Chlorine	12	20000	3.22
29	12	7440-32-6	Ti	Titanium	10000	38000000	3.58
30	8	7429-91-6	Dy	Dysprosium	782	16000	1.31

(1) or CAS No. 16984-48-8 (2) or Cr(total) based on an assumed Cr^{+6}:Cr^{+3} ratio of 1:6

For As, Be, and Ag it is difficult to claim that the fuzzy mode bounds "typical" regulatory guidance values. For As, (see Fig. 16) the fuzzy mode bounds 21of the 69 values, but these are clustered at the low end of the value distribution. For Ba and Ag, the reverse is true. The Be (see Fig. 17) fuzzy mode bounds 18 of the 64 values, but these are clustered near the high end of the value distribution.

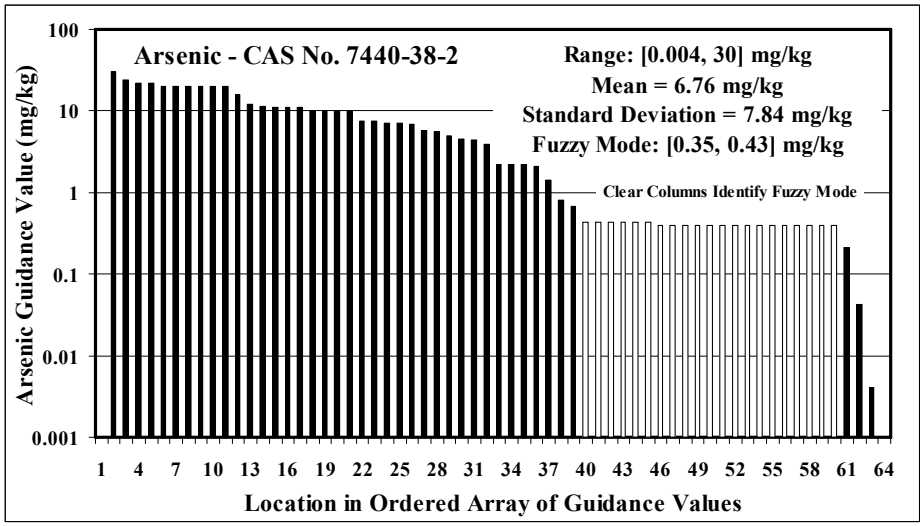

Figure 16. LOCD of Residential Surface Soil Regulatory Guidance Values for Arsenic

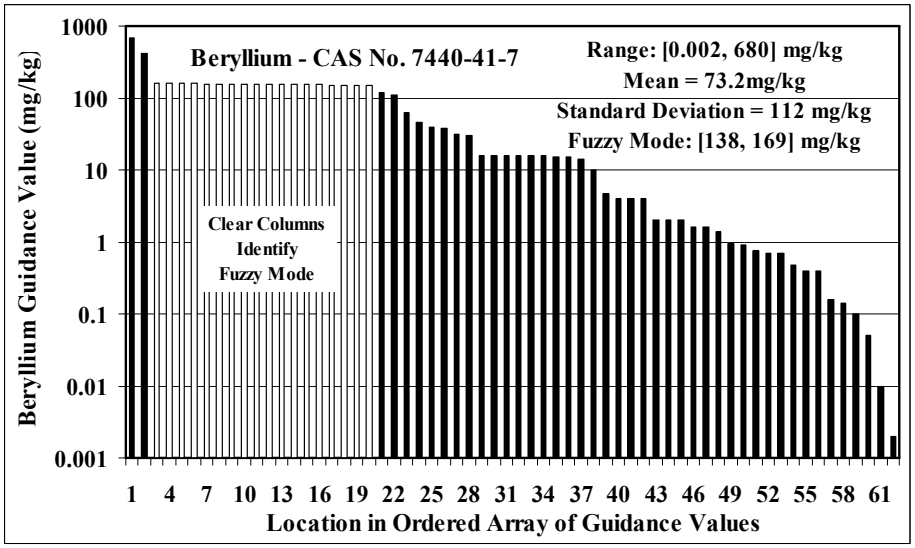

Figure 17. LOCD of Residential Surface Soil Regulatory Guidance Values for Beryllium

The Ag (See Fig. 18) fuzzy mode bounds 25 of the 63 values but these are also clustered near the high end of the distribution. This pattern is repeated for Se (29 of 62) (see Fig. 20) and Sb (24 of 60) (see Fig. 21). Only Ba (see Fig. 23) has a fuzzy mode that contains 21of 63 values and occurs near the central portion of the value distribution.

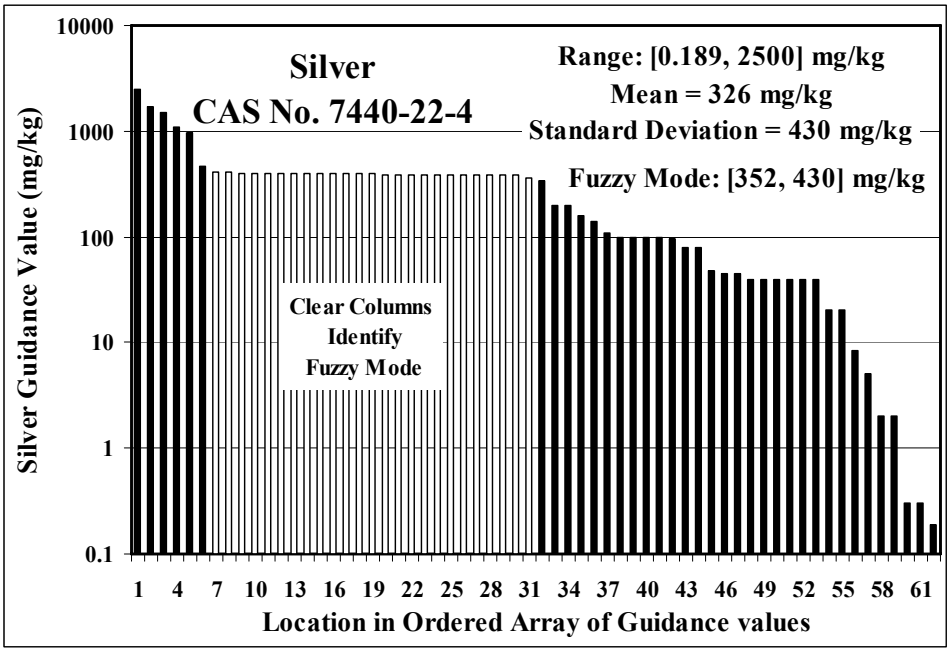

Figure 18. LOCD of Residential Surface Soil Regulatory Guidance Values for Silver

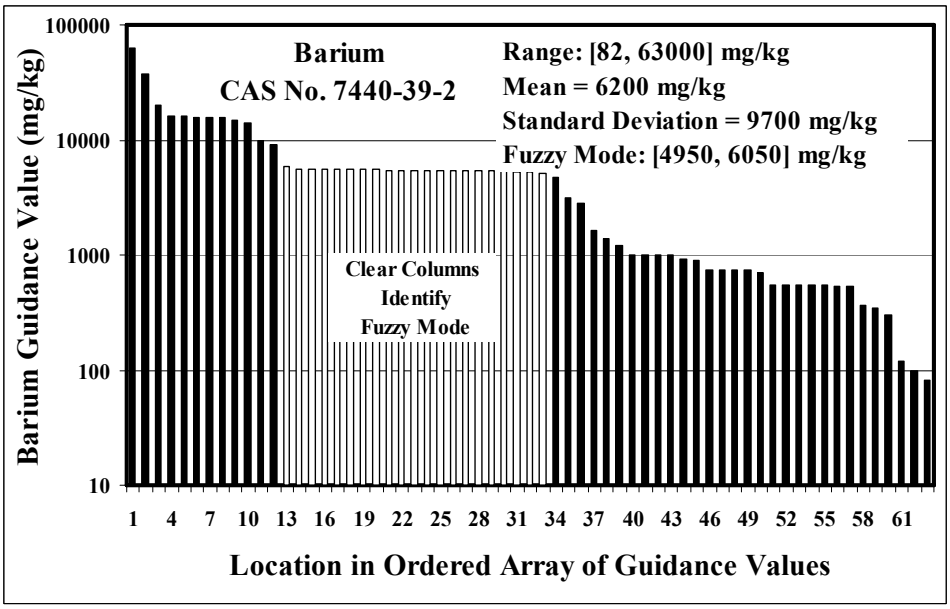

Figure 19. LOCD of Residential Surface Soil Regulatory Guidance Values for Barium

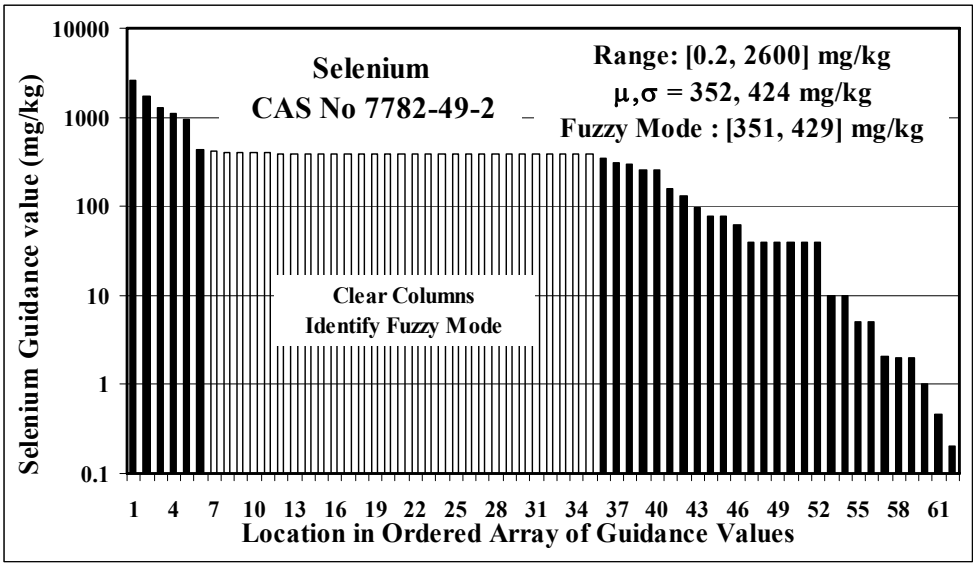

Figure 20. LOCD of Residential Surface Soil Regulatory Guidance Values for Selenium

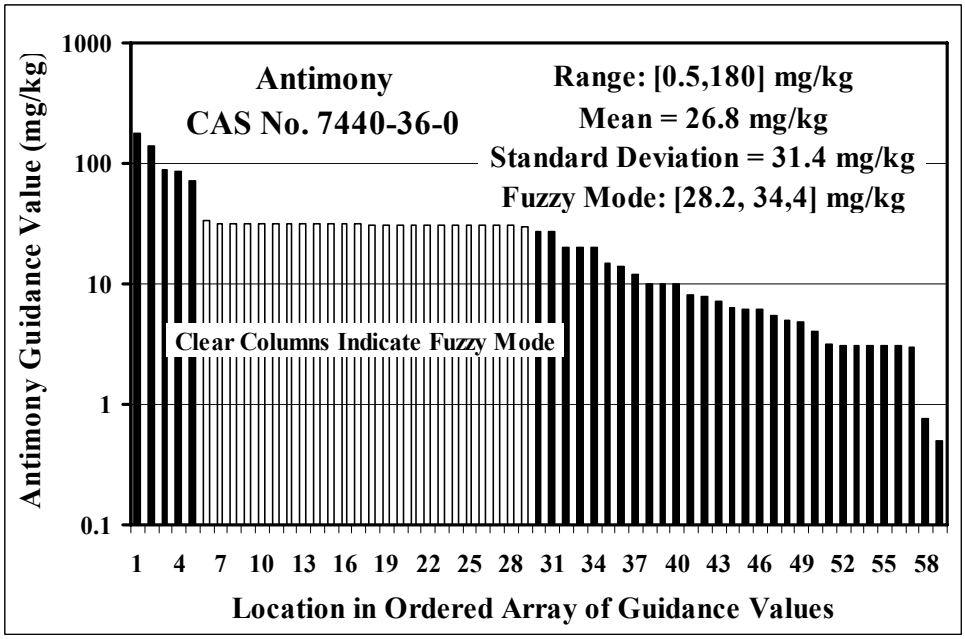

Figure 21. LOCD of Residential Surface Soil Regulatory Guidance Values for Antimony

2.8 Infeasible Guidance

The vast majority of the guidance values in S^3GVD (99.2%) are feasible. Some of them are quite high, and there is a great deal of variability for each regulated pollutant, but the values are physically possible. However, there are 144 guidance values that are not feasible because they

have numerical values ≥1,000,000 mg/kg. It is not possible for a mass burden to exceed this value, and it is not likely that anything approaching this value could be observed. Table 9 provides examples of nonfeasible guidance values for both residential and commercial/industrial site classifications.

There appear to be 3 explanations for nonfeasible guidance values. First, these may be errors such as typographical errors in number exponents. This appears to be the case for the 6.39E+33 phosphoric acid guidance value of MS. Others appear to be the result of automated value generation software. This appears to be the case for the 7.45 E+09 guidance value for 1,1-difluoro,1-chloloethane (and several others) of WI. Apparently the algorithm used resulted in unusual values for highly volatile contaminants. However, there is a large fraction of these infeasible values that appear to be intentional. Jennings et al. (2002) noted that, at the time, USEPA Region III was using an infeasible Cr (III) guidance value of 3,100,000 mg/kg and that discussions with their staff confirmed that this was the value intended. The number originated emerged from a rat feeding study estimate of toxicity to which a safety factor of 1000 was applied. The value has since been revised, but has lingered on in state guidance that was based on EPA Region III guidance.

3. DISCUSSION

The overriding observations that can be made about the state-of-the-art in regulatory guidance for residential surface soil contamination is that the values in current use are extremely variable. For many of the most commonly regulated contaminants, the range of values is 5 or 6 orders of magnitude, and there is modest "common" agreement among the values more central to the distribution. There appear to be several reasons why some of these values would differ.

i. Guidance values may be based on fundamentally different approaches. For example, values based on "background" are likely to be much lower than values based on human health risk analysis. This may explain some of the differences observed in the element or inorganic standards, but is more difficult to extend to organics. Most of the regulated organics should have a background of zero since they are not naturally-occurring.

ii. Guidance values may be based on alternative risk assessment formulations, exposure scenarios and/or coefficient value sets. Any of these could yield modest variations in the values calculated for any one pollutant.

iii. Guidance values may be based on different levels of acceptable risk. In most instances, the values are based on cancer risk (for known carcinogens ?) of 1E-06 or a hazard quotient (HQ) of 1.0 for non-carcinogenic pollutants. However, some jurisdictions use higher levels of risk for known carcinogens (e.g. 1E07) or lower levels (1E -05) suspected carcinogens. Some jurisdictions also use alternative HQ values of 0.5, 0.2 or 0.1. These differences could yield an order of magnitude difference in computed guidance values.

iv. Guidance values are often "rationalized" after they are computed. States use varying numbers of significant figures for this, and the results can be numbers that vary in the second or third digit.

v. Some guidance values are inherited from elsewhere in a state's legislative or regulative history. These values may be inconsistent with the methods used to generate most of the state's other guidance values.

Table 9. Soil Contaminants with Infeasible Surface Soil Guidance Values (mg/kg)

CAS No.	Compound	Residential * or C/I Guidance Value in mg/kg (State)
107-21-1	Ethylene glycol	2,040,000 (VA,VT); 2,000,000 (TX); 1,000,000(WV); 7,000,000 (WA)
107-98-2	Propylene glycol monomethyl ether	1,400,000(TX); 1,000,000 (WV); 2,500,000 (WA)
108-05-4	Vinyl acetate	1,020,000 (VA,VT) ; 1,000,000 (WV); 3,500,000 (WA)
108-38-3	m-Xylene	1,000,000 (WV); 7,000,000 (WA)
108-94-1	Cyclohexanone	5,110,000 (VA,VT); 1,000,000 (WV); 18,000,000 (WA)
108-95-2	Phenol	1,000,000 (WV); 2,100,000 (WA)
110-91-8	Morpholine	140,000,000 (TX)*; 1,000,000,000 (TX)
111-46-6	Diethylene glycol	2,000,000(TX); 7,000,000 (WA)
111-90-0	Diethylene glycol, monoethyl ether	1,000,000 (WV); 7,000,000 (WA)
120-12-7	Anthracene	1,100,000 (WA)
123-33-1	Maleic hydrazide	1,000,000 (WV); 1,800,000 (WA)
131-11-3	Dimethyl phthalate	1,000,000 (WV,IN,VA); 1,000,000 (IN)*; 3,500,000 (WA)
141-78-6	Ethyl acetate	1,000,000 (WV); 3,200,000 (WA)
39148-24-8	Fosetyl-al	1,000,000 (WV); 11,000,000 (WA)
52125-53-8	Propylene glycol monoethyl ether	2,500,000 (WA); 1,000,000 (WV)
57-55-6	Propylene glycol	3100000 (TX)*; 1,560,000 (MS)*; 1,000,000 (AZ,WV)* 1,600,000 (WA)*; 20,000,000 (TX); 1,000,000 (WV); 70,000,000 (WA)
65-85-0	Benzoic acid	14,000,000(WA); 4,100,000 (TX); 4,090,000 (VA,VT); 1,000,000 (IN, WV)
76-13-1	1,1,2-Trichloro-1,2,2-trifluoroethane	2,350,000(VA)*; 30,700,000 (VA); 2,350,000 (VT)* 30,700,000(VT); 1,000,000 (WV)*; 1,000,000 (WV); 2,400,000(WA)*; 110,000,000 (WA)
78-93-3	Methyl ethyl ketone	1,000,000 (WV); 2,100,000 (WA)
79-10-7	Acrylic acid	1,800,000 (WA); 1,000,000 (WV,TX)
79-20-9	Methyl acetate	1,020,000 (VA,VT); 1,000,000 (WV); 3,500,000 (WA)
80-62-6	Methyl methacrylate	4,900,000 (WA); 1,439,000 (VA,VT)
84-66-2	Diethyl phthalate	1,000,000 (WV); 2,800,000 (WA)
84-72-0	Ethylphthalyl ethyl glycolate	1,000,000 (WV); 11,000,000 (WA)
95-47-6	o-Xylene	1,000,000 (WV); 7,000,000 (WA)
95-70-5	Toluene-2,5-diamine	1,000,000 (WV); 2,100,000 (WA)
10102-44-0	Nitrogen dioxide	1,000,000 (WV)
7647-01-0	Hydrogen Chloride	2,980,000 (WI)*
7664-38-2	Phosphoric Acid	1,490,000 (WI)*

Table 9 continued

CAS No.	Compound	Residential * or C/I Guidance Value in mg/kg (State)
7664-41-7	Ammonia	14,900,000 (WI)*
16065-83-1	Chromium III	1,530,000 (VT, VA); 1,000,000 (IN, WV); 5,300,000 (WA)
7429-90-5	Aluminum	1,000,000 (TX, WV)
7439-95-4	Magnesium	1,000,000 (MI)*
7440-24-6	Strontium	2,100,000 (WA); 1,000,000 (WV)
7440-31-5	Tin	2,100,000 (WA); 1,000,000 (WV)
7440-32-6	Titanium	38,000,000 (TX)*; 240,000,000 (TX)
7440-66-6	Zinc	1,100,000 (WA)
7723-14-0	Phosphorus (Total)	1,000,000 (MI)*

It is easy to envision these considerations impacting a few numbers at the extremes of a guidance value number distribution. It is much more difficult to see how these differences can impact so many of the guidance values across the heart of the distribution. There are examples where literally no two states agree on the magnitude of a contaminant's guidance value.

The analysis presented here has concentrated on residential soil guidance values. S^3GVD also contains commercial and industrial site guidance values. The total number of contaminants covered is less than those for residential (or generic, unrestricted) site classifications, and the number of values per CAS designations is lower (not all states provide guidance for alternative site designations), but values specifically designated for commercial or industrial sites may be found for 809 distinct CAS numbers. On average, these are a factor of 20 times higher than the corresponding residential value. This is expected since the values are generally calculated from less conservative exposure scenarios (e.g. fewer hours per day and days per year) and for adults with larger body mass. Beyond this, the guidance value distributions for each CAS number appear to be similar to those for residential guidance values. If anything, there is a bit more agreement among the commercial and industrial values because there are less per chemical and because they more often approach the feasibility upper bound.

4. CONCLUSIONS

There is a great deal of variability in the states' surface soil contamination guidance values currently being applied. This variability leads to several questions, including questions (see Question #4) about the adequacy of current risk assessment methodology.

4.1 Question #1 – Comparability ?

Variability is observed by comparing guidance values taken from many sources and developed by several alternative methods applied over several years. Is this appropriate? The answer is yes. Although guidance values are developed by different methods, using different strategies, exposure scenarios and coefficient data, they were all developed for the same purpose. They were developed to identify levels of soil contamination that are high enough to be of health

concern, or high enough to prompt additional ecosystem assessment. It is the results of the methods that are applied (the actual guidance value mass burdens) that are comparable. This is not like comparing apples to oranges. This is like comparing the cost of apples to the cost of oranges (or taste or color or…) which are valid comparison criteria used daily by shoppers across the nation.

4.2 Question #2 – Feasibility ?

Some regulatory jurisdictions have promulgated guidance values that are not physically possible. Is this appropriate? The answer is no. No regulatory guidance value greater than 1,000,000 mg/kg is physically possible and it is very difficult for mass burdens to approach this value. Organic liquids may exist in pure form which, given a density greater than water, might yield a concentration above 1,000,000 mg/l. However, for these to become a soil contaminant, they must be mixed with soil, and in soil their mass burden would be limited by the soils porosity (often <0.4). This is a question because at least 11 jurisdictions (AZ, GA, IN, MI, MS, TX, VA, VT, WA, WI, and WV) publish guidance values that exceed the 1,000,000 mg/kg.

When a contaminant's guidance value exceeds 1,000,000 mg/kg, it is not possible for a single component risk analysis to yield an unacceptable result. For example, when hazard quotient (HQ) analysis is applied to contaminant "i", the calculation must yield a value less than 1.0 since the measured mass burden (Ci) cannot exceed the guidance value (Csi).

$$HQ_i = \frac{C_i}{C_{Si}} < (?)1.0 \qquad (1)$$

Unfortunately, at many sites, humans and ecosystems experience multiple contaminants and risk analysis must consider cumulative impacts. In index (HI) analysis, this is done by summing HQi exposures across the set of contaminants likely to inflict similar organism or ecosystem damage.

$$HI = \sum_{i=1}^{I} \frac{C_i}{C_{Si}} < (?)1.0 \qquad (2)$$

Guidance values in excess of 1,000,000 mg/kg make it nearly impossible for contaminants to impact cumulative risk assessments. Even in the presence of other contaminants, they cannot significantly contribute to the HI result. If this is not the desired effect, the values should be lowered. Many states cap guidance values at 100,000 mg/kg. If this is the desired impact, then the "contaminant" should be dropped from regulation. When there is no way for a chemical to exceed the allowable maximum value, there is no need for the guidance value and no need for chemical analysis to quantify the site mass burden. The chemical should join the huge number of unregulated chemicals.

4.3 Question # 3 - Appropriate Value Set Size ?

Some jurisdictions provide guidance on hundreds of contaminants. Others do not. Is there a "correct" number of chemicals that should be regulated? The answer is unclear. There is probably a set of soil contaminants that should be regulated and jurisdictions should provide guidance values for all of the contaminants of this set. The size of this set is debatable, but it should probably include the 200 of the most common pollutants (the average state currently contains guidance on 291 contaminants). Some jurisdictions go far beyond this. Although promulgation of hundreds of additional guidance values may appear to be admirable human health and/or environmental vigilance, this can also have less desirable implications. One must wonder about how often these less common contaminants are encountered and how often their guidance is applied. If they are rarely encountered, is it cost-effective to require their analysis? If analysis is not mandated, how does a jurisdiction know that its guidance is being followed?

4.4 Question #4 – Risk-Assessment Implications of Guidance Value Variability?

There is a high degree of variability in the guidance values applied to surface soil contamination. This is the soil that humans come into contact with most frequently, and it is children who experience the critical exposure. We are unable to explain why there is so much disagreement about regulatory guidance values, but would offer the following observations.

(i) The differences between guidance values cannot be attributed to disagreements about acceptable risk levels, risk models, or coefficient values. The magnitudes of differences are far too great for this.

(ii) The differences between guidance values imply questions about economic equity and environmental justice. How can it be acceptable to expose children to a concentration of 10,000 mg/kg in one jurisdiction if it is unacceptable to expose them to more than 1 mg/kg in an adjacent jurisdiction? How can it be equitable to require analysis for hundreds of compounds and remediation to low mass burden levels in one jurisdiction if the same compounds are unregulated elsewhere?

(iii) The differences imply questions about the reliability of current risk assessment practices. Jurisdictions using the same levels of risk compute vastly different guidance values.

With this much uncertainty in the analysis process, it is difficult to see how risk-based guidance can be adequately protective of human health and the environment.

Jennings (2005) discussed one method of mitigating these problems. There are few examples of strong national leadership on acceptable levels of surface soil contamination, but there is one. In 2001, the U.S. EPA established "national standard" guidance of 400 mg/kg for Pb in residential surface soil (USEPA, 2001). There are limitations on the application of this value, but its existence has done a great deal to reduce the variability of Pb regulatory guidance. All of the residential soil Pb guidance values fall within 2 orders of magnitude and, with the exception of two low values (2 mg/kg in OR, 16.5 mg/kg in WV), are within one order of magnitude. At

least 35 jurisdictions share 400 mg/kg as their residential Pb value. This suggests that, if the USEPA would provide stronger leadership on the number of contaminants for which guidance should be provided, and on appropriate mass burdens for these contaminants, states would have more incentive and justification for tightening the bounds about regulatory guidance variability.

5. ACKNOWLEDGMENT

This research was conducted with the support of National Science Foundation Grants CMS 99-01108 and CBTE-0650675. The authors also wish to acknowledge the contributions of Dr. Jun Ma and Mr. Elijah Petersen in helping to identify, acquire, and analyze soil guidance values.

6. REFERENCES

ACS (American Chemical Society), (2005), CAS Registry, http://webbook.nist.gov/chemistry/cas-ser.html, [2/1/06].

Chemexper, (2006), ChemExper Chemical Directory, http://www.chemexper.com/, [2/1/06].

Hanna, A. (2007), Frequency and Variability of Regulatory Guidance for Surface Soil Contamination, Thesis, Department of Civil Engineering, Case Western Reserve University, Cleveland, OH.

Jennings, A.A and Ma, J, (2007), Variation in North American Regulatory Guidance for Heavy Metal Surface Soil Contamination at Commercial and Industrial Sites. Journal of Environmental Engineering and Science, (in press).

Jennings, A.A, (2005), The Need to Rationalize North American Regulatory Guidance for Soil Contamination, Journal of Residuals Science & Technology, 2(4).

Jennings, A.A. and Petersen, E.J, (2006), Variability of North American Regulatory Guidance for Heavy Metal Contamination of Residential Soil. Journal of Environmental Engineering and Science, 5(6), 485-508.

Jennings, A.A., Cox, A.N., Hise, S.J. and Petersen, E.J., (2002), Heavy Metal Contamination in the Brownfield Soils of Cleveland, Soil and Sediment Contamination, 11(5): 719-750.

Jennings A.A. and Hanna, A., (2007), Database Analysis of U.S. State Regulatory Guidance for Organic Surface Soil Contamination, International Journal of Environment and Waste Management, (submission in review).

NCBI (National Center for Biotechnology Information), (2006), Pubchem, http://pubchem.ncbi.nlm.nih.gov/.

NIST (National Institute of Standards and Technology), (2007), httl://webbook.nist.gov/chemicsty/cas-cer.html, [6/25/07].

OEPA (Ohio Environmental Protection Agency), (1999), Closure Plan Review Guidance for RCRA Facilities – March 1999, http://www.epa.state.oh.us/dhwm/cprg.html, [6/20/03].

OEPA (Ohio Environmental Protection Agency), (2002), 3745-300-08 Generic Numerical Standards http://www.epa.state.oh.us/derr/vap/docs/rule-8.pdf, [3/31/07].

USEPA (U.S. Environmental Protection Agency), (2001), 40CFR Part 745. Lead: identification of Dangerous Levels of Lead; Final Rule. ***Federal Resister,*** Jan 5, 2001.

USEPA (U.S. Environmental Protection Agency) (2006) Substance Registry System. http://aspub.epa.gpv/srs/srs_proc_qry_search_sort, [7/27/07].

Chapter 9

FISHERVILLE MILL – A CASE STUDY – COST EFFECTIVE REMEDIATION THROUGH COLLABORATION

Paul Ollila[1§], Jim Soukup[2], Dean Brammer[2], Bette Nowack[2], Eugene Bernat[3], Eric Hultstrom[4], Janis Tsang[5]

[1]MassDEP, 627 Main Street, Worcester, MA 01608 [2]Weston Solutions, Inc., 1 Wall Street, Manchester, NH 03101, [3]Fisherville Redevelopment Corporation, 95 State Street, Suite 812, Springfield, MA 01103 [4]Woodard & Curran, Inc., 980 Washington Street, Dedham, MA 02026, [5]USEPA, Region I, One Congress Street, Suite 1100, Boston, MA 02114

ABSTRACT

The Fisherville Mill site is located on the Blackstone River in Grafton, MA. Soil and groundwater are contaminated with chlorinated VOCs and petroleum. The mill and a groundwater recovery system designed to prevent VOCs from migrating to a public water supply well (Well # 3) located approximately 1000 feet southwest of the site were destroyed by fire in August 1999. In November 2000, TCE was detected in Well #3. After notification, site investigation efforts focused on evaluating potential migration pathways to Well #3.

Based on site investigation results, the USEPA installed a temporary dam to alter groundwater flow directions and reduce risk to Well # 3. In Situ Chemical Oxidation (ISCO) using sodium permanganate was selected to decrease TCE concentrations in the source area and provide long-term protection for Well # 3.

Fisherville Redevelopment Company (FRC) took ownership of the site in 2004. A collaborative approach and strategy was developed between FRC, MassDEP and the Town of Grafton that would encourage significant remedial actions while environmental assessment and engineering activities were ongoing. Work completed includes installation of a # 6 oil interception and collection infrastructure, and encapsulation of asbestos impacted debris and lead contaminated soil in flowable fill.

Keywords: Fisherville, Grafton, trichloroethene, permanganate, flowable fill, Brownfields

§ Corresponding Author: Paul Ollila, MassDEP, 627 Main Street, Worcester, MA 01608, E-mail: Paul.Ollila@state.ma.us

1. INTRODUCTION

The Fisherville Mill Site is located between the Blackstone River and Blackstone Canal in the southern part of Grafton, Massachusetts (Figure 1). The original mill produced textiles from 1831 to the late 1870s, was destroyed by fire, and replaced by a much larger mill that produced cotton goods until 1949. From 1949 to 1986, the mill was used for manufacture of tool and die parts, machine tool stamps, lawn furniture, and foam rubber and fabrics for car seats. The mill was destroyed by fire in 1999 shortly after ownership passed from the Town of Grafton to the

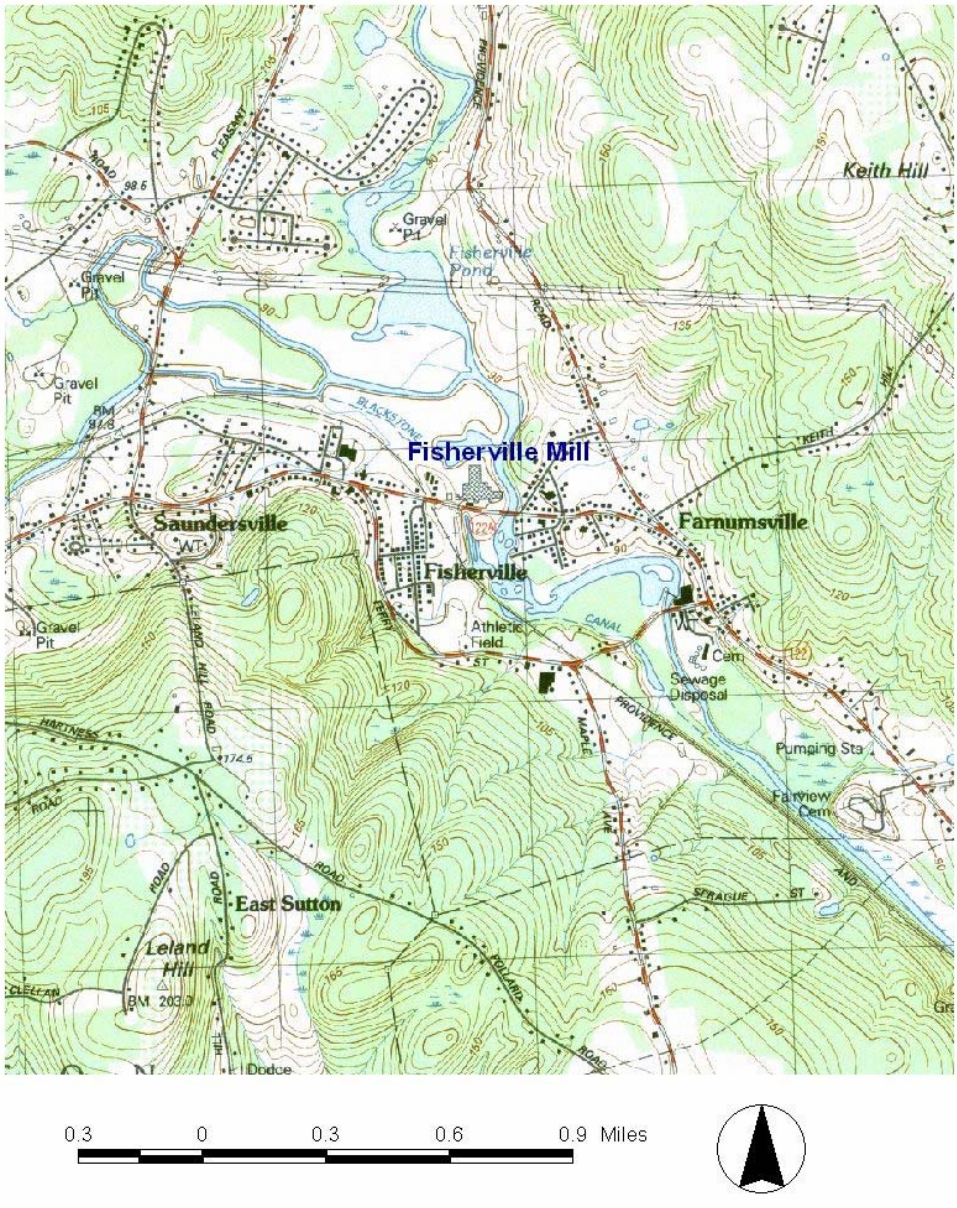

Figure 1. Site location map. Base map is a portion of the USGS 7.5 x 15' Milford, MA quadrangle.

Central Massachusetts Economic Development Authority (CMEDA). Main Street (Route 122A) divides the site into two roughly equal areas (Figure 2). The mill occupied the area north of Main Street. The area south of Main Street (the "peninsula") is undeveloped and is bounded by the Blackstone River on the east and the Blackstone Canal on the west and south.

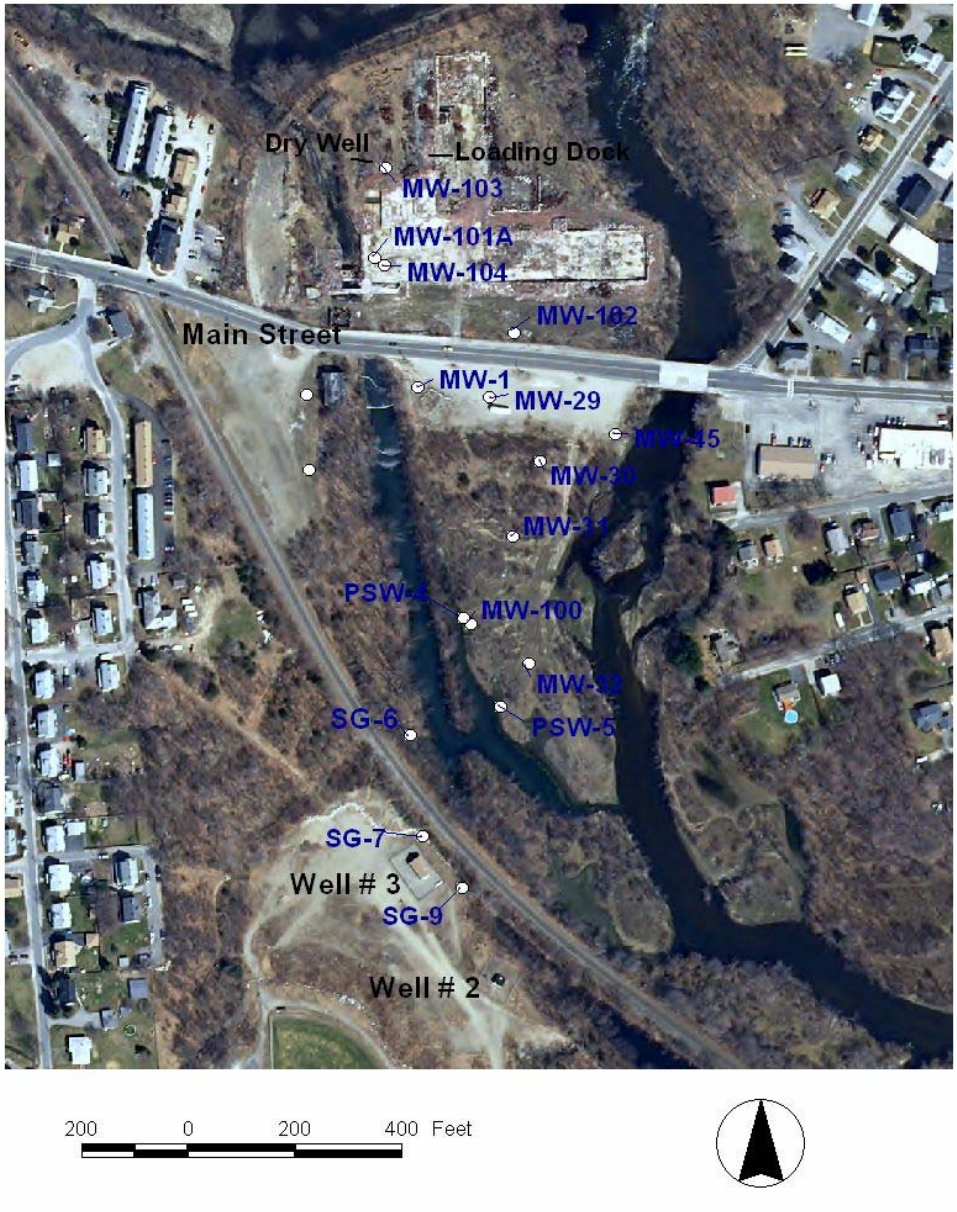

Figure 2. Orthophoto showing the former mill, the peninsula and monitoring well locations.

Major environmental problems include No. 6 oil in soils, sediment and surface water, and chlorinated volatile organic compounds (CVOCs) in soil and groundwater. The mill owners began capturing oil in the canal in the early 1970's and removed two 20,000-gallon underground storage tanks in 1987. Oil-saturated soils in the subsurface are a continuing source of oil in the

canal. CVOCs were first reported in 1986 and threatened a public water supply well located approximately 1200 feet south (Well # 2) of the Site. MassDEP installed a groundwater recovery system in 1996, at the same time that the South Grafton Water District (SGWD) installed a second water supply well (Well # 3) approximately 1000 feet south of the site. The SGWD only used Well # 3 in the late summer and fall after the fire destroyed the groundwater recovery system. MassDEP requested assistance from the EPA after receiving notification from the SGWD that TCE had been detected in a sample collected from Well #3 in November 2000, 15 months after the fire.

Work conducted prior to the 1999 fire is summarized in Handex (1997) and included deployment of absorbent booms in the Blackstone Canal, excavation of petroleum contaminated soils, removal of two 20,000-gallon underground storage tanks, and installation of a groundwater recovery system. MassDEP maintained absorbent booms in the canal from 1990 to 2004, conducted numerous site investigations to evaluate the extent of oil and CVOC contamination, and operated the groundwater recovery system between 1996 and 1999. The U.S. Environmental Protection Agency, Region 1, Emergency Planning and Response Branch (EPA), CMEDA, and MassDEP cleaned up most of the asbestos-contaminated debris after the fire and the EPA removed lead-contaminated ash from the former building foundation. However, the fire at the mill had significantly complicated cleanup efforts, primarily with respect to two aspects of site cleanup. The fire dispersed asbestos fibers throughout the property commingling asbestos with other debris and destruction of the MassDEP groundwater recovery system allowed CVOCs to migrate from the source area toward the SGWD wells.

The EPA Superfund Innovative Technology Evaluation (SITE) program and CMEDA conducted a pilot project for enhanced bioremediation of CVOCs from 2000 to 2002. After trichloroethene was detected in SGWD Well #3 in November 2000, the EPA, SGWD, and MassDEP evaluated potential migration pathways between the site and the SGWD well. Based on these investigations, the EPA installed a temporary dam between the Blackstone Canal and Blackstone River in 2002, and began chemically oxidizing CVOCs under the former mill in June 2003.

Fisherville Redevelopment Corporation (FRC) took ownership of the site in 2004 and is preparing the site for redevelopment while continuing the cleanup. To date, FRC has encapsulated asbestos contaminated soils with flowable fill, installed an oil recovery system and begun installation of a soil vapor extraction system designed to address shallow CVOC contamination. FRC efforts also involved public relations, community outreach, and public planning for this project.

The first part of this paper describes site investigation efforts after the 1999 fire. The second part describes risk reduction measures implemented to minimize risk to SGWD Well #3. The third part discusses cleanup and redevelopment issues after FRC took ownership of the site.

2. SITE INVESTIGATION

2.1 Methods

Site investigation activities conducted after the 1999 fire include advancement of borings and installation of monitoring wells using hollow stem augur, drive and wash, and direct push techniques. Borings for bedrock monitoring wells were advanced with an air hammer and wells were completed as standard two-inch monitoring wells. Direct push techniques were used to collect groundwater samples at five-foot vertical intervals in the former mill and on the western side of the peninsula. Piezometers installed in the Blackstone River and Canal consisted of 1.25-inch diameter clear plastic tubes installed such that the bottom end of the tube was 1-2 feet below the sediment surface and the upper end was above the water surface.

Soil samples were collected using split-spoon samplers or direct-push techniques. Soils were screened in the field for VOCs using the jar-headspace method. Soil samples collected for VOC analysis were preserved in methanol and analyzed using EPA Region I's Standard Operating Procedure for Head Space Screening for Volatile Organic Compounds (USEPA, 1998) and/or EPA Method 8260b.

Groundwater samples were collected with bailers, submersible centrifugal and bladder pumps, peristaltic pumps, and inertial pumps. Polyethylene diffusion bag samplers (ITRC, 2004) were deployed in selected monitoring wells. Peristaltic and inertial pumps primarily were used during vertical profiling. Results for samples collected using conventional three-volume purge and low-flow (EPA, 1996) techniques were similar and sampling method did not appear to cause bias in long-term monitoring results. Results from polyethylene diffusion bag samplers agreed with pumped sample results in some cases. In other cases, particularly in a bedrock monitoring well, vertical concentration gradients made placement of the sampler critical to achieving good agreement between sampling methods. Groundwater and surface water samples were analyzed for VOCS in mobile laboratories using headspace techniques (Pine & Swallow, 2000a; USEPA, 1998) and/or in fixed laboratories via EPA Method 624 or 8260b.

Passive vapor diffusion samplers (PVDS) were constructed and deployed following methods described by Church et al. (2002). Air samples from the VOA vials were analyzed in the field with a portable gas chromatograph (Pine & Swallow, 2000b).

Pumping tests were conducted by pumping SGWD Well #3 at a rate of 450 gallons per minute. Eight pressure transducer data loggers (In-Situ Troll or Mini-Troll) were installed and collected water level/pressure and temperature measurements every 15 minutes for ten days prior to an initial 4-hour pumping test. Ten additional data loggers were installed one month prior to 4 hour per day and 8 hour per day, 5-day pumping tests. Data was collected at 2-minute intervals during the 5-day pumping tests.

2.2 Hydrogeology

Fill and alluvial deposits overlie a discontinuous peat layer, approximately 30-60 feet of stratified sand and gravel, and 0-17 feet of dense sand, silt and cobbles (till) over bedrock (Figure 3). Hydraulic conductivity estimates for the sand and gravel aquifer near the SGWD wells exceed 400 ft/day. Till overlies bedrock on hills located on either side of the Blackstone River Valley and granitic gneiss is exposed on the east bank of the Blackstone River near the Fisherville Dam. Based on boring and seismic refraction data, the center of a bedrock depression is located under the peninsula (HMM, 1993). Depth to bedrock exceeds 60 feet in this area. Fill materials consist of sand and gravel, peat, and minor amounts of brick and other debris. Fill may be as much as 25 feet thick near the Blackstone Canal in the former mill area.

Prior to 1995, groundwater elevations and gradients were strongly influenced by dams located north (Fisherville Dam) and south (Farnumsville Dam) of the site. The Farnumsville Dam was used to generate electricity and releases from the dam caused an approximate 2-foot daily change in surface and groundwater levels on the peninsula. The USGS (1995) documented that fluctuations in groundwater levels were similar to fluctuations in stream stage (Figure 4). The Farnumsville Dam has not been used to generate power since 1995 and has deteriorated over

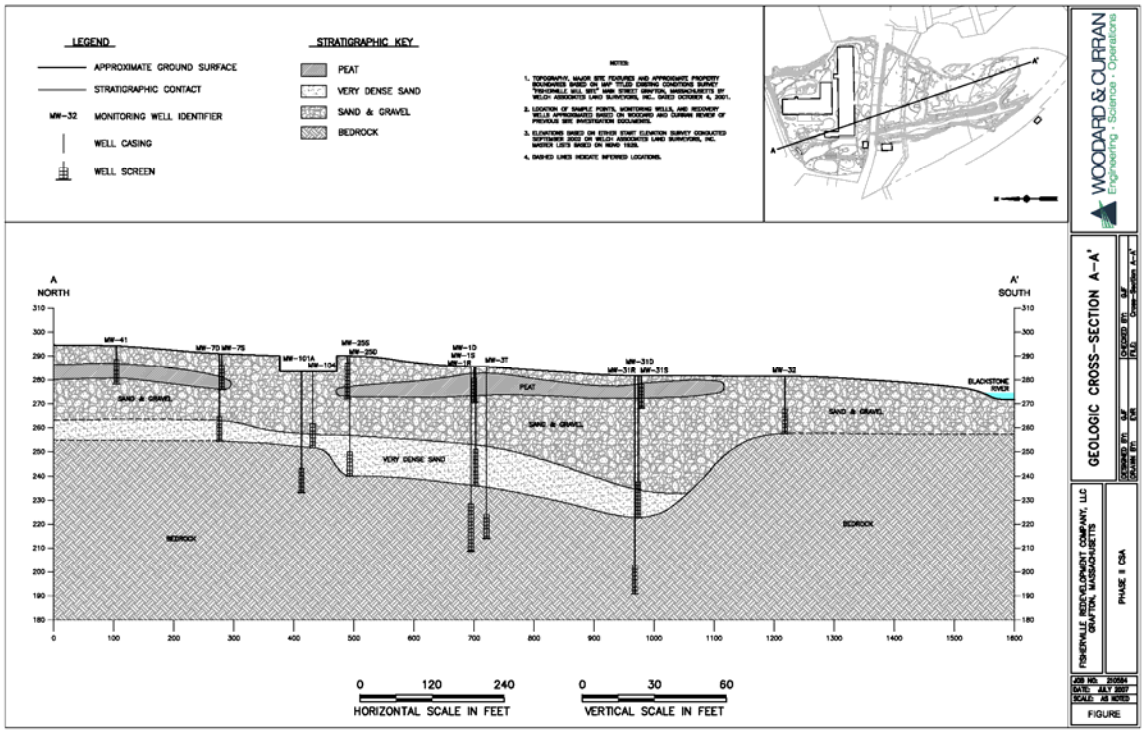

Figure 3. Geologic cross section from Fisherville Pond to the southern end of the peninsula.

time. Average water levels behind the dam decreased by about 2 feet between 1994 and 1996 and average horizontal groundwater gradients under the peninsula are probably slightly steeper than in the past because of the deterioration of the Farnumsville Dam and intermittent pumping of SGWD Well #3.

The Fisherville Dam created the impoundment (Fisherville Pond) that fed the mill canal. In 1995 the dam's spillway gates were welded open and water only flowed through the mill canal during wetter parts of the year. However, debris jams intermittently have restricted flow in the spillway and increased water flow through the canal. Water generally was not present in the mill canal during the summer and fall from 2000 until 2005. During 2006 and 2007 water has been present in the mill part of the canal during most of the summer. South of Main Street (Figure 2), groundwater discharge maintains flow in the canal except under very dry conditions in the late summer and fall. Water elevations in the canal strongly influence groundwater flow directions under the peninsula.

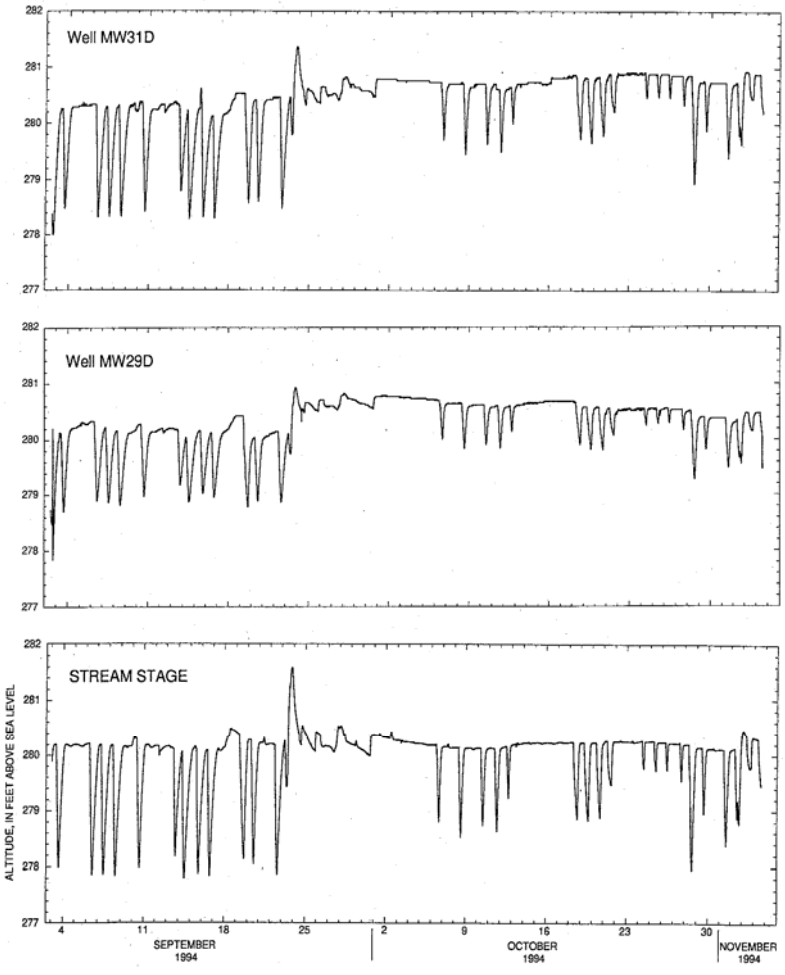

Figure 4. Groundwater and surface water elevations measured in 1994 by the USGS (Desimone and Barlow, 1995).

In order to evaluate potential migration pathways to Well #3, the EPA (Weston, 2002) installed ten overburden and three bedrock monitoring wells, and installed eighteen pressure transducer data loggers in new and existing monitoring wells and surface water gauges. Three overburden (SG-7S, SG-9S, SG-9D) and two bedrock wells (SG-7R, SG-9R) were installed near SGWD Well #3, three overburden wells (MW-100S,M,D) were installed near PSW-4, and three overburden wells (MW-102, 103, and 104) and one bedrock well (MW-101A) were installed in or near the former mill (Figure 2). These wells supplemented an existing network of monitoring wells.

Figure 5 is a potentiometric contour map based on July 2001 gauging data for deep overburden monitoring wells. On July 16, 2001, deep groundwater was flowing under the canal towards the Blackstone River. Based on gauging data from monitoring wells near the canal, and piezometers and surface water gauges installed in the canal, shallow to intermediate depth groundwater was discharging to the canal. This is not the case during dry parts of the year when Well #3 is in use.

Figure 5. Potentiometric contours (277.6 and 277.4 feet) based on water elevations measured in deep overburden monitoring wells on July 16, 2001.

Water levels in piezometers installed in the Blackstone River and Canal in the summer and fall of 2000 indicated that the Blackstone River was neutral or losing near Main Street and became a gaining stream as it dropped in elevation south of Main Street. The canal was gaining except when SGWD Well #3 was pumping. Upward gradients decreased and eventually reversed under parts of the canal when Well #3 was in use.

Monitoring well gauging data also indicated relatively steep downward gradients in the former mill area. Recent investigation in the mill area identified perched water under the former mill and apparent downward gradients may be artifacts of subsurface structures and the nature of the fill material.

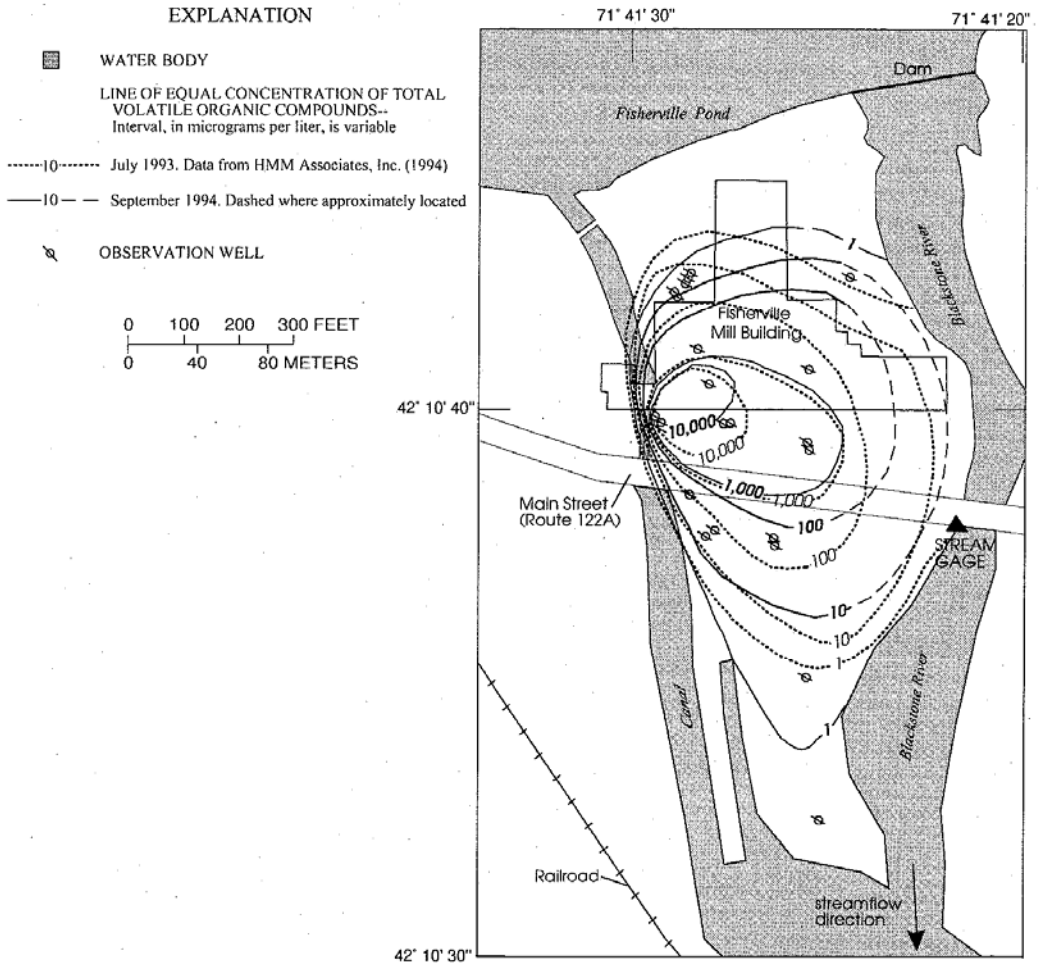

Figure 6. Total VOCs (ug/l) measured in groundwater samples collected in July 1993 (HMM, 1994) and in September 1994 (Desimone and Barlow, 1995).

2.2.1 Contaminant Distribution

Probably the best indicator of the change of hydrologic conditions between 1994 and 2000 is the change in contaminant distribution patterns. Figure 6 shows total VOC concentrations in 1993 and 1994. VOCs were either not detected or at very low concentrations in wells located on the southern part of the peninsula. Figure 7 shows the changes in TCE concentrations in selected peninsula monitoring wells after the fire. TCE is the principal VOC in all the selected wells. After the fire, TCE concentrations first increased in MW-1D followed by MW-31R, MW-1R, MW-31D, MW-31S, and MW-32D. In the fall of 2000, VOC concentrations in peninsula monitoring wells were higher and VOC contamination extended further south than in 1993 and 1994.

MassDEP conducted a passive vapor diffusion sampler (PVDS) study in June 2000 in order to provide more information about the fate of the VOC plume on the peninsula (Figure 8). TCE contaminated water was discharging to the Blackstone River and Canal but VOCs were not detected in samplers located near the southern end of the peninsula. CVOC concentrations in surface water samples collected from the canal near the former mill have been as high as 574 ug/l. CVOCs have not been detected in surface water samples collected from the Blackstone River.

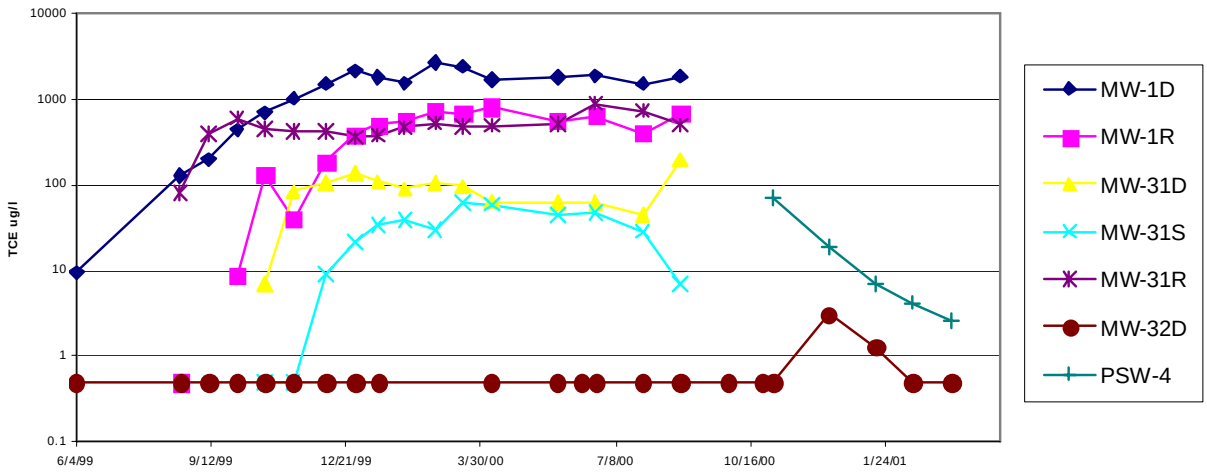

Figure 7. VOC concentrations measured in groundwater samples after the August 1999 fire.

Figure 8. TCE concentrations measured in passive vapor diffusion samplers (ppbv) in June 2000.

MassDEP (Pine & Swallow, 2000) advanced 17 one-inch microwells at the site in October 2000 in order to further evaluate groundwater contamination in the presumed source area and to evaluate the vertical distribution of VOCs under the peninsula near the locations where the PVDS indicated contaminated groundwater was discharging to the canal. The presumed sources of contamination at the site are a dry well located north of the former boiler room and a loading dock area to the east of the former drywell (Figure 2). Shallow groundwater samples collected during vertical profiling near the dry well contained high concentrations of cis-1,2-dichlorothene and relatively low concentrations of TCE. High TCE concentrations (>1000 ug/l) were limited to the deep aquifer in an area south of the former dry well and loading dock and under the western end of the former mill with the highest concentrations (>50,000 ug/l) limited to the area near the western end of the former mill.

Figure 9 shows TCE concentrations measured in groundwater samples collected at five-foot vertical increments on the western side of the peninsula near (PSW-4) and south (PSW-5) of the MW-100 location. CVOCs were present in the upper part of the aquifer, CVOCs were not present at intermediate depths, and concentrations were highest near the bottom of the overburden aquifer.

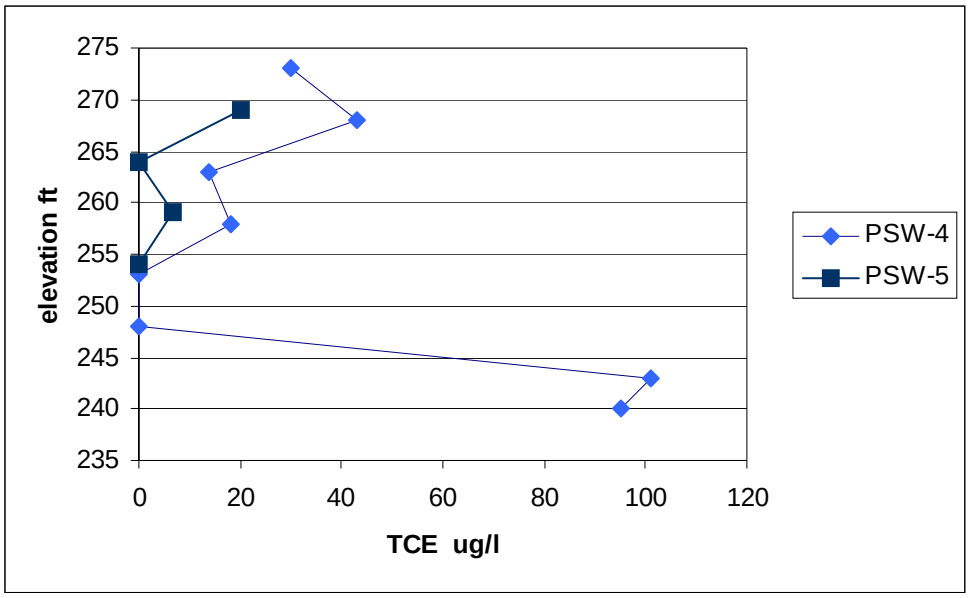

Figure 9. TCE measured in groundwater samples collected at five-foot intervals on the western side of the peninsula at locations PSW-4 (near MW-100) and PSW-5.

SGWD Well #3 is screened at the base of the sand and gravel aquifer from 37 to 43 feet below grade and has a maximum permitted yield of 450 gallons per minute. In January 2001, the SGWD reported that 0.7 ug/l of TCE had been detected in a sample collected from Well #3 in November 2000. The SGWD stopped using Well #3 shortly after the November sample was collected because water levels had recovered at a well (Well #1) located in another part of the town. Interpretation of the November sampling results for Well #3 was difficult because TCE was not detected in a sample collected from monitoring well SG-7 that is located between Well #3 and the Fisherville Mill Site. After the SGWD stopped using Well #3 and after water levels increased, TCE concentrations in PSW-4 decreased compared to concentrations measured in November 2000 (Figure 7).

2.2.2 Pumping Tests

The SGWD, EPA and MassDEP jointly conducted pumping tests in July 2001. The SGWD pumped Well #3 at a rate of 450 gallons per minute for 4 hours per day from July 16 to July 20, 2001, and 8 hours per day from July 23 to July 27, 2001. Figures 10 and 11 show water levels in monitoring wells on the west and east sides of the canal respectively. Pumping had little, if any,

effect on water levels on the eastern side of the canal (Figure 11). Daily oscillations in water levels in wells located on the eastern side of the canal and in MW-9R, a bedrock well located on the western side of the canal, are related to water level changes in the Blackstone River. Drawdown during the eight hour pumping test briefly created an upward vertical gradient from bedrock into the overburden aquifer near Well #3, but did not induce infiltration of surface water near SG-6 (Figures 2 and 10). However, extrapolation of trends observed during the pumping tests indicated that continued pumping would induce surface water infiltration near SG-6.

In October 2001, the SGWD began using Well #3 because of low water levels at Well #1. Well #3 operated for approximately 10 hours each day from October 23 to October 25. A total of 792,000 gallons of water was pumped over the three days. The SGWD gauged wells at the beginning and end of pumping on each day. Figure 12 is based on water elevations measured prior to the pumping test conducted in July 2001. Figure 13 is based on water elevation data collected at the end of pumping on October 25. Sampling results and water level measurements from October 25, 2001 are consistent with deep flow under the canal. TCE was detected in SG-6 but was not detected in DP-4A despite downward gradients between the canal and DP-4A.

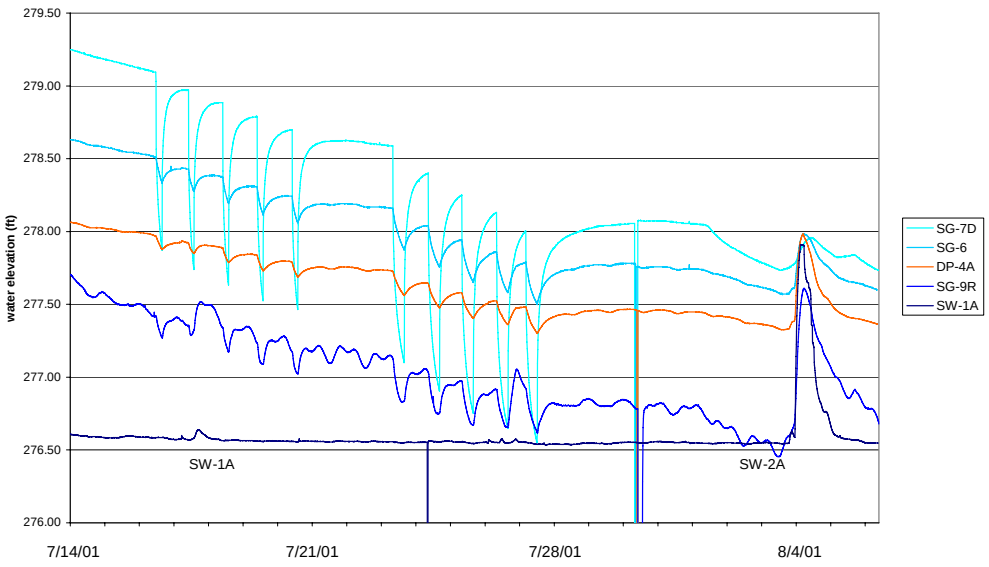

Figure 10. Water elevations measured in monitoring wells located on the western side of the canal.

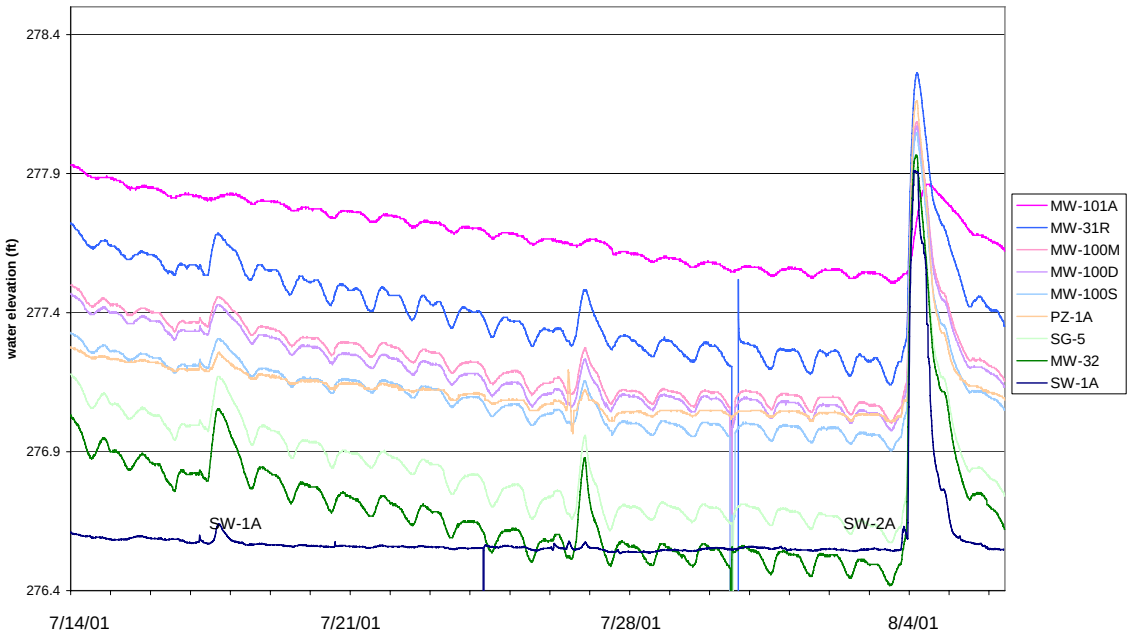

Figure 11. Water elevations measured in monitoring wells located on the eastern side of the canal.

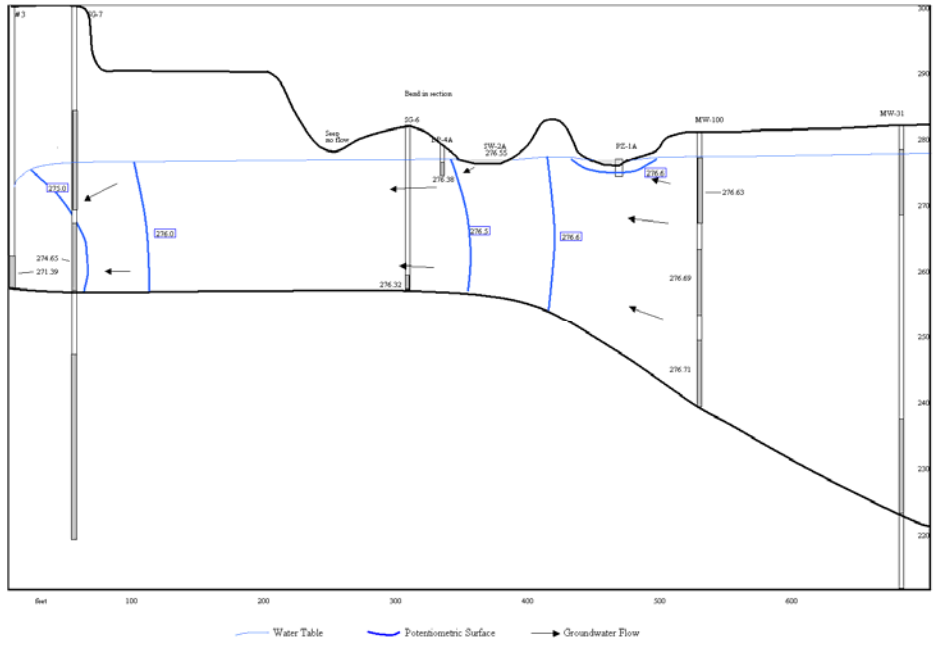

Figure 12. Potentiometric contours between SGWD Well #3 and MW-100S, M and D based on water elevations measured on July 16, 2001.

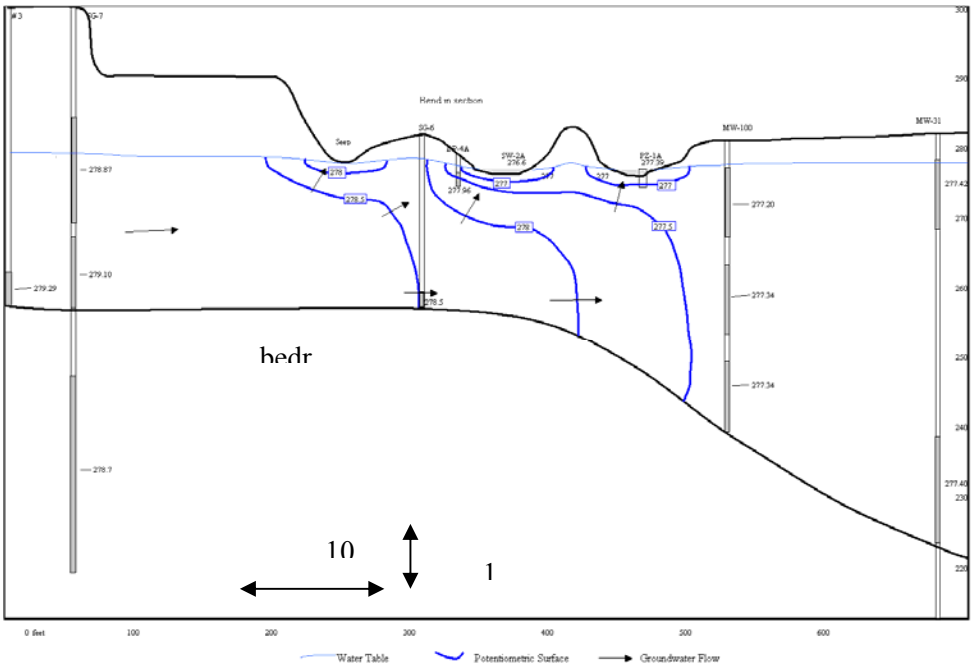

Figure 13. Potentiometric contours between SGWD Well #3 and MW-100S, M and D based on water elevations measured on October 25, 2001.

2.2.3 Conceptual Model

Based on the pumping tests, water level measurements, and groundwater sampling data, it appears that TCE migrated from a deep overburden source located under the western end of the former mill to Well #3. The PVDS study (Figure 8), vertical profiling results (Figure 9), surface water and groundwater sampling results, and gauging data (Figure 12) indicate that contaminated water in the shallow overburden aquifer discharges to the canal and that a deeper CVOC (mostly TCE) plume migrates to the south and southeast towards the Blackstone River during the wetter parts of the year. However, during the dry part of the year when Well #3 is in use, the deep plume shifts westward and is drawn under the canal (Figure 13). A bedrock pathway may be possible, but pumping Well #3 had little or no effect on groundwater elevations on the peninsula where bedrock contamination is known to be present and very high TCE concentrations would have to present in bedrock in the area of influence of Well #3 in order to be detected in water produced from Well #3. Based on sampling results for DP-4A it also appears unlikely that CVOCs are migrating towards Well #3 via a shallow pathway. However, it is possible that shallow contaminated groundwater from the eastern side of the canal could migrate underneath DP-4A. It is uncertain why TCE was not detected in a sample collected in November 2000 from SG-7D. However work conducted in the former mill has shown that there are strong preferential pathways in the overburden aquifer.

3. RISK REDUCTION

In June 2000, the EPA SITE program and CMEDA initiated a pilot study evaluating use of Hydrogen Release Compound (HRC®, Regenesis, 2004) to treat the CVOC plume. Monitoring well MW- 1D is located immediately upgradient of the HRC® injection area and sampling results (Figure 14) are typical of results from the treatment zone. After trichloroethene was detected in SGWD Well #3 in November 2000, the EPA and MassDEP determined that reduction in contaminant mass within the Fisherville Mill source area was needed to reduce TCE concentrations in groundwater on the peninsula to levels that would no longer represent a threat to the well field. Because high concentrations of cis-1,2-dichloroethene were still present more than one year after injection of the HRC®, MassDEP, EPA, and SGWD concluded that other risk reduction measures would be required to minimize risk to Well #3.

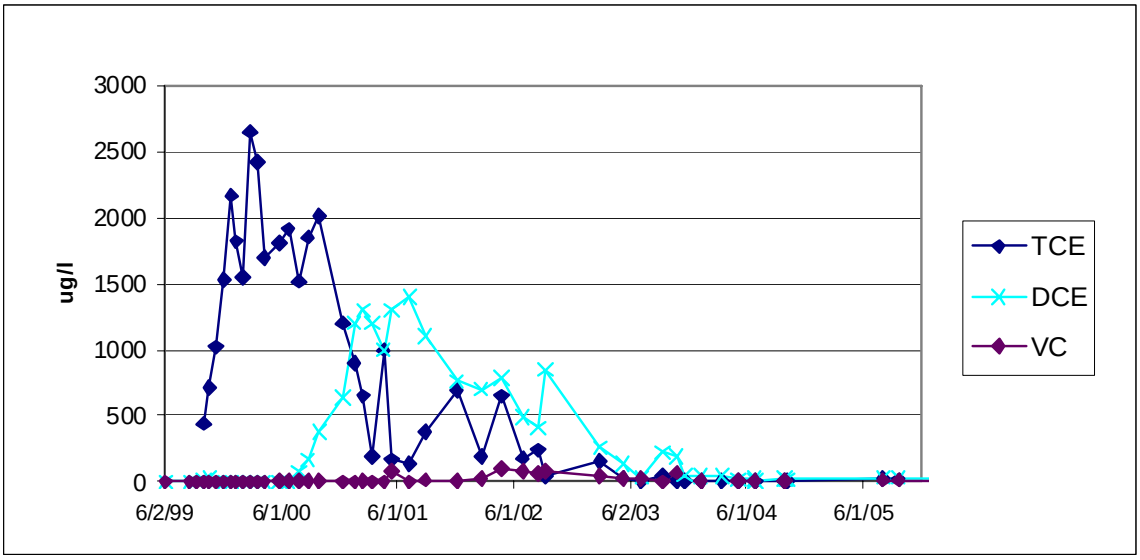

Figure 14. Trichloroethene (TCE), cis-1,2-dichloroethene (DCE) and vinyl chloride (VC) concentrations measured in groundwater samples from monitoring well MW-1D.

Based on TCE concentrations, the project team concluded that residual DNAPL in the deep overburden and shallow bedrock under the western end of the former mill was the most likely source of groundwater contamination threatening SGWD Well #3. Calculations by the project team suggested that a reduction of dissolved TCE concentrations in source area groundwater by two orders of magnitude would reduce down-gradient concentrations to the point that the SGWD well field would no longer be threatened.

After evaluating several remedial options including enhanced in-situ bioremediation, groundwater extraction and treatment, and point of withdrawal treatment, In-Situ Chemical Oxidation (ISCO) was selected by the project team as the preferred alternative. ISCO treatment would destroy contaminant mass in the source area resulting in eventual decreases in the size and contaminant concentrations of the downgradient plume. However, based on the seepage velocity across the site, it was anticipated that there would be a delay in achieving improvements to downgradient water quality, so a temporary method of protecting the SGWD well field in the

near term was needed. A temporary dam was constructed in the Blackstone Canal to address this concern.

3.1 Temporary Dam

The EPA completed installation of a temporary sand bag dam (Figure 15) near the confluence of the Blackstone River and Canal south of the former Fisherville Mill (Figure 2) on June 28, 2002 and replaced the sand bag dam with a sheet-piling dam (Figure 16) during December 2003. The dam was installed to deflect the CVOC plume away from Well #3. Figure 17 shows potentiometric contours after the dam was installed. Average groundwater elevations, except for the area influenced by the dam, were similar on July 16, 2001 (Figure 5) and July 12, 2002 and comparison of Figures 5 and 17 illustrates the dam's effect on potentiometric gradients in the deep overburden aquifer. After installation of the dam, water elevations in monitoring wells near the canal (MW-1D, MW-100D) increased relative to monitoring wells located in the center of the peninsula (MW-29D, MW-31D, MW-32D). Installation of the dam enhanced flow to the east towards the Blackstone River. During the late summer of 2002, when water elevations in the canal dropped below the crest of the dam, potentiometric gradients were similar to pre-dam conditions. This pattern persisted until water levels increased during late October 2002.

Figure 15. Sand bag dam installed in June 2002.

Figure 16. Sheet-piling dam installed in December 2003.

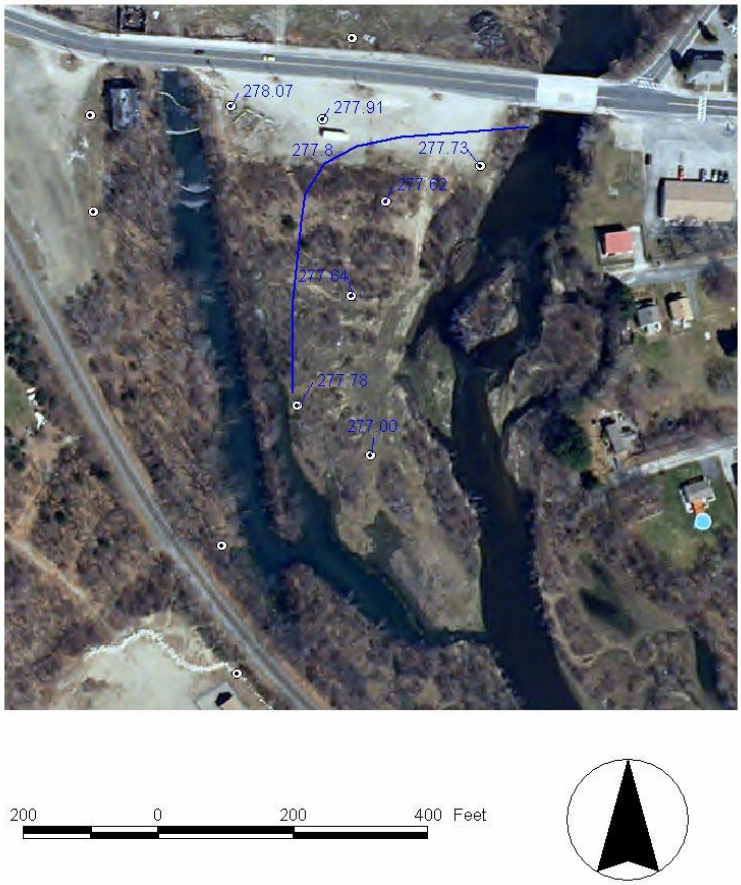

Figure 17. Potentiometric contour (277.8 ft) based on water elevations measured in deep overburden monitoring wells on July 12, 2002.

Gauging data for MW-31D and 100D are summarized in Figure 18. Gauging data for MW-1D and 29D exhibited a similar pattern. After the dam was installed in late June 2002, gradients between MW-31D and100D, and MW-1D and 29D reversed. Gradients reversed again in mid-August 2002 as water levels in the canal dropped and have reversed numerous times during the five years since the dam was installed. Water elevations in MW-100D and MW-1D were greater than elevations in MW-31D and MW-29D respectively during most of the winters, springs and early summers of 2003 2004 and 2005, and this pattern has been more persistent since a flood in October 2005 deposited up to two feet of sediment on the peninsula and deepened the Blackstone River channel. When the water elevation in MW-100D is higher than the elevation in MW-31D and the elevation in MW-1D is higher than in MW-29D (i.e. the difference is > 0 in Figure 18), the VOC plume migrates to the southeast away from South Grafton Water District (SGWD) Well #3.

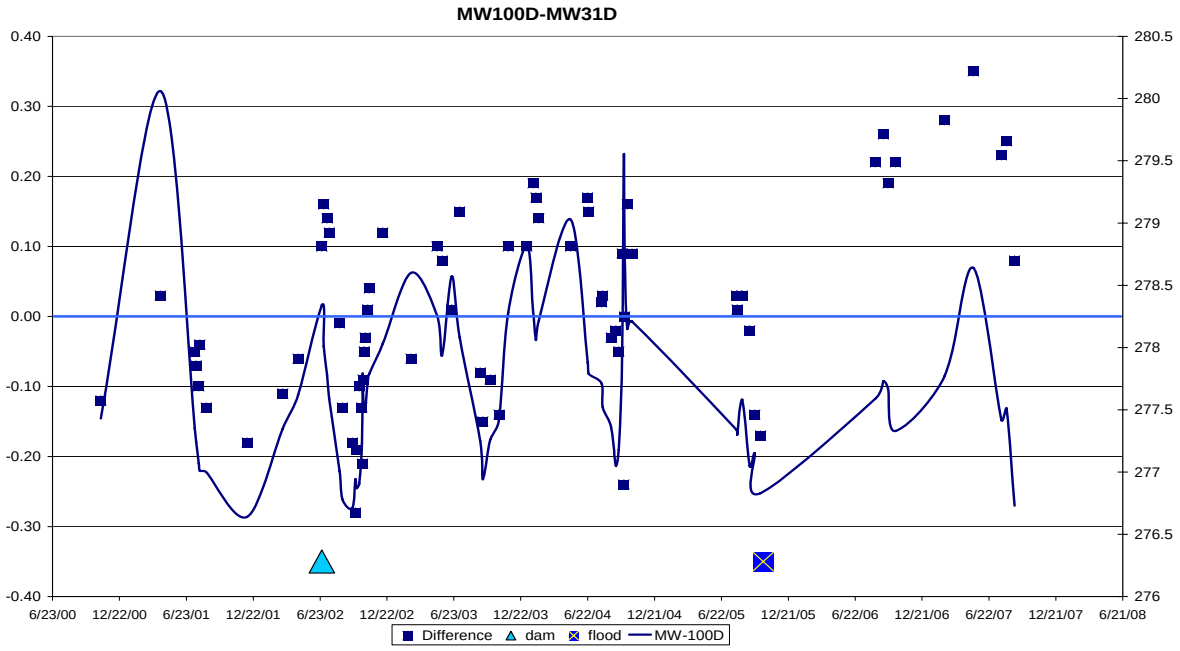

Figure 18. The difference in groundwater elevations between MW-100D and MW-31D and the groundwater elevation measured in MW-100D. The dam was installed on June 28, 2002 (blue triangle) and a major flood occurred on October 14, 2005 (dark blue square).

In the month following installation of the dam, TCE concentrations decreased in MW-1D, 31D and 100D. Concentration changes shown in Figures 14 and 19 are similar in all three wells. However, during the late summer of 2002 when water levels dropped below the crest of the dam and the SGWD started using Well #3, TCE concentrations increased in all three monitoring wells. After water levels rose in the winter and spring of 2003, TCE concentrations decreased in the three wells and remained low until the fall of 2003. The increases in concentrations during the fall of 2003 were less than in 2002. This was the case even though the SGWD pumped

approximately 226,000 gallons per day from Well #3 from mid-April to December 2003. TCE concentrations have been less than 1 ug/l in samples from MW-100D since January 2004 and less than 7 ug/l in samples from MW-31D since October 2004. A groundwater sample collected from monitoring well SG-6 on October 24, 2003 contained 1.9 ug/l TCE. TCE has not been detected in SG-6 since October 2003.

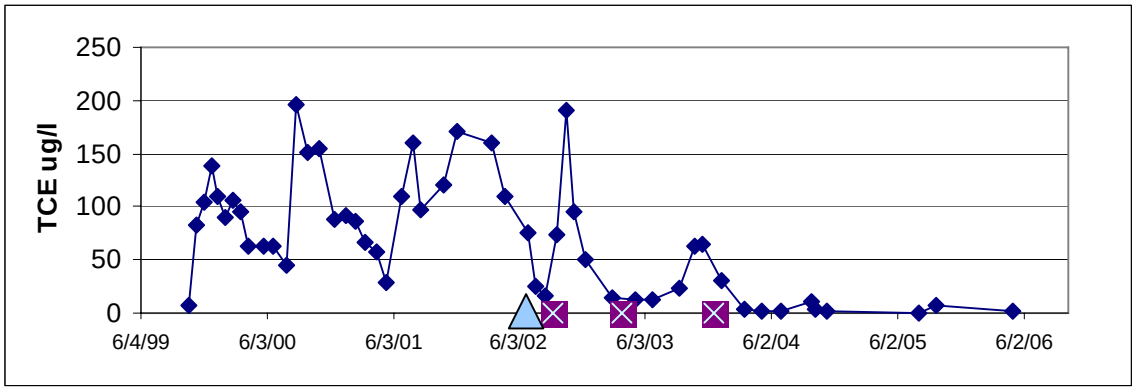

Figure 19. TCE concentrations measured in groundwater samples collected from MW-31D.

TCE concentrations in bedrock monitoring wells on the peninsula decreased in MW-1R and remained relatively constant in MW-31R (Figure 20). Monitoring well MW-31R is approximately 90 feet deep with a screen 15 to 30 feet below the bedrock surface. Based on polyethylene diffusion bag sampler results, contaminated water is present at the top of the screened interval. The different responses in MW-31D and MW-31R following installation of the temporary dam indicates that hydrologic changes in the overburden aquifer have little effect on contaminant migration in MW-31D.

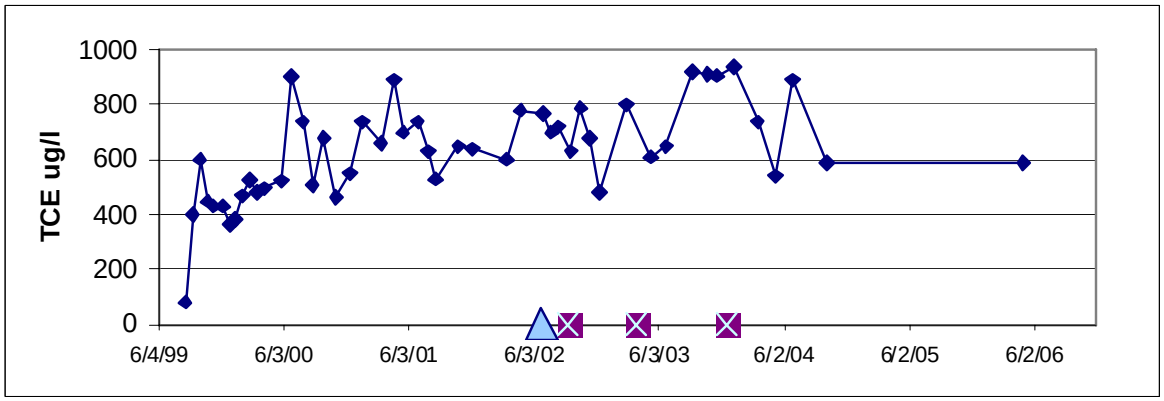

Figure 20. TCE concentrations measured in groundwater samples from MW-31R.

Total precipitation was greater during August, September and October of 2002-2006 than during 2000 and 2001. Because of this, it remains uncertain how effective the dam will be during dry years similar to 2000 and 2001. However, it does appear that a series of years with

near (2002, 2006) or above average (2003-2005) precipitation do have a cumulative effect and have minimized risk to Well #3. TCE was not detected in Well # 3 after November 2000 and the dam allowed use of Well #3 while ISCO was implemented in the source area.

4. IN-SITU CHEMICAL OXIDATION (ISCO)

The advantages of implementing ISCO as the long-term solution at this site were that it:

- Had been shown to be effective for the contaminants of concern (TCE and its breakdown products),
- Chemically degraded contaminants upon contact, without producing more toxic compounds like vinyl chloride,
- Could be implemented within the timeframe dictated by USEPA under the time-critical removal action program, and
- Did not require any long-term operations and maintenance, for which there was no funding or proprietor.

A number of chemical oxidants were evaluated for use at the site including hydrogen peroxide (or Fenton's Reagent), permanganate (either NaMnO4 or KMnO4), and ozone, but sodium permanganate was selected as the preferred approach. Sodium permanganate had several key advantages over the other oxidants considered including:

- Permanganate is more persistent in the subsurface than peroxide or ozone. Therefore, it has a wider range of options for field application/subsurface delivery.
- Because of the higher stability of permanganate, diffusive transport through low permeability zones, such as the till unit at the Fisherville Mill Site, is possible.
- Permanganate has a strong affinity for oxidizing organic compounds containing carbon-carbon double bonds, aldehyde groups, or hydroxyl groups. The other oxidants are less selective oxidizers. The effective radius of treatment will likely be greater for permanganate than it would be with other oxidants, because it is less likely to be consumed as quickly by natural organic matter in the subsurface.
- Permanganate is a more stable oxidizing agent, so dangers of rapid decomposition are not as great as with peroxide and ozone. However, fire or explosion hazards still exist if the permanganate comes in contact with combustible or flammable compounds.
- The optimum pH range for chemical oxidation with permanganate is 7 to 8, but it is effective over a wide pH range. Therefore, no pH adjustment is required.

- Laboratory and field studies have demonstrated that permanganate has the highest oxidation efficiency for destruction of TCE and PCE, as compared to Fenton's Reagent or ozone. (West, et al., 1997).

- The density of the proposed 20% sodium permanganate solution is close to that of the DNAPL contamination and thus would likely seek the same contaminant migration pathways through the subsurface, targeting residual DNAPL.

Permanganate can be applied to the subsurface in the form of potassium permanganate (KMnO4) or sodium permanganate (NaMnO4). Potassium permanganate is less expensive, but less soluble in water. Solutions of potassium permanganate can be readily mixed in concentrations of 3 to 4 % (by weight), whereas sodium permanganate is available in liquid form at a 40% concentration. The higher solubility of sodium permanganate increases the ease of application, reducing labor costs, and making it cost effective at some sites. However, because of the higher concentration of the NaMnO4 solution, there are greater health and safety concerns.

The reaction is as follows:

$2NaMnO_4 + C_2HCl_3 \Rightarrow 2CO_2 + 2MnO_2 + 2Na^+ + 2Cl^- + HCl$

Stoichiometrically, a ratio of 2:1 permanganate to TCE is required to oxidize TCE to carbon dioxide. However, laboratory studies have indicated that the reaction is optimized at a ratio of 5:1. (Dichloroethene and vinyl chloride are also amenable to oxidation by permanganate with stoichiometric ratios of 8:3 and 10:3, respectively.) The presence of naturally occurring organic matter and inorganic chemicals that exert an oxygen demand will further increase the dosage of oxidant required.

5. TREATABILILITY TESTING

5.1 Treatability Study

A treatability study was conducted in spring of 2002 to verify that sodium permanganate would effectively destroy the site contaminants, to determine the amount of oxidant required, and to evaluate various methods of delivering the oxidant to the subsurface. The treatability study consisted of 1) in-situ injection testing to evaluate injection rates and injection point design and spacing; and 2) bench scale treatability tests to evaluate the effectiveness of various doses of permanganate in destroying site contaminants.

The injection testing was conducted by injecting potable water into the subsurface using three different injection point designs including: 1) 1" diameter PVC well points installed using direct-push methods, 2) 2-inch diameter monitor wells installed using conventional rotary drilling methods, and 3) direct injection via direct push drilling rods.

The injection tests were performed by pumping potable water into a single injection point, and monitoring the injection flow rate, volume and backpressure. Water level measurements were also made in nearby monitor wells and injection points to assess the radius of the treatment zone. The injection was continued for 10 to 20 minutes based on the response of water levels in nearby wells. In most cases, a large rise in water levels (0.5 to 1-ft) in adjacent wells was noted within five minutes, with only slight increases (few hundredths of a foot) after that.

Of the various injection points tested, the 1-inch diameter PVC well point performed best. Although injection through the drill rods was possible at high flow rates (up to 20-gpm) with little or no back pressure, better water level response in adjacent wells was observed using the PVC well points. In addition, installation of PVC well points would enable them to be used as future monitoring points to help assess the effectiveness of the treatment and for subsequent oxidant injections, if deemed necessary.

The injection rates varied from 3-gpm to 23-gpm. The lower flow rates were confined to shallow injection points where the flow had to be reduced to prevent surface breakout of the injected water in the annulus around the well point. Intermediate and deeper well points were able to accept flow rates of 15 to 20-gpm with little or no backpressure. The volume of water injected into the intermediate and deep well points ranged from 250 to 450-gallons. The data indicated that the injection system and aquifer capacity would not be limiting factors for the oxidant delivery system design.

5.2 Bench-Scale Testing

To confirm the effectiveness of sodium permanganate at reducing site contaminants to below the cleanup goal and to assess the required dosage, a bench-scale treatability test was conducted. Four composite samples of site soil and groundwater were collected. The soil was collected using direct push drilling methods from the area of highest known contamination. Two of the composite samples were composed of outwash, and two were of till. This was done to account for potential differences in the amount of natural organic carbon between the two formations.

The treatability test was conducted by dividing the four composite samples into seven oxidation test jars labeled “a” through “g”. Each test jar contained 500 grams of soil and 180 ml of groundwater collected from the monitoring well that contained the highest observed concentration of TCE at the site (370,000 ug/L). The oxidation test jars were then treated with sodium permanganate in a range of dosages from 2 to 40g permanganate/kg of soil (approximately 5 to 120 lbs permanganate per cubic yard of soil)**.** Water samples were collected for VOC analysis from each composite soil sample prior to allocation into the oxidation test jars. VOC samples were also collected from each oxidation test jar one week after introduction of the sodium permanganate.

The results of the treatability testing showed that the required dosage to achieve the treatment goal (reduce the TCE concentrations in the source area by two orders of magnitude) is between 2 and 6-grams (g) of sodium permanganate for every kg of soil. Figure 21 shows the oxidation test jars from one of the composite samples. Water and soil samples from the concentrations of contaminants in two of the three water and soil samples that had been treated with a dosage of 2

g/kg were less than two orders of magnitude lower than the original concentrations. The concentrations of contaminants in all of the water and soil samples that had been treated with a dosage of 6 g/kg were two orders of magnitude lower than the original concentrations and, with the exception of one soil sample, were below the analytical detection limits.

5.2.1 Conceptual Design

Conceptual design of the full-scale ISCO application was conducted following completion of the treatability testing and based on its result.

The area targeted for application of the oxidant is shown on Figure 22 and was chosen based on soil and groundwater quality data collected during historical site characterization work. The treatment area was approximately 100-ft by 200-ft, with the long axis parallel and abutting the Blackstone Canal, and a southern terminus at Main Street. This area was considered a conservative estimate of all areas with groundwater and/or soil with concentrations greater than 1 mg/L total volatile organic compound (VOCs). A total of 100 injection points are included within the treatment area. The injection point grid consisted of 10 rows spaced 20-ft apart in the direction parallel to groundwater flow (roughly north to south). Each row consisted of 10 injection points spaced 10-ft apart in the direction perpendicular to groundwater flow (roughly east-west). The spacing of the injection points was greater in the direction parallel to groundwater flow because of the convective transport that will occur in that direction. Each row was offset from the previous row by 5-ft so that the rows did not line up in the downgradient direction. This was done to prevent untreated zones from developing between the injection points.

Figure 21. Sodium Permanganate Bench-Scale Treatability Testing

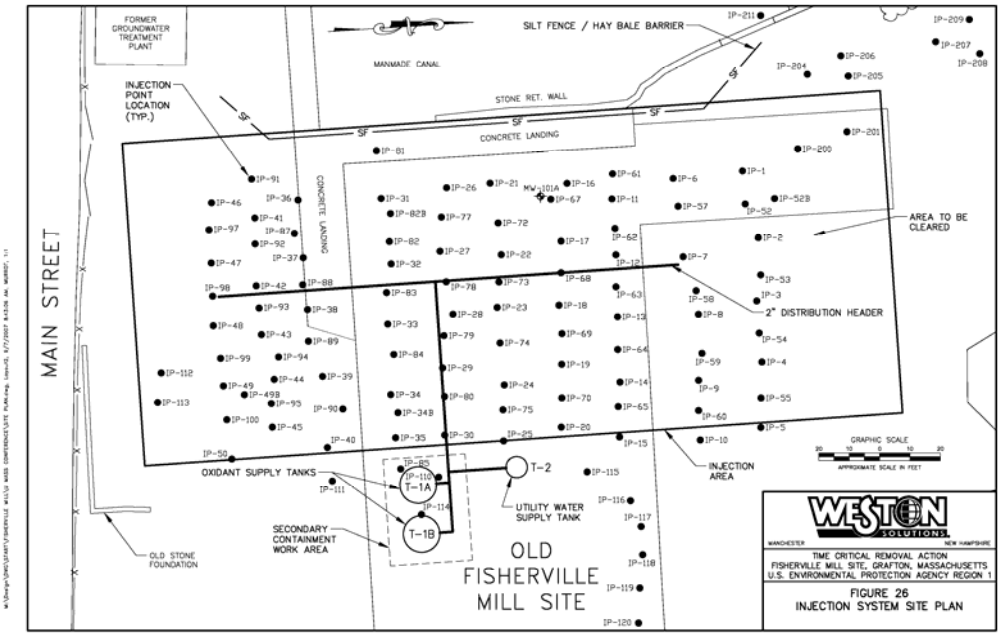

Figure 22. Injection System Layout

Based on the bench scale treatability test results, the recommended dosage rate was 4 g of sodium permanganate for every kg of soil. For purposes of full-scale implementation of ISCO at the site, this equated to injection of 1,244-pounds of $NaMnO_4$ per injection point. Permanganate dosage rates for ISCO are highly dependent on the amount of naturally occurring organic matter present in the site soils. During the treatability testing, soil samples were collected and analyzed for TOC. TOC concentrations in the untreated soil samples varied from 1,541-milligram/kilogram (mg/kg) in the till sample to 3,283-mg/kg and 4,483-mg/kg in the outwash samples. More than 50% of the TOC remained in the samples after treatment with permanganate. The relationship between soil TOC concentrations and permanganate demand was evaluated by Siegrist, et al. In the studies reviewed, the ratio of permanganate to TOC varied from 2-mg to over 100-mg of permanganate per milligram of TOC. Dosages of 2-mg to 10-mg permanganate per milligram TOC were most common. Increases in oxidant consumption were observed with increases in the oxidant dose concentration. Based on a minimum theoretical dosage of 2 mg permanganate per mg of TOC, and an average TOC concentration of 3,000 mg/kg, a theoretical dosage of 7.2 g $NaMnO_4$ per kg of soil, or 2,240-pounds of $NaMnO_4$ per injection point, was calculated. This is approximately 1.8 times the dosage estimated above, which is based on the VOC destruction observed during the treatability testing.

A direct calculation of permanganate demand per gram of TCE, DCE, and PCE was also made to evaluate the contaminant oxidant demand directly related to the site contaminants. The oxidant demands for TCE, DCE, and PCE are 1.81, 3.28, and 0.96-grams permanganate per gram of contaminant, respectively. This results in a demand of approximately 5 to 40 pounds of permanganate per injection point assuming a concentration of 9 to 40 mg/kg of TCE in the treatment area soils. Converting from the mass of permanganate ion (MnO_4^-) to the mass of sodium permanganate salt ($NaMnO_4$), this equates to 11 to 48-pounds of $NaMnO_4$ per injection point. This dosage is significantly less than the required dosage observed during the treatability

study because it does not take into account the oxidant demand of the naturally occurring organic materials in the soil. Less than 3% of the oxidant demand required to treat the soils at the site is likely to be directly related to the chlorinated contaminants.

Although the treatability study results provided valuable site-specific information regarding the mass of $NaMnO_4$ that would likely be required during full-scale implementation of ISCO, conditions varied throughout the treatment area. Therefore, the calculated dosages provided a good starting point for the full-scale design, but were not expected to predict exact oxidant demands for ISCO application. For this reason, it was recommend that application of the oxidant be conducted using a phased approach; with three or more injections. By injecting 50% of the calculated dosage during the initial injection, and 25% of the calculated dosage for subsequent injections, dosage rates could be adjusted based on performance. If monitoring indicated that concentrations of the contaminants had been attained, or were close to attaining, cleanup goals in certain areas, oxidant dosages injected in those areas could be reduced or eliminated. Conversely, if contaminant concentrations in some areas did not appear to be decreasing significantly, oxidant dosages could be increased in those areas.

5.2.2 Full-Scale Application of ISCO

Full-scale implementation of ISCO was begun in July 2002 with the installation of the injection points. The original design included installation and injection into 100 wells, however several injection points had to be relocated due to cultural interferences and one location was deleted altogether. To monitor the penetration of the permanganate into the bedrock, five bedrock wells (IP-52B, -82B, -34B, -49B, and MW-3T-B) were installed. Although direct push drilling methods were originally planned for installation of the injection points, they were ultimately installed using standard rotary drilling methods after it was determined that direct push methods were unsuccessful at reaching the design depth. The injection points are constructed of 1-inch diameter PVC with 10 ft of 10-slot well screen at the bottom, an appropriately-sized filter pack, and bentonite pellet seal installed 2 ft above the top of the well screen. The annulus was backfilled with native material to the ground surface.

Prior to full-scale injection of permanganate, a comprehensive baseline groundwater sampling round was conducted. This included sampling all 99 injection points and all accessible monitoring wells at the site. The injection point samples were analyzed for VOCs only, but the monitoring well samples were analyzed for metals as well as VOCs so that potential mobilization of metals by the oxidant could be assessed.

In August 2002 permanganate injections were initiated at the site with placement of the injection storage and pumping equipment including: three 6,500 gallon polyethylene storage tanks, three 250-gallon stainless steel tanks, two temporary containment structures, and two 3.5-horsepower centrifugal pumps. Two of the 6,500-gallon tanks used for the sodium permanganate solution storage were placed within containment structures. The third 6,500-gallon tank and the three 250-gallon tanks were utilized for clean water storage. Figure 23 is a schematic diagram of the injection system and Figure 24 is a photograph of the system as constructed.

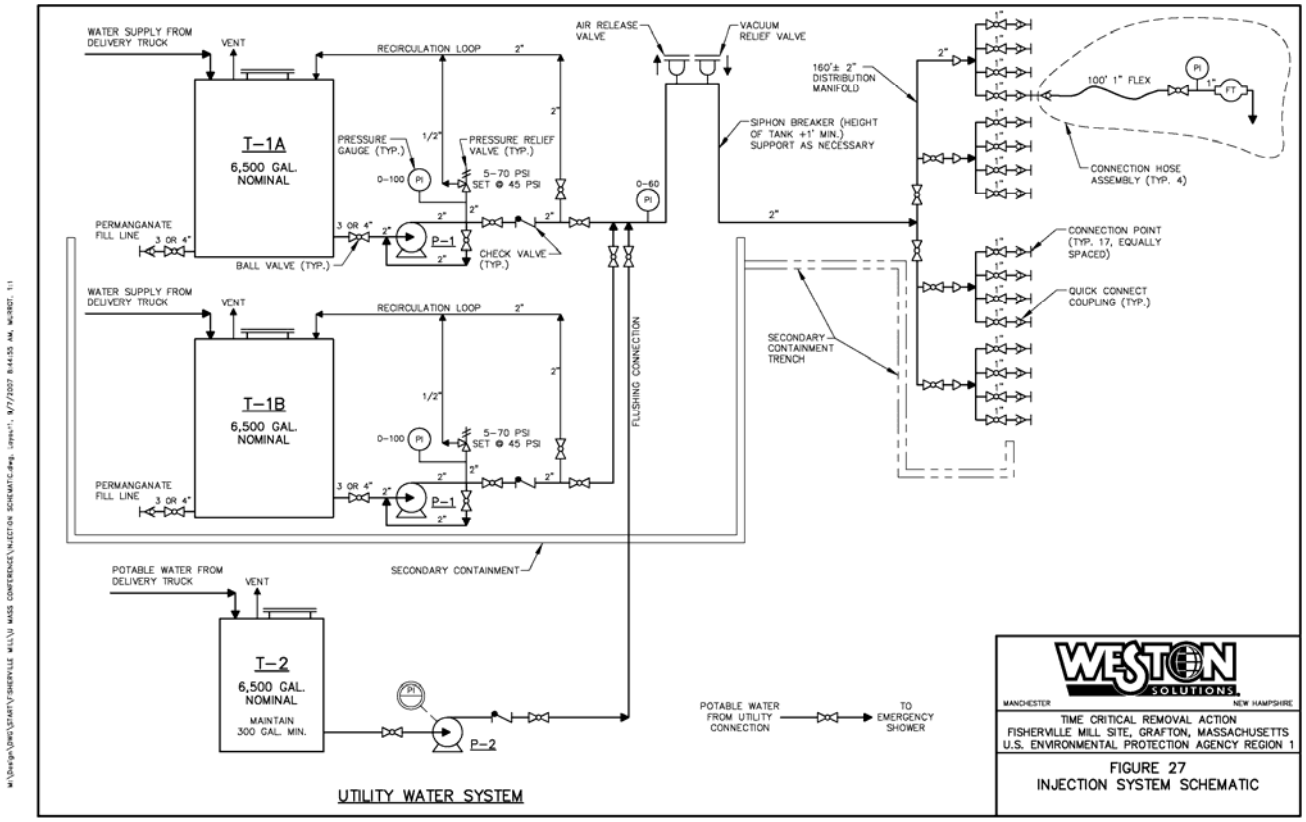

Figure 23. Injection System Schematic

Figure 24. Permanganate Mixing Tanks and Distribution Manifold.

After setup of the injection system, potable water was injected into a series of 4 injection points to test the equipment and to verify that the design injection rate of 10 gpm per well could be achieved. Water levels in adjacent wells were monitored to determine the extent of groundwater mounding caused by this injection rate. Minimal mounding was observed in adjacent wells, even after the complete injection volume of 373 gallons was injected into each of the 4 wells. The mounding dissipated within minutes after the injections were curtailed.

The first injection round began on August 28, 2002. A solution of 40% (by weight) sodium permanganate was delivered to two 6500-gallon polyethylene tanks at the site. The solution was diluted to 20% (by weight) before being injected into each of the injection points. A total of 373 gallons of the 20% solution was injected into each of the wells at a rate of about 10 gallons per minute, typically pumping into 4 to 6 wells at a time. A solution of 20% sodium permanganate contains 1.92 pounds per gallon, so each well received 716 pounds of pure sodium permanganate. This represents approximately 58% of the total design dosage.

The injection was begun at the upgradient (north) end of the treatment grid, working downgradient. Initially, the 20% sodium permanganate solution was injected into every other point in each row. After the first pass through the injection grid, oxidant was injected into the remaining wells, again progressing from upgradient to downgradient acres the grid. This “every other well” sequence allowed us to monitor for the presence of permanganate in the uninjected wells to evaluate permanganate distribution between injection points before completing the injection round. By the time injection of the first half of the wells was complete, permanganate was observed in the majority of the uninjected wells, indicating that the permanganate was quite well distributed throughout the treatment area.

Upon completion of the initial injection, permanganate levels were monitored in the injection points as well as in a series of monitoring wells located throughout and adjacent to the treatment area on a weekly basis. The monitoring wells included both overburden and bedrock wells. Once the permanganate concentrations dropped to less than 1% (10,000 ppm) in a sufficient number of points within the treatment area, samples were collected for VOC analysis using an on-site GC.

Permanganate concentrations remained very high in the center and downgradient portions of the treatment grid, but only trace levels of permanganate were observed south of Main Street. An increase in dissolved oxygen and oxidation/reduction potential (ORP) was noted in monitoring wells south of Main Street. The lack of significant migration of the permanganate was attributed to the fact that although the permeability of the aquifer is very high, the hydraulic gradient across most of the treatment grid is very low. It is likely that increased water levels in the Blackstone Canal after installation of the temporary dam decreased hydraulic gradients in the treatment grid. This set of conditions allowed high concentrations of permanganate to stay within the treatment area for an extended period of time, thereby facilitating diffusion into lower permeability layers within the formation.

Although permanganate was not injected in bedrock monitoring wells within and/or adjacent to the treatment area, permanganate did eventually migrate into the bedrock. Permanganate was first observed in bedrock monitoring wells in late September, about 1 month after the initial injection. By the end of October, nearly two months after the initial injection, permanganate was observed in MW-101A, the most highly contaminated well at the site. Permanganate then persisted in the bedrock for the duration of the project. MW-101A differs from the other source area bedrock wells in that it is extremely "tight" and has limited connection with the overburden aquifer. It remains uncertain how TCE migrated to MW-101A. Permanganate was detected in MW-101A but concentrations were significantly less that in other wells and VOCs have persisted even with low concentrations of permanganate. Because of the limited connection with the overburden aquifer and the lack of transmissive fractures, high concentrations of TCE measured in MW-101A were not viewed as a significant threat to SGWD Well #3.

After approximately 6 months of permanganate and VOC monitoring it was noted that while the majority of the treatment area still contained high concentrations of permanganate, several injection points in the northwest corner of the treatment grid no longer contained permanganate and that VOC concentrations had rebounded to near pre-injection levels. As a result, a second more limited injection was performed in March 2003. Approximately 100 gallons of 20% sodium permanganate was injected into 10 injection points (IP-1, IP-2, IP-3, IP-6, IP-7, IP-12, IP-52, IP-53, IP-57, and IP-63). Because of the limited size of this injection, the manifold system was not used and the permanganate solution was mixed in 55-gallon drums and gravity fed into the individual injection points. Weekly permanganate monitoring was resumed after the second injection was completed.

Shortly after this injection, permanganate was observed seeping into the surface water within the adjacent canal near the Main Street Bridge. This area is heavily contaminated with #6 fuel oil from a former underground storage tank associated with the mill. Upon entering the surface water, the permanganate was immediately reacting with the fuel oil and/or natural organics. Surface water samples collected from the canal and screened using the spectrophotometer did not

show detectable levels of permanganate. The permanganate seepage stopped after a few days and was never observed again.

In August 2003, approximately 1 year after the initial injection and about 6 months after the limited second injection, monitoring again suggested that the permanganate has dissipated within a number of injection points and monitoring wells in the northwest corner of the injection grid. Subsequent VOC monitoring confirmed that contaminant concentrations remained above 1 mg/L total VOCs in this area. Many of the wells now exhibiting VOCs were the same ones that had been subjected to the second permanganate dose in March 2003. It was suggested that impacted groundwater might have been migrating into the treatment grid from a previously unidentified upgradient source. To assess this possibility, a series of vertical profile borings were advanced to the north and east of the treatment grid. A Waterloo Profiler was used to collect discrete groundwater samples at 5-foot intervals. The samples were analyzed for VOCs using an EPA mobile laboratory. Although some TCE and its breakdown products was found in groundwater upgradient of the treatment grid, the concentrations were generally very low and did not exceed the cleanup goal. As a result, it was concluded that the injection points within the treatment grid where the permanganate did not persist as long as in other areas must be a zone of higher permeability where more flushing with upgradient groundwater was taking place, not allowing the permanganate sufficient contact time with contaminants adsorbed to the aquifer matrix.

Permanganate continued to persist in nearly 90% of the injection points at very high concentrations, which was viewed as positive because it allowed the oxidant to diffuse into the lower permeability layers within the aquifer and also allowed extended contact time with the contamination. However, the continued flushing of selected areas of the treatment grid was not allowing those areas to be adequately treated. As a result, it was decided that a temporary recirculation system would be implemented to move the permanganate from areas with high levels to the northwest corner, where the permanganate did not persist very long. The objective was to re-circulate approximately one pore volume of groundwater estimated to be contained within the aquifer beneath the injection grid.

The initial groundwater/permanganate re-circulation was conducted in October 2003. During a 2-week period, approximately 384,000 gallons of groundwater containing permanganate was re-circulated. The extraction and re-injection points were varied almost daily based on observations of permanganate concentrations, groundwater mounding, and injection point yields

In December 2003, MassDEP installed eight steel injection points (IP-116 through IP-123) east of the original injection grid using direct-push methods. These additional injection points were installed to investigate possible additional VOC source areas and serve as a line of permanganate injection locations to treat any VOC contamination flowing east from the injection grid. The steel injection points were installed to variable depths depending on refusal of the direct push equipment.

Based on the results of the vertical profiling and recirculation study, and continued permanganate and VOC monitoring since the second injection, a limited third injection of sodium permanganate was performed in December 2003. Approximately 100 gallons of 20% sodium permanganate was injected into 16 injection points (IP-6, IP-7, IP-11, IP-12, IP-16, IP-

21, IP-57, IP-63, IP-67, IP-116 through IP-120, IP-122, and IP-123). Weekly permanganate monitoring was resumed after the third injection was completed.

Lastly, in late December 2003, a second groundwater re-circulation event was conducted in an effort to transfer high permanganate concentration groundwater from the southern end of the treatment grid to flush IP locations that had received the third sodium permanganate injection. Between 5,000 and 7,000 gallons of permanganate-containing groundwater was re-circulated from southern injection points to IP-7, IP-116, IP-117, IP-118, IP-119, IP-120, IP-122, and IP-123.

6. RESULTS

The cleanup objective for the Fisherville Mill ISCO project was to decrease trichloroethylene (TCE) concentrations in the source area by two orders of magnitude, thereby reducing the size of the downgradient plume, and reducing the risk of drawing TCE into the downgradient municipal water supply wells. This meant reducing the average concentration of TCE in the overburden source area from approximately 4000 ug/L and average concentrations in transmissive source area bedrock wells from approximately 16,000 ug/L to less than 100 ug/L. In March 2003, six months after completing the first injection of permanganate, detectable concentrations of TCE remained in 10 of the injection points and concentrations in two points exceeded 1 mg/L. The second round of injections into the 10 injection points was conducted in April 2003. The third round of injections into 16 injection points was completed in December 2003. Upon completion, over 18,000 gallons of 20% sodium permanganate solution had been injected into the subsurface at this site. Performance monitoring confirmed that the cleanup objectives had been attained in both overburden and in all transmissive source area bedrock wells. An increase in sodium concentrations was observed in source area groundwater as a result of the injections, but mobilization of naturally occurring metals, sometimes cited as a potential concern with implementation of this technology, was not observed. Figure 25 shows the distribution of TCE in the source area before and after implementation of ISCO. Figure 26 presents graphs of the average TCE concentration within the treatment area in both the bedrock and overburden. Attainment of cleanup goals was achieved within 16 months of implementation of ISCO and the project was completed under the $2M budget.

6.1 Creating a shared vision: Recognizing shared goals

FRC recognized an opportunity in the Fisherville Mill remediation project to utilize its accumulated knowledge and operational experience to clean up a highly impaired property and return it to a valuable economic and community use.

Through extensive consensus building, public visioning and detailed collaboration between the project stakeholders and the company, agreement in principle with regard to our fundamental prerequisites for a successful cleanup project to be undertaken was achieved. The development of consensus on the remedial approach and end use vision of the site were the primary deciding

factors that motivated FRC to complete the acquisition of the property and begin implementing its remediation strategy.

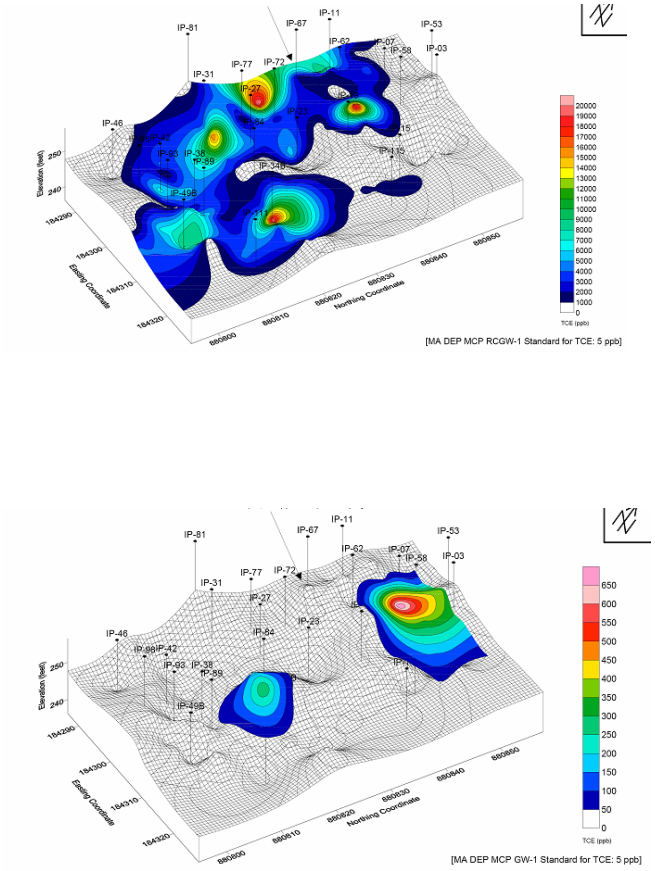

Figure 25. Distribution of TCE in Treatment Grid before and after ISCO (note change in concentration scale between figures).

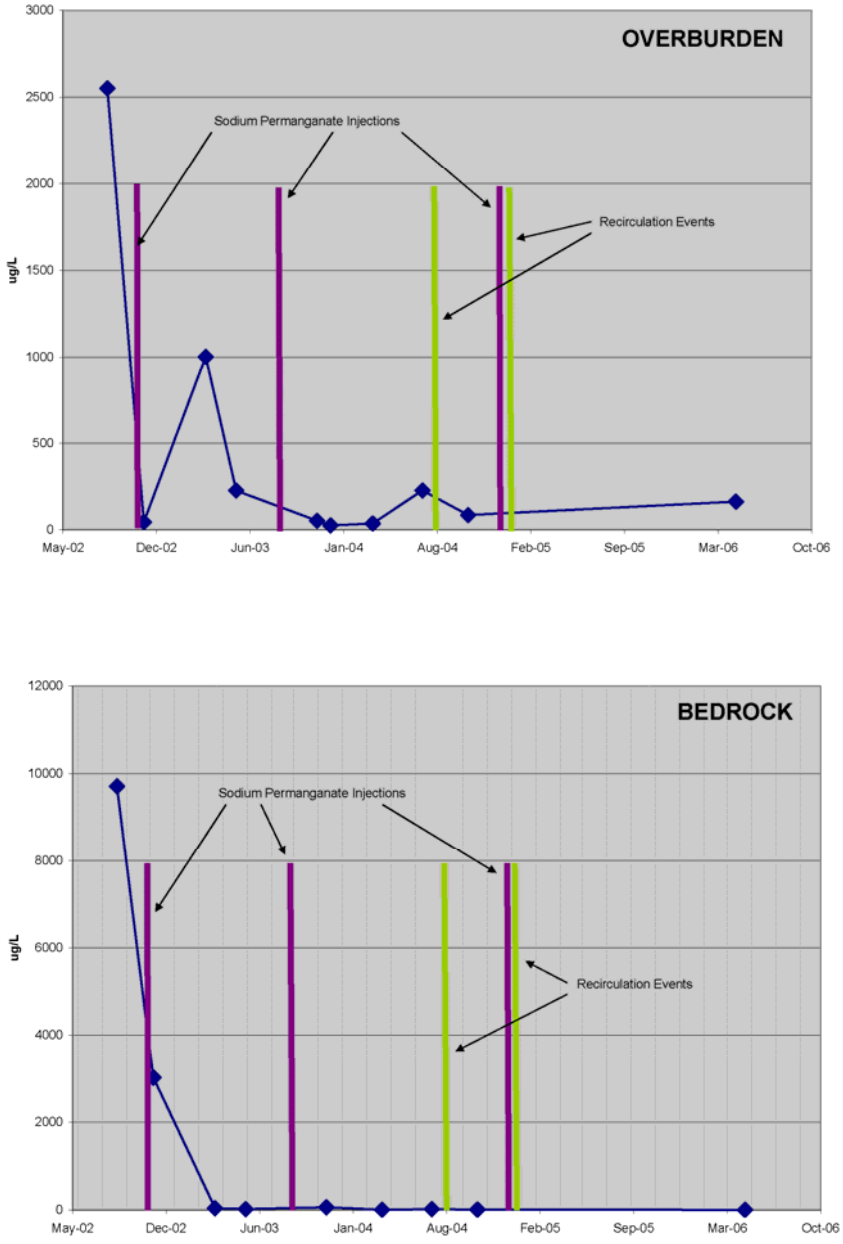

Figure 26. Average Total VOC concentration in source area in overburden and bedrock.

Figure 27. Rendering of mixed-use redevelopment of property with large amounts of open-space and public access for recreational activities.

To achieve the successful remediation and redevelopment of the Fisherville Mill site FRC recognized a need to create a vested community of regulators and public stakeholders with common goals and a shared vision. The implementation of complex cleanups and redevelopment projects in an adversarial or indifferent political environment are extremely difficult and often too risky for the private sector to undertake.

It was recognized that the dominant impediments to the cost-effective redevelopment of the Fisherville Mill site was the presence of tremendous volumes of visually offensive and environmentally sensitive asbestos impacted materials, poor underlying real estate value under then existing zoning, and time consuming and expensive regulatory requirements that would retard implementation of our remedial approach. Additional environmental impediments included the heavy metal impacted surficial soils, bunker oil contamination and residual CVOC contamination were also recognized but determined to be surmountable if the asbestos, zoning and regulatory issues could be adequately addressed. The primary source of the CVOC

contamination had been addressed by the implementation of ISCO by EPA in 2003 through 2005, as described in the second part of this paper.

Figure 28. Fisherville Mill Site before encapsulation with flowable fill.

In FRC's opinion, the key to establishing an effective collaboration lies in identifying and acknowledging the shared goals of the stakeholders in a cleanup project and creating a shared vision of final outcomes. In the case of the Fisherville Mill redevelopment project this involved the following:

- Developing a compelling end use vision
- Recognizing that the number one goal of all the stakeholders is a cleaned up site.
- Recognizing that the number one goal of most of the public is a visibly cleaned up site.
- Understanding the perceived value or lack thereof to the affected public of environmental engineering and the regulatory process.
- Focusing on implementing remedial activities wherever possible.
- Understanding and communicating owner / redeveloper risk

FRC determined that it would need to reach agreements on the following fundamental issues prior to assuming ownership of, and responsibility for, the cleanup of the Fisherville Mill Site:

- MassDEP agreement to allow encapsulation of the potential asbestos containing material at the site as an acceptable remediation strategy, thus allowing cost effective implementation of company remediation concepts.
- Town of Grafton agreement to pursue and support changing the underlying zoning for the site to allow higher value use by right, thus justifying remediation expense.

- MassDEP agreement to allow immediate remedial activities to be undertaken prior to completion of Phase 2 Comprehensive Site Assessment, thus allowing rapid tangible improvement in site economic value and appearance.

A collaborative approach and strategy was developed between FRC and our environmental consultants (Woodard & Curran), MassDEP, EPA, the Town of Grafton and several other stakeholder groups including, Mass Audubon, US Park Service, Mass Fish and Wildlife, Blackstone Heritage Corridor Commission and the Blackstone Headwaters Coalition, that would encourage significant remedial actions while environmental assessment and engineering design activities were ongoing.

The tangible benefits of our collaborative approach has been:

- An accommodating public with a vested interest in the success of the project and a willingness to tolerate truck traffic and noise associated with the remedial activities.
- Public support that encourages and facilitates a cooperative regulatory environment.
- A collaborative remedial strategy developed and supported through frequent communication and the shared knowledge and skills of site owners, environmental consultant and the regulatory community.
- Lower remediation cost due to:
    - Reduced filings: collaborative approach eliminates and or minimizes repeated submission of expensive environmental engineering documents and remedial approaches that may be unacceptable to the public, the owners and the regulatory community.
    - Efficient application of technical skills, knowledge and remedial actions.
    - Greatly reduced time to effect remedial outcome

The “on the ground” results of this approach has been:

- The expedited management of visible uncontaminated debris including bricks and steel.
- The encapsulation of the asbestos impacted debris and lead containing soil with flowable fill.
- The installation of a bunker oil interception and collection infrastructure.
- The clean up and partial restoration of a portion of the historic Fisherville canal.
- The removal and disposal of contaminated soil.
- The installation of soil vapor extraction piping infrastructure.
- The recovery and preservation of historic and architecturally valuable cut granite elements of the original mill building.
- The partial restoration Fisherville Dam.
- The re-grading, re-vegetation and stabilization of the site for future construction.

All of the above achievements have been realized without impeding the completion of comprehensive site assessment activities as dictated by the Massachusetts Contingency Plan (MCP). Additional site assessment activities conducted during the implementation of the remedial activities have focused on developing an accurate understanding of subsurface soil conditions in the CVOC source area, additional site investigation of the limits and extent of shallow CVOC impacted soils and evaluating options to complete remediation of the site. The remedial action plan is anticipated to be completed by the spring of 2008.

Additional innovative remedial alternatives that have been explored during this period include completing a pilot study that has demonstrated that fungi and higher plants may be a feasible approach remediation of oil contaminated sediments and the oil impacted surface waters of the canal. This novel, in-situ, remediation concept involves the use of selected higher plants and fungi in an engineered ecosystem that is capable of metabolizing petroleum compounds and converting them to living biomass.

6.2 Encapsulation of Debris with Flowable Fill

Though significant money had been spent by the EPA and MassDEP, CMEDA and others to stabilize the site and remove grossly contaminated waste immediately following the 1999 fire; enormous piles of asbestos containing materials containing, ash, contaminated soil, wood, steel, brick, concrete debris as well as remnant piping, machinery, and foundations virtually covered

Figure 29. Debris piles at Fisherville Mill before remediation

the entire site. As the cleanup of this visual and environmental blight was the highest priority of the community expressed during the consensus building process, the company determined that addressing this problem should form the foundation of the remedial approach at the site. Immediately addressing this high visibility issue at the outset of the remediation process reinforced and validated the company's core remedial concept of rapidly implemented improvement in site environmental conditions from both a public and regulatory perspective.

As the various debris materials were intermixed, the high costs for disposing of these materials without segregation and safety risks associated with their re-handling and segregation had prevented other interested developers in taking on this project.

FRC believed that it could best address this challenge and achieve multiple related goals in the redevelopment process through encapsulation of the asbestos impacted soils and debris in "flowable fill", an engineered low strength semi-liquid pozzolanic material.

The application of flowable fill to encapsulate the debris would accomplish the following:

- The desired immediate improvement in the visible appearance of the site.
- Immediate reduction in the potential environmental hazard posed to the public and site personnel from airborne asbestos.
- Reduction in the costs, risk, and complexity associated with excavation and disposal of potential asbestos impacted material at an off site facility.
- Creation of a high strength, level, subsurface pad suitable for use as a foundation for a multistory residential mill complex.
- Reinforcement of the earthen Fisherville Mill Dam allowing future re-watering of Fisherville Pond that in turn would improve subsurface hydrological conditions at the site by providing a constant water supply for the Blackstone canal.

By working with various regulatory officials, it was agreed that the application of flowable fill to encapsulate debris was a much better, safer method to handle the asbestos impacted material at this site.

In the first twelve months of the remediation project the former foundation holes of the mill buildings and the associated debris were encapsulated with a commercially available flowable fill product. A few discrete areas of debris piles with heights that exceeded the depth of flowable fill were relocated under a MassDEP approved asbestos work plan that included the use of wetting techniques and perimeter monitoring for asbestos fibers.

To prepare areas for flowable fill, concrete slabs were removed both to explore for pipes, tanks or other unknown sources of contamination but also to access vaults and voids for filling. Additionally, berms were created using soil to contain the flowable fill until setting. As described in further detail below, off-site soil from regional construction projects was evaluated by Woodard & Curran (W&C) for suitability, in accordance with soil acceptance criteria approved by MassDEP, and used at the site to form many of the berms.

Figure 30. Encapsulation of debris with flowable fill.

The flowable fill was prepared on-site using a portable batching systems in general accordance with the Massachusetts Highway Department (MHD) specifications for Type 1E (very flowable and excavatable) Controlled Density Fill as described in the December 11, 2002 "MHD Supplemental Specifications for Highways and Bridges" in subsection M4.08.0. The materials for flowable fill were processed in a mobile batching plant in an elevated location immediately adjacent to the application area. The flowable fill pours directly down the chutes from the portable batching system. The flowable fill is self-leveling and generally does not require any grading or reshaping to fill each application area.

Figure 31 (left). Application of flowable fill to encapsulate debris. *Figure 32 (right).* Flowable fill after setting and curing.

Infrastructure for a soil vapor extraction (SVE) system was installed in the shallow overburden soil in the front foundation area to allow for the potential future treatment of this area by SVE, as necessary. Due to the presence of shallow groundwater in this area, SVE wells were installed in a horizontal configuration. Vertical risers were run to the top of the foundation wall and capped. Existing monitoring and injection wells were extended above the final grade of the flowable fill to allow access for future monitoring and remedial actions.

Figure 33. Application of flowable fill in front foundation area in conjunction with SVE piping, monitoring wells and injection points.

6.3 Innovative Oil Control and Recovery

Since FRC's purchase of the property in 2004, one of the areas of the site that required continuous attention was the accumulation of bunker (No. 4 and No. 6) oil in the canal. Underground storage tanks (USTs) adjacent to the canal, used by the former mill owners were found to have leaked and were removed from the site in 1987. Subsurface investigations conducted on the fuel oil release area determined that there were large volumes of oil-saturated soil at depths of 10 to 25 feet below the ground surface adjacent to the vertical granite block canal walls. Massive granite blocks used as former building foundations limited excavation of these soils due to the risk of collapse of the canal walls. It had been observed that oil was seeping into the canal through gaps between the granite blocks within a fairly localized, 50-foot span adjacent to the western tailrace.

In 2004, the primary oil recovery technique was the containment of oil in the canal downstream of the tailraces, with absorbent booms and the periodic skimming of accumulated oil with a vacuum truck. This technique was expensive, labor intensive, and prone to occasional failure if there were large volumes of water flowing through the canal.

Figure 34. Oil absorbent boom change out in canal near tailraces

In 2005, a channel diversion wall and oil containment barrier was designed and installed at the canal tailraces. The diversionary structure routed canal water towards the eastern tailrace away from the source of oil at the western tailrace.

A platform was installed above the tailraces to allow for the installation of an adjustable hanging containment wall to contain floating oil for collection and allows water to pass under the wall. An Abanaki "Oil Grabber" belt skimmer was installed on the platform with the belt hanging into the containment area to skim oil. A section of drain piping surrounds the belt to prevent excessive movement due to wind or vibration.

Two recovery wells were installed using sections of perforated concrete leaching basins in an area adjacent to the location of the former USTs. During excavation of the recovery wells oil saturated soil and oil were observed. The excavation area was backfilled with coarse stone and oil-impacted soil was segregated for off-site disposal. Following installation, the recovery wells were fitted with Abanaki belt skimmers.

6.4 Cost Effective Re-use of Off-Site Soil

Off-site soil was reused at the site as berm, grading, shaping and cover material. Though approximately 30,000 cubic yards of flowable fill was used to encapsulate the debris, significant volumes (approx. 30, 000 cubic yards) of off-site soil was needed to create the berms, to cover above the flowable fill, and as grading material in transitional areas. As the cost to purchase virgin fill materials would be cost-prohibitive, a creative approach was developed for accepting off-site soils (that met MCP S-1/GW-1 standards) from urban construction sites.

Figures 35 and 36. Channel diversion wall installed in 2005 to direct canal water away from the oil-impacted western tailrace.

Figures 37 and 38. A containment wall was installed at the western tailrace to corral the oil and allow for collection with a belt skimmer.

Figure 39(left). Installation of one of two recovery wells using perforated leaching basin sections.; *Figure 40(right)*. Recovery wells fitted with belt skimmers.

FRC's and W&C's experience and existing relationships with business partners on similar projects provided the framework for a soil acceptance program that could be implemented at this site. FRC required generators of soil to characterize soil in accordance with acceptance criteria approved by the MassDEP. The acceptance criteria, required documentation of the source of the soil including a review of the historical use of the construction site and specific analytical testing requirements. The analytical results were compared to a set of acceptance standards developed for the site.

Prior to acceptance of soil at the site, a representative of W&C reviewed the analytical data, shipping records and opinion statements from the generator, to ensure conformance with the requirements outlined in the MassDEP approved soil acceptance criteria.

Figure 41. View of the site to the northeast across Main Street following application of flowable fill and re-use of offsite soil.

7. ACKNOWLEDGEMENTS

Dr. Paul W. Ollila was originally the corresponding author of this paper before he passed away on May 19, 2008. The Fisherville Mill Project Team dedicates all our efforts in the memory of our beloved friend. Dr. Ollila graduated from the Wachusett Regional High School in 1967 and the University of Rochester in 1972, where he earned a BA in Fine Arts. He received a Ph.D. in Geology from the University of Massachusetts Amherst in 1984 based on his work mapping the Santanoni Quadrangle in the Northern Adirondacks. Dr. Ollila taught at Vassar College, worked in environmental consulting, and served as a contractor for the Massachusetts Department of Environmental Protection. He was prolific in his field, presenting at professional conferences and publishing multiple articles on geologic and geo-chemical topics. Dr. Ollila contributed tremendously to the Fisherville Mill project, both as a leader and friend. We will miss him greatly!

8. REFERENCES

Church, P.E., Vroblesky, D.A., Lyford, F.P., and Willey, R.E. 2002. Guidance on the Use of Passive-Vapor-Diffusion Samplers to Detect Volatile Organic Compounds in Ground Water-Discharge Areas, and Example Applications in New England: United States Geological Survey Water-Resources Investigations Report 02-4186.

Desimone, L.A. and Barlow, P.M. 1995. Water-Quality and Hydrologic Conditions at a Site of Ground-Water Contamination by Volatile Organic Compounds, South Grafton, Massachusetts, September and October 1994. U.S. Geological Survey Open-File Report 95-425

Handex (Handex Environmental, Inc.). 1997. Comprehensive Site Assessment, Fisherville Mill, Route 122A, Grafton, Massachusetts. July, 1997.

HMM (HMM Associates, Inc.). 1993. Investigation of Groundwater Contamination Final Report; Prepared for MADEP. March, 1993.

ITRC. 2004. Technical and Regulatory Guidance for using Polyethylene Diffusion Bag Samplers to Monitor Volatile Organic Compounds in Groundwater: Interstate Technology and Regulatory Council. February, 2004.

Pine & Swallow Associates 2000a. Limited Subsurface Investigation, Fisherville Mill Grafton, Massachusetts. December 2000.

Pine & Swallow Associates 2000b. Fisherville Mill, Grafton, MA, PSA Reference Number: 00210. August 2000.

Regenesis, Inc. 2004. Case Study H-118. Regenesis, 1011 Calle Sombra, San Clemente, CA.

Siegrist, R.L., M.A. Urynowicz, O.R. West, M. L. Crimi, and K.S. Lowe (2001). Principals and Practices of In-situ Chemical Oxidation Using Permanganate. Batelle Press, Columbia NJ.

USEPA. 1998. Headspace screening for volatile organic compounds in aqueous, soil, and drum samples: Region I, Internal Standard Operating Procedure no. EIAFLDVOA1. SOP, U.S. Environmental Protection Agency, March 1998.

West, O.R., S.R. Cline, W.L. Holden, F.G. Gardner, B.M. Schlosser, J.E. Thate and D.A. Pickering. 1997. A Full-scale Demonstration of In Situ Chemical Oxidation Through Recirculation at the X-701B Site: Field Operations and TCE Degradation. ORNL/TM-13556. Oak Ridge National Laboratory, Oak Ridge, Tennessee.

Weston (Roy F. Weston, Inc.) 2002. Removal program Hydrogeologic Investigation Report for the Fisherville Mill Site Grafton, Massachusetts May 2001 Through December 2001; Prepared for U.S. EPA Region 1 Emergency Planning and Response Branch, Contract No. 68-W-00-097; April 2002.

PART IV: Chemical Oxidation

Chapter 10

EVALUATION OF IN SITU CHEMICAL OXIDATION OF SOILS AT A MIXED WASTE SITE AND ASSESSMENT OF EFFECTS ON GROUND WATER QUALITY

Richard C. Bost[§] and Robert G. Perry
Environmental Resources Management (ERM), Houston, Texas, USA

ABSTRACT

In Situ Chemical Oxidation (ISCO) entails the introduction of chemical oxidant into the subsurface for the oxidation and treatment of organic constituents of concern (COCs). This paper presents a case study that involved bench-scale testing and field demonstration of ISCO via Mechanical Auger Mixing (MAM) that resulted in over 95% removal of chlorinated and non-chlorinated chemicals identified as recalcitrant. Also presented are ISCO's effects on dissolved oxygen levels in the underlying aquifer. Mechanical mixing of soils with an oxidant solution is an improved remedial strategy that facilitates more effective mixing of reagants with affected soils and hence in more effective treatment than from injection of oxidant. Based on the apparent effectiveness of persulfate in bench-scale tests, ISCO utilizing persulfate and a source of alkalinity was then applied to the demonstration site. The site is a 1970s era waste disposal area where a multitude of different types of wastes were disposed. Six chemical constituents comprised the most abundant COCs at the subject site. These compounds are: 1,1-dichloroethane, vinyl chloride, acetone, 1,2-dichloroethane, benzene, and tertiary butyl alcohol. Solutions of 20% sodium persulfate and 2% of different alkaline sources were found to be most effective in bench scale tests. After the successful field demonstration, it was noted that dissolved oxygen levels increased in the underlying aquifer within about one month and persisted for about nine months. Ground water data as well as field test and bench-scale test data are presented in the paper.

Keywords: in-situ chemical oxidation, organic constituents of concern, aquifer, persulfate

[§] Corresponding Author: Richard C. Bost, 15810 Park Ten Place, Ste. 300, Houston, Texas, Tel: 281-600-1218, Email: rick.bost@erm.com

1. INTRODUCTION

In Situ Chemical Oxidation (ISCO) is a method for the introduction of chemical oxidants into the subsurface for the oxidation and destruction/mineralization of organic constituents as a remedial technology. However, for ISCO to be effective, the oxidant has to come into contact with the chemicals of concern (COCs). Typically this means injecting an oxidant into the affected soils and/or aquifer. While ISCO has been demonstrated to be effective at remediation of COCs within a subsurface zone of higher permeability, in areas where COCs have migrated into more clayey zones with low hydraulic conductivity, diffusion of the COCs out of the clayey zones following ISCO aquifer treatment has resulted in the rebounding of ground water concentrations following treatment.

This paper presents the results of a case study involving bench scale tests and a field-scale pilot test of the ISCO technology at a site to treat a mixture of compounds, many of which have been identified as recalcitrant. In addition, to address the issue of also treating clayeyer areas with low hydraulic conductivity, this paper presents the results of a field-scale pilot study that demonstrated the effectiveness of Mechanical Auger Mixing (MAM) using large six-foot diameter light augers as a means to incorporate ISCO into a predominately clayey subsurface to a depth of 25 feet below ground level.

1.1 Site Hydrogeology

Investigations at the site previously identified the local geology to be comprised of a surficial clayey zone found from approximately 0 to 18 feet below ground surface (bgs), a shallow transmissive zone from about 18 to 22 feet bgs, another clayey zone from about 22 to 30 feet bgs, a deeper transmissive zone from about 30 to 80 feet bgs, and a deeper clayey zone below 80 feet to approximately 180 feet bgs. The shallow transmissive zone is generally comprised of silts and clayey silts with occasional lenses of silty sand up to 2.5 feet thick. In contrast, the deeper aquifer is predominantly sand and is typically 50 to 55 feet thick. The shallow aquifer is confined by the surficial clay above and the underlying clay below while the deeper aquifer is confined by the overlying clay above and the deeper aquitard below. Aquifer tests indicate that the best conceptual model for the intermediate intervening clay unit is that of a “leaky” confining layer.

1.2 Site COCs and Mass Distribution

The constituents found in at the site were predominately chlorinated hydrocarbons, petroleum related hydrocarbons, and tert-butyl alcohol (TBA) and acetone. The predominated constituents found at the site, in order of mass, were 1,1-dichlorethane (1,1-DCA), vinyl chloride, benzene, TBA and acetone. While these five constituents accounted for most of the constituent mass at the site, over 20 other compounds had been reported present in soil and ground water samples. A mass balance of COC constituents in the soil indicated that in the source area about 40% of the mass was in the surficial clay, about 30% in the shallow sand, about 24% in the underlying clay and less than 1.0% in the dissolved phase in the shallow and deeper aquifer. Because of the large

percentage of overall mass in the surficial and intermediate clays, ISCO treatment in only the transmissive aquifers would only result in a small overall percentage reduction in COC mass and would leave significant mass in the clays that would over time migrate by infiltration or diffusion back into the sands. Therefore, the challenge is to effectively mix an oxidant into the clays. The method that was investigated in this case study was to use MAM to liquefy the upper clay while injecting an oxidant.

2. LITERATURE SEARCH

Prior to conducting the pilot test, an extensive literature search was conducted to assess the applicability of ISCO and to determine which of the oxidants on the market today would be the most effective at treating the constituents of concern (COCs) found in the shallow soils and ground water at the subject site. Based on the literature search, several studies were found that identified sodium persulfate as the oxidant that would be most effective at treating the site COCs. Two of the primary sources utilized include:

- Philip A. Block, Ph.D., Richard J. Watts, Ph.D., Amy L. Teel, Ph.D., Richard A. Brown, Ph.D: An Examination of Persulfate Activation and Reactivity, presented at the fourth International Conference on Oxidation and Reduction Technologies for In-Situ Treatment of Soil and Groundwater Marriott Chicago O'Hare, Chicago, Illinois, USA.
- Richard Brown, George Skladany, David Robinson; Joe Fiacco, John McTigue: Comparing Permanganate and Persulfate Treatment Effectiveness for Various Organic Contaminants, presented at The First International Conference on Oxidation and Reduction Technologies for In-Situ Treatment of Soil and Groundwater (ORTs-1) Niagara Falls, Ontario, Canada, June 25-29, 2001.

Based on these studies, bench-scale testing was conducted using samples of the site soil and ground water to assess the effectiveness of the persulfate on treating the site COCs in each media. Other oxidants, including percarbonate, were used to compare the effectiveness of the treatment. In addition, the bench-scale testing evaluated the use of cement mixing to stabilize the treated soils and the effects of cement on the oxidation process. The study also evaluated the effects of the soil mixing process on volatilization.

3. BENCH SCALE TESTING

Bench-scale studies were conducted to evaluate the effectiveness of ISCO and to provide additional data necessary for the design of the full scale implementation of MAM ISCO at the site.

The results of the bench-scale studies demonstrate that persulfate in an alkaline environment was more effective than persulfate alone at treating the site-specific COCs. While the reaction rate using persulfate was slower for some compounds (several days), the rates for reducing two of the more abundant COCs, benzene and vinyl chloride, to non-detectable levels were relatively rapid (a few hours). In the subsequent field studies, persulfate also proved to be more persistent

than percarbonate, lasting several days, whereas the percarbonate was used up very rapidly, making it ineffective for treating the slower reacting compounds.

3.1 Bench Scale Test Methodology and Results

The first study was conducted to demonstrate the effectiveness of In Situ Chemical Oxidation (ISCO) using alkaline persulfate to treat volatile organic compounds (VOCs) present at the site. The bench tests were conducted on the soil-ground water slurry under the following three conditions: 1) persulfate alone; 2) pH adjusted persulfate [with potassium hydroxide (KOH)]; and 3) a staged approach with an initial dose of persulfate followed by a dose of persulfate at an alkaline pH. These three conditions were measured against a control, which consisted of soil and ground water only. The tests were run in a sealed 500 mL centrifuge bottle. They were charged with 150 g of soil (sieved with a 4.75 mm screen) and 200 mL of ground water and the appropriate amounts of chemicals. Each test jar had about 200 mL of headspace. The headspace was not analyzed during the test for VOCs. The VOC data for the initial soil and ground water samples used to charge the bottles are listed in Table 1 as are the concentrations of the soil and water phases for the initial test conditions after mixing.

Table 1. Summary of T=0 Soil and Ground Water Analytical Results

ISCO Bench Scale Test		**Initial Char.**		**T=0**	
Parameter	**Units**	**Value**		**Value**	
Vinyl Chloride	ug/kg	<560	U	590	J
Acetone	ug/kg	3400		12000	
1,1-DCA	ug/kg	160	J	29000	J
1,2-DCA	ug/kg	<220	U	2500	
Benzene	ug/kg	<110	U	630	
Toluene	ug/kg	<560	U	<2500	U
TBA	ug/kg	1400	J	5100	J
2-Chloropropene	ug/kg	<560	U	5100	

Ground Water		**Initial Char.**		**T=0**
Parameter	**Units**	**Value**		**Value**
Vinyl Chloride	ug/L	8700		18000
Acetone	ug/L	59000		66000
1,1-DCA	ug/L	140000	J	220000
1,2-DCA	ug/L	10000		14000
Benzene	ug/L	1900		4800
Toluene	ug/L	<5000	U	<12000
TBA	ug/L	<100000	U	<250000
2-Chloropropene	ug/L	48000		98000

Notes: U = Not Detected J = Estimated Concentration

The supernatants from each of the three bench test slurries and the control were analyzed for pH, oxidation reduction potential (ORP), residual persulfate, and VOCs after 14 days and 28 days, respectively. Soils from the samples were analyzed for pH and VOCs. Table 2 presents the VOC data for the three test conditions in terms of the percent removal for each constituent relative to the control. The percent removal is given for both the aqueous phase and the total constituent mass.

Residual persulfate was also measured after 14 and 28 days by titration. The persulfate data is presented in Table 3, which also includes pH and ORP data. After 14 days, there was a 14 to 28% loss of persulfate. The persulfate/KOH test had the highest initial loss. The percent loss of persulfate after 28 days was 17 to 32%, which was not significantly greater than the initial loss. The persulfate loss was much less in the 14-28 day period than in the 0-14 day period, only 3.6 to 5.8% was lost. The results indicated that a persulfate/alkaline mix was more effective than persulfate only.

The data suggests that there was an initial consumption of persulfate. The iron present (12,000 mg/Kg) is probably reduced and reacted with the persulfate. Once the iron was oxidized, the persulfate appears to be fairly stable. On a stoichiometric basis, the iron present would have consumed about 10% of the persulfate added. This would account for the initial loss of persulfate.

The effectiveness of the persulfate/KOH requires that the pH be kept at 10 or above. This is generally accomplished by adding 0.5 moles of the alkaline, in this case KOH, per mole of persulfate. In addition, the natural soil acidity needs to be compensated for. This is generally done by titrating the soil to a pH of 10 and adding extra KOH to neutralize the soil based on this titration. It took 70 mL of 0.05 N KOH to raise the pH of 50g of soil to 10. The pH of the test jars was measured at 14 and 28 days (Table 3). The soil appears to be buffered as the pH of the persulfate only jar was 6.9 after 28 days. Typically, in the water phase only, the addition of persulfate drops the pH to < 2.0 due to the production of sulfuric acid.

The soil seems also to buffer the KOH. In the setup of the persulfate/KOH test, a 4-fold excess of KOH (based on a 0.5 mole ratio) was added. The pH of the jar was 12.5. With the staged test, after 14 days, KOH was added at a 0.5 mole ratio with a 50% excess. The pH only rose to 8.8 after 28 days, less than the expected pH of 10 – 11.

Table 2. Percent Change from Control ISCO Bench Scale Test

Aqueous Phase							
		Persulfate Only		Persulfate/KOH		Staged	
Constituent	**Units**	**14 Day**	**28 Day**	**14 Day**	**28 Day**	**14 Day**	**28 Day**
Vinyl Chloride	ug/L	86.7	--	96.1	97.8	65.7	9.1
Acetone	ug/L	-7.3	-54.3	98.6	99.5	-9.1	20
1,1-DCA	ug/L	34.1	61.3	99	98.7	-24.4	33.3
1,2-DCA	ug/L	7.4	28.1	99.5	99.4	-3.7	50
Benzene	ug/L	21.9	--	86.6	79	21.9	--
TBA	ug/L	-5.9	--	95.9	95	-41.2	--
2-Chloropropene	ug/L	92.3	80.2	97	97.1	96.9	91.9

Total COC Mass							
		Persulfate Only		Persulfate/KOH		Staged	
Constituent	**Units**	**14 Day**	**28 Day**	**14 Day**	**28 Day**	**14 Day**	**28 Day**
Vinyl Chloride	ug/L	86.7	--	96.1	97.8	65.7	--
Acetone	ug/L	-7.3	-48.4	98.6	99.4	-9.1	40.4
1,1-DCA	ug/L	34.1	61.3	99	98.7	-24.4	40.6
1,2-DCA	ug/L	7.4	31.5	99.5	99.5	-3.7	58.2
Benzene	ug/L	--	--	86.6	44.1	--	--
TBA	ug/L	-5.9	79	95.9	94	-41.2	--
2-Chloropropene	ug/L	90.6	78	97	97.3	96.9	92.7

NOTES:

Highlight denotes that one-half the detection limit was used for calculation.

"--" denotes that detection limit was too high to use in calculations

Table 3. Summary of pH, ORP, and Residual Oxidant Measurements

Day 14 Results					
Treatment		**pH**	**ORP**	**Persulfate (mg/L)**	**% Loss Persulfate**
1	Persulfate	6.7	528	42962	14.1
2	Persulfate + KOH	12.5	325	35801	28.4
3	Staged	7.1	518	41768	16.5
4	Control	7.8	427	0	--

NOTES:

1. 6.0 g sodium persulfate and 1.056 g KOH added to treatment 3.

Day 28 Results							
Treatment		**pH**	**ORP**	**Persulfate (mg/L)**	**% Loss Persulfate**	**% Loss Persulfate**	**Soil pH**
					0 – 28 days	**14 – 28 days**	
1	Persulfate	6.9	556	41172	17.7	3.6	7
2	Persulfate + KOH	12.5	347	34011	32	3.6	11.2
3	Staged	8.8	533	76224	22.2	5.8	8.8
4	Control	7.5	421	0	--		7.8

NOTES:

Soil pH measured with 10 g soil and 40 mL deionized water.

Based on the results of this bench scale test, it was observed that:

- A loss of VOCs in the controls was observed over the course of the tests, with the exception of TBA. This was likely due to volatilization into the headspace.
- The second observation was that the persulfate plus KOH was effective in oxidizing each of the VOCs present. In general this system resulted in a greater than 90% reduction of the VOCs.
- Vinyl chloride was easily oxidized, responding to both persulfate alone and persulfate/KOH. 1, 1-DCA and 1, 2-DCA, were resistant to oxidation and were only completely oxidized by the persulfate/KOH.

The persulfate/KOH worked well on each of the COCs. Persulfate alone did not have better reactivity for the COCs than the persulfate/KOH. In addition, there was no apparent benefit to staging the treatment. Based on the results of the initial bench scale study, a field scale pilot study was conducted.

4. FIELD SCALE PILOT TEST

The purpose of the MAM ISCO pilot study was to demonstrate the feasibility of in-situ soil mixing using a chemical oxidant and to provide information for preparing full scale remediation specifications. The objectives of the MAM ISCO pilot test were to assess whether:

- MAM would be effective at liquefying the clayey soil and achieving a small clod size;
- MAM would be capable of auger mixing to a depth of 25 feet in a reasonable time frame;
- MAM would be capable of injecting a chemical oxidant solution proven to be effective based on bench-scale testing;
- The resultant soil slurry created by the soil mixing with chemical oxidant solution can be amended with lime, cement or fly ash to restore its bearing strength; and
- Vapors and air emissions from a MAM pilot hole can be controlled via available control technologies and provide an emission rate to assess whether air emission controls are necessary.

4.1 Pilot Test Procedures

A specialized auger rig was used for the pilot test; it was capable of mixing oxidant and water with the site's clayey soils as it augered through them to create a slurry of treated soil. The equipment used was similar to that typically used for full-scale implementation of the remedy using this technology. The augers were 6 feet in diameter and created a 6-foot diameter treated column to 25 feet below ground surface (bgs). An initial test boring was completed to demonstrate the feasibility of the augering technology with a candidate oxidant mix followed by the completion of four additional borings to provide design information and data for alternative oxidant formulations.

Prior to drilling, a 5-foot deep pit was excavated at each drilling location to accommodate the expansion of the soils (fluff) due to the mixing process. Some of the excavated surficial soil was used to create small berms to divert stormwater from entering the excavations. The surficial soils, although they exhibited no odors or field OVM (flame ionization detector, FID OVM) readings above background, were placed in roll-off boxes for transport and disposal.

The following test mixtures and solidification agents were used for the test borings:

- Test Hole PT-1 - Initial Feasibility Test Case - 4 percent persulfate, 2.5 percent lime, and upper 5 feet mixed slowly with dry cement by the rig or backhoe;
- Test Hole PT-2 – Alternate Solidification Agent - 4 percent persulfate, 2.5 percent lime, and upper 5 feet mixed slowly with fly ash cement by the rig or backhoe;
- Test Hole PT-3 – Base Case – 4 percent persulfate, 2.5 percent lime, and 5 percent cement slurry in full column;
- Test Hole PT-4 - Alternative Oxidant – 2 percent percarbonate, 3 percent persulfate, 2.5 percent lime, and 5 percent cement slurry in full column; and
- Test Hole PT-5 – High Persulfate Effect on Solidification – 6 percent persulfate, 4 percent lime is increased to keep same ratio to persulfate), and 5 percent cement slurry in full column.

To restore the bearing strength of the ground surface, a 5% cement mixture was injected into the slurry. After mixing, samples of the fluff were collected to estimate clod size and to assess the extent of the slurry set-up as a result of cement addition.

Prior to initiating the pilot test, each MAM location was cored and sampled to provide baseline information for geotechnical parameters and initial VOA organic concentrations.

Following the injection phase of the pilot test, soil borings were installed in each of the pilot test pits to collect samples of the treated soil. Samples were collected at three depths and at three time intervals following the injection/mixing: Initial [T_1] (immediately following injection/mixing); Time 2 [T_2] (one week after injection/mixing); and Time 3 [T_3] (28 days after injection/mixing). These samples were collected to assess the effectiveness of different stabilizing agents (e.g., Portland cement and fly ash). These stabilizing agents are required to re-establish the bearing strength of the soil after mixing and treatment.

Samples of the soil mixtures were tested for VOA organics to test the effectiveness of the mixing process relative to the different mixtures injected. Samples were also collected to assess the amount of excess oxidant remaining in each test boring.

4.2 Pilot Test Results

The first objective of the pilot test entailed liquefying and breaking down the clayey soils to a clod size of approximately 4 to 5 inches or less in diameter. The following clod sizes were measured in the field for samples collected from the boring at the surface of the slurry, 10 ft bgs, and 20 ft bgs:

Sample Depth	Clod Size (inches)
Surface	Mostly less than 1 in. but ranges up to 2 in.
10 ft bgs	0.25 in to 1 in.
20 ft bgs	1.5 to 2 in.

Based on field observations, approximately 75% of the soil was liquefied and was present in the mixed slurry. Large clods (up to 1 foot in diameter) were observed on the auger bit when retrieved; however, the samples of the slurry collected at all three depths showed much smaller clod sizes.

Following mixing, the fluff filled four of the five pits to within one foot of the surface. The pit for boring PT-4 (fifth pit) overflowed due to the reaction of the percarbonate with the ground water creating carbon dioxide gas. This resulted in greater expansion of the soil mixture than was observed in the other test borings. The overall fluff expansion observed at each test boring indicated that the treated soil volume was approximately two (2) times the in situ soil volume.

The second and third objectives of mixing the soil with a chemical oxidant solution to a depth of 25 feet in a reasonable time frame were also achieved. The above results were obtained after augering to a depth of 25 feet and mixing during a total augering time period of approximately one hour. No impediments were encountered during the injection of oxidant solution through the auger jets.

A summary of the persulfate and COC analyses relative to the original design mixtures for each boring are provided in Tables 4 and 5. The data show that oxidant was effectively delivered to the applicable test boring depths. Higher concentrations of oxidant were found in several of the treated soil samples than anticipated from the initial design estimates. This finding is primarily attributed to the soil having a lower bulk density than was originally estimated.

Table 4. Summary of Persulfate and Percarbonate Analytical Results

		5-7 ft			15-17 ft			23-25 ft		
	Constituents	T_1	T_2	T_3	T_1	T_2	T_3	T_1	T_2	T_3
PT-1	Persulfate	0.89	1.79	1.19	6.54	1.19	0.56	8.92	1.79	2.38
PT-2	Persulfate	7.73	1.19	0.60	6.54	1.79	4.76	7.14	4.17	4.17
PT-3	Persulfate	6.54	1.79	2.98	7.73	2.38	2.08	7.14	1.79	2.38
PT-4	Persulfate	8.33	2.98	2.38	7.44	2.38	1.49	5.36	4.17	2.98
	Percarbonate	5.60	2.00	1.60	5.00	1.60	1.00	3.60	2.80	2.00
PT-5	Persulfate	1.79	2.98	2.38	5.06	6.55	2.68	6.54	4.76	2.98

Table 5. Comparison of Shallow Pilot Test Soil Results

	PT-1			PT-2		
Constituents	To 2/14/2006	T_1 2/20/2006	T_3 3/28/2006	To 2/14/2006	T_1 2/21/2006	T_3 3/28/2006
1,1-DCA	1.7	8.2	0.02	22	14	U
Acetone	U	0.17	U	U	3.7	U
Benzene	0.038	0.040	U	0.63	0.11	U
TBA	U	0.24	U	0.41	0.14	U
Vinyl chloride	2.7	0.91	0.003	4.9	1.3	0.0029
	PT-3			**PT-4**		
Constituents	To 2/14/2006	T_1 2/22/2006	T_3 3/28/2006	T_0 2/14/2006	T_1 2/22/2006	T_3 3/28/2006
1,1-DCA	20	27	U	76	U	U
Acetone	0.016 J	9.4	U	3.5	U	U
Benzene	0.2	0.58	U	2.3	U	U
TBA	0.4	0.41	U	0.47	U	U
Vinyl chloride	4.4	4.0	U	7.3	U	U

Table 5 Continued

	PT-5		
	T_0 2/14/2006	T_1 2/22/2006	T_3 3/28/2006
Constituents			
1,1-DCA	20	5.7	U
Acetone	U	0.18	U
Benzene	0.63	0.048	U
TBA	0.36	0.12	U
Vinyl chloride	2.8	0.39	U

NOTE: The typical detection limit for the COC analyses was 0.001 mg/kg

The fourth objective was also achieved. Fly ash, an inexpensive pozzolanic alternative to cement, was mixed with the slurry at the surface to solidify the slurry and re-establish the approximate bearing strength of the ground surface. Based on field observations the fly ash augmented slurry set up as expected.

The fifth objective of the pilot study was to conduct it safely and effectively while controlling air emissions. Previous site investigation test results were used to allow an initial excavation of five feet to create a bowl to contain the "fluff" (volume expansion) created by liquefying the soil column. No odors or sustained readings above background levels were noted during the excavation or augering. FID readings were also collected from the rig operator's cabin and no readings above background were observed.

During the pilot study the boring location, excavation, and auger were enclosed within a plastic shroud and air within the shroud was routed to a series of activated carbon canisters to remove organic from the emissions prior to discharge. A week after the injection tests, no sustained FID readings above background (0 ppm) were observed in the carbon canister exhaust. The influent monitoring results showed that a maximum sustained vapor concentration in the carbon canister influent was 84 ppm. Only an ephemeral 1.2 ppm was detected in the effluent. This data documents the effectiveness of the carbon canisters at adsorbing the vapors from the soil mixing prior to air discharge from the hood.

Additional observations made during the pilot test indicated the following:

- Treated soil volume was approximately two (2) times the in situ soil volume.
- Treated soil will not have sufficient strength to support reconstruction of a road over the treated area.
- Analytical results indicate that injection of persulfate as the oxidant can destroy in practice greater than 90% of the COCs in the ground water and soil. This estimate is based on bench-scale tests that demonstrate over 90% destruction of the most predominant COCs in a laboratory setting and on analytical results for soil samples collected before and after the pilot test that demonstrated nearly 100% destruction after treatment.

4.3 Post Pilot Ground Water Dissolved Oxygen Data Evaluation

Following the application of MAM ISCO to the upper 25 feet of soil, subsequent ground water monitoring indicated that the dissolved oxygen content of the shallow aquifer increased as expected, but data also indicated that the concentration of dissolved oxygen increased in the deeper aquifer within six weeks of the pilot study in a area underneath and adjacent to the location of the pilot study. Based on quarterly sampling data, the dissolved oxygen concentrations in the underlying deeper aquifer remained elevated for at least six months but had returned to pre-pilot study levels within a total of nine months. Table 6 summarizes the dissolved oxygen data for three wells in the S2 sand.

Table 6. Summary of Deep Aquifer Dissolved Oxygen Data

Date	Wells		
	A	B	C
11/22/05	0.47	0.35	0.60
02/02/06	0.42	0.40	0.35
03/29/06	5.46	1.25	0.55
09/07/06	2.54	2.20	0.17
12/07/06	0.24	0.18	0.17

Wells A and B are located just up gradient and down gradient, respectively, to the pilot study location with well A being located closer to the pilot study than well B. Well C is another deeper aquifer well, but it is located further away from and cross gradient to the pilot study location and is representative of other deeper aquifer wells further away from the location of the pilot study that did not show an increase of dissolved oxygen concentrations. The MAM ISCO field pilot study was conducted in mid-February 2006, shortly after an early February 2006 ground water sampling event. Such an increase in dissolved oxygen may have potentially acted to temporarily increase the aerobic biodegradation of some of the constituents present in the deeper aquifer.

5. CONCLUSIONS

The following conclusions can be drawn from the test results:

- Most remedial technologies would not be effective in treating the case study site due the inherent difficulty of inducing oxidant, water, or air/vapor penetration and transport through soils and sediments of low conductivity in which most of the site contaminants are bound.
- Mechanical auger mixing with a chemical oxidant represents a viable alternative for addressing sites where most of the mass is located in low permeability soils and sediments.
- Persulfate with an alkaline source for controlling pH and activating persulfate is effective in treating a complex mixture of oxygen-containing hydrocarbons, and chlorinated and non-chlorinated COCs.
- Mechanical auger mixing provided an effective means of introducing the oxidant and activator into clayey soils resulting in effective removal of over 95% of the COCs using persulfate at the demonstration site.
- The addition of cement does not impact the oxidation efficiency of the persulfate. There was not a significant difference observed between the COC reduction attained with alkaline activated oxidant with/or without cement addition.

Chapter 11

MUNICIPAL SOLID WASTE USED AS BIOETHANOL SOURCES AND ITS RELATED ENVIRONMENTAL IMPACTS

A. Li[1§], M. Khraisheh[1]
[1]*University College London, Department of Civil, Environmental & Geomatic Engineering, London WC1E 6BT, UK*

ABSTRACT

An investigation into the possibility of replacing the conventional biomass with biodegradable municipal solid waste, which provides an alternative solution for preventing the biodegradable fraction of municipal solid waste (BMSW) going into landfill required by EU Landfill Directives (1999/31/EC) was carried out. However, as every type of energy have some advantages as well as disadvantages. The use of BMSW as biomass sources for the production of bio-ethanol was investigated. The experimental results have shown that more than 90% of the cellulose from the waste can be converted to glucose which can be easily fermented to ethanol production. The potential impacts on related environmental issues, such as sustainable waste management, climate change, water issues, land use and biodiversity, are discussed. Sustainable waste management solutions are also discussed under different environmental, economic, and social scenarios.

Keywords: Biodegradable municipal solid waste (BMSW), bio-ethanol, biomass, sustainable waste management, environmental impacts

1. INTRODUCTION

Traditionally, ethanol is made from biomass such as corns, sugar canes and energy crops etc. Issues such as food shortage, land-use, and the needs of biofuel for transportation have been raised. The replacement of biomass with BMSW can bring the environmental advantages particularly in waste management, carbon dioxide cut, water quality and quantity control, land use and biodiversity.

This paper discusses the potential environmental impacts of using BMSW as bio-ethanol resources from both prospects of energy development and waste management as well as sustainable waste management solutions.

2. MATERIALS AND METHODS

§ University College London, Department of Civil, Environmental & Geomatic Engineering, London WC1E 6BT, UK, Email: aiduan.li@ucl.ac.uk

The BMSW-to-ethanol process is shown in Figure 1 which includes sample collection, pre-treatment, hydrolysis, fermentation, product recovery ad product distribution. The BMSW used in this study was selected from typical biodegradable waste, such as kitchen waste, garden waste and paper waste. The sample consists of 20% carrot peelings, 20% potato peelings, 20% grass, 20% newspaper, and 20% scrap paper. The selected waste was milled to small particles with size of 0.2mm-1.2mm, and then followed by pre-hydrolysis with sulphuric acid and steam treatment, and then enzymatic hydrolysis. Full details of the experimental procedures including sample preparation, pre-hydrolysis and enzymatic hydrolysis was given in Li et al., 2007.

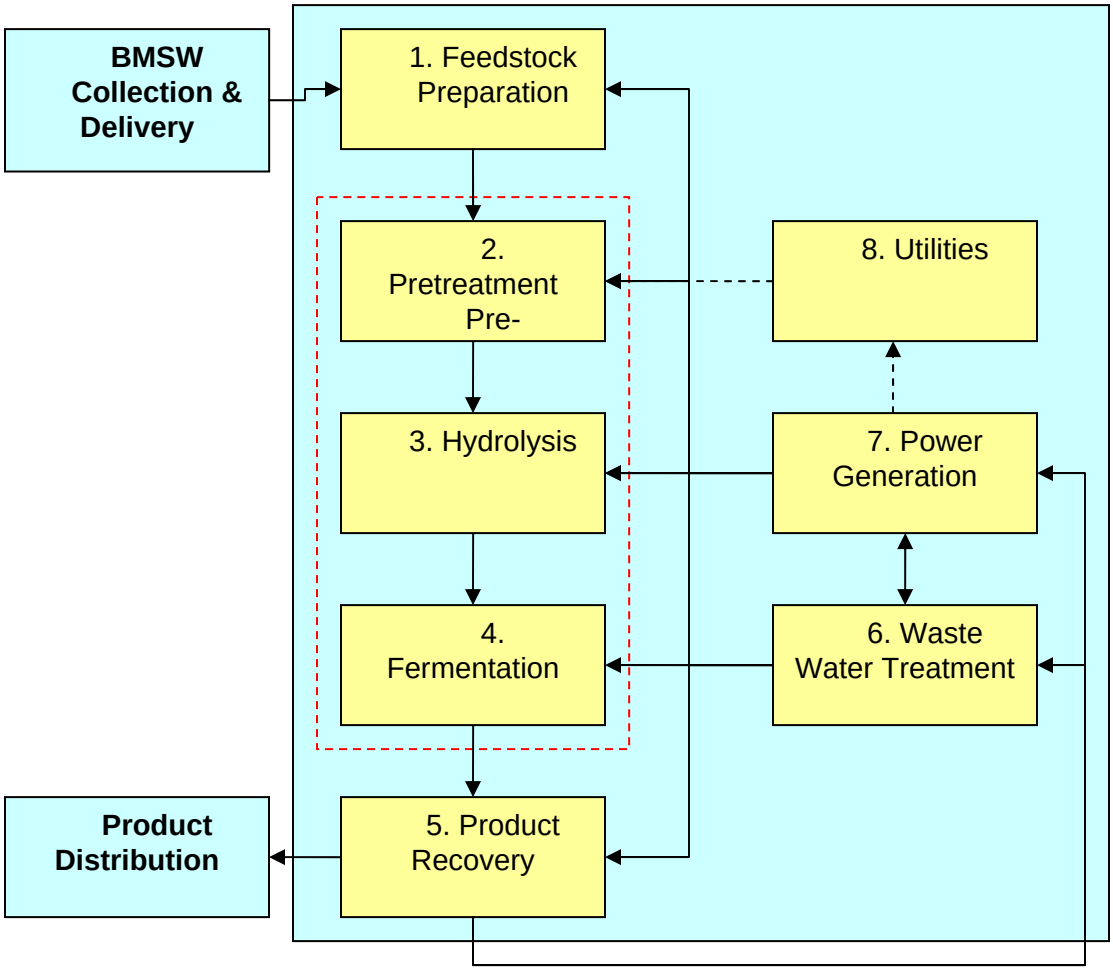

Figure 1. Simplified BMSW-to-ethanol process

The mass balances were calculated for two main steps: 1- from raw material to pre-hydrolysed biomass, and 2-to enzymatic hydrolysis residues, with consideration of the weight loss during each step.

The environmental impact assessment is based on the results from the laboratory work. The assessment covers a number of environmental issues such as waste management, carbon dioxide emission, water issue, land-use, biodiversity etc, by comparing with traditional biomass such as corn and energy crops.

The assessment of sustainable waste management is based on the sustainability of the application of this technology, by considering the environmental sustainability, economic viablity and social acceptance.

3. RESULTS AND DISCUSSIONS

A previous study (Li et al., 2007) showed that BMSW as a feedstock produced about 52% glucose for the production of ethanol. Recent studies on hydrolysis optimization showed that about 90% of glucose yield can be reached under the optimal conditions (lower substrate concentration, higher enzyme concentration, temperature 50˚C and pH 4.8).

Results from the mass balance revealed that about 0.25g biomass remained after pre-hydrolysis and 0.1g remained after the enzymatic hydrolysis process when 0.5g BMSW was used as feedstock. This indicated that about 80% of the biodegradable waste fractions were removed by using this BMSW-to-ethanol process.

The environmental impacts were assessed from the following areas: waste management, climate change, water issues, land use, biodiversity and others.

3.1 Waste management

Using BMSW as a resource for bio-ethanol production will reduce the biodegradable fraction from MSW going to landfill which is one of the requirements of EU Landfill Directives. According to the mass balance from the laboratory plant, the amount of waste will be massively reduced by 80% and the main composition of solid residues from the hydrolysis process are acid insoluble lignin, ash content, protein absorbed and dead cells, which can be used as compost. This technology can be used as an alternative solution for sustainable waste management and material/energy recovery.

3.2 Climate change

Ethanol represents the closed carbon dioxide cycle because after burning of ethanol, the released carbon dioxide is recycled back into plant material because plants use carbon dioxide to synthesize cellulose during the photosynthesis cycle (Wyman, 1999; Chandel et al., 2007). Ethanol production process only uses energy from renewable energy sources; no net carbon dioxide is added to the atmosphere, making ethanol an environmentally beneficial energy source. In addition, the toxicity of the exhaust emissions from ethanol is lower than that of petroleum sources (Wyman and Hinman, 1990). Apart from these, using BMSW as ethanol resources will

avoid the biodegradable fraction going to traditional waste disposal plant such as landfill or incineration which often causes green gas emissions.

3.3 Water issues

A large quantity of water is required to be used for growing energy crop which causes water shortage problems but there are also cases where there is plentiful water. One of the advantages is that irrigation can increase productivity surrounding plantations. For the ethanol process itself from both BMSW and energy crops, to produce 1 litre ethanol, 4-8 litres of water are required (Lang, 2007). And 13 litres of sewage effluent are produced per 1 litre of ethanol produced because of the water that has to be added to the ground corn grain for the fermentation process (Geotimes, 2005). Water remains a big issue for bio-ethanol process.

3.4 Land use

Growing energy crop for bio-ethanol purpose required lots of land use. Harvesting corn stover may result in lowering soil organic carbon levels and soil nitrogen content, and may also increase soil erosion (Mann et al., 2002). If agricultural prices are increasingly linked to energy prices then impacts on food security will also be more volatility in the markets. World prices usually account for less than 25% for any variation at country level. It is currently hard to model the effect of bio-fuels (ODI, 2007). Using BMSW as biomass can free the land used for landfill and growing energy crops.

3.5 Biodiversity

Input intensive energy crop production involves the movement of agrichemicals, especially nitrogen, phosphorus, and pesticides from farms to other habitats and aquifers. The use of BMSW for bio-ethanol purpose can avoid this problem.

Apart from the environmental impacts discussed above, this BMSW-to-ethanol system has its economic and social benefits. The end product: bio-ethanol is a valuable market product, which brings economic benefits from the non-valuable waste and meets the requirement of current energy market demands. However, this process requires the biodegradable waste fraction to be separated from non-biodegradable wastes from the households. The economic benefits with bio-fuel product will encourage waste separation. Waste management varies from developing nations to developed countries. Under different economic and social environment, different types of waste management methods from re-use, recycle, and energy/material recovery to disposal etc are used.

4. CONCLUSIONS

In conclusion, bioconversion of BMSW to bio-ethanol production has its environmental and economical advantages compared with traditional process with agriculture product. It can be

used as an alternative sustainable waste management option. Sustainable waste management needs to involve different type of waste management methods in order to minimize the waste produced, and maximize energy/material recovery and to meet the needs of environmentally, economically and socially sustainable.

5. REFERENCES

Chandel, A.K., Chan E.S., Rudravaram.R., Narasu, M.L., Rao. L, V., and Ravindra, P. 2007. Economics and environmental impact of bioethanol production technologies: an appraisal. Biotechnology and Molecular Biology Review 2 (1): 014-032

European Commission (EC). 2003. Directive 2003/30/EC of the European Parliament and of the Council of 8 May 2003 on the promotion of the use of biofuels or other renewable fuels for transport. Official Journal of European Union 123: 42–46.

Geotimes, 2005. Weighing in on Renewable Energy Efficiency.

Kathy Lang. 2007. Shellulosics – The Next Generation? Canada.

Li, A., Antizar-Ladislao, B., and Khraisheh, M. 2007. Bioconversion of municipal solid waste to glucose for bio-ethanol production. Bioprocess and Biosystems Engineering 30(3): 189-196.

Mann, L., Tolbert, V., and Cushman, J. 2002: Potential environmental effects of corn (Zea mays L.) stover removal with emphasis on soil organic matter and erosion. Agr Ecosyst Environ 89 (3): 149–166.

Overseas Development Institute (ODI). 2007. Biofuels and poverty reduction: Is there a way through the maize? London, UK.

Wyman, C.E., and Hinman, N.D.1990. Fundamentals of production from renewable feedstocks and use as transportation fuel. Appl Biochem. Biotechnol. 24/25: 735-75.

Wyman, C.E. 1999. Biomass ethanol: technical progress, opportunities, and commercial challenges. Annual Review Energy Environment 24: 189–226.

PART V: Environmental Fate

Chapter 12

EFFECTS OF REDUCING CONDITIONS ON THE FATE AND TRANSPORT OF RDX IN GROUNDWATER; A MULTIVARIATE APPROACH

Michael W. Morris[§] and Lonnie Fallin
Jacobs Engineering, 6 Otis Park Drive, Bourne, Massachusetts 02532

ABSTRACT

Groundwater investigations conducted at the Massachusetts Military Reservation (MMR) show the impact of historic activities on the development of groundwater contaminant plumes emanating from military ranges. Several of the plumes, located on the southeastern side of the reservation, contain elevated concentrations of hexahydro-1,3,5-trinitro-1,3,5-triazine (RDX). In most cases, these plumes show continuity from the source to the leading edge, indicating that very little attenuation of RDX is occurring in the aquifer. Interesting exceptions to this trend are locations where plumes consisting of RDX and perchlorate intercept part of the aquifer that was previously impacted by a fuel spill; reducing conditions due to biological activity resulted from this spill. RDX concentrations show a significant positive correlation with both dissolved oxygen and oxidation-reduction potential, and a significant negative correlation with specific conductivity. The distribution of RDX is more consistent upgradient from the oxygen depleted zone and implies that RDX is degrading in the aquifer near the fuel spill. A factor analysis yielded two geochemical (44 percent variability explained) and two contaminant (30 percent variability explained) factors. This suggests that the geochemical nature of the aquifer is the primary source of groundwater parameter variability determined by this investigation.

Keywords: RDX, perchlorate, groundwater contamination, correlation matrix, factor analysis

1. INTRODUCTION

Investigations of groundwater chemistry and contamination have been conducted on the Massachusetts Military Reservation (MMR) since the mid-1970s. These studies have focused on

[§] Michael W. Morris, Jacobs Engineering, 6 Otis Park Drive, Bourne, MA 02532, Tel: 508-743-0214, ext. 232, Email: mike.morris@jacobs.com

characterization and remediation of contaminated groundwater. The groundwater plumes are located in a sole source aquifer called the Sagamore Lens that occupies the northwestern portion of Cape Cod (Figure 1). The Sagamore Lens is an unconfined aquifer that occupies a series of glacial deposits primarily consisting of outwash as thick as 400 feet over bedrock. The sandy nature of the glacial deposits has created a groundwater setting that is highly transmissive. Therefore, much of the remediation for MMR contamination has focused on source control and groundwater plume extraction and treatment. Efforts to characterize these plumes are of particular interest to this study.

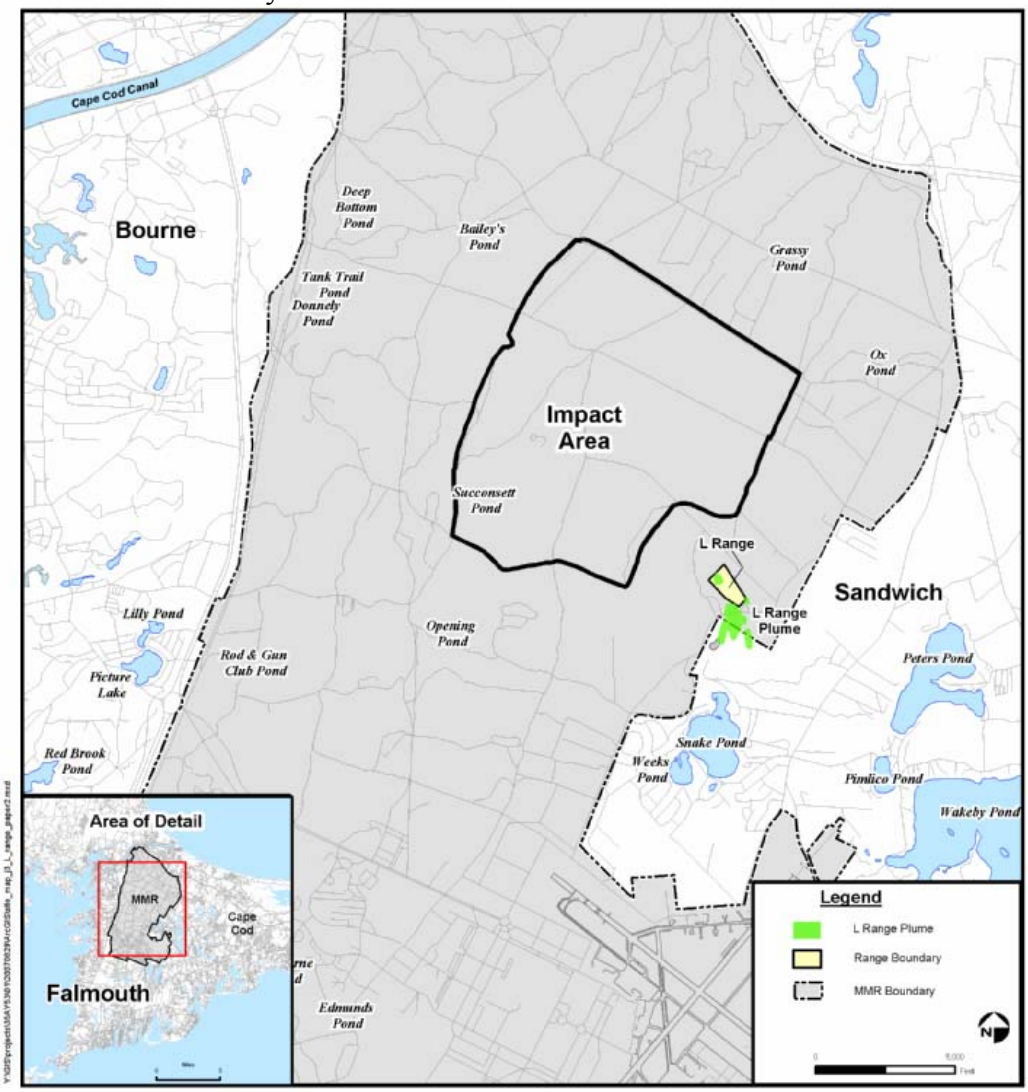

Figure 1. Location of L Range and L Range Plumes on the Massachusetts Military Reservation.

Both the MMR and areas outside the reservation are replete with groundwater wells. These wells have been placed to characterize contaminants in groundwater. Because these wells represent a heavily biased sampling, it is reasonable to ask what these wells are actually characterizing. The example in this investigation consists of a series of contaminant plumes emanating from a military test range on the MMR. This range exhibits groundwater contamination from the explosives hexahydro-1,3,5-trinitro-1,3,5-triazine (RDX) and octahydro-

1,3,5,7-tetranitro-1,3,5,7-tetrazocine (HMX), and from the propellant perchlorate. Since the groundwater monitoring network was designed to capture the variability of these three contaminants in the aquifer, it is reasonable to ask if this is actually what is shown within the groundwater data set. The purpose of this investigation is to explore what variability is actually characterized and what factors are responsible for this variability.

1.1 Site Setting

The MMR is a military training facility located in the western portion of Cape Cod that covers approximately 22,000 acres (Figure 1). The military began using portions of the MMR in the early 1900s; however, the majority of activity has occurred since 1935. The most intensive military activity at the MMR occurred during World War II.

The geologic setting of the MMR is dominated by Late Pleistocene deposits from processes attributed to the Late Wisconsinan ice front advance and retreat. Deposits on Cape Cod normally date no older than 18,000 to 22,000 years ago when the Laurentide Ice Sheet reached its maximum southward extent to the islands of Martha's Vineyard and Nantucket (Oldale, 2001; Dyke and Prest, 1987; Fletcher, 1993). The geology of the MMR is dominated by an outwash plain known as the Mashpee Pitted Plain. The Mashpee Pitted Plain was formed by streams that drained the Buzzards Bay and Cape Cod Bay glacial lobes (Oldale, 2001). The MMR is located within the Sagamore Lens of the Western Cape Cod aquifer. The Sagamore Lens is an unconfined freshwater aquifer bounded on three sides by salt water: Cape Cod Bay and Cape Cod Canal to the north, Buzzards Bay to the west, and Vineyard Sound to the south.

The L Range was primarily and most recently used as a grenade launcher range. The southern end of the range contains a berm upon which eight firing points are located along the southeastern boundary. The range extends northwest from the berm and there are multiple targets positioned at varying distances around the northern portion of the range. The L Range had been used historically as an infiltration range in the 1940s and 1950s and was converted to a grenade launcher range in the late 1970s. From the late 1980s the L Range was used exclusively as a grenade launcher range until activities were discontinued in 1997. These military activities resulted in the development of groundwater contamination plumes containing elevated levels of perchlorate and RDX downgradient from the range. The top of the groundwater mound is located a short distance northwest of the L Range and the general flow direction is south-southeast from the L Range. The perchlorate and RDX groundwater plumes are diffuse and occur as isolated, noncontiguous zones or lobes detached from upgradient source areas. The maximum perchlorate and RDX concentrations detected in the plumes are 2.8 µg/L and 9.2 µg/L, respectively. HMX has been detected at and less than 1 µg/L. The spatial and temporal distribution of perchlorate and RDX concentrations indicate very stable and attenuating plumes. The varying distance and depth of contamination lobes relative to the L Range footprint between the two primary contaminants suggest that there were multiple source areas, multiple release events, or differences in the chemical-specific subsurface migration and attenuation rates. The data do not indicate a continuing source. These plumes are believed to have been formed from low order detonations of grenades near target areas and subsequent particulate deposition of explosives across the soil surface (ECC, 2005). This particulate deposition has been noted in other range studies (Jenkins et al., 2000a; 2000b; 2001a; 2001b).

An interesting compounding factor is the development of the FS-12 plume. This plume was formed when an aviation fuel pipeline was breached and approximately 70,000 gallons of fuel leaked into the aquifer just south of the L Range. This plume consists primarily of ethylene dibromide and benzene with minor amounts toluene, ethylbenzene, and xylenes (AFCEE, 2001). The L Range plume is co-mingling with the FS-12 plume remnants, and the biological interaction between the former and latter plumes creates a unique geochemical environment that may influence the nature and extent of the L Range plume.

Once in the groundwater, perchlorate, RDX, and HMX are variably subject to transformations based on geochemical conditions. Perchlorate is relatively soluble and is not easily transformed once it reaches the aquifer. Susarla et al. (1999) has shown that the distribution coefficient (Kd) values for perchlorate range from 8.91 L/kg to 0.76 L/kg based on the type of organic matter and particle size in the matrix. Perchlorate does not adsorb readily to the soil matrix mineral fraction or organic fraction, and its transport is relatively rapid when it reaches groundwater. Perchlorate is not readily degraded by chemical or biological means. There is some indication of microbial reduction of perchlorate (Logan et al., 2001), but conditions in nature are relatively rare. In some bench scale tests, perchlorate has been shown to biodegrade under anaerobic conditions (AFCEE, 2002a). Regardless, perchlorate is a compound that migrates rapidly through groundwater with little degradation and is the most mobile contaminant in groundwater at the MMR.

RDX and HMX are not readily retained in the soil fraction and migrate to groundwater relatively rapidly. Reported Kd values for RDX under variable soil conditions ranged from 0 to 6.75 L/kg (Selim and Iskander, 1995; Townsend and Meyers, 1996; McGrath, 1995), and Kd values for HMX ranged from 0 to 13.25 L/kg (Townsend and Meyers, 1996). The highest Kd values for HMX are associated with reducing environments (Price et al., 2001). RDX and HMX are transformed anaerobically in the groundwater environment (Price et al., 1998; McCormick 1984). RDX and HMX are cyclic nitrogen-containing compounds that are moderately resistant to aerobic degradation and undergo ring cleavage and extensive mineralization (Hawari, 2000). Anaerobic degradation of RDX and HMX involves direct microbial reduction of the nitro functional groups on the cyclic structure. This process has been used to develop remedial strategies employing microbial degradation to address RDX and HMX contamination in groundwater (Kwon and Finneran, 2006; Young et al., 2006; Morley et al., 2002; Doppalapudi et al., 2002).

1.2 Background

Samples from the L Range groundwater study area were initially investigated using a correlation assessment. Correlation is a statistic that measures the strength of a relationship between two variables, quantified by the correlation coefficient (r). The correlation coefficient is a linear association between variables x and y. Correlation coefficients range from -1.0 to 1.0 with these extremes being the strongest negative and positive correlations respectively. No correlation between two variables would be represented by a correlation coefficient of 0.0. These correlation coefficients are then arranged in a correlation matrix to provide an overall perspective of how all of the variables in a dataset relate to each other. Correlation analyses are

sensitive to non-normality, and mathematical transforms are recommended to normalize non-normal data sets.

An integrated multivariate investigation was used to provide an overall picture of contaminant trends in the L Range plumes. Unlike a series of independent comparisons involved in constructing a correlation matrix, a multivariate investigation compares several variables in a single analysis with the goal of isolating trends in complex environmental data sets. This is accomplished with a multivariate factor analysis.

Factor Analysis, like the statistically similar Principal Components Analysis, is an exploratory multivariate method that can be used to explain the relationships among several variables. In the simplest sense, the Factor Analysis method arranges the sites and environmental variables in multidimensional space. Factor Analysis captures variability through the use of eigenvectors, which define linear factors that capture the maximum variability (i.e., environmental gradients) in a multivariate data set. Factor Analysis calculations result in clustering of sites (wells) based on their environmental similarity. In such an analysis, samples that occur close together have similar environmental characteristics, and samples that plot far apart are environmentally different. Likewise, environmental variables that lie near a specific variable tend to be "high" in that variable, and lower in others. Factor Analysis is particularly useful because it can provide a visual assessment of a large matrix of complex data by displaying relationships among variables and sites.

The Factor Analysis method extracts "principal components," also known as "factors" that explain variation in the data. The first axis explains the greatest amount of variance (i.e., has the highest eigenvalue). The second axis captures the second most important amount of variance orthogonal to the first axis. The third axis is orthogonal to the first two axes, and it captures the next most important component of the remaining variance. Factor Analysis deviates from Principle Components Analysis in that after the eigenvectors are defined, the factors are "rotated" to optimize the capture of the variability in the data set. This is accomplished through a varimax rotation that maintains the same orthogonal relationship as the original eigenvectors. If desired, Factor Analysis calculations may continue until only random variation remains, but in most environmental data sets, four or fewer factors often explain most, if not all, of the nonrandom variation. In turn, the factor scores can be calculated for each data point (well), and predicted factor scores can be calculated for each well and plotted in multiple dimensions. Generally, eigenvalues that are greater than one are retained, and factors that explain a cumulative variation between 80 and 90 percent are considered important (Manly, 1991).

Statistical analyses of groundwater have long provided insight into the distribution of analytes within a defined aquifer or groundwater location of concern. Gonçalves et al. (2007) used a factor analyses to determine the effect of agricultural practices on distribution of pesticides and their impacts on water quality in Portugal. They found that five principal components were attributed to environmental and agrochemical managing factors. The distribution of pesticides detected in groundwater was related to the character of local agricultural practices. Chen et al. (2006) examined 17 trace elements in groundwater samples from Shenzhan, China. Their principal components analysis found that the oxidizing and reducing conditions in the aquifer were primarily responsible for the distribution of metals in the aquifer and that the seasonality of the groundwater sampling was of lesser importance in defining

this variability. A Factor Analysis study of groundwater at a landfill site in Nagpur, India (Pujari and Deshpande, 2005) showed that five factors (including geological setting, leaching from host rock, leachate of heavy metals from the landfill, and bacterial contamination from the landfill) were responsible for the variability in this aquifer. A Factor Analysis conducted on groundwater in the Everglades National Park (Muñoz-Carpena et al., 2005) examined the variability of nitrate, phosphate, fluoride, and chloride anions. They found that nitrate and phosphate compounds were affected by water table depth, enriched topsoil, and occurrence of a leaching rainfall event. The Factor Analysis indicated that leaching by rainfall was the main mechanism explaining concentration peaks in groundwater. A groundwater Factor Analysis was applied to 13 hydrochemical parameters in Taiwan to determine the causes of variability in a blackfoot disease area (Liu et al., 2003). The study isolated two factors (seawater salinization and arsenic pollutant) that explained almost 78 percent of the variability. This study found that overpumping of groundwater led to subsidence, which caused introduction of more saline seawater into the water supply, thus possibly causing complicating health problems. A study by Reghunath et al. (2002) of groundwater in Karnataka, India showed that variability, defined by a Factor Analysis, could be attributed to various degrees of mixing between river and groundwater. A study in northwest Peloponnesus, Greece used Factor Analysis to explain the variability in a Plio-Pleistocene aquifer (Voudouris, et al., 1997). This study found that seawater intrusion and possible groundwater-halite interaction was responsible for the variability of analytes in the aquifer. A study of groundwater in Western Nigeria (Olobaniyi and Owoyemi, 2006) used factor analysis to understand the variability in the deltaic plain sands aquifer, and study isolated three factors: the first factor was interpreted to reflect the signature of saline water incursion resulting from seepages into the aquifer from the tide-influenced River Warri. The second factor was attributed to the processes of natural rainwater recharge and water-soil/rock interaction. The third factor was related to the dissolution of sulfides from interstratified peat within the geological formation. A Factor Analysis study in the Mogi-Pardo watershed in Brazil (Invernizzi and Barros de Oliveira, 2004) found that two factors explained the variability in the groundwater dataset. The first factor represented the flushing of evaporate minerals, and the second factor represented the progressive interaction between the water and the Botucatu Formation along the flow gradient from the recharge zone to the zone confined by basalt lavas. It is interesting to note that the theme among all of these studies is that geochemical variability in the aquifer is often the most important factor in defining the variability, particularly among contaminants in groundwater.

2. METHODS AND MATERIALS

Data for the multivariate investigation were collected from monitoring wells and groundwater screening borings in the vicinity of the L Range. Groundwater samples were collected in accordance with approved workplans (AMEC, 2004) and were analyzed for explosives by U.S. Environmental Protection Agency (EPA) Method SW846/8330 and for perchlorate by EPA Method E314.0. Metals analyses were conducted using EPA Method SW846/60108/7470A, and field parameters were collected using a Yellow Springs Instrument water analyzer with a flow through cell. Wells used in the study were installed as part of the L Range characterization and are presented on Figure 2. All monitoring well locations were surveyed, and horizontal position was referenced to the North American Datum of 1983,

Universal Transverse Mercator Zone 19 North in meters. The vertical datum was referenced with an accuracy of 0.005 ft vertical/horizontal control to the North American Datum of 1927 in feet. Summary statistics for L Range groundwater is presented in Table 1.

Table 1. L Range Groundwater Summary Statistics

Parameter	n	Mean	Median	Range
RDX (µg/L)	354	0.58	ND	ND to 9.2
HMX (µg/L)	352	ND	ND	ND to 0.8
Perchlorate (µg/L)	315	ND	ND	ND to 2.8
Total Fe (µg/L)	20	23,800	74.25	ND to 99,400
Total Mn (µg/L)	20	475	60.8	ND to 2,260
Temperature (°C)	335	11.37	11.10	4.5 to 18.7
pH	344	5.77	5.78	4.06 to 7.17
DO (mg/L)	362	6.98	8.66	0.08 to 15.97
ORP (mV)	99	192	213	-238 to 507
SpC (µS/cm)	343	105	74	38 to 554
Turbidity (ntu)	289	3.08	1.22	0 to 65.9
Elevation (ft msl)	423	3.80	8.74	-127.84 to 70.04
Northing (m)	423	-	-	484
Easting (m)	423	-	-	1230

Data from 425 groundwater samples collected from 42 well locations (many of which contain multiple screens) between January 1998 and May 2007 were used in this investigation. For the statistical analyses, the non-detect data were transformed to one-half the detection limit. The data were screened for outliers; however, none were removed from the dataset. After these treatments, the data were subjected to Correlation Analysis and Factor Analysis.

Intervariable comparisons were made for analyte pairs (e.g., RDX vs. perchlorate, or HMX vs dissolved oxygen [DO]) measured in the L Range study area. A correlation matrix was generated to address information about relationships among specific parameters. These parameters included RDX, HMX, perchlorate, total iron, total manganese, DO, oxidation-

reduction potential (ORP), pH, temperature, specific conductivity (SpC), turbidity, easting coordinate, northing coordinate, and elevation. Because not all locations were analyzed for all parameters, there were a number of null data points in the measured data set, so the number of pairwise comparisons in correlation calculations ranged from 423 (northing vs easting) to 13 (manganese vs. ORP). The Spearman Ranked Correlation procedure was used for this analysis. This is a nonparametric procedure used when data distributions express nonlinearity that would affect parametric tests. This procedure was used because many of the data points for perchlorate, RDX, and HMX were below the detection limits, assuring a non-normal distribution of values. In general, a greater number of pairwise comparisons increases the statistical strength of the correlation analysis. A value of 0.0 indicates no correlation between variables. A value of $\alpha = 0.05$ was chosen as the significance level for this analysis.

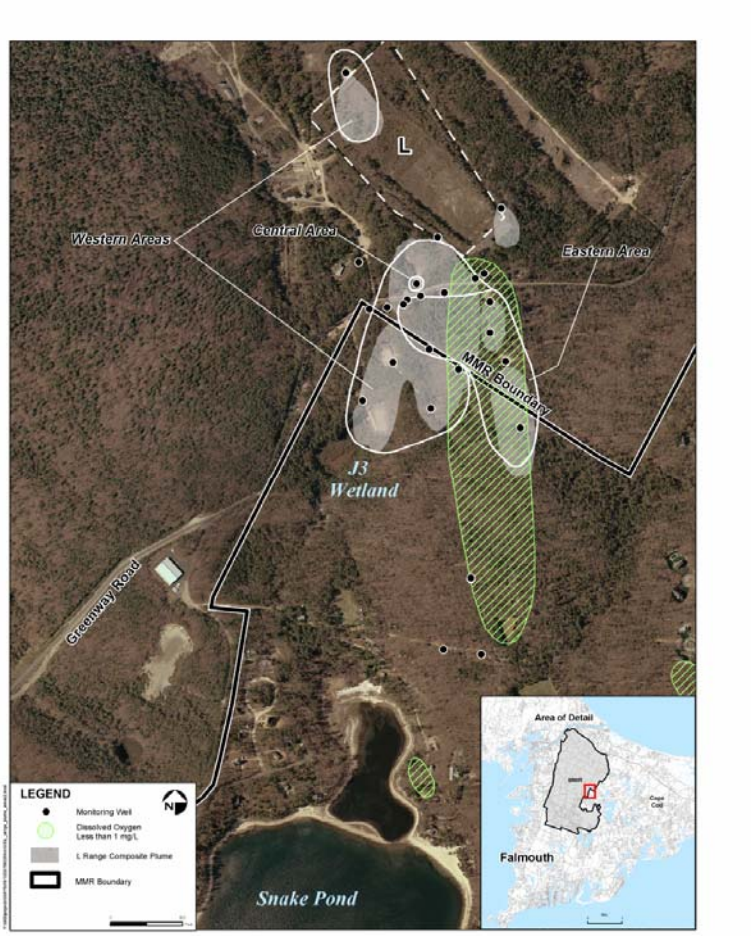

Figure 2. Location of L Range Groundwater Study Area, Factor Analysis Groundwater Zones, and anoxic zone.

The Factor Analysis procedure for this investigation used the following variables: perchlorate, RDX, HMX, pH, temperature, DO, ORP, SpC, turbidity, northing, easting, and elevation. The Factor Analysis procedure required that all cells be filled for each row; therefore, a missed analyte removed that sampling point data from the analysis. Because sampling of explosives and perchlorate were sometimes on different schedules, a large number of observations were removed from the analysis because perchlorate was frequently sampled on a different date than explosives. A total of 48 observations were retained for the Factor Analysis due to their data completeness.

3. RESULTS

The statistical analyses performed for groundwater samples from L Range indicated that the chemistry of the aquifer was the primary factor affecting the variability that is observed within the aquifer. The distribution of contaminants (perchlorate, RDX, HMX) is not only a result of anthropogenic deposition, but also the result of post-depositional processes that govern the nature of these groundwater plumes.

The correlation analysis for perchlorate indicated that this analyte had a significant relationship to a few other parameters (Table 2). Perchlorate was significantly positively correlated with RDX (r = 0.l67), temperature (r = 0.183), and DO (r = 0.126). This relationship reveals that there is some co-location of perchlorate (a propellant) with RDX (an explosive) and indicates either similar depositional processes or extensive co-mingling of the plume. The high correlation with temperature is primarily a result of the shallow nature of the perchlorate contamination because the temperature in the aquifer decreases with depth. The high correlation with DO indicates that the perchlorate contamination, found mainly in the western portion of the L Range plumes (Figure 2) is located in an area not affected by the reducing conditions caused by the FS-12 Plume farther east.

The correlation analysis shows that RDX and HMX are significantly positively correlated with each other (r = 0.635), indicating that these two explosive compounds are likely from the same source(s) (Table 2). RDX and HMX are significantly negatively correlated with SpC (r = -0.186 and -0.128, respectively) and temperature (r = -0.133 and -0.209, respectively). The negative correlation between SpC and each of these explosives is likely due to the contaminants' preference for the more oxic portions of the aquifer and, therefore, lower concentrations of soluble metals and lower SpC values. The negative correlation with temperature could be an indication of the location of these compounds in the deeper portions of the aquifer where temperatures are cooler. This is also observed in the negative correlation between RDX and elevation (r = -0.322), confirming the higher occurrence of RDX in the deeper portions of the aquifer. This could be the result of RDX source areas farther upgradient and thus occupying the lower portions of the aquifer with increasing distance from the source. In addition, RDX has high positive correlations with DO and ORP (r = 0.157 and 0.233, respectively). Because RDX is likely to decompose under reducing conditions, this correlation is reasonable (Table 2)

Table 2. Correlation Matrix for L Range Groundwater

	Perc	RDX	HMX	Fe	Mn	pH	Temp	DO	ORP	SpC	Turb	North	East	Elev
Perc	**1.000**													
RDX	**0.167**	**1.000**												
HMX	-0.018	**0.635**	**1.000**											
Fe	-0.313	-0.393	-0.379	**1.000**										
Mn	**-0.567**	-0.050	-0.359	**0.756**	**1.000**									
pH	-0.101	-0.088	-0.051	**0.620**	**0.736**	**1.000**								
Temp	**0.183**	**0.133**	**0.209**	0.111	0.430	**0.187**	**1.000**							
DO	**0.126**	**0.157**	0.039	**0.681**	**0.893**	**0.465**	0.030	**1.000**						
ORP	0.077	**0.233**	0.079	0.453	0.445	**0.440**	0.013	**0.676**	**1.000**					
SpC	-0.086	**0.186**	**0.128**	**0.775**	**0.552**	**0.329**	0.011	**0.643**	**0.640**	**1.000**				
Turb	-0.115	-0.025	0.077	**0.912**	**0.750**	**0.266**	0.033	**0.241**	0.131	**0.181**	**1.000**			
North	0.094	0.072	0.022	**0.491**	**0.511**	0.026	0.001	**0.228**	**0.300**	**0.240**	0.020	**1.000**		
East	-0.007	**0.116**	**0.110**	**0.628**	**0.861**	**0.240**	0.068	**0.540**	**0.363**	**0.439**	**0.209**	0.031	**1.000**	
Elev	-0.095	**0.322**	0.103	**0.660**	0.373	0.054	0.034	**0.146**	**0.299**	**0.381**	0.097	**0.232**	**0.187**	**1.000**

Notes: Coefficients in **BOLD** are considered significant at alpha = 0.0

Total iron and manganese concentrations were included in the correlation analysis because these metals are sensitive to reducing conditions and are generally more common in anoxic portions of an aquifer. The development of the FS-12 plume, located downgradient from the L Range, provided a carbon source for bacteria; from its benzene, toluene, ethylbenzene, and xylenes (AFCEE, 2001). This fuel spill created an anoxic to suboxic zone in the aquifer (Figure 2). As expected, total iron and manganese are significantly positively correlated with SpC and each other, and are significantly negatively correlated with ORP and DO (Table 2). There is also a significant positive correlation with both pH (which is interpreted as an indicator of biological activity) and turbidity. The turbidity could be related to fines in the aquifer that bear these metals, but it could also be attributed to by-products of biological degradation. The correlation coefficients for these two metals are much higher than the correlation coefficients for the explosives and perchlorate. This is partially due to a lower number of samples, which makes higher correlation coefficients necessary to meet the level of significance. It is also important to note that there is only one significant correlation between total manganese and perchlorate. In fact all of the correlations between these metals and the explosives are negative but insignificant, indicating that these analytes do not necessarily occupy the same portions of the aquifer. This analysis confirms that there is an active anoxic zone in the aquifer located downgradient from the L Range that has a significant effect on the aquifer's geochemistry.

The Factor Analysis also showed that the aquifer's geochemistry is the primary factor dictating the distribution of contaminants in the aquifer (Table 3). A total of five factors were identified that explained more than 87 percent of the variability in the data set. The first factor explains approximately 25 percent of the total variability, and this factor is loaded on two geochemical parameters. Factor 1 is mostly influenced by the easting of the well with contributions from both DO and SpC (Table3). The negative easting and SpC and the positive DO factor loadings demonstrate that increasing DO is negatively associated with easting and SpC which shows that the areas of the aquifer with low SpC and high DO occupy the more western portion of the site. This indicates that the presence (or absence) of reducing conditions in the aquifer is primarily responsible for the variability of the parameters used in this Factor Analysis. One of the unique qualities of a Factor Analysis is that the varimax rotation strengthens the factor loadings, and these combinations of variables can be interpreted and named (Manly, 1991). In this case, Factor 1 would be the oxic/anoxic water quality factor.

Factor 2, which explains almost 20 percent of the variation in the dataset, has factor loadings on the pH and turbidity parameters (Table 3). The pH in this aquifer has two major sources of variability. First, there is a low to high pH gradient with depth that has been noted in other MMR studies (ECC, 2006). This gradient has been attributed to recharge by acid rain and the influx of organic acids released by the predominantly acid-soil tolerant vegetation on the MMR. Higher pH values are also noted in other areas of the MMR exhibiting elevated biological activity, such as near fuel spills and sewage discharge areas (AFCEE, 2001; 2002b). Factor 2 is determined to be biological because the combined higher pH and turbidity are associated with biological activity in the reducing zone (i.e., the remnants of the former fuel spill). The pH in the reducing zone can be raised by iron bacteria, which form ammonia by metabolizing certain protein or protein derived materials and synthesize alkali hydroxyl groups by consuming the salts of organic acids. The presence of these bacteria and by-products can lead to occlusion and increased turbidity.

Table 3. Eigenvalues and Factor Loadings for L Range Groundwater

Factor	1	2	3	4	5
Eigenvalue	1.90593	1.51169	1.36542	1.02061	0.89083
Variability Explained (%)	24.65	19.55	17.66	13.20	11.52
Cumulative Variability (%)	24.65	44.2	61.86	75.06	86.58
Factor Loadings After Varimax Rotation					
Perchlorate	0.162871	-0.045954	**0.775064**	0.063321	-0.063346
RDX	0.034555	-0.165173	0.027123	**-0.528309**	-0.138301
HMX	0.186822	-0.115209	-0.22436	-0.201112	-0.144153
pH	-0.211025	**0.859164**	-0.011842	-0.053552	-0.056475
Temperature	-0.377075	-0.293366	**0.457436**	0.017534	-0.251397
DO	**0.713282**	-0.144288	0.012391	-0.241942	-0.350318
ORP	0.232568	-0.156122	-0.200806	-0.249305	-0.344063
SpC	**-0.594435**	-0.017736	**0.663904**	0.186991	0.234547
Turbidity	-0.105161	**0.662933**	-0.096222	0.143898	-0.123877
Northing	0.115200	0.234282	0.057466	-0.087637	**-0.676596**
Easting	**-0.845562**	0.248292	-0.091189	-0.038476	-0.018001
Elevation	-0.032654	-0.208017	0.227928	**0.712981**	-0.104661

A plot of factor scores between Factor 1 and Factor 2 shows how the wells in the eastern, central and western portions of the study area arrange themselves in two-dimensional space (Figure 3). The wells were organized according to their location (east, central, west) or whether they had measurable levels of contaminants (i.e plume vs. non-plume wells). In general, the eastern area contained the RDX plumes, the western area contained the perchlorate plumes, and the central area contained one location (two wells) that had measurable levels of HMX (as shown in Figure 2). Figure 3 shows how the eastern areas (i.e., the RDX plumes) plot to the left in the direction of higher SpC values and lower DO values, and the western areas (i.e., the perchlorate plumes) plot toward the lower right quadrant in the direction of higher DO and lower SpC values. A line divides the eastern portion into two sections on Figure 2. The left side of the line represents eastern portion wells where RDX has not been detected since 2002 and the right side of the line represents eastern portion wells that have had RDX detected after 2002. The eastern portion wells on the left had side of the dividing line are all located within the portion of the aquifer characterized by reducing conditions. This is the reason the eastern portion wells plot in the same direction as the non-plume wells because RDX is degrading over time. The Factor 2 axis is weighted with pH and turbidity, therefore, as expected, the western portion of the study area plots in the lower half of the graph and the eastern, perchlorate free zones plot in the upper half. The central portion plots as a subsection of the western portion and this part of the aquifer is likely related to the western portion based on Factors 1 and 2. The non-plume portion plots in the upper left quadrant, indicating that these wells are high primarily in pH and turbidity. It is important to note that there is a relationship between non-plume areas and the presence of biologically active reducing conditions.

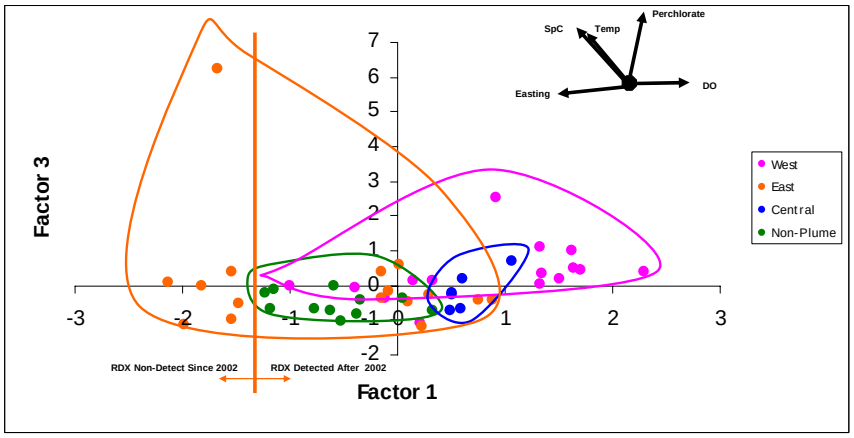

Figure 3. L Range Groundwater Factor Analysis, Factor 1 vs. Factor 2

Factor 3 is weighted mostly on perchlorate concentrations, temperature, and SpC, making this the perchlorate factor (Table 3). This factor accounts for approximately 16 percent of the variability in the groundwater dataset; and indicates that portions of the aquifer with elevated perchlorate, groundwater temperatures, and SpC differentiate from lower perchlorate, lower temperature, and lower SpC portions of the aquifer. An examination of the plots of Factor 1 vs. Factor 3 (Figure 4) with Factor 1 on the x-axis and Factor 3 on the y-axis shows how Factor 3 helps define the groundwater areas. The central area, with measurable HMX concentrations, plots as a subset of the western area. The western portion of the study area plots to the upper right quadrant toward high perchlorate and high DO, while the eastern portion plots to the left toward low perchlorate and high SpC. The non-plume area plots as a subset of the eastern portion of the study area. This graph mainly shows the difference between areas with measurable levels of perchlorate and areas devoid of perchlorate.

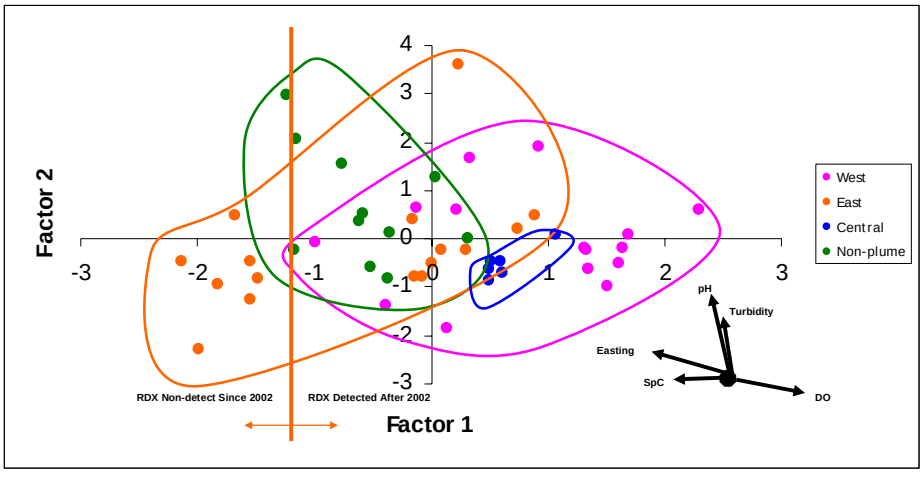

Figure 4. L Range Groundwater Factor Analysis, Factor 1 vs. Factor 3

Factor 4 is negatively loaded on the RDX parameter and positively loaded on the elevation parameter (Table 3). Factor 4 is the RDX factor, and implies that there is a general increase in RDX values with depth. This factor explains almost 13 percent of the variability in the dataset.

Figure 5 shows a plot between Factor 1 and Factor 4. While much of the discrimination is along the x-axis (Factor 1), the eastern portion of the aquifer shows a tendency to plot in the direction of high RDX and increased depth. The western, central, and non-plume areas plot more in the direction of the upper half of the graph. It is interesting to note that the left hand side of the eastern portion dividing line shows that the wells where RDX was not detected after 2002 plots similarly to non-plume wells. Therefore, the variability explained by Factor 4 is primarily due to the increased presence of RDX with depth in the plume.

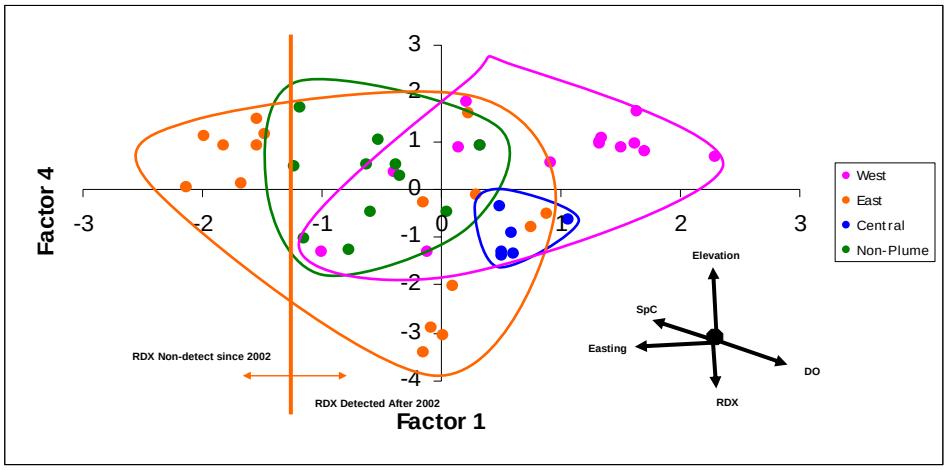

Figure 5. L Range Groundwater Factor Analysis, Factor 1 vs. Factor 4

The remaining Factor 5 explains almost 12 percent of the variability and is weighted on a single variable, northing (Table 3). This factor is negatively weighted with all other factors based on a comparison to the contaminants and indicates that there is a relationship between the north to south well location and decreasing to increasing contaminant concentrations. The correlation analysis (Table 2) indicates that the DO, ORP, and SpC have the strongest relationship to the northing parameter with decreasing values of DO and ORP and increasing values of SpC from north to south.

4. DISCUSSION

The results of the Correlation and Factor Analyses indicate that there is a relationship between the geochemistry of the aquifer and the distribution of contaminants in the aquifer downgradient from the L Range. The correlations between the contaminants (i.e., perchlorate, RDX, and HMX) and geochemical parameters (e.g., DO, ORP, and SpC) indicate that the geochemical parameters are of primary importance in determining the distribution of the contaminants in the aquifer. Significant correlations between RDX and the parameters related to oxidizing and reducing conditions in the aquifer show the importance of a former fuel spill in characterizing the distribution of the contaminants. The biological interaction with the fuels from the FS-12 plume has created a zone of water that, due to oxygen depletion by biological organisms, is a chemically reduced area in the aquifer. In turn, these reducing conditions create an environment conducive to reducible metal solubility. Under oxygen depleted conditions, easily reducible metals such as iron and manganese, tend to go into or remain in solution rather

than precipitate into the solid phase. This increases the electrical conductivity of the water downgradient from the fuel spill. The relationship between perchlorate, RDX, and HMX with these geochemical conditions has potential implication for the distribution of these contaminants in the aquifer. Generally, the concentrations of perchlorate, RDX, and HMX are lower inside and higher outside of the FS-12 source area. This relationship implies that RDX and HMX are degrading in the aquifer near the fuel spill. Perchlorate is absent in the area of the fuel spill mainly because it occupies a flow path that is west of the low DO area. Biodegradation is one explanation for the decreasing levels of RDX and HMX near the fuel spill. An alternative explanation is the reduction of nitroaromatic compounds to primary amines by an oxidation-reduction reaction with metals where the reduced metals act as a reducing agent and the nitro-compounds are reduced. A third explanation for higher RDX and HMX concentrations north of the FS-12 plume could be the attenuation of explosives through dispersion.

The primary source of contamination at the L Range area is probably from historical use of grenades and possibly mortars to produce localized discrete areas of contamination. A conceptual site model for the L Range is presented in Figure 6. During use, explosives would have detonated near targets and propellants would have accumulated near the firing points. The sources would have accumulated particulates on or near the ground surface. Groundwater modeling (ECC, 2005) suggests that rather than a widespread diffuse source, fewer small area sources of higher concentration may have dispersed particles or larger pieces, and infiltration would act to dissolve the constituent compounds and transport them to groundwater. The heterogeneous nature of the source deposition combined with the episodic pattern of infiltration would have resulted in a heterogeneous (in both space and time) contaminant source to groundwater. On the soil surface or in the aerobic vadose zone, little degradation of RDX, HMX or perchlorate would have occurred.

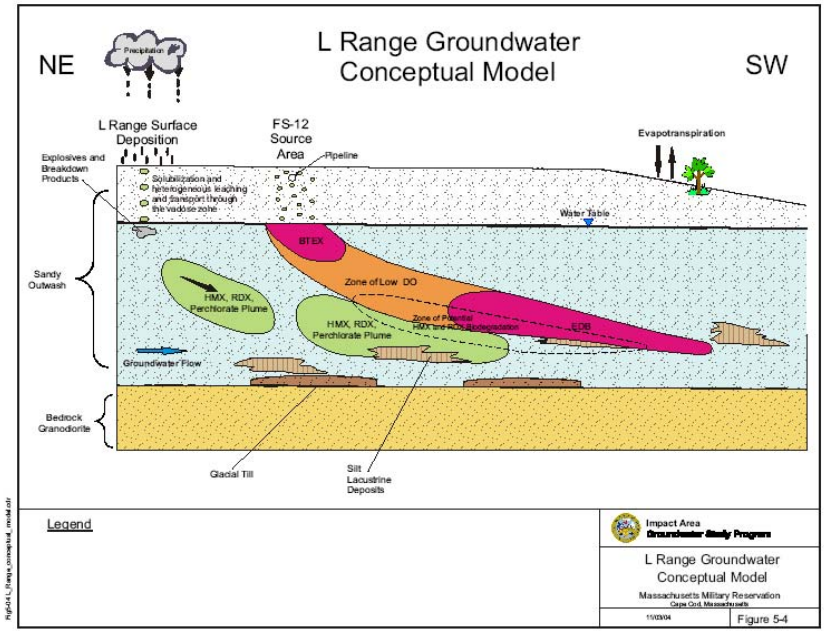

Figure 6. L Range Site Groundwater Conceptual Model (Source: ECC 2005).

Once in the saturated zone, RDX, HMX, and perchlorate migrate under the influence of the flow patterns, which are generally south to southeast. Because both RDX and HMX can be degraded under anaerobic conditions, any local anaerobic conditions due to the FS-12 plume may facilitate the degradation of the RDX and HMX, and hence contribute to the laterally and vertically discontinuous distribution of RDX and HMX in L Range groundwater. Statistical correlations between RDX and HMX with parameters such as DO and ORP (positive) and SpC (negative) indicate these compounds' preference for the more oxic portions of the aquifer. This may also indicate that the absence of these compounds in the anaerobic portions of the aquifer means the breakdown of these compounds. The results of the Factor Analysis show that Factor 1, the oxic/anoxic aquifer quality factor, is the primary factor that defines the variability of the parameters within the L Range aquifer. The second derived factor is a biological factor weighted on pH and turbidity. These geochemical properties explain more than 44 percent of the variation in the groundwater dataset. The third and fourth factors are perchlorate and RDX factors and explain more than 30 percent of the variation. Although they are of lesser importance, their contribution to variability is significant based on the Factor Analysis. Therefore, the sampling design for the L Range groundwater not only accomplished its goal of defining the distribution of contaminants in the aquifer, but also managed to show that the geochemical parameters are of the utmost importance in defining the distribution of all parameters within the aquifer.

5. CONCLUSIONS

Many of the investigations on the MMR, including those on the L Range, have emphasized the placement of groundwater wells in order to characterize the contamination emanating from the various source areas. It has been assumed that this monitoring design is biased toward capturing the variability of contaminants within each of the plumes. However, multivariate studies of groundwater indicate that the primary factors regarding variability of parameters in groundwater are related to the geochemical nature of the groundwater. This is important in L Range groundwater because a known area of the aquifer is characterized by low DO, low ORP, and high SpC downgradient from the L Range. A correlation analysis of groundwater parameters shows that there is a significant correlation between RDX and several geochemical parameters. In general, RDX is positively correlated with DO and ORP and negatively correlated with SpC. One of the implications is that RDX is preferentially found in the more oxic portions of the aquifer. Because the RDX plumes in the eastern portion of the study area co-mingle with the reducing conditions promulgated by a former fuel spill, it is possible that RDX is breaking down when this contaminant migrates into the portion of the aquifer where reducing conditions prevail. A multivariate factor analysis showed that the first two factors that explained 44 percent of the total variability were related to the reducing conditions in the aquifer and the biological activity associated with these reduced zones. The contaminants perchlorate and RDX were captured in the next two most important factors and accounted for approximately 30 percent of the variability in the data set. Therefore, the geochemical nature of the aquifer is the most important influence on the distribution of contaminants in the L Range plumes. While the monitoring well placement design functions well in defining the nature and extent of perchlorate, RDX, and HMX contamination downgradient from the L Range, the sampling design was instrumental in demonstrating how important the geochemistry of the aquifer is in defining the distribution of contaminants.

6. ACKNOWLEDGEMENTS

The authors wish to thank the Army Environmental Center Impact Area Groundwater Study Group, Camp Edwards, Massachusetts; and the U.S. Army Corps of Engineers, New England District, Concord, Massachusetts, for access to the data collected in the L Range studies and for their comments on the manuscript. These agencies provide the technical expertise and funding for the past and continuing L Range groundwater monitoring program.

7. REFERENCES

AFCEE (Air Force Center for Engineering and the Environment). 2002a (August). *Perchlorate Treatment Technology Fact Sheet: In Situ Anerobic Bioremediation*. www.afcee.brooks.af.mil/products/techtrans/perchloratetreatment/anaerobicbiormemdiation

AFCEE (Air Force Center for Engineering and the Environment). 2002b (March). *Final Ashumet Valley Axial 2000 Annual System Performance and Ecological Impact Monitoring Report*. A3P-J23-35Z01513-M31-0004. Prepared by Jacobs Engineering Group for AFCEE/MMR, Installation Restoration Program, Otis ANG Base, MA

AFCEE (Air Force Center for Engineering and the Environment). 2001 (December). *Final Fuel Spill-12 2000 Annual System Performance and Ecological Impact Monitoring Report*. A3P-J23-35Z01503-M31-0005. Prepared by Jacobs Engineering Group for AFCEE/MMR, Installation Restoration Program, Otis ANG Base, MA

AMEC (AMEC Earth & Environmental Inc) 2004 (February). *Final L Range Supplemental Groundwater Workplan, Camp Edwards Massachusetts Military Reservation*. EDMS No. 4797. Prepared by AMEC for NGB and USACE. Westford, MA.

Chen, K. J.J. Jiao, J. Huang, and R. Huang. 2006. Multivariate statistical evaluation of trace elements in groundwater in a coastal area in Shenzhen, China. *Environ. Pollut*. 147(3):771-780.

Doppalapudi, R.B. G.A. Sorial, and S.W. Maloney. 2002. Electrochemical reduction of simulated munitions wastewater in a bench-scale batch reactor. *Env. Eng. Sci*. 19(2):115-130.

Dyke, A.S. and V.K. Prest. 1987. Late Wisconsinan and Holocene history of the Laurentide Ice Sheet. *Geographie Physique et Quaternaire* 41(2): 237-263.

ECC (Environmental Chemical Corporation). 2006 (December). *Draft J-3 Range Groundwater Remedial Investigation and Feasibility Study*. ECC-J23-35AY5301-M14-0006. Prepared by Environmental Chemical Corporation for U.S. Army Corps of Engineers, New England District, Concord, MA.

ECC (Environmental Chemical Corporation). 2005 (November). *Final L Range Groundwater Characterization Report*. ECC-J23-35AY5302-M14-0003. Prepared by Environmental Chemical Corporation for U.S. Army Corps of Engineers, New England District, Concord, MA.

Fletcher, P.C. 1993. *Soil Survey of Barnstable County, Massachusetts*. United States Department of Agriculture soil Conservation Service. U.S. Government Printing Office, Washington, D.C.

Gonçalves, C.M., J.C. Silva, and M.F. Alpendurada. 2007. Evaluation of the pesticide contamination of groundwater sampled over two years from a vulnerable zone in Portugal. *J. Agric Food Chem.* 55(15): 6227-6235.

Hawari, J., S. Beaudet, A. Halasz, S. Thiboutot, G. Ampleman. 2000. Microbial degradation of explosives: biotransformation versus mineralization. *App. Microbiology Biotechnology*. 54:605-618.

Invernizze, A.L. and S.M. Barros de Oliveira. 2004. Hydrochemical characterization of a watershed through factor analysis. *Rev Aguas Subterraneas*. 18:67-77.

Jenkins, T.F., J.C. Pennington, T.A. Ranney, T.E. Berry, P.H. Miyares, M.E. Walsh, A.D. Hewitt, N.M. Perron, L.V. Parker, C.A. Hayes, and E.G. Wahlgren. 2001a (July). *Characterization of Explosives Contamination at Military Firing Ranges*. U.S Army Corps of Engineering Engineer Research and Development Center (ERDC). ERDC-TR-01-5. Hanover, NH.

Jenkins, T.F., T.A. Ranney, A.D. Hewitt, M.E. Walsh, J.A. Stark, and J.C. Pennington. 2001b. *Use of Snow-Covered Ranges to Determine the Amount of Explosives Residues Deposited from High-Order Detonations of Army Munitions*. Geological Society of American National Meeting. November 1-10, Boston, MA.

Jenkins, T.F., T.A. Ranney, M.E. Walsh, P.H. Miyares, A.D. Hewitt, and N.H. Collins. 2000a. *Evaluating the Use of Snow-Covered Ranges to Estimate the Explosives Residues that Result from Detonation of Army Munitions*. U.S. Army Corps of Engineers Engineer Research and Development Center (ERDC)/ Cold Regions Research and Engineering Laboratory (CRREL) TR-00-15. Hanover, NH.

Jenkins, T.F. T.A. Ranney, P.H. Miyares, N.H. Collins, and A.D. Hewitt. 2000b. *Use of Surface Snow Sampling to Estimate the Quantity of Explosive Residues Resulting from Land Mine Detonations*. U.S. Army Corps of Engineers Engineer Research and Development Center (ERDC)/ Cold Regions Research and Engineering Laboratory (CRREL) TR-00-12. Hanover, NH.

Kwon, M.J, and K.T. Finneran. 2006. Microbially mediated biodegradation of hexahydro-1,3,5-trinitro-1,3,5-triazine by extracelluar electron shuttling compounds. *App. and Env. Microbiology* 72(9):5933-5941.

Liu, C.W., K.H. Lin, and Y.M. Kuo. 2003. Application of factor analysis in the assessment of groundwater quality in a blackfoot disease area in Taiwan. *Sci Total Environ*. 313(1-3):77-89.

Logan, B.E. H. Zhang, P. Mulvaney, M.G. Milner, I.M. Head, and R.F. Unz. 2001. Kinetics of Perchlorate and Chlorate-Respiring Bacteria. *App. and Env. Microbiology* 67:2499-2506.

Manly, B.F.J. 1991. *Multivariate Statistical Methods*. Chapman and Hall, London.

McCormick, N.G., J.H. Cornell, and A.M. Kaplan. 1984. *The Fate of Hexahydro-1,3,5-trinitro-1,3,5-triazine (RDX) and Related Compounds in Anaerobic Denitrifying Continuous Culture Systems Using Simulated Wastewater*. NATICK/85/008. United States Army Natick Research and Development Laboratory. Natick, MA.

McGrath, C.J. 1995. *Review of Formulations for Processes Affecting Subsurface Transport of Explosives*. Report IRRP-95-2. U.S. Army Corps of Engineers, Waterways Experiment Station. Vickburg, MS.

Morley, M.C., S.N. Shammas, G.E. Speitel. 2002. Biodegradation of RDX and HMX mixtures: Batch screening experiments and sequencing batch reactors. *Env. Eng. Sci* 19(4):237-250.

Muñoz-Carpena, R., A. Ritter, and Y.C. Li. 2005. Dynamic factor analysis of groundwater quality trends in an agricultural area adjacent to Everglades National Park. *J. Contam. Hydrol*. 80(1-2):49-70.

Oldale, R.N. 2001. *Cape Cod, Martha's Vineyard & Nantucket, The Geologic Story*. On Cape Publications, Yarmouthport, MA.

Olobaniyi, S.B. and F. B. Owoyemi. (2006). Characterization by factor analysis of the chemical facies of groundwater in the Deltaic Plain Sands aquifer of Warri, Western Niger Delta, Nigeria. *African Journal of Science and Technology*. 7(1):73-81.

Price, C.B., J.M. Brannon, and C.A. Hayes. 2001. Relationship between redox potential and pH on RDX transformation in soil-water slurries. *J. of Env. Eng*. 127:26-31.

Price, C.G., J.M. Brannon, and S.L. Yost. 1998. *Transformation of RDX and HMX under Controlled Eh/pH Conditions*. IRRP-98-2. U.S. Army Corps of Engineers, Waterways Experiment Station, Vicksburg, MS.

Pujari, P.R. and V. Deshpande. 2005. Source apportionment of groundwater pollution around landfill site in Nagpur, India. *Environ Monit Assess* 111(1-3):45-54.

Reghunath, R., T.R. Sreedhara Murthy, B.R. Raghavan. (2002). The utility of multivariate statistical techniques in hydrogeochemical studies: an example from Karnataka, India. *Water Res*. 36(10):2437-2442.

Selim, H.M., and I.K. Iskandar. 1995. Transport of 2,4,6-trinitrotoluene and hexahydro-1,3,5-trinitro-1,3,5-triazine in soils. *Soil Sci*. 160:328-339.

Susarla, S. T.W. Collette, A.W. Garrison, N.L. Wolfe, and S.C. McCutcheon. 1999. Perchlorate identification in fertilizers. *Env Sci and Tech*. 33:3469-3472.

Townsend, D.M. and T.E. Meyers. 1996. Recent Developments in Formulating Model Descriptors for Subsurface Transformation and Sorption of TNT, RDX, and HMX. Technical Report IRRP-96-1. United States Army Corps of Engineers, Waterways Experiment Station, Vicksburg, MS.

Voudouris, K.S., N.J. Lambrakis, G. Papatheothorou, and P. Daskalaki. 1997. An application of factor analysis for the study of the hydrogeological conditions of Plio-Pleistocene aquifers of NW Achaia (NW Peleponnesus, Greece). *Mathematical Geology* 29(1):43-59.

Young, T.S.M., M.C. Morley, and D.D. Snow. 2006. Anaerobic biodegradation of RDX and TCE: single- and dual-contaminant batch tests. *Pract. Periodical of Haz., Toxic, and Radioactive Waste Mgmt*. 10(2):94-101.

PART VI: Environmental Forensics

Chapter 13

THE CASE ON ASSESSMENT OF SPILLED OIL WITH MIXED FREE PRODUCT IN SEOUL

Seog-Won Eom[1§], Il-Sang Bae[2], Jae-Seung Lee[3]
[1]Seoul Metropolitan Govern Research Institute of Public Health and Environment, 202-3, Yangjae-Dong Seocho-Gu, Seoul, Korea, [2]Seoul Metropolitan Govern Research Institute of Public Health and Environment, 202-3, Yangjae-Dong Seocho-Gu, Seoul, Korea, [3]Seoul Metropolitan Govern Research Institute of Public Health and Environment, 202-3, Yangjae-Dong Seocho-Gu, Seoul, Korea

ABSTRACT

The purpose of this study is to assess sources of contamination by analyzing the free product and oil compounds in groundwater near the Subway Station, located adjacent to the Yongsan Garrison in Seoul, Republic of Korea. All of the samples collected twice were groundwater and free product in a monitoring well. Analysis items are TPH fingerprinting, pristine/phytane ratio, alkylbenzene pattern, PAH&alkyl PAH, antioxidant, icing inhibitor, PIANO, element(C, N, H), and sulfur. Using ratio of pristine/phytane, we were able to distinguished fuel type between kerosene and JP-8 samples, which was impossible by GC/FID pattern. Alkyl benzene pattern was very effective in distinguishing between JP-8 and kerosene. It is very important that 2,4-dimethyl-6-tert-butyl phenol, an antioxidant used only for JP-8, was detected in free product samples. The concentration of sulfur in kerosene fuel is much lower than that of JP-8, and the total contents of sulfur in environmental samples can be used to differentiate the fuel type of spilled oil between kerosene and JP-8. In conclusion, according to the result of a variety of analytical methods to find the source of spilled fuel, it had been found that the fuel type detected in the tunnel of subway station and monitoring wells outside of Yongsan Garrison and the monitoring wells inside of Yongsan Garrison are the same.

Keywords: Oil; Free product; groundwater; alkylbenzene; sulfur

§ Corresponding Author: Seog-Won Eom, Seoul Metropolitan Govern Research Institute of Public Health and Environment, 202-3, Yangjae-Dong Seocho-Gu, Seoul, Korea, Tel: 82-2-570-3221, Email: sweom@seoul.go.kr

1. INTRODUCTION

The Noksapyong Subway site is located north of the Yongsan Garrison, in the city of Seoul, ROK. The investigation area includes approximately 50,000 square meters of paved ground, wooded ground, and sloped terrain that extends from the AAFES Gas Station to Noksapyong Subway Station.

Construction on the Noksapyong segment of Subway Line Number 6 began in December 1995 and was completed in July 2000. In January 2001, the free product was found in seepage water within the Noksapyong Subway tunnels, located to the northwest of the army garrison in Seoul, Korea. The service station within the army garrison has been in use since 1974 when the underground storage tanks (USTs) were installed. In 1990, water was observed in premium gasoline tanks and the tanks were replaced. In July 2000, the use of the premium fuel line was suspended when the line failed a routine pressure test. The fuel line was subsequently replaced in January 2001.

In February 2001, two USTs located within the Housing Area failed leak tests and were subsequently removed and replaced with aboveground storage tanks (ASTs). The tanks at these locations are used to store diesel or JP-8 fuel for heating purposes. After an additional leak test was performed on USTs near the Service Station area, a UST was also removed from the area immediately adjacent to the Military Dog Training Ground in August 2001. This UST purportedly contained kerosene for heating purpose(Samsung, 2002).

The U.S. forces in Korea (USFK) and the Seoul City (SC) have been confused over the source of the fuel contamination near Noksapyong Subway Station. The fuel type was found to be gasoline and kerosene. The USFK recognized that the gasoline was from the Yongsan Garrison but not the kerosene. This led to reinvestigation of the source for identifying the kerosene.

To confirm the source of the contamination, the type of fuel in the contaminated area should be identical to the potential source of the contamination. A simple pattern analysis of hydrocarbon cannot provide the answer. Fuel is a quite complicated compound ranging from a simple straight chain-type saturated hydrocarbon (n-alkane), unsaturated hydrocarbon and aromatic hydrocarbon, etc. Once exposed to the environment, oil undergoes various chemical processes including volatilization, dissolution, microbial or chemical decomposition, which drastically transforms the saturated hydrocarbon. This makes it impossible to accurately identify the type of fuel with the simple hydrocarbon pattern analysis.

In particular, as for the one at the center of controversy, kerosene, most oil refineries in Korea use a similar-quality crude oil; the fuel used at the U.S. Army base has been also supplied from a Korean refinery, which makes it very difficult to identify the source of contamination. But it is believed that a very thorough and detailed analysis of the chemical features of the oil could identify the subtle difference between oil types. This will enable us to identify the source of contamination. Most oil goes through volatilization, dissolution and microbial or photochemical decomposition processes but the compounds which were not transformed can be utilized as a very important marker. Therefore development of the most reliable and accurate analytical method is essential.

Required is a method that allows the most reliable and accurate analysis. Especially, the pattern analysis of the difficult-to-decompose contained in the oil can be used as a very useful index to distinguish the oil type and analysis of additives added for different purposes can provide a clue to determine the source of contamination.

The USFK recognized that the gasoline component in the contaminated groundwater at Noksapyong Station tunnel came from the Yongsan Garrison but not for Kerosene. Therefore, this research is to identify the source of contamination by analyzing the free product and groundwater samples near the Noksapyong station and tunnel.

2. MATERIALS AND METHODS

2.1 Sample Collection and Analysis Items

Commercial gasoline, white kerosene, boiler kerosene and diesel control standard samples were taken from LG and SK gas stations near the Noksapyong station. At the same time, gasoline, kerosene and diesel control standard samples were taken from the AAFES gas station located within the Yongsan Garrison and two JP-8s from the AST, and they are used as a reference.

All of the samples collected twice jointly by SC and USFK were ground water and free product and its details are as follows: Analysis items are: TPH fingerprinting, TPH (gasoline and kerosene), pristane/phytane ratio, BTEX, alkylbenzene pattern, PAH & Alkyl PAH, PIANO, element (C,N,H), sulfur, antioxidant and icing inhibitor. It was attempted to identify the contamination source by analyzing each item using the best possible analytical method for them and combining all the findings.

When it comes to the groundwater samples, SC and USFK team together gathered in the following order: anti-oxidant, icing inhibitor, biomarker (alkylbenzene included), TPH fingerprinting (gasoline, kerosene included), and stable isotopes.

The first-phase samples were collected from November 21, 2002 to November 26, 2002 and the groundwater samples taken from 12 wells near New Veterinary Clinic in Yongsan Garrison (NVC) (B01-729, B01-730, B01-788, B01-868, B01-869, B01-870, B01-874, B01-875, B01-877, B01-880, RW02-103, and RW02-106) and from 8 wells on monitoring well installed by the Seoul City(MSC) (BH-1 to 8), and from 8 spots within the Noksapyong Station tunnel(20K-187C, 20K- 230C, 20K-217C, 20K-230C, 20K-246C, 20K-260C, and 20K-525C). Two samples were taken from BH-7 and 20K-187C as duplicate sample. The free product samples were taken from 8 monitoring wells where free product was accumulated (NVC: B01-730, B01-868, B01-874, B01-880 and MSC near Noksapyong station (BH-5, BH-6, BH-7), and 19K-890 in the direction of Itaewon from the south tunnel of Noksapyong station. Twelve samples were taken from four locations on November 22 as fuel control standard (ASTs-1 near 52nd Medical Battalion; ASTs -2 in front of the building S4348 within the housing area; premium gasoline, regular gasoline, kerosene, diesel at AAFES gas station, white kerosene, boiler kerosene from

SK Namkyung gas station and LG Daesung gas station). As a result, there were a total 30 groundwater samples (duplicates included), 8 free product samples, 5 soil samples and 12 reference samples for the first-phase underground sample collection.

In the second phase, samples were collected from February 14, 2003 and February 24 throughout 26, 2003. On February 22 Korea and U.S.A. jointly collected samples on 10 locations inside the underground tunnels of Noksapyong station (20K-187C, 20K-230C, 20K-217S,

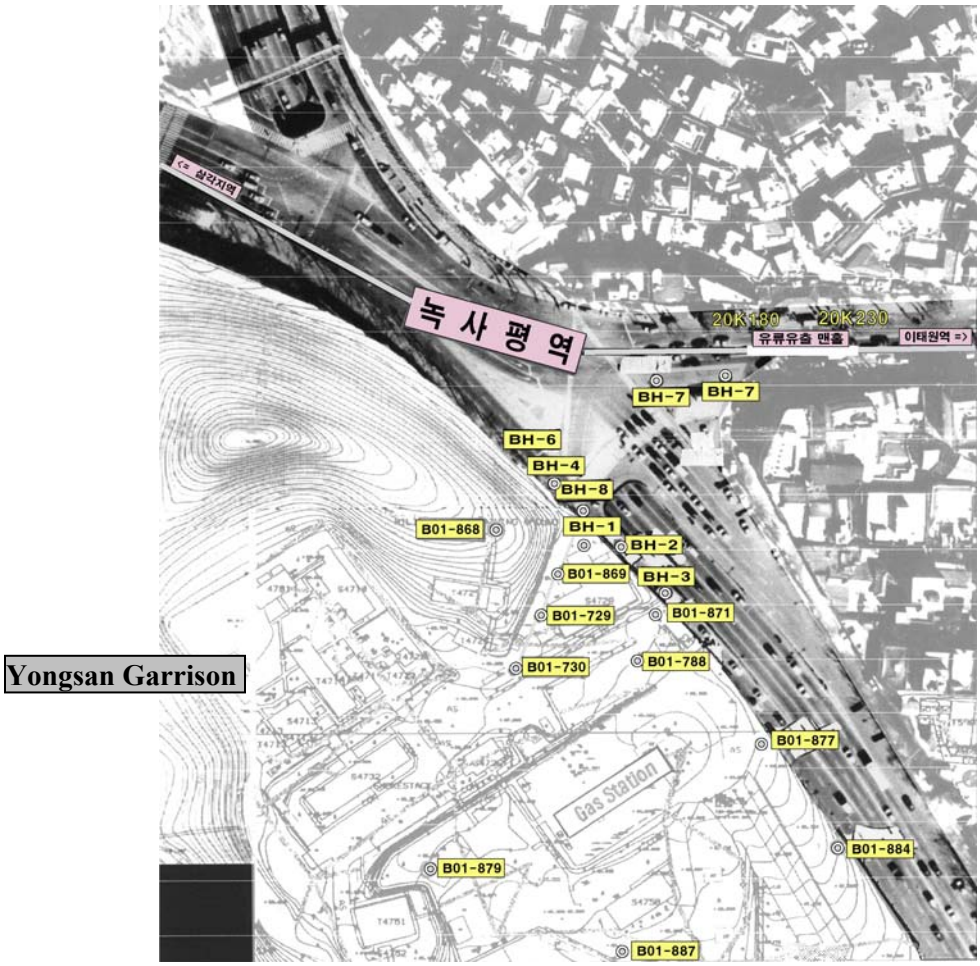

Figure 1. Site map near Noksapyong Subway Station

20K- 230S, 20K-246S, 20K-260C, 20K-525C, BH-32, BH-33) and three locations on the 19K area (19K-810C, 19K-755C, 19K-550C) and on February 24 on 20 MSC on the outer track of NVC (BH-1 to 16, BH-18 to 21), on February 25 on 13 locations within the USFK base near NVC (B01-729, B01-788, B01-868, B01-869, B01-870, B01-874, B01-875, B01-877, B01-880, RW02-103, RW02-106, RW02-107, RW02-108). Four fuel control standards were collected on two spots on February 25 (ASTS: JP-8, gas station: premium gasoline, regular gasoline,

kerosene) and for duplicates two samples were picked per item on BH-6, B01-874, B01-880 and 20K-260S. Free fuel control standards were taken from eight monitoring wells (monitoring well near NVC: B01-788, B01- 874, B01-877, B01-880 and monitoring wells for Korean side on outer block of NVC: BH-5, BH-6, BH-7 and 19K-890 in the direction of Itaewon from the south tunnel of Noksapyong station). Therefore, the total number of groundwater samples collected in the second phase was 61 including duplicate samples, along with 8 free product samples and 4 reference fuel control standards. Fig 1 is Site map near Noksapyong Subway Station.

Samples were collected using the disposable, bottom discharging bailer (ASTM D4489) and it was transferred into the newly purchased clean brown-colored 1000 ml(1L) glass bottle along with the Teflon-coated cap without washing them. Free product samples were contained in the newly purchased clean brown-colored 500 ml glass bottle (or 40 ml to1ml VOC bottle, size varies depending on the quantity of the oil collected) along with the Teflon-coated cap without washing them.

Those samples were stored in a dark area in the temperature of 4-5℃ and pretreatment was made within 7 days and then analysis was completed within 30 days (ASTM D3325).

2.2 Chemicals and Analysis Methods

The methylene chloride used for this study was solvent used for analyzing residual agricultural chemicals produced by Merck and standard materials were purchased from Aldrich or Sigma. Other reagents were used special reagents whose seal is not broken.

Sodium sulfate (Na2SO4, Kanto, Japan, for pesticide residue) were used as reagents. Water was purified in milli-Q (Millipore Corp., Milford, MA). Table 1 shows methods for analysis of free product and groundwater samples.

3. RESULTS AND DISCUSSION

3.1 TPH pattern and pristane/phytane

Unknown oil component show different patterns depending on oil type and origin. n-alkanes and isoprenoids of saturated hydrocarbon are feeble in toxicity; however, they are the components that are used very often as a tracing material in spilled oil because they are the primary component. GC-FID chromatogram shows the pattern of these n-alkanes and isoprenoids. They have specific fingerprint in accordance with pertroleum hydrocarbon type. However, environmentally contaminated oil changes its pattern by weathering, distribution between phases and vaporation(Wang, Z 1995).

GC-FID chromatograms were obtained by analyzing water phase and free product according to each analysis method after distributing fuel control standard sample of LG, SK, GS and ASTs into groundwater that is not contaminated with oil for a certain amount of time. If we compare

Table 1. Method for Analyses of Free Product and Groundwater Sample

Items	Free Product		Ground Water	
	Pre	**Method**	**Pre**	**Method**
TPH Fingerprinting	EPA 3580	EPA 8015	EPA 3510	EPA 8015
PAH & Alkyl PAH	EPA 3580	EPA 8270	EPA 3510	EPA 8270
Alkyl Benzene	EPA 3580	EPA 8270A	EPA 3510	EPA 8270A
Antioxidant	EPA 3630A	EPA 8470	EPA 3510A	EPA 8270
Icing Inhibitor	ASTM D5006 mod	EPA 8270	EPA 3510 mod	EPA 8270
PIANO	ASTM D5134		-	-
Sulfur	ASTM D4294&D3120*		-	-
C, H, N	ASTM D5291		-	-

*: D3210 for determination of trace concentrations of sulfur/ D4294 for determination of sulfur at 0.015 to 5% mass of hydrocarbon
Pre: Pre-treatment of sample, mod: modified
REF: Bull. Geol Surv Japan Vol 30pp 241-245, 1979&Anal. Chem. Vol 47pp 1179-1185, 1975&ASTM Method D129-64

these materials, we can find out that they have different TPH patterns depending on their fuel type. Some of the differences were found in even TPH pattern kerosene and JP-8. But even though there were some differences in TPH pattern of C-9 part and C-15 part, the pattern could be identified only when the fuel type was singular, while it was impossible when they were mixed. However, we could not find differences among patterns of GS kerosene, SK kerosene and LG kerosene.

GC-FID pattern analysis of the samples collected was identified that 15 samples were contaminated by gasoline, 2 samples were contaminated by kerosene (or JP-8), 7 samples of BH-4, BH-5, BH-6, BH-7, BH-8, B01-868, 20K-217S were contaminated by mixture of gasoline and kerosene (or JP-8), and 2 samples of B01-877, B01-880 were contaminated by mixture of gasoline, kerosene (or JP-8) and diesel. However, GC-FID pattern analysis was impossible to distinguish between kerosene and JP-8.

Homogeneity of oils can be traced using the ratio between pristane and phytane of oil components. This is due to the fact that pristane and phytane, of branched saturate isoprenoids, are not decomposed easily by microorganisms, and their ratios remain the same environmentally for a long time. Seoul City obtained data of m/z 85 GC-MS (SIM) by extracting free products and groundwater samples which were collected twice.

SC measured the ratio of pristane/phytane of oil components and found that the ratio of LG-white kerosene was 3.10, that of SK-white kerosene was 3.58 and that of GS-kerosene was 3.76, all of which double the value of JP-8 (1.77). It was useful in distinguishing between similar two fuel types in the pattern of TPH. And, the pristane/phytane ratio of LG-boiler kerosene with significant differences between JP-8 and TPH pattern was 1.3, SK-boiler kerosene was 1.55 and diesel was 0.79. As for the analytical result of the first free product sample, the ratio of pristane/phytane in most of the sample identified as kerosene(or JP-8) in TPH pattern analysis was 1.67-1.86 and the ratio for the second sample was 1.71-1.78, very similar to the ratio of JP-8.

3.2 Alkyl benzene and alkyl PAH

SC carried out pattern analysis of alkyl benzene to identify contaminated fuel type of groundwater around Noksapyong subway station. The pattern of alkyl benzene was very useful in identifying fuel type in the environmental sample transformed by weathering. SC used SIM mode of GC-MS for the pattern analysis of alkyl benzene in samples and chose ions of C6-benzene (162), C7-benzene (176) and C8-benzene (190). An additional peak group was found behind the alkyl benzene pattern of kerosene in the alkyl benzene pattern of JP-8. In general, kerosene passes through a desulfurization process unlike JP-8 under the condition of heating and resolution. Because of that, it is assumed that there were partial removals or modifications in the tail of kerosene. Therefore the additional tag that appears in alkylbenzene pattern of JP-8 takes an important role in differentiating kerosene and JP-8. Alkyl benzene pattern was very effective in distinguishing between JP-8 and kerosene and was not greatly interfered by the presence of a large amount of other fuel type. Using alkyl benzene pattern, 30 samples of BH-1, BH-2, BH-3, BH-4, BH-5, BH-6, BH-7, BH-8, BH-16, BH-31, BH-32, B01-730, B01-788, B01-868, B01-869, B01-870, B01-874, B01-875, B01-880, RW02-103, RW02-106, RW02- 107, RW02-108, 19K-890, 20K-187C, 20K-203C, 20K-217S, 20K-230C, 20K-230S, 20K-246S (Fig. 89) were identified as JP-8 rather than kerosene. Fig 2 showed a comparison of alkylbenzene patterns of JP-8 and kerosene.

Alkyl PAH pattern including peaks of n-C9-, n-C10-, n-C11-, n-C12-, n-C13-alkane was used to distinguish between kerosene and JP-8. The results of sample analysis showed that BH-5, BH-6, BH-7, B01-868, 19K-890 and RW02-106 were contaminated by JP-8.

3.3 Antioxidants and icing inhibitor

Detection of antioxidants in environmental sample can be the evidence that the kerosene found in groundwater around Noksapyong subway station is JP-8, since antioxidant of phenol type is used in JP-8 only as an oil additive domestically. Detection of JP-8 can be considered as a clue that the polluter is American Army since JP-8 is used only in American Army Base around Noksapyong subway station.

The antioxidants used in JP-8 domestically are 2, 4-dimethyl-6-tert-butylphenol (DMTBP). we obtained the result of measurement of GC-MS (SIM) by extracting - according to test methods - free product samples and groundwater samples which have been collected twice and

analyzed the antioxidants out of gasoline, white kerosene, boiler kerosene, JP-8 and diesel control standard sample from LG oil station and SK oil station, and a gas station (GS) in American Army Base and ground ASTs around Noksapyong subway station. According to the analytical result of the fuel control standard sample obtained from oil stations, 12.3 mg/L of DMTBP was measured in AST(JP-8) sample in American Army Base, while DMTBP was not detected in gasoline, white kerosene, boiler kerosene and diesel control standard samples from LG oil station and SK oil station.

The fact that high concentrations of 180-2,890ug/L of 2,4 -dimethyl-6-tert-butyl phenol were detected in the free product samples, BH-6, BH-7,19K-890, B01-874, B01-877 and B01-880. This is an unavoidable evidence to show that they were contaminated by JP-8. An antioxidant, 2,4-dimethyl- 6-tert-butyl phenol was detected from BH-5, BH-6, BH-7, 19K-890, B01-788, B01-874, B01-877 and B01-880 samples.

Of JP-8 additives for jet fuel, icing inhibitor is a representative additive. A frequently used icing inhibitor is DEGME (diethylene glycol monoethyl ether). As for JP-8 obtained from ASTs samples in American Army Base, DEGME was 1,951.8ppm. Icing inhibitors of free product samples and groundwater samples were analyzed, but any icing inhibitor was not detected.

3.4 Sulfur Content, PIANO

Analysis of sulfur content found in fuels can be used to identify kerosene and JP-8.

The difference between kerosene and JP-8 with different quality standards of sulfur content is in their production processes. Kerosene requires deep desulfurization through hydrorefining, while JP-8 uses Merox process eliminating only mercaptane with a bad smell to get rid of sulfur. The hydrorefining process of kerosene involves mixing hydrocarbon base oil and hydrogen, and then contacting the mix to a catalyst under high pressure and temperature to eliminate sulfur constituent, separated into H_2S, and nitrogen constituent, separated into NH_3, when olefins are transformed into saturated hydrocarbons. Therefore, kerosene has relatively more saturated hydrocarbons and hydrogen content and less nitrogen content than JP-8.

While sulfur content of kerosene produced by domestic 5 petroleum companies in 2002 was as low as 5~40 mg/L, sulfur content of JP-8 with below 3,000 mg/L of quality standard (KS, ASTM, MIL-DTL-83133X Quality Standard) showed actually 400~2,000 mg/L. JP-8 rich-sample(BH-5, BH-6, BH-7, B01-868, 19K-890) contain high concentration of sulfur. Sulfur content was observed from 195 up to 1416mg/L in 1st survey, and from 120 up to 13861416mg/L in 2st survey.

PIANO compounds mainly take an important role in determining the physical characteristics of gasoline constituent. However, since increasing boiling point makes complete analysis of components leading to lower identification ratio, those compounds are not so meaningful in kerosene (jet fuel) constituent and beyond.

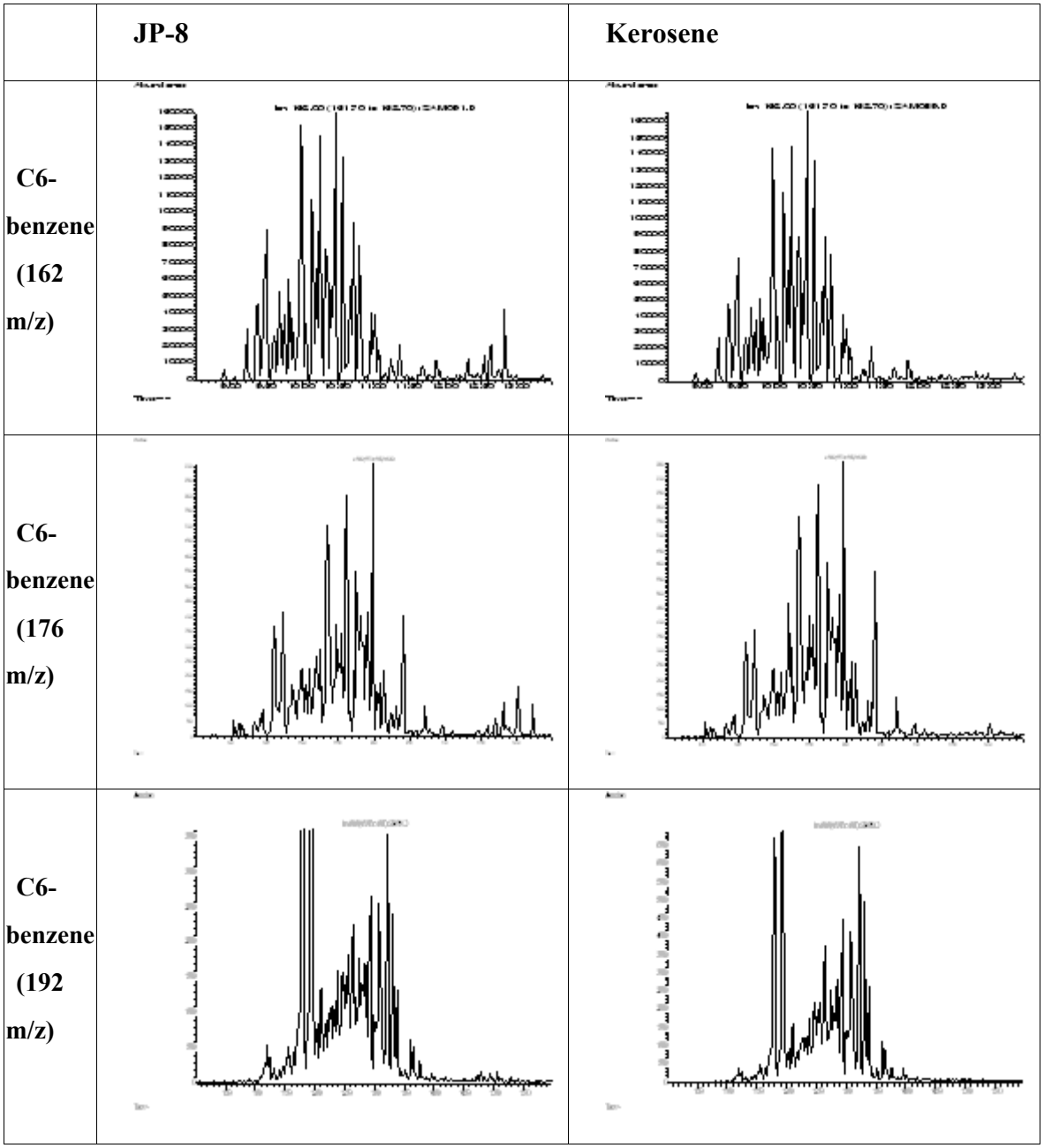

Figure 2. Comparison of alkylbenzene patterns of JP-8 and kerosene

4. CONCLUSION

According to the result of a variety of analytical methods to find the source of spilled fuel, i.e. the contaminant that caused fuel contamination of groundwater in tunnel of Noksapyong subway station in Seoul City, it has been found that the fuel type detected in the tunnel of Noksapyong subway station and the monitoring wells outside of Yongsan Garrison and the one

well inside of Yongsan Garrison are the same. The USFK did not recognize it before, but the exact fuel type was JP-8. Since JP-8 has been only by the USFK, we conclude that the source of fuel contamination in the groundwater wells around Noksapyong area and Subway tunnel is identified as the same source as the fuel discovered in the Yongsan Garrison.

5. REFERENCES

Samsung. 2002. Site history and contaminations. In: Assessment report for contaminated water sumps at Noksapyong Subway Station, located adjacent to the Yongsan Grrison, korea, pp. 1-50.

ASTM (American Society for Testing and Materials). 1996. Standard Practice for Preservation of Waterborne Oil Samples. 100 Barr Harbor Dr., West Conshohocken, PA 19428. ASTM D3325-90, Reapproved 1996.

ASTM (American Society for Testing and Materials). 1996. Standard Test Method for Trace Quantities of Sulfur in Light Liquid Petroleum Hydrocarbons by Oxidative Microcoulometry. 100 Barr Harbor Dr., West Conshohocken, PA 19428. ASTM D 3120-96.

ASTM (American Society for Testing and Materials). 1998. Standard Test Method for Enumeration of Candida albicans in Water. ASTM D 4249-93, Reapproved 1998.

Wang, Z, M. Fingas. 1995. Differentiation of the source of spilled oil and monitoring of the oil weathering process using gas chromatography-mass spectrometry. J.chromatogr. A, 712, 321-343.

Chapter 14

FACT OR FICTION: THE SOURCE OF PERCHLOROETHYLENE CONTAMINATION IN GROUNDWATER IS A MANUFACTURING IMPURITY IN CHLORINATED SOLVENTS

Valerie Lane[1§] and James S. Smith, Ph.D.[2]
[1]GeoTrans, Inc., One Monarch Drive, Suite 101, Littleton, MA, 01460, [2] CPC, Trillium, Inc., 28 Grace's Drive, Coatesville, PA 19320

ABSTRACT

Manufacturing impurities in chlorinated solvents have been considered to be sources of contamination in groundwater. Chlorinated solvents are manufactured in a variety of grades; the technical grade is used at many industrial and manufacturing facilities. Compounds present as manufacturing impurities in technical grade chlorinated solvents vary, and their quantity is extremely small or not measurable, because chlorinated solvents historically have been manufactured to a high degree of purity. The purity of currently manufactured TCE ranges from 99.9% for reagent grade to 98.0% for the technical grade. Impurities in technical grade 1,2-dichloroethane, also known as ethylene dichloride (EDC), manufactured within the last 10 years with purities of 99.9991% and 99.9955% contained PCE between about 0.0001% and 0.0006%, respectively.

In a number of litigation cases where TCE released from a vapor degreaser is the major contaminant in groundwater, there is an accompanying minor concentration of PCE. The assumption made in these cases is that the PCE impurity in technical grades of TCE is the source of the PCE in groundwater. This assumption is based on the release of these two compounds together from a distillation bottom residue where PCE is concentrated, relative to the TCE, because of its much higher boiling point at atmospheric pressure.

There is no peer reviewed literature that can be cited to prove that PCE is a significant impurity in either the distillation bottoms produced from a vapor degreaser or technical grade TCE. PCE, if present as a manufacturing impurity, is present in such small amounts that significant concentrations would not be generated in groundwater. When PCE and TCE are present together in groundwater, the source of the PCE is likely not an impurity in the manufactured TCE.

Keywords: PCE, Manufacturing impurity, Vapor degreasing

§ Corresponding Author: Valerie Lane, GeoTrans, Inc., One Monarch Drive, Suite 101, Littleton, MA, 01460, 978-952-0120, vlane@geotransinc.com

1. INTRODUCTION

When chlorinated solvents are manufactured, the resulting product often contains less than 100% of the chlorinated solvent itself. Very small amounts of other chlorinated solvents may also be present as "impurities." Manufacturing impurities (MIs) in chlorinated solvents have been considered to be sources of contamination in groundwater. One chlorinated compound in particular, tetrachloroethylene (PCE), has been identified as a MI source of groundwater contamination.

PCE, as a manufacturing impurity (PCEMI), has been identified as the source of PCE at sites where trichloroethylene (TCE) releases from vapor degreaser operations occurred. In a number of litigation cases, in which TCE released from a vapor degreaser is the major contaminant in groundwater, there has been an accompanying minor concentration, relative to the TCE, of PCE in groundwater. The assumption made in these cases is that the PCEMI in technical grades of TCE is the source of the PCE in groundwater.

There is no peer-reviewed literature documenting studies that can be cited to show that PCE is a significant MI in either the distillation bottoms produced from a vapor degreaser or in technical grade TCE. Furthermore, there is a dearth of available data that quantifies the MIs in chlorinated solvents. There is some data available for the purity of manufactured TCE, but, to date, no quantifying data has been found in the literature for the PCE MI in TCE.

Although no published quantifying data for the PCEMI in TCE has been found to date, there is some quantifying data available for the PCEMI in TCE and in 1,2-dichloroethane (1,2-DCA). The data for the quantity of PCEMI in TCE is from a chlorinated solvent manufacturer. The data for the quantity of PCEMI in 1,2-DCA, also from a chlorinated solvent manufacturer, is from a site investigation performed at a single-component dense non-aqueous phase liquid (DNAPL) release site. These data provide further insight into the amount of PCE MI present in manufactured chlorinated solvents.

The purpose of this paper is to facilitate a more thorough understanding of the fate of MIs at sites where groundwater contamination has resulted from releases of chlorinated solvents. Two cases are examined: a conceptual model where TCE is used as the solvent in a vapor degreaser and an actual case study where 1,2-DCA, known to contain PCE MI, was released to the ground surface. Preliminary conclusions regarding the fate of MIs, such as PCE, can be made by examining these two cases.

2. CONCEPTUAL MODEL: VAPOR DEGREASER OPERATION USING TCE

The function of a vapor degreaser is to remove process oil, grease, other residues, and small particulate from non-porous materials such as metals. A solvent is heated to boiling to create a solvent vapor that condenses on a cooler metal object. Through this process, the oil, grease, other residues, and particulate, such as sand and metal grit, are stripped from the metal as the

solvent condensate drips from the metal object back into the boiling solvent. Over time, sludge forms in the bottom of the degreaser. This sludge, commonly referred to as distillation bottoms, contains the solvent plus the materials formerly coating the degreased objects. Figure 1 shows the design of a basic vapor degreaser (ASTM 1989).

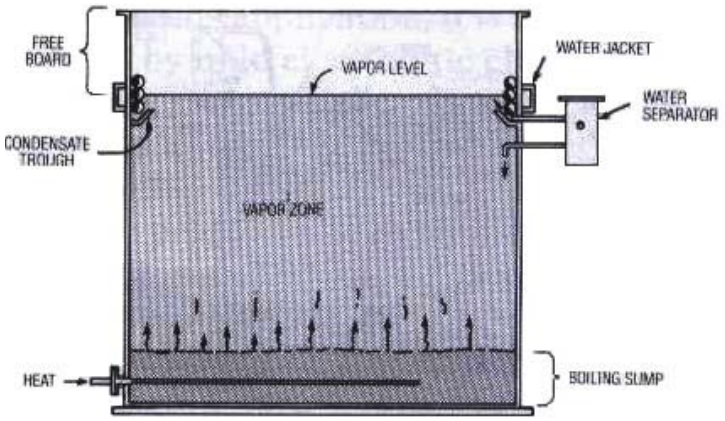

ASTM 1989

Several chlorinated solvents have historically been used in vapor degreasers. They include methylene chloride, PCE, TCE, 1,1,1-trichloroethane, and trichlorotrifluoroethane (ASTM 1989). By 1991, 90% of the TCE produced was used for metal cleaning and degreasing (Doherty 2000).

At some sites where TCE was used as the vapor degreasing solvent and where PCE was detected in conjunction with TCE in groundwater, the assumption has been that PCEMI in TCE was the source of the PCE groundwater contamination. This assumption is based on a common sense approach to the release of these two chemicals together from a distillation bottom residue where PCE is concentrated, relative to the TCE, because of its much higher boiling point at atmospheric pressure.

Groundwater concentrations of PCE relative to TCE at vapor degreaser sites have been reported in the 0.5 to 5 percent range (ODHHS 2003). Assume a maximum concentration of 100 ppm PCEMI in TCE. Also assume the distillation bottoms contain 20% TCE and 500 ppm PCE relative to the TCE. The equilibrium solubility of PCE and TCE in water are 200 mg/L and 1,100 mg/L, respectively (Schwille 1988). TCE is five and a half times more soluble in water than PCE at equilibrium, and it is 2,000 times higher in concentration than PCE. This is an effective multiplier of 11,000. In terms of a rough estimate for a concentration of 100 μg/L TCE in groundwater, it would be expected that the maximum PCE concentration generated from a manufacturing impurity would be about 0.01 μg/L or 0.01% of the TCE in the groundwater.

Another approach to evaluation of the potential for PCEMI contamination of groundwater from distillation bottom residue is as follows: If there is 1% PCE in the groundwater relative to TCE, then the amount of PCEMI in the TCE representing the distillation bottoms would be in the neighborhood of 20%. This represents approximately 4% PCEMI in the manufactured TCE. This is three to four orders of magnitude greater than the 0.0001% (Table 1) to 0.001% of measured PCEMI, discussed in the next section.

2.1 Purity and Composition of Manufactured TCE

Chlorinated solvents are manufactured in a variety of grades; the technical grade is used at many industrial and manufacturing facilities. The purity of manufactured TCE is usually greater

than 99% (CCOHS 1999), and TCE purity in the technical grade has been cited as high as 99.97% (Morrison 2000). Other chlorinated solvents, such as PCE, dichloroethylene isomers, and trichloroethane isomers, may be present in TCE as MIs (CCOHS 1999, IPCS 1985). The quantity of these MIs is extremely small or nonexistent. Manufactured TCE may also contain stabilizers and additives. Stabilizers may be present in amounts between 0.1 to 0.5% and as much as 2.0% (Doherty 2000). Neu-Tri*E is TCE that has been manufactured specifically for vapor degreasing. The purity of TCE in Neu-Tri*E is 99.4%; stabilizers and additives comprise 0.1% and 0.5%, respectively (The Dow Chemical Company 1991, 1994, 1999).

For the past 10 to 15 years, TCE produced by a major manufacturer has contained less than the PCE detection limit, which is one ppm by weight PCEMI (Table 1) (Terry 2006). The PCEMI represents less than 0.0001% of the manufactured TCE solvent. Prior to that time, the greatest quantity of PCMI in TCE was 10 ppm, or 0.001%, which rarely occurred (Terry 2006). Because the boiling points of PCE and TCE are 121.5º C and 87.2º C, respectively (CRC 1995), separation of PCE from TCE by atmospheric distillation is easily accomplished. This is strongly supported by manufacturer product quality test results.

Table 1. Manufacturer's Quantification of PCEMI in TCE for the Past 10 to 15 Years

Compound	***MW*** (g/mol)	***Quantity*** (ppm w/w)[a]	***Fraction by Mass***	***Moles***	***Mole Fraction***	***Solubility*** (mg/L)	***Solubility$_{eff}$*** (mg/L)
TCE solvent	131.5	1,000,000		7.6046E+03	1.0000E+00	1100	1099.9991
PCE	165.8	1	1.00E-06	6.0314E-03	7.9312E-07	200	0.0002
Other MIs				unknown	unknown		
Stabilizers				unknown	unknown		
Additives				unknown	unknown		
Total				7.6046E+03			

[a] Number of grams of impurity per 10^6 grams of EDC

3. CASE STUDY: 1,2-DCA RELEASE AT A MAJOR CHEMICAL MANUFACTURING FACILITY

The field site for this case study (Lane 2001) is situated in an area of petrochemical production facilities in the city of Sarnia in southwestern Ontario (Figure 2). The study site is located at a major chemical manufacturing facility situated on an extensive area of clayey deposits between 130 and 230 feet thick that exist along the St. Clair River. It is a location where leaks from 1955 to 1972 from an above-ground product line connected to a tank of 1,2-dichloroethane (1,2-DCA), the monomer used to produce vinyl chloride, resulted in the cumulative input of a considerable 1,2-DCA volume to the subsurface (Figure 3).

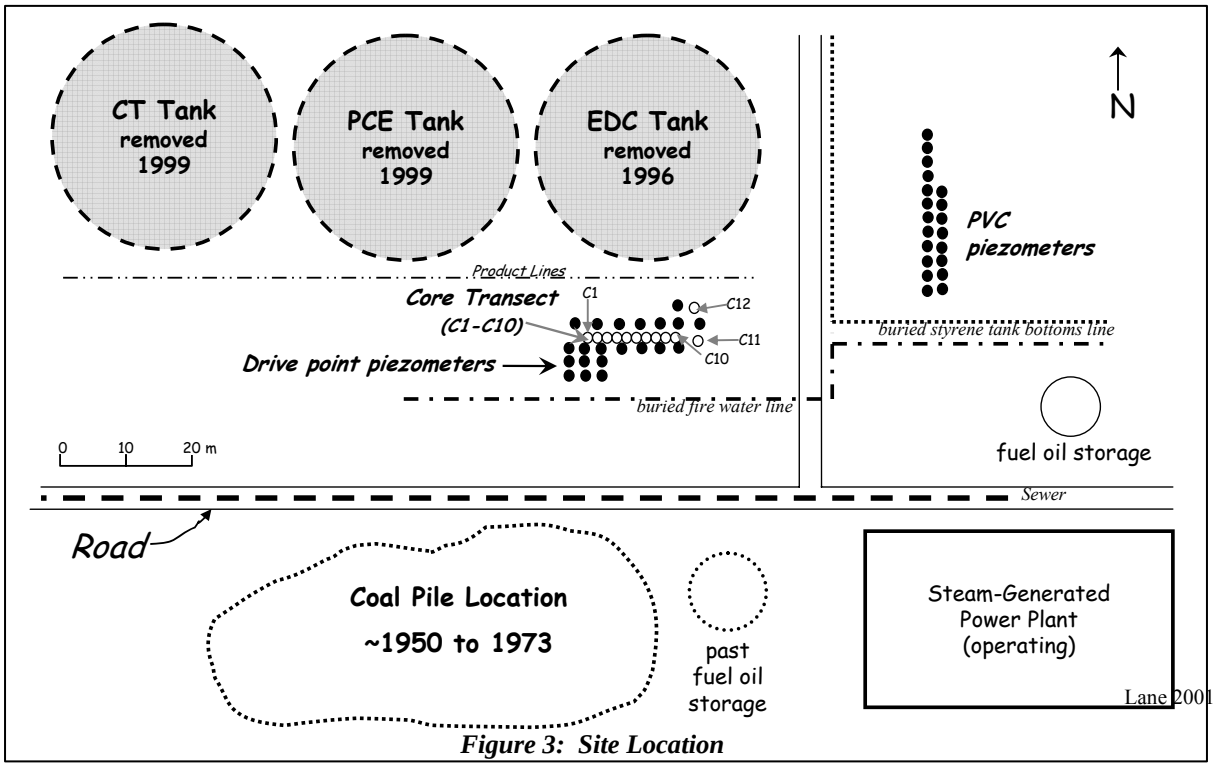

Figure 3: Site Location

The 1,2-DCA site was initially considered to be a site where only 1,2-DCA DNAPL had been released. However, analytical results from soil and groundwater samples showed that several compounds are present at this site, including PCE, TCE, cis-1,2-dichloroethylene (c-1,2-DCE), 1,1-dichloroethylene (1,1-DCE), and vinyl chloride (VC). Like 1,2-DCA, the PCE most likely originated as DNAPL from other product line or storage tank leaks in the area, and the TCE, cis-1,2-DCE, 1,1-DCE, and VC appear to be degradation or transformation products of PCE.

Concentrations of c-1,2-DCE and of 1,1-DCE were similar in most groundwater samples, with the concentration of 1,1-DCE exceeding that of c-1,2-DCE in several samples. Because c-1,2-DCE is typically the more predominant isomer, the source of the 1,1-DCE was evaluated. This evaluation included investigation of whether the detected 1,1-DCE was from a MI in 1,2-DCA solvent or a product of degradation.

3.1 Purity and Composition of Manufactured 1,2-DCA

In order to identify the MIs present in 1,2-DCA, a sample was retrieved in 1998 from a tank car containing recently manufactured 1,2-DCA. Table 2 shows the results from the manufacturer's product quality analysis (Lane 2001). Nine other chlorinated compounds were detected in this sample as manufacturing impurities, but 1,1-DCE was not present.

3.2 Use of Manufacturing Impurities to Identify Degradation Mechanisms

The data identifying MIs in the 1,2-DCA sample were used to conclude that the presence of TCE (degradation product and MI), significant amounts of 1,1-DCE, and the absence of 1,1-DCE in the 1,2-DCA solvent indicated that abiotic degradation of TCE may have occurred at this site. 1,1-DCE was not manufactured or used by the site owner; therefore, it was not disposed at this site, and it is not known to occur as an impurity in any of the DNAPLs that were disposed at this site (Prine 1999, Creber 2000). Studies (Klecka et al. 1990, Kastner 1991) indicated that 1,1-DCE in groundwater can occur as a product from the abiotic degradation of TCE.

Kriegman-King and Reinhard (1992) observed that abiotic degradation of another chlorinated solvent (carbon tetrachloride) was enhanced by the presence of iron sulfide (pyrite) and iron vermiculite. The clays at this site contain both pyrite and iron vermiculite (Abbott 1987, Quigley and Ogunbadejo 1976). TCE occurs in nearly all core samples where 1,1-DCE was found, and the mole fraction of 1,1-DCE was observed to increase as the mole fraction of TCE decreases, which is consistent with 1,1-DCE production from TCE. Therefore, it is likely that abiotic degradation of TCE produced the 1,1-DCE.

Table 2. Manufacturer's Analysis of 1,2-DCA Solvent: 1998 Sample

Compound	***MW*** (g/mol)	***Quantity*** (ppm w/w)[a]	***Fraction by Mass***	***Moles***	***Mole Fraction***	***Solubility*** (mg/L)	***Solubility$_{eff}$*** (mg/L)
EDC Solvent	99	1,000,000		1.0101E+04	9.9955E-01	8,500	8,496
1,1,2-TCA	133.4	210.9	2.11E-04	1.5810E+00	1.5645E-04	4,400	0.6884
cis-1,2-DCE	97	180.1	1.80E-04	1.8567E+00	1.8373E-04	3,500	0.6431
TCE	131.5	19.8	1.98E-05	1.5057E-01	1.4900E-05	1,100	0.0164
PCE	165.8	9.9	9.90E-06	5.9710E-02	5.9087E-06	200	0.0012
1,1-DCA	99	9.7	9.70E-06	9.7980E-02	9.6957E-06	8,100	0.0785
H_20	18	5.3	5.30E-06	2.9444E-01	2.9137E-05		
NVM[b]	--	5	5.00E-06	unknown	unknown		
HCL	13	1.73	1.73E-06	1.3308E-01	1.3169E-05	miscible	miscible
CA	64.51	1	1.00E-06	1.5501E-02	1.5340E-06	6,040	0.0093
trans-1,2-DCE	97	0.8	8.00E-07	8.2474E-03	8.1613E-07	6,300	0.0051
VC	62.5	0.8	8.00E-07	1.2800E-02	1.2666E-06	3,000	0.0038
1,1,2,2-TECA	167.9	0.8	8.00E-07	4.7647E-03	4.7150E-07	2,900	0.0014
Iron	55.847	0.064	6.40E-08	1.1460E-03	1.1340E-07		
Total				1.0106E+04	1.0000E+00		

[a] Number of grams of impurity per 10^6 grams of EDC

[b] Non-volatile materials

3.3 PCEMI in Manufactured 1,2-DCA

The original use of the 1,2-DCA MI data was to evaluate degradation mechanisms at the site. This data also may be used to evaluate the potential impact to groundwater by PCEMI. PCEMI comprises, by mass, about 0.001% of this particular sample of 1,2-DCA.

3.1.1 Solubility of PCEMI

The solubility of PCE in water has been reported at 150 mg/L (CRC 73rd Ed) and 200 mg/L (Pankow and Cherry 1996). This solubility is valid for PCE present as a single component. When PCE is present in a mixture, its solubility must be calculated with respect to the other components of the mixture, based on Raoult's Law (Feenstra et al. 1991). The solubility of a component in a mixture is calculated by the following formula, where Csat,m is the aqueous solubility of a component in a mixture, Xm is the mole fraction of the component, and Cosat is the aqueous solubility of the compound as a single component:

$$C_{sat,m} = X_m C^o_{sat}$$

$C_{sat,m}$ is known as the "effective solubility" of a component in a mixture (Pankow and Cherry 1996).

Table 1 shows the calculated effective solubility of PCEMI in manufactured TCE, when the higher solubility is considered. For the past 10 to 15 years, the maximum effective solubility of PCEMI in manufactured TCE has been 0.0002 mg/L (0.2 µg/L), based on PCEMI present in an amount equal to the detection limit of 1 ppm w/w. Prior to that time, the effective solubility of PCEMI would have been, sporadically, as high as 0.002 mg/L (2.0 µg/L). Table 2 shows that the calculated effective solubility for PCEMI in the 1998 sample of 1,2-DCA solvent is 0.0012 mg/L (1.2 µg/L). These effective solubilities represent the calculated maximum possible groundwater concentrations of PCEMI from manufactured TCE and 1,2-DCA, because attenuating mechanisms, such as sorption, dilution, and degradation, will reduce the concentration in groundwater.

An aliquot of a different sample of 1,2-DCA, produced by the same manufacturer at about the same time as the sample analyzed in 1998, was dissolved in deionized water to determine, under laboratory conditions, aqueous concentrations of the chlorinated components present in the manufactured 1,2-DCA. The results from this analysis are tabulated in Table 3. These results show the presence of four MIs — cis-1,2-dichloroethylene (c-1,2-DCE), PCE, TCE, and 1,1,2-trichloroethane (1,1,2-TCA).

Table 3. Analysis of Impurities in 1,2-DCA Solvent Dissolved in Water: 1999 Sample

Compound	***Concentration*** (mg/L)	***Fraction of EDC***
EDC	8,562	
cis-1,2-DCE	0.0641	7.4866E-06
PCE	0.0065	7.5917E-07
TCE	0.0061	7.1245E-07
1,1,2-TCA	Not Quantified	

The aqueous concentration of PCEMI generated under laboratory conditions was 0.0065 mg/L (6.5 ppb), which is about 5.5 times the calculated effective solubility. This high concentration is likely inaccurate due to the formation of an emulsion of NAPL in the water

during mixing of the sample (Feenstra et al. 1991, Billington et al. 1988). It is unlikely that this high concentration is a result of differences in 1,2-DCA batch production. PCEMI would have to be present in the manufactured 1,2-DCA at 50 ppm to generate a concentration of 6.5 ppb in water, which far exceeds the amount of PCEMI typically generated during solvent manufacturing.

4. CONCLUSIONS

The calculated maximum groundwater concentrations of PCEMI that might be generated from its presence in manufactured TCE or 1,2-DCA, are likely no more than 0.2 to 2.0 μg/L for PCEMI in TCE and 1.2 μg/L for PCEMI in 1,2-DCA. These concentrations, which are overestimated, are below or near the method detection limit (MDL) for some analytical methods (Table 4).

Table 4. Detection Limits for PCE

Method	Method Detection Limit μg/L	
5032	1.4	Vacuum Distillation – Internal Standard
5032	1.8	Vacuum Distillation – External Standard
8021B	0.05	PID (photoionization detector)
8021B	0.04	HECD (electrolytic conductivity detector)
8260B	0.14	Wide-Bore Capillary Column
8260B	0.05	Narrow-Bore Capillary Column

Estimating groundwater concentrations generated by MIs from effective solubility calculations results in overestimation of the groundwater concentration of the MI, because processes such as sorption, dilution, and degradation reduce groundwater concentrations. Another important process in the generation of groundwater concentrations of PCEMI is the rate of dissolution for PCE and the chlorinated solvent. When these processes are considered, it is likely that the groundwater concentrations generated by PCEMI are much less than its effective solubility and are below the detection limit of commonly used analytical methods. This is supported by the evaluation of the vapor degreaser conceptual model based on reported field concentrations. The results of this evaluation indicate that the groundwater concentration that could realistically result is 0.01 μg/L, which is below all of the analytical methods listed in Table 4. PCEMI likely does not significantly contribute to groundwater contamination, as PCEMI is either not detectable or groundwater concentrations generated are likely below the maximum contaminant level of 5 μg/L.

This work represents an initial step toward greater understanding of the potential impact to groundwater from MIs and, as a result, better source identification. Greater participation from chemical manufacturing partners in research related to the issues presented here is necessary to better quantify the MIs in manufactured solvents, particularly over the history of their manufacture. Laboratory and field studies designed to improve our understanding of solubility issues related to manufactured solvents and site specific effective solubilities are also necessary

to understand the environmental impact from chlorinated solvents and MIs. This is important, because even minor concentrations of PCE may indicate sources of PCE contamination other than MIs. At sites where chlorinated solvent releases have occurred, better source identification and quantification of the resulting environmental impact are required for thorough site characterization, selection of effective remediation technologies, reliable forensic investigations, fair cost allocation, and presentation of sound, justifiable technical opinions for litigation support.

5. REFERENCES

Abbott, D.E., 1987, The Origin of Sulphate and The Isotope Geochemistry of Sulphate-Rich Shallow Groundwater in the St. Clair Clay Plain, Southwestern Ontario, University of Waterloo, Waterloo, Ontario, 1-134.

Agency for Toxic Substances and Disease Registry, 2006, Toxicological Profile for Trichloroethylene: 4. Production, Import/Export, Use, and Disposal, http://www.atsdr.cdc.gov/toxprofiles/tp19-c4.pdf, accessed May 21, 2006, 185-189.

American Society for Testing and Materials, 1989, Manual on Vapor Degreasing, Baltimore, June.

Billington, J.W., et al., 1988, Preparation of Aqueous Solutions of Sparingly Soluble Organic Substances: I. Single component Systems, Environmental Toxicology and Chemistry, v. 7, 117-124.

CRC, 1994/1995, Handbook of Chemistry and Physics, 75th Edition, CRC Press.

Canadian Center for Occupational Health and Safety, 1999, Basic Information on Trichloroethylene, http://www.ccohs.ca/oshanswers/chemicals/chem_profiles/trichloroethylene/basic_trichlor.html, accessed May 15, 2006.

Creber, C., 2000, Personal Communication, April 16.

Doherty, R.E., 2000, A History of the Production and Use of Carbon Tetrachloride, Tetrachloroethylene, Trichloroethylene and 1,1,1-Trichloroethane in the United States: Part 1 — Historical Background; Carbon Tetrachloride and Tetrachloroethylene, Journal of Environmental Forensics, 1, 69-81.

Doherty, R.E., 2000, A History of the Production and Use of Carbon Tetrachloride, Tetrachloroethylene, Trichloroethylene and 1,1,1-Trichloroethane in the United States: Part 2 — Historical Background; Trichloroethylene and 1,1,2-Trichloroethane, Journal of Environmental Forensics, 1, 83-93.

Feenstra, S., et al, 1991, A Method for Assessing Residual NAPL Based on Organic Chemical Concentrations in Soil Samples, Ground Water Monitoring and Remediation, Spring, 128-136.

International Program on Chemical Safety, 1985, Environmental Health Criteria 50, Trichloroethylene, http://www.inchem.org/documents/ehc/ehc/ehc50.htm, accessed August 18, 2005 and May 20, 2006.

Kästner, M., 1991, Reductive Dechlorination of Tri- and Tetrachloroethylenes Depends on Transition from Aerobic to Anaerobic Conditions, Applied and Environmental Microbiology, July, 2039-2046.

Klecka, G.M., et al.,1990, Biological Transformations of 1,1,1-Trichloroethane in Subsurface Soils and Ground Water, Environmental Toxicology and Chemistry, 9, 1437-1451.

Kriegman-King, M.R. and M. Reinhard, 1992, Transformation of Carbon Tetrachloride in the Presence of Sulfide, Biotite, and Vermiculite, Environmental Science and Technology, 26(11), 2198-2206.

Lane, V., 2001, Distribution of Chlorinated Solvent Contamination in a Surficial Clayey Aquitard: Evidence for Fractures and Attenuation, Master of Science Thesis, The University of Waterloo, Canada.

Mohr, T.K.G., 2001, Solvent Stabilizers, White Paper, Prepublication Copy, Santa Clara Valley Water District, http://www.valleywater.org/Water/Water_Quality/Protecting_your_water/_Lustop/_Publications_and_Documents/_PDFs_Etc/SolventStabilizers.pdf, accessed May 21, 2006, 52 pp.

Morrison, R.D., 2000, Critical Review of Environmental Forensic Techniques: Part 1, Environmental Forensics, 1, 157-173.

Morrison, R.D., 2000, Critical Review of Environmental Forensic Techniques: Part 2, Environmental Forensics, 1, 157-173.

Quigley, R.M. and T.A. Ogunbadejo, 1976, Till Geology, Mineralogy and Geotechnical Behavior, Sarnia, Ontario, In: Legget, R.F., (Ed.), Glacial Till an Inter-Disciplinary Study, The Royal Society of Canada, 336-345.

Oregon Department of Health and Human Services, 2003, Questions and Answers from the View-Master Public Meeting held on January 28, 2003 and released on April 2, 2003.

Prine, B., 1999, Personal Communication, August 18.

Schwille, F., 1988, Dense Chlorinated Solvents in Porous and Fractured Media, CRC Press, Inc.

Terry, D., 2006, Personal Communication, June 5.

U.S. Environmental Protection Agency, 1999, Final Listing Background Document for the Chlorinated Aliphatics Listing Determination (Proposed Rule), Office of Solid Waste, http://www.epa.gov/epaoswer/hazwaste/id/chlorali/backgrnd/final_lb.pdf

PART VII: Ethics in Environmental Practice

Chapter 15

THE PUBLIC TRUST AND AIR QUALITY

Norman Anderson, M.S.P.H.[§]
American Lung Association of New England, 122 State Street, Augusta, ME

ABSTRACT

As we approach the fortieth anniversary of the Clean Air Act, it is worthwhile to review the basic philosophical underpinnings that place limits on private ownership for the public good. This presentation will examine the Public Trust Doctrine, which dates back to the time of the Emperor Justinian, in relationship to protecting the public from the harmful effects of air pollution. It will focus on issues that have emerged since the 1970 Clean Air Act, such as exposures to environmental tobacco smoke. It will also focus localized situations in which significant exposures can occur in the surrounding population, such as the emerging health threat of outdoor wood boilers. A central concern in all these instances is what the primary responsibility of government should be as the keeper of the public trust.

1. INTRODUCTION

This paper addresses an area of environmental health within its broader ethical and philosophical context. It is, therefore, departing from the established format of hypothesis generation and consequent testing and interpretation. The field of environmental ethics is an increasingly important one (c.f., Newton et al, 2006), and parallels efforts to incorporate philosophical concerns in other scientific fields as well, (e.g., Sen, 1987, in the field of economics). Here, we examine some specific concerns regarding the applications of the Public Trust Doctrine to air pollution issues.

[§] Norman Anderson, M.S.P.H., American Lung Association of New England, 122 State Street, Augusta, ME 04330, Tel: 207-621-4059 x109; 1-888-241-6566 x109, Fax: 207-626-2919, Email: nanderson@lungme.org

2. TWO CONCEPTIONS OF JUSTICE

We start first with two different and opposing conceptions of justice. One is based on subjective relativism and the other on an ethical aspiration towards a well-ordered society. With subjective relativism, as described by Newton et al. (Newton et al., 2006), there are: a) no absolute or unchanging moral principles; b) rules that govern each situation are to be determined in relation to something else; and c) the sole source of knowledge or authority is in the perception of the individual. This idea is consistent with the fact that we live in a pluralistic society in which tolerance and acceptance of other people is a clearly accepted expectation. (Newton et al., 2006). Unfortunately, the notions of tolerance and acceptance, particularly regarding actions of private citizens, may often fail to recognize the ramifications in the form of public health and environmental externalities.

A well-ordered society, according to John Rawls (Rawls, 2001), is regulated by: a) a public conception of justice; b) one system of cooperation; and c) a normally effective sense of justice among the citizens. As in a condition of subjective relativism, one recognizes the existence of a pluralistic society. A well-ordered society, however, contains certain fundamental ideas from which it is possible to work up a political conception of justice. The environment as a consideration of justice was not directly addressed by Rawls. On the other hand, he did posit the requirement of basic rights and liberties as being needed and required by individuals to be fully cooperating members of society.

It is this construct that not only makes our laws possible both to establish and enforce. It also makes it possible to approach conditions of justice from an ethical perspective. Debates concerning environmental issues entail a great deal of analysis regarding risk assessment and the scientific basis for risk assessment. While these are important considerations, it is possible that an important perspective may be lost if the protection of the environmental protection is considered solely as a scientific matter. In that respect, environmental laws and policies should be no less subject to a discussion of ethics than more identifiable forms of civil justice. The basis of our environmental laws, in other words, stems from "a public conception of justice" and not an ever-changing compromise among different subjective realities. It compels regulatory thinking to reach beyond subjective relativism towards a more encompassing vision. This exercise for a public health organization is not a trivial one. It influences how such an organization should advocate for a particular environmental law, or even for a broader regulatory policy.

3. THE PUBLIC TRUST

In searching for a fundamental principle to guide this discussion, none seems as compelling as the notion of the *public trust*.

> By the law of nature these things are common to all mankind, the air, running water, the sea, and consequently all the shores of the sea.
>
> Codex Justinian, 529 A.D.

Specifically, Justinian ruled that navigable water was the common property of a nation's citizens, owned by everyone and no one at once, an unwritten public easement protected by their steward, the state (Dowie, 2005). The Public Trust Doctrine, as applied currently, is founded on this concept regarding the public nature of our rivers, the sea, and the seashore (Sax, 1970).

Through its evolution in English common law, the idea of "sovereign" property was born, and with this came the duty of state stewardship (Dowie, 2005). There are two co-existing interests to trust lands: the *jus publicum* is the public's right to use and enjoy trust lands; the *jus privatum* is the private property rights that may exist in the use and possession of trust lands. The Public Trust Doctrine says that the State must recognize the *jus privatum* or private property rights so long as they remain subservient to the inalienable public trust over land and water (Dowie, 2005). In essence, the problem that the Public Trust Doctrine is addressing is the political imbalance created when the interests of a diffuse majority is made subject to the will of a concerted minority (Saxe, 1970).

Throughout much of the last century, the Public Trust Doctrine was used primarily against obstacles to commerce and navigation (Dowie, 2005). The concept was reinvigorated, however, in 1970 with a landmark article by Joseph Sax (Sax, 1970). In this article, he advocated that the Public Trust Doctrine be expanded far beyond navigable water to protect the soil, air, and other species – things "so particularly the gifts of nature's bounty that they ought to be preserved for the whole of the populace."

An example of the impact of Sax's thinking can be found in the Hawaii state constitution.

> For the benefit of present and future generations, the State and its political subdivisions shall conserve and protect Hawaii's natural beauty and all natural resources, including land, water, air , minerals and energy sources, and shall promote the development and utilization of these resources in a manner consistent with their conservation and in furtherance of the self-sufficiency of the State. All public natural resources are held in trust by the State for the benefit of the people." – Hawaii State Constitution, Article XI, Section I (Added 1978).

On a more grassroots level, in 1970 over 20 million people celebrated the first Earth Day a national demonstration of support for public protection of common resources (Dowie, 2005). Shortly thereafter, President Nixon signed into law the National Environmental Protection Act, the Clean Water Act, the Coastal Zone Management Act, the Endangered Species Act, and legislation creating the Environmental Protection Agency. It could be argued that during this historical moment the interests of the *diffuse majority* to which Sax referred found a collective voice that subsequently impelled a new constellation of environmental laws.

As a guiding philosophic principle, the Public Trust Doctrine addresses two major environmental policy concerns. The first is that our ambient environment is a public resource given in trust to the State to protect. The second is that with respect to the public trust, private interests are subservient to public interests (note, for instance, examples of wetlands laws and fishing or hunting regulations). The counter-argument, that of *takings*, applies when the State appropriates private property without adequate compensation. The balancing of these interests has a long history in the implementation of environmental and nuisance laws. Yet, it is critical to recognize that there are two competing interests, and the important role of the State as the guardian of the *diffuse* public interest, as noted by Sax.

4. PROTECTION OF AIR QUALITY

Application of the Public Trust Doctrine to air quality concerns involves three inter-related components: 1) the enactment of laws to limit or eliminate exposure to air pollutants; 2) the use of nuisance provisions for situations in which environmental exposure limits are either lacking or insufficiently address the variety of circumstances that could create harm**;** and 3) the development of a research and education plan to provide a stronger basis for encouraging effective exposure reduction alternatives. Despite the fact that most of the Public Trust Doctrine's history has focused on navigable waters and the seashore, the underlying principle, that there are resources "owned by everyone and no one" (see Dowie, 2005) should certainly apply to something as fundamental to life as the air we breathe.

4.1 Environmental Laws

The Public Trust Doctrine is not a set of laws. Rather, we can view it as a political concept that can guide the nature and intensity of actions to support the preservation of the public good. It can be argued, for example, that the strong sense of public empowerment surrounding the first Earth Day was motivated in at least some fundamental way by our collective desire to have the State exert its police power to enforce environmental protections. This sentiment is reflected as well in the legislation creating the Bureau of Air Quality in Maine.

> "The Legislature by this chapter intends to exercise the police power of the State in a coordinated state-wide program to control present and future sources of emission of air contaminants to the end that air polluting activities of every type shall be regulated in a manner that reasonably insures the continued health, safety, and general welfare of all of the citizens of the State; protects property values and protects plant and animal life." (MRSA, Title 38, Chapter 4, Section 581).

Over the past fifteen years, one of the most important advances in public health has been the enactment of clean indoor air laws in workplaces and public environments. These laws were motivated in large part by the U.S. Environmental Protection Agency finding that environmental tobacco smoke (ETS) is a human carcinogen (USEPA, 1992). Prohibitions on smoking were enacted in Maine and throughout the country on the premise that there is no safe level of exposure, and that the interests of smokers must be subservient to the basic public obligation of protecting health. While not explicitly stated, this is an application of the public trust doctrine, in that the public's right to healthy air cannot be compromised by private decisions to allow smoking. Indeed, the enforcement of these laws are largely self-enforced, based on the cultural expectation that smoking is not acceptable in indoor environments accessible to the public.

4.2 Public Nuisance: Outdoor Wood Boiler Example

Wood smoke has long been considered a health concern, particularly for people with lung and heart diseases (Naeher et al, 2007). In addition, as a combustion mixture, wood smoke also contains many toxic compounds that can increase the risk of cancer. Increasing attention is focused on the fine particulate fraction of wood smoke. These particles can penetrate deep into

the lungs where they can cause damage locally or cause systemic effects due to absorption into the bloodstream.

Under ideal conditions, there is the expectation that the laws preventing or restricting air pollutant emissions would be sufficient to avoid any public harm. Performance standards now exist for wood stoves, and there are many educational resources available to consumers on how to burn wood efficiently and with the minimum of emissions. With the advent of outdoor wood boilers (OWBs), however, there is an emerging and serious concern regarding the ability of the State to protect the public from harm. OWBs have become increasingly popular over the past several years because they use a renewable resource, can provide a cheaper source of space heating and domestic hot water than fossil fuels, and are exempt from federal regulation. The advantages are particularly evident in rural areas such as Maine.

Unfortunately, the features that make outdoor wood boilers so appealing also contribute to their potential to adversely affect health. Reports and studies conducted in the past few years have documented the significant air pollution exposure problems that these boilers can create (Attorney General of New York State, 2005; NESCAUM, 2006; Johnson, 2006), and that exposures resulting from OWB use can far exceed health criteria (Brown et al., 2007). For most OWBs, their large fireboxes, the cyclic nature of their operations (in response to intermittent demands for hot water), relatively low temperatures compared to other combustion devices, and short stack heights are among the features that have been cited as reasons why their hourly emissions substantially are higher than wood stoves (NESCAUM, 2006). In the absence of federal regulation, states are beginning to adopt regulations to control emissions of new units based on guidance from the Environmental Protection Agency (USEPA, 2007) and the Northeast States for Coordinated Air Use Management (NESCAUM, 2007).

This regulatory activity gives rise to the often misleading perception that the State is providing the public sufficient protection from the harmful effects of OWBs. Although regulatory guidance has been developed, this perception may be misplaced for a number of reasons. First, the air quality standard used to measure acceptable air quality, the PM 2.5 standard (or particulate matter 2.5 microns in diameter), has been criticized as being not stringent enough and for not focusing on a short enough time period (e.g., two hours) to protect against acute health effects. Moreover, the regulatory analysis could have adopted a more conservative air quality criterion than compliance with the PM 2.5 air quality standard, such as one focused on Prevention of Significant Deterioration, but it did not. Second, there are questions as to whether the exposure assessment techniques used by the regulatory agencies to develop their guidance were sufficiently protective even when this arguably lax standard is used (for example, by the omission of multiple OWBs in the modeling estimates). Third, the potential adverse health consequences associated with the full range of harmful air pollutants in the combustion mixture were not addressed. Fourth, there is little if any air quality monitoring data on which to evaluate the current public health dimensions of the problem and consequently, the extent of risk reduction which will be afforded by regulations based on these recommendations. Fifth, there is little protection in these regulations afforded to those living near existing boilers

States are recognizing the potential limitations regarding the protection of public health by incorporating nuisance language into the OWB regulations. This language is focused primarily on evidence of visible emissions without any specific reference to health impacts. In this context,

enforcement is under the purview of state environmental agencies. While promising in concept, it is too early to determine whether this mechanism will prove effective.

It is within this regulatory and policy context that those seeking relief now have to make their case regarding evidence of health harm. Absent helpful state regulation, those affected by OWBs could seek relief through recourse to general nuisance provisions that have existed for the past two centuries. Generally, nuisances constitute conditions that may endanger life or health, or obstruct reasonable and comfortable use of property. Thus OWBs could theoretically be included among the state's list of particular nuisances. In a recent legal proceeding, however, harm to health was not assumed but had to be demonstrated. The perceptions surrounding this case framed the matter more as a dispute among neighbors. From a philosophic point of view, the context for decision making appeared to be more along the lines of a subjective relativism argument than one related to "a public conception of justice," at least with respect to the protection of health or the environment.

The difficulty faced by affected individuals is further magnified by the 1993 Supreme Court Daubert decision. This decision set a standard for actions to protect public health to areas that are highly researched according to rigorous peer review standards. Such a bar is effectively prohibitive for individual private citizens who seek some sort of relief from the boiler emissions.

Thus, a major barrier to the satisfactory resolution of health problems in this context is the difficulty in demonstrating a specific connection between the air pollution and the impairment of health or well being. This is a well-known dilemma in risk assessment, which relies on epidemiological and toxicological studies to determine acceptable levels of exposure, and is not focused to ascribing causation in particular instances. Inferences can be drawn from population based studies using statistical methods that are useful for setting public policy. These types of studies overcome the uncertainties associated with the inability to reject alternative hypotheses when applied to individual cases.

There are also significant barriers when trying to implement traditional public health approaches to nuisances. Such approaches focus more on vector borne diseases, where a particular illness can be ascribed to a particular cause and where nuisance can be determined qualitatively (e.g., the simple presence of an offending agent). On the other hand, air pollution tends to aggravate pre-existing conditions rather than cause illness outright. Also, nuisances in theses circumstances often rely on some quantitative assessment of exposure, which may often be both difficult to obtain and difficult to interpret, creating even further disincentives for enforcement by local health officers.

Sadly, without nuisance provisions, affected individuals are left with few options for seeking relief. In some cases these individuals have argued for basic constitutional protections focused on life, liberty and the pursuit of happiness.* This is a relatively rare approach. Yet, there are documented cases of families being forced to leave their homes as a result of a neighbor's outdoor wood boiler to protect their health and well being. Further, they do so with the knowledge that their property might be very difficult to sell, at least without taking a significant loss because of the neighboring boiler.

Despite its current limitations, however, a nuisance-based approach provides a valuable backstop for ensuring public health protection in individual circumstances. Strong nuisance provisions would not only address instances in which broader air quality laws may prove ineffective. They would also create the means by which emerging health threats could be identified and resolved through additional public policy initiatives. A robust interaction between nuisance enforcement and a re-invigorated Public Trust Doctrine could provide the ideal context for ensuring protection of the ambient air.

In time, the Public Trust Doctrine might prove useful to this situation as set of criteria from which to evaluate the adequacy of environmental regulations. The circumstance of outdoor wood boilers, however, like that of many localized air pollution problems, does not apply to a defined geographical area, such as a seashore or waterway. Instead, it applies to a commonly accepted public resource, our ambient air, which is being compromised in separate, generally isolated situations. Here, the diffuse majority Sax described is randomly selected from the general population whenever a neighbor may decide to install an OWB.

4.3 The Importance of Research and Education to the Public Trust Doctrine

Finally, the concept of the public trust recognizes that an ever changing dynamic exists when deciding the degree of protection that should be accorded to our natural resources. Because of this, there is always the opportunity for the public dialogue and consequently, the opportunities for citizen action, to be transformed by new research. Research on the harmful effects of environmental tobacco smoke ultimately led to the consensus regarding its role in the development of lung cancer, as well as variety of other respiratory and cardiovascular diseases. This consensus regarding its role as a human carcinogen, led to the deletion of the ventilation standard recommendation by the American Society of Heating, Refrigeration, and Air Conditioning Engineers (ASHRAE) for buildings where smoking was present. ASHRAE based this recommendation on the fact that a safe level of exposure to ETS had not been determined by any recognized credible authority. A variety of legislative initiatives on indoor smoking prohibitions followed which, in addition to the specific policy objectives, provided substantial opportunities for public education and mobilization. While focused predominantly on the air in public *indoor* environments, the success of such advocacy can provide hope for a renewed sense of protection for our outdoor air as well, particularly given the similarity of health concerns between ETS and outdoor air pollution.

We are just beginning to develop a research and information base on outdoor wood boilers (e.g., Johnson, 1006; Brown et al., 2007). The importance of efforts such as these to political advocacy is to recognize the interactive framework in which we are working. The challenge before us is how to promote a meaningful public health agenda on air quality that reconnects us with these basic public underpinnings of a democratic society.

Beyond the specific cases, an advocacy framework based on protecting the public trust also provides a means by which we can develop a collective sense of ownership regarding our air. In the context of a general framework, the lessons and accomplishments of individual cases become cumulative in nature. They are consequently amenable to public policy research, as well as ongoing educational opportunities.

5. CONCLUSION

This paper has outlined the beginnings of a dynamic strategy for advocacy regarding air quality. It involves the interaction of public laws and nuisance abatement, motivated by a robust research and education agenda. Recent public policy successes in the area of tobacco control, particularly with respect to smoking in public places, can engender a renewed sense of air as a public trust. Outdoor wood boilers are an example of an emerging health threat requiring the interplay of all the major components of this strategy. It is hoped that through this example, we may develop a more generalized model for public health protection.

*See, for example, the following sections of Maine's constitution. Section 1. Natural rights. All people are born equally free and independent, and have certain natural, inherent and unalienable rights, among which are those of enjoying and defending life and liberty, acquiring, possessing and protecting property, and of pursuing and obtaining safety and happiness; Section 6-A. Discrimination against persons prohibited. No person shall be deprived of life, liberty or property without due process of law, nor be denied the equal protection of the laws, nor be denied the enjoyment of that person's civil rights or be discriminated against in the exercise thereof; Section 19. Right of redress for injuries. Every person, for an injury inflicted on the person or the person's reputation, property or immunities, shall have remedy by due course of law; and right and justice shall be administered freely and without sale, completely and without denial, promptly and without delay.

6. REFERENCES

Attorney General of New York State, 2005, Smoke Gets in Your Lungs: Outdoor Wood Boilers in New York State, 32 pages.

Brown, D.R., et al., 2007, "An Assessment of Risk from Particulate Released from Outdoor Wood Boilers," Human and Ecological Risk Assessment, Vol. 13, pp. 191-208.

Dowie, M., 2005, "In Law We Trust," Orion Magazine, July/August, http://www.orionmagazine.org/index.php/articles/article/122/

Johnson, Philip, 2006, "In-Field Ambient Fine Particle Monitoring of an Outdoor Wood Boiler: Public Health Concerns," Human and Ecological Risk Assessment, Vol. 12, pp. 1153-1170.

NESCAUM (Northeast States for Coordinated Air Use Management), 2006, Assessment of Outdoor Wood-Fired Boilers, June 2006 Revision. http://www.nescaum.org/documents/assessment-of-outdoor-wood-fired-boilers

NESCAUM (Northeast States for Coordinated Air Use Management), 2007, Outdoor Hydronic Heater Model Regulation, January 29, 2007. 19 pp. http://www.nescaum.org/topics/outdoor-hydronic-heaters

Newton, LH, et al., 2006, Green Ethics: An Introduction to Environmental Ethics, Fairfield University, 67 pp.

Naeher, L.P., et al., 2007, Woodmoke Health Effects: A Review, Inhalation Toxicology, Vol. 19, pp. 67-106.

Rawls, John, 2001, Justice as Fairness: A Restatement., Harvard University Press, Cambridge, Massachusetts. 214 pp.

Sax, Joseph, 1970, "The Public Trust Doctrine in Natural Resources Law: Effective Judicial Intervention," Michigan Law Review, Vol. 68, pp. 471-570.

Sen, Amartya, 1987, On Ethics and Economics, Blackwell Publishing, Malden, MA, 131 pp.

USEPA (U.S. Environmental Protection Agency), 1992. Respiratory Health Effects of Passive Smoking: Lung Cancer and Other Disorders, U.S. EPA Office of Research and Development, Publication No. EPA/600/6-90/006F.

USEPA (U.S. Environmental Protection Agency), 2007, EPA Outdoor Wood-fired Hydronic Heater Program, 41 pp. March 16, 2007 Revision, http://www.epa.gov/owhh/pdfs/Partnership_Agreement_3_16_07.pdf

Chapter 16

DECEPTION AND FRAUD IN THE PUBLICATION OF SCIENTIFIC RESEARCH: ARE THERE SOLUTIONS?

Christopher M. Teaf[1§] and Barry L. Johnson[2]

[1]Center for Biomedical & Toxicological Research, Florida State University, 2035 East Dirac Dr., Tallahassee, FL, 32310; [2]Rollins School of Public Health, Emory University, 2618 Riverglenn Circle, Atlanta, GA, 30338

ABSTRACT

A number of events in the U.S. and abroad have refocused the scientific community on historical issues of whether, and how, integrity of our technical literature can be assured. Solutions to this problem are neither simple nor certain. Professional societies have addressed scientific misconduct, and effective responses by the research community will require cooperation of scientific publications. While the incidence of scientific fraud is difficult to estimate with precision and certainly varies with discipline, identified and publicized recent cases beg attention from editorial boards. Several egregious cases are described. The peer review system serves the function of examination and critique by scientists in relevant disciplines to assess submitted papers prior to publication. There is even a developing literature and several specific journals dedicated to the subject of fraud, professional integrity and ways to monitor or correct existing conditions. Underlying the field of professional and scientific publication is a fundamental assumption that data are real and that research actually occurred. Typically, the process is "blind" in both directions, although some journals permit "author-directed" reviews. A reviewer's responsibilities include ensuring that text properly reflects data, that tables and figures are necessary/appropriate, and that conclusions fairly and reasonably reflect results and the body of information. Thus, existing peer review systems probably cannot detect anything but the most obvious fraud. In addition to imposing or perpetuating stringent review protocols, journals also can amend author guidelines to speak explicitly about publishing requirements. Cases of properly documented fraud warrant immediate public announcement, followed by official withdrawal or retraction. Reflection on these issues led editors of one journal to institute changes in editorial policies and develop a code of ethics for authors, reviewers, and editors. Prevention of dishonest research is already difficult, and we should ensure that this remains the case. Editors should formally commit reviewers/authors to ethical conduct in technical publications prior to publication and review.

Keywords: Fraud, scientific research, peer review

§ Corresponding Author: Christopher M. Teaf, 2035 East Dirac Dr, Tallahassee, FL 32310, Tel: 850-644-5524, Email: cteaf@mailer.fsu.edu

1. INTRODUCTION

To quote Sir Winston Churchill: "Truth is incontrovertible. Malice may attack it and ignorance may deride it, but, in the end, there it is." Mark Twain looked at this question from the darker side and concluded: "One of the most striking differences between a cat and a lie is that a cat has only nine lives." With the huge stakes that ride on technical, medical or engineering decisions every day, it seems quite obvious that veracity in the scientific literature (… our literature) is essential. However, multiple events over the last several years in Norway, South Korea and elsewhere have refocused the scientific community on the unpleasant issue of whether, and by what means, we can ensure the continued integrity of our technical literature. Many scientific journals have set aside significant time and effort to address this thorny problem, and have struggled to find practical and effective solutions that may be suitable to their respective disciplines.

2. DISCUSSION

Potential scientific misconduct and fraud can come in many colors, and may include fabrication/falsification of data (aka "fudging", "culling", "massaging"), plagiarism, nondisclosure, violation of standards for human or animal research, and "ghostwriting" or "gift authorship." These events in principle should be clearly and quickly distinguished from honest error or scientific sloppiness, though in practice that distinction may be very difficult to accomplish.

In a recent Norwegian case which received international attention (Pincock 2006; Sudbo et al. 2005), regarding a publication in the prestigious medical journal The Lancet, the primary author confessed to the complete fabrication of all data in a clinical study investigating the influence of nonsteroidal anti-inflammatory drugs on oral cancer incidence. Even more highly publicized was the recent case of W.S. Hwang, who reported the laboratory cloning of human embryos in a mainstay of the scientific publishing world, the journal Science (Hwang et al. 2004; Hwang et al. 2005). These events involved several separate articles, each of which had many co-authors, ranging from 13 in the Sudbo et al. paper to more than 20 in one of the Hwang reports. A related but distinct part of the problem was identified by Schulz (2008), who discussed the case of a researcher from India who reportedly published 70 papers in 25 journals in three years. Evidently, the tactic was to "flood journals with manuscript submissions in the hopes of wearing down editors".

Whether an instance of scientific fraud is conducted for financial gain or for professional advancement, reports of such academic dishonesty are by no means novel, nor are they limited to any particular field of research. Medicine, physics, chemistry, physiology, anthropology, psychology and other disciplines all can claim a share of the bad news. Not surprisingly, the subject even has prompted at least a scholarly book or two (e.g., Lock et al. 2001; Judson 2004), a few in the popular literature also (e.g., Park 2001; Rivlin, 2004), an ongoing electronic bibliography (Pearson, 2005),and some official interest in government circles as well (Office of Research Integrity, 2000).

Prominent historical examples of scientific fraud, going back to Piltdown Man in the early-1900s (anthropology), also include the Schon case at Bell Labs in 2001 (physics), the Darsee (Harvard Medical School), Slutsky (UC-San Diego) and Breuning (NIMH) cases involving biomedical research in the early to mid-1980s, and the Industrial Bio-Test case of the late-1970s (involving laboratory testing procedures). One of the most famous cases, involving distinguished faculty and a postdoc at Massachusetts Institute of Technology (MIT), often colloquially referred to as the "Baltimore case", emphasized the inequitable division of responsibility and blame that inevitably follows when such unfortunate events come to light. The very recent Blair case, involving a reporter for the New York Times, included many articles purportedly, but falsely, attributed to interviews with the families of Iraqi war veterans. Even the names Newton, Mendel, Darwin, Pasteur, Haeckel, and Freud have been implicated in greater or lesser sins of adjusting, improving or even fabricating their data, information and scientific conclusions (Judson 2004). In 2006, Eric Poehlman (University of Vermont) became the first researcher in the U.S. to be jailed for scientific misconduct that was unrelated to the deaths of patients (Couzin, 2006).

Simply pointing out that there is a problem is neither surprising nor helpful, and the solutions in this situation are neither simple nor certain. A number of professional societies in our field, such as the Society of Toxicology, the Society for Risk Analysis, and the Society for Environmental Toxicology and Chemistry have addressed the issue of scientific misconduct, and effective responses by the research community will require intense introspection on the part of scientific publications worldwide.

While few would argue that the practice of scientific fraud is common, there is precious little empirical data to support a conclusion either way. This remains true despite the development of a series of specific journals that address the issue directly (e. g., Science and Engineering Ethics, Ethics and Behavior, Accountability in Research, and the Journal of the Society of Research Administrators). The mere existence of this growing body of literature illustrates the existence of the problem, though it also emphasizes that it is far from resolved. Further, the ability to truly understand the magnitude of the issue was questioned by Greenberg (2008) in the Chronicle of Higher Education, when he critically addressed surveys which seek to quantify "misconduct". Irrespective of what the true incidence may be, the presented cases and others beg several questions of editorial boards across the scientific community. This issue is crystallized in the comments of the Editor-in-Chief of Science, and former President of Stanford University, Dr. Donald Kennedy, who opined that "Scientific fraud is not new and is not rare. Luckily its not common either" (Kennedy, 2006). On the heels of Science's retraction of the Hwang papers, Kennedy's comments underscore the difficulties faced by the review process.

It is worth noting that a distinction is often made, albeit a subjective one, between formal, federally articulated "misconduct" and the other forms of unethical behavior. Federal misconduct formally is defined as activity that transgresses moral or civil law, while other unethical behavior can take on many meanings. Tough it may be useful to recognizing the more negative connotation of that specific category of unethical behavior, the distinction is not particularly important, nor emphasized, in this paper.

In its present form, the peer review system serves the valuable function of examination and critique by scientists in relevant disciplines, for the purpose of vetting and improving submitted

papers prior to their acceptance and publication. Implicit in that review process is the fundamental assumption that the reported data are real and that the research actually occurred. There really is "no workable alternative to starting with the assumption that authors are trying to offer a faithful depiction of the facts" (Sox and Rennie 2006). Typically, as is the case with manuscripts submitted to the international journal Human and Ecological Risk Assessment (HERA), the process is intentionally "blind" in both directions, and neither the author nor the reviewer is aware of the identity of the other. A reviewer's responsibilities, among others, include ensuring that the text properly reflects the tabular data, that the tables and figures are necessary and appropriate, and that the conclusions fairly and reasonably reflect the analytical results and the body of previous information available on the subject. Thus, the existing review system probably is not capable of detecting anything but the most obvious instances of fraud. Absent an inherently impractical system where peer reviewers visit laboratories, review lab notebooks and interview research personnel or secondary authors, substantive change in this area is unlikely.

While the intent of a blind review process is laudable and technically valid, it may be that the time honored practice fosters an unhealthy anonymity on the part of both the writer and the reader. Disclosure of both identities arguably would inhibit the temptation to submit manufactured or manipulated data. For example, HERA has employed an author-directed element of the review system for several years. This system requests that authors nominate potential reviewers, with concurrence from HERA's Managing Editor, who typically supplement the list of reviewers. All reviewers of such manuscripts are identified in the final printed article. Remarkably, this kind of review system is seldom used by authors. In our view, journals should amend their author guidelines to speak explicitly about publishing requirements. As a part of that step, it may be beneficial to require authors to sign a legally binding disclosure that clearly identifies the process and penalties that will accompany detection of fraudulent data or misrepresentation. In order to be effective, this disclosure would require signature by all coauthors on a submitted manuscript. Such a step may influence the growing phenomenon of papers with 10, 15 or even more co-authors, some of whom have had little direct knowledge of the results presented or the conclusions drawn. It is that type of "gift authorship" which has been put forth as a potential contributor to some of the fraudulent articles.

Innuendo and speculation regarding suggestions of academic dishonesty clearly are not sufficient to warrant action, and can do great harm. Jealousies and competition certainly could distort fair review. However, cases of properly documented fraudulent research warrant immediate public announcement, which would include identification of the full original citation in the announcement, so that subsequent database searches will pull up both of the references. Such an announcement would be followed by official withdrawal or retraction of the article or articles from the journal. As professionally embarrassing and technically inconvenient as these actions may be to the journal and to its editors, failure to do so is untenable if the allegations against the author(s) are substantiated. Further, in at least one case (Smith, 2005), the entire previous body of work by an author or group may rightly come under retroactive review as a result of proven or demonstrated fraud.

Reflection on these kinds of difficult issues led the editors of HERA to institute some changes in applicable editorial policies. While we acknowledge that the prevention of fraudulent research is a daunting proposition, we are committed to a course of action that will make it more

difficult to publish fraudulent science in our journal. Effective in August 2006, authors who submit manuscripts to HERA are advised that multiple authorship manuscripts explicitly acknowledge that all authors are aware of and in agreement with findings and conclusions in the manuscript. To provide further emphasis for this point, the e-mail addresses of all listed authors are required, and editorial decisions regarding a manuscript are communicated directly to all authors of that paper.

In addition, the HERA Instructions to Authors were revised to notify authors that fraudulent data or other improprieties in a manuscript will result in the manuscript being returned to all authors and notification sent to the authors' institution(s). Moreover, authors are alerted to the need for all authors to be identified for the purpose of trying to avoid preparation of manuscripts by "ghost" authors who might have a conflict of interest in the conduct of the study or in its publication. As a further measure, the HERA guidance to technical reviewers now contains language explicitly asking that any suspected fraudulent data be made known to HERA's editors. Finally, HERA's new Code of Ethics was published for the first time in the August 2006 issue. The Code is provided to all peer reviewers and authors during the manuscript review process. We commit ourselves and our reviewers to ethical conduct in review and publication of independently peer-reviewed science.

These editorial changes in policy were achieved through active dialog and debate amongst members of the HERA Editorial Board and the journal's Senior Editors. We are indebted to those editors who have helped to shape HERA's efforts to prevent fraudulent science from reaching publication in our journal. Many other journals have taken similar steps in this area, and they are to be commended as well.

3. REFERENCES

Couzin, J. 2006. Breakdown of the Year: Scientific Fraud. Science 314(5807): 1853.

Greenberg, D. 2008. Detecting scientific fraud. Chronicle of Higher Education. June 26, 2008.

Hwang, W.S., Y. J. Ryu, J. H. Park, E. S. Park, E. G. Lee, J.M. Koo, H. Y. Jeon, B. C. Lee, S. K. Kang, S. J. Kim, C. Ahn, J. H. Hwang, K. Y. Park, J. B. Cibelli, S. Y. Moon. 2004. Evidence of a pluripotent human embryonic stem cell line derived from a cloned blastocyst. Science 303: 1669-74.

Hwang, W.S., I.S. Roh, B.C. Lee, S.K. Kang, D.K. Kwon, S. Kim, S.J. Kim, S.W. Park, H.S. Kwon, C.K. Lee, J.B. Lee, J.M. Kim, C. Ahn, S.H. Paek, S.S. Chang, K.J. Koo, H.S. Yoon, J.H. Hwang, Y.Y. Hwang, Y.S. Park, S.K. Oh, H.S. Kim, J.H. Park, , S.Y. Moon, G. Schatten. 2005. Patient-specific embryonic stem cells derived from human SCNT blastocysts. Science 308: 1777-83.

Judson, H.F. 2004. The Great Betrayal: Fraud in Science. Harcourt Trade Publishers, San Diego, CA, USA.

Kennedy, D. 2006. Opening remarks at the January 20, 2006 symposium, "Beyond the Embryo", hosted by the Stanford Center for Biomedical Ethics' Program on Stem Cells and Society. As reported in the January 25, 2006 Stanford Report. http://news-service.stanford.edu/news/2006/january25/med-kennedy-012506.html

Lock, S., F. Wells. and M. Farthing. 2001. Fraud and Misconduct in Biomedical Research (3rd Edition). BMJ Publishing Group, London, UK.

Office of Research Integrity. 2000. Managing Allegations of Scientific Misconduct. Office of Public Health and Science, United States Department of Health and Human Services. Washington, D.C.

Park, R.L. 2001. Voodoo Science: The Road from Foolishness to Fraud. Oxford University Press. New York, NY.

Pearson, G. 2005. Bibliography of Resources on Scientific Misconduct. Available at http://www.lemoyne.edu/library/plagiarism/scientific_plagiarism_bib.htm.

Pincock, S. 2006. Lancet study faked. The Scientist, January 16, 2006.

Rivlin, S. 2004. Scientific Misconduct and Its Coverup: Diary of a Whistleblower. Unpublich.com Publishers.

Schulz, W.G. 2008. A massive case of fraud. Chemical & Engineering News 88(7): 37-38.

Smith, R. 2005. Investigating the previous studies of a fraudulent author. British Medical Journal 331:288-291.

Sox, H.C. and D. Rennie. 2006. Preventing scientific fraud. Annals of Internal Medicine 145(6): 473-474.

J. Sudbø, J. Lee, S. Lippman, J. Mork, S. Sagen, N. Flatner, A. Ristimäki, A. Sudbø, L. Mao, X. Zhou. 2005. Non-steroidal anti-inflammatory drugs and the risk of oral cancer: a nested case control study. The Lancet, October 15, 2005.

PART VIII: Heavy Metals

Chapter 17

EXPERIMENTAL AND BIOGEOCHEMICAL MODELING STUDIES ON ARSENIC RELEASE IN SOIL UNDER ANAEROBIC CONDITION

Md. Abdul Halim[§], Kenji Jinno, Abdur Razzak, Keita Oda and Yoshinari Hiroshiro
Institute of Environmental Systems, Graduate School of Engineering, Kyushu University, 744 Motooka, Nishi-ku, Fukuoka 819-0395, Japan

ABSTRACT

The identification of release mechanisms of arsenic may assist in designing safe and effective remediation strategies, due to its severe toxicity effect for the human body. In this regards, investigations were carried out to observe the release of As from soil into water. It was found that As concentration increased with decreasing oxidation reduction potential. Arsenic concentrations demonstrated negative covariation with the concentrations of NO_3^- but strongly correlated with DOC and Fe concentrations. Batch leaching tests at different pH conditions showed a strong pH dependence on arsenic and iron leaching. A numerical simulation of arsenic transport model, coupled with microbially mediated biogeochemical processes was developed for describing the release of As in soil under reducing environment. The simulation concentrations of Mn, Fe and As were well matched those found experimentally. The results of this study suggested that the microbially mediated degradation of organic matter and reductive dissolution of Fe-oxyhydroxide are considered to be the dominant processes to release As in aquifers.

Keywords: Arsenic, oxidation reduction potential, Fe-oxyhydroxide, Organic matter, Microbial reduction and biogeochemical arsenic transport model.

[§] Corresponding author: Md. Abdul Halim, Institute of Environmental Systems, Graduate School of Engineering, Kyushu University, 744 Motooka, Nishi-ku, Fukuoka 819-0395, Japan Tel.: 81-92-802-3427, Fax: 81-92-802-3427, E-mail address: hyd09@civil.kyushu-u.ac.jp

1. INTRODUCTION

Groundwater is the major source of water supply for domestic consumption, agriculture and industrial development, due to its inherent features. Unfortunately, groundwater is affected by arsenic (As) and now it is a major concern on a global scale due to its severe toxicity to the human body. The chemical species arsenate [As(V)] and arsenite [As(III)] of As controlling its chemistry and toxicity in the environment. Arsenate is the thermodynamically stable form under aerobic conditions, and it is mainly adsorbed onto iron and manganese oxides. Arsenite is the predominate species under anaerobic conditions; it is a neutral species at neutral pH values and is more soluble, mobile and phytotoxic than arsenate (Carbonell-Barrachina et al., 1999). The mobilization of arsenic from soil to groundwater and groundwater to soil is dependent on soil-water interaction in the subsoil environment. Although the geogenic source of As in the groundwater is generally accepted, the primary source and mechanism of release of As from soils and aquifer sediments into the groundwater is still not well understood (Wagner et al. 2005). However, the notion that reductive dissolution of arsenic-rich iron and manganese oxyhydroxides deeper in the aquifer may lead to the release of arsenic into the ground water is highly accepted (Smedley and Kinniburgh, 2002). On-site hydro-chemical investigations of aquifers have led to the hypothesis that the mobility of arsenic is primarily controlled by the availability of organic matter, which drives this process forward through microbial degradation of organic matter after consumed dissolved-O_2 and NO_3^- (Nickson et al., 2000), although this hypothesis has not been rigorously proven. It is not clear if these organic substances are derived from decomposing buried peat beds or from hydrologic seasonal drawdown of agricultural and other organic waste from the surface (McArthur et al. 2004).

The oxidation reduction potential (ORP) can affect the degradation and solubility of organic material living in soil and then influence the release of As in groundwater. Arsenic is chemically and microbiologically mediated oxidation-reduction, and methylation reaction in soils (Masscheleyn et al., 1991). It is necessary to develop a comprehensive reactive transport model that can simultaneously describe microbially-mediated biogeochemical reactions as well as other advection-dispersion processes. However, some studies on arsenic reactive transport have considered either adsorptive transport under anaerobic conditions or equilibrium sorption (Darland and Inskeep, 1997; Williams et al., 2003). None of these studies have considered the effects of microbial reaction kinetics.

The main objectives of this study are: (i) to conduct the experiments for elucidating the effect of oxidation reduction potential, pH and dissolved organic matter on release of arsenic from soil into groundwater, and (ii) to develop a biogeochemical arsenic transport model that consider microbially mediated redox processes for evaluating experimental results.

2. MATERIALS AND METHODS

2.1 Laboratory Experiments

A column experiment was carried out to observe the release of arsenic from soil to water in an anaerobic environment. An air-dried sediment sample was added with original soil at around 5% of total samples to enhance organic matter, manganese, iron and arsenic. The major physicochemical properties of the study soil together with original soil are given in Table 1. The pH of these samples was measured in 1:2 soil to deionized water ratio.

A schematic diagram of the experimental setup is shown in Fig. 1. The apparatus consisted of transparentacryl Resin column of 10 cm in diameter and 30 cm in height. The column was packed with study soil of 3.5 kg and its surface area, bed volume and total bed porosity were 78.54 cm^2, 2356 cm^3 and 44%, respectively. The top and the bottom of the column were closed using glass transparentacryl Resin plates with tubes for the flowing of influent and effluent, respectively. The water flow was continuous from feeding tank point 1 to overflow tank point 3 to create the anaerobic environment in the soil column and average temperature was measured at 24 ^{0}C.

Table 1. Main physicochemical properties of the study soil together with original soil

Parameter	Original soil	Study soil
TOC (%)	1.70	1.95
pH	6.2	6.2
ORP (mV)	345	359
Fe (mg/kg)	17000	39400
Mn (mg/kg)	2.3	1130
As(III) (mg/kg)	BDL	BDL
As(V) (mg/kg)	6.4	9.4
As_{total} (mg/kg)	6.4	9.4

TOC: Total Organic Carbon, ORP: Oxidation Reduction Potential
BDL: Bellow Detection Limit (0.5 mg/l)

At point 5, effluents were collected in the clean air tied disposable syringe coupled with filtration unit of 0.45 μm pore size. All effluents were kept in the refrigerator at 4 ^{0}C for analyzing. The pH and oxidation reduction potential (ORP) of the examined water were 7.9 and

301 mV, respectively. The amounts of total As, Fe and Mn in this water were 1.2, 1.6 and 2.3 µg/l respectively.

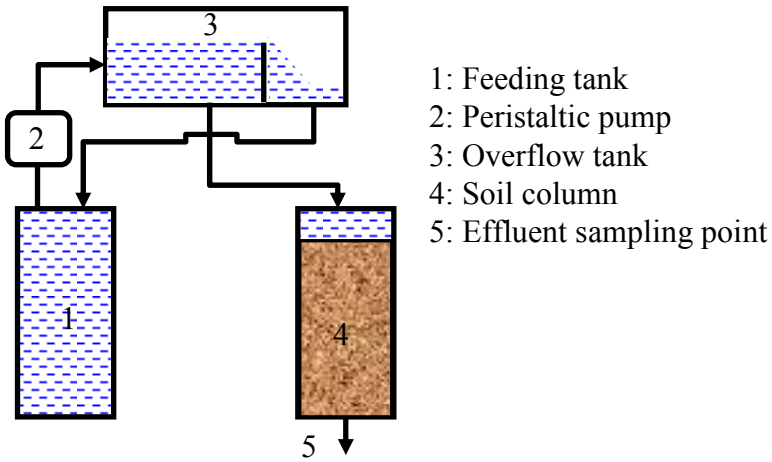

Figure 1. Schematic diagram of the experimental setup for the column tests.

Batch experiments at different pH values of 1 to 13 were carried out to observe the As release from soil to groundwater. Supra-pure grads HNO_3 and ultra-pure grade NaOH were used for adjusting the pH of solutions. All experiments were conducted by combining 30 ml of pH solution with 0.5 g of soil in 60 ml polypropylene bottle at a liquid:solid ratio of 60:1. The samples were then shaken for 48 hours at room temperature. The suspensions were subsequently sampled and flitted through 0.45 µm pore size filtration unit and the supernatants were analyzed for iron and arsenic.

2.2 Analytical Determinations

The measurements of oxidation reduction potential (ORP), conductivity (EC), temperature and pH were performed immediately after effluent collection. The Redox Meter (TOA, RM-20P) using two electrodes (Ag/AgCl and platinum) was employed for the measurement of ORP. Dissolved organic carbon (DOC) was measured by high-temperature catalytic oxidation method using a Shimazu TOC 5000A, total organic carbon analyzer. The total concentrations of As, Fe and Mn in the samples were measured by inductively coupled plasma and mass spectrometry (ICP-MS) (Agilent 7500, Octopole reaction system). The mass resolution was low that produced high-peak intensities. The instrument was linearly calibrated from 10 to 100 µg l-1 with custom multi-element standard (SPEX CertiPrep, Inc.). The detection limit of the instrument for As was 6 ng/l. The average relative standard deviation for all the samples was 5%. All of the samples were diluted several times to adjust for the operating range and were analyzed.

2.3 Biogeochemical Modeling

2.3.1 Conceptual Model

The model developed in this study was based on the reactive solute transport and biogeochemical reaction processes. This model takes into account three different phases: mobile pore water phase, immobile bio phase, and matrix phase, which is shown in Fig. 2 with chemical species considered in the model. All biogeochemical reactions take place inside the bio phase. Five different species of bacteria *X1*, *X2*, *X3*, *X4* and *X5* are assumed to grow in this bio phase.

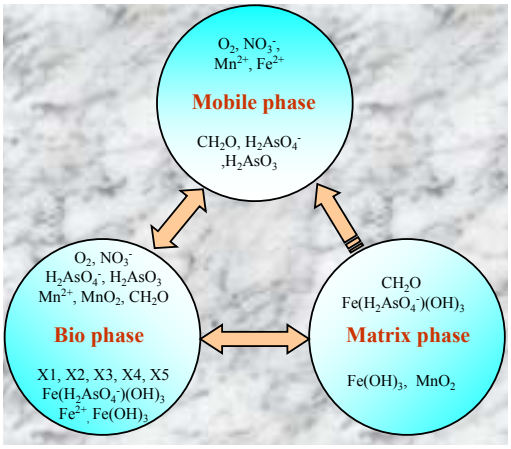

Figure 2. Conceptual biogeochemical model of arsenic mobilization in soil.

In the conceptual model, the arsenic transformation reaction is modeled as an oxidation-reduction process, where a carbonaceous substrate is oxidized to supply the required electrons and As(V) is reduced by acting as an electron accepter. The As(V) reduction process is incorporated within a sequential terminal electron acceptor reaction modeling framework, including aerobic, denitrifying, Mn(IV)-reducing, Fe(III)-reducing, dissolution of surface complexation and As(V)-reducing processes. Using organic matter as the ultimate electron donor and O_2, NO_3^-, Mn(IV), Fe(III) and As(V) as electron acceptors, the different degradation biochemical reaction processes are shown in Table 2.

Table 2. Microbials and biochemical reactions used for simulation of As reduction in soil

Bacteria		Reaction
X1	Aerobic	$CH_2O + O_2 \rightarrow CO_2 + H_2O$
	Denitrifying	$5CH_2O + 4NO_3^- + 4H^+ \rightarrow 5CO_2 + 2N_2 + 2H_2O$
X2	Manganese reducing	$CH_2O + 2MnO_2 + 3H^+ \rightarrow HCO_3^- + 2Mn^{2+} + 2H_2O$
X3	Iron reducing	$CH_2O + 4Fe(OH)_3 + 7H^+ \rightarrow HCO_3^- + 4Fe^{2+} + 10H_2O$
X4	Dissolution of surface	$CH_2O + 4Fe(OH)_3(H_2AsO_4^-) + 2H_2O \rightarrow HCO_3^- + 4Fe^{2+} +$

	complexation	$2H_2AsO_4^- + 6H^+$
X5	Arsenic reducing	$CH_2O + H_2AsO_4^- + H^+ \rightarrow HCO_3^- + 2H_3AsO_3$

2.3.2 Mathematical Model

The transport part of the model solves the one dimensional advection dispersion partial differential equation for each chemical species. Following mass transport equation is used for the numerical modeling of the pollutants transport (Bear, 1972):

$$\frac{dC_i}{dt} = \frac{\partial C_i}{\partial t} + \frac{\partial}{\partial x_m}\left(C_i V_m\right) = \frac{\partial}{\partial x_m}\left(D_{L_{mn}} \frac{\partial C_i}{\partial x_n}\right) + f(C_j) \quad (1)$$

where, Ci = target concentration of dissolved species i(ML-3), DLmn = coefficient of hydraulic dispersion (L2T-1), Vm = qm / ne = pore velocity of the ground water in the direction of xm(LT-1), Cj = concentration of interacting species through source/sink term f(Cj) representing bio-chemical reactions term.

Exchange processes are considered between the different model phases. The exchange between two phases is modeled by a linear exchange term. Mass exchange of dissolved species is governed by the concentration difference of the species in the pore water phase [Cj]mob, the bio phase [Cj]bio, the matrix phase [Cj]mat, and the exchange coefficients α, β, and γ formulated as (Schäfer et al., 1998; Lensing et al., 1994):

$$C_1 = \frac{\alpha\theta_{bio}}{\theta_{bio} + \theta_w}\left(\left[C_i\right]_{bio} - \left[C_i\right]_{mob}\right) \quad (2)$$

$$C_2 = \frac{\beta\theta_{mat}}{\theta_{mat} + \theta_w}\left(\left[C_i\right]_{mat} - \left[C_i\right]_{mob}\right) \quad (3)$$

$$C_3 = \frac{\gamma\theta_{mat}}{\theta_{mat} + \theta_w}\left(\left[C_i\right]_{bio} - \left[C_i\right]_{mat}\right) \quad (4)$$

where, C1 is the term of exchange reaction at the concentration difference between the pore and the bio phase, C2 is the exchange reaction term at the concentration difference between pore water and soil matrix, and C3 is the exchange reaction term between matrix phase and the bio phase. θ_w, θ_{bio} and θ_{mat} are the specific volume of mobile phase, bio phase and matrix phase, respectively.

For the chemical species related to As(III) and As(V) the following equations are formulated:

Mobile phase: $H_2AsO_4^-$:

$$\frac{\partial[H_2AsO_4^-]_{mob}}{\partial t}+\bar{v}\frac{\partial[H_2AsO_4^-]_{mob}}{\partial x}=D_L\frac{\partial^2[H_2AsO_4^-]_{mob}}{\partial x^2}+\frac{\alpha\theta_{bio}}{\theta_{bio}+\theta_w}\left([H_2AsO_4^-]_{bio}-[H_2AsO_4^-]_{mob}\right) \quad (5)$$

H_3AsO_3:

$$\frac{\partial[H_3AsO_3]_{mob}}{\partial t}+\bar{v}\frac{\partial[H_3AsO_3]_{mob}}{\partial x}=D_L\frac{\partial^2[H_3AsO_3]_{mob}}{\partial x^2}+\frac{\alpha\theta_{bio}}{\theta_{bio}+\theta_w}\left([H_3AsO_3]_{bio}-[H_3AsO_3]_{mob}\right) \quad (6)$$

Bio phase: $H_2AsO_4^-$:

$$\frac{\partial[H_2AsO_4^-]_{bio}}{\partial t}=\frac{1}{P_{H_2AsO_4^-}}\left[\frac{\partial X_4}{\partial t}\right]_{growth}-\frac{1}{U_{H_2AsO_4^-}}\left[\frac{\partial X_5}{\partial t}\right]_{growth}-\frac{\alpha\theta_w}{\theta_{bio}+\theta_w}\left([H_2AsO_4^-]_{bio}-[H_2AsO_4^-]_{mob}\right) \quad (7)$$

H_3AsO_3:

$$\frac{\partial[H_3AsO_3]_{bio}}{\partial t}=\frac{1}{P_{H_3AsO_3}}\left[\frac{\partial X_5}{\partial t}\right]_{growth}-\frac{\alpha\theta_w}{\theta_{bio}+\theta_w}\left([H_3AsO_3]_{bio}-[H_3AsO_3]_{mob}\right) \quad (8)$$

Fe $(H_2AsO_4^-)(OH)_3$:

$$\frac{\partial[Fe(H_2AsO_4^-)(OH)_3]_{bio}}{\partial t}=-\frac{1}{U_{Fe(H_2AsO_4^-)(OH)_3}}\left[\frac{\partial X_5}{\partial t}\right]_{growth}-\frac{\gamma\theta_{mat}}{\theta_{bio}+\theta_{mat}}\left([Fe(H_2AsO_4^-)(OH)_3]_{bio}-[Fe(H_2AsO_4^-)(OH)_3]_{mat}\right) \quad (9)$$

Matrix phase: $Fe(H_2AsO_4^-)(OH)_3$:

$$\frac{\partial[Fe(H_2AsO_4^-)(OH)_3]_{mat}}{\partial t}=\frac{\gamma\theta_{bio}}{\theta_{bio}+\theta_{mat}}\left([Fe(H_2AsO_4^-)(OH)_3]_{bio}-[Fe(H_2AsO_4^-)(OH)_3]_{mat}\right) \quad (10)$$

Bacteria: Bacteria X_4:

$$\left[\frac{\partial X_4}{\partial t}\right]_{Total\_growth}=\left[\frac{\partial X_4}{\partial t}\right]_{growth}+\left[\frac{\partial X_4}{\partial t}\right]_{decay} \quad (11)$$

$$\left[\frac{\partial X_4}{\partial t}\right]_{growth} = \nu_{\max}^{Fe(H_2AsO_4^-)(OH)_3} \cdot \frac{IC_{(O_2,NO_3^-)}}{IC_{(O_2,NO_3^-)} + [O_2, NO_3^-]_{bio}} \cdot \frac{IC_{Fe(OH)_3}}{IC_{Fe(OH)_3} + [Fe(OH)_3]_{bio}} \times \frac{[CH_2O]_{bio}}{K_{CH_2O} + [CH_2O]_{bio}} \cdot \frac{[Fe(H_2AsO_4^-)(OH)_3]_{bio}}{K_{H_2AsO_4^-} + [Fe(H_2AsO_4^-)(OH)_3]_{bio}} \cdot X_4 \quad (12)$$

$$\left[\frac{\partial X_4}{\partial t}\right]_{decay} = -\nu_{X_4 dec} \cdot X_4 \quad (13)$$

Bacteria X_5:

$$\left[\frac{\partial X_5}{\partial t}\right]_{Total\_growth} = \left[\frac{\partial X_5}{\partial t}\right]_{growth} + \left[\frac{\partial X_5}{\partial t}\right]_{decay} \quad (14)$$

$$\left[\frac{\partial X_5}{\partial t}\right]_{growth} = \nu_{\max}^{H_2AsO_4^-} \cdot \frac{IC_{(O_2,NO_3^-)}}{IC_{(O_2,NO_3^-)} + [O_2, NO_3^-]_{bio}} \times \frac{[CH_2O]_{bio}}{K_{CH_2O} + [CH_2O]_{bio}} \cdot \frac{[H_2AsO_4^-]_{bio}}{K_{H_2AsO_4^-} + [H_2AsO_4^-]_{bio}} \cdot X_5 \quad (15)$$

$$\left[\frac{\partial X_5}{\partial t}\right]_{decay} = -\nu_{X_5 dec} \cdot X_5 \quad (16)$$

The values of the stoichiometric, kinetic, switching function, and denitrification parameters are listed in Table 3. Most of these parameters were taken from previous studies (Schäfer et al., 1998; Eljamal et al., 2007).

3. RESULTS AND DISCUSSION

3.1 Relationship of As with ORP, pH and NO_3^-

Geochemical factors exert an important role in the release of arsenic in the soil. The redox conditions observed in the present study can be classified (1) highly aerobic conditions (>250 mV), (2) moderately aerobic (100 to 250 mV) and moderately anaerobic (-100 to +100 mV). In the system, water flow was continuous from the feeding tank to the overflow tank for creating the anaerobic condition in the soil column. The leaching profile of arsenic as a function of oxidation reduction potential (ORP) is presented in Fig. 3a. Leaching of As in aerobic conditions is insignificant and coprecipitation or sorption of As on to Fe precipitates can limit arsenic solubility (Nikolaidis et al. 2004). Dissolved As concentration increased gradually from 2.84 to 4.76 μg/l over range of ORP (73 to -37 mV). The influence of redox on As solubility in soils was found (Masscheleyn et al. 1991) to be governed by (i) reduction of arsenate to arsenite followed by desorption and (ii) the dissolution of Fe-oxyhydroxides and concurrent release of

coprecipitated arsenate. The increase of As solubility in moderately reducing condition was probably linked to the reductive dissolution of hydrated iron oxides. However, unfortunately, the speciation of As could not perform due to the low concentration.

Table 3. Parameters used for the simulation of arsenic reduction in the soil column

Biochemical parameter		Value
Exchange coefficient	α	10.0 day^{-1}
	β	0.005 day^{-1}
	γ	0.00005 day^{-1}
Half velocity concentration	Half velocity of CH_2O	0.01 mmol/l
	Half velocity of O_2, NO_3^- and FeAs	0.001 mmol/l
	Half velocity of Mn, Fe and As	0.0001 mmol/l
Aerobic bacteria (*X1*)	Yield coefficient for organic carbon	0.3 mol cell-C/mol OC
	Maximum growth rate	3.0 day^{-1}
	Constant decay rate	0.3 day^{-1}
Denitrifying bacteria (*X1*)	Yield coefficient for organic carbon	0.027 mol cell-C/mol OC
	Maximum growth rate	1.125 day^{-1}
	Constant decay rate	0.1125 day^{-1}
Manganese reducing bacteria (*X2*)	Yield coefficient for organic carbon	0.21 mol cell-C/mol OC
	Maximum growth rate	0.26 day^{-1}
	Constant decay rate	0.026 day^{-1}
Iron reducing bacteria (*X3*)	Yield coefficient for organic carbon	0.16 mol cell-C/mol OC
	Maximum growth rate	0.75 day^{-1}
	Constant decay rate	0.025 day^{-1}
Dissolutive bacteria (X4)	Yield coefficient for organic carbon	0.01 mol cell-C/mol OC
	Maximum growth rate	0.89 day^{-1}
	Constant decay rate	0.089 day^{-1}
Arsenic reducing	Yield coefficient for organic carbon	0.01 mol cell-C/mol OC

bacteria (*X5*)	Maximum growth rate	0.1 day^{-1}
	Constant decay rate	0.01 day^{-1}
Switching function parameter	Threshold concentration of O_2	0.015 mmol/l
	Slope of switch function	40.0
Soil properties	Porosity	44.0%
	Longitudinal dispersion length	0.001 cm

The effluent of soil column pH is circum-neutral and ranges between 6.6 and 7.3 (Fig. 3b). The influence of pH on As release in soil is discussed later in this section. The concentration of NO_3^- decreased from 14.91 mg/l to 0.01 mg/l with elapsed time and demonstrated negative correlation with As (Fig. 3c). The concentration of NO_3^- decreased with time in the effluent may be due to process resulting from microbially mediated reduction in presence of organic matter in the soil (Komor and Anderson 1993). Bhattacharya et al. (2002) suggests that the organic matter rich sediments mostly reducing in nature can create favorable conditions for forming reducing bacteria, thereby decreasing the concentrations of NO_3^- in water (Akai et al. 2004).

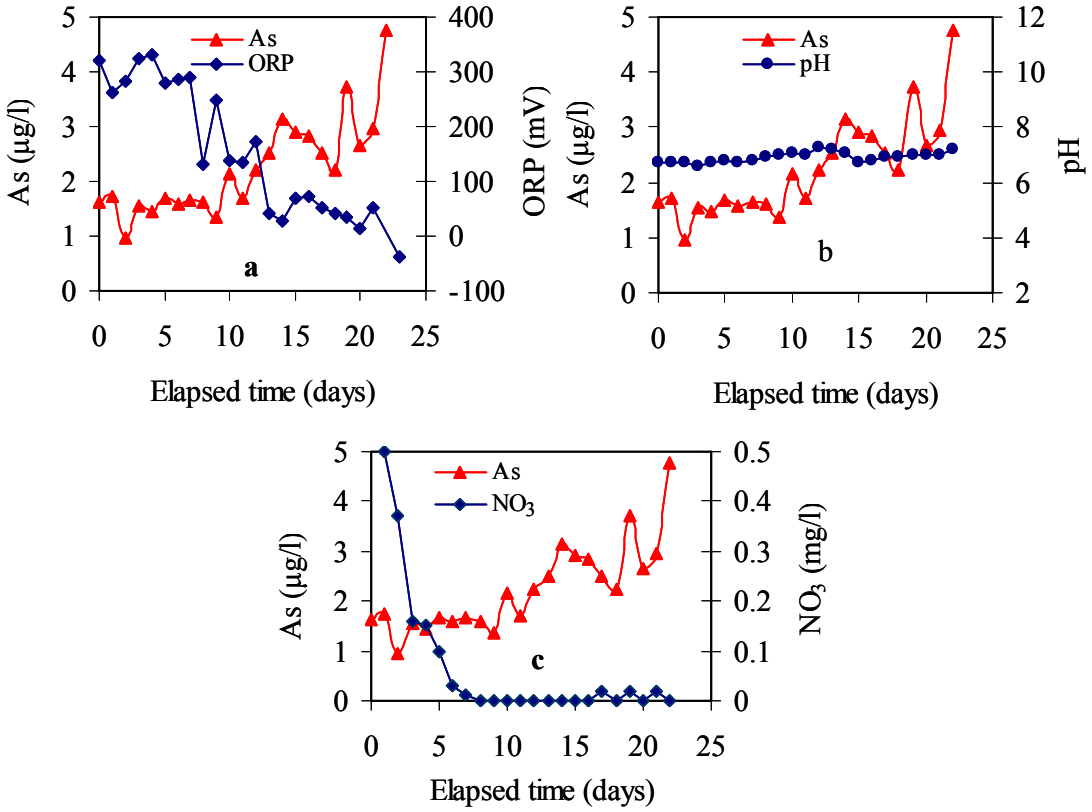

Figure 3. Relationships of As with **a** ORP, **b** pH and **c** NO_3^- in the effluent.

Batch experiments were carried out at pH of 1-13 with a liquid:solid ratio of 60:1 to observe the influence of pH on the solubility of As in the soil. Though the solution concentration, reaction time and soil-to-liquid ration can strongly influence As extraction patterns (Chappell et al. 1995), the different reaction conditions have also been observed in the previous studies (Carbonell-Barrachina et al., 1999; Cai et al., 2002; Ruiz-Chancho et al., 2005; Alam and Tokunaga, 2007). Results from present experiments for arsenic and iron are shown in Fig. 4. The extracted contents of As and Fe are generally much lower than the total metal concentration and exhibited a strong pH dependence. With an increase in pH from 1 to 7, As and Fe concentrations drops an order in magnitude with the total dissolved As and Fe concentrations decreasing from 271.3 µg/l and 750.7 mg/l to 18.73 µg/l and 92.6 mg/l, respectively. Further increase in pH to 13 of the suspension increased the dissolved metal concentration by two orders of magnitude. Maximum As and Fe leaching was observed at highly alkaline conditions (pH 13), with dissolved concentrations as high as 2651.03 µg/l and 1003.2 mg/l, respectively.

The content of As and Fe extracted from soil can be attributed to either dissolution of less resistant minerals or sorption/desorption mechanisms which are influenced by the pH. The dissolved As concentration at very low pH indicating either release of weakly sorbed As on Fe oxides or dissolution of carbonates driven by cation exchange (Pierce and Moore 1982; Masscheleyn et al. 1991; Bayard et al. 2006) The similarities in the leaching profiles of As and Fe due to their releases from their acid extractable phases suggested a strong association between them. With an increase in pH to neutral pH, precipitation of Fe as hydroxides can result in coprecipitation of arsenic on to the solid matrix, resulting in lower concentrations of dissolved arsenic.

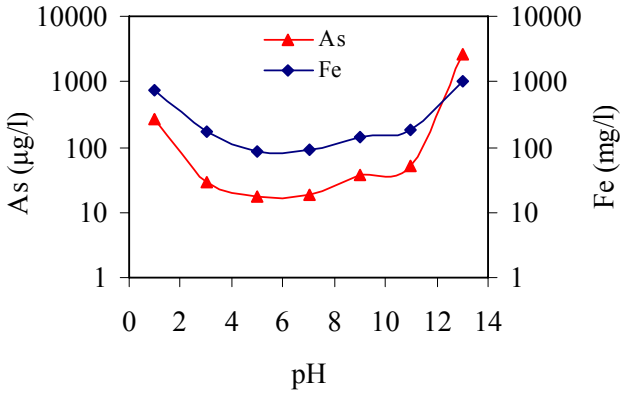

Figure 4. Influence of pH on the release of arsenic and iron in the soil.

With an increase in pH beyond neutral pH, almost 0.55% of the total As was released at pH 11, while 28.2% of total As was released at pH 13. In contrast, less than 2.6% of total Fe was released under alkaline conditions. As the suspension pH increases, hydroxyl ions replace As on the iron oxide sorption sites, facilitating the desorption of As oxyanions (Pierce and Moore 1982; Masscheleyn et al. 1991; Yang et al. 2002). The relatively small amount of Fe released is due to the reductive dissolution of iron oxides, which may contribute to As solubilization (Stumm and Morgan 1996; Carbonell-Barrachina et al. 2004). While, McArther et al. (2004) found that pH

dependent desorption of As is likely to be insignificant in groundwaters for which pH is greater than 8.5, and only occur via contact of high pH (10) landfill leachates with aquifer substrate.

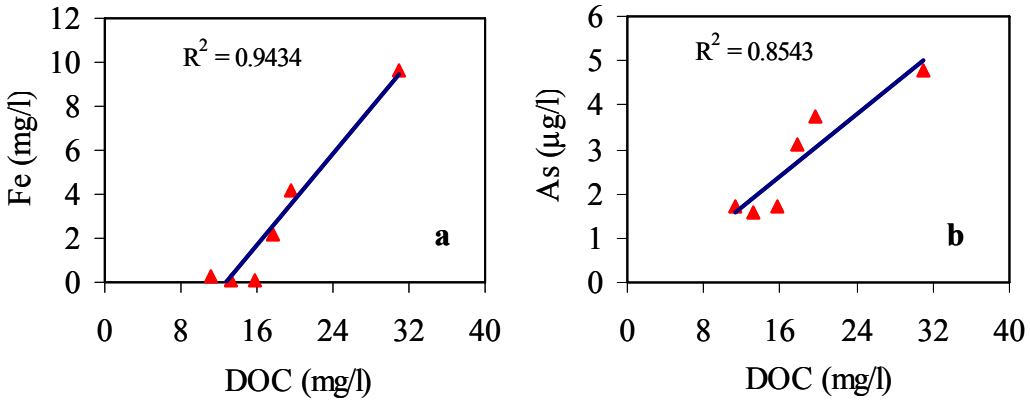

Figure 5. Relationship between the concentrations of DOC with **(a)** Fe and **(b)** As in the effluent.

3.2 Correlation of As With Other Parameters

Degradation of organic matter could drive the sequence of redox reactions in the aquifer and may, thereby enhance As mobilization (Ravenscroft et al. 2001; Anawar et al. 2003; McArthur et al. 2004). Elevated level of Fe due to biodegradation of organic matter (Harvey et al. 2002, Bhattacharya et al. 2006) are also indicated by strong correlation (R2 = 0.9434) of DOC with Fe (Fig. 5a). Strong correlation (R2 = 0.8543) between DOC and As (Fig. 5b) in effluent of soil column suggests that the microbial degradation of organic matter in the soil results in an moderately reducing environment and facilitates the release of As in the water (McArthur et al. 2001). Aiken (2002) pointed out that the DOC produce through the biodegradation of organic matter in the aquifer. A significant portion of the refractory DOC remains for a longer time in the liquid phase. Enhanced microbial activity accelerates the diagenetic process, involving mobilization of As from soils and sediments with high organic matter (Akai et al. 2004; Bhattacharya et al. 2006).

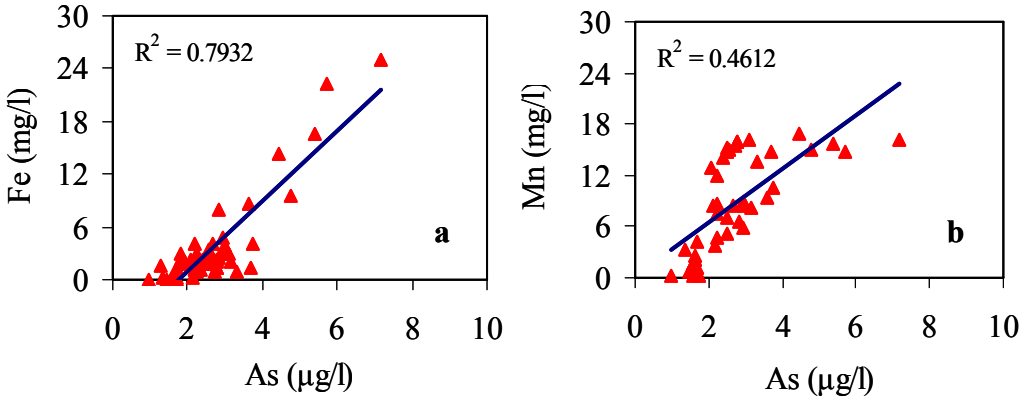

Figure 6. Relationship between the concentrations of As with **a** Fe and **b** Mn in the effluent.

Biodegradation of organic matter drives extreme degrees of reduction of Fe-oxyhydroxide and supplies high concentrations of As to groundwater (Ravenscroft el al. 2001). The correlation of As with Fe (R^2 = 0.7932) is stronger than that of the correlation between As and Mn (R^2 = 0.4612); it again suggests that As is released in effluent due to reductive dissolution of Fe-oxyhydroxide and this reduction is coupled to the microbial degradation of organic matter in the soils (Fig. 6a, b).

3.3 Comparison Between Measured and Simulated Concentrations

The measured concentrations of Mn, Fe and As in the effluent of soil column compared with the output of microbially-mediated biogeochemical arsenic transport model, which is shown in Fig. 5. The measured and simulated concentrations of Mn, Fe and As increased with elapsed time and fairly agreements with each other (Fig. 7a, b and c, respectively). However, some discrepancies exist between measured and simulated concentrations of them. A possible explanation for these discrepancies is that the aerobic and denitrifying bacteria X1 (Table 2) completely reduced oxygen and nitrate in the model, however, the observed oxidation-reduction potential values (Fig. 3a) indicated that the moderated reducing conditions present in the experimental soil column. Moreover, the reduction of As(V) is generally inhibited in presence of oxygen, nitrate, Mn(IV) or Fe(III), because oxygen, nitrate, Mn(IV) and Fe(III) reducers derive more energy from the organic matter than the As(V) reducers.

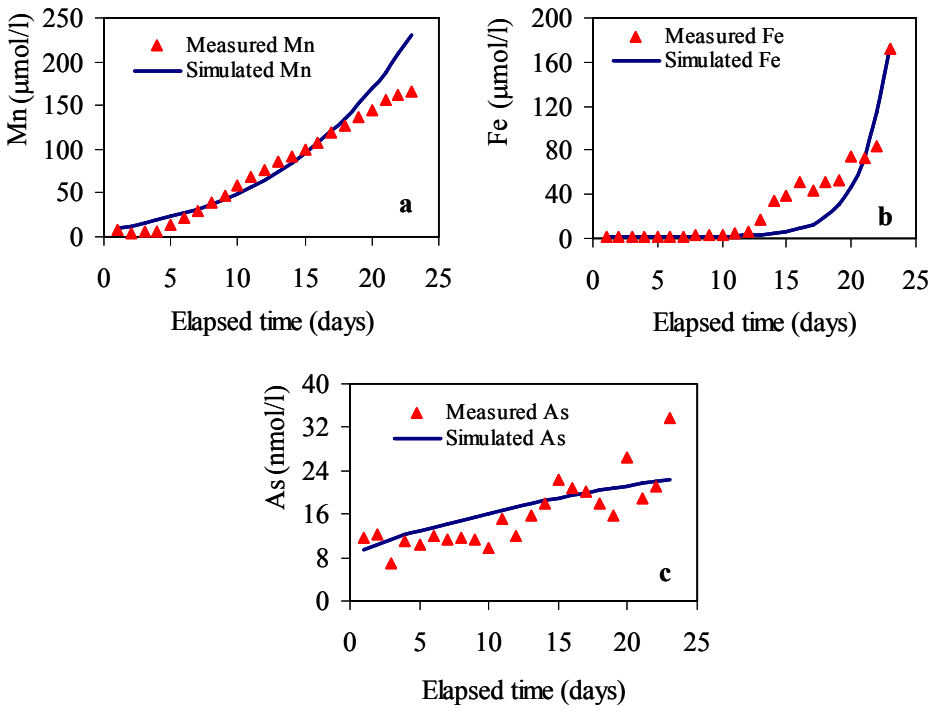

Figure 7. Comparison of the measured concentrations of Mn, Fe and As with those obtained from the microbially-mediated biogeochemical model in **a**, **b** and **c**, respectively.

The oxidation of degradable organic carbon with solid Mn(IV) as an electron accepter is catalyzed, e.g., by the anaerobic bacterial GS-15 or by Alteromonas Putrefaciens (Lovely and Phillips, 1988). These microorganisms are also able to reduce solid Fe(III) (Schäfer et al. 1998). In the model, manganese and iron reducers are two different bacterial groups. Manganese reducer in the model oxidizes CH2O to carbon dioxide and reduces Mn(IV) from MnO2 to Mn(II) ions. The bacteria growth rate and exchange coefficient were tuned until the simulated manganese reduction resulted in the observed dissolved Mn(II) concentration became close.

The microbial Fe(III) reduction rate cannot directly be determined from observed dissolved Fe(II) concentration. Von Gunchten and Zobrist (1993) determined a microbial Fe(III) reduction rate in an additional column experiment, where no Fe-As compound was present. The most important model parameter was the exchange coefficient between solid Fe-As and microbially available Fe-As in the biophase (Fig. 2). Again the bacteria growth rate was tuned until the simulated arsenic concentration became close to the observed dissolved arsenic concentration (Fig. 7c). Several controlled laboratory studies have been performed to understand the release mechanism of arsenic species in groundwater from various types of soil minerals and sediments. Islam et al. (2004) suggested that arsenic adsorbed onto sediment surfaces could be mobilized into groundwater by anaerobic respiration of Fe(III) reducing bacteria. In another study, Newman et al. (1998) found that the As(V) reducing bacterium, D. auripigmentum could reduce As(V) to As(III).

4. CONCLUSIONS

Experiments were carried out to observe the influence of geochemical factors on As mobilization from soil into water. The concentration of total As and As(V) measured in study soil was the same that indicated As remained primarily as As(V) in soil. The results of this study demonstrate that the moderately reducing condition of the soil column and strong correlation of As with DOC and Fe suggests that the microbially mediated degradation of organic matter and reductive dissolution of Fe-oxyhydroxide is considered to be the dominant processes to release As in aquifers.

Batch pH leaching studies showed a strong dependence of pH on both As and Fe leaching. Arsenic mobilization was high under highly acidic conditions and maximum in the alkaline pH region. Its mobilization was strongly correlated with that of iron, indicating that As release occurred either via (i) dissolution of the Fe-oxyhyroxide bearing phase in the acidic region or; (ii) desorption or reductive dissolution of Fe oxide in the alkaline region. Near the neutral pH region, significantly low As and Fe release was observed, due to As re-precipitation on Fe.

A reactive transport model for describing the microbially mediated transformation of arsenic species and their subsequent transport was developed. Simulation results of this model well matched those found experimentally. The developed model can serve as a useful tool for predicting the fate and transport of arsenic species in groundwater systems considering bacteria mediated oxidation and reduction bio-chemical processes.

5. ACKNOWLEDGEMENTS

The authors would like to gratefully acknowledge the Japan Society for the Promotion of Science for funding on the simulation and remediation model for the groundwater contaminated by arsenic and multi-geochemical species (No. 18-06396, 2006-2007) and Dr. Watanabe, Center of Advanced Instrumental Analysis, Kyushu University, Japan for her kind cooperation in the analytical determinations.

6. REFERENCES

Aiken, G. 2002. Organic matter in groundwater. US Geological Survey Artificial Recharge Workshop Proceedings, Sacramento, California, 2-4 April 2002, pp. 21-23.

Akai, J., Izumi, K., Fukuhara, H., Masuda, H., Nakano, S., Yoshimura, T., Ohfuji, H., Anawer, M.H. and Akai, K. 2004. Mineralogical and geomicrobiological investigations on groundwater arsenic enrichment in Bangladesh. Appl. Geochem. 19, 215-230.

Alam, M.G.M. and Tokunaga, S. 2006. Chemical extraction of arsenic from contaminated soil. J. Environ. Sci. Health Part A. 41, 631-643.

Anawer, M.H., Akai, J., Komaki, K., Terao, H., Yoshimura, T., Ishizuka, T., Safiullah, S. and Kato, K. 2003 Geochemical occurrence of arsenic in groundwater of Bangladesh: sources and mobilization processes. Appl. Geochem. Explor. 77, 109-131.

Bayard, R., Chatain, V., Gachet, C., Troadec, A. and Gourdon, R. 2006. Mobilization of arsenic from a mining soil in batch slurry experiments under bio-oxidative conditions. Water Res. 40, 1240-1248.

Bear, J. 1972. Dynamics of fluids in porous media, American Elsevier publishing Company, Inc., New York.

Bhattacharya, P., Ahmed, K.M., Hasan, M.A., Broms, S., Fogelstrom, J., Jacks, G., Sracek, O., Bromssen, M. and Routh, J. 2006. Mobility of arsenic in groundwater in a part of Brahmanbaria district, NE Bangladesh. In: Naidu R, Smith E, Owens G, Bhattacharya P, Nadebaum P (eds) Managing arsenic in the environment: from soil to human health. CSIRO, Melbourne, Australia, pp. 95-115.

Bhattacharya, P., Jacks, G., Ahmed, K.M., Khan, A.A. and Routh, J. 2002. Arsenic in groundwater of the Bengal Delta Plain aquifers in Bangladesh. Bull. Environ. Cont. Toxicol. 69, 538-545.

Cai, Y., Cabrera, J.C., Georgiadis, M. and Jayachandran, K. 2002. Assessment of arsenic mobility in the soils of some golf courses in South Florida. Sci. Total Environ. 291, 123-134.

Carbonell-Barrachina, A.A., Jugsujinda, A., Sirisukhodom, S., Anurakpongsatorn, P., Burló, F., DeLaune, R.D. and Patrick, Jr.W.H. 1999. The influence of redox chemistry and pH on chemically active forms of arsenic in sewage sludge-amended soil. Environ. Int. 25, 613–618.

Carbonell-Barrachina, A.A., Rocamora, A., Garcia-Gomis, C., Martinez-Sanchez, F., Burlo, F. 2004. Arsenic and zinc biogeochemistry in pyrite mine waste from the Aznalcollar environment disaster. Geoderma. 122, 195-203.

Chappell, J., Chiswell, B. and Olszowy, H. 1995. Speciation of arsenic ina contaminated soil by solvent extraction. Talanta. 42, 323-329.

Darland, J.E. and Inskeep, W.P. 1997. Effects of pH and phosphate competition on the transport of arsenate. J. Environ. Qual. 26, 1133-1139.

Eljamal, O., Jinno, K. and Hosokawa, T. 2007. Modeling of biologically mediated redox processes using sawdust as a matrix. Annual J. Hydro. Eng. 51, 19-24.

Harvey, C.H., Swartz, C., Badruzzaman, A.B.M., Keon-Blute, N., Yu, W., Ali, M.A., Jay, J., Beckie, R., Niedan, V., Brabander, D., Oates, P., Ashfaque, K.N., Islam, S., Hemond, H.F. and Ahmed, M.F. 2002. Arsenic mobility and groundwater extraction in Bangladesh. Science 298, 1602-1606.

Islam, F., Gault, A., Boothman, C., Polya, D., Charnock, J., Chatterjee, D., Lyond, J. 2004. Role of metal reducing bacteria in arsenic release from Bengal delta sediments. Nature. 430, 68-71.

Komor, S.C. and Anderson, H.W. Jr. 1993. Nitrogen isotope as indicators of nitrate source in Minnesota sand-plain aquifers. Ground Water 31, 260-271.

Lensing, H.J., Vogt, M. and Herrling, B. 1994. Modeling of biologically mediated redox processes in the subsurface. J. Hydro. 159, 125-143.

Lovley. D.R. and Phillips, E.J.P. 1988. Novel model of microbial energy metabolism: organic carbon oxidation coupled to dissimilatory reduction of iron and manganese. Appl. Environ. Microbial. 54, 1472-1480.

Masscheleyn, P.H., DeLaune, R.D. and Patrick, Jr. W.H. 1991. Effect of redox potential and pH on arsenic speciation and solubility in a contaminated soil. Environ. Sci. and Tech. 25, 1414–1419.

McArthur, J.M., Banerjee, D.M., Hudson-Edwards, K.A., Mishra, R., Purohit, R., Ravenscroft, P., Cronin, A., Howarth, R.J., Chatterjee, A., Talukder, T., Lowry, D., Houghton, S. and Chadha, D.K. 2004. Natural organic matter in sedimentary basins and its relation to arsenic in anoxic ground water: the example of West Bengal and its worldwide implications, Appl. Geochem. 19, 1255-1293.

McArthur, J.M., Ravencroft, P., Safiullah, S., Thirlwall, M.F. 2001. Arsenic in groundwater: testing pollution mechanism for sedimentary aquifers in Bangladesh. Water Resour. Res. 37, 109-117.

Newman, D.K., Ahmann, D. and Morel, F.M.M. 1998. A brief review of microbial arsenate respiration. Geomicrobiol. J. 15, 255–268.

Nickson, R.T., McArthur, J.M., Ravenscroft, P., Burgess, W.G. and Ahmed, K.M. 2000. Mechanism of arsenic release to groundwater, Bangladesh and West Bengal. Appl Geochem 15, 403-413.

Nikolaidis, N.P., Dobbs, G.M., Chen, J. and Lackovic, J.A. 2004. Arsenic mobility in contaminated lake sediments. Environ. Pollut. 129, 479-487.

Pierce, M.L. and Moore, C.B. 1982. Adsorption of arsenite and arsenate on amorphous iron hydroxide. Water Res. 16, 1247-1253.

Ravencroft, P., McArthur, J.M. and Hoque, B.A. 2001. Geochemical and paleohydrological controls on pollution of groundwater by Fourth International Conference on Arsenic Exposure and Health Effects, San Diego, California, 18-22 June 2000.

Ruiz-Chancho, M.J, Sabe, R., Lopez-Sanchez, J.F., Rubio, R. and Thomas, P. 2005. New approaches to the extraction of arsenic species from soils. Microchim. Acta. 151, 241-248.

Schäfer, D., Schafer, W. and Kinzelbach, W. 1998. Simulation of reactive processes related to biodegradation in aquifers. 2. Model application to a column study on organic carbon degradation. Cont. Hydro. 31, 187-209.

Semdley, P.L. and Kinniburgh, D.G. 2002. A review of the source, behavior and distribution of arsenic in natural waters. Appl. Geochem. 17, 517-568.

Stumm, W. and Morgan J. 1996. Aquatic Chemistry, third ed. Wiley-Interscience, New York.

von Gunten, U. and Zobrist, J. 1993. Biogeochemical changes in groundwater-infiltration systems: column studies. Geochim. Cosmochim. Acta. 57, 3895–3906.

Wagner, F. Berner, Z.A. and Stuben, D. 2005. Arsenic in groundwater in Bengal Delta Plain: geochemical evidences for small scale redox zonation in the aquifer. In: Bundschuh J, Bhattacharya P, Chandrasekharam D (eds) Natural arsenic in groundwater: Occurrence, remediation and management. Taylor & Francis Group, London, pp. 3-15.

Williams, L.E., Barnett, M.O., Kramer, T.A. and Melville, J.G. 2003. Adsorption and transport of arsenic(V) in experimental subsurface systems. J. Environ. Qual. 32, 841-850.

Yang, J.K., Barnett, M.O., Jardin, P.M., Basta, N.T. and Casteel, S.W. 2002. Adsorption, sequestration and bioaccessibility of As(V) in soils. Environ. Sci. Technol. 36, 4562-4569.

Chapter 18

IN SITU STABILIZATION OF ZINC IN SOIL AND GROUNDWATER

Bernd W. Rehm[1§], Robert Kondelin[2], Steve Markesic[3],
[1]*ReSolution Partners LLC, PO BOX 44181, Madison, WI 53570* [2]*Environmental Alliance Inc., 1812 Newport Gap Pike, Wilmington, DE 19808* [3]*Redox Technology LLC, 1441 Branding Lane, Suite 100, Downers Grove, IL 60515*

ABSTRACT

A 21-acre parcel in the east coast region of the United States hosted several industrial operations from 1907 to 1982. Groundwater at a pH of 5 SU and containing as much as 30 mg/L of zinc discharges to a small stream on one edge of the facility. The site surface was remediated and redeveloped into an apartment complex. Groundwater remediation was not a requirement at the time that the apartment complex was built. Subsequent ecological studies indicated that surface water impacts were occurring from zinc discharging from groundwater, and therefore remediation was required. *In situ* stabilization technologies that could be applied to groundwater with minimal interference with site use were evaluated in bench-scale and in-field pilot tests. The bench scale testing using site soil and groundwater samples determined that a 4 weight percent (wt. %) slurry of magnesium hydroxide [$Mg(OH)_2$] reduced zinc concentrations from 14.7 to 0.013 mg/L. Multiple extractions found a pH of 8.5 SU and a zinc concentration of 0.088 mg/L of zinc following about 1,200 aquifer pore volumes of leaching, equivalent to 400 years at the site groundwater flow rate. Pilot testing was completed with direct-push injection methods. Approximately 7.3 tons of reagent slurried in 4,205 gallons of water was injected at six points. Temporary well samples within the injection zone had post-injection zinc concentrations of <0.020 mg/L. A monitoring well downgradient of the injection zone yielded 21 mg/L of zinc prior to the injection. Within two weeks the concentration had decreased to 10 mg/L and at 8 months following injection the zinc concentration was 0.99 mg/L and the pH was 9.3 SU. The proposed remedial design took the form of a reactive zone at the edge of the facility, which treats groundwater prior to its discharge to surface water. Regulatory approval for the full-scale implementation was received in July 2007 and injection was begun in August 2007.

Key words: zinc, soil, groundwater, remediation, injection, stabilization

§ Corresponding Author: Bernd W. Rehm, ReSolution Partners, LLC, P.O. BOX 44181, Madison, WI 53570, Tel: 608.669.1249 Email: brehm@resolutionpartnersllc.net

1. INTRODUCTION

A 21-acre parcel in the east coast region of the United States hosted a number of industrial operations from 1907 to 1982. In the 1990's, interest in developing the site as residential housing lead to brownfield investigations, which identified petroleum hydrocarbon, chlorinated solvent, and zinc contamination in soil and groundwater. Soil removals from the site resulted in a recommendation for no further action with respect to surface soil by the regulatory agency. The site was redeveloped into 12 apartment buildings, recreational facilities, parking areas, and a stormwater basin. However, the regulatory agency required continued monitoring of groundwater and surface water after the development was completed. Upon review of surface water impacts from zinc, remediation of groundwater that discharges to surface water was required. This paper describes the remediation of zinc in the saturated soil and groundwater beneath the site in order to protect aquatic organisms in the surface water that receives the discharge of the zinc-bearing groundwater.

2. SITE CHARACTERIZATION

The shallowest soil beneath the site includes heterogeneous fill material consisting of clay to sand to gravel with varying amounts of debris. The fill overlies heterogeneous alluvium that grades downward into saprolite. The alluvium consists of layers and lenses ranging from silty and sandy clay to silty fine sand to gravelly sand with pebbles. Most of the soil is micaceous. The layers and lenses are typically less than two feet in thickness, with some sand units as thick as five feet. There is little lateral continuity evident in borings with spacings as little as 100 feet. At many locations there was a pattern of fining upwards (i.e., the gravelly sands were typically found at the base of the alluvium). The saprolite is typically clayey sand with gravel.

The water table is on the order of six feet below ground surface. Groundwater flow in the alluvium is generally from north to south. Groundwater discharges into two perpendicular culverts that bound the southern and southeastern edges of the former industrial parcel. The north-south culvert and the west-east culvert join to form a southward flowing stream at the southeastern corner of the site (see Figure 1). The hydraulic conductivity of the alluvium as measured in monitoring wells is on the order of 14 ft/d, yielding flow rates on the order of 100 ft/yr.

Zinc concentrations in soil are highly variable over short horizontal distances. However, there appear to be three general areas where concentrations of zinc greater than >750 mg/kg are found in soil. These are as follows: south of and beneath Building A, to the north-south culvert (range of 1,300 to 18,200 mg/kg; average of 5,420 mg/kg; n=8); beneath the north wing of Building A (range of 1,600 to 5,780 mg/kg; average of 3,020 mg/kg; n=5); and beneath the south wing of Building B (range of 890 to 3,000 mg/kg; average of 1,640 mg/kg; n=13). Other samples exceeding 750 mg/kg zinc were collected from west of the north-south culvert but do not generally form spatially contiguous or extensive "hotspots". The zinc in the soil forms a continuing source of dissolved zinc in the groundwater.

The groundwater has a low dissolved solids content (<500 mg/L). There are no dominant cations or anions in the groundwater, with the groundwater classified as a Ca+Mg, Na+K :: $Cl+SO_4$, HCO_3 geochemical facies. The groundwater contains 1 to 2 mg/L of dissolved oxygen and is acidic, with an average pH of 5.6 SU. Zinc concentrations in groundwater samples collected in January 2006 were as high as 25.6 mg/L at MW-3A (see Figure 1). Zinc concentrations in the southern portion of the site are typically greater than 1 mg/L. Concentrations have been relatively unchanged over the last ten years of monitoring.

Groundwater discharges to the culverts crossing the site. Zinc concentrations in the surface water collected at and immediately down stream of the culvert confluence ranged from 1.44 to 2.35 mg/L in January 2006. The zinc concentration in the stream decreased to 0.819 mg/L as the stream left the site.

3. REMEDIAL OBJECTIVES AND APPROACH

The regulatory agency required that groundwater remediation be undertaken to reduce the zinc concentrations in groundwater to the extent feasible in order to reduce the flux of zinc from groundwater to surface water. Although a regulatory groundwater standard of 2.0 mg/L exists, the lack of nearby groundwater wells precluded a need for groundwater remediation for the drinking water receptor pathway. The objective of the remediation is to reduce the zinc concentrations in the stream to approach the surface water quality standards for the protection of aquatic organisms, which incorporate hardness and range between 0.1 and 0.2 mg/L.

Groundwater remediation was deferred until after the apartment complex was built. The remedy, therefore, had to be implementable within the constraints posed by the existing facilities. These facilities precluded direct access to the zinc-bearing soils beneath the site. An injection treatment barrier (ITB) was selected as the most feasible approach for reducing the zinc flux from the groundwater to the surface water.

4. BENCH-SCALE TESTING

Bench-scale treatment trials were completed using soil and groundwater samples collected by Environmental Alliance (Alliance) on 17 January 2006. The soil sample was collected from between depths of 12 to 20 feet below ground surface (bgs) near a location where previous sampling had found 18,200 mg/kg of zinc in the soil. The soil sample was homogenized and used in the treatability studies with its as received wet weight (moisture content) of 23 percent. The soil was a yellow-brown fine to medium sand with some silt and clay and occasional coarse gravel. Sieving of a representative sample found 6 percent coarse sand and fine gravel, 84 percent fine and medium sand, and 10 percent silt and clay.

The groundwater was collected from monitoring wells MW-3A and MW-12. Approximately 12 litres of groundwater were collected from each well. Equal volumes of water from the two wells were mixed to form the leaching solution (the extractant) in the treatment studies. The

groundwater chemistry from the two wells sampled in October 2004 is summarized in Table 1. The mixed groundwater pH was 6.4 SU.

The treatment procedure placed 10.0 g of as received soil in a container with 200 mL of blended groundwater to achieve a nominal liquid to solid ratio of 20 to 1[2]. The samples were not dried prior to use to minimize potential geochemical changes drying may cause. The samples were then tumbled for approximately 16 to 18 hours, filtered at 0.7 μm and acidified prior to analysis by USEPA Method 6010B at CT Laboratories, Baraboo, Wisconsin.

The remediation had to reduce aqueous zinc concentrations using reagents that were amenable to injection. Two approaches were considered:

- Zinc sequestration as a hydroxide [$Zn(OH)_2$] can achieve the necessary concentration reductions with an increase of pH from the acidic site conditions to pH values in the range of 8 to 10 SU (Cortina et al., 2003). AquaMag®, a commercial magnesium hydroxide [$Mg(OH)_2$] slurry, was selected as a pH buffer for zinc stabilization. A comparable approach was evaluated by Cortina and others (2003) in column experiments using granular magnesium oxide [MgO] that formed a layer of $Mg(OH)_2$ on the MgO when placed in the column. They found that reagent would maintain a pH on the order of 8.5 to 10.0 SU and zinc concentrations would be reduced from 75 mg/L to less than 0.04 mg/L for 100's of pore volumes.
- Zinc can also be sequestered as a zinc sulfide mineral [ZnS] to low aqueous concentrations (Ayres, et al., 1994; Langmuir et al., 2003). Sulfide application is commonly used in waste water treatment systems as calcium polysulfides [CaS_x]. The material has a very high pH and has the potential to create hydrogen sulfide odors. A slurry consisting of native sulfur and a pH buffer would produce polysulfides after injection (and thereby mitigate potential odor issues) was also evaluated.

The results of the treatment trials are presented in Table 2. The untreated soil leached with groundwater produced 14,700 μg/L of zinc. Addition of all three reagents produced comparable results, with leachable zinc concentrations reduced by more than 99.9 percent. The sulfur-based reagents both increased the pH of the leachate to levels that could have formed $Zn(OH)_2$, therefore we cannot be certain as to the degree to which the zinc was sequestered as hydroxide or sulfide minerals.

Following a review of the data presented above, a consensus was reached between Environmental Alliance and ReSolution Partners that AquaMag should be carried forward into a multiple groundwater leaching test to evaluate the long-term stability of the treatment when exposed to site groundwater.

A sample of soil treated with a 2 weight percent (wt %) dose of AquaMag was exposed to a 200 to 1 liquid to solid ratio applied in a single step. The pH of the extracted liquid was 7.5, and the zinc concentration was 8.1 mg/L. This result was well above a concentration in groundwater that was felt to be protective of the surface water quality standard between 0.1 and 0.2 mg/L. The multiple extractions were therefore carried out at a 4 wt % dose of AquaMag to improve upon the longevity of the buffering capacity. A 20 to 1 groundwater to solids ratio was used

[2] Based on the one sample of soil tested for moisture content, the liquid to solid ratio based on dry soil weight was on the order of 27 to 1 for the treatment trials.

Table 1. Groundwater chemistry.

Total Analytes (mg/L unless noted otherwise)	MW-3A	MW-12	Average
pH (SU)	5.35	5.35	5.35
Calcium	18.8	50.5	34.7
Magnesium	10.3	17.2	13.8
Sodium	25.6	29.1	27.4
Potassium	2.45	2.29	2.37
Iron	4.82	1.01	2.92
Manganese	2.66	3.36	3.01
Zinc	**29.0**	**7.37**	**18.2**
Alkalinity, as CaCO3	37.4	47.2	42.3
Sulfate	71.9	97.8	84.9
Chloride	67.7	93.7	78.7
Nitrate	2.5	1.5	2.0

Table 2. Bench-scale reagent evaluation.

Reagent Dose	Leached Zinc (μg/L)	Final pH (SU)
0	14,700	7.4
2 wt % $Mg(OH)_2$	12.3	10.2
2 wt% CaS_x	39.2	9.1
4 wt% buffered S	9.5	11.1

for each of 10 sequential extractions in which the initial treated aquifer mass was retained and leached repeatedly. The results are summarized in Table 3. Repeated leaching of 10 g of treated aquifer material with a cumulative 2,000 g of groundwater slowly reduced the pH of the resulting solution from 9.7 to 8.6 SU. The zinc concentrations were not detectable in the first extraction, a reduction of greater than 99.97 percent. Zinc concentrations rose to 0.088 mg/L as the pH slightly declined to 8.6 SU. The final zinc concentration still represented a 99.40 percent decrease over the initial concentrations and is still well below the 2.0 mg/L goal. The sequential extractions were estimated to be equivalent to about 400 years of leaching at the site groundwater flow rate.

Treated groundwater will discharge to the stream that leaves the site. The initial pH of the treated aquifer and groundwater is above the 8.5 pH surface water quality criterion. The stream contains a mixture of groundwater and surface water. The titration of a surface water sample collected from location SG-3 (pH of 6.9 SU) using treated groundwater (pH of 9.8 SU) demonstrated that the surface water pH criterion was not exceeded until about equal volumes of groundwater and surface water were mixed. The discharge of the groundwater would have to more than double the stream flow across the site before the pH criterion is exceeded.

5. PILOT-SCALE TESTING

ReSolution Partners and Redox Tech mobilized to the site in September 2006 to perform a pilot test designed to determine the feasibility of injecting AquaMag to create an in situ treatment barrier. The test was conducted on the south side of the site in the immediate vicinity of monitoring well MW-3A (Figure 1). This location was selected due to the relatively high zinc concentrations previously identified in the groundwater in MW-3A and its accessibility.

Soil borings and temporary 1-inch diameter PVC wells advanced by direct push techniques were installed and sampled prior to slurry injection (Figure 2). Filtered groundwater samples were collected MW-3A and the temporary wells using a peristaltic pump. The temporary wells were removed and all boreholes were plugged with bentonite to minimize potential short circuiting through the boreholes during slurry injection. Following the completion of the injection, five additional borings and two temporary monitoring wells were advanced to evaluate the effects of the reagent injection (Figure 2). Well MW-3A was also re-sampled 8 months following the injection. As a planned precautionary measure, the surface water in the unnamed tributary flowing through the culvert along the south edge of the site was sampled at the point the water leaves the culvert. No evidence of direct AquaMag discharge or pH increase in the stream was observed.

Approximately 7.3 tons (1,100 gallons) of AquaMag as a 61 weight percent aqueous suspension of magnesium hydroxide Mg(OH)2, was delivered in drums and staged in the parking lot near the test site. Potable water used to make up the injection solution to yield the equivalent of a 2 wt % dose was obtained from the site maintenance facility. Injections were completed through 1.5-inch direct-push tooling advanced with a truck-mounted Geoprobe 6600. A 1.5-inch drive tool was advanced to 20 feet and pulled back to 19, 16, 13, and 11 feet for injections in the same borehole. A support trailer with a 550-gallon tank and two air-driven diaphragm pumps

was used to mix the AquaMag with potable water and inject the solution through the downhole tooling.

Table 3. Multiple groundwater extraction results.

Extraction Number	Post-Extraction pH (SU)	Zinc Concentration (µg/L)
Untreated	7.4	14,700
1	9.7	<4.00
2	9.7	5.70
3	9.2	5.90
4	8.8	12.0
5	8.6	17.2
6	8.6	9.4
7	8.6	13.8
8	8.6	23.9
9	8.5	46.8
10	8.6	88.4

In general, the pilot test area was underlain by silty clay and clay to a depth of 9 to 10 feet below ground surface. Debris (e.g., brick, wood, and rubber fragments) were found to depths of at least 5 feet. Sand with varying amounts of gravel and silt was found below the silty clay. This sand zone was the target of the reagent injections. The analyses of the pre-injection soil samples' average zinc concentrations of 347 mg/kg with a range of 313 to 423 mg/kg. Leachable zinc concentrations ranged from <0.020 to 0.0552 mg/L and averaged 0.0390 mg/L. However, the concentration of <0.020 mg/L appears to be a low outlier, with 5 of 6 samples ranging from 0.0192 to 0.0552 mg/L.

The zinc concentration in MW-3A was 21.2 mg/L and the pH was 4.91 SU. The groundwater samples from the temporary wells (PIB-1 and PIB-2) yielded zinc concentrations about 60 times less than the zinc concentration in MW-3A and the pH was higher (5.71 to 5.79 SU). The well screens of the temporary wells were about 5 feet higher than the MW-3A well screen. It may therefore be possible that the chemistry difference is a result of vertical

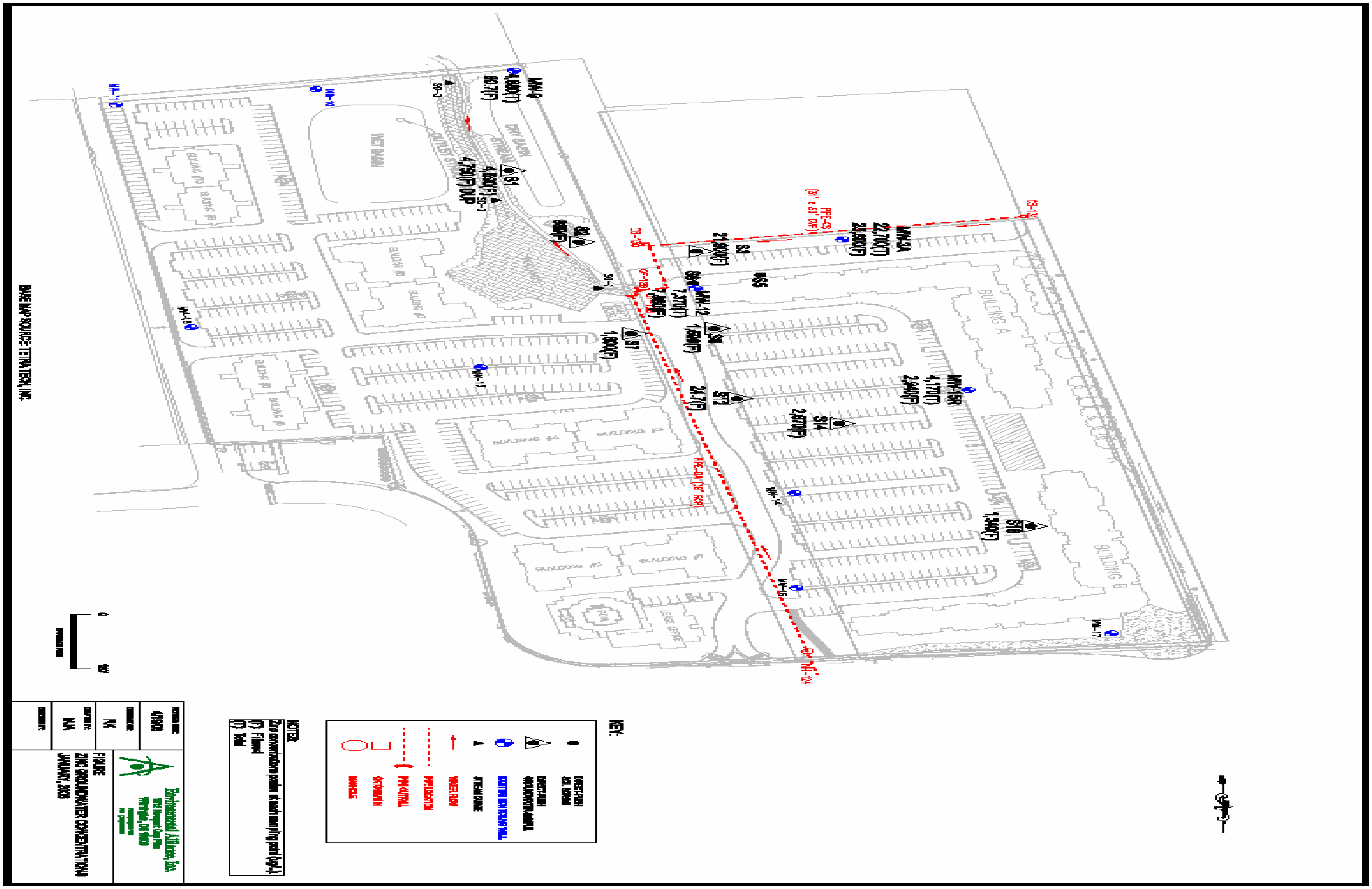

Figure 1. Site map.

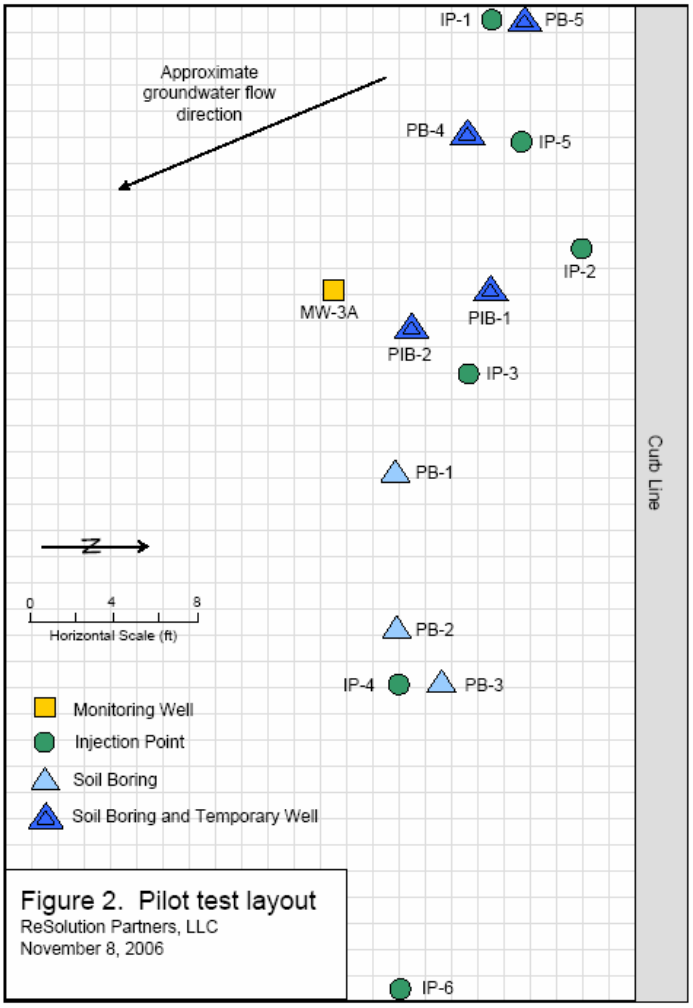

Figure 2. Pilot test map.

stratification of the zinc plume. The borings suggest that the permeability of the soil may increase with depth (i.e., increasing gravel and decreasing silt content). This suggests that zinc was present in a preferential flow zone in the deeper sandier soil.

The plan was to inject the AquaMag into two locations with four injection depths per location. The injection of 4,200 gallons of diluted AquaMag was completed in two days. Injection flow rates were typically on the order of 5 to 10 gallons per minute (gpm) at injection pressures of about 20 to 40 pounds per square inch (psi). Injected volumes ranged from 30 to 550 gallons per interval due to break-through of the injection solution at the ground surface. A total of six injection points were advanced to complete the test. Some of the breakthroughs occurred at the boreholes advanced prior to the injection. These could often be plugged by driving 3-in diameter direct push tools into the original 2-in diameter boreholes. However there were also breakouts at locations not associated with earlier borings these could not be plugged and resulted in the cessation of injection.

The portion of the area immediately upgradient of monitoring well MW-3A received about 66-percent of the total injection with approximately 240 tons of soil receiving a 2 wt % of reagent. The shallowest injection zones received the lowest doses because of slurry discharge at the ground surface. However, if the hypothesis that the zinc plume is mostly at depth is correct, the incomplete injection at shallower depths should have little effect on the performance of the remedy as measured at MW-3A.

Soil borings were advance approximately 10 feet, 3 feet, and 2 feet from the injection locations to evaluate the distribution of treatment reagents in the soil. Visual observations and soil pH measurements found evidence of the injection in discreet thin seams. The pH at the seams was between 9 and 10 SU and a "halo" of pH greater than 7 SU commonly extended about 1 foot from the seam (compared to untreated soil pH that ranged from 5.5 to 6.5 SU). The AquaMag seams were no thicker than 0.03 ft. Soil samples from PB-4 and PB-5 for laboratory analyses were compared to the pre-injection data from borings PIB-1 and PIB-2, the average magnesium concentrations approximately doubled as a result of the injections but the concentration range was comparable to the pre-injection levels of about 2,600 mg/kg to as high as 11,800 mg/kg. This is consistent with the visual observations and pH screening that indicates the reagent distribution is spatially heterogeneous. Temporary wells in post-injection borings PB-4 and PB-5 found the post injection groundwater pH at 8.00 and 8.94 SU. The bench scale testing indicated that pH values in this range would result in zinc precipitation. This was confirmed by the field results where the zinc concentrations determined by the laboratory analyses of two groundwater samples were <0.020 and an estimated 0.0094 mg/L. The post-injection groundwater sample results from PB-4 and PB-5 indicated successful treatment of the groundwater in these locations.

The post-injection results of the monitoring well MW-3A re-sampling are summarized in Table 4. Within about two weeks following the injections, the pH began to increase at the monitoring wells and the zinc concentration decreased from 21.4 to 8.44 mg/L. From October 2006 through February 2007 the pH rose slowly and the zinc concentrations decreased slowly. From February to May 2007 the pH rose by 2.5 SU to 9.3 SU and the zinc concentration fell by 650 percent to 0.986 mg/L.

Table 4. Post-injection groundwater chemistry.

Sample Date	Zinc (mg/l)	pH (SU)
9/28/2006	21.4	5.0
10/12/2006	8.44	5.7
10/27/2006	6.54	6.5
11/22/2006	5.74	7.0
12/20/2006	7.87	5.8
1/25/2007	7.63	6.1
2/12/2007	6.43	6.8
3/9/2007	4.68	7.6
4/13/2007	0.614	8.6
5/10/2007	0.986	9.3
6/13/07	6.60	8.2
8/10/07	13.2	6.2

In spite of the apparent heterogeneous spatial distribution of AquaMag suggested by the post-injection soil borings, the groundwater results from the monitoring well downgradient of the injection area clearly shows a decrease in the dissolved zinc concentrations through the first nine months of treatment as a result of the injections. On the basis of this performance the regulatory agency approved the full-scale implementation of an IRB upgradient of the surface water receiving the zinc-bearing groundwater.

A rebound of the zinc concentrations (and lower pH) was observed since May 2007. This increase suggests that the limited spatial distribution and dose applied during the pilot test may be affected by the continued flux of acidic and zinc-bearing groundwater. Additional injections were planned in the area of the pilot test as part of the full-scale remedy.

6. FULL-SCALE IMPLEMENTATION

Approval for the full-scale implementation of the remedy was received on 25 July 2007. Vironex, Inc. was retained by Environmental Alliance to provide injection services. Site preparation including staging area construction, utility clearance, and additional monitoring well installations began the first week of August and injection began on 6 August.

An estimated total of 35,000 gallons of undiluted reagent was successfully injected into the zinc treatment barrier (Figure 3). An estimated total volume of 45,000 gallons of diluted and undiluted reagent was injected on-site in 63 injection locations. The injections were performed over a 4-week period. Groundwater monitoring will continue for a period of 2 years.

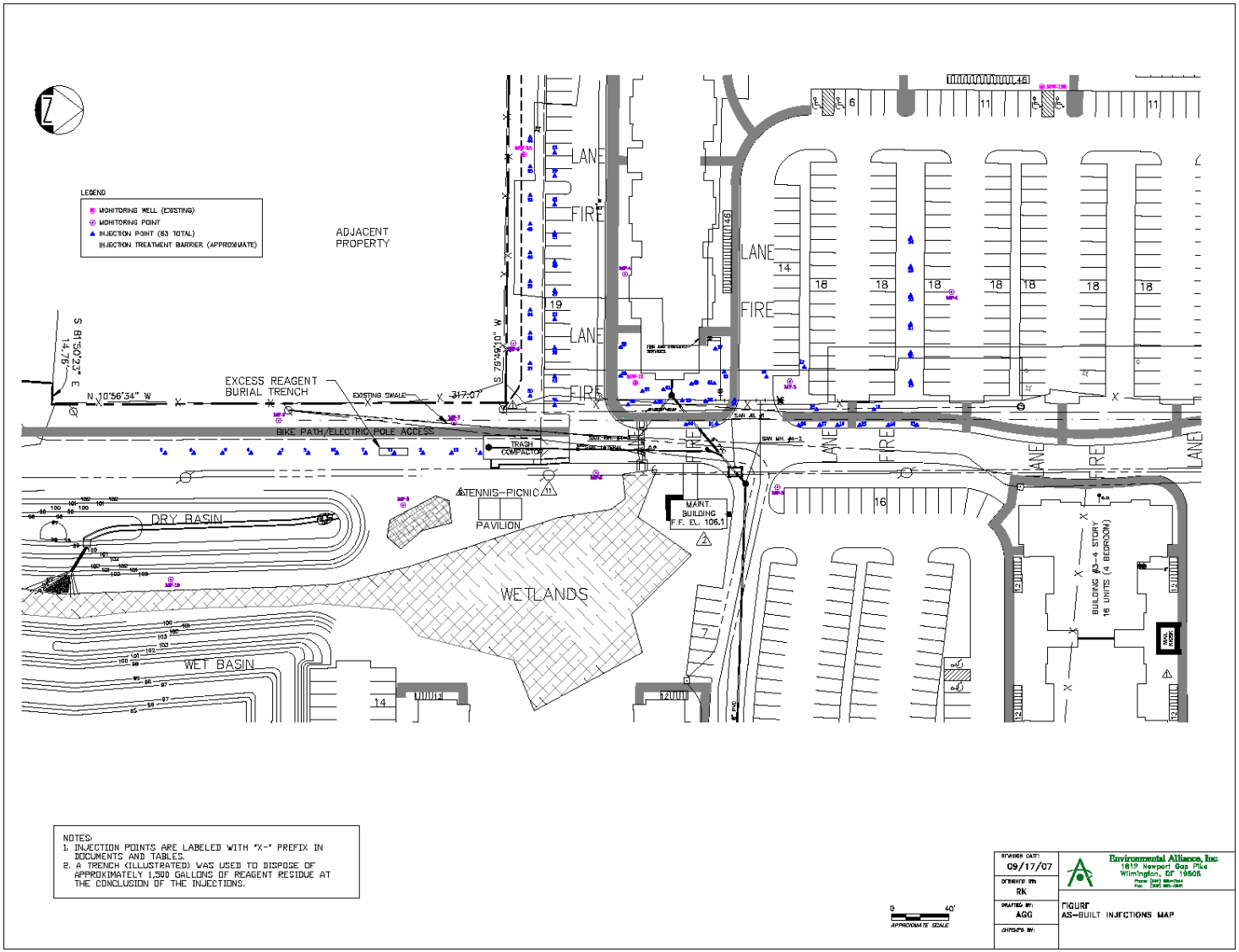

Figure 3. Full-scale injection locations.

7. REFERENCES

Ayres, D. M., Davis, A. P., and Gietka, P. M. 1994. Removing heavy metals from wastewaters. University of Maryland, Engrg. Res. Center Rept. 21 pp.

Cortina, J.-L., Lagreca, I., De Pablo, J., Cami, J., and Ayora, C. 2003. Passive *in situ* remediation of metal-polluted water with caustic magnesia: Evidence from column experiments. Environ. Sci. Technol., 37(9):1971-1977.

Langmuir, D., Chrostowski, P., Chaney, R., and Vigneault. 2003. Issue paper on the environmental chemistry of metals. USEPA, Risk Assessment Forum. 105 pp.

Chapter 19

EFFECT OF PHOSPHOROUS, ORGANIC AND SAPROPEL AMENDMENTS ON LEAD, ZINC AND CADMIUM UPTAKE BY TRITICALE FROM INDUSTRIALLY POLLUTED SOILS

Krasimir I. Ivanov[§], Violina R. Angelova, and Stefan V. Krustev
Department of Chemistry, Agricultural University, Mendeleev Street 12, 4000 Plovdiv, Bulgaria

ABSTRACT

A comparative study has been carried out on the effect of some soil amendments (phosphorus compounds, organic fertilizers and sapropel) on the quantity of the phytoaccessible forms of Pb, Zn and Cd and the accumulation of these elements by the Triticale. The effect of the used soil amendments on the mobile forms of the Pb, Zn and Cd is specific without clearly expressed tendencies. Only with the natural fertilizer there is a clear tendency for their reduction in all of the three studied elements. No direct relation between the quantity of the mobile forms and the absorption of Pb, Zn and Cd by the Triticale was established.

The superphosphate and KH_2PO_4 are effective phytostabilizing amendments for soils contaminated with lead. In combined contamination, however, adding superphosphate is not appropriate, as it increases the content of zinc and cadmium in the overground parts of the plants, while KH_2PO_4 can be used successfully.

Keywords: phytostabilization, heavy metals, soil amendments

1. INTRODUCTION

Chemical immobilization is a promising technique for decreasing the mobility of the contaminants in the ecosystems, in which chemical and mineralogical materials are added to the contaminated soils in order to decrease the solubility and phytoaccessibility of the metals, through absorption and/ or sedimentation.

The additives, used in phytostabilization, should quickly deactivate the metals; they have long-lasting effects, should not be expensive, and are easily added to the soil. Most often, for decreasing the phytoaccessibility of the metals, phosphorus and organic fertilizers such as ferrous and manganese hydroxides and natural or synthetic clay minerals are used. The

[§] Corresponding Author: Krasimir I. Ivanov, Department of Chemistry, Agricultural University, Mendeleev Street 12, 4000 Plovdiv, Bulgaria

mechanisms, through which the additives affect the polluters, differ depending on the §type of the additives and the degree and the nature of the pollution. The suggested mechanisms include sedimentation, complex formation, sorption and change in the degree of oxidation (Berti and Cunninggham, 1997; Hettiarachi et al., 2001; Yang et al., 2001; Hettiarachchi and Pierzynski, 2002; Geebelen et al., 2002; Cao et al., 2003; Seaman et al., 2003; Walker et al., 2003).

One of the most progressive directions in phytostabilization of toxic metals in the soils is the use of phosphorus fertilizers and phosphorus containing compounds, such as hydroxyapatit and phosphorus minerals (Chloplecka and Adriano, 1997; Boisson et al., 1999; Basta et al., 2001; Knox et al., 2001, 2003; Scheckel and Ryan, 2003). This method has gotten much more attention in recent years. The immobilization of lead with phosphorus containing compounds is a result of the formation of lead phosphate (pyromorphite), which is very stable even at low pH. The formation of pyromorphite significantly reduces the mobility of Pb in the soil (McGowen et al., 2001; Cao et al., 2003; Zhu et al., 2004), and, as a final result, its phytoaccessibility for the plants and the human digestion systems (Cheng and Hseu, 2002). Chemical immobilization with phosphorus compounds is preferable because of their relevantly low price and also because of the fact that adding phosphates in the soil is normal practice in the agriculture. Achieving a significant effect, however, requires the quantity of the additives to be much higher than the normal fertilization (5 g P/kg soil for deactivation of the lead, compared to 15-30 mg P/kg in most crops) (Hettiarachchi and Pierzynski, 2002). While the positive effect of the phosphorus additives on the reduction of the phytoaccessibility of the lead is indisputable, the evaluation of their complex effect on the absorption of the important nutrients for plants' microelements and the rest of the toxic metals requires further study.

There have been attempts for immobilization of heavy metals in the soil through the use of different organic additives (Berti and Cunninggham, 1997; Geebelen et al., 2002; Cao et al., 2003; Seaman et al., 2003, Jamode et al., 2003, Walker et al., 2003, 2004). It has been established that more of the organic materials, such as composites, fertilizers, and waste, can inactivate more toxic metals (lead, cadmium, copper, zinc, etc) as a result of sorption or complex formation. For some of the organic additives, it has been established that they reduce their solubility and obstruct their transition into the soil solution (Ciecko et al., 2001). The tests on soils polluted with lead, however, prove that its decreased solubility after the organic additives does not always lead to its decreased absorption by the plants.

The idea, for the use of Black-sea deepwater organogene-mineral sediments (DOMS) in agriculture and the environment is based on the experience of the use of lake and swamp sapropels in the agricultural practice (Dimitrov and Velev, 1988). They were formed 8000 ago as result of an ecological catastrophe cause by the inflow, through the Bosporus, of oceanic waters, which were mixed with the Black sea waters. Then occurred the mass development and dying of plankton organisms and the bottom of the sea were precipitated sediments with thickness of 1-3 m, know as DOMS. The source substances of DOMS is the dying flora and fauna of Black sea, which, as a result of the activity of anoxia bacteria, undergo the process of turning into animal

and plant planktons and bentos and form biolite mineral substances with special physical-mechanic and biogeochemical characteristics.

It is known that adding sapropel in the soil leads to neutralization of the soil acidity, increases the moisture capacity of the soils and the content of microelements, and stimulates the growth of the plants by accelerating their maturity and increases the yields in some crops (Lopotko et al, 1992). Our preliminary study shows that DOMS stimulate the vegetation and the growth of the root system of the cereal crops – wheat, corn and barley, and lead to increase of the chlorophyll content and soluble protein in the leaves. It is also known that the sapropel has the ability to inactivate and restrict the entrance of heavy metals in the plants (Vashkov, 1996). Its quality evaluation as a heavy metals and radionuclides absorbent is at initial stage. There are no systematic and profound studies in this direction in science literature. Despite this, it is suggested (Maskalchuk and Klimava, 2003; Shnyukov and Ziborov, 2004; Maskalchuk and Pozilova, 2005) that DOMS could be successfully used as absorbents for recultivation of tailing dumps from uranium production and lead-zinc and copper mines.

Taking into consideration the positive effect of the sapropels on the growth of the plants, we believe that it is useful to clarify the issues, regarding their use as phytostabilizers of toxic elements in the soil.

The present study has the following three objectives: (i) to broaden and increase the knowledge of effect of the different soil additives (phosphorus compounds, organic fertilizers and sapropel) on the quantity of the phytoaccessible forms of Pb, Zn and Cd (ii) to compare the effect of the selected additives on the accumulation of heavy metals by the Triticale and (iii) to estimate the effect of the introduction of additives on the phytostabilization of contaminated with heavy metals soils.

2. MATERIALS AND METHODS

2.1 Soils

Soil used in this experiment was sampled from the vicinity of the area contaminated by the NFMW (Non-Ferrous-Metal Works) near Plovdiv, Bulgaria. The soil needed for the pot experiments was collected from the surface (0-20 cm depth) of fields located at 0.5 km from the NFMW. It characterizes by alkaline reaction, moderate calcium carbonate content, loamy texture and moderate content of organic matter (Table 1).

Table 1. Soil properties

Classification	Depth, cm	pH, (H_2O)	Humus, %	$CaCO_3$, %	Clay, %
Calcaric Fluvisol	0 - 20	7.72	2.19	7.30	29.35

The soil characteristics are favourable to low metal availability to plants, and DTPA-extractable Pb, Zn and Cd concentrations are low for Zn, and moderate for Pb and Cd. The total

content of Pb, Zn and Cd is high and considerably exceeding the maximum permissible concentrations (Table 2).

Table 2. DTPA - extractable and total content of Pb, Zn and Cd in the soil.

Element	DTPA extractable	Total content	DTPA - extractable/ total content, %	MPC*
Pb	106.8	217.7	39.3	80
Zn	145.0	621.8	23.3	340
Cd	3.4	7.6	44.7	2,5

*MPC - maximum permissible concentration (approved for Bulgaria)

2.2 Soil amendments

Several amendments belonging to different categories were tested. The main reason for their selection was the requirement not to contaminate additionally the soil and to contribute for the soil fertility.

2.2.1 Phosphorus additives

KH_2PO_4 and superphosphate were chosen as phosphor soil amendments. The analysis of superphosphate showed that it does not contain lead, while the zinc and cadmium content reached 163.5 and 9.55 mg/kg, respectively. KH_2PO_4 did not contain detectebale Pb, Zn and Cd.

2.2.2 Organic additives

Rotten natural fertilizer and biomanure were chosen as organic soil amendments, obtained in the process of natural fertilizer and other organic waste by the Californian worm. In Table 3 are shown the agrochemical characteristics of the used organic fertilizers.

2.2.3 Sapropel

The deep-water organogen mineral slimes from the Black sea are at peat stage in their development. Because of the anaerobic environment in which they precipitate, they do not pass the stage of complete decomposition and in semi-decomposed state are preserved in suppurated hydrogen zone. Considering the fact that the cocolitophoryde, diatom, and sapropel slimes stratify each other and are a relatively homogeneous mixture, they could be treated as a complex organogen-mineral fertilizer, of which the sapropels represent 80 % of the general volume of the raw material.

Table 3. Agrochemical characteristics of the used organic fertilizers

Fertilizer	pH (H_2O)	Organic content %	N %	P_2O_5 %	K_2O %	CaO %	MgO %	Pb mg/kg	Zn mg/kg	Cd mg/kg
Natural fertilizer	7.46	17.65	0.850	0.42	0.77	1.10	0.37	23.1	162.4	0.80
Biomanure	7.80	34.94	1.963	0.74	1.37	1.25	0.68	38.8	111.0	0.38

The organogen mineral slimes are valuable not only for their organic substance, but also for their carbon ingredient and the amorphous silicates. In their mineral part, which is homogeneous with the organic, there are nutrients macroelements such as calcium, magnesium, potassium, the microelements ferrous, chrome, manganese, etc. In the sediments, there are quartz, plagioclase and volcanic glass, opal and chalcedony (rare grains), marcasite, calcite and aragonite, there also particles of shell detrite.

For the experiments with Triticale were use samples from DOMS, taken from the bottom of the Black sea at a depth of 1500-1800 m. The sapropel, used by us, has the following chemical content: Organic content - 3%, SiO_2 – 3.15%, CaO – 14.5%, MgO - 2.73%, Fe_2O_3 - 4.57%, Al_2O_3 -11.5, P_2O_5 -1.32%, Cu - 0.03%, Cr - 0.0125%, Mn - 0.0365%, Zn - 0.0085%, Mo - 0.0175%, Co - 0.0155%, Ni - 0.0073.

2.3 Pot experiment

2.3.1 Experimental design

The pot experiment was conducted on investigated soils with phosphorus additives, organic additives, and sapropel at 5% addition rates (calculated on soil dry weight basis). Soils were passed through a 1-cm sieve. Amendments were added and thoroughly mixed by hand. The pots were filled with 9 kg soil. All treatments were performed in triplicates. Three control pots were also set up without amendment. Pots were watered and stored in a greenhouse, where they were left to settle a minimum of 6 weeks at room temperature before planting the Triticale.

2.3.2 Plants

Triticale was chosen as a test-plant for greenhouse pot experiment. Ten seeds of Triticale were sown in pots and, after germination, thinned to three plants per pot. The plants were harvested 78 days after germination separated into aboveground parts (stems, leaves and seeds) and roots. The latter were washed free of all adhering soil in distilled water.

2.4 Sample preparation and analysis

Soils: (i) *Total content* of heavy metals in soils was determined in accordance with ISO 11466. The soil sample was decomposed on a sand bath heater for 3 h with 21 ml of concentrated HCI + 7 ml of concentrated HNO_3. After cooling the sample, the residue was transferred into a 50-ml flask, and water was added to the mark. (ii) *The mobile heavy metals* contents have been determined in 0.005 M diethylentriaminepentaacetic acid (DTPA) and 0.1 M triethanolamine (TEA) buffered at pH 7.3 (ISO 14870). Soil samples were shaken for 2 hours at 20°C. After shaking, the soil- solution system was centrifuged and filtered. The ratio soil to liquid was 1:2 by weight to volume.

Plants: The samples were treated by the method of dry ashing. A 1 g sample was weighed into a quartz crucible and put into a furnace (400°C) until ashing occurred. After cooling to a room temperature 1 ml HNO_3 (1:1) was added, evaporated in a sand bath and put again into the furnace (400°C). The procedures were repeated until the ash was white. It was finally dissolved in 2 ml 20 % HCl (v/v), transferred in a graduated 25 ml flask and brought to volume with doubly distilled water.

Soil amendments: Total heavy metal analysis was performed on finely ground samples of soil amendments (phosphorus additives, organic additives and sapropel) by using the same procedure, described for the soil samples.

Equipment: To determine the heavy metal content in the samples, inductively coupled emission spectrometer (Jobin Yvon Horiba "ULTIMA 2", France) was used. The working wave lengths were as follows: Zn - 213.9 nm; Pb - 220.4 nm; Cd - 214.4 nm. Detection limit for Pb was 1.5 µg/l, for Cd - 0.09 µg /l, for Zn - 0.15 µg /l. A commercial multielement standard solution (Merck) with concentration 100 mg/L was used as a stock solution. The calibration standard solutions have the following concentrations: 0; 0.2; 0.5; 2.0 and 5.0 mg/L. The acidity of the standard and sample solutions was the same.

Data were evaluated using analyses of variance (ANOVA) procedures.

3. RESULTS AND DISCUSSION

3.1 Effect of soil amendments on the mobile forms of Pb, Zn and Cd

In most of the plants, there is a direct connection between the content of microelements in the soil solution and their assimilation by the plants. This relation is most evident with the cadmium and less evident with zinc and lead (Kabata Pendias, 2001).

In many plants there is a direct relation between the content of microelements in the soil solution and their absorption by the plants. This relation is most evident with the cadmium and less evident with the zinc and the lead. (Kabata Pendias, 2001). The soil amendments used for the phytostabilization may have a significant effect in the mobile forms of Pb, Zn and Cd as a

result of sedimentation, absorption and change in the degree of oxidation. This effect, however, is not unidirectional, which makes necessary the testing of every single case.

Table 3 shows the quantities of the mobile forms of Pb, Zn and Cd in the control sample from naturally contaminated soil, used in the experiment and their change 6 weeks after the soil amendments were added.

Table 3. Influence of the soil amendments on the quantity of the mobile forms of Pb, Zn and Cd

Element mg/kg	Control	Soil amendments				
		KH_2PO_4	Superphosphate	Natural fertilizer	Biomanure	Sapropel
Pb	106.8	84.6	84.8	77.2	113.2	123.2
Zn	145.0	108.4	196.2	79.6	112.8	79.6
Cd	3.36	3.54	3.7	2.44	3.66	4.92

The results in Table 3 show, that the effect of the soil amendments on mobile forms of lead is in various directions and relatively weak, as the deviations from the control are up to 28 %. The phosphorus additives and the natural fertilizer decrease the quantity of the mobile lead with about 21% and 28 %, respectively. This is explainable, considering the high pH in the soil solution and the fact that the lead easily forms the hard to dissolve pyromorfite with degree of solubility at 25^oC 4.10^{-12} (Ma et al., 1995; Zhang et al., 1997; Laperche et al., 1997). Adding biomanure practically does not affect the quantity of the mobile lead, and the sapropel increases it with about 15 %.

The tendency of decreasing the mobile forms under the influence of the additives is more evident in the case of zinc, as in the natural fertilizer it is almost double. Only the superphosphate is an exception in which the content of the mobile zinc increases with 35%.

In the change of the mobile forms of the cadmium the tendency is reverse. In most of the cases their quantity increases, as this is most evident with the biomanure (46 %). Only with the natural fertilizer the quantity of the mobile cadmium decreases with 27 %.

The results in Table 3 show that the effect of the used soil amendments on the mobile forms of the Pb, Zn and Cd is in various directions and hard to explain. Only with the natural fertilizer there is a clearly expressed tendency for decreasing the quantity of the mobile forms of the three studied elements.

3.2 Effect of phosphorous amendments on the Pb, Zn and Cd accumulation in Triticale

The results for the influence of the phosphorous additives on the accumulation and distribution of Pb, Zn и Cd in the test-plant investigated are presented in Table 4. The change of the heavy metals content in comparison with the control (in %) is presented too.

The results presented in Table 4 show that the lead content in the roots of the Triticale decreases by 24% after adding KH_2PO4, while when superphosphate is added the decrease is much less. The obtained results are in accordance with the results of other authors who investigated the influence of the phosphorous compounds as a soil amendments. According to Laperche et al. (1997) adding apatite in the soil has a significant effect on the Pb content in plants roots. The authors have established the presence of Ca-substituted pyromorphites in the plants, grown in soils treated with apatite. Such particles were not found on the surface of the roots of the plants, grown in untreated soil. Apparently, adding apatite to the contaminated soils leads to sedimentation of pyromorphite particles on the root surface (on the outer layer). The local acidity in the risosphere may increase the local solubility of the apatite granules or other phosphorous compounds, which makes easier the sedimentation of the pyromorphite. Cotter-Howells and Capron (1996) also establish sedimentation of the Ca-substituted pyromorphites on the plants roots (*Agrostis capillaris),* grown in soils contaminated with Pb. In this case, their sedimentation is a result of root-exudate phosphates, which increases the phosphorus quantity in the risosphere. In any case, however, the formation of pyromorphite decreases the phytoaccessibility of the Pb. The tendency to decrease the lead content in the formation of phosphorous amendments is more evident with the aboveground parts of the plants - stem, leaves and seeds. Adding more superphosphate decreases the quantity in the stems (79% decreasing compared to the control), while KH_2PO_4 – in the stems (78%). Similar results were obtained by Laperche et al. (1997). Adding apatite to lead contaminated soil decreases the Pb content in the stems of sudax grass (*Sorghum bicolor* L. Moench) a hybrid of sorgum (Sor*ghum vulgare* L. Moench) and sudan grass (*Sorghum vulgare* var. *sudanese*) from 87% to 96%.

It is different with the zinc and the cadmium. Adding KH_2PO_4 decreases both their mobile forms and their content in all the parts of the plant, while when adding supephosphate we see the opposite tendency. The possible reason for this is the additional introduction of these elements in the soil with the superphosphate. As it was mentioned above, the superphosphate does not contain lead, while its content of zinc and cadmium is 163.5 и 9.55 mg/kg. The obtained results show the in the cases of soils contaminated with lead, KH_2PO_4 and superphosphate are effective soil amendments for the purpose of phytostabilization. The main reason for this is the formation of insoluble phosphates in the plant tissues and the soil. In combined contamination of the soil, however, adding superphosphate is not appropriate, as it increases the content of zinc and cadmium in the overground parts of the plants, KH_2PO_4 can be used successfully.

3.3 Effect of organic amendments on the Pb, Zn and Cd accumulation in Triticale

The results for the influence of the organic additives on the accumulation and distribution of Pb, Zn и Cd in the test-plant investigated are presented in Table 5.

Table 4. *Influence of the phosphorous amendments on the quantity (mg/kg) and distribution of Pb, Zn and Cd in the Triticale*

Element	Plant material	Control	KH_2PO_4		Superphosphate	
			Result	Change, %	Result	Change, %
Pb, mg/kg	Roots	32.1	24.4	- 24	31.0	- 3
	Stems	1.9	0.82	- 57	0.40	- 79
	Leaves	7.8	1.75	- 78	4.5	- 42
	Seeds	0.9	0.9	-	n.d	-
Zn, mg/kg	Roots	192.4	120.2	- 38	132.9	- 31
	Stems	69.5	61.4	- 12	99.3	+ 43
	Leaves	131.8	93.7	- 29	280.0	+ 112
	Seeds	46.7	30.0	- 36	72.6	+ 55
Cd, mg/kg	Roots	2.4	2.0	- 17	1.7	- 29
	Stems	0.45	0.32	- 29	0.6	+ 33
	Leaves	3.2	0.28	- 91	3.4	+ 6
	Seeds	0.44	0.06	- 86	0.5	+14

*Not detectable.

The content of organic substance in the soil has a significant effect on the absorption and the carrying of heavy metals in the soil and their assimilation by the plants. The zinc, the lead and the cadmium are absorbed in the organic substance and form stable forms, which leads to their accumulation in the organic horizons of the soil and the peat (Kabata Pendias, 2001). The stability of the metal-organic compounds and their participation in the carrying and the absorption of heavy metals, however, strongly depends on pH environment. Gambus and Gorlach (1996) prove that organic fertilizers have a favorable effect on oats as they reduce the content of the cadmium in the overground parts of the crop with 24%. Gambus and Gorlach (1996) and Ciecko et al. (2001), also establish decrease of the absorption of the cadmium by he plants when peat amendments are used.

As it can be seen from the data, presented in Table 5, the tendency for reduction of the quantity of the lead and the cadmium in all parts of the studied crop is well evident in both soil amendments. The lead content in the roots decreases with 59% with manure and 61 % with biomanure, and the cadmium content decreases respectively with 50% and 49%. In the stems and the leaves the reduction is less, as for the lead it is 21 and 30%, and for the cadmium - 38 and

25%. The content in the seeds remains the same when natural fertilizers are used, and decreases with 62% when biofertilizer is used, while the content of the cadmium decreases drastically in both cases.

Table 5. *Influence of the organic amendments on the quantity (mg/kg) and distribution of Pb, Zn and Cd in the Triticale*

Element	Plant material	Control	Natural fertilizer		Biofertilizer	
			Result	Change, %	Result	Change, %
Pb, mg/kg	Roots	32.1	13.3	- 59	12.6	- 61
	Stems	1.9	1.2	- 38	1.5	- 21
	Leaves	7.8	7.0	- 10	5.5	- 30
	Seeds	0.9	0.9	-	0.34	- 62
Zn, mg/kg	Roots	192.4	81.4	- 58	98.9	- 49
	Stems	69.5	34.0	- 51	67.8	- 3
	Leaves	131.8	130.1	-1	92.0	- 30
	Seeds	46.7	45.5	-3	32.9	- 30
Cd, mg/kg	Roots	2.4	1.2	-50	1.5	- 49
	Stems	0.45	0.3	- 33	0.28	-38
	Leaves	3.2	2.4	- 25	2.4	- 25
	Seeds	0.44	0.10	-77	0.11	- 75

The obtained results regarding the absorption and the localization of the zinc are different. Although mobile forms in the soil decrease after manure is added, its content in the leaves and the seeds stays practically unchanged. The biofertilizer significantly decreases the zinc in the roots, the leaves, and the seeds, while its content in the stems stays unchanged. The obtained results show that the organic fertilizers are effective soil amendments for the soils, contaminated with Pb, Zn and Cd. Regarding the zinc, however, the results are unconvincing, especially when natural fertilizer is used.

3.4 Effect of sapropel on the Pb, Zn and Cd accumulation in Triticale

The deep-water marine slimes are in the pea stage of their development. Because of the anaerobic environment in which they precipitate, they do not pass the stage of complete decomposition and in semi-decomposed state are preserved in suppurated hydrogen zone.

In the sediments of the sapropel horizon the content of the organic carbon varies within a wide range - from 5 to 18% (Dimitrov and Velev, 1988). In their mineral part, which is homogeneous with the organic, there nutrient macroelements (K, Ca and Mg) and number of microelements (Cr, Mn, Fe etc.). The X-ray analyses show the presence of hydromica, caolite, vermiculite, and montmorillonite. From the carbonate minerals the most evident are calcite, dolomite, and aragonite; there are also amorphous oxides of the silicium.

Table 6. Influence of the sapropel on the quantity (mg/kg) and distribution of Pb, Zn and Cd in the Triticale

Element	Plant material	Control	Sapropel	
			Result	Change, %
Pb, mg/kg	Roots	32.1	24.0	- 25
	Stems	1.9	1.3	- 32
	Leaves	7.8	4.3	- 45
	Seeds	0.9	0.7	- 22
Zn, mg/kg	Roots	192.4	124.2	- 35
	Stems	69.5	3.1	- 67
	Leaves	131.8	24.9	- 81
	Seeds	46.7	17.5	- 63
Cd, mg/kg	Roots	2.40	1.50	- 38
	Stems	0.45	0.06	- 87
	Leaves	3.20	0.3	- 91
	Seeds	0.44	0.13	- 70

The possibilities to use the sapropel, independently or mixed with other substances, in agriculture as a mineral stimulator is a subject of an increasing interest. The studying of its potential for the purposes of phytostabilization is at initial phase. The results we obtained on the effect of the sapropel on the absorption and the localization of Pb, Zn and Cd in the Triticale are presented in Table 6.

As can be seen from the results presented in Table 6, the tendencies are the same for the three elements. The lead content decreases in all organs of the plant, as this is most evident in the stem (32%) and in the leaves (45%). With the zinc and cadmium, this process intensifies in all the parts of the plant, as in this case also, the reduction is less in the roots and the stems and more in the leaves (81% with Zn and 91% with Cd).

Most likely, the reason for the observed processes is the strongly developed surface and the big absorption capacity of the sapropel. The obtained results give us reason to believe, that the sapropel is of great interest for the purposes of phytostabilization. The final answer to this question requires studying of its effect in wider range of agricultural crops both independently and mixed with other soil amendments.

4. CONCLUSIONS

A comparative study has been carried out on the effect of some soil amendments (phosphorus compounds, organic fertilizers and saprople) on the quantity of the phytoaccessible forms of Pb, Zn and Cd and the absorption of these elements by Triticale. It was established that:

1. The effect of the used soil amendments on the mobile forms of the Pb, Zn and Cd is specific without clearly expressed tendencies. Only with the natural fertilizer there is a clear tendency for their reduction in all of the three studied elements. No direct relation between the quantity of the mobile forms and the absorption of Pb, Zn and Cd by the Triticale was established.

2. The superphosphate and KH_2PO_4 are effective phytostabilizing amendments for soils contaminated with lead. In combined contamination, however, adding superphosphate is not appropriate, as it increases the content of zinc and cadmium in the overground parts of the plants, while KH_2PO_4 can be used successfully.

3. The organic fertilizers are effective soil amendments for the soils contaminated with Pb and Cd. Regarding the zinc, however, the results are not convincing enough, especially when natural fertilizer is used.

4. The sapropel presents a great interest for the purposes of phytostabilization. The evaluation of its potential, however, requires further studying of both the physical-mechanical and chemical characteristics, as well as its effect on wider range of agricultural crops.

5. REFERENCES

Basta, N. T., Gradwohl, R., Snethen, K. L., and Schroder, J. L. 2001. Chemical immobilization of lead, zinc, and cadmium in smelter-contaminated soils using biosolids and rock phosphate. J. Environ. Qual. 30, 1222 -1230.

Berti, W.R., and Cunninggham, S.D. 1997. In-place inactivation of Pb in Pb-contaminated soils. Environ Sci Technol. 31, 1359–1364.

Boisson, J., Ruttens, A., Mench, M., and Vangronsveld, J. 1999 Evaluation of hydroxyapatite as a metal immobilizing soil additive for the remediation of polluted soils. Part 1. Influence of hydroxyapatite on metal exchangeability in soil, plant growth and plant metal accumulation. Environ. Poll. 104, 225 - 233.

Cao, R.X., Ma, L.Q., Chen, M., Singh, S.P., and Harris, W.G. 2003. Phosphate-induced metal immobilization in a contaminated site. Environ Pollut. 122,19– 28.

Ciecko, Z., Wyszkowski, M., Krajewski, W., and Zabielska, J. 2001. Effect of organic matter and liming on the reduction of cadmium uptake from soil by Triticale and spring oilseed rape. The Science of the Total Environment 281, 37- 45

Cheng, S.F., and Hseu, Z.Y. 2002. In-situ immobilization of cadmium and lead by different amendments in two contaminated soils. Water Air Soil Pollut. 140, 73–84.

Chlopecka, A., and Adriano, D.C. 1997. Influence of zeolite, apatite and Fe-oxide on Cd and Pb uptake by crops. Sci. Tot. Environ. 207, 195-206.

Cotter-Howells, J., and Capron, S. 1996. Remediation of contaminated land by formation of heavy metal phosphates. Appl. Geochem. 11, 335-342.

Dimitrov, P., and Velev, V. 1988. Opportunities of using of deep-water sapropeloide slimes of Black Sea for agrobiological and industrial purposes. Ocealology 17, 92-95

Gambus, F., and Gorlach, E. 1996. Wplyw obornika, slomy i wegla ´brunatnego na fitoprzyswajalnosc metali ciezkich. Zesz.˙Ž . Ž Nauk AR Szczec Rol. 172, 131-137.

Geebelen, W., Vangronsveld, J., Adriano, D.C., Carleer, R., and Clijsters, H. 2002. Amendment-induced immobilization of lead in a lead-spiked soil: evidence from phytotoxicity studies. Water Air Soil Pollut.140, 261–277.

Hettiarachchi, G.M., and Pierzynski, G.M. 2002. In situ stabilization of soil lead using phosphorus and manganese oxide: influence of plant growth. J Environ Qual. 31, 564–572.

Hettiarachi, G.M., Pierzynski, G.M., and Ransom, M.D. 2001. In situ stabilization of soil lead using phosphorus. J Environ Qual. 30,1214– 1221.

ISO 11466. 1995. Soil Quality- Extraction of trace elements soluble in aqua regia.

ISO 14870. 2001. Soil Quality- Exxtraction of trace elements by buffered DTPA solution.

Jamode, A. V., Rao, M., Chandak, B. S., Jamode, V. S., and Parwate, A.V. 2003. Applications of the inexpensive adsorbents for the removal of heavy metals from industrial wastewater: a brief review. J. Ind. Poll. Control. 19, 114 -134.

Johnston, A.E., and Jones, K.C. 1992. The cadmium issue long-term changes in the cadmium content of soils and the crops grown on them. Proc. Int. Workshop, Phosphate fertilizers and the environment, International Fertilizer Development Center, Tampa, 255 - 269.

Kabata-Pendias, A. 2001. Trace Elements in Soils and Plants, 3rd ed. CRC Press LLC, Boca Raton.

Knox, A S., Kaplan, D. I., Adriano, D. C., Hinton, T. G., and Wilson, M. D. 2003. Apatite and phillipsite as sequestering agents for metals and radionuclides. J. Environ. Qual. 32, 515 - 525.

Knox, A S., Seaman, J. C., Mench, M., and Vangronsveld, J. 2001. Remediation of Metal- and Radionuclides-Contaminated Soils. In: Environmental Restoration of Metals-Contaminated Soils, pp. 21 -60 (Iskandar, I.K., Ed.). CRC Press LLC, Boca Raton Florida.

Laperche, V., Logan, T.J., Gaddam, P., and Traina, S.J. 1997. Effect of apatite amendments on plant uptake of lead from contaminated soil. Environ Sci Technol. 31, 2745– 2753.

Lopotko, M.Z., Kuzmitski, P.L., and Evdokimova, G.A. 1992. Sapropels in agriculture. Minsk, Belarus.

Ma, Q.Y., Logan, T.J., and Traina, S.J. 1995. Lead immobilization from aqueous solutions and contaminated soils using phosphate rocks. Environ. Sci. Technol., 29,1118-1126.

McGowen, S.L., Basta, N.T., Brown, G.O. 2001. Use of diammonium phosphate to reduce heavy metal solubility and transport in smelter-contaminated soil. J Environ Qual. 30, 493–500.

Moskalchuk, L.N., and Klimava, N.G. 2003. Recovery of Chernobyl-affected soils in the Republic of Belarus: Tendencies and trends, pp. 126-131 (IAEA-J9-CN-109 International Conference on the Protection of the Environment from the Effects of Ionizing Radiation: Stockholm, Sweden).

Maskalchuk, L.N., and Pozilova, N.M. 2005. Radioactive Contamination of Soils in Belarus: Experience and Trends of Rehabilitation, pp. 169-173 (IAEA-CN-135 International Conference on the Safety of Radioactive Waste Disposal: Tokyo, Japan).

Scheckel, K.G., and Ryan, J.A. 2003. In vitro formation of pyromorphite via reaction of Pb sources with soft-drink phosphoric acid. Sci Total Environ. 302, 253–65.

Seaman, J.C., Hutchison, J.M., Jackson, B.P., and Vulava, V.M. 2003. In situ treatment of metals in contaminated soils with phytate. J Environ Qual. 32, 153– 61.

Shnyukov, E.F., and Ziborov, A. P. 2004. Mineral resources of the Black Sea. Kiev, Naukova Dumka.

Yang, J., Mosby, D.E., Casteel, S.W., and Blanchar, R.W. 2001. Lead immobilization using phosphoric acid in a smelter-contaminated urban soil. Environ Sci Technol. 35, 3553– 3559.

Vashkov, H. 1996. Sapropel as an improver of soils contaminated by heavy metals. Himija v Selskom Hozyaistve 4, 5-7

Walker, D.J., Clemente, R., Roig, A., and Bernal, M.P. 2003. The effect of soil amendments on heavy metal bioavailability in two contaminated Mediterranean soils. Environ Pollut. 122, 303– 12.

Walker, D.J., Clemente, R., and Bernal, M.P. 2004 Contrasting effects of manure and compost on soil pH, heavy metal availability and growth of Chenopodium album L. in a soil contaminated by pyritic mine waste. Chemosphere 57, 215 - 224.

Zhang, P., Ryan, J.A., and Yang J. 1997. In vitro soil Pb solubility in the presence of hydroxyapatite. Environ Sci Technol. 32, 2763– 2768.

Zhu, Y. G., Chen, S. B., Yang, J. C. 2004. Effects of soil amendments on lead uptake by two vegeTable crops from a lead-contaminated soil from Anhui, China. Environment International 30, 351– 356

PART IX: Modeling

Chapter 20

EVALUATING THE IMPACTS OF UNCERTAINTY IN GEOMORPHIC CHANNEL- CHANGES ON PREDICTING MERCURY TRANSPORT AND FATE IN THE CARSON RIVER SYSTEM, NEVADA

R.W.H. Carroll[§] and John J. Warwick
Division of Hydrologic Sciences, Desert Research Institute, Reno, NV

ABSTRACT

The Carson River is one of the most mercury-contaminated fluvial systems in North America. Most of its mercury is affiliated with channel bank material and floodplain deposits, with the movement of mercury through this system being highly dependent on bank erosion and sediment transport processes. Mercury transport is simulated using three computer models: RIVMOD, WASP5, and MERC4. Model improvements include the addition of a bank package that accounts for flow history. The rates at which river stages are rising or falling will, in turn, impart time-dependant and vertically variable MeHg concentrations within the channel banks along the Carson River. Also, Lahontan Reservoir's geomorphic characteristics have been refined along with the explicit tracking of a temporally and spatially varying colloidal fraction. The augmented and refined modeling approach results in more accurate and realistic simulation of mercury transport and fate. An extensive uncertainty analysis, involving characterizing the co-variance of two calibration parameters used to define bank erosion and overbank deposition, will define the degree of expected variation in model predictions relative to limitations posed by available field data.

Keywords: Monte Carlo, mercury modeling, Carson River, Lahontan Reservoir

1. INTRODUCTION

The United States Environmental Protection Agency (US EPA) designated the Carson River as part of a Superfund site in 1991 due to contamination by mercury. It is estimated that

[§] Corresponding Author: Rosemary W.H. Carroll, Assistant Research Hydrologist & Graduate Student, Desert Research Institute, Division of Hydrologic Sciences, 2215 Raggio Parkway, Reno, NV 89512, Tel: 970-349-0356, Email: Rosemary.Carroll@dri.edu

approximately 6.36 x 10^6 kg (7,000 tons) of residual mercury is now distributed throughout the river's bank sediments and floodplain deposits (Miller et al, 1998; Smith and Tingley, 1998). It has also been found that more than 95% of the mercury transported in the Carson River is affiliated with particulate matter (Bonzongo et al., 1996). During January 1997 a rare, high magnitude flood generated significant geomorphic change and resulted in an estimated $1.81x10^8$ kg (200,000 tons) of sediment and 1,360 kg (3,000 lbs.) of mercury to be transported downstream into Lahontan Reservoir (Hoffman and Taylor, 1998). These quantities far exceed the amount of sediment and mercury transported in the decade prior to the flood. Consequently, any useful model of mercury transport in the Carson River system requires an accurate simulation of bank erosion and floodplain sedimentation mechanisms during extreme flood events. The January 1997 flood is the largest recorded event on the Carson River (1911 to present) and provides a unique opportunity to assess sediment cycling and mercury transport as a result of a rare-magnitude event. Modeling procedures use data collected by Miller et al. (1999) on channel widening and overbank deposition as a result of the 1997 flood as well as mercury data collected by the University of Nevada, Reno (UNR) and the United States Geological Survey (USGS) before, during and after the flood.

2. SITE DESCRIPTION

The Carson River flows eastward out of the Sierra Nevada Mountains just to the south of the Lake Tahoe Basin. Figure 1 shows a map of the Carson River with several reference locations marked. The section of the Carson River under investigation extends from the USGS gaging station near Carson City, Nevada (CCG, point 0 in Figure 1 detail) downstream through Lahontan Reservoir. The river's delta is located approximately 80 km from CCG and is located approximately 10 km below the Fort Churchill gaging station (FCH). Miller et al. (1999) conducted an extensive survey of the Carson River in the early spring following the 1997 flood. Both bank erosion and overbank deposition were evaluated using geomorphic techniques of aerial photography (taken in 1991 and 1997) and floodplain mapping. Data were discretized into ten river reaches (refer to Figure 1) defined by valley slope and floodplain width. For a complete discussion on techniques and results of the geomorphic survey read Miller et al. (1999).

Flow in the Carson River is typical of most semi-arid fluvial systems in that it is highly variable. Flow is predominately from snowmelt in the Sierra Nevada with peak discharge generally occurring in the spring with a sustained moderately high hydrograph. Catastrophic floods, such as the January 1997 flood, however, are generated with rain-on-snow events that can occur during the winter months. Peak mean daily discharge during the 1997 flood was estimated at 630 m^3/s. For comparison, the designated 100-year event occurred in 1986 with a peak discharge of 470 m^3/s. In contrast, the summer and fall months are dominated by low flows and these flows can cease all together during extended periods of drought.

3. MODELING PROCEDURES

3.1 Model Description

Three computer models (RIVMOD, WASP5 and MERC4) were used to simulate the transport of sediment and mercury in the Carson River. RIVMOD (Hosseinipour and Martin, 1990) is a U.S. EPA 1-dimensional hydrodynamic and sediment transport routine that simultaneously solves standard fluid equations of continuity and momentum. Finite difference equations are solved by the Newton-Raphson method to determine fluid velocity and depth given unsteady flow conditions. WASP5 (Ambrose et al., 1991) is the U.S. EPA

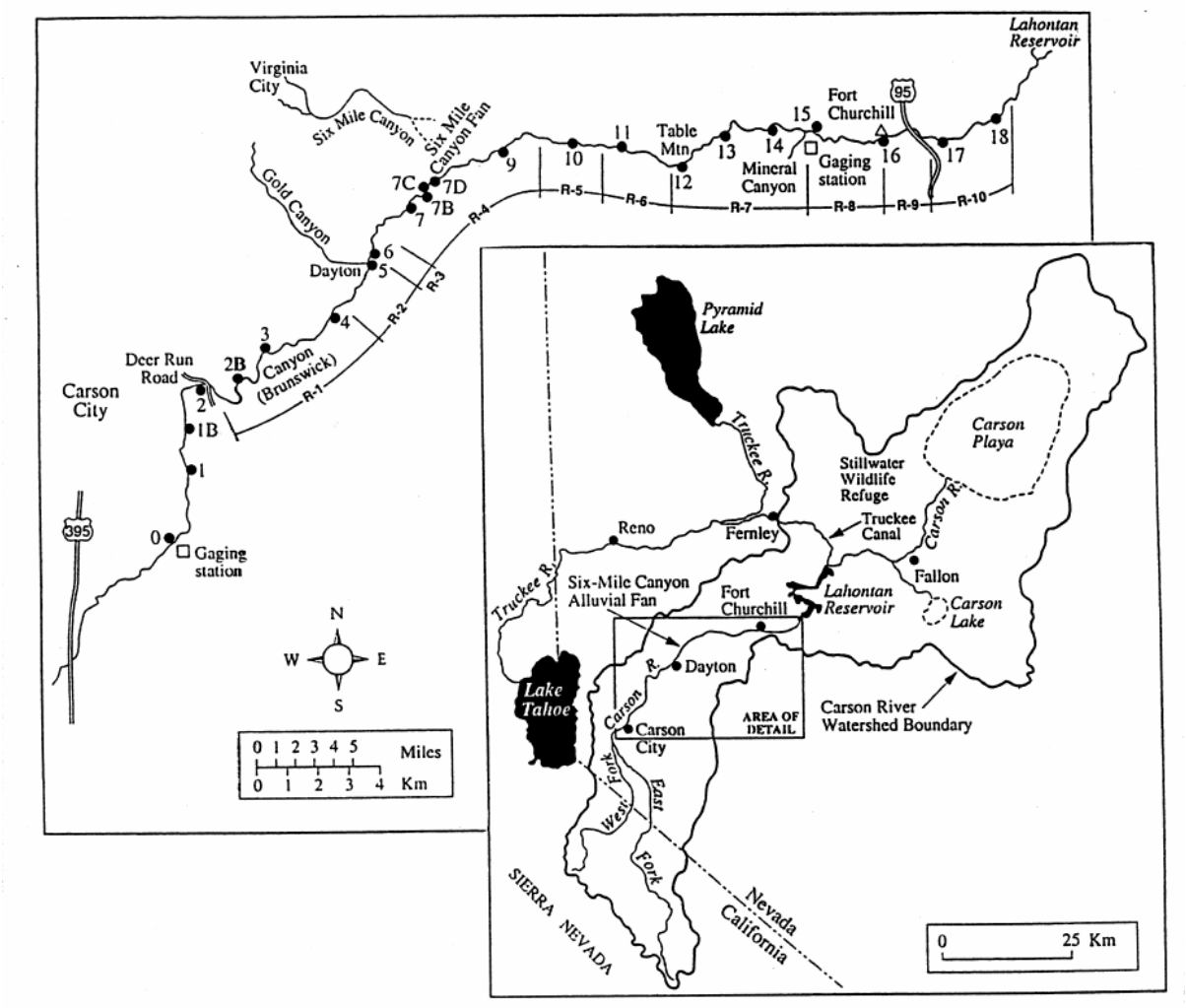

Figure 1. The Carson River – Lahontan Reservoir system with the detail showing the ten river reaches used by Miller *et al*. (1999) for geomorphic analysis.

Water Quality Analysis Simulation Program-5 that was developed to simulate the transport and transformation of various water body constituents. Mass balance equations account for all

material entering and leaving model segments through direct and diffuse loading, advective and dispersive transport, and any physical or chemical transformation. MERC4 (Martin, 1992) is a subroutine contained within WASP5. It was developed to specifically compute mercury speciation and kinetic transformation. MERC4 is capable of simulating up to four mercury species and three distinct solid types. Five state variables are modeled in this study: inorganic mercury (Hg^{2+}), methylmercury (MeHg), washload, coarse suspended sediment (CSS) and bedload. Elemental mercury (Hg0), while very toxic, is highly volatile with only very low concentrations detected in the surface waters of the Carson River (Bonzongo et al., 1996) and so was excluded from analysis.

Washload constitutes the smallest fraction (diameter< 0.063 mm) and is considered uniformly distributed from the riverbed to the water surface. Concentrations of CSS (diameter> 0.063 mm) are greatest near the riverbed and diminish upward toward the water surface. This is a direct reflection of the exchange of bed material into suspension and visa-versa (Meade, 1990). Bedload is the third type of solid modeled. It is defined as coarse material that travels by rolling, skipping and/or sliding along the riverbed. In addition to these three sediment fractions, the colloidal material (diameter less than 0.002 mm) was assumed to occupy a fraction of the washload. Colloids represent fine material that will not settle despite a decrease in stream velocities either on the river's floodplain or within the reservoir. The colloidal upstream boundary condition at the CCG was set to 11% of the total washload based on site data. The modeled fraction of colloidal material was then allowed to vary downstream such that when washload was deposited the fraction of colloids increased. The colloidal fraction increases to 100% of the fine material following sedimentation in the reservoir's delta region.

RIVMOD, WASP5 and MERC4 were originally chosen, linked and modified by Warwick and Heim (1995) and Heim and Warwick (1997) with further modification by Carroll et al. (2000) and Carroll et al. (2004). It is acknowledged an updated WASP7 and mercury module exist, however dynamic linking of WASP5 with RIVMOD as well as extensive code modifications to WASP5 done by previous studies prohibit its use. An attempt has been made to briefly summarize modeling procedures, however one is encouraged to refer to these previous studies for a complete discussion on model development.

The Carson River - Lahontan Reservoir model contains 307 water column segments starting at the CCG and ending at Lahontan Dam. The river is defined as segments 1 through 203 with segment spacing equal to 0.5 km. Reservoir segments (204 to 307) encompass the entire reservoir during peak capacity and are discretized smaller (0.25 km) to improve numeric stability during summer and fall drawdowns. All water column segments contain a corresponding bed segment for sediment and mercury exchange, but only river segments contain a representative bank element (described in the section Methylation in Bank Segments) for a total of 817 modeled segments. Carroll et al. (2004) modeled daily flows from 1991 to 1997 to simulate estimated erosion by Miller et al. (1999). Carroll et al. (2004) found no significant geomorphic change occurred during the drought years of 1991, 1992 and 1993. Therefore, this study will only focus only on daily flows beginning October 1, 1993 and extend through the 1998 water year to include University of Nevada, Reno (UNR) and USGS data collected near FCH in the model's analysis (refer to Figure 2).

3.2 Previous Modifications to RIVMOD

Early alterations to RIVMOD include a revision of the simple rectangular channel geometry to a more complex shape (Warwick and Heim, 1995). Past research along the Carson River considered cross sectional geometry spatially variable but temporally fixed (Carroll *et al.,* 2000). Subsequent modifications allowed dynamic width adjustment in which the modeled mass eroded was used to update channel width every timestep by assuming the entire vertical face of the bank was susceptible to erosion (Carroll *et al.,* 2004). The divided channel approach was also applied to the momentum equation contained within the RIVMOD numeric code to estimate floodplain depths and velocities during overbank flows (Carroll *et al.,* 2004).

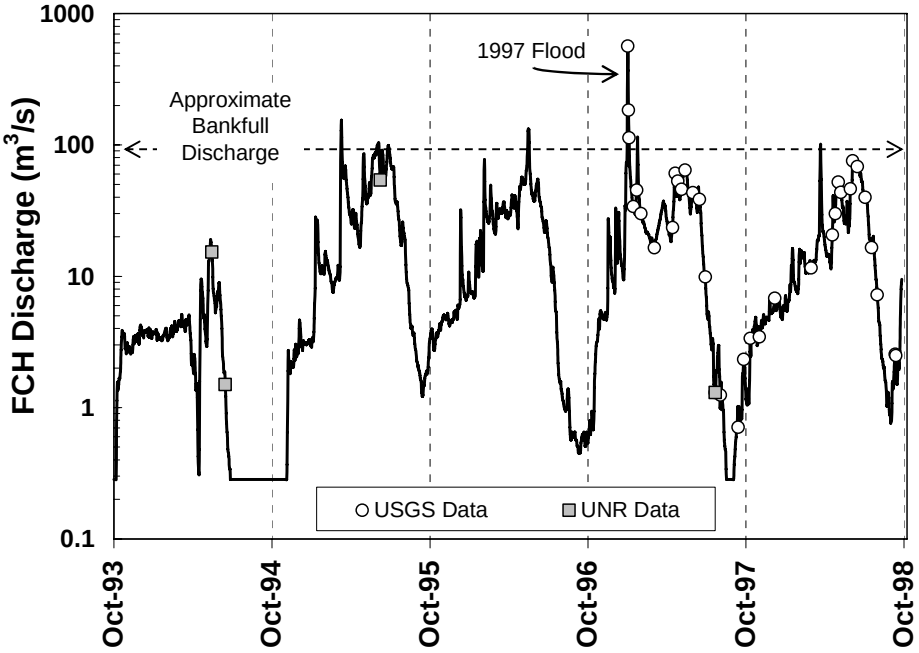

Figure 2. Modeled discharge at the Fort Churchill gage, with water column sampling dates marked. (UNR = collected by the University of Nevada, Reno; USGS = collected by the United States Geological Survey).

3.3 Modeling Bank Erosion and Overbank Deposition

Carroll *et al.*, (2004) developed an empirical relationship in WASP to describe bank erosion during in-channel flows as well as during over-bank flows. These relationships assume the rate of erosion is proportional to the shear stress applied to the bank (Darby and Thorne, 1996) and is indirectly related the average velocity, or square-root of the channel bottom slope. Using

Manning's wide channel relationship Carroll et al. (2004) developed the following relationship for bank erosion,

$$MER = \frac{\psi_1 \rho_s \gamma_w n^2 D^{2/3} v^2 L_s}{S_0^{1/2}} + \frac{\psi_2 \rho_s \gamma_w n^2 (D-h) v^2 L_s}{h^{1/3} S_0^{1/2}} \quad (1)$$

Where *MER* is the total bank mass eroded (kg) γ_w is the specific weight of water ($kg/m^2/s^2$), *h* is the height of the vertical bank face along the river's edge (*m*), *D* is the water depth starting at the vertical face of the channel bank (*m*), S_f is the friction slope, *v* is the water velocity (*m/s*), *n* is Manning's coefficient, L_S is the segment length (*m*), and ψ_1 and ψ_2 are constants of proportionality (m^2 *s/kg*). The first term on the right-hand-side of equation 1 was used to model mass eroded from the banks when river discharge was below bank-full, while both terms on the right-hand-side of equation 1 were used to model mass eroded during over-bank discharge. Carroll et al. (2004) calibrated ψ_1 using measured water column concentrations of washload material at FCH when flows were below bankfull discharge and calibrated ψ_2 such that total modeled mass eroded (*MER*) from the banks fell within the range presented by Miller et al. (1999). It is only possible to match observed values by allowing significantly more erosion to occur when flows surpass bankfull discharge than when flows are confined to the main channel. Carroll et al. (2004) modeled results show that nearly 87% of bank mass eroded in a 6-year time span occurred during the single 1997 flood event. These results agreed with Miller et al. (1999) who attributed all geomorphic change along the Carson River from 1991-1997 to this single high-magnitude event. Verification of this approach showed the model fell within the 95% confidence interval of the observed mean channel width increase in seven of the ten reaches (reaches shown in Figure 1 detail), with trends well predicted in two of the remaining three reaches.

Overbank deposition was modeled using separate, but related, approaches for CSS and washload (Carroll et al., 2004). CSS was modeled by coupling analytical approaches presented by Thomann and Mueller (1987) and Walling and He (1997) in order to relate the amount of sediment deposited to the distance from the main channel. With no calibration, modeled values of CSS deposition on the floodplain agreed quite well with observed values by matching observed values in five out of ten reaches (Carroll et al., 2004).

Carroll et al. (2004) modeled washload deposition using a functional relationship developed for the model WEPP (Foster et al., 1995) that relates the rate of washload deposition to the difference between the actual concentration of sediment in the water column and the theoretical transport capacity (Johnson et al., 2000). The rate of washload deposition R_s^w (kg/s/m^2) is given by,

$$R_s^w = \frac{\bar{\beta} V_s^w}{q_f} \left(G_{main}^w - T_c \right) \quad (2)$$

where V_s^w is the average fall velocity for washload material (m/s) and q_f (m^2/s) is the discharge per unit width on the floodplain. Using Stoke's Law and assuming an average washload particle diameter of 0.033 mm (non-colloidal washload 0.002 mm to 0.63 mm), V_s^w

equals 0.001 m/s. G^{w}_{main} is the water column non-colloidal washload (kg/s/m) in the main channel and T_c is the transport capacity (kg/m/s). β is a dimensionless turbulence coefficient and is assumed to decay exponentially with distance from the channel across the floodplain. To estimate T_c, a modified form of the model applied by Johnson et al. (2000) was used (Carroll et al., 2004),

$$T_c = \psi_3 q^2 S_0^{1.66} \tag{3}$$

where ψ_3 is a calibration constant (kg s/m^5) adjusted to match washload water column concentrations at FCH during overbank flows. These functions were able to predict washload concentrations at FCH, but over predicted washload deposited on the floodplain for most modeled reaches and over predicted total washload deposited by a factor of 2.7 (Carroll *et al*., 2004). Carroll *et al*. (2004) calibration of ψ_1, ψ_2, and ψ_3 to model bank erosion and overbank deposition was maintained in this study.

3.4 Modeling Lahontan Reservoir

Lahontan Reservoir consists of three distinct basins with water from the Carson River entering the south basin and moving northward through the middle basin and into the north basin (refer to Figure 1). The north basin terminates at Lahontan Dam with inputs from the Truckee Canal occurring at the north side of the dam. Lahontan Reservoir is almost 30 km in length when filled to maximum capacity. Past modeling of the Carson River-Lahontan Reservoir system used 0.5 km model segment lengths throughout the study site, but allowed for a finer discretization of segments (0.25 km) in the region of the reservoir delta. Rediscretization of the entire reservoir into 0.25 km segments was done to improve model stability during the drought of 1994 when drawdown in the reservoir allowed the delta to migrate into the north basin. Model stability was similarly improved by smoothing reservoir channel bottom slopes. Detailed cross sections of each modeled segment in the reservoir were developed using an updated United States Bureau of Reclamation (USBR) bathymetry map. Reservoir segments were redefined using these cross sections and the geometric definitions required by the modified RIVMOD (Carroll et al., 2004). Groundwater inflows/outflows were added to the reservoir to force modeled reservoir stages to match observed values. In particular, this was important to match massive drawdown in the reservoir during the drought of 1994 and allowed for accurate movement of the delta region which is important in simulating sediment and mercury deposition.

3.5 Modeling Mercury Transport

Boundary conditions, initial conditions, methylation - demethylation rates, particle reaction coefficients and the diffusion from bottom sediments are discussed in detail by Carroll et al. (2000). Carroll et al. (2000) developed a relationship describing river bank Hg concentrations ($[Hg^{2+}]_{bank}$) as a function of channel bed slope (S_0) (equation 4a) in which λ_1 (µg/kg) was adjusted to match observed pre-1997 flood water column concentrations along the Carson River. To accommodate a newly developed bank package where the concentration of MeHg would be

computed as time varying based upon bank moisture history, a spatially variable (simple linear function) inorganic mercury bank concentration was imposed as shown in equation 4b,

$$[Hg^{2+}]_{bank} = \frac{\lambda_1}{S_0^{0.5}} \qquad [Hg^{2+}]_{\max} = \frac{\lambda_1}{S_0^{0.5}} \tag{4a}$$

$$[Hg^{2+}]_{bank} = [Hg^{2+}]_{bot} + \frac{\left([Hg^{2+}]_{\max} - [Hg^{2+}]_{bot}\right)D}{2h} \tag{4b}$$

where $[Hg^{2+}]_{max}$ = maximum inorganic bank mercury concentration ($\mu g/Kg$), $[Hg^{2+}]_{bot}$ = measured channel bottom inorganic mercury concentration ($\mu g/Kg$) based on data collected by Miller and Lechler (1998) and described by (Carroll et al., 2000), D is water depth beginning at the vertical face of the bank (m) and h = the vertical height of the bank (m). The factor of two in the denominator of equation 4b accounts for banks on both sides of the river. It is also assumed that banks related to the low flow inner channel as well as the low to medium flow transition slope (roughly flow depths less than 1 m) have Hg^{2+} bank concentrations similar to channel bottom sediments. For this study, the calibration of λ_1 was accomplished using Hg^{2+} water column data collected during flow conditions just below bankfull (June 10, 1995).

3.6 Methylation in the Bank Sediments

Laboratory experiments conducted by Dr. Mark Hines (University of Massachusetts, Lowell) demonstrated that methylation activity was nonexistent when the bank soils were dry but quickly became significant after approximately four days of soil saturation (http://biogeochemistry.uml.edu/pages/Hg.html). To implement these findings, the newly developed bank package tracks the depth of vertical bank that has been saturated for four or more days, computes the average Hg^{2+} concentration in the saturated bank sediments (equation 4b), and then computes a MeHg bank concentration based on the computed amount of Hg^{2+} and the methylation-demethylation ratio. Rapid increases in flow will actually cause a "dilution" of in-stream MeHg concentrations since the bank concentrations will not increase by the time of significant erosion. On the other hand, if flow rises more gradually such that a majority of the bank remains saturated for four or more days, then the concentration of MeHg in the banks will be substantial as will be the potential mass loading rate into the river due to bank erosion and possibly bank diffusion. No calibration was performed using MeHg bank concentrations to match water column concentrations.

3.7 Uncertainty Analysis

Carroll and Warwick (2001) performed the first comprehensive uncertainty analysis of the Carson River mercury transport model. Specifically, uncertainty in the methylation-demethylation ratio and the diffusion rate of mercury from channel bottom sediments were evaluated in the river channel from the CCG to the FCH region. This study used a similar

approach to uncertainty, but focused only on impacts of geomorphic change on mercury transport while incorporating channel widening and dynamic bank methylation rates into the analysis. The Monte Carlo simulation was employed using the computing power of the Desert Research Institute's Advanced Computing in Environmental Sciences (ACES) program. This is a sophisticated research grid among the three University and Community College System of Nevada campuses. Grid computing power comes from a SGI Altix 3700 from Silicon Graphics with the shared –memory high performance supercomputer boasting 40 Intel Itanium2 CPUs, 80 GB of RAM and 3 TB of disk space and the Linux kernel. Five hundred simulations were run on ACES (taking three months computing time) simultaneously adjusting the parameters λ_1 and ψ_1. Results were then ranked to establish the 80% confidence interval of Hg and MeHg water column concentrations across the modeled domain and over the entire course of the simulation.

4. RESULTS AND DISCUSSION

Hg water column concentrations measured June 1995 were calibrated using a λ_1 value equal to 6,000 µg/kg. This value is approximately double that presented by Carroll et al. (2000), which is explained by the relationships between equation 4a used by Carroll et al. (2000) and equations 4b used herein. Figure 3a shows that while water column Hg^{2+} concentrations are slightly over-predicted in the upper river reaches, river Hg^{2+} concentrations at FCH (segment 140) and the river's delta region were well predicted. No calibration was attempted to match Hg^{2+} reservoir concentrations. Figure 3a suggests that the model may either over-estimate the importance of the over-bank flow event earlier in 1995 (refer to Figure 2) and its ability to transport Hg^{2+} into the reservoir, or has not moved the pulse of Hg^{2+} through the reservoir quickly enough. Verification of λ_1 used pre- and post-1997 flood data collected by UNR (refer to Figure 2 for sampling dates and flow regimes). Excellent results suggest equation 4b is fairly robust and capable of modeling systematic trends seen in mercury water column concentrations. No calibration was attempted to match MeHg water column data. Modeled MeHg water column concentrations for June 10, 1995 are compared to observed values in Figure 3b. Given no calibration, modeled results show excellent correlation with observed concentrations. Similar to Hg^{2+} results, MeHg concentrations in the reservoir show a large pulse of MeHg. Lack of data in the reservoir prevents judgment on the existence of this pulse.

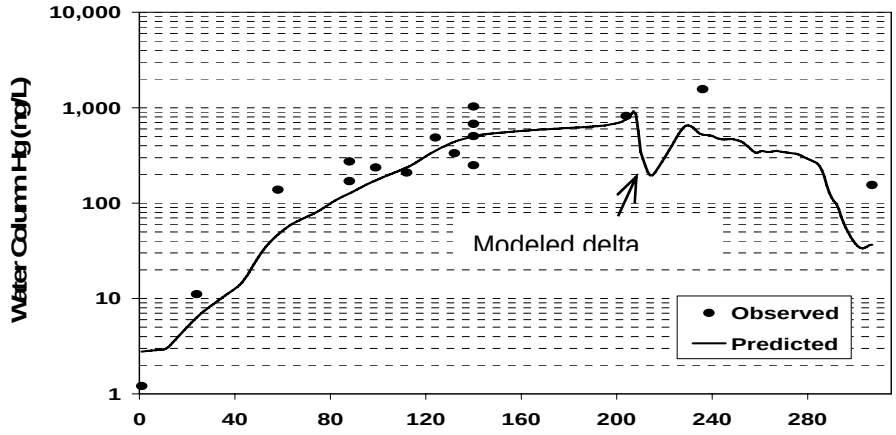

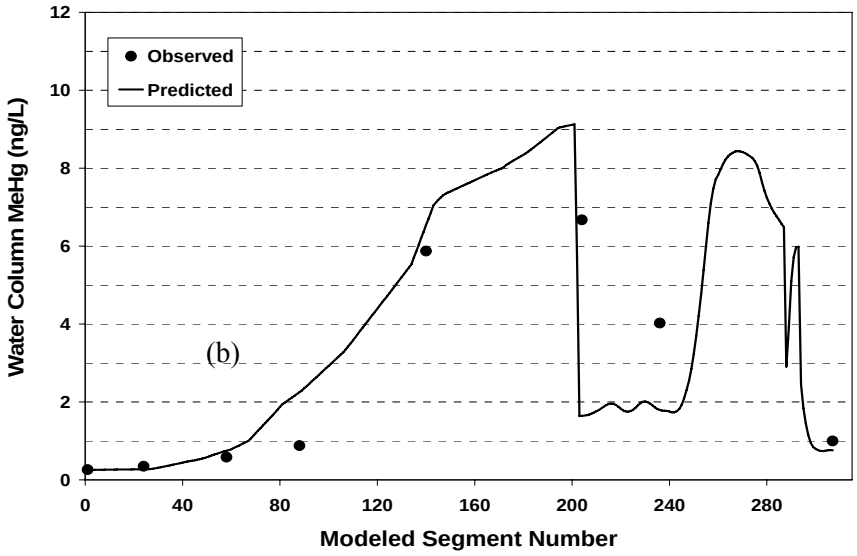

Figure 3: Water column mercury concentrations collected June 10, 1995 along the Carson River and Lahontan Reservoir, (a) Calibration of λ_1 (Hg^{2+} bank concentrations) to best match observed Hg^{2+} water column concentrations, (b) comparison of modeled and observed MeHg with no calibration.

The Monte Carlo simulation was conducted running 500 realizations with confidence intervals calculated from ranked results. λ_1 was varied ±33% from its calibrated value to assess uncertainty in Hg^{2+} and MeHg bank concentrations and their subsequent impact on water column concentrations due to bank erosion and bank diffusion processes. A triangle distribution was used with a mean (maximum probability of occurring) equal to thecalibrated value (6,000 µg/kg) and the upper and lower bounds set to a probability of zero. On the other hand, a half-triangle distribution was used to define ψ_2 with maximum probability set to the calibrated value (8,000 m^2·s/kg) and 4,000 m^2·s/kg set to zero probability. This lower bound was established by matching the minimum estimated total mass eroded (*MER*) by Miller et al. (1999). Maximum values of each probability distribution function (*PDF*) were computed such that the area under each *PDF* equaled 1.0. Note that *MER*, as determined by ψ_2 and the amount of fine material deposited on the floodplain, as defined by the transport capacity (ψ_3), are indirectly related to each other. The relationship between these variables was developed (equation 5) by adjusting ψ_3 to match the highest observed washload concentration (2,250 mg/L at 514 m^3/s) given different values for ψ_2. The resultant strong correlation (r^2 = 0.99) allows for excellent auto-calibration during the Monte Carlo simulation

$$\Psi_3 = 1.96\times10^6 - 13.694(\Psi_2 - 40{,}000) \quad (5)$$

Setting the maximum limit of the ψ_2 distribution to the original calibrated value excludes the upper bound of *MER* as defined by Miller et al. (1999). This was done because Carroll et al.

(2004) found the model over predicted washload deposition on the floodplain (i.e. transport capacity (ψ_3.) was too small). To bias the Monte Carlo realizations toward less over-bank deposition, it was necessary, according to equation 5, to bias the model toward less bank erosion (i.e. smaller values of ψ_2.).

Figure 4 shows that the resultant 80% confidence interval for expected variation due to bank erosion near FCH does not encapsulate all available data. Marked in Figure 4 are data collected during a flash flood event in Mineral Canyon (refer to Figure 1). Elevated Hg^{2+} and MeHg concentrations in the Carson River during this event are not related to modeled processes in the Carson River and, while shown in Figure 4, are excluded from analysis. Figure 4a shows bank erosion processes dominate Hg^{2+} inputs during spring melt (and rain-on-snow events) with peak Hg^{2+} concentrations occurring during over-bank discharge events. Hg^{2+} data collected prior to, and during, the 1997 flood fall within the estimated bounds.

Unlike inorganic mercury, modeled MeHg in the river's water column appears dominated by diffusion and not necessarily bank erosion processes. This is evident during the drought of 1994 when MeHg experiences its highest water column concentrations (Figure 4b) and the greatest range in the 80% confidence interval. The large range in uncertainty modeled in 1994 is a reflection of uncertainty in λ_1, the associated MeHg bank concentrations and resultant bank diffusion since significant bank erosion does not occur before or during 1994. In contrast, the second largest range in MeHg uncertainty occurs during the first over-bank flow event in 1995. This demonstrates that while diffusion appears more important, bank erosion is still a viable mechanism for MeHg loading to the river with significant impacts on MeHg water column concentrations. The 1997 flood event, which is so important to loading of Hg^{2+}, actually dilutes MeHg due to the flashy nature of the flood and the lag in peak MeHg bank concentrations relative to bank erosion.

(a)

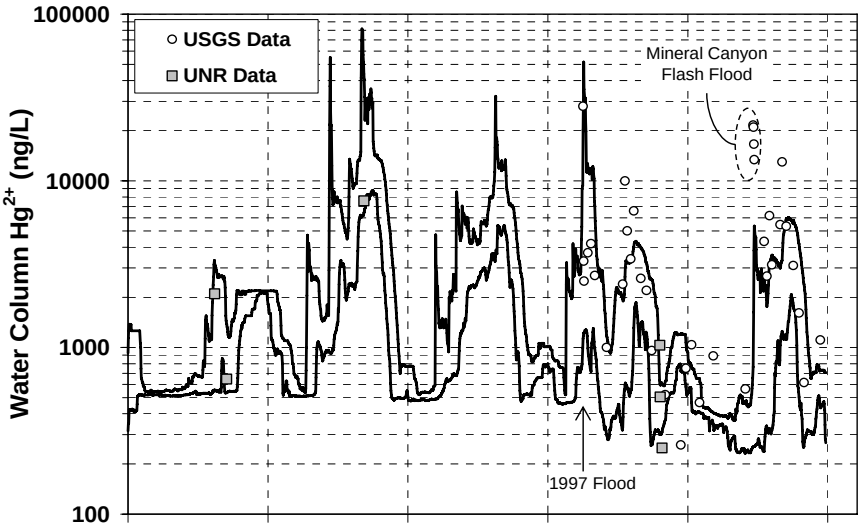

(b)

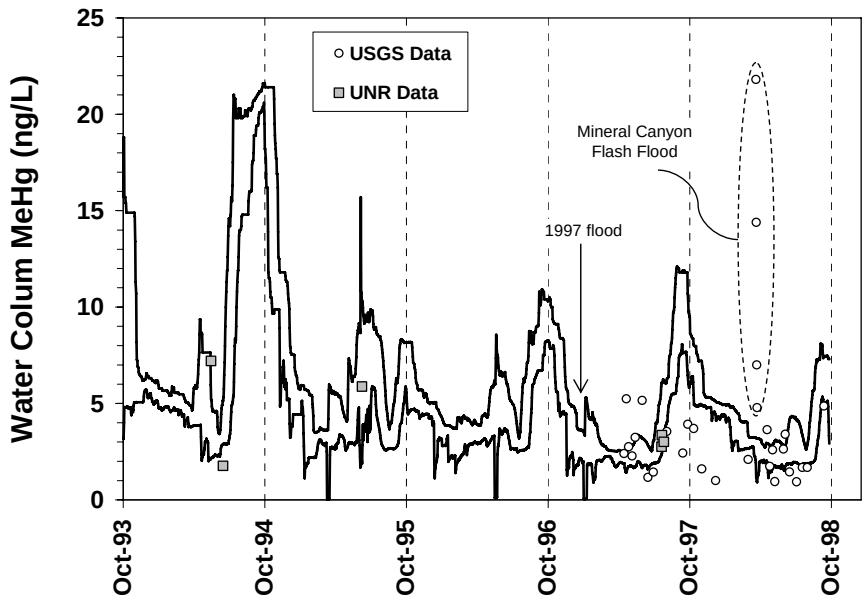

Figure 4: 80% confidence intervals given uncertainty related to geomorphic change near FCH for (a) Hg^{2+} and, (b) MeHg. Model results compared to data collected by UNR and the USGS.

However, modeled MeHg uncertainty decreases over time such that MeHg loading via bank erosion or bank diffusion diminishes with each successive over-bank flow event as a result of increased channel widths.

System-wide upper 80% bounds of uncertainty due to bank erosion processes are presented in Figure 5. The 1997 flood occurred on day 1193 in the simulation and model segment 304 represents the furthest upstream extent of Lahontan Reservoir. Settling of contaminated sediment at the reservoir delta causes a rapid decrease in mercury concentrations (Hg^{2+} and MeHg) and allows quick delineation of the delta region. During the drought of 1994 the reservoir (day 350 to 400) reverted back to river-status as it was nearly drained. Hg^{2+} and MeHg concentrations were relatively high throughout the reservoir during the drought since water column velocities remained high and sedimentation was limited. MeHg concentrations throughout the system were highest during the drought of 1994 with diffusion dominated loading (Figure 5b). MeHg concentrations during the 1997 flood were much lower as the result of dilution.

System-wide Hg^{2+} results (Figure 5a) agree, in part, with those presented for FCH in Figure 5a, such that erosion is important during 1995 when flows first go over bank, and to a lesser degree in 1996. However, system-wide, the 1997 flood appears the dominate Hg^{2+} loading event into the reservoir and not 1995 as suggested by FCH results. During the 1997 flood the Hg^{2+} upper 80% confidence interval is significantly elevated throughout most of the system, including the reservoir where velocities remained high despite the reservoir reaching its maximum capacity. The discrepancy between FCH results and system-wide results has to do with the very

shallow channel bottom slope (S_0) defined at FCH and its indirect relationship to MER defined by equation 1. The FCH site, marked in Figure 5a, shows a significant dip in Hg^{2+} concentrations during the 1997 flood relative to steeper river segments above and below its location. A similar dip is not evident in 1995 during peak flows. FCH illustrates that segments with shallow river bottom slopes place greater emphasis on earlier over-bank flow events than steeper river segments.

5. CONCLUSIONS

n summary, uncertainty related to modeled geomorphic processes of bank erosion and over bank deposition describe observed variation in Hg^{2+} water column concentrations prior to and during the 1997 flood. The model places relatively greater uncertainty in modeled behavior on earlier over-bank discharge events than later events. This is most evident in river reaches that have shallow channel slopes, which experience the greatest increases in channel widths during the earliest modeled over-bank flow events. Despite this limitation, the model is able to capture all of the measured variation in the Hg^{2+} concentrations during the 1997 flood arguably the largest Hg^{2+} loading event ever recorded in the Carson system. However, a change in the system appears to occur during the 1997 flood that is not adequately modeled since uncertainty in modeled parameters alone cannot explain Hg^{2+} variation following the flood. MeHg loading appears dominated by diffusion as opposed to geomorphic changes to the river channel. Diffusion from river banks is indirectly included in the uncertainty analysis via the amount of Hg^{2+} (and subsequent MeHg) in the river banks. Bank diffusion appears as an important mechanism for MeHg loading as evidenced by the large amount of MeHg uncertainty in during the drought of 1994. However, its influence diminishes with time because of increased channel widths and the resultant decrease in river depths. Uncertainty in geomorphic channel change, including Hg^{2+} and MeHg bank concentrations, are not enough to capture observed variation in MeHg water column concentrations at FCH. Future work will need to include uncertainty in diffusion rates as well as methylation and demethylation rates to encompass all observed variability.

(a)

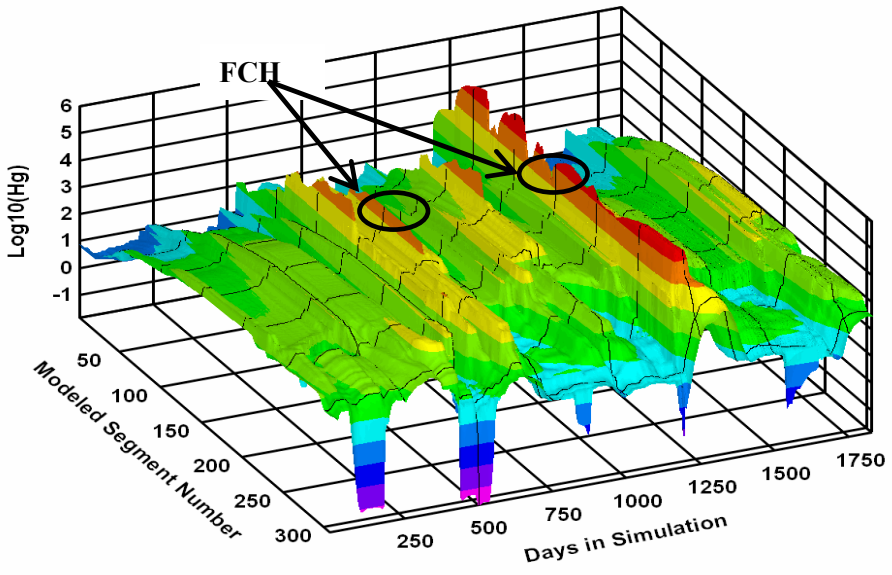

(b)

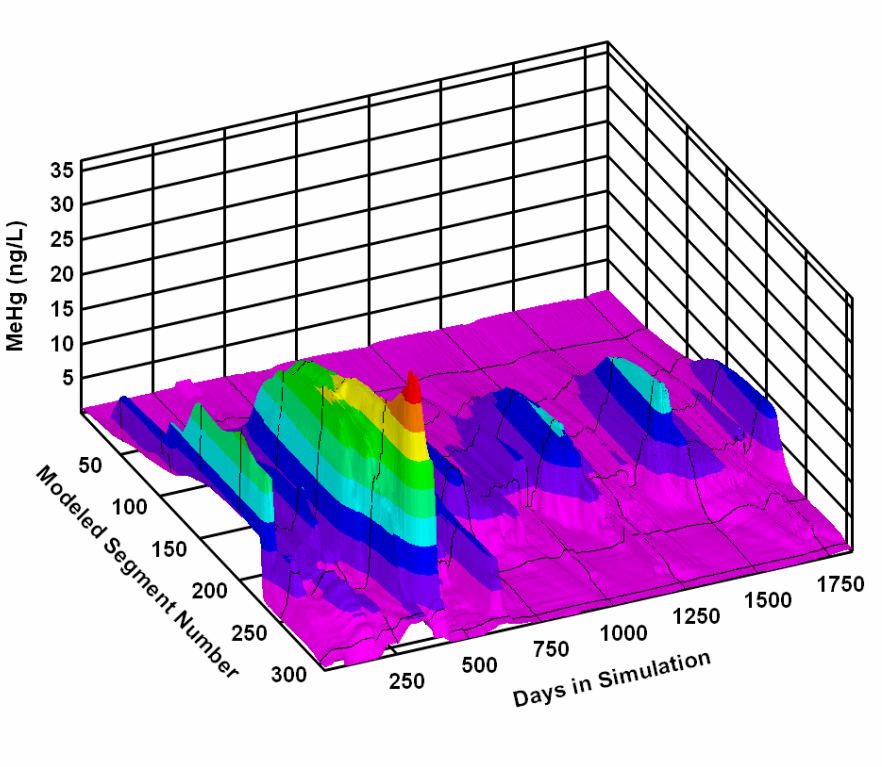

Figure 5: Upper 80% confidence interval for entire model domain over entire simulation given uncertainty in geomorphic changes to the river channel. (a) Hg^{2+}, (b) MeHg. Note that Hg^{2+} is plotted in log10-units.

6. ACKNOWLEDGMENTS

This work was partially funded by the National Science Foundation (EAR-9712857). Also, the authors wish to thank Ms. Karen Thomas (USGS Carson City) for sharing data and associated explanations from field observations.

7. REFERENCES

Ambrose, R.B., Wool, T.A., Martin, J.P. and Schanz, R.W., 1991. WASP5.X: A Hydrodynamic and Water Quality Model: Model Theory, User's Manual and Programmer's Guide. U.S. E.P.A., Athens, Georgia.

Bonzongo, J.C., Heim, K.J., Warwick, J.J. and Lyons, W.B., 1996. Mercury Levels in
Surface waters of the Carson River-Lahontan Reservoir system, Nevada: influence of historic mining activities. Environ Pollution, 92(2): 193- 201.

Carroll, R.W.H., Warwick, J.J., Heim, K.J., Bonzongo, J.C., Miller, J.R. and Lyons, W.B., 2000. Simulating Mercury Transport and Fate in the Carson River, Nevada. Ecological Modeling, 125:255-278.

Carroll, R.W.H. and Warwick, J.J., 2001. Uncertainty analysis of the Carson River mercury transport model. Ecological Modeling, 137: 211-224.

Carroll, R., Warwick, J.J., James, A., and J. Miller, 2004. Modeling Erosion and Overbank Deposition During Extreme Flood Conditions on the Carson River, Nevada. Journal of Hydrology. 297:1-21.

Darby, S.E. and Thorne, C.R., 1996. Numerical simulation of widening and bed deformation of straight sand-bed rivers. I: Model development. Journal of Hydraulic Engineering, 122(4): 184-193.

Foster, G.R., Flanagan, D.C., Nearing, M.A., Lane, L.J., Risse, L.M., and Finkner, S.C., 1995. Chapter 11: Hillslope erosion component. *In* USDA-Water Erosion Prediction Project (WEPP) Technical Documentation, NSERL Report No. 10, National Soil Erosion Research Laboratory, USDA-ARS-MWA, W. Lafayette, IN.

Heim, K.J. and Warwick, J.J., 1997. Simulating sediment transport in the Carson River and Lahontan Reservoir, Nevada. Journal of the American Water Resources Association, 33(1): 177-191.

Hoffman, R.J. and Taylor, R.L., 1998. Mercury and suspended sediment, Carson River
basin, Nevada- loads to and from Lahontan Reservoir in flood year 1997 and deposition in reservoir prior to 1983. FS-001-98, USGS

Hosseinipour, E.Z. and Martin, J.L., 1990. RIVMOD: a one-dimensional hydrodynamic sediment transport model: model theory and user's guide. U.S. E.P.A, Athens, Georgia.

Johnson, B.E., Julien, P.Y., Molnar, D. K., and Watson, C.W., 2000. The two-dimensional upland erosion model CASC2D-SED. Journal of the American Water Resources Association 36(1): 31-42.

Martin, J.L., 1992. MERC4: A mercury transport and kinetics model: model theory and user's guide. U.S. E.P.A., Athens, Georgia.

Meade, J.R., 1990. Movement and storage of sediment in rivers of the United States and Canada. In: M.G. Wolman and H.C. Riggs (Editors), Surface water hydrology. The geology of North America. Geological Society of America, Boulder, CO, pp. 255-280.

Miller, J.R. and Lechler, P.J., 1998. Mercury partitioning within alluvial sediments of the Carson River valley, Nevada: implications for sampling strategies in tropical environments. In: J.W.e. al. (Editor), Geochemistry of tropical environments. Springer-Verlag, pp. 211-233.

Miller, J.R., Lechler, P.J., and Desilets, M., 1998. The role of geomorphic processes in the transport and fate of mercury in the Carson River basin, west-central Nevada. Environmental Geology, 33(4): 249-262.

Miller, J.R., Barr, R., Grow, D., Lechler, P., Richardson, D., Waltman, K. and Warwick, J., 1999. Effects of the 1997 flood on the transport and storage of sediment and mercury within the Carson River valley, west-central Nevada. Journal of Geology, 107(3): 313.

Smith, G.H. and Tingley, J.V., 1998. The history of the Comstock Load, 1850-1997. Nevada Bureau of Mines and Geology in association with the University of Nevada Press.

Thomann, R.V. and Mueller, J.A., 1987. Principles of Surface Water Quality Monitoring and Control. Harper Collins Publishers, Inc, New York, NY, 549 pp.

Walling, D.E. and He, Q., 1997. Investigating spatial patterns of overbank sedimentation of river floodplains. Water, Air and Soil Pollution, 99: 9-20.

Warwick, J.J. and Heim, K.J., 1995. Hydrodynamic modeling of the Carson River and Lahontan Reservoir, Nevada. Water Resources Bulletin, 31(1): 67-77.

Chapter 21

BIOSCREEN, AT123D, AND MODFLOW/MT3D, A COMPREHENSIVE REVIEW OF MODEL RESULTS

Robert A. Schneiker, P.G. [§2] and Liliana Cecan, P.E., Ph.D.[§1]
[1]McLane Environmental, LLC, 707 Alexander Road, Suite 206, Princeton, NJ 08540, [2], Environmental Software Consultants, Inc. P.O. Box 2622, Madison, Wisconsin 53701-2622

ABSTRACT

The Domenico equation is commonly used to evaluate long term risks associated with contaminated groundwater. Numerous groundwater models are based on it, including BIOSCREEN and BIOCHLOR. This paper compares the results from BIOSCREEN, AT123D and MODFLOW/MT3D groundwater models. Results from the AT123D and MODFLOW/MT3D models indicate that BIOSCREEN significantly underestimates contaminant mobility and thus exposure risks. This was unexpected as BIOSCREEN results are commonly assumed to be extremely conservative. In fact BIOSCREEN did produce the highest downgradient concentrations; however it took unreasonably long periods of time to achieve them. Such lengthy time periods are not typically evaluated as part of a risk evaluation. Even more surprisingly, BIOSCREEN produced the same peak concentration for all contaminants and for all aquifer types tested. Both contaminant concentration and travel times from AT123D and MODFLOW/MT3D models were almost identical. Furthermore, these results varied with contaminants and aquifer properties as expected. The influence of biodegradation was also evaluated. Inclusion of conservative biodegradation rates made BIOSCREEN the least conservative model by far. This is because the lengthy travel times produced by BIOSCREEN provide a longer period of time over which biodegradation works.

Keywords: AT123D, BIOSCREEN, MODFLOW, MT3D, SESOIL

§ Corresponding Author: Robert A. Schneiker, P.G., Environmental Software Consultants, Inc., P.O. Box 2622, Madison, Wisconsin 53701-2622, Phone: (608) 240-9878, rschneiker@seview.com

§ Corresponding Author: Liliana Cecan, P.E., Ph.D., McLane Environmental, LLC, 707 Alexander Road, Suite 206, Princeton, NJ 08540, Phone: 609) 987-1400, lcecan@mclaneenv.com

1. INTRODUCTION

Groundwater transport modeling can be useful in making informed and defensible remedial decisions. It has been prevalent in the field of environmental hydrogeology because of its wide application in the risk-based decision making process. Often this involves the use of the Domenico equation as a first step of the risk-based process. Selection of an appropriate transport model is of paramount importance in this process, as capabilities and ease of use can vary greatly. This paper compares three commonly used transport models, BIOSCREEN, AT123D, and MODFLOW/MT3D. These models are used to predict groundwater contaminant concentrations, which in turn can determine the amount of contamination that can remain in place while assuring the protection of human health and environment. The three models reviewed in this paper were selected based on their past use and availability.

1.1 Model Description

There are two basic types of computer-based groundwater transport models: analytical and numerical. Analytical models use equations to calculate exact solutions for simple hydrogeological systems, while numerical models provide approximate solutions for complex hydrogeologic conditions.

1.1.1 Analytical Models

AT123D and BIOSCREEN are both analytical groundwater models, and as such they use equations to calculate concentrations at specific locations and times. Results at any point are established independently of results at adjacent points or upon previous time steps. This makes analytical models much easier to use, and eliminates many common problems associated with numerical modeling. For instance, there is no need to design a three-dimensional grid prior to running the model. Furthermore, there is no need to calibrate analytical models. This ease of use has sometimes been misinterpreted as indicating that analytical models are less accurate than numerical models; however, this is not necessarily the case. Instead, the downside related to analytical models is that they are restricted to uniform flow conditions.

1.1.2 Numerical Models

Numerical models, such as MODFLOW/MT3D, provide approximate solutions for complex hydrogeologic conditions. Unlike analytical models, numerical model results depend upon many factors including cell (grid) size and the length of the model stress periods. This makes setting up MODFLOW/MT3D far more complicated than running either BIOSCREEN or AT123D. In general, numerical modeling consists of several steps. First, the area of interest must be divided into a grid of three-dimensional cells. These cells can vary in length, width and thickness. Thus, the grid must be carefully designed, as results are dependent upon cell size. Properties are then assigned to each cell. These properties are assumed to be uniform within a cell, although they can vary from cell to cell. Second, once the grid is established, a method (i.e., Preconditionate

Conjugate Gradient - PCG, Slice Implicit Procedure - SIP, etc.) is selected to solve the finite-difference equations.

It should be noted that results are produced for all model cells, not just the cells of concern, which means that cell size should be small enough to represent a point of compliance but large enough to minimize model run times. In general, accuracy is increased as grid cell sizes decrease. At the same time, the grid must accommodate the contaminant release coordinates. It is not advisable to simply increase the size of the time steps to shorten run times as this may also alter the results. Specifically, if the time step or the grid spacing is too large, the simulation results are poor. Furthermore, the simulation results rely greatly upon the results obtained in adjacent cells and at earlier times. Reducing the values of these parameters may improve the results at the expense of lengthily model run times.

The advantage of numerical models is that they are valid over a wide range of complex hydrological conditions. However, prior to predictive modeling, groundwater flow must be calibrated to site conditions. This means that additional information, including pump tests data, are required for calibration. Calibration is performed by carefully varying input parameters until model results match the observed head values. It should be pointed out that most sites have insufficient data for proper calibration, making it impossible to assure that the models are properly set up. Once MODFLOW is calibrated, the MT3D transport and fate model can be run. Contaminant load in MT3D can be introduced in any of the model cells or at the top of a cell (Figure 1). MT3D results may often indicate a need for further calibration. Finally budgetary constraints and project deadlines may further restrict the use of numerical models.

1.2 BIOSCREEN

In recent years there has been a significant increase of the use of groundwater models based on the Domenico (1987) analytical equation (Table 1). This includes BIOSCREEN (1996), which was developed for the US Air Force by Ground Water Services, Inc. With over 6,000 downloads it may be the most widely used groundwater model in the world. BIOSCREEN is a public domain, two-dimensional screening level groundwater transport and fate model, that is used by many regulatory agencies as a screening model. Contaminant transport is simulated under one-dimensional horizontal groundwater flow. Version 1.4 of the BIOSCREEN model was utilized to perform the modeling in this review.

Table 1. Domenico Equation Based Groundwater Models

RBCA Tool Kit for Chemical Releases v 1.3b	Texas - Update from RBCA for Chemical Releases
RNA Tool Kit for the Florida Petroleum Cleanup Program	FATE5
RBCA Tool Kit for Atlantic Canada v 2.0	BIOSCREEN
Update from version 1.0.1	BUSTR-Screen
Delaware - DERBCAP Module	BIOCHLOR
Delaware - Update from RBCA for Chemical Releases	Illinois EPA TACO
Texas - RBCA Tool Kit for TRRP	

There is only one type of load configuration in BIOSCREEN, in which the contamination is applied as a plane perpendicular to groundwater flow (Figure 1). Processes simulated in this model are advection, dispersion, adsorption, and biological decay (Table 2). Biodegradation can be simulated either a first-order decay or an instantaneous reaction process. The results can be displayed as both area and centerline graphs. However, BIOSCREEN cannot produce a point of compliance report. Aquifer boundaries are set to infinite in BIOSCREEN.

The Domenico equation on which the BIOSCREEN model is based assumes that the source contaminant concentration remains constant through time (i.e. the source mass is infinite) (Figure 2). This means that the source concentration remains constant no matter how long the model is run. The infinite source is an inherent limitation of the Domenico equation that does not depict any real world release scenario. It does however simplify the math thus significantly reducing the computational time. In an attempt to overcome this limitation of the Domenico equation, a declining source concentration term was added to BIOSCREEN. This was accomplished by reducing the source concentration at a rate based on an estimate of the total mass in the source volume (even though actual load is still only a plane). However, the rate at which the source declines is not explicitly determined based on contaminant migration. As stated in the BIOSCREEN User's manual: "this is an experimental relationship, and it should be applied with caution". Most regulatory agencies are aware of the problems associated with the declining source in BIOSCREEN and require that it only be run using the infinite source option.

1.3 AT123D

AT123D (G.T. Yeh 1981) is an acronym for the Analytical Transient 1-, 2-, and 3-Dimensional Simulation of Waste Transport in the Aquifer System. It is a public domain three-dimensional analytical groundwater transport model. Contaminant transport is simulated under one-dimensional horizontal groundwater flow. Transport processes simulated are advection, dispersion, adsorption, diffusion, and biodegradation (Table 2). The aquifer can be simulated as either confined or unconfined.

On the surface AT123D and BIOSCREEN appear to be very similar, yet there are significant differences in the basic model assumptions. For instance BIOSCREEN is written in Excel, which although powerful is not designed to optimize mathematical calculations. On the other hand, AT123D and MODFLOW/MT3D are all written in FORTRAN, which is specifically created for the development of scientific applications. This provides a dramatic improvement in performance, which allows AT123D and MODFLOW/MT3D to simulate a wider array of processes and load configurations.

There are a total of eight load configurations in AT123D, in which the load can be established as a point, line, area or volume (Figure 1). The source concentration in AT123D declines as contamination migrates downgradient (Figure 2). In addition to simulating a single instantaneous release, a separate load for each time-step can be applied in AT123D. This feature allows AT123D to be linked to the SESOIL vadose zone model. The SESOIL - AT123D link is one of the reasons why the SESOIL and AT123D models have been used by a number of state agencies to develop baseline cleanup objectives. Modeling was performed using Version 6.0 of AT123D in the SEVIEW 6.3 Integrated Contaminant Transport and Fate Modeling System

Load		BIOSCREEN	AT123D	MODFLOW MT3D	Load		BIOSCREEN	AT123D	MODFLOW MT3D
Point	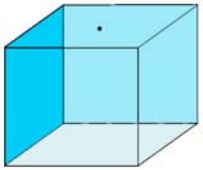		✓		Area	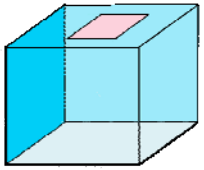		✓	✓
Line	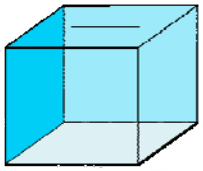		✓			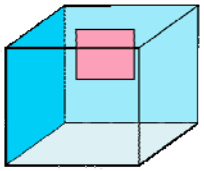		✓	
	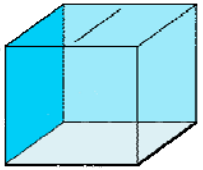		✓			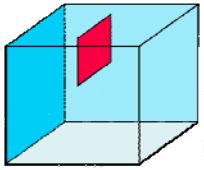	✓	✓	
	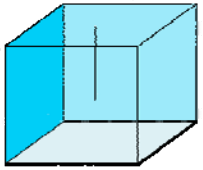		✓		Volume	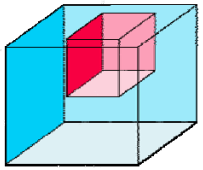		✓	✓

Figure 1. Model Load Configurations

Table 2. Model Processes

Process	BIOSCREEN	AT123D	MODFLOW/MT3D
Volume source		✓	✓
Declining source		✓	✓
Advection	✓	✓	✓
Dispersion	✓	✓	✓
Adsorption	✓	✓	✓
Biological Decay	✓	✓	✓
Water Diffusion		✓	✓

(ESCI, 2005). SEVIEW was used to setup and run the AT123D model. The SEVIEW point of compliance report was used to determine the peak groundwater concentrations.

1.4 MODFLOW and MD3D

MODFLOW (McDonald and Harbaugh 1984) is a public domain three-dimensional numerical groundwater model. Groundwater flow can be simulated for both steady state and transient conditions. It can also simulate flow based on external stresses, such as wells, recharge, evapotranspiration, rivers, and lakes. Hydraulic conductivities, storage coefficients, and groundwater flow parameters may differ spatially (horizontal–specific for each cell, vertical–specific for each layer), thus accounting for anisotropic conditions (heterogeneous aquifers). Specified head and flux boundaries can be used to simulate head inside the boundary domain. The aquifer can be simulated as confined or unconfined. MODFLOW is currently the most widely used numerical model in U.S. for groundwater flow problems.

MT3D (C. Zheng 1990) is a public domain three-dimensional transport model. It was developed independently from MODFLOW and was designed to work with any cell-centered numerical groundwater flow model. Transport processes simulated are advection, dispersion, adsorption, diffusion, and biodegradation (Table 2). As with AT123D varying contaminant loads can be applied for each time step. The feature means that MT3D can also be link to the SESOIL model. In addition, MT3D can simulate time-dependent aquifer conditions. Contaminant load can be established as a volume of contaminated groundwater in any of the cells or as a plane at the top of the water table (Figure 1). As with AT123D, MT3D simulates a declining source as an integral part of the transport and fate process. Together MODFLOW and MT3D represent the gold standard in modeling.

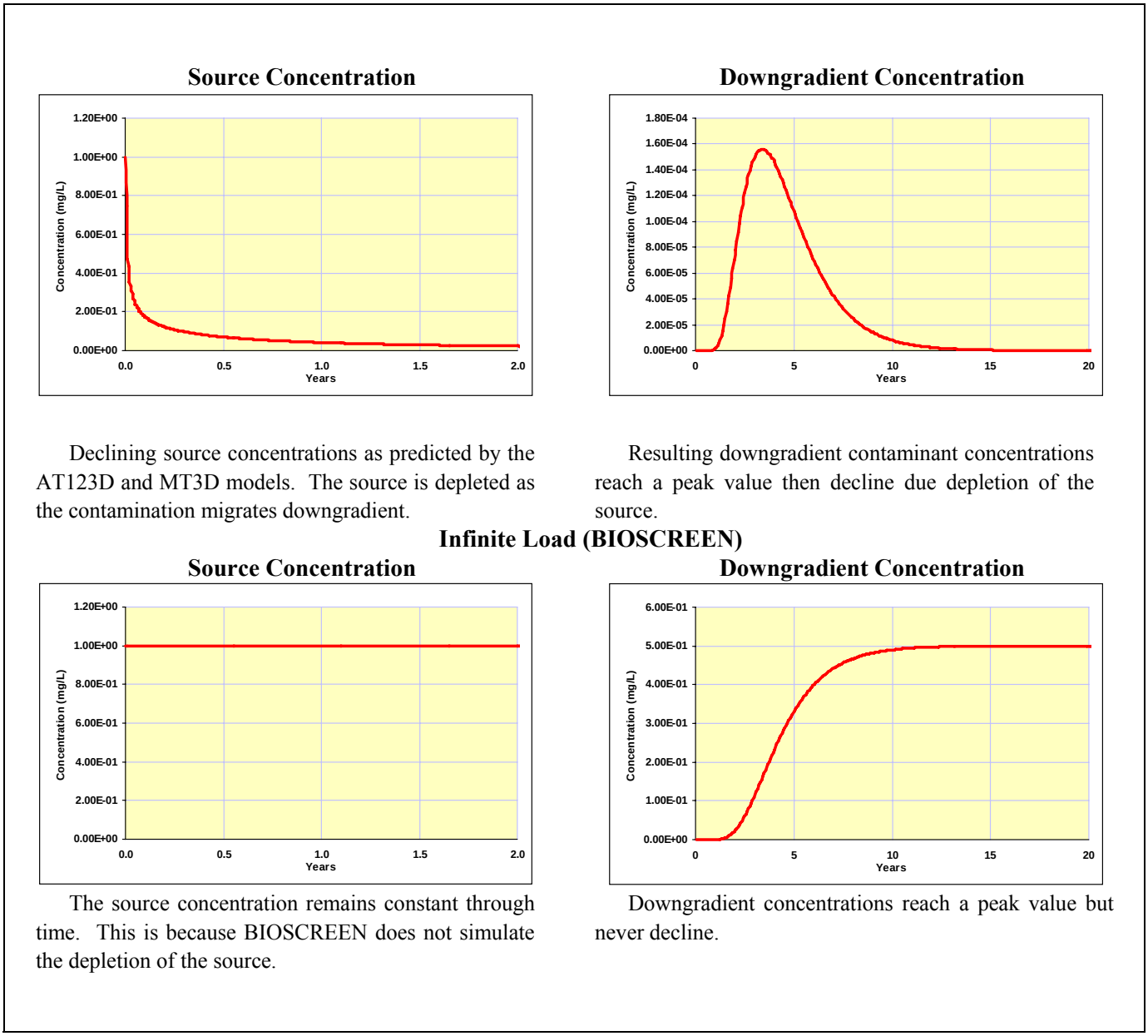

Figure 2. Instantaneous Load (AT123D and MODFLOW/MT3D)

1.5 Transport and Fate Processes

Groundwater models use various methods to simulate contaminant transport and fate processes. A summary of transport and fate processes simulated by the models is displayed in

Table 2. There can be substantial differences in the total number of processes simulated and in the methods used to simulate a particular process. All of the models tested simulate advection, dispersion, adsorption, and biological decay processes. The AT123D and MT3D models simulate two additional processes. The first is the declining source concentration as the contamination mass migrates downgradient. The second is the water diffusion process. Water diffusion produces migration of contamination from areas of higher concentration to areas of lower concentration. This process is not dependent upon groundwater flow and as such it even occurs in stagnant groundwater. Diffusion becomes progressively more important as groundwater flow decreases. Inclusion of this process means that AT123D and MODFLOW/MT3D can be used for lower permeability aquifers than BIOSCREEN. Inclusion of the water diffusion coefficient is not an issue, as many regulatory agencies have published values. In addition values can be quickly located in the chemical literature or even calculated based on molecular weight.

1.6 Input Parameters

Model input parameters (Tables 3 and 4) were obtained from default values specified by the Ohio Department of Commerce, Bureau of Underground Storage Tank Regulations (BUSTR, 2003). These input parameters were designed for use in the BUSTRScreen transport and fate model. BUSTRScreen is a variation of BIOSCREEN specifically developed for BUSTR. A tight clay aquifer scenario was added. This produced a wide range of conditions over which model responses could be evaluated. A gradient of 0.001 ft/ft was used for all aquifers. Modeling was performed for benzene and methyl tertiary-butyl ether (MTBE). We decided to use these chemicals as they often control remediation of contaminated sites. Chemical specific parameters for organic carbon partition coefficient (Koc) and water diffusion coefficient were obtained from the SEVIEW 6.3 chemical database. Biodegradation rate values were also obtained from the BUSTR data. Biodegradation of MTBE was not considered, as it is not assumed to readily degrade. Dispersivity values utilized in this evaluation are presented on (Table 5). AT123D and BIOSCREEN input parameters are almost identical with the exception of two additional parameters in AT123D: the distance of the load in the x direction and the water diffusion coefficient (Table 6).

This evaluation consisted of determining predicted groundwater concentrations at a point ten meters (32 feet) downgradient of the source. Hydraulic conductivities simulated ranged from 1.0E+1 cm/sec to 1.0E-6 cm/sec. A total of 54 model scenarios were completed to evaluate results over a wide range of conditions.

1.7 Model Parameters

The source dimensions were set to 6 by 10 by 5 feet in AT123D and MT3D, while the source in BIOSCREEN was set to a plane perpendicular to groundwater flow with a width of 10 feet and a depth of 5 feet (Table 7). Modeling was performed using an initial concentration of 1.0 ppm.

Table 3. Aquifer Parameters

Aquifer Type	Hydraulic Conductivity	Porosity	Bulk Density	Soil Organic Carbon	Gradient
units	cm/sec	dimensionless	kg/L	fraction	ft/ft
Tight Clay	1.0E-6	0.20	1.9	0.001	0.001
Clay	1.0E-5	0.20	1.8	0.001	0.001
Silt	1.0E-3	0.30	1.7	0.001	0.001
Silty Sand	1.0E-1	0.30	1.6	0.001	0.001
Clean Sand	1.0E+0	0.30	1.5	0.001	0.001
Gravel	1.0E+1	0.35	1.4	0.001	0.001

Table 4. Chemical Parameters

Chemical of Concern	Partition Coefficient (K_{oc})	Solute Half-Life	Water Diffusion Coefficient	Maximum Contaminant Level (MCL)
units	L/kg	years	cm^2/sec	mg/L
Benzene	58.9	1.97	9.80E-6	0.005
Methyl-tertiary Butyl Ether	6.0	- -	8.70E-6	0.040

Table 5. Aquifer Dispersivities

units	ft
Longitudinal	3.28
Transverse	0.328
Vertical	0.0328

Table 6. AT123D and BIOSCREEN Input Parameters

1.7.1.1.1 Parameter		BIOSCREEN	AT123D	MODFLOW/MT3D
Hydraulic Conductivity		✓	✓	✓
Gradient		✓	✓	✓
Dispersivities		✓	✓	✓
Porosity		✓	✓	✓
Bulk Density		✓	✓	✓
Organic Carbon Content		✓	✓	✓
Partition Coefficient		✓	✓	✓
Biodegradation	**Half-Life**	✓	✓	✓
	Instantaneous Reaction	✓		
Water Diffusion Coefficient			✓	✓

1.8 Model Setup And Run Times

It took less than 5 minutes to set up each of the BIOSCREEN and AT123D scenarios. It took about two hours to setup the MODFLOW/MT3D models. Modeling was performed using a 2.4 GHz Pentium 4 computer using the Microsoft Windows XP operating system. BIOSCREEN was run in Microsoft Excel 97. Among all three models, BIOSCREEN was the fastest, producing almost instantaneous results for all aquifer types. AT123D came in second taking a maximum of 10 seconds to run. It took MODFLOW/MT3D up to 28 minutes to run the tight clay simulations. Even then, rather than waiting for hours for the run to finish, some of the MODFLOW/MT3D runs were terminated once the peak concentration was observed.

Table 7. Contaminant Load Coordinates

Models	**AT123D & 1.8.1.1 MODFLOW/MT3D**	**BIOSCREEN All**
units	ft	ft
x-axis*	-6.0	0.0
y-axis	10.0 (± 5.0)	
z-axis	-5.0	

1.9 Reports

All three models present results as area reports (Table 8). These reports depict concentrations over the entire area at a specific time. Although the area reports are nicely presented, they provide little relevant data for the evaluation of exposure risk. Both AT123D and BIOSCREEN have centerline reports. This report is particularly useful when calibrating contaminant concentrations to measured values.

Table 8. Model Reporting Capabilities

Parameter	**BIOSCREEN**	**AT123D**	**MODFLOW/MT3D**
Area	✓	✓	✓
Centerline	✓	✓	
Point of compliance		✓	*
* MT3D data is saved as a text file that can be imported in to Excel.			

Both AT123D and MT3D present results at a point of compliance. Called an observation point in MT3D, this report depicts predicted concentrations over time at a specific location, which meets the requirement for the development of risk-based evaluations. BIOSCREEN does not contain a point of compliance report and as such, it had to be run over and over until sufficient output data was produced to create a point of compliance report. It should be noted that this process made BIOSCREEN the slowest model by far.

2. RESULTS

Results show a strong agreement in the peak concentrations and travel times produced by AT123D and MODFLOW/MT3D for all hydraulic conductivities and contaminants tested. However BIOSCREEN results were at least one order of magnitude higher than the other models for hydraulic conductivities between 1.0E+1 cm/sec and 1.0E-3 cm/sec. Predicted concentrations for BIOSCREEN and the other models diverged further as hydraulic conductivities were reduced, reaching a maximum of three orders of magnitude at a hydraulic conductivity of 1.0E-6 cm/sec. It should be noted that BIOSCREEN produced the same peak downgradient concentration for both contaminants and for all hydraulic conductivities. Travel times to peak downgradient concentrations predicted by BIOSCREEN were significantly longer, reaching a maximum of 39,000 years for benzene with a hydraulic conductivity of 1.0E-6 cm/sec. However, based on AT123D and MODFLOW/MT3D predicted travel times were 310 and 572 years respectively.

Results were evaluated at a point located 10 meters (32 feet) downgradient from the source. The 10-meter distance was selected because some regulatory agencies have used this distance in the development of default cleanup objectives. Modeling results are presented not only as peak groundwater concentrations, but also as maximum allowable source concentrations. The resulting groundwater concentrations are shown in Tables 9 and 10 (as well as in Figures 3 and 4). Due to the significant difference between the BIOSCREEN results and the other models, concentrations are displayed as both linear and logarithmic plots. Travel times to the peak concentrations are presented in Tables 11 and 12.

In general, the AT123D model results match well with the MODFLOW/MT3D simulations. These models produced almost identical peak concentrations and at nearly the same time. Observed variations may be related to differences in the way in results are established. For example results in AT123D are calculated for a specific point, where as results in MODFLOW/MT3D are generated for an entire cell.

Peak concentrations produced by BIOSCREEN did not vary at all. In fact, BIOSCREEN produced the same peak downgradient concentration for all aquifer types and chemicals tested (Figures 3a to 4b). Additional modeling using benzo-a-pyrene confirmed that BIOSCREEN produces the same peak concentration regardless of the contaminant properties or aquifer type. Travel times varied significantly from the other models taking up to 39,000 years for benzene to reach a point 10 meters downgradient. Where as, AT123D and MODFLOW/MT3D predicted it would only take 310 and 572 years respectively.

According to BIOSCREEN it would take benzene 40 years to reach a point 10 meters downgradient with a hydraulic conductivity of 1.0E-3 cm/sec. However, the other two models indicate it would only take 10 years for benzene to reach this point. BIOSCREEN produced a travel time for benzene of 3,980 years at a hydraulic conductivity of 1.0E-5 cm/sec. While the other models indicated to would only take between 311 and 329 years to reach the peak concentration.

1.0E+1 (cm/sec)

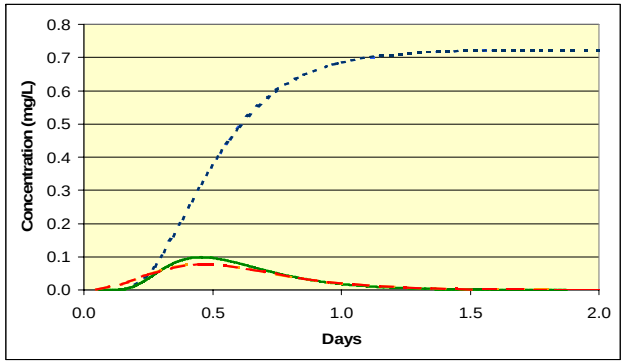

1.0E+0 (cm/sec)

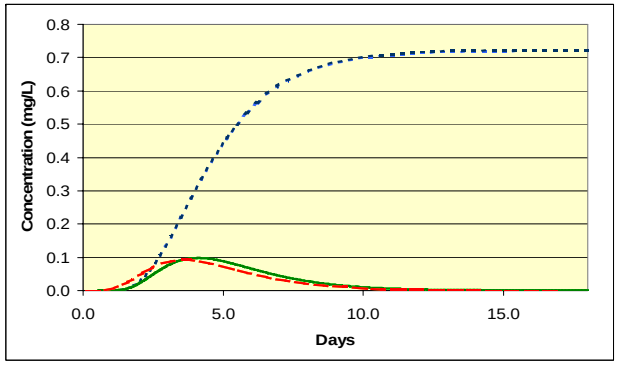

1.0E-1 (cm/sec)

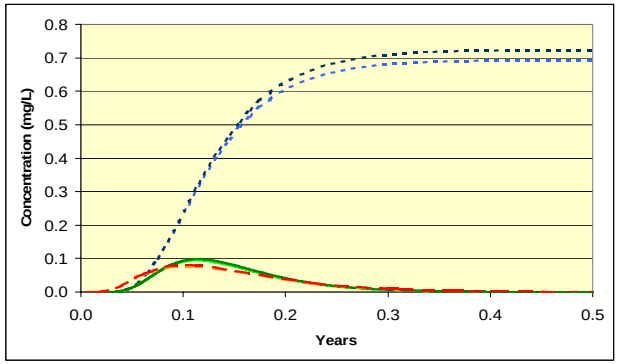

1.0E-3 (cm/sec)

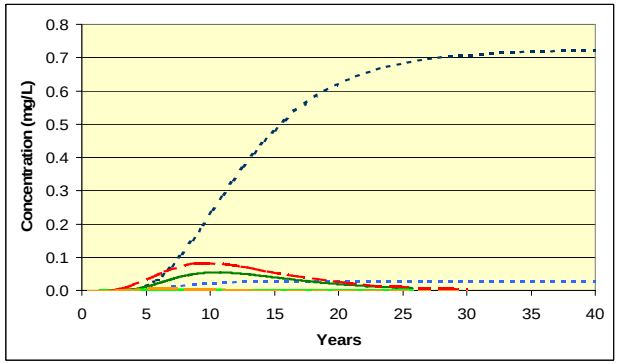

1.0E-5 (cm/sec)

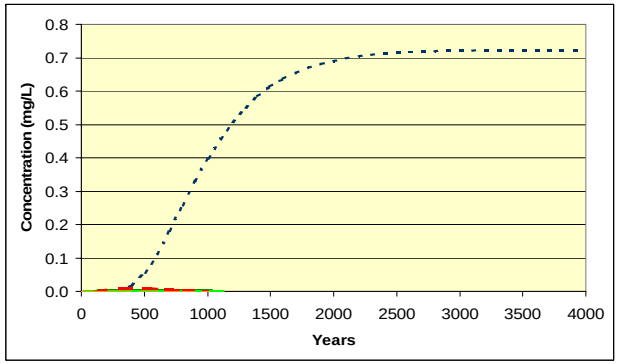

1.0E-6 (cm/sec)

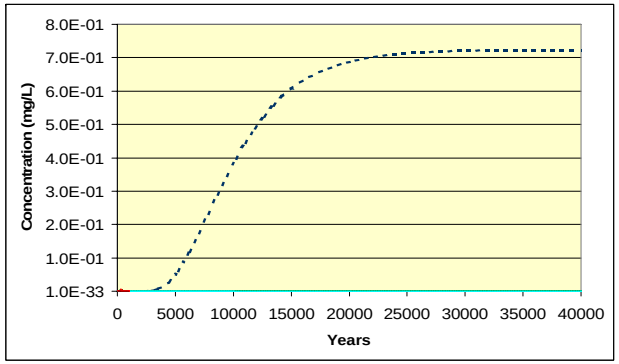

Linear plot of benzene results. BIOSCREEN produced the same peak concentration for all aquifer types. Predicted peak concentrations for the AT123D and MODFLOW/MT3D models were almost identical.

Table 9 Benzene Peak Concentrations						
Permeability	**BIOSCREEN**		**AT123D**		**MODFLOW/MT3D**	
	No Bio	**w/Bio**	**No Bio**	**w/Bio**	**No Bio**	**w/Bio**
cm/sec	mg/L	mg/L	mg/L	mg/L	mg/L	mg/L
1.0E+1	**0.724**	**0.724**	**0.0985**	**0.0985**	**0.0791**	**0.0791**
1.0E+0	**0.724**	**0.721**	**0.0982**	**0.0978**	**0.0934**	**0.0931**
1.0E-1	**0.724**	**0.694**	**0.0982**	**0.0943**	**0.0817**	**0.0788**
1.0E-3	**0.724**	**0.0277**	**0.0543**	**0.00293**	**0.0836**	**0.00581**
1.0E-5	**0.724**	**1.37E-23**	**0.00272**	**3.96E-11**	**0.0108**	**1.05E-12**
1.0E-6	**0.724**	**8.47E-78**	**0.00108**	**8.47E-15**	**0.00242**	**1.48E-15**

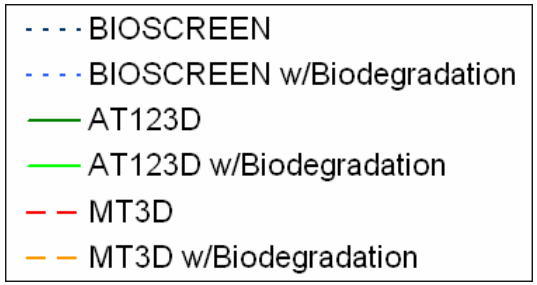

Figure 3a. Linear plots – Benzene Results for Varying Hydraulic Conductivities

1.0E+1 (cm/sec)

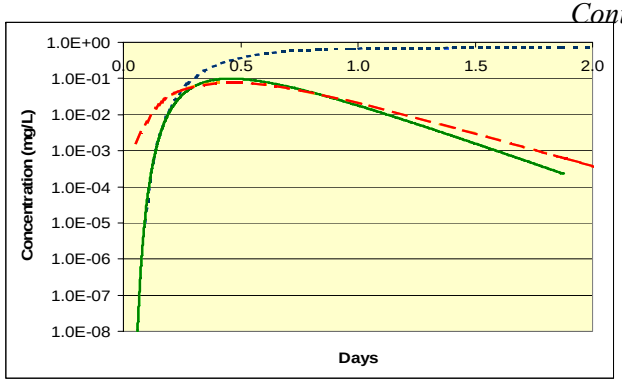

1.0E+0 (cm/sec)

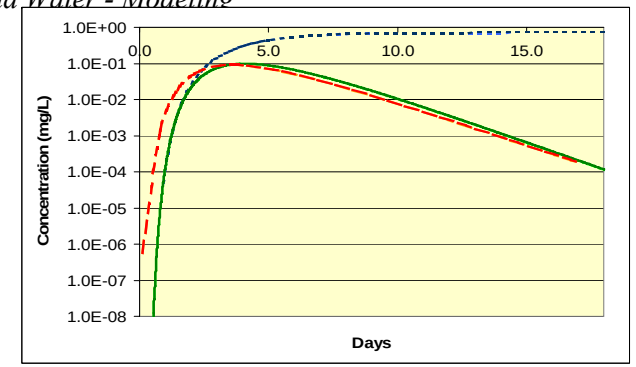

1.0E-1 (cm/sec)

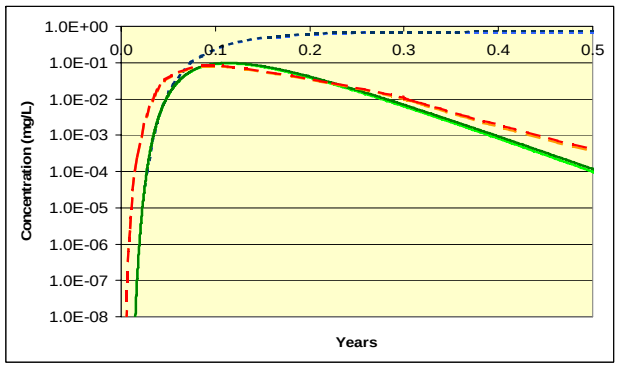

1.0E-3 (cm/sec)

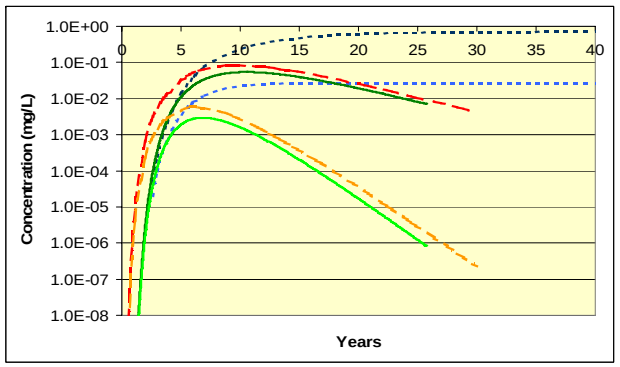

1.0E-5 (cm/sec)

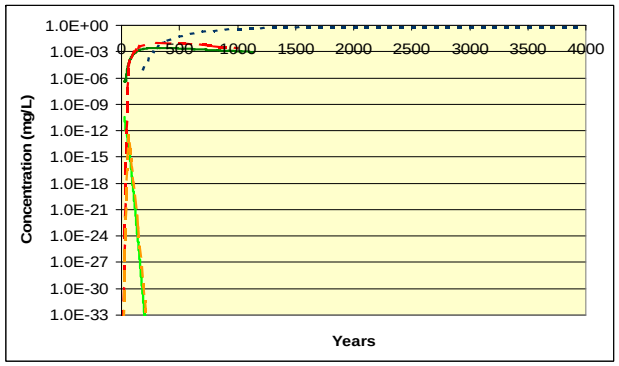

1.0E-6 (cm/sec)

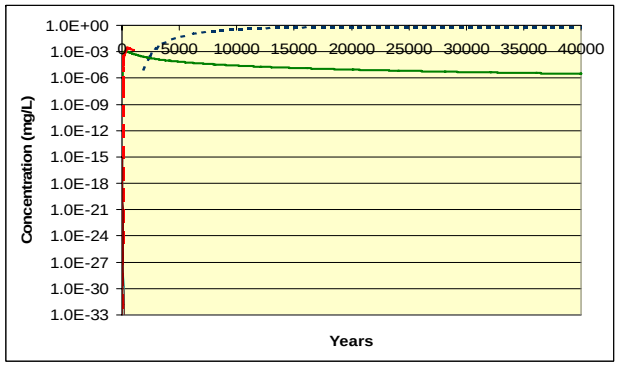

Logarithmic plot of benzene results. BIOSCREEN produced the same peak concentration for all aquifer types. Predicted peak concentrations for the AT123D and MODFLOW/MT3D models were almost identical.

Table 9 Benzene Peak Concentrations						
Permeability	**BIOSCREEN**		**AT123D**		**MODFLOW/MT3D**	
	No Bio	**w/Bio**	**No Bio**	**w/Bio**	**No Bio**	**w/Bio**
cm/sec	mg/L	mg/L	mg/L	mg/L	mg/L	mg/L
1.0E+1	**0.724**	**0.724**	**0.0985**	**0.0985**	**0.0791**	**0.0791**
1.0E+0	**0.724**	**0.721**	**0.0982**	**0.0978**	**0.0934**	**0.0931**
1.0E-1	**0.724**	**0.694**	**0.0982**	**0.0943**	**0.0817**	**0.0788**
1.0E-3	**0.724**	**0.0277**	**0.0543**	**0.00293**	**0.0836**	**0.00581**
1.0E-5	**0.724**	**1.37E-23**	**0.00272**	**3.96E-11**	**0.0108**	**1.05E-12**
1.0E-6	**0.724**	**8.47E-78**	**0.00108**	**8.47E-15**	**0.00242**	**1.48E-15**

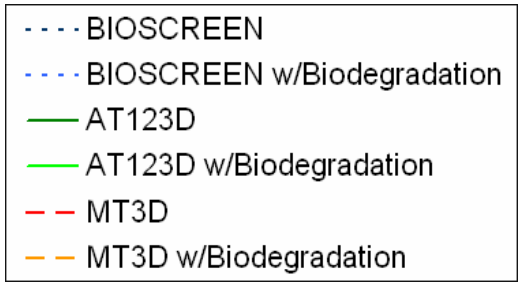

Figure 3b. Logarithmic Plots – Benzene Results for Varying Hydraulic Conductivities

1.0E+1 (cm/sec)

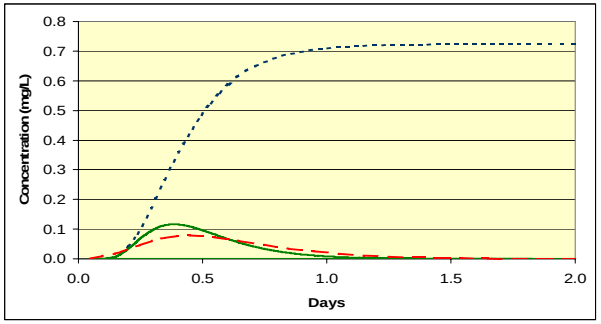

1.0E+0 (cm/sec)

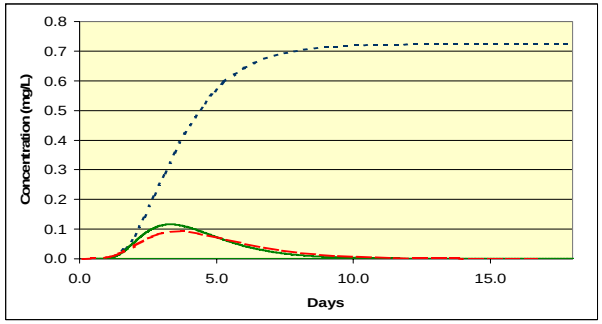

1.0E-1 (cm/sec)

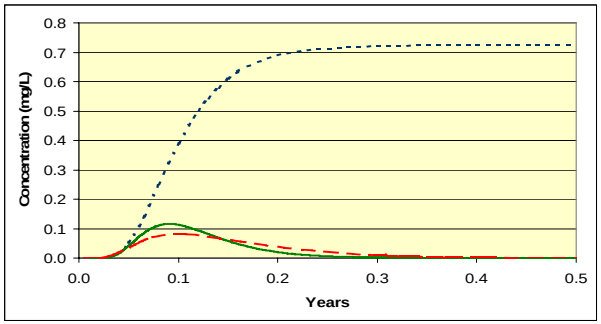

1.0E-3 (cm/sec)

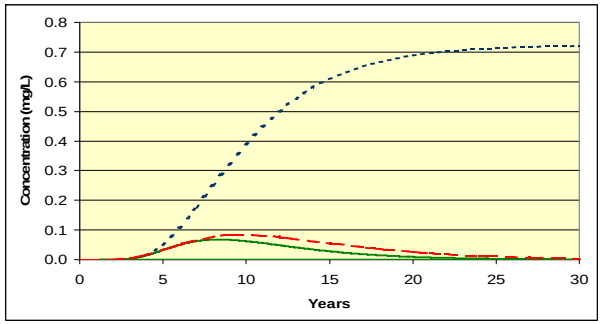

1.0E-5 (cm/sec)

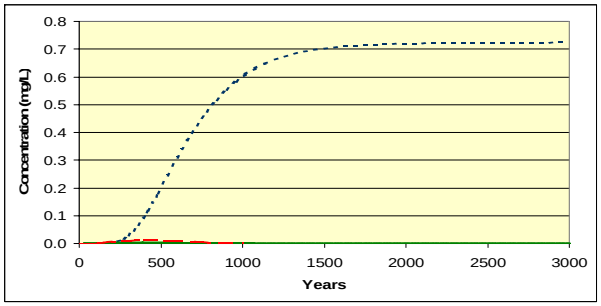

1.0E-6 (cm/sec)

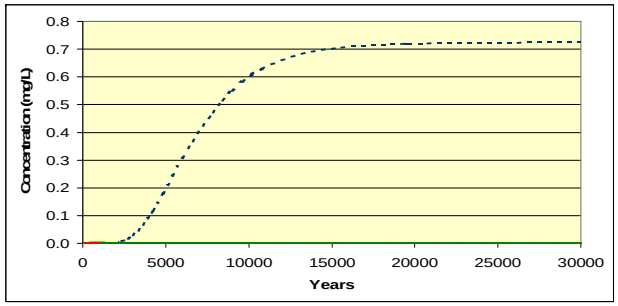

Linear plot of MTBE results. BIOSCREEN produced the same peak concentration for all aquifer types. Predicted peak concentrations for the AT123D and MODFLOW/MT3D models were almost identical.

Table 10 MTBE Peak Concentrations			
Permeability	**BIOSCREEN**	**AT123D**	**MODFLOW/MT3D**
cm/sec	mg/L	mg/L	mg/L
1.0E+1	**0.724**	**0.116**	**0.0791**
1.0E+0	**0.724**	**0.116**	**0.0934**
1.0E-1	**0.724**	**0.116**	**0.0817**
1.0E-3	**0.724**	**0.0676**	**0.0847**
1.0E-5	**0.724**	**0.00415**	**0.0120**
1.0E-6	**0.724**	**0.00136**	**0.00251**

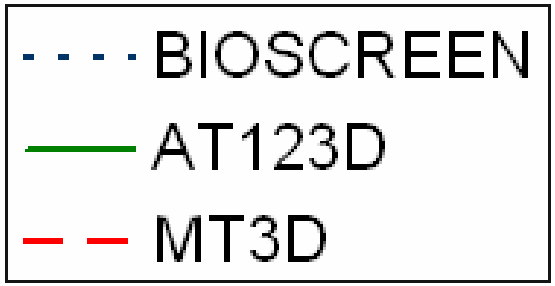

Figure 4a. Linear plots – MTBE Results for Varying Hydraulic Conductivities

1.0E+1 (cm/sec)

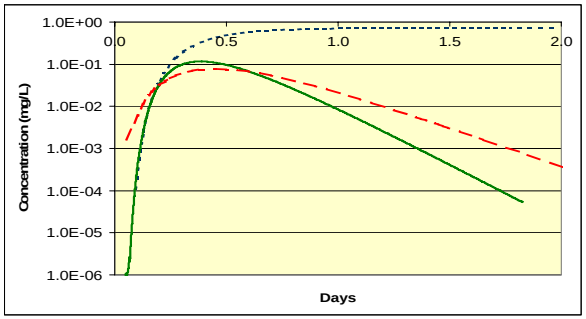

1.0E+0 (cm/sec)

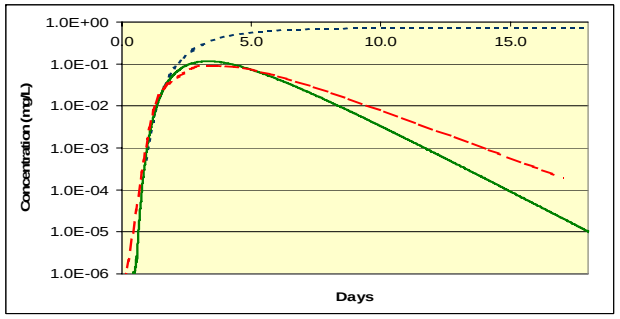

1.0E-1 (cm/sec)

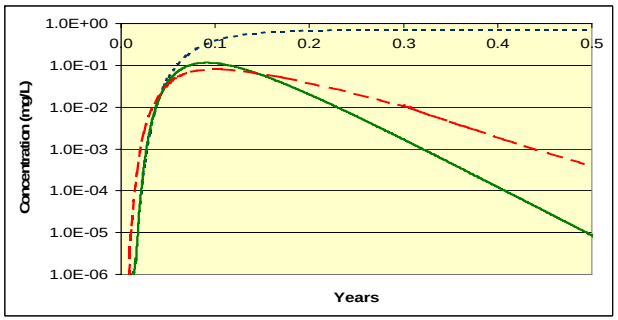

1.0E-3 (cm/sec)

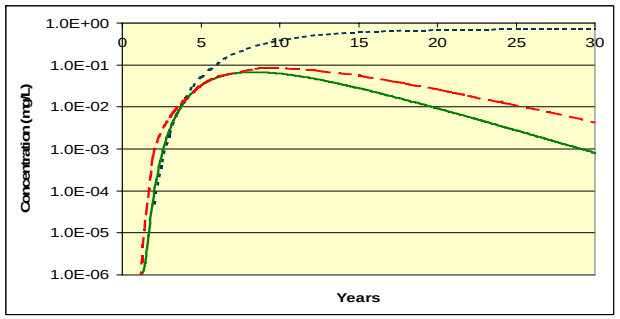

1.0E-5 (cm/sec)

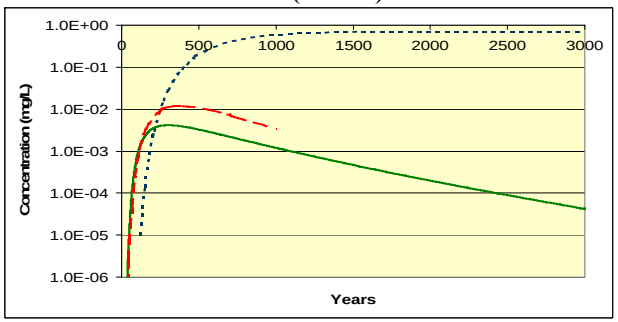

1.0E-6 (cm/sec)

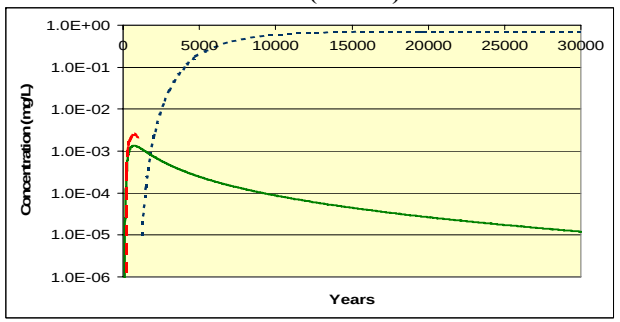

Logarithmic plot of MTBE results. BIOSCREEN produced the same peak concentration for all aquifer types. Predicted peak concentrations for the AT123D and MODFLOW/MT3D models were almost identical.

Table 10 MTBE Peak Concentrations			
Permeability	**BIOSCREEN**	**AT123D**	**MODFLOW/MT3D**
cm/sec	mg/L	mg/L	mg/L
1.0E+1	**0.724**	**0.116**	**0.0791**
1.0E+0	**0.724**	**0.116**	**0.0934**
1.0E-1	**0.724**	**0.116**	**0.0817**
1.0E-3	**0.724**	**0.676**	**0.0847**
1.0E-5	**0.724**	**0.00415**	**0.0120**
1.0E-6	**0.724**	**0.00136**	**0.00251**

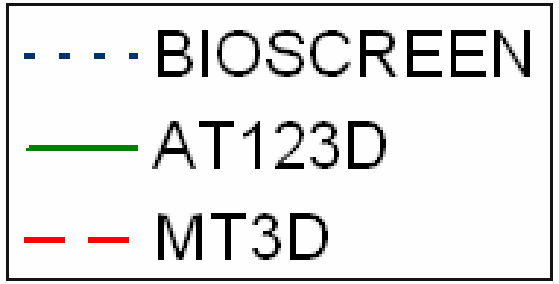

Figure 4b. Logarithmic Plots – MTBE Results for Varying Hydraulic Conductivities

Table 11. Time to Peak Benzene Concentrations

Permeability cm/sec	units	**BIOSCREEN**		**AT123D**		**MODFLOW/MT3D**	
		No Bio	**w/Bio**	**No Bio**	**w/Bio**	**No Bio**	**w/Bio**
1.0E+1	days	**1.82**	**1.82**	**0.45**	**0.45**	**0.45**	**0.45**
1.0E+0	days	**17.3**	**17.3**	**4.05**	**4.05**	**3.57**	**3.57**
1.0E-1	years	**0.48**	**0.47**	**0.11**	**0.11**	**0.11**	**0.11**
1.0E-3	years	**40**	**23.4**	**10.5**	**6.70**	**9.67**	**6.22**
1.0E-5	years	**3980**	**105**	**311**	**26.3**	**329**	**31.5**
1.0E-6	years	**39000**	**600**	**310**	**50.0**	**572**	**35.9**

Table 12. Time to Peak MTBE Concentrations

Aquifer Type cm/sec	units	**BIOSCREEN**	**AT123D**	**MODFLOW/MT3D**
1.0E+1	days	**1.82**	**0.36**	**0.45**
1.0E+0	days	**15.7**	**3.15**	**3.57**
1.0E-1	years	**0.43**	**0.089**	**0.107**
1.0E-3	years	**43.0**	**8.25**	**9.67**
1.0E-5	years	**2940**	**289**	**359**
1.0E-6	years	**29300**	**680**	**630**

Biodegradation had almost no impact on results for hydrologic conductivities from 1.0E+1 cm/sec to 1.0E-1 cm/sec in any of the models. This is not surprising as it took less than half a year to reach the peak concentration in these aquifers. Such short time frames do not provide enough time for any significant amount of biodegradation. However, at hydraulic conductivities of 1.0E-3 cm/sec and below, biodegradation significantly reduced the resulting peak downgradient concentrations. This is expected as the longer travel times associated with lower permeabilities would give biodegradation a longer period of time over which to work. Given that BIOSCREEN produced the longest travel times, it produced the highest amounts of biodegradation.

2.1 Maximum Allowable Concentrations

The maximum allowable contaminant concentration in the source area is another key point in comparing the results of the three models. Regulations typically require that the predicted groundwater concentrations do not exceed the Maximum Contaminant Level (MCL) at the point of compliance. As demonstrated in (Tables 13 and 14), AT123D and MODFLOW/MT3D allow at least one order of magnitude more benzene and MTBE to remain in place in the source, as did BIOSCREEN for aquifers with hydraulic conductivities of between 1.0E+1 cm/sec and 1.0E-1 cm/sec. As hydraulic conductivities were lowered to 1.0E-6 cm/sec, AT123D and MODFLOW/MT3D allowed up to three orders of magnitude more contamination to remain in the source than BIOSCREEN did.

Table 13. Maximum Allowable Benzene Source Concentrations

Permeability	MCL	BIOSCREEN		AT123D		MODFLOW/MT3D	
		No Bio	w/Bio	No Bio	w/Bio	No Bio	w/Bio
cm/sec	Mg/L	mg/L	mg/L	mg/L	mg/L	mg/L	mg/L
1.0E+1	**0.005**	**0.00691**	**0.00691**	**0.0508**	**0.0508**	**0.0632**	**0.0632**
1.0E+0	**0.005**	**0.00691**	**0.00693**	**0.0509**	**0.0511**	**0.0535**	**0.0537**
1.0E-1	**0.005**	**0.00691**	**0.00720**	**0.0509**	**0.0530**	**0.0612**	**0.0634**
1.0E-3	**0.005**	**0.00691**	**0.180**	**0.0921**	**1.71**	**0.0598**	**0.860**
1.0E-5	**0.005**	**0.00691**	**3.65E+20**	**1.84**	**1.26E+08**	**0.463**	**4.76E+09**
1.0E-6	**0.005**	**0.00691**	**5.90E+74**	**4.63**	**5.90E+11**	**2.07**	**3.38E+12**

Table 14. Maximum Allowable MTBE Source Concentrations

Permeability	MCL	BIOSCREEN	AT123D	MODFLOW/MT3D
cm/sec	mg/L	mg/L	mg/L	mg/L
1.0E+1	**0.040**	**0.0552**	**0.345**	**0.506**
1.0E+0	**0.040**	**0.0552**	**0.345**	**0.428**
1.0E-1	**0.040**	**0.0552**	**0.345**	**0.490**
1.0E-3	**0.040**	**0.0552**	**0.592**	**0.472**
1.0E-5	**0.040**	**0.0552**	**9.64**	**3.33**
1.0E-6	**0.040**	**0.0552**	**29.4**	**15.9**

Inclusion of biodegradation for benzene had no effect on the maximum allowable source concentration for hydraulic conductivities between 1.0E+1 cm/sec and 1.0E-1 cm/sec in any of the models. This is because the travel times were too short to for biodegradation to produce any effect. However, the influence of biodegradation increased significantly as hydraulic conductivity was lowered. This is due to lengthy travel times associated with the lower hydraulic conductivities. As BIOSCREEN produces the longest travel times it became the least conservative model when biodegradation was included.

2.2 Influence Of Model Capabilities

Discrepancies observed between BIOSCREEN and the other models are not a result of the input parameters. In fact, AT123D and BIOSCREEN use almost identical parameters. Instead the differences are a result of the original model design specifications. BIOSCREEN was designed for ease of use and computational speed. This goal was achieved by limiting contaminant load options, as well as the transport and fate processes. Computation speed was deemed an important design criterion due to limited computer capabilities at that time. Other models, such as AT123D and MODFLOW/MT3D, were initially designed with increased model capabilities, such as additional load options and additional transport and fate processes. Inclusion of these processes in AT123D and MODFLOW/MT3D means that they can be

confidently used over a wider range of aquifer types and release scenarios, which in turn, improves confidence in the results. Only recently have computer capabilities improved to the point where run times are no longer an issue for AT123D. Although there has been a significant improvement in performance, model run times still restrict use of the MODFLOW and MT3D models. BIOSCREEN was clearly the fastest model. As far as reporting capabilities both AT123D and MT3D have point of compliance reporting capabilities, making it much faster and easier to evaluate the results.

3. DISCUSSION

With its infinite source concentration, BIOSCREEN produced the most conservative results, if run until the peak concentration is observed. However, even with the infinite source, inclusion of conservative biodegradation rates caused BIOSCREEN to produce the least conservative results. This is because BIOSCREEN does not simulate diffusion, which can become a significant process as gradients and hydraulic conductivities are lowered. Under such conditions BIOSCREEN significantly underestimates contaminant mobility, thus increasing travel times and the amount of biodegradation. Perhaps the most interesting observation is that BIOSCREEN produced the same peak downgradient concentrations for all aquifer types and different chemicals tested. This appears to be intuitively wrong and calls the results in question the basic model assumptions.

There was a strong correlation between the AT123D and MODFLOW/MT3D results. As aquifer and chemical properties changed so did the results. These results are consistent with real world observations.

Ease of use has always been a concern in the process of model selection. Of the three models tested, BIOSCREEN was slightly easier than AT123D to set up and run, while MODFLOW/MT3D is the most challenging. It has often been assumed that more accurate modeling would require additional site characterization to obtain the required input parameters. However, even though AT123D and BIOSCREEN use almost identical input parameters they produce very different results. Our study indicates that improved accuracy is also dependent upon which model is used. That AT123D and MODFLOW produce similar results improves confidence in the reliability of both models.

4. CONCLUSIONS

BIOSCREEN results are not consistent with the other models. When compared to AT123D and MODFLOW/MT3D it significantly under estimates contaminant mobility and over estimates downgradient concentrations. Lengthy travel times produce by BIOSCREEN produce a false sense of security that underestimates exposure risks. Furthermore, given the lengthy travel times, inclusion of even conservative biodegradation rates significantly reduces downgradient concentrations, thus, making BIOSCREEN the least conservative model. Exposure risk is often considered inconsequential at sites where modeling predicts it will take more than 100 years to

reach a downgradient point of compliance. Based on our results BIOSCREEN may not be an appropriate model to evaluate such risks.

Risk-based evaluations are established using the peak concentrations and the travel times to reach those peak concentrations. Peak concentrations are used to establish risk-based cleanup levels protective of groundwater quality at the point of compliance. It is typically assumed that risks to groundwater quality decrease as contaminant travel times increase. Therefore, BIOSCREEN, which underestimates contaminant mobility, may not provide an adequate assessment of downgradient risks. Given the lengthy travel times produced by BIOSCREEN, it should always be run until the peak concentration is observed. Even conservative biodegradation rates should be used with caution in BIOSCREEN, as the lengthy travel times produce significantly higher amounts of biodegradation. On the other hand, cleanup objectives based on peak concentrations from BIOSCREEN in which biodegradation is not used are extremely conservative and may result in costly remedial actions, which may not be justified.

Discrepancies are not a result of the model input parameters as AT123D and BIOSCREEN use almost identical parameters. Rather they are a result of inherent limitation associated with BIOSCREEN model and the Domenico equation. Given today's powerful computers, it is difficult to justify the use of BIOSCREEN, especially when AT123D can be safely used over a wider range of aquifer conditions. AT123D produces MODFLOW/MT3D results, yet it takes much less time to use. MODFLOW/MT3D modeling could be performed as an alternative to AT123D modeling. Taking in consideration the costs and complexities associated with numerical modeling may also be advisable to use AT123D to verify the MODFLOW/MT3D results.

5. ACKNOWLEDGEMENTS

We would like to thank James Rumbaugh of Environmental Simulations, Inc. for the use of the Groundwater Vistas software. His assistance was invaluable in the preparation of this paper.

6. REFERENCES

Bureau of Underground Storage Tank Regulations. 2003. Using the BIOSCREEN Fate & Transport Model for BUSTR Corrective Action Sites. Ohio Department of Commerce.

Domenico, P.A. 1987. An Analytical Model for Multidimensional Transport of a Decaying Contaminant Species. Journal of Hydrology. 91, 49-58.

Newell, C.J., McLeod R.K. and J.R. Gonzales, 1996. BIOSCREEN Natural Attenuation Decision Support System, Users Manual Version 1.3. National Risk Management Research Laboratory, Office of Research and Development, USEPA.

Rumbaugh J.O. and D. Rumbaugh, 2005. Groundwater Vistas. User's Guide, Version 4, Environmental Simulations, Inc.

Schneiker, R.A. 2005. SEVIEW Integrated Contaminant Transport and Fate Modeling System, User's Guide, Version 6.3, Environmental Software Consultants, Inc.

Yeh, G.T. 1981. AT123D: Analytical Transient One-, Two-, and Three-Dimensional Simulation of Waste Transport in the Aquifer System. ORNL-5602, Oak Ridge National Laboratory.

Part X: Regulatory

Chapter 22

URBAN POLYCYCLIC AROMATIC HYDROCARBONS (PAHS): A FLORIDA PERSPECTIVE

Christopher M. Teaf[1,2§], Douglas J. Covert[1], Srikant R. Kothur[1]
[1]Hazardous Substance & Waste Management Research, Inc., 2976 Wellington Circle West, Tallahassee, FL 32309; [2]Center for Biomedical & Toxicological Research, Florida State University, 2035 E. Dirac Dr., Tallahassee, FL 32310

ABSTRACT

Over the past decade, polycyclic aromatic hydrocarbons (PAHs) have steadily climbed in importance on the CERCLA list of hazardous substances. Though the listing does not necessarily imply that these chemicals exhibit the greatest degree of toxicity, such recognition by ATSDR and USEPA is predicated at least in part on their overwhelming ubiquity in association with many very common sources, coupled with toxicity considerations. Regulatory agencies increasingly are under pressure to define and interpret data describing urban background levels, and to appropriately determine the relative importance of waste-producing activities and concentrations resulting from typical natural and/or human activity. Three case studies from Florida are presented that confirm the ubiquity of the PAHs at low levels, and that demonstrate the need for more sophisticated and transparent treatment by regulatory agencies. We discuss assessment and risk assessment activities related to two urban redevelopment projects, as well as one property transaction project. In each case, considerable sampling of surficial soils and sediment identified total benzo(a)pyrene-equivalent concentrations in the range of less than one ppm to about 5 ppm. Although those concentrations frequently exceeded the default Florida cleanup target level for both residential and commercial/industrial land use by a wide margin, it was concluded that they are completely consistent with levels reported in a great many urban settings. There is an ongoing need to consider the development of a default urban background level for PAHs in areas characterized by busy roadways or multiple industrial facilities, in much the same way that geological or anthropogenic background levels are established for some inorganics.

Keywords: Polycyclic aromatic hydrocarbons, soil, sediments, water, background, health risk assessment, urban, toxicology, PAH

§ Corresponding Author: Christopher M. Teaf, Center for Biomedical & Toxicological Research, Florida State University, 2035 East Dirac Dr., Tallahassee, FL, 32310, Tel: 850-681-6894, 850-644-3453, Email: cteaf@res.fsu.edu, cteaf@mailer.fsu.edu

1. INTRODUCTION

Over the past decade, polycyclic aromatic hydrocarbons (PAHs) have climbed towards the top of the Comprehensive Environmental Response, Compensation, and Liability Act (CERCLA) list of hazardous substances (ATSDR, 2006). In the biennial ranking comprised of chemicals deemed to pose the greatest possible risk to human health, PAHs placed a meager tenth before moving to fifth in 2001 and settling in at seventh in 2005. Both the Agency for Toxic Substances and Disease Registry (ATSDR) and US Environmental Protection Agency (EPA) recognize the potential importance of PAHs due to their ubiquity in many urban and rural environments. Acknowledgment of their burgeoning presence means regulatory agencies must define and interpret urban background levels to appropriately determine whether industrial facilities or contaminated sites are damaging the environment beyond concentrations resulting from typical natural and human activity.

PAHs are a collection of over 100 different fused benzene ring chemical compounds with varying prevalence and regulatory concern. Background is defined as concentrations in a common area, such as a road, residential yard or non-industrialized locale, due to sources independent of a known waste site (IEPA, 2005b). The multitude of non-point, diffuse, and mobile sources of PAHs ranges from automobile exhaust to road asphalt to cigarette smoke (NPI, 2004). In tandem, they create an urban background concentration that often exceeds health based regulatory recommendations for generally accepted PAH-producers (Delgado, 2000). This paradox undermines environmentalists' desires to contain carcinogenic PAHs, the true threat to public safety. Heightened awareness of this potentially costly inconsistency has increased the vigor of efforts to determine local background levels before targeting sites for remediation. Local and state agencies like the Illinois EPA have begun to more actively rely on background as a means to establish risk-based objectives to determine realistic goals (IEPA, 2005).

In Florida, the Department of Environmental Protection (FDEP) is increasingly aware of and potentially receptive to site-specific demonstrations of urban background, rather than site-related activities, being the cause of observed PAH impacts. However, at this point, procedural constraints, political climate, or financial considerations dictate a strict adherence to the much lower default cleanup guidelines.

1.1 Human Health Effects

The potential carcinogenicity of seven common PAH list compounds [benzo(a)anthracene (B(a)A), benzo(a)pyrene (B(a)P), benzo(b)fluoranthene (B(b)F), benzo(k)fluoranthene (B(b)F), chrysene, dibenz(a,h)anthracene, indeno(1,2,3-c,d)pyrene] warrant reasonable regulation and remediation. Due to their ubiquity, PAH exposure occurs constantly whether an individual breathes roadside air, comes into contact with a hazardous waste site, eats grilled food, or drinks contaminated water (NPI, 2004). In the US, lifestyle considerations represent the greatest exposure potential to carcinogenic PAHs for an individual, with general population estimates indicating daily intake averages of 0.207 ug from air, 0.027 ug via water, and 0.16-1.6 ug through food (ATSDR, 1995). Inhalation of tobacco and wood smoke, and residence near a hazardous waste site may increase the 2 to 3 ug/day of total carcinogenic PAHs an adult male encounters (ATSDR, 1995). Significant time spent in metropolitan areas boosts risk since

several studies indicate PAHs in urban ambient air exceed rural air by ten times (ILDPH, 2005). Once PAHs have entered the body, the kidneys, liver, fat, spleen, adrenal glands and ovaries can store them until they are released in urine and feces within a few days (ATSDR, 1995; Grosenheider et al. 2005). Short-term effects have yet to be determined since other chemicals that commonly co-occur with PAHs (e.g., volatile hydrocarbons) often cause immediate symptoms such as eye irritation, nausea, diarrhea, and confusion (ILDPH, 2005). Detrimental long-term, high-level exposure may lead to consequences including cataracts, kidney and liver damage, jaundice, and skin irritation and redness, specifically for naphthalene contact. The immune system also is vulnerable and B(a)P in large doses suppresses the system and damages erythrocytes. Moreover, sufficient doses may cause developmental and reproductive deficiencies in animal studies (BCERF, 2001).

The above effects, though more likely, seem inconsequential in most literature because of the overwhelming focus on cancer from long-term exposure. Laboratory research on female rats indicates breast tissue injection and consistent high dose ingestion of B(a)P and dibenzo(a,l)pyrene caused a significant increase in the development of breast cancer (BCERF, 2001). However these results have not been proven with any consistency in human studies. One of the pioneering PAH cancer studies began in the early 1980's after Long Island, New York appeared to have a 30% higher breast cancer rate than the national average (NBCC, 2002). The first of the 12 studies forming the Long Island Breast Cancer Study Project considered PAHs since these compounds bind to DNA and form DNA adducts, the sites of tissue damage. Detectable adducts increased the chance of breast cancer by 35%, a statistically significant figure; however, a threshold effect was observed in the observed endpoints.

1.2 Sources of PAHs in Urban Environments

1.2.1 Natural Sources

Petroleum and coal formations contain PAHs, and forest fires, volcanic eruptions, and plant and animal pigments (Delgado, 2000) also release PAHs. Volcanoes and forest fires are by far the most common means by which natural producers release PAHs into a given environment (ATSDR, 1995). Coal tar, crude oil, and shale oil are all important repositories of PAHs, and human conversion and incomplete combustion of fuels increases their abundance in the contemporary environment (NPI, 2004). Products, including creosote and asphalt, derived from these fossil fuels also contribute (ILDPH, 2005).

1.2.2 Anthropogenic Sources

Although readily identifiable point sources garner the wealth of federal and government attention and budget, diffuse and mobile sources strongly influence total PAH concentrations in a given medium (NPI, 2004). Non-point sources are unavoidable with virtually every citizen culpable. Common daily anthropogenic contributions include cigarette smoke, internal combustion engines, oil-based heating, indoor and outdoor grilling, jet engines, acetylene torches, and road paving (Delgado, 2000).

PAH concentrations, especially indoors, can rise significantly as a result of smoking. One study conducted in Durham, North Carolina observed that smoking increased indoor levels to alarming heights in smoking households, ranging from 0.08 to 3,600 ng/m^3, while outdoor levels in Durham were between 0.03 and 1,700 ng/m^3 (USEPA, 1997). Fire production resulting from agricultural, home heating and cooking purposes also causes widespread PAH emissions. These are difficult to control since nearly every urban edifice contributes (NPI, 2004). In fact, the largest anthropogenic source is reportedly residential wood combustion (Grosenheider et al., 2005). Motor vehicle exhaust, the main mobile source, supplements PAHs' expanding presence alongside several vital consumer products. However, US mobile sources such as vehicular emissions contribute only a small quantity, estimated to be 25% in the 1980's, of total PAH emissions (Li, 2003).

Regardless of the source type, PAHs behave similarly in the environment. Once discharged, most enter the air before atmospheric deposition deposits them in other notable mediums. Surface water receives its share primarily from airborne deposition, but other major contributors include urban runoff, effluents from industrial plants, petroleum processing, and occasionally oil spills. Urban runoff, a common non-point source of residential communities, accounted for an estimated 36% of the total PAH input into Rhode Island's Narragansett Bay, as well as an atypical 71% of all high molecular weight toxins found (McCarthy, 2003; LBNL, 2004). Heavy hydrocarbons in water environments tend not to venture far from their anthropogenic source, and thus, aquatic areas near extensive human activity have a propensity to be excessively taxed (ATSDR, 1995).

Soil is the most complex in regard to principal source determination (Delgado, 2000; Hellmann, 1999). Local and long-range transport follows initial atmospheric entrance; therefore, areas seemingly unfettered by direct industrial activity could harbor significant baseline PAH concentrations. Soils adjacent to roadways and parking lots tend to have higher concentrations than rural soil due to auto and asphalt emissions and associated stormwater runoff (Mahler et al., 2005; Wagrowski and Hites, 1997). Additional contributors include public sewage treatment plants, bituminous coal leachate from storage sites, and compost-based fertilizers (ATSDR, 1995). Furthermore, higher organic carbon content and sorbent particle surface area have been associated with increased absorption and accumulation in sediments. For example, Karckhoff (1979) and Gardner (1979) established that silt and clay are twice as likely to amass B(a)P and B(a)A than a sand composition (ATSDR, 1995).

1.3 Reported Ambient Levels of PAHs

Establishing a universal baseline has occupied numerous researchers over the course of the past three decades. Intra-town levels can vary two or three-fold depending on different prevailing sources (traffic vs. domestic coal burning), heating fuels (coal vs. oil), and position relative to an industrial zone (downwind vs. upwind; EU, 2001). Urban and industrial land-use adjacent to river systems is just one example of the complications associated with source attribution and risk assessment (Costa and Gensky, 2001). Another hurdle in standardizing literature relates to whether individual or total PAHs are measured and reported. Furthermore, some researchers utilize BaPeq to create values based on carcinogenic potency in relation to B(a)P, the most often measured and regulated PAH (Grosenheider et al., 2005).

1.3.1 Air

In the ATSDR's 1995 toxicological profile for polycyclic aromatic hydrocarbons, ambient air's unique role as a feeder to soil and water is identified and background ranges are provided. Rural ambient air for some individual PAHs ranged between 0.02-1.2 ng/m^3, and urban background fluctuated between 0.15-19.3 ng/m^3 (ATSDR, 1995). The extent of this urban-rural discrepancy is once again noted in a New Jersey project from 1981 and 1982. This study showed a 3-5 times higher concentration for urban air and also discovered a 5-10 times higher concentration in winter as opposed to summer. Another early 1980's project found that B(a)P had an urban baseline of 0.64 ng/m^3 in Los Angeles. B(g,h,i)PER, a byproduct of automobile emissions on LA's notorious freeways, had a mean geometric concentration of 3.27 ng/m^3. Legzdins et al., and Tan and Ku independently determined in 1994 that B(g,h,i)PER was the highest individual PAH concentration among hydrocarbons measured in Hamilton, Ontario and New York City. The specific values, 4.3 ng/m^3 in Hamilton and 4.05 ng/m^3 in New York City, furthered the notion that urban ambient air levels follow a general pattern when free of point source contributions.

Other research efforts have had more specific goals that were reached by focusing on select media. Addressing urban air pollution is a frequently attempted task that requires PAH background information. A worldwide study of 60 towns in the mid-1970's determined the range of B(a)P in European and US ambient air. For Europe, a range of 1-20 ng/m^3 was reported and the US appeared to contain approximately 1 ng/m^3 (Menichini, 1992). However, Europe in the 1990's exhibited significantly improved the value ranges for B(a)P (EU, 2001). Rural background varied between 0.1 and 1 ng/m^3, and urban baselines ranged from 0.5 to 3 ng/m^3. The EU reported 30 ng/m^3 as the commonly accepted background in zones close to industrial processes.

1.3.2 Soil

PAH compounds found in soil have been an increasing problem since the Industrial Revolution's promotion of PAH-producing anthropogenic behavior. A compilation of data by the ATSDR confirms the expected: urban background concentrations are greatest, followed by agricultural and rural soil (ATSDR, 1995). Thomas' 1986 survey indicated that even remote Wyoming woods contained 210 ug/kg of total PAHs; whilst, Black et al. (1989) later in the 1980's provided a counterpoint by measuring New York City's Fountain Avenue Landfill, which contained concentrations between 400 and 10,000 ug/kg.

Several of the studies conducted allow a general understanding of urban baseline levels through analysis of samples from several locations throughout an urban domain. The lowest observed levels were in rural soil located far from major highways (Lagoy and Quirk, 1994). According to the IARC, these concentrations were between 0.01-10 mg/kg for all PAHs, while urban background ranged from 1-100 mg/kg. Among the more volatile carcinogenic PAHs, Menzie et al. (1992) noted a variation of 0.01 to 1.3 mg/kg in forest and rural soil. Based on the 15 samples used in this determination, urban soils ranged from 0.06 to 5.8 mg/kg with a median of 1.1 mg/kg.

A mid-90's analysis in New England focused on the relationship between proximity to pavement and toxicity in conjunction with background range determinations (Bradley, 1994). The study found state regulatory standards difficult to reconcile, with background levels of urban surface soils dwarfing the cleanup levels for the weighted total concentration of carcinogenic PAHs [B(a)P-T], which commonly ranges from 0.1 to 0.66 mg/kg. As suggested by the EPA, a 95% confidence interval was utilized to serve as the baseline value. The values were 12.4 mg/kg for total carcinogenic PAH value, and 3.3 mg/kg for B(a)P-TE. The B(a)P-TE at urban background was 30 times greater than the 0.1 mg/kg target level advocated by the CERCLA risk assessment guidance of 1993. Statistical analysis of pavement proximity involved tests for homogeneity of variance and equality of means. The mean for near pavement was 21.9 ppm total PAHs and 2.9 ppm B(a)P-TE, while samples away from pavement had means of 8.3 ppm total PAHs and 1.1 ppm B(a)P-TE. These tests proved there is statistical significance at the 0.05 level on all accounts, but emphasized that ppm levels of PAHs were ubiquitous.

The Massachusetts DEP in 1995 attempted to interpret background concentrations in "natural soil," a term used to denote the 90th percentile value (MADEP, 2002). Lower than 90th percentile values were commonly applied when site-specific background information was absent. A general stipulation when establishing literature background is consideration for the nature of the soil and past uses, but the MADEP's 1996 background levels identified still serve as a solid foundation. Notable "natural" concentrations identified were B(a)P at 3 mg/kg, B(g,h,i)PER at 1 mg/kg, and chrysene at 2 mg/kg (MADEP, 2002).

Subsequently in 2005, the Illinois EPA, as part of their risk-based tiered remediation, established their own carcinogenic PAH background in soil (IEPA, 2005b). Their study separated locales based on population. Areas with over 50,000 residents were branded "Metropolitan Statistical Areas (MSA)," the equivalent of an urban area. Since they deemed the data lognormally distributed, a lognormal 95th percentile concentration, shown on Table 1, represented their conclusions regarding background.

Table 1. Background concentrations of carcinogenic PAHs in IL (mg/kg)

Individual PAH	Chicago	MSA	Non-MSA
B(a)A	1.1	1.8	0.72
B(b)F	1.5	2.0	0.70
B(k)F	1.0	1.7	0.63
B(a)P	1.3	2.1	0.98
Chrysene	1.1	2.7	1.1
Dibenzo(a,h)A	0.20	0.42	0.15
Indeno(1,2,3-c,d)P	0.86	1.6	0.51

*Derived from IEPA, 2005b

1.3.3 Watershed/Sediment

Emissions from a host of mechanisms including stormwater runoff, direct deposition, surface runoff from roadways, and discharges from boats contribute heavily to aquatic sediment contamination (US Navy, 2003; Abrajano and Bopp, 2001). A US Navy review of properties along the Elizabeth River in Virginia examined 20 sediments, and concluded that urban

background was 16 mg/kg for a 16-PAH list of priority pollutants and 26 mg/kg for all detectable PAHs. With those statistics in hand, the researchers proposed that 30 mg/kg of priority pollutants should be the cutoff above which urban background alone cannot account for the PAH concentration. Conversely, Stout et al (2004) reported on surficial sediments and reiterated the lack of one representative urban baseline value. Regardless, there was general consistency, with 96% of the 280 sampled sediments containing below 20 mg/kg of the16-PAH list of pollutants.

Low solubility and high organic carbon affinity in particulate matter makes sediments a major player, often with a total concentration in the "parts per billion" (ug/kg) or "parts per million" (mg/kg). Water usually only musters a measly "parts per trillion" (ng/kg) concentration due to low water solubility.

Surface water, however, can be a major sink for PAHs. Total PAHs in drinking water, a final destination for PAHs via effluents, was shown to have background between 4 and 24 ng/L. However, in 1978, Basu and Saxena found total mean background concentrations in Pittsburg, Pennsylvania to be 600 ng/L. Additionally, Basu and Saxena (1978) identified groundwater levels between 3-20 ng/L in the bordering states of Ohio, Indiana, and Illinois. A 1986 analysis of the Mississippi River acknowledged that phenanthrene was the highest individual PAH with a high of 34 ng/L. The New Orleans industrial zone sample supports the notion that effluents and surface runoff are some of the most significant contributors to water background (McCarthy, 2003). Several studies presented by the ATSDR have uniformly shown the importance of urban runoff's role.

The United States Fish and Wildlife Service's (USFWS) 1987 report on PAHs is another comprehensive attempt to compile and evaluate cross-generational and cross-geographic background data to form remediation plans. Lee and Grant's 1981 development of the idea that total PAHs in air are approximately 10 times higher than B(a)P levels is a helpful barometer to estimate total PAH concentrations, even with the observed statistical variation (USFWS, 1987).

Coal tar road sealants, 10-18% PAH in weight, have had 500 to 600 times greater quantities of PAHs than asphalt sealant (Mahler et al., 2005). Coal tar sealant's high PAH composition yields direct effects in river sediments near asphalt parking lots sealed with coal tar (Grosenheider et al., 2005). This knowledge fostered research of asphalt runoff because of the known severity of runoff particulates being caught by sediment traps. The United States Geological Survey determined PAH concentrations using 13 parking lots in Austin, Texas, where 600,000 gallons of coal tar sealant were applied each year (USGS, 2005a). Particles in runoff from unsealed lots, serving as the control, contained 54 mg/kg, a concentration 65 times lower than the 3,500 mg/kg resulting from coal tar-based sealants (Mahler et al., 2004). The study also found asphalt-sealed parking lots produced 620 mg/kg in runoff. Due to vehicle exhaust, tire particles, motor oil, and atmospheric deposition, all values surpassed the 22.8 mg/kg sediment Probable Effects Concentration (PEC) used to assess risks from sediment. This hazard prompted Austin officials to ban coal tar sealants and penalize violators with $2,000 fines (Richardson, 2006).

According to a stormwater analysis in coastal Massachusetts, fluoranthene, phenanthrene, pyrene, and chrysene were the most pervasive PAH compounds (McCarthy, 2003). The authors then deciphered the source of origin by associating the various land uses capable of producing

such a composition. Researchers concluded that "localized bulk increases" of PAHs in coastal sediment were primarily due to stormwater discharges (McCarthy, 2003). Additionally, a long-term study of the Lower Hudson Watershed found the highest PAH concentrations near the Western NY/NJ Harbor in Newark Bay occurred during the early 1950's, a period marked by petroleum's prevalence and use in the area (Abrajano and Bopp, 2001). By the mid-1960's, the 180 ppm of total PAHs in sediments in the 1950's dropped to 25 ppm.

In 2003, the Ohio EPA conducted a detailed assessment on the Mad River Basin in order to shed more light regarding PAH concentrations in the State's aquatic environments (OH EPA, 2005). The results varied, but a large proportion of the samples were greater than measured above PEC values suggested by McDonald et al. (2000). Samples, summarized in Table 2, below, were collected at various junctions and tributaries in the Massachusetts River ecosystem.

Table 2. PAH concentrations in Mad River Basin sediments (mg/kg)

PAH name	Moore Run	Dugan Run	St. Paris Tributary	Buck Creek
B(a)A	**1.62**	**3.18**	**1.27**	**2.22**
B(a)P	**2.04**	**2.99**	1.38	**2.39**
B(b)F	2.81	3.09	1.55	2.67
B(g,h,i)PER	1.75	2.04	1.09	1.81
B(k)F	2.31	2.96	1.45	2.10
Chrysene	**2.57**	**3.84**	**1.77**	**2.94**
Fluoranthene	**5.41**	**6.98**	**3.31**	**5.92**
Indeno[1,2,3-cd]pyrene	2.08	2.20	1.15	2.04
Phenanthrene	**2.07**	**3.60**	**1.43**	**2.91**
Pyrene	**4.24**	**5.75**	**2.64**	**4.60**
Total PAH	**26.90**	**37.26**	17.04	**29.60**

***Bolded values indicate a level above the PEC.**
**Derived from OH EPA (2005).

Chrysene, fluoranthene, phenanthrene, and pyrene all were above PEC levels in all four locations in the Mad River area. B(a)P crossed the threshold in three of the sites, and passed the TEC in the St. Paris Tributary (1.38 mg/kg). Similarly, the total PAHs were above the PEC in all but the aforementioned tributary where it did exceed the TEC. Values higher than the TEC indicate harmful effects for benthic-dwelling organisms being more likely, but not quite probable (WI DNR, 2003). These levels are not novel to urban watersheds since effluents from anthropogenic activity inevitably enter these aquatic environments.

The main stressors impacting the Lewis Creek Watershed in a Virginia study were lead, total PAHs and sediments (VADEQ, 2006). Sediments often accumulate PAHs due to surface runoff, streambank erosion, and other natural erosion; however, human activity catalyzes these natural processes. This sediment movement transferred a significant amount of PAHs into previously uncontaminated areas in the watershed. With direct contamination a minor threat, the majority of hydrocarbons entered via urban areas such as the city of Staunton and point sources like the

Beverly Exxon site. In 2001, an initial sampling of only one site showed several PAHs above PEC guidelines. During the subsequent 2005 sampling sweep, all except one of the 13 sites showed concentrations above the PEC, and more of them exceeded the TEC. Though none of the PAHs at the other sites posed a threat individually, their toxicity has an additive effect that warrants interest since four sites showed gerater than a 1.0 Hazard Index (VADEQ, 2006). The hazard index equals the sum of the hazard quotients (measured result/ PEC or screening level), and a score above 1.0 signifies a potentially toxic condition. Unfortunately, measurements taken five months later showed that half of the impending problem areas experienced statically significant reduction in biological survival or reduction in growth.

1.4 Florida Perspective

1.4.1 Florida Case Study #1

During investigations related to a former manufactured gas plant destined for urban redevelopment project in north-central Florida, PAHs were discovered in soils and roadside ditch sediments at levels that exceeded the site-specific park user scenario soil cleanup target level (SCTL) of 0.35 ppm, as well as the default Florida SCTL for industrial/commercial sites of 0.7 ppm. The 95% upper confidence limit on the mean benzo(a)pyrene-equivalent concentration for on-site soil samples was approximately 1.2 ppm. Site impacts were observed to be sporadic and not specifically associated with historical activities that may have resulted in PAH releases. Further, upstream roadside ditch samples contained higher levels of PAHs than those observed on the site, implicating general urban conditions.

The consultant demonstrated through literature review and site-specific data analysis that the observed concentrations were quite consistent with urban background for PAHs in such a setting. The federal and state agencies involved with the site concurred in principle, but procedurally required the enactment of an institutional control to notify future property owners of the presence of impacted soil and to prevent exposure.

1.4.2 Florida Case Study #2

A local housing authority in central Florida undertook the redevelopment of a decades old urban neighborhood bracketed by major roadways and an interstate highway. Surface soil investigations detected PAHs in excess of default residential SCTLs (0.1 ppm for B(a)P-eq) over most areas of the site. A statistical analysis of the data revealed a mean concentration of 0.6 ppm and a 95% UCL of the mean concentration of 1.1 ppm for 68 surface soil samples.

A background study was proposed by the consultants, and encouraged by the state, to support the literature-based and site-specific evidence of an urban background phenomenon. However, out of an abundance of caution, and in light of available funding for the remediation, it was decided to excavate, and or cap with two feet of clean soil, the exposed areas of the site (i.e., those areas not covered by roads, driveways or buildings).

1.4.3 Florida Case Study #3

As part of the due diligence involved in a property transaction in west-central Florida, PAH impacts were discovered in soils adjacent to and beneath an asphalt parking lot of a former retail shopping center. The investigation was expanded multiple times in an attempt to delineate the impacts. No clear delineation was evident for samples beneath the asphalt, but concentrations adjacent to the parking lot decreased with increasing distance from the parking lot. This was a fairly obvious example of the ubiquity of PAHs, and, specifically was concluded to be related to vehicle emissions and parking lot runoff causing low level impacts.

With a maximum benzo(a)pyrene-equivalent concentration of 2.1 ppm, and mean and 95% UCL concentrations of 0.4 ppm and 0.8 ppm, respectively, site concentrations were well within the widely published range of urban background PAH levels (i.e., typically 1-10 ppm, with some areas as high as 100 ppm). Once again, even though all parties agreed that historical site-related activities were not likely the cause of the observed PAH impacts, in order to facilitate the property transaction process, it was decided that soils adjacent to the parking lot would be excavated and replaced with clean fill. The soils beneath the parking lot were left in place, but an institutional control was enacted to notify future property owners of the presence of impacted soils.

2. DISCUSSION

- Stationary and mobile sources account for as much as 80% of PAHs. Let's worry about the other 20% (background).
- Remediation should not commence without establishing a site-specific background, if possible.
- "While natural events cannot be controlled they do contribute to the background and can have an important local impact. They may therefore affect the ability of a member state to meet any emission limit." (EU, 2003)
- Due to incongruity of nature and the variability in activity among people inhabiting a given area, background values vary a great deal.
- CERCLA [Section 104(3)(A)] addresses the impracticality and unfeasibility of remediation to guideline levels if naturally occurring background exceeds the maximum allowable value. It deems remediation unnecessary and unproductive in such scenarios.
- Those monitoring health risks and PAH concentrations should first identify and control the principal point sources contributing to ambient levels.
- Urban background may be detrimental to human health, but the inability to directly control diffuse and mobile sources makes the threat difficult to manage.
- The main goal is returning a site to urban background, which is relatively stable throughout a city. For this reason, baseline measurements should be determined by utilizing samples from an assortment of locations (parks, roadside, suburbia) throughout a city.
- A tier-based guideline system such as the Illinois TACO or ALARA is often ideal since minor contamination can be addressed with through a nominal response.
- ALARA system: "A tier 1 level of 1 mg/kg of PAHs measured as B(a)P eq. is recommended as a remediation goal; if PAHs are below this level, no further action is

required. A tier 2 level of 10 mg/kg of PAHs measured as B(a)P eq. is recommended as well; if PAHs are below this level, a subjective evaluation of likely current and potential future land use is required. If it appears unlikely that frequent exposure would occur, no further action is required." (Lagoy and Quirk, 1994)

3. REFERENCES

Abrajano, TA, and Bopp, RF., 2001. Sources and Chronology of Polycyclic Aromatic Hydrocarbon Deposition in Sediments from the Lower Hudson Watershed. Goldschmidt Conference, Hot Springs, VA.

ATSDR (Agency for Toxic Substance and Disease Registry). 1995. Toxicological profile for polycyclic aromatic hydrocarbons (PAHs). Available at http://www.atsdr.cdc.gov/toxprofiles/tp69.html.

ATSDR (Agency for Toxic Substance and Disease Registry). 2006. 2005 CERCLA Priority List of Hazardous Substances. Available at http://www.atsdr.cdc.gov/cercla/05list.html.

BCERF (Program on Breast Cancer and Environmental Risk Factors). 2001. Polycyclic Aromatic Hydrocarbons and Breast Cancer Risk. Available at http://envirocancer.cornell.edu/FactSheet/general/fs41.pah.cfm.

Beyond Pesticides. 2004. New York becomes the first state to pass a creosote ban. Available at http://beyondpesticides.org/news/daily_news_archive/2004/07_07_04.htm.

Black, W.V., D.S. Kosson, R.C., Ahlert. 1989. Characterization and evaluation of environmental hazards in a large metropolitan landfill. In: Bell, J.M., ed. Proceedings of the Industrial Waste Conference. Chelsea, MI: Lewis Publishers, Inc. 147-152.

Bradley LJN, Magee BH, and Allen SL. 1994. Background Levels in Hydrocarbons (PAH) and Selected Metals in New England Urban Soils. Journal of Soil Contamination 3(4): 349-61.

Costa H and Gensky N. 2001. Concentration or composition? Defining PAH background in sediments. Society for Environmental Toxicology and Chemistry.

Delgado T. 2000. The occurrence and regulation of PAHs in groundwater and soil. Smart News: 2(5): 1-3l

EU (European Union). 2001. Ambient air pollution by Polycyclic Aromatic Hydrocarbons (PAH): Position Paper. ISBN 92-894-2057-X. Office for Official Publications of the European Communities, Luxembourg.

EU (European Union). 2003. Proposal for a Directive of the European Parliament and of the Council Relating to Arsenic, Cadmium, Mercury, Nickel and Polycyclic Aromatic Hydrocarbons in Ambient Air. 2003/0164 (COD). Commision of the European Communities, Brussels, Belgium.

Grosenheider KE, Bloom PR, Halbach TR, et al. 2005. A Review of the Current Literature Regarding Polycyclic Aromatic Hydrocarbons in Asphalt Pavement. Mn/DOT Contract No. 81655. University of Minnesota, Minneapolis, MN, USA.

Hellmann, H. 1999. PAH background levels in contaminated soils. Wasser Boden, no. 51(10): 26-29.

ILDPH (Illinois Department of Public Health). 2005. Environmental health fact sheet: polycyclic aromatic hydrocarbons. Available at http://www.idph.state.il.us/envhealth/factsheets/polycyclicaromatichydrocarbons.htm.

IEPA (Illinois Environmental Protection Agency). 2005a. Intergovernmental Agreement Between the Illinois EPA and the Illinois Department of Transportation Regarding the Reuse of Soil from IDOT's Dan Ryan Expressway Reconstruction Project. 35 Ill. Adm. Code 742. IEPA Bureau of Land, Springfield, IL, USA.

IEPA (Illinois Environmental Protection Agency). 2005b. Urban area polycyclic aromatic hydrocarbons study tiered approach to corrective action objectives. Available at http://www.epa.state.il.us/land/site-remediation/urban-area-pah-study.pdf.

LaGoy PK and Quirk TC. 1994. Establishing generic remediation goals for the polycyclic aromatic hydrocarbons: critical issues. Environ Health Perspec 102(4): 348-52.

LBNL (Lawrence Berkeley National Laboratory). 2004. Constraining Uncertainties about the Sources and Magnitude of Ambient Air Exposures to Polycyclic Aromatic Hydrocarbons (PAHs): the State of Minnesota as a Case Study. Paper LBNL-54473. University of California, Berkeley, CA, USA.

Li, M. 2003. Ambient concentrations and measurement precision of molecular markers in fine particles from Philadelphia, PA. Drexel Theses and Dissertations.

MADEP (Massachusetts Department of Environmental Protection). 2002. Technical Update: Background Levels of Polycyclic Aromatic Hydrocarbons and Metals in Soil. 310 CMR 40.0006. MADEP, Boston, MA, USA.

Mahler, BJ, Van Metre, PC, and Wilson, JT. 2004 [revised 2007], Concentrations of polycyclic aromatic hydrocarbons (PAHs) and major and trace elements in simulated rainfall runoff from parking lots, Austin, Texas, 2003 (version 3). U.S. Geological Survey Open-File Report 2004–1208.

Mahler BJ, Van Metre PC, Bashara TJ, et al. 2005. Parking lot sealcoat: An Unrecognized Source of Urban Polycyclic Aromatic Hydrocarbons. Environ Sci Technol 39(15): 5560- 66.

Mannino, I. 2004. Extraction and Analysis of PAHs in Surface Soils Near Freeways in Los Angeles. American Geophysical Union.

McCarthy B. 2003. Polycyclic aromatic hydrocarbons (PAHs) in urban runoff. The GEI MGP Reporter: 1,3.

Menichini E. 1992. Urban air pollution by polycyclic aromatic hydrocarbons: levels and sources of variability. Sci Total Environ 116(1-2): 109-35.

NBCC (National Breast cancer Coalition). 2002. The Long Island Breast Cancer Study Project. Available at http://www.natlbcc.org/bin/index.asp?strid=536& depid=9&btnid=2.

NPI (National Pollution Inventory). 2004. Polycyclic aromatic hydrocarbons. Available at http://www.npi.gov.au/database/substance-info/profiles/74.html.

OH EPA (Ohio Environmental Protection Agency). 2005. Biological and Water Quality Study of the Mad River Basin, 2003. EAS/ 2005-5-5. Division of Surface Water, Columbus, OH, USA.

Richardson DC. 2006. Parking lot sealants: on the trail of urban PAHs. Stormwater, The Journal for Surface Water Quality Professionals 7 (4): pp unknown.

Stout SA, Uhler AD, and Emsbo-Mattingly SD. 2004. Comparative evaluation of background anthropogenic hydrocarbons in surficial sediments from nine urban waterways. Environ Sci Technol 38(11): 2987-94.

USEPA (US Environmental Protection Agency). 1997. Field Methods Evaluation for Estimating Polycyclic Aromatic Hydrocarbon Exposure: Children in Low-Income Families that Include Smokers. EPA/600/SR-97/029. National Exposure Research Laboratory, Research Triangle Park, NC, USA.

USEPA (US Environmental Protection Agency). 2000a. National Air Toxics Program: The Integrated Urban Strategy Report to Congress. EPA-453/R-99-007. Office Of Air Quality Planning And Standards, Research Triangle Park, NC, USA.

USEPA (US Environmental Protection Agency). 2000b. Prediction of sediment toxicity using freshwater sediment quality guidelines. EPA-905/R-00/007. Great Lakes National Program Office, Chicago, IL, USA.

USFWS (US Fish and Wildlife Service). 1987. Polycyclic Aromatic Hydrocarbons Hazards to Fish, Wildlife, and Invertebrates: A Synoptic Review. Biological Report 85(1.11). Patuxent Wildlife Research Center, Laurel, MD, USA.

USGS (US Geological Survey). 2005. Parking-lot sealcoat: a major source of PAHs in urban and suburban environments. Available at http://water.usgs.gov/nawqa/asphalt_sealers.html.

US Navy. 2003. A User's Guide for Determining the Sources of Contaminants in Sediments. TECHNICAL REPORT 1907. SPAWAR Systems Center, San Diego, CA, USA.

VADEQ (Virginia Department of Environmental Quality). 2006. Total Maximum Daily Load Development for Lewis Creek, General Standard (Benthic). New River-Highlands RC & D, Wytheville, VA, USA.

Wagrowski DM and Hites RA. 1997. Polycyclic aromatic hydrocarbon accumulation in urban, suburban, and rural vegetation. Environ Sci Technol 3f: 279-282.

WI DNR (Wisconsin Department of Natural Resources). 2003. Consensus-based Sediment Quality Guidelines: Recommendations for Use & Application. WT-732 2003. WI DNR, Madison, WI, USA.

Part X: Remediation

Chapter 23

ORGANOCLAYS TRAP RECALCITRANT METALS AND ORGANIC COMPOUNDS IN SEDIMENTS SIMULTANEOUSLY

George R. Alther[§]
Biomin, Inc., Ferndale, MI. 48220

ABSTRACT

The capability of organoclays as components of permeable sediment barriers has been researched extensively over the past several years.

Organoclays have been used in permeable walls to block the movement of a DNAPL plume from an abandoned wood treating site, and for sediment stabilization at an old MGP site (from a power and light company).

Laboratory column tests and batch tests with organoclays have revealed that a standard, non-polar organoclay fixates all heavy metals, including lead, zinc, nickel, chrome and cadmium, but also inorganic aqueous mercury. In terms of organic hydrocarbons, such diverse compounds as dioxin and nitro-benzenes, as well as PCP, PCB, PNHA and BTEX are trapped effectively.

Studies with polar organoclays, which can easily be blended with the non-polar types, fixate arsenate, selenite, chromate, perchlorate, etc.

This article presents data showing these capabilities, as well as case histories.

1. INTRODUCTION

When used as a sediment barrier, the organoclay is present as a granule of about 20 x 50 mesh size. The purpose of that size is so that the granules blend in with the sediments, which are usually sand or sandy silt. The organoclay functions as a cap to retard the upward movement of

[§] Corresponding Author: George R. Alther, Biomin, Inc., Ferndale, MI. 48220 Email: Biomin@aol.com

contaminants into the surface water. Groundwater discharges into rivers and lakes. The plume is then either intercepted in this manner by capping the river sediments with organoclay, or a slurry wall intercepts it, where organoclay is blended in with the back fill. Slurry walls are used either as a permeable barrier for new landfills or superfund type sites, or they are placed as secondary barriers around old, existing walls, which are leaking. In that case, the vibrating beam type slurry wall is used because it is only 10 inches wide, vs. the three feet of conventional types, and they are much easier and quicker to construct. The backfill of the vibrating beam type consists of powdered cement, bentonite, and organoclay, with the emphasis of the design being creation of a permeable barrier (Alther et al, 2003). Landfill liners can be constructed with granular or powdered organoclay, depending on the existing soil type (Alther, et al, 1988).

Soil stabilization is conducted by admixing with the soil a blend of Portland cement, fly ash, powdered organoclay, and powdered activated carbon. Such a system, which has to pass the TCLP test, fixates organic hydrocarbons and heavy metals. There are two mechanisms by which organoclay and the contaminants are fixated:

In micro-encapsulation, at the microscopic level, the organoclay and the organic contaminants are entrapped within the crystalline matrix of the solidified mass. This prevents degradation of the organoclay into ultra fine particles, which migrate and potentially release organic contaminants. Without the organoclay the organic contaminants are not bound to the crystalline structure created by the cement and are easily released back into the environment.

In macro-encapsulation, at a larger scale, the organoclay with the sorbed organic contaminants is physically entrapped within the voids of the cementitious matrix inside the discontinuous pores. Only extreme freezing or thawing could break down this structure (Alther, et al, 1991).

1.1 Description of Organoclay

Organically modified clays consist of bentonite, which is modified with quaternary amines (Theng, 1974). The major constituent of bentonite, which is a chemically altered volcanic ash, is the clay mineral montmorillonite. It has a cation exchange capacity of 70-95 meq/g. The quaternary amines, which are used for this purpose, are of the cationic ammonium chloride type, which have a positive charge on one end of the chain. This charge, derived from the nitrogen ion at the carboxylic head, ion exchanges with sodium, calcium, and magnesium ions on the surface of the montmorillonite. In this fashion the hydrophilic clay becomes hydrophobic or organophilic, and the entire structure becomes a non-ionic surfactant with a solid base. Upon introduction of some moisture, the amine chain, which hitherto lies on the clay platelet surface like the hair of an animal's fur lies on its body, extends now vertically into the water. As organic hydrocarbons of low solubility pass by the particle, they dissolve into the organic phase where they are more soluble. This process is called "partitioning" (Smith & Jaffe, 1994). When an immiscible organic solvent such as octanol is added to water, which includes contaminants of low solubility such as PCB, a portion of this compound will move out of the water and into the octanol, where it is more soluble. The relative solubility determines the amount retained in each phase. The concentration ratio of this compound in the two phases is constant over a wide range.

This is known as the "partition coefficient, k", in this case the "Kow" octanol-water coefficient (Mortland et al, 1986).

This terminology can now be extended to contaminants partitioning from the water phase onto a solid phase, such as organic cations sorbed onto clay surfaces. The higher the solution concentration of a compound and the lower its solubility, the larger the quantity removed by the organoclay through partition. For example, the removal efficiency of organoclay for phenolic compounds is inversely related to the water solubility and amount of chlorination of the compound. Therefore, pentachlorophenol (PCP, 14 mg/kg solubility in water) is removed in much larger amounts than straight phenol (77,500 mg/kg solubility). By plotting the solubility vs. the n-octanol water partition coefficient onto a graph, the relative ease of removal of organic hydrocarbons by organoclays can be estimated.

Since there are always more amine chains available than can be stoichiometrically affixed to the montmorillonite, the remainder tends to adhere to the fixated surfactant chains by a "tail-tail interaction". That means that a non-ionic organoclay does have a small positive charge, which allows it to remove some anions, such as hexavalent chrome. Therefore, the organoclay has a slight anion removal capacity; it has become polar.

Since the bentonite, which makes up the bulk of the organoclay, is a natural cation exchange resin, it retains some cation exchange capacity, which helps in reducing the heavy metal content of the groundwater, which passes through the barrier (Alther, 2004).

1.2 Laboratory Testing Methods:

1.2.1 The "Mini-Column" Technique

One gram of powdered organoclay is packed into a small vial or mini-column. A spiked solution of water is pumped through this column until the influent concentration of the contaminants equals that in the effluent. In this manner, the effectiveness of the organoclay for removing a certain organic hydrocarbon from water can be quickly determined. The advantage of this method is that the equilibrium concentration is the same as the influent concentration, and therefore under ready control (Alther, 2,002).

1.2.2 The Jar Test

This test describes a single point isotherm, which is created by contacting a known weight of sorbent with the contaminated water. A known weight of sorbent, for example 1 gram, is slowly added into a 1000 ml jar filled with the contaminated water. The sorbent is then dispersed in the water by a shaking mechanism, a magnetic stirrer, or a paddle. After a predetermined time, usually 10 minutes, the solids are allowed to settle, followed by centrifugation. The amount of the remaining contaminant in the water is then determined. This test provides a quick performance evaluation, without having to perform the 10-point ASTM Isotherm test.

1.2.3 Column Test

The capacity of granular (8x30 U.S. mesh size) organoclay to remove heavy metals was also tested by means of a column test. A 30-inch long and 3 inch diameter column was constructed from poly-vinyl-chloride (PVC) and filled with the organoclay. A large amount of water was poured into a container and spiked with 6 metals, in this case Cu, Cd, CrIII, Ni, Zn, and Pb, and the solution was forced through the column with a peristaltic pump. The column was first backwashed for several hours to displace air in pores and remove any fines. Once in operation, samples of the water where periodically collected and analyzed by means of Acetylene-Air Flame/ Atomic Adsorption (at the laboratory of the Dept. of Environmental Engineering, University of Virginia). Anions were also passed through columns in a separate set of tests.

2. RESULTS OF LABORATORY TESTS

2.1 Mini-Column Tests

In this test, powdered organoclay (1 gram), powdered activated carbon (1 gram), and a combination of powdered organoclay (0.5 gram) followed by powdered activated carbon (0.5 gram, in the same vessel), were tested by passing distilled water spiked with benzene, toluene and naphthalene through the vessel (Alther, 2002). The results are shown in Figure 1. Benzene breaks through first, followed by toluene and then naphthalene. This sequence is expected based on the solubility of these compounds.

2.2 Soil Stabilization

Table 1 below shows the results of tests conducted by mixing a sample of the solidification ingredients in a Hobart mixer with the contaminated soil.

An interesting observation is that the organoclay totally fixated highly soluble compounds such as vinyl and methylene chloride, acetone and chloro-ethylene compounds.

Two organoclays were evaluated for their removal capacity of Pb from water, using EPA 6010 method. The organoclay included 23% of quaternary amine. Testing it with water, which contained 5 ppm and 10 ppm of Pb, respectively, showed that the organoclay removed Pb to less than 0.05 ppm in either case.

Another organoclay that contained 28% quaternary amine was tested for its capability to remove Zn and Cd from water (EPA 6010 method), using 2 grams of clay, 100 ml water, pH 3-5; mixed in jar for 20 minutes.

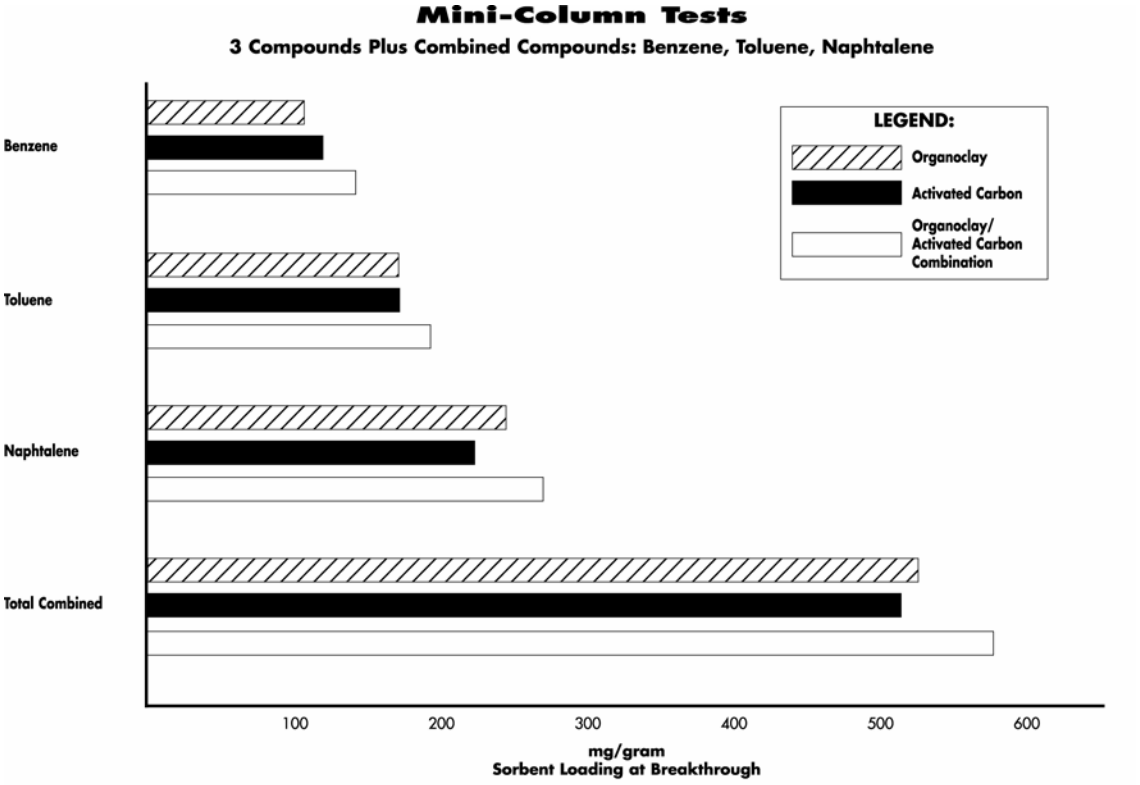

Figure 1. Mini-column tests showing the efficiency of non-ionic organoclay for removing organics from water, followed by activated carbon, followed by the two sorbents in sequence in the same vial, in the removal of petroleum hydrocarbons from water.

Table 1. Results of Laboratory Tests on Soil Stabilization. Jar tests for removal of heavy metals by non-ionic organoclay.

Reagent: 90 percent silicates including cement 10 percent organoclay		Mix Ratio: 80 percent soil sludge 20 percent reagent (i.e. 2 percent organoclay)	
Test Number	**Contaminant**	**Contaminant Concentration**	
		Before Treatment	**After Treatment**
1	Vinyl Chloride	24 ppm	ND
	Methylene Chloride	38 ppm	7 ppb
	Acetone	2600 ppm	151 ppb
2	PCB (Alchor 1260)	320 ppm	ND
3	Total Grease & Oil	15,000 ppm	5 ppm
4	Creosol	7.5 ppm	0.4 ppm
5	Dichloroethylene	26-110 ppm	0.8 ppm
	Trichloroethylene	17-95 ppm	0.1 ppm
	Toluene	110-320 ppm	1.2 ppm
	Xylene	20-55 ppm	0.2 ppm
	Napthalene	22-43 ppm	0.02 ppm
	PCB	5-20 ppm	ND

The results are:

Input: 1 ppm Zn	Retained: less than 0.05 ppm;	Input: 2 ppm Cd	Retained 0.11 ppm
5	0.71	5	1.5
10	7.2	10	7.1
1 ppm Cu:	0.03	2 ppm Ni	0.2
5	0.09	5	1.8 ppm
10 ppm	4.4 ppm		

These data show that 2 gram (sample size) of the organoclay can remove about 1.5 ppm of the metal.

Mercury was removed from water with an organoclay containing 29% of quaternary amine, using EPA 7470 testing method:

Inflow: 1 mg/l mercury;	outflow: 0.04 mg/l
0.5 mg/l	0.026
0.1.1	0.004 mg/l
0.2	

2.3 Column Tests, Heavy Metals Removal

Table 2 shows the results of a column test conducted with granular non-ionic organoclay, on a composite sample of 6 different metals. The U.S. mesh size of these granules is +8x-30 mesh, with a porosity of 36% (0.36). Calculations show that some 17% of the surface area of the bentonite is still available for ion exchange after conversion to an organoclay. Therefore the ion exchange capacity of the granular organoclay is about 0.16 meq/100 grams.

Table 2a. Sorbent mass, porosity, flowrate and residence time information for each of the column experiments.

		Mass		Porosity	Flow Rate		Residence Time
Metal	Sorbent	(kg)	(lbs)		(mL/min)	(gal/hr)	(min)
Pb	Organoclay	2.8	6.2	0.32	135	216	8.40
Cd	Organoclay	2.3	5.17	0.42	125.5	199	11.2
Cu	Organoclay	2.9	6.4	0.27	114	182	8.05
Zn	Organoclay	2.9	6.4	0.31	133	213	8.10
Cr	Organoclay	2.54	5.6	0.37	164.4	263	8
Ni	Organoclay	2.41	5.3	0.38	147.3	236	9.09

Table 2b. 95% Breakthrough of each metal for the sorbent material given in pore volumes and minutes with estimated mass of metal sorbed per mass of sorbent in mg/kg, lb/lb and percent basis.

		Breakthrough		Mass Sorbed		Mass Sorbed/Mass of Sorbent		
Metal	Sorbent	(pore vol.)	(min)	(mg)	(lb)	(mg/kg)	(ln/lb)	% by weight
Pb	Organoclay	31.56	264	12,164	0.02682	4,321	0.004321	0.432%
Cd	Organoclay	13.9	162.9	4,319	0.0095	1841	0.0018	0.18%
Cu	Organoclay	48*	386*	3,580	0.00789	1,233	0.001233	0.12%
Zn	Organoclay	15.8	128	2,771	0.00611	950	0.000950	0.095%
Cr	Organoclay	6.2	67.77	820	0.00180	323	0.000323	0.032%
Ni	Organoclay	8.1	73.68	1,382	0.0029	572	0.000572	0.0572%

Below is a bar graph that shows the effectiveness of non-ionic organoclay to remove heavy metals from water. In graph A the water was spiked with various metals to determine which ones are removed preferentially. In graph B, ion exchange tests were conducted with each metal in a separate test.

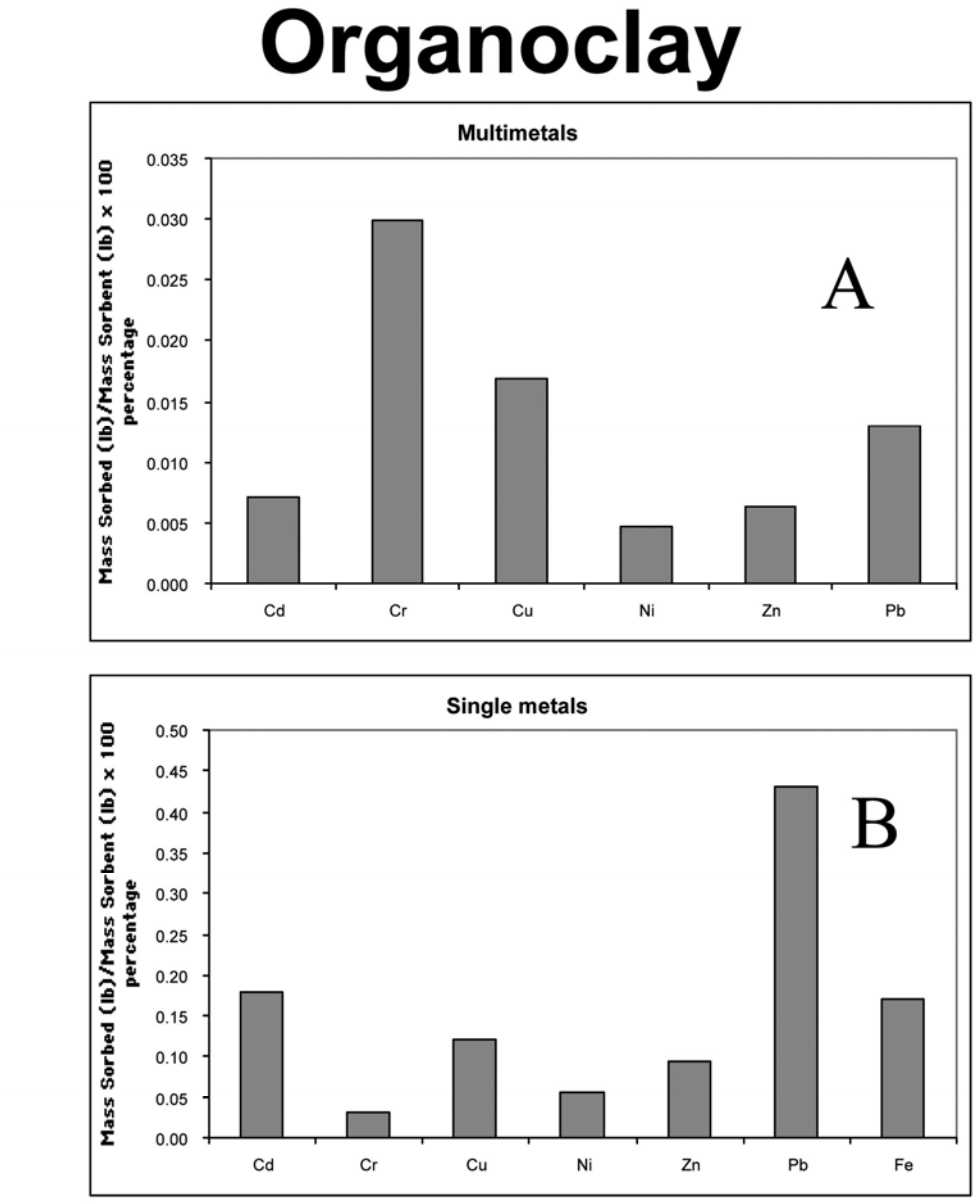

Figure 2. The next page shows the effectiveness of polar organoclay to remove anions from water.

Table 3a. Column tests with arsenate, perchlorate and chromium (VI)
(same description as Table 2a).
TC75 = Polar Organoclay

Sorbent	Mass Sorbent		Porosity	Flow Rate		Residence
	(kg)	(lb)		(mL/min)	(gal/hr)	(min)
TC-75 arsenate	0.396	0.88	0.33	8.3	0.133	20
TC-75 perchlorate	0.389	0.87	0.32	8.3	0.133	20
TC-75 chromium (VI)	0.391	0.87	0.33	8.3	0.133	20

Table 3b. Column tests with arsenate, perchlorate and chromium (VI)
(same description as Table 2b).

Sorbent	Breakthrough		Mass Sorbed		Mass Sorbed/Mass Sorbent		
	PV	Min	(mg)	(lb)	(mg/kg)	(lb/lb)	(% by sorbent)
TC-75 arsenate	27	540	715	0.0017	1896	0.0017	0.18
TC-75 perchlorate	10	200	259	0.0006	655	0.0007	0.07
TC-75 chromium (VI)	25	500	2319	0.005	5858	0.0058	0.58

Table 4a. Sorbent mass, porosity, flow rate and residence time information for the removal of selenium IV column experiments.

Sorbent	Mass Sorbent		Porosity	Flow Rate		Residence
	(kg)	(lb)		(mL/min)	(gal/hr)	(min)
TC-75 Selenite	2.1	4.7	0.26	50.5	0.81	20

Table 4b. 95% breakthrough for the sorbent given in pore volumes and minutes along with estimated mass of selenium IV sorbed per mass of sorbent in mg/kg, lb/lb and percent basis.

Sorbent	Breakthrough			Mass Sorbed		Mass Sorbed/Mass Sorbent		
	PV	BV	Min	(mg)	(lb)	(mg/kg)	(lb/lb)	(% by sorbent)
TC-75 Selenite	50.5	14.1	1,005	5,107	0.01	2,431	0.01	1.15

Table 5a. Sorbent mass, porosity, flow rate and residence time information for TC-75 sorbent column experiments.

Sorbent	Mass Sorbent		Porosity	Flow Rate		Residence
	(kg)	(lb)		(mL/min)	(gal/hr)	(min)
TC-75	2.3	5.1	0.34	59	0.94	20

Table 5b. 95% breakthrough for TC-75 sorbent materials given in pore volumes (PV), bed volumes (BV) and minutes along with estimated mass of CR(III) and Cr(VI) sorbed per mass of sorbent in mg/kg, lb/lb and percent basis.

Sorbent	Breakthrough			Mass sorbed		Mass Sorbed/Mass Sorbent		
	PV	BV	min	(mg)	(lb)	(mg/kg)	(lb/lb)	(% by sorbent)
Cr(VI) before regeneration	31	10.5	620	9768	0.022	4247	0.004	0.425
Cr(VI) after regeneration	24	8.2	480	3657	0.0081	1590	0.0016	0.159
Cr(III) before regeneration	8	2.7	160	736	0.0016	320	0.0003	0.031
Cr(III) after regeneration	4	1.4	80	586	0.0013	255	0.0003	0.025

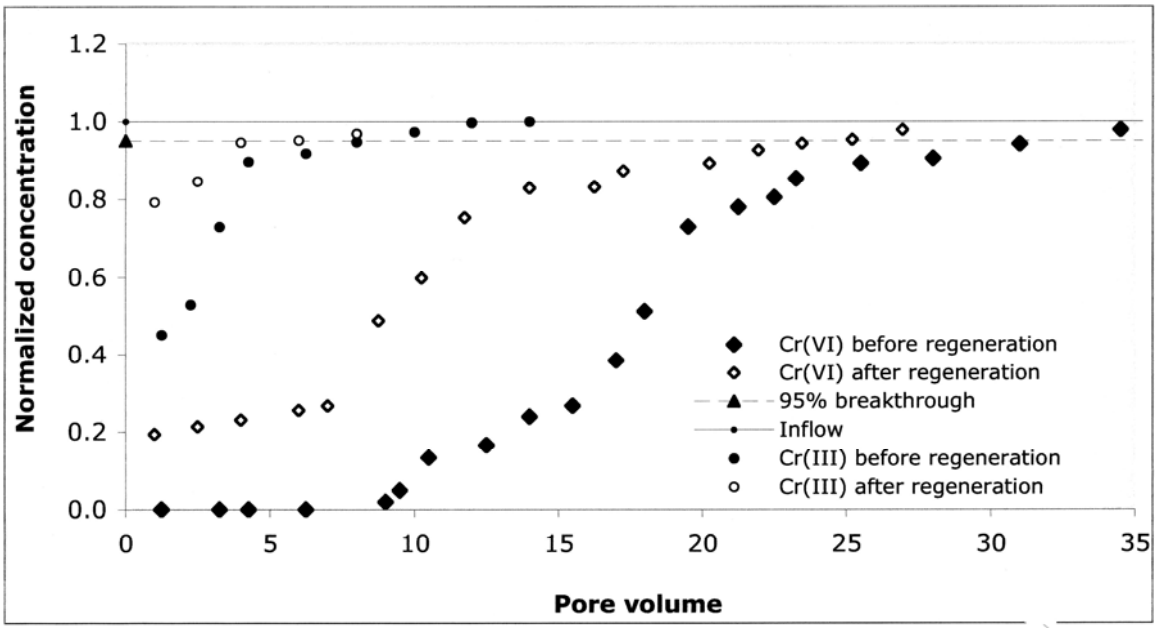

Figure 3a. Breakthrough curves (in terms of pore volume) of Cr(III) and Cr(VI) through TC-75.

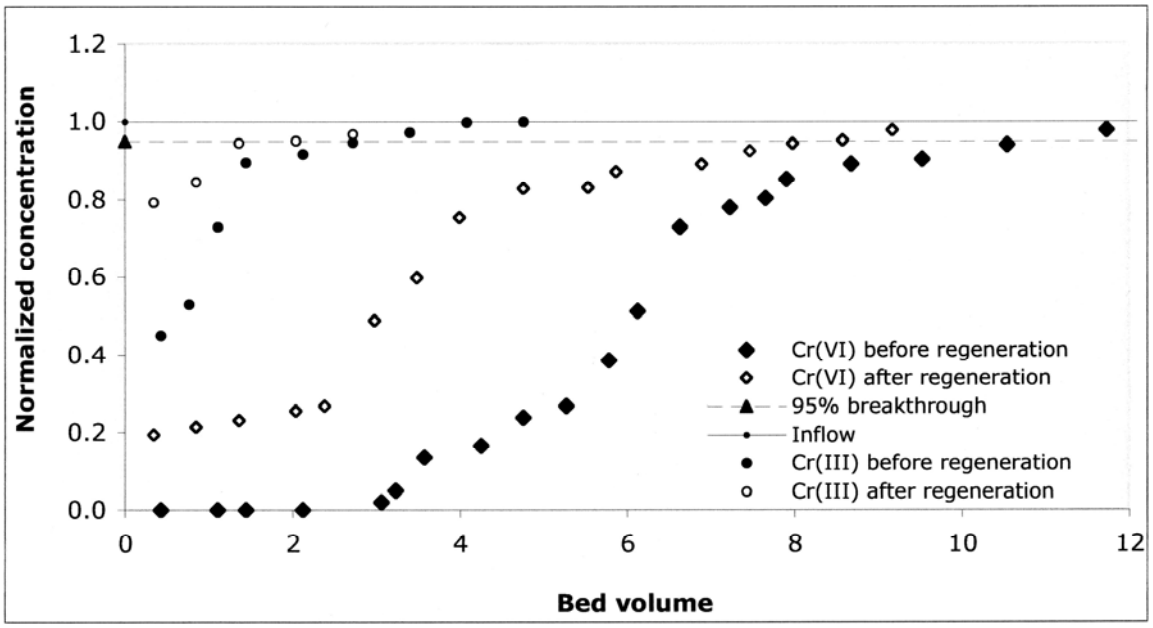

Figure 3b. Breakthrough curves (in terms of bed volume) of Cr(II) and Cr(VI) through TC-75.

3. CASE HISTORIES: SOIL STABILIZATION

A rolling mill sludge, which contained 10% oil and grease, was stabilized with a mixture of cement, silica additives and organoclay. This resulted in a mixture of 80% sludge, 17.7% cement blend, and 2.3% organoclay. Treated with these compounds, the sludge had unconfined compression strength of greater than 50 psi (after 28 days of curing per TCLP), and the TCLP yielded less than 5-ppm oil and grease. Powdered organoclay has the capability of removing 80% or more oil and grease from water.

A large Midwestern utility company, which owned property that included a former manufactured gas plant (MGP) site next to a river, had soil on its site stabilized. This soil was contaminated with coal tar, which includes heavy oils (Bunker C) and pitch. This mixture included benzene, toluene, naphthalene, phentathrine, pyrene and phenolic compounds. The coal tar contaminated the soil below the groundwater table to a debt between 12 to 25 feet. Sediments in the river where contaminated at the sediment/water interface, to a debt of 3 feet

The mixture that was blended with the soil and sediments consisted of fly ash, Portland cement, powdered organoclay and powdered activated carbon. 22 truckloads of both organoclay and activated carbon were used.

The mixing mechanism consisted of an in-situ drilling system whereby the mixture was injected into the soil, and soil/mixture columns were constructed. The mixing of the additives was performed with a pug mill (asphalt type) mixer. At the bottom of each column sodium silicate was added to ensure maximum strength. The columns showed consistently more than 50 psi unconfined compression strength and passed the TCLP test.

3.1 Barrier Construction Next to a Refinery

A refinery next to the terminal of the Port of Portland in Oregon was responsible for an oil contaminated Superfund site, from which oils oozed into the estuarine and coastal waters. A 15 feet wide wall was constructed; the contaminated soil was excavated and disposed of in a Subtitle D disposal site. A backfill, blended with 1% of powdered organoclay, was installed to function as a permeable sorption barrier. Laboratory tests had established that such a system would prevent oil from passing through the barrier, without creating a "bathtub" filled with water. Other authors have since conducted scientific studies, confirming the feasibility of this method (Lo et al, 1997).

3.2 Landfill Liner Design

Such liners, which include organoclay, where first discussed by Alther et al (1989), and later by Smith et al, 2000. The short of it is that a permeable barrier is created which allows clean water to pass, but retards and prevents inorganic and organic contaminants from ever leaving the site (Young Yoo et al, 2004). If such a barrier ever starts leaking, a thin slurry wall using the vibrating beam technology can be constructed around the landfill at economical costs.

4. CONCLUSIONS

This brief description of methods to establish permeable barriers around contaminated sites establishes the feasibility of the concept. This technology is a system, which has been long in coming, but should now be accepted as "state of the art" technology.

The tests have also proven that a polar organoclay is capable of removing cations, anions and non-ionic organic compounds from water simultaneously. Organoclay is the only sorbent which has this capability.

5. REFERENCES

Alther, G.R., 2005. Sediment Stabilization and Permeable Barriers with Organoclay. Battelle Conference on Sediment Remediation, New Orleans, LA.

Alther, G.R., 2004. Some Practical Observations on the Use of Bentonite. Environmental & Engineering Geoscience, Vol.X, No.4, pp. 347-359, GSA, Boulder, CO.

Alther, G.R.,Wesolek, D., and Schmednecht, F., 2,003. Permeable Sorption Barriers. Proceedings, NGWA Conference, New Orleans, Nov. 2,003. NGWA, Westerville, OH.

Alther, G.R., Evans, J.C., and Pancoski, E.S., 1988. Organically modified clays for stabilization of organic hazardous waste. In HMCRI's 9th National Conference, Superfund 88, Silver Spring, MD. Pg 440-445.

Alther, G.R., Evans, J.C., and Tarites, R., 1991. The use of Organoclays for stabilization of hazardous wastes. In Proceedings of Fourth Annual Hazardous Management Conference/Central, Glen Ellyn, Il, pp. 547-552.

Alther, G.R., 2002. Using Organoclays to enhance carbon filtration. Waste Management, Vol. 22, Pergamon Press (Elsevier), NY, pp. 507-513.

Alther, G.R., Evans, J.C., and Pancoski, E.S., 1989. A composite liner system to retain inorganic and organic contaminants. In Superfund 89, HMCRI, Washington, DC.

Lo, I.M., Mak, R.K.M, and Lee, S.C.H., 1997. Modified Clays for Waste Containment and Pollutant Attenuation. Journal of Environmental Engineering, Vol. 123, No.1, pg 25-32, ASCE.

Mortland, M.M., Shaobai, S., and Boyd, S.A., 1986. Clay-organic complexes as adsorbents for phenols and chloro-phenols. Clays and Clay Minerals, Vol. 34, No.5, pp. 581-585.

Smith, J.A., Li, J., and Galan, A., 2,000. Organobentonites as components of Earthen Landfill Liners to minimize contaminant transport. Geoenvironment 2,000, Vol. 11, pp. 806-814.

Theng, B.K.G., 1974. The chemistry of Clay-organic reactions: Halstead Press, NY., 343 pg.

Young Yoo, JL; Choi, J., Lee, T., and Park, J.W., 2004. Organobentonite for Sorption and degradation of phenol in the presence of heavy metals. Water, Air and Soil Pollution, Vol. 154, Kluwer Academic Publishers, The Netherlands. Pp 225-237.

Chapter 24

ELECTRICAL RESISTANCE HEATING OF SOILS AT C-REACTOR AT THE SAVANNAH RIVER SITE

Mark E. Farrar[3], Michael R. Morgenstern[1], Joseph A. Amari[2], Annamarie MacMurray[3], Terry P. Killeen[2] and Robert F. Blundy[2§]

[1]Bechtel Savannah River Co, Savannah River Site, Aiken South Carolina 29808, USA; [2] Washington Savannah River Co, Savannah River Site, Aiken, South Carolina 29808, USA, [3]Savannah River National Laboratory, Savannah River Site, Aiken South Carolina 29808, USA.

ABSTRACT

Chlorinated solvent contamination of soils and groundwater is an endemic problem at the Savannah River Site (SRS), and originated as by-products from the nuclear materials manufacturing process. Five nuclear reactors at the SRS produced special nuclear materials for the nation's defense program throughout the cold war era. An important step in the process was thorough degreasing of the fuel and target assemblies prior to irradiation. Discharges from this degreasing process resulted in significant groundwater contamination that would continue well into the future unless a soil remediation action was performed. The largest reactor contamination plume originated from C-Reactor and an interim action was selected in 2004 to remove the residual trichloroethylene (TCE) source material by electrical resistance heating (ERH) technology. This would be followed by monitoring to determine the rate of decrease in concentration in the contaminant plume. Because of the existence of numerous chlorinated solvent sources around SRS, it was elected to generate in-house expertise in the design and operation of ERH, together with the construction of a portable ERH/SVE system that could be deployed at multiple locations around the site. This paper describes the waste unit characteristics, the ERH system design and operation, together with extensive data accumulated from the first deployment adjacent to the C-Reactor building. The installation heated the vadose zone down to 62 feet bgs over a 60 day period during the summer of 2006 and raised soil temperatures to over 200 ^{o}F. A total of 730 lbs of trichloroethylene (TCE) were removed over this period, and subsequent sampling indicated a removal efficiency of 99.4%.

Keywords: Electrical Resistance Heating, Savannah River Site, Reactor, trichloroethylene

§ **Corresponding Author:** Robert F. Blundy, Washington Savannah River Company, Savannah River Site, Building 730-4B, Aiken, South Carolina 29808. E-mail address robert.blundy@srs.gov

1. INTRODUCTION

The Savannah River Site (SRS) is a 310 square mile Federal facility located near to Aiken, South Carolina. The site is owned by the U.S. Department of Energy (DOE) and is operated by the Washington Savannah River Company with Bechtel Savannah River Company being responsible for the Environmental Restoration program. SRS was built in the early 1950's to produce special nuclear materials for the nation's defense program. SRS operated throughout the Cold War era until the late 1980's when the site transitioned to environmental clean up activities. The central components of the production process at SRS, were the 5 nuclear reactors which irradiated special target materials to generate the plutonium and tritium. The nuclear fuel and target materials were fabricated into assemblies in the manufacturing area (M-Area) of SRS and were then transported to the reactor areas for processing. An important part of the fuel loading step was a thorough initial degreasing of the reactor fuel and target assemblies, prior to loading into the reactor vessel. In the early years, this degreasing step was performed within the reactor building itself. The degreasing operation consisted of a large vapor degreasing tank located in the assembly area of the reactor and contained 2,300 gallons of trichloroethylene (TCE). After the early 1970's this step was transferred back to M-Area. However, while degreasing was still being performed at the reactor areas, the inevitable spillage resulted in a source of solvent contamination to the groundwater that persisted until recently.

A remedial investigation of C Area (WSRC, 2003) was conducted between 1996 and 2000, with a subsequent investigation conducted in 2002. These investigations revealed the presence of two TCE contaminated groundwater plumes, that are shown in Figure 1. The northern plume emanates from a construction waste pit (C Area Burning Rubble Pit), which has been under a separate remediation action since 1999 (WSRC, 2003a), and initially utilized conventional soil vapor extraction (SVE), but has since reverted to passive SVE (i.e. Baroballs^{R}). The southern plume, which emanates from a source near to the reactor building, discharges into Castor Creek at concentrations above the maximum contaminant levels (MCLs) for groundwater. Due to the extended period of operation of the SVE units, it was determined that an accelerated technique for source removal would be the most desirable method to address the southern plume, and in 2003 an agreement was reached with the site environmental oversight regulatory agencies, the U.S. Environmental Protection Agency and South Carolina Department of Health and Environmental Control, to execute an interim source removal action using Electrical Resistance Heating (ERH) (WSRC, 2003b).

A remedial investigation conducted in 2002, identified the TCE source as being adjacent to the assembly building of the reactor, in a near vertical column descending from an area near to storm drain. The vertical distribution is shown in Figure 2. The ERH action would take place in a partially disturbed soil region that had been excavated and then backfilled during the reactor construction phase. The stratigraphy consisted of two clayey-sand layers (Engineering Unified Soil Classification system) that were believed to be relatively electrically conductive, interspersed in a sandy-clay matrix that would be less electrically conductive but conducive to SVE. The upper electrically conductive clayey-sand layers is located between -8 to -28 feet below ground surface (bgs), and was designated as the A zone; the lower zone is located between -52 to -64 feet bgs, and was designated as the C zone. The local area water table is located at around -70 feet bgs. The majority of the TCE inventory was believed to be contained in the

upper clay-sand layer from approximately -15 to -39 feet bgs. Further investigation for the presence of buried utilities in the area, revealed the area to be crisscrossed with several steel utility water pipes and steel reinforced concrete storm drainage pipes. All these utilities were connected to the internal piping systems within the building. This feature of the location could present both a significant safety hazard for personnel within the building, and also a source of power drain while the ERH system was operating.

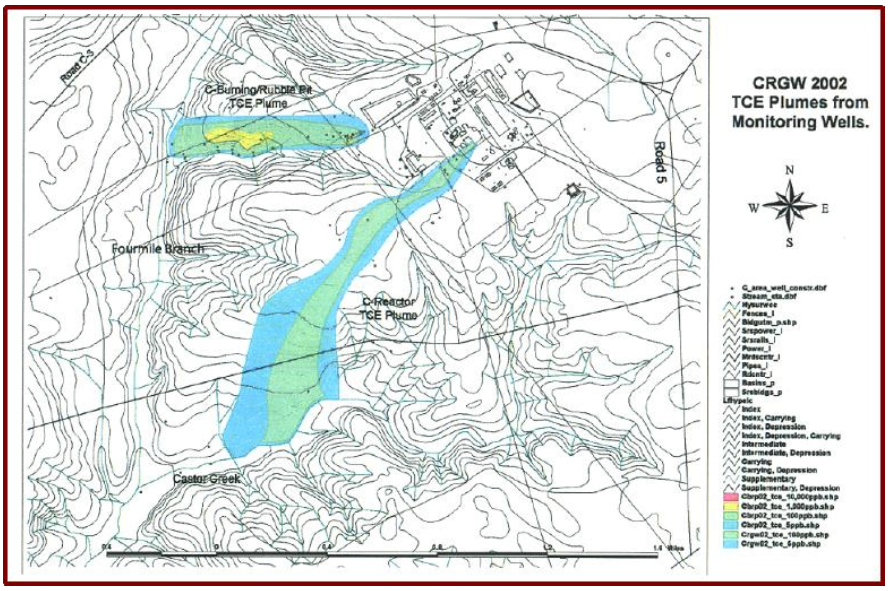

Figure 1. Groundwater TCE plumes emanating from C Area

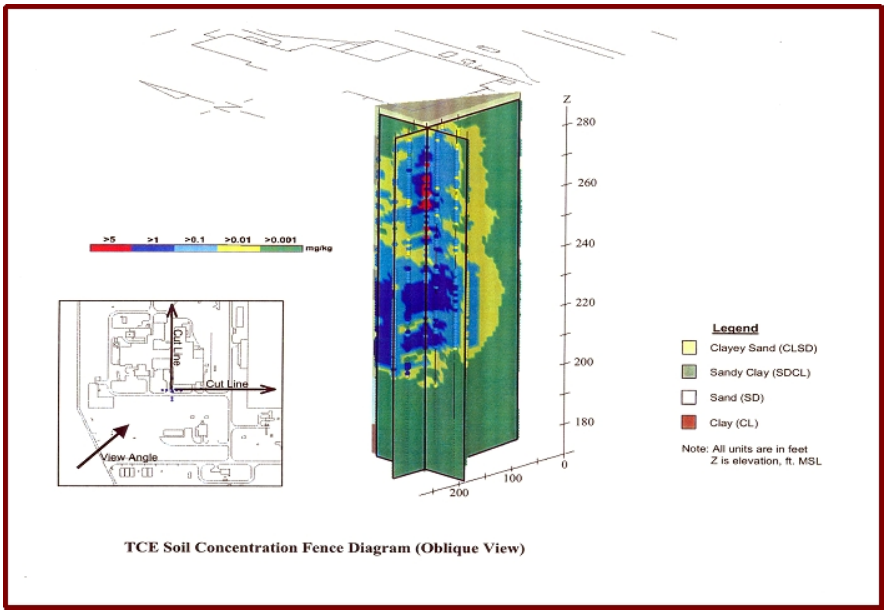

Figure 2. TCE soil contamination fence diagram

The negotiated remedial goals for the interim action were basically two fold. The first objective was to sustain an average soil temperature in excess of 189 ^{o}F within the heated zones for a minimum of 30 continuous days. As 189 ^{o}F is the boiling temperature of pure TCE, this would ensure that all of the solvent was transformed into the vapor phase. The second goal would be to reduce TCE concentrations in the source zone to the point where any further leaching would not cause groundwater concentrations to exceed the regulatory MCL limit of 5.0 μg/L. This reduction would be determined by taking soil cores after heating had been terminated.

2. MATERIALS AND METHODS

ERH technology was originally developed by Pacific Northwest National Laboratory (Heath et al., 1992) in the early 1990's with DOE funding, and has since been proven to be a highly successful technology with licenses being held by a number of commercial vendors. Chlorinated solvents are a soil contamination problem at many SRS waste units, and although conventional SVE had previously been deployed, it has been found to require extended operating time frames to achieve an effective level of source reduction. ERH has the potential to greatly accelerate the rate of solvent removal in low permeability soils, therefore it was concluded that ERH could potentially be deployed at other locations at SRS following the deployment at C Reactor. With the prospect of accelerating the SRS clean up program, it was decided to develop an in-house capability in ERH technology, which included obtaining a site specific license, designing and constructing portable ERH equipment together with developing internal operating expertise.

Electrical power was obtained from the reactor 13.8kV electrical distribution system. The voltage was simultaneously stepped down and split from 3 phase 60 Hz AC, to 6 phase, 60 Hz AC via a 1,250 kVA capacity mobile power supply manufactured by Spang Power Electronics. Six phase electrical power provides for more even heating than 2 or 3 phase power (Carrigan and Nitao, 2000). In operation, the power supply could maintain a preset voltage between 0 and 1,100 volts at each electrode by multi step transformer tap changes. The constant voltage at each electrode was set by a remote computer and controlled within the range of the tap setting by automatic control of the applied current by silicon controlled rectifiers. The desired voltage was set at the start of each day, based on the trend in change of soil resistance.

The ERH design consisted of six electrodes placed in a 30 foot diameter circle, effectively surrounding the soil column to apply the electrical heating. A central neutral electrode was installed to absorb the electrical imbalance generated by differences in soil resistance. The design of the neutral electrode was the same as the power electrodes, even though the power transmitted through the neutral would be less. As the power supply effectively operated in an ungrounded arrangement, the central neutral electrode enabled the power supply to provide more stable overall voltage control from a well defined electrical reference. The SVE vapor extraction wells were co-located internally within the electrode boreholes.

Soil is effectively an electrical insulator, and in applying electrical power to the subsurface, significant "stray" voltages can appear outside of the six power electrode array. These "stray" voltages can energize any metal in contact with the ground, resulting in step-touch potentials and

potentially significant safety issues. Therefore a number of safety features were implemented to mitigate potential electrical safety issues:

- A wood fence was erected around the electrodes with a single gate that was administratively locked out with the power supply. The power to the electrodes had to be turned off before personnel could enter the electrode field.
- A grounding ring consisting of a bare No. 4 bare copper wire was buried at a depth of approximately one foot and circled the installation. All metal parts in the above ground equipment were grounded to this ring, thus effectively eliminating any potential differences between components.
- A wire mesh equipotential mat was placed over the energized zone and was also connected to the grounding ring. This effectively eliminated any possible step-touch potentials.
- During ERH start up and operation, stray voltage checks were performed weekly at strategic locations around the ERH site, including test points within the building and also whenever the applied voltage was increased. The highest stray voltage recorded between a metal structure and the ground, was 12 volts which was well below the OSHA limit of 50 volts.

During operation, the offgas vapor was withdrawn from the SVE wells through a gas treatment system supplied by REP Inc, before being released to the atmosphere, where the TCE is degraded by ultra violet sunlight (Corbo, 1985). The above ground gas treatment train collected the hot vapor from each electrode/SVE well via a manifold system and then into a primary water droplet/particulate separator. The gas temperature was reduced to 140 ^{o}F by a heat exchanger and the condensate removed in the secondary condensate separator. Cool water to the heat exchanger was maintained by a packaged Delta 100 ton capacity cooling tower. The offgas vapor then passed through a Dresser Roots type blower which had the capability of drawing up to 300 acfm at a vacuum of up to 12 inches of mercury. TCE concentrations between the vapor and condensate phases partitioned according to Henry's Law or roughly 100 to 1. However TCE concentrations in the condensate were too high for immediate discharge, therefore the condensate was stored in two 7,500 gallon tanks, and was finally dispositioned to the large M-1 air stripper, that is located elsewhere on site. To maintain good electrical contact between the electrodes and the subsurface soil, an electrolyte consisting of 0.1M Mg_2SO_4 was drip fed to each electrode.

In the ERH process, the Joule heating effect is generated by utilizing electrical resistance of the soil as a heating element. The electrodes themselves merely transmit the electrical power to the soil, and do not get any hotter than the surrounding soil. The electrodes are therefore the most critical component of the ERH system and must be designed carefully to ensure continuing electrical contact with the soil and focus the electrical power to the most contaminated region as the soil heats up. The electrode design schematic is shown in Figure 3.

Each electrode borehole was drilled to a depth of 62 feet using a 10 inch diameter Rotosonic rig. The upper heating zone was located from -16 to -32 feet bgs and the lower heating zone from -42 to -58 feet bgs. The upper elevation was set so that the electrically energized zone was below the underground pipes, and the lower elevation was set to be just above the water table.

The intervening space between the two heating zones in the electrodes was filled with bentonite pellets to achieve electrical separation. The electrode connection was accomplished by running 4/0 Teflon^{R} insulated electrical cables from the surface down to a 12 feet long by 3 x 3 inch, 304 grade stainless steel angles, placed in the center of each heating zone. Electrical contact between these angles and the soil was maintained by filling the intervening gap with coarse graphite

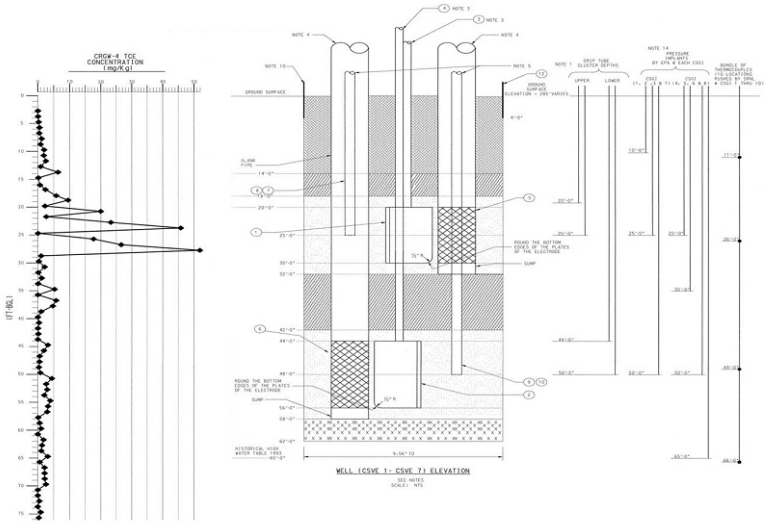

Figure 3. Individual electrode design schematic (both power and neutral)

powder. The upper and lower heating zones were electrically connected at the surface so that in normal operation, the two zones were connected in parallel. However power could be applied separately to either zone if necessary. The co-located vapor extraction wells were fabricated from spirally wound 2 inch epoxy fiberglass pipe that was capable of withstanding temperatures of up to 300 ^{o}F. The vapor extraction screens were 10 feet long and were slotted directly into the epoxy pipe which was located at the same elevations as the electrodes. The graphite also acted as the well packing media. Even though six-phase power provides fairly even soil heating, the power density is still highest in the soil immediately surrounding the electrode. To maintain good electrical conductivity in the soil in this area, each electrode zone was equipped with two ¼ inch internal diameter Kynar^{R} drip tubes to allow electrolyte to saturate the graphite and the adjacent soil. Electrolyte flow rate was adjustable, but was set at a nominal 0.1 gallons per minute to each electrode including the neutral.

The earlier geotechnical investigation (WSRC, 2003c) showed that the backfilled soil around the reactor, where the ERH array was located, to be highly compacted and it was suspected that the co-located electrode SVE wells would not be able to capture all of the vapor that would be generated. Therefore three additional 6 inch diameter SVE only wells were drilled on a 35 feet diameter circle, centered on the neutral electrode, using the Rotosonic drill rig. These wells were screened from -27 feet to -67 feet bgs, and the TX-50 sand filter extended from -18 feet to -70 feet bgs. Post construction flow testing revealed that these SVE only wells yielded negligible air flow, even after extensive well development. The cause of the low flow was believed to be due to the action of the Rotosonic drill concentrating the soil fines on the surface of the well bore. Gas sampling of the SVE wells after installation, also revealed that the highest TCE gas concentrations were located in the south west quadrant of the array, possibly indicating the

location of the highest soil contaminant concentrations. As good operation of these outer SVE wells was believed to be essential for efficient TCE removal, three additional wells were drilled using a hollow stem auger. Two of these wells were located in the south west quadrant and one was located to the north of the array. The flow performance of these hollow stem auger drilled wells proved to be satisfactory. The above ground equipment arrangement is shown schematically in Figure 4 below.

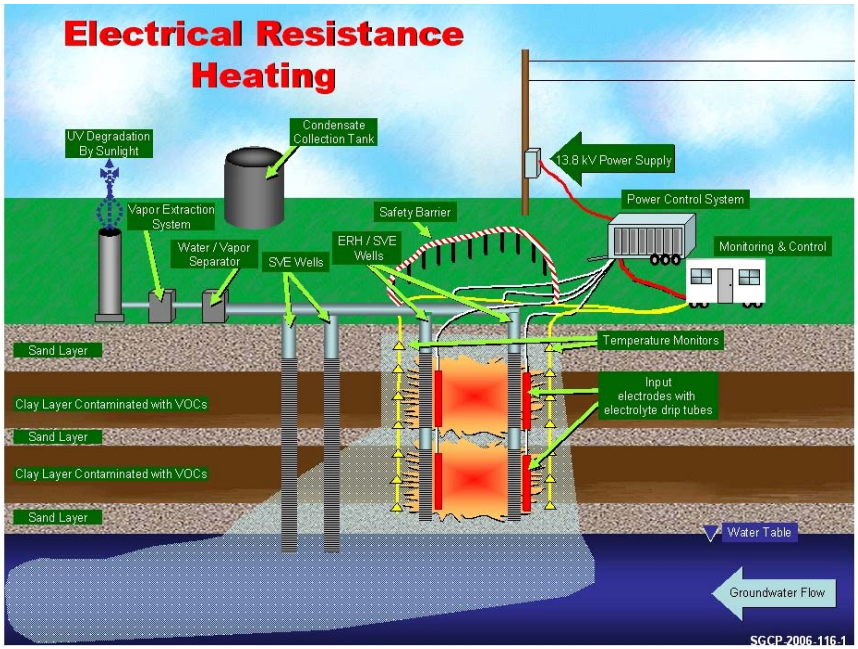

Figure 4. Layout of electrode array, SVE wells, piping and sensors

Figure 5 shows the ERH installation with the assembly building of the reactor building in the background. Two process monitoring systems were placed in the subsurface to facilitate control of heating. Thermocouples were placed at 10 locations around the array, with individual thermocouples at 4 elevations (-11, -26, -49 and -66 feet bgs). In addition a series of pressure measurement implants were placed at 8 locations around the array with the ability to sense the vacuum in the subsurface at 5 depths: -10 feet bgs (AA zone), -25 feet bgs (A zone), -35 feet bgs (B zone), -50 feet bgs (C zone) and -65 feet bgs (D zone). These were used to verify that, while the vapor extraction system was operating, the heating zones were consistently under negative pressure, thus minimizing TCE migration out of the heating volume.

Although not strictly required by the remedial goals, the quantity of TCE extracted was an important indication of the effectiveness of the treatment process. Due to the rapid heating provided by the ERH process, an innovative approach was introduced to measure TCE and PCE concentrations in the off gas, and hence measure the quantity of contaminants removed. The conventional monitoring approach employed with SVE systems at SRS, takes weekly Tedlar bag samples, followed by analysis in a laboratory gas chromatograph/mass spectrometer. Because of the rapid heating rate with ERH, the expected erratic rate of TCE evolution and the possibility of an air discharge permit excursion, it was believed that the low sampling frequency combined

with normal laboratory turn around time, would be too slow to obtain an accurate measurement of mass removal rate and also give advanced warning of an impending permit excursion.

The continuous off gas monitoring system consisted of a gas diffusion sampling probe to separate the TCE vapor from the water vapor, a photoacoustic gas analyzer manufactured by California Analytical, a Rosemont Annubar mass flow meter which were all linked by a dedicated computer. The photoacoustic analyzer measured off gas concentrations of TCE and PCE every minute. The algorithm in the computer integrated the concentrations with the mass flow rates to give both instantaneous and cumulative read outs of the mass of solvent removal. The photoacoustic analyzer was calibrated weekly against the weekly bag sample/gas chromatograph technique.

Figure 5. The ERH installation looking east. The electrode array is at top right, the electrical power supply is in the right foreground, the hut housing the control equipment is in the center foreground and the condensate tanks in the left foreground.

3. RESULTS

Heating commenced on June 15, 2006, and continued uninterrupted until September 7, 2007. The planned operating strategy was to maintain 30 kW of power at each electrode until the soil dried out and the electrical resistance became too high.

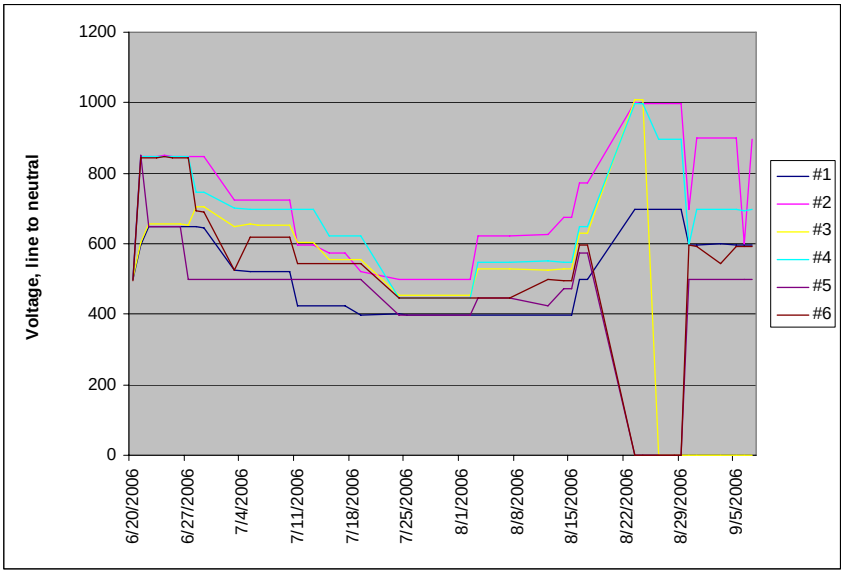

Figure 6. Individual electrode phase voltages (line to neutral)

Figure 6 shows the voltage at each electrode (measured line to neutral) and Figure 7 shows the electrical power delivered to each of the six electrodes over the duration of the project. Figure 8 shows the change in phase resistance measured at each electrode over the duration of the project. In Figure 8, phase resistance is defined as the line voltage at each electrode with respect to the neutral, divided by the current applied to that electrode. Initially the array exhibited a wide variation in soil resistance, which was accommodated by daily power adjustments to obtain a consistent power distribution at each electrode. As the array area heated up, the soil resistance initially decreased. This is due to the electrical conductive path being via the interstitial soil moisture, and the electrical conductivity of aqueous solutions decreases as temperature increases. The electrical resistance remained stable until the middle of August, when soil moisture had been reduced by evaporation to a level where electrical continuity within the soil began to break down and resistance increased sharply. Electrical contact was then lost at one electrode after another. Some limited success was achieved in recovering electrode operation by increasing the electrolyte drip rate, but on September 7, the power supply was switched off.

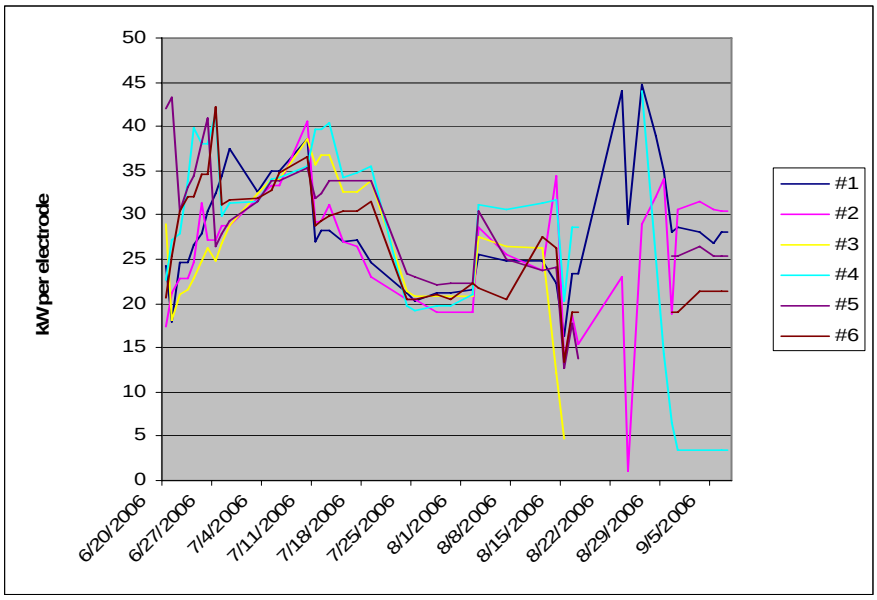

Figure 7. Individual electrode power levels

Figure 9 shows the resulting average temperature recorded by the thermocouples located in the upper and lower heating zones. The lower C heating zone reached the target temperature of 189 ^{o}F after two weeks of heating, this was followed by the upper A zone reaching the target temperature one week later. When the average temperature reached the theoretical maximum of 212 ^{o}F, power was reduced to around 20 kW per electrode to conserve soil moisture. Heating continued past the 30 day target, as gas concentration measurements made at each electrode and SVE well indicated that the majority of the TCE source was located in the upper A zone in the south west quadrant of the array, but that region proved reluctant to ramp up to the 189 ^{o}F target temperature. From archived photographs of the reactor construction, it appeared that the array location straddled the transition between the area native soil and the sand fill that had been used

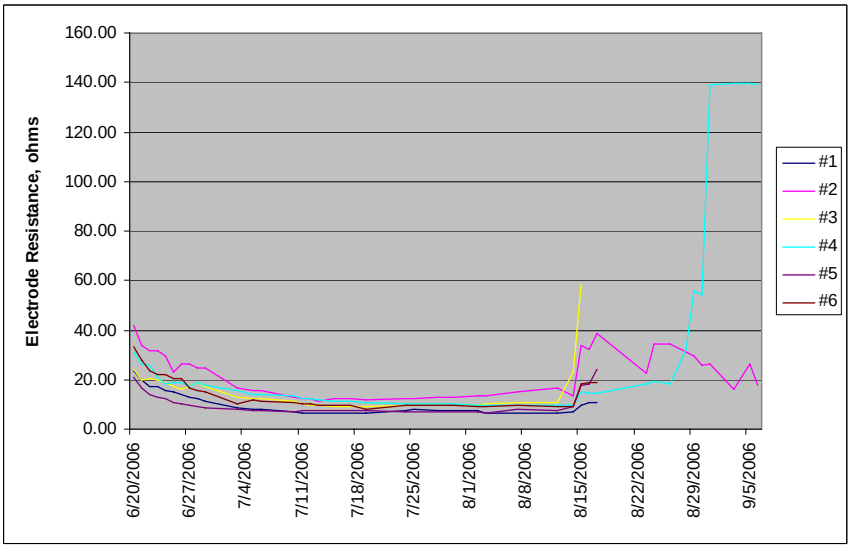

Figure 8. Individual electrode phase resistance

to backfill around the building after the 40 feet deep foundation had been completed. This produced a disparity in soil resistance between the north-east and south-west segments of the array, which resulted in channeling of the power towards the northern segment of the array. The underground piping did not have a significant effect on the ERH operation until the applied voltage exceeded 700 volts, when the N-S steel pipe that passed close to electrodes CSVE-01 and CSVE -03, began to act as a parallel conductor, which resulted in an excessive current draw.

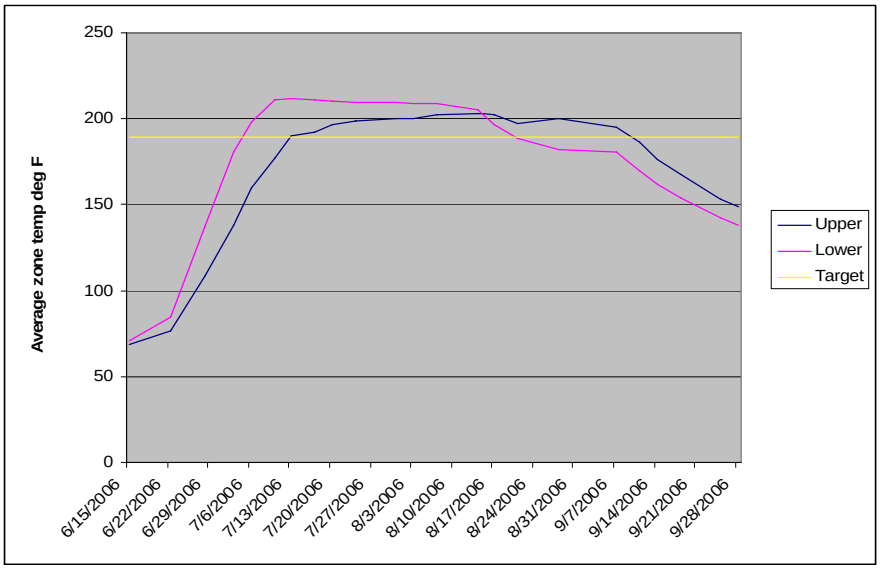

Figure 9. Average heating zone temperature timeline

Figure 10 shows the cumulative mass of TCE and PCE removed over the duration of the project. The extraction rate peaked as each heating zone approached the boiling temperature of TCE, with the majority being removed as the upper A zone, heated up. A total of 730 pounds of solvents were removed. As anticipated, the rate of solvent removal was too rapid during these peaks, for the conventional bag sampling technique to permit representative sampling. Although the measured gas concentrations between the continuous system and the Tedlar bag - GC/MS technique did not differ by more than 10%, the continuous system recorded a mass of TCE removed to be 3 times greater.

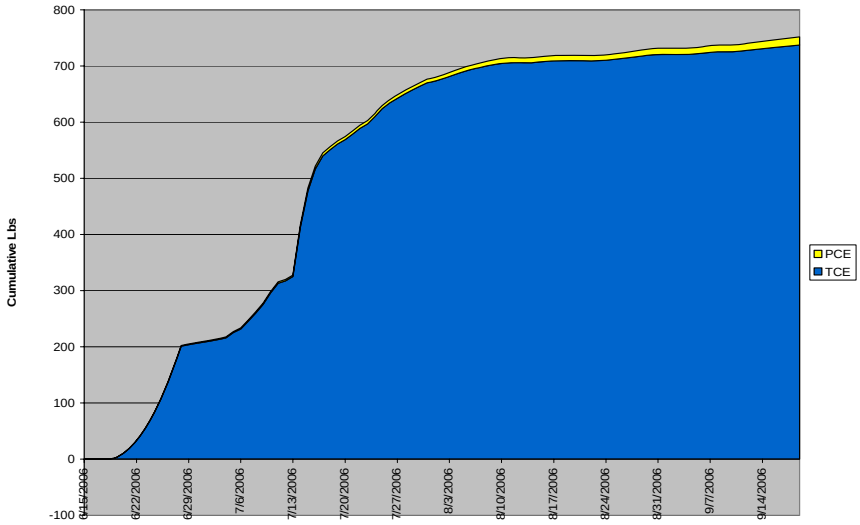

Figure 10. Cumulative mass of solvent extracted

4. DISCUSSION

A total of 229 MW hours of electrical energy was consumed over the duration of the project, which included the energy required to heat the soil, power the blower and the other above ground equipment.

A total of 55,619 gallons of electrolyte was injected over the heating period. The initial soil resistance was found to be quite high due to the soil around the electrode boreholes drying out during construction. Therefore the injection rate was higher over the first two weeks the first two weeks of heating. A total of 47,300 gallons of condensate was collected, mostly overt the latter stages of heating when the whole heating zone was close to 212 ^{o}F.

The combined air flow from the SVE wells is shown in Figure 11 and averaged 90 scfm throughout the heating period at an average manifold vacuum of 10 ins Hg. Air flow was kept to a minimum to the SVE wells in the SW quadrant of the array in the middle part of the heating period to facilitate heating. As this area reached the target temperature, air flow was then increased. The range of vacuum levels in the 5 subsurface zones are given in Table 1 and confirm that relatively high vacuums occurred at the beginning of heating which fell quite sharply as the soil dried out. Nevertheless, the heated region remained under negative pressure, particularly beneath the lower heating zone (D zone) thus minimizing TCE vapor migration to the groundwater.

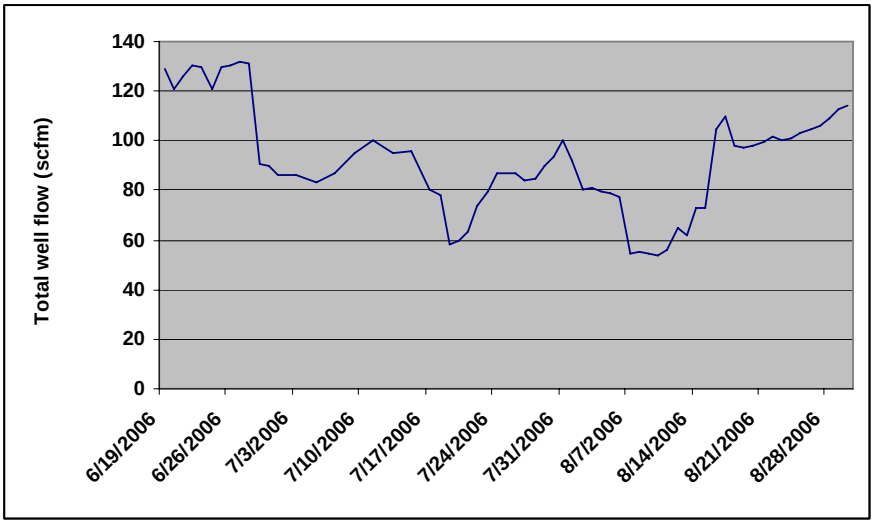

Figure 11. Air flow from the SVE wells throughout heating period

The initial soil core TCE concentration profile is shown in Figure 3 and the final soil concentrations in the two confirmatory soil cores are shown in Table 2. Substantial concentration reductions throughout the heating zone can be seen. Integrating the before and after profiles indicate a reduction of over 99% was achieved.

Table 1. Subsurface vacuum levels in the five zones

Zone	Depth (feet bgs)	Zone Type	Vacuum range (ins W.C.)
AA	-10	Above Heating	-1.5 to -0.1
A	-25	Upper Heating/SVE	-20 to -1.0
B	-35	Intermediate	-22 to -6.0
C	-50	Lower Heating/SVE	-32 to -1.0
D	-65	Beneath Heating	-17 to -3.5

5. CONCLUSIONS

ERH proved to be a very effective technology for accelerating the removal of chlorinated solvents that had proven to be tightly bound to the SRS clayey soils. The previous solvent removal action at C-Burning Rubble Pit, required 5 years of operation with a conventional SVE system followed by an ongoing passive SVE using Baroballs^{R} before the rate of removal reached an acceptable asymptotic condition. ERH achieved a similar solvent removal condition in just 12 weeks of operation. The increased cost of power and capital equipment with ERH was more than compensated by the reduction in operating costs.

Table 2. Soil core results

Depth bgs (feet)	Concentration in 2002 (µg/Kg)	Conc. at CRGW-13 in 2006 (µg/Kg)	Conc. at CRGW-14 in 2006 (µg/Kg)
16	6,360	656	25
18	670	427	40
20	5,780	111	29
22	2,220	3	19
24	2,640	0	6
26	45,760	4	2
28	17,630	2	1
30	51,840	4	0
32	310	0	0
34	140	1	0
36	70	0	0
38	NA	0	0
40	5,740	0	0
42	1,030	0	0
44	360	0	0
46	160	0	1
48	NA	1	1
50	3,160	3	1
52	570	3	1
54	340	0	10
56	4,440	10	26
58	NA	20	35
60	2,970	11	22
62	3,940	7	32
64	2,980	NA	60
66	610	2	18
68	0	0	44
70	1,330	20	50
72	3,140	106	399
Average	6,310	50	28
TCE/PCE Removal Efficiency %		99.2	99.5

The ERH design allowed sufficient power to be applied to reach the target temperature within 2 to 3 weeks and hold the temperature at or close to 212 ^{o}F for 30 days, thus meeting the regulatory remedial goals.

The TCE removal efficiency, in excess of 99%, was very high throughout the heating zone, as indicated by the two soil cores. The vacuum implant readings confirmed that negative pressure was sustained throughout the heating zone, despite the highly compacted soils and the possibility of air channeling via the sandy strata, the buried sewer systems and drains.

Despite the presence of electrically conductive underground pipes and drains running through the heating area and the close proximity of the reactor building basement, no significant stray voltages were detected in any metallic components in the vicinity of the project or within the building itself.

6. REFERENCES

Carrigan, C. R. and Nitao, J. J., Predictive and Diagnostic Simulation of In Situ Electrical Heating in Contaminated, Low-Permeability Soils, Environ. Sci. Technol. Vol. 34, No. 22, 2000.

Corbo, P., Atmospheric Fates of Trichloroethylene, Tetrachloroethylene and 1,1,1-Trichloroethane, Savannah River National Laboratory Internal Memorandum, DPST-85-240, February 8, 1985.

Heath, W. O., Roberts, J. S., Lessor, D. L., and Bergsman, T. M., Engineering Scale Up of Electrical Soil Heating for Soil Decontamination, SPECTRUM '92, Boise ID, August 23-27, 1992.

WSRC, 2003. RCRA Facility Investigation/remedial investigation report for the C Area Reactor Groundwater (CRGW) Operable Unit, WSRC-RP-2003-4073, Revision 0, December 2003.

WSRC,2003a. Report on the Effectiveness of the C-Area Burning Rubble Pit
(CBRP) Interim Remedial Action, WSRC-RP-2003-4043, Revision 0, June 2005.

WSRC, 2003b. Interim Action Proposed Plan for the C-Reactor Groundwater
Operable Unit, WSRC-RP-2003-4041, Revision 0, October 2003.

WSRC, 2003c. Rendering and Visualization of C-Reactor Soil Contamination, WSRC-RP-2003-4006, Revision 0, January 2003.

ACKNOWLEDGEMENTS

The authors would like to acknowledge Mr. William Heath of Current Environmental Solutions for valuable consultations on the ERH system design and operation, and also the U.S Department of Energy for funding this work under Contract Number DE-AC09-96SR18500.

Chapter 25

APPLICATION OF ELECTROCHEMICAL TECHNIQUES FOR THE REMEDIATION OF SOILS CONTAMINATED WITH ORGANIC POLLUTANTS

Elisa Ferrarese[§], Gianni Andreottola
Università degli Studi di Trento, Dipartimento di Ingegneria Civile e Ambientale, Via Mesiano 77, I-38050 Trento (TN), Italy

ABSTRACT

Direct Current Technologies (DCTs) are remediation techniques for contaminated soil, in which an electrical field is created in the polluted medium by applying a low-voltage direct current across electrodes placed in the ground. This study aimed at evaluating the feasibility of using DCTs for the remediation of different organic contaminants from various types of fine grain soils and sediments. For this purpose, a one-dimensional experimental setup for bench scale testing was assembled and several laboratory tests were performed. The experimental setup included an electrochemical cell, two stainless steel plate electrodes, a stabilized DC generator and tanks for the pore fluid collection. Two types of soils contaminated by diesel fuel and river sediments polluted by polycyclic aromatic hydrocarbons (PAHs) were considered in the investigation. In the experiments, the contaminant removal was evaluated under the influence of the electric current generated by a constant potential difference (0.5-6 V/cm) for a fixed period of time. The results showed that a high efficiency of organic pollutant removal could be achieved via electrochemical methods. About 90% contaminant removal was achieved for PAH-contaminated sediments after a one month treatment, while the diesel fuel contaminated soils resulted in about 45-55% TOC removal and in 70-85% TPH removal. The main factors influencing the process seem to be the process duration and the soil mineralogy, especially the iron content of the treated medium. On the opposite, the applied voltage seems to have a limited influence on the contaminant removal efficiency, good results being achieved with specific voltages as low as 1 V/cm. The results suggest that DCTs can be effectively used for the mineralization of many organics with low energy expenditure, especially in very fine soils, like clays, which are often more difficult to treat with conventional chemical methods, because of their low permeability and high sorption capacity.

Keywords: Electrochemical remediation, electrooxidation, polycyclic aromatic hydrocarbons, diesel fuel

§ Corresponding Author: Elisa Ferrarese, Università degli Studi di Trento, Dipartimento di Ingegneria Civile e Ambientale, Via Mesiano 77, I-38050 Trento (TN), Italy, Tel: +39 0461 88263, Email: elisa.ferrarese@ing.unitn.it

1. INTRODUCTION

The remediation of fine grain soils contaminated with sorbed organic pollutants is as far as today a challenging task. Despite the fact that many techniques have been developed to remediate contaminated soils, sediments and groundwater, it is still difficult to remove hydrophobic organic compounds (HOCs), which are often strongly sorbed onto soil particles. These pollutants are in fact difficult to remove by biological methods, while the low permeability of clayed soils limits the applicability of flushing and chemical oxidation. On the other hand, conventional ex situ methods, as the disposal in sanitary landfill or incineration are discouraged because they are very expensive and may represent a source of air pollution. Electrochemical treatments are emerging technologies for the in situ or ex situ remediation of fine grain soils: they seem amenably applicable especially for silts and clays, in which the low permeability constrains the applicability of conventional remediation techniques.

1.1 Electrochemical Oxidation

The base method for the current research, the electrochemical oxidation, is a branch of Direct Current Technologies (DCTs), which are remediation techniques for contaminated soils, in which an electrical field is created in the polluted medium by applying a low-voltage direct current (DC) to electrodes placed in the ground. Usually, for real scale in situ DCT applications, the applied electric current density is of the order of milliamperes per square centimeter (1 mA/cm^2) and the electric potential difference is on the order of a few volts per centimeter across the electrodes (1 V/cm) (Van Cauwenberghe, 1997; USAEC, 2000; Chung and Kamon, 2005; Reddy et al., 2006).

At first, DCTs were used mainly for the remediation of metals, radionuclides and polar inorganic pollutants from soil and groundwater, the method being named electrokinetic remediation. Many researchers demonstrated the feasibility of electrokinetic remediation for many hazardous inorganic pollutants, as lead, chromium, copper, zinc and cadmium (Acar et al., 1995; Puppala et al., 1997; Chung and Kamon, 2005; Zhou et al., 2005; Reddy et al., 2006; Lynch et al., 2007). In recent years, research has been developed about DCTs and their effectiveness in the removal of organic pollutants, such as polycyclic aromatic hydrocarbons (PAHs) and chlorinated solvents, from soils and sediments (Röhrs et al., 2002 ; ECP, 2003; Chung and Kamon, 2005; Reddy et al., 2006; Isosaari et al., 2007; Szpyrkowicz et al., 2007 ; Zheng et al., 2007). These studies seem to suggest that DCTs can be effectively used for the mineralization of many organics, with lower energy expenditure than traditional electrokinetic methods (Acar et al., 1995). Empirical evidences indicate that the reaction rates are inversely proportional to grain size (Acar et al., 1995), such that this remediation technique is particularly effective in saturated low permeability soils (like clays and silts), which are often more difficult to treat with conventional remediation methods, such as chemical oxidation or soil flushing, because of their low permeability and their high sorption capacity.

The application of an electrical field to a soil environment has several complex physical and chemical effects that involve soil particles, water and contaminants. The most important electrochemical phenomena are electrolysis, electroosmosis, electromigration, electrophoresis, changes in soil pH and geochemical reactions (Acar et al., 1995; Puppala et al., 1997; USAEC,

2000; Rahner et al., 2002; Alshawabkeh et al., 2004; Chung and Kamon, 2005; Reddy et al., 2006). On the whole, the processes induced by electric field can be distinguished into two categories: electrokinetic transport (including electroosmosis, electromigration and electrophoresis), and electrochemically induced chemical reactions within the soil matrix (Rahner et al., 2002), responsible of the destruction of immobile organic contaminants.

Under the influence of the electrical field, water electrolysis reactions take place at the electrodes, also resulting in pH changes: oxidation of water occurs at the anode and generates hydrogen ions (H^+). On the opposite, reduction of water occurs at the cathode and generates hydroxyls ions (OH^-). The hydrogen ions H^+ generated at the anode create an acid front which moves towards the cathode, while hydroxyls ions OH^- generated at the cathode create a base front which moves towards the anode (Acar et al., 1995; USEPA, 2004; Chung and Kamon, 2005; Reddy et al., 2006). Since the transport of H^+ is faster than the transport of OH^- the acid front moves faster (approximately two times faster) than the base front; unless the H^+ transport is not retarded by the soil buffering capacity, this difference in the fronts' moving rates leads to an acidification of the soil between the electrodes (Acar et al., 1995; Puppala et al., 1997; USAEC, 2000). The migration of the acid and basic front also depends on the buffering capacity of the soil, which may neutralize H^+ or OH^- ions (Reddy et al., 2006).

Electroosmosis is a bulk transport of water, which flows through the soil as a result of the applied electrical field (Acar et al., 1995; USAEC, 2000; Chung and Kamon, 2005, Reddy et al., 2006; Lynch et al., 2007). The electric field causes fluids to flow from the anode compartment to the cathode compartment, producing a flow, called electroosmotic flow, and forcing the water table to arise in the cathode compartment (Acar et al., 1995). Electrophoresis consists in a movement of charged particles under the influence of an electrical field, as a result of Lorentz force: cations, like most of metals, tend to migrate towards the cathode and anions tend to migrate towards the anode. Electromigration is the transport of particles induced by the gradual movement of the ions (electrophoresis) due to the momentum transfer between charged particles and nearby particles. Because of electrophoresis and electromigration (the whole process being often named as electroosmotic transport), ions tend to concentrate near the opposite charged electrode (Acar et al., 1995; Alshawabkeh et al., 2004; USAEC, 2000; Chung and Kamon, 2005; Reddy et al., 2006); this process is the principle of electrokinetic remediation. The electroosmotic transport depends on many parameters, including the soil pH, the zeta potential, the soil activity coefficient and the ionic concentration (Lynch et al., 2007). In particular the pH changes, regulated by water electrolysis, play an important role in contaminant migration, since they can influence metal solubility and mobility in the soil (Acar et al., 1995). Since neutral or acid pH may favor the metal migration and prevent metal precipitation (Lynch et al., 2007), the electrokinetic remediation is commonly enhanced by the addition of conditioning agents to adjust the soil pH. Various reactions involving ions can occur nearby the electrodes; for example, metals ions can be plated onto the electrodes (electrodeposition), or can precipitate or co-precipitate, while gaseous compounds can be liberated (USAEC, 2000).

As far as the geochemical reactions are concerned, during the electrochemical treatment of a contaminated soil, the soil-pore water system can be considered as an electrochemical cell, in which oxidation and reduction reactions occur. Water electrolysis provides the partners for redox reactions. In an electrochemical cell, hydrogen peroxide (H_2O_2) can be produced as a result of redox reactions, and in particular by the reduction of O_2 from air at the cathode (Da Pozzo et al.,

2005; Meinero and Zerbinati, 2006; Laine and Cheng, 2007), according to the following reaction:

$$O_2 + 2H^+ + 2e^- \rightarrow H_2O_2 \quad (1)$$

In soils, redox reactions are supposed to occur not only nearby the electrodes as in a traditional electrochemical cell, but also simultaneously at any and all interfaces between soil and pore water, thus leading to a contaminant removal within the treated medium. In fact, according to the "microconductor principle" (Rahner et al., 2002), electrochemical reactions can be induced within the soil matrix if the soil contains particles of films with electronic conducting properties (microconductors). In the presence of microconductors, the electric current can induce the wet soil to act as a diluted electrochemical solid bed reactor and allow the occurrence of the redox processes.

The microconductors that can be found in soils are mainly weathering products of rocks and minerals, such as fine particles or films of iron, manganese or titanium compounds, carbonaceous particles and humic substances (Rahner et al., 2002). Their occurrence, abundance and distribution depend on the soil type and origin. When an electric filed is applied to a soil, the microconductors are polarized and may act as microelectrodes (both monopolar or bipolar microelectrodes), able to induce redox reactions in their vicinity (Rahner et al., 2002). The composition, size, electronic conductivity and electrochemical activity of microconductors may vary from type to type. For example, among iron compounds, graphite was found to be able to enhance redox reactions, as wells as iron ions, while magnetite seems inactive (Rahner et al., 2002). The reactions that are induced by the microconductors depend on the nature of the contaminant, on the nature of the microconductor itself, and on the characteristics of the electrolyte solution (such as the solution pH), which may enhance or constrain the redox reactions. Therefore, the degradation of organic contaminants depends on the occurrence of the suitable microconductors in combination with a proper redox system (Rahner et al., 2002). Also, the prediction of the degradation products is difficult since they can include a large number of by-products and reaction intermediates, some of which may be mobile and be influenced by the electrokinetic processes, besides the geochemical reactions.

Since soils commonly contain significant amounts of iron, once hydrogen peroxide has been created (reaction (1)), hydroxyl radical ($^{\bullet}OH$) can be produced, according to the Fenton's reaction:

$$Fe^{2+} + H_2O_2 + H^+ \rightarrow Fe^{3+} + H_2O + {}^{\bullet}OH \quad (2)$$

This catalytic reaction is propagated by the Fe^{3+} reduction, which leads to the Fe^{2+} regeneration, which is enhanced by the electrochemical process itself (Meinero and Zerbinati, 2006). Hydroxyl radicals are strong non-selective oxidant agents (standard oxidation potential about 2.8 V) that are able to react with most organic pollutants (Watts et al., 2002; ITRC, 2005; Rivas, 2006), and they are considered the main entities responsible for the organic matter mineralization. In fact, this radical-based redox process (also addressed as indirect oxidation) seem the most probable mineralization mechanism for electrooxidation, as the alternative pathway (i.e. the direct oxidation or reduction at the soil microconductor surface) may be

effective on mobile contaminants, but seems unlikely for immobile organic pollutants due to its very high activation energies of the reactions involved (Rahner et al., 2002).

It must be pointed out that since the pore fluid plays a very important role in all electrochemical processes, the presence of a pore fluid in soil pores is required in order for the electrochemical remediation to be effective, both to conduct the electric field and to transport target species across the soil mass (Acar et al., 1995). Moreover, the soil must be wet to keep the resistance low and provide significant currents flowing (Röhrs et al., 2002). Theoretically, it may be possible to saturate a partially saturated soil by electroosmotic flux of the pore fluid, but this process must be carefully engineered and controlled (Acar et al., 1995).

Different configurations can be used for real scale outdoor applications of DCTs. The electrodes can be made of different materials such as stainless steel or carbon, and they can be placed in the soil either in a vertical or horizontal array. A significant interest in the effectiveness of different electrode materials has recently arisen for the application of electrochemical remediation techniques, especially in aqueous systems, as groundwater and wastewater treatment, with the use of platinum, PbO_2, titanium compounds, boron doped diamond, graphite and ceramics (Röhrs et al., 2002; Meniero and Zerbinati, 2006; Laine and Cheng, 2007). Nevertheless, since all electrodes in soil remediation applications undergo corrosion, fouling and passivation, the use of low cost materials, as stainless steel or graphite, is commonly preferred for real scale applications.

For in situ electrokinetic applications, the electrodes are usually placed in wells with permeable walls and filled with processing fluid to promote the pollutant extraction (Röhrs et al., 2002), while when electrooxidation is used, the contaminant recovery is not necessary. Usually, a spacing of a few meters between cathodes and anodes is used (Alshawabkeh, 2001). Because of their rather simple setup, electrochemical systems are often considered less environmentally intrusive than traditional chemical remediation methods, such as chemical oxidation or soil flushing (Laine and Cheng, 2007).

When the remediation of heavy metals and radionuclides is performed, the electrokinetic transport is commonly enhanced by flushing the soil with chelating agents, complexing agents or conditioning fluids, i.e. acid solutions which adjust soil pH to promote metal solubilization and transport (Puppala et al., 1997; Alshawabkeh, 2001; Zhou et al., 2005). Solvents, surfactants or cyclodextrins can be used to enhance the mobilization and flushing of apolar organic pollutants (Reddy et al., 2006; Isosaari et al., 2007). Moreover, recent research has shown that direct currents can lead to better contaminant removal than alternate or pulsing currents, probably because alternate currents cause continuous changes in the soil polarization and consume a relatively high energy to discharge or recharge the double layer of soil particles (Röhrs et al., 2002).

In some recent studies traditional chemical oxidation was used in combination with electrochemical methods. Different reactants were tested, including hydrogen peroxide, Fenton's reagent (the method being named electro-Fenton or EK-Fenton), chlorine species or persulfate (Yang and Liu, 2001; Kim et al., 2005; Park et al., 2005; Kim et al., 2006; Isosaari et al., 2007; Szpyrkowicz et al., 2007, Zheng et al., 2007), with good results on different organic contaminants, as chlorinated solvents and PAHs. Significant benefits seems to be possible by

integrating electrokinetic remediation with in situ chemical oxidation, because the electrokinetic treatment is supposed to facilitate oxidant delivery and promote the production of radicals (Isosaari et al., 2007).

To date, there are several examples of application of DCTs to real cases of contamination in Europe and North America (USAEC, 2000; USEPA, 2002; ECP, 2003; USEPA, 2004), but a deep knowledge of the phenomena ruling the remediation process has not been reached yet. In particular, it is not clear what processes play the most important roles in organic mineralization, and what factors can affect the results of this technique. Therefore, at the moment the calibration of the remediation action is mainly based on empirical data and on the results of field preliminary tests. Further investigation is needed to better understand the mechanisms of electrooxidation.

1.2 Research Objectives

This experimental investigation aimed at evaluating the effectiveness of electrochemical oxidation for the remediation of different organic pollutants from fine grain soils and sediments, in case of unenhanced electroremediation, i.e. when the application of the electric field is not supported by the addition of conditioning fluid to adjust soil pH, help contaminant transport or promote soil conductivity.

Other objectives of the study were to assess the most important design parameters that can affect the system's efficiency (as applied voltage, treatment duration or soil mineralogy) and to understand any link between removal efficiency and macroscopic electrochemical phenomena, as electroosmotic flux and changes in soil pH. A better knowledge of these processes will help to design more efficient and more effective remediation actions.

During the first phase of this experimental investigation, a systematic study was conducted to assess the effects of electrooxidation on fine grain soils contaminated with diesel fuel. Two types of soil were considered in the study: a silty clay (Speswhite kaolin) and a clay, mainly composed of montmorillonite, to evaluate the influence of soil type and mineralogy on the effectiveness of the electrochemical processes. During the second phase of the research, a feasibility study was carried out to assess the applicability of electrochemical oxidation to degrade sorbed PAHs in river sediments, in case of old date contamination. In all the tests performed, the contaminant removal was evaluated under a constant voltage gradient of 0.5-6 V/cm in unenhanced conditions.

The contaminants considered in this study are typical pollutants that derive from petroleum product spills. Diesel fuel is a mixture of hydrocarbon produced from crude oil. It is composed of about 75% saturated hydrocarbons (mainly paraffins) and 25% aromatic hydrocarbons. In this study diesel fuel was chosen as soil contaminant to represent the environmental pollution due to spills of oil and various petroleum products. Oil spills are a frequent source of contamination that may derive from underground fuel leaks, industrial activities or oil refinery. Due to the high occurrence of these events, petroleum spills have contaminated many large areas and are widely recognized as posing a strong environmental threat (Saner et al., 1996; Watts and Dilly, 1996; Curtis and Lammey, 1998; Iturbe et al., 2005; Powell et al., 2007).

PAHs are a group of organic molecules composed of fused benzene rings, classified among HOCs. PAHs are released during the incomplete combustion of coal, petroleum products and wood. Their presence in environmental matrices is of great concern due to their high toxicity, carcinogenic effects and environmental persistence (IARC, 1983; IARC 1984; Wild and Jones, 1995; Harvey, 1997; Henner et al., 1997; Cupyers et al., 1998; Haapea and Tuhkanen, 2006; O'Mahony et al., 2006). A summary of the main physico-chemical properties of the 16 PAH species considered in this study is reported in Table 1.

Table 1. Summary of the main physico-chemical properties of the PAHs considered in this study (Wild and Jones, 1995; Muller, 2002).

PAH specie	Chemical formula	Molecular weight	Partition coefficient Log(Kow)	Number of aromatic rings
naphthalene	$C_{10}H_8$	128,2	3,28	2
acenaphtylene	$C_{12}H_8$	152,2	4,07	2
acenaphtene	$C_{12}H_{10}$	154,2	3,98	3
fluorene	$C_{12}H_{11}$	166,2	4,18	3
phenantrene	$C_{14}H_{10}$	178,2	4,45	3
anthracene	$C_{14}H_{11}$	178,2	4,45	3
fluoranthene	$C_{16}H_{10}$	202,3	4,90	4
pyrene	$C_{16}H_{10}$	202,3	4,88	4
chrysene	$C_{16}H_{12}$	228,2	5,16	4
benzo(a)anthracene	$C_{18}H_{12}$	228,2	5,61	4
benzo(b)fluoranthene	$C_{20}H_{12}$	252,3	6,04	5
benzo(k)fluoranthene	$C_{20}H_{12}$	252,3	6,06	5
benzo(a)pyrene	$C_{20}H_{12}$	252,3	6,06	5
dibenzo(a,h)antracene	$C_{22}H_{14}$	278,4	6,84	6
benzo(g,h,i)perylene	$C_{22}H_{12}$	276,3	6,50	6
indeno(1,2,3-cd)pyrene	$C_{22}H_{13}$	276,3	6,58	6

Several remediation techniques can be applied for the remediation of petroleum products and PAHs from contaminated sites. The bioremediation of many types of hydrocarbons has been well documented by several authors (Luthy et al., 1994; Saner et al., 1996; Curtis and Lammey, 1998; Höhener et al., 1998; Hunkeler et al., 1998; Taylor and Jones, 2001; Namkoong et al., 2002; Rivera-Espinoza and Dendooven, 2004; Sarkar et al., 2006), but the strong hydrophobicity of many hydrocarbons constrains their bioavailability, so that their biologic degradation rates are often too slow for bioremediation to be amenably applied to real scale remediation actions (Luthy et al., 1994; Saner et al., 1996; Taylor Jones, 2001). Moreover, many high-molecular weight hydrocarbons have proven to be recalcitrant to biological degradation (Luthy et al., 1994; Henner et al., 1997; Antizar-Ladislao et al., 2005; Haapea and Tuhkanen; 2006). Among physical and chemical remediation techniques, soil venting is usually ineffective for the remediation of the low volatility hydrocarbons. Chemical oxidation seems to be effective on a wide range of organic pollutants (Watts and Dilly, 1996; Masten and Davies, 1997; Kong et al.,

1998; Watts et al., 2002; Flotron et al., 2005; ITRC, 2005; Haapea and Tuhkanen; 2006; O'Mahony et al., 2006; Rivas, 2006; Bissey et al., 2006), but in saturated fine grain soils its application is constrained by the soil low permeability and by the limited mass transfer of hydrophobic compounds.

A few Authors (Chung and Kamon, 2005; Kim et al., 2005 ; Park et al., 2005 ; Kim et al., 2006; Reddy et al., 2006; Isosaari et al., 2007) have studied the removal of PAHs from soils by electrochemical methods, while the application of electrooxidation to nonhalogenated aliphatic contaminants is still limited. The results of these studies are encouraging, and suggest that PAHs can be effectively removed from clay soils (ECP, 2003; Isosaari et al., 2007), with a removal efficiency dependent on the soil type (Isosaari et al., 2007). Most of these studies investigated the combined effect of electrooxidation and electrokinetic removal, i.e. aimed at removing PAHs by flushing them or by decomposing them by electrochemical oxidation. Despite the fact that PAHs are apolar molecules and do not carry an electric charge, they can in fact be transported with the electroosmotic flux (Reddy et al., 2006; Isosaari et al., 2007). However, the low recovery of organic compounds in the catholyte solution during combined electrokinetic-electrochemical tests suggests that the main part of the pollutant removal was achieved via electrooxidation rather than via electromigration (Röhrs et al., 2002; Reddy et al., 2006; Isosaari et al., 2007).

2. MATERIALS AND METHODS

2.1 Materials

Two types of fine grain soils were used to carry out the experimental investigation on diesel fuel remediation.

The first soil (Speswhite kaolin) could be classified as a silty clay (BSI, 1999), being mainly composed of particles having dimensions ranging between 2 μm and 75 μm (40%) or lower than 2 μm (60%). From a chemical point of view, it was mainly composed by SiO_2 (47%) and Al_2O_3 (38%), its Cation Exchange Capacity (CEC) was 8.3 m_{eq}/100g and its pH was about 6.

The second soil was essentially composed by montmorillonite (65%), the remaining part being quartz (12), mica (12%) and kaolin (11%). The granulometric analysis led to the following results: 2-10 μm 33%, 0.5-2 μm 16%, <0.5 μm 42%, thus the soil could be classified as clay. Also this soil was mainly composed of SiO_2 (58%) and Al_2O_3 (38%); its CEC was 34.2 m_{eq}/100g and its pH was about 10.

In order to assess any influence of the metal content on the system efficiency, the iron and manganese concentrations of the addressed soils were determined. The kaolin proved to be characterized by a iron content about 2794 mg/kg_{SS}, and a manganese content about 34 mg/kg_{SS}. The montmorillonite clay showed a much higher metal content, with an iron concentration of 10180 mg/kg_{SS} and a manganese concentration of 44 mg/kg_{SS}. Before being mixed with diesel fuel, the TOC of the two soils was negligible (about 0.01 mg/kg_{SS} for kaolin and 0.12 mg/kg_{SS} for montmorillonite).

The diesel fuel used in this study was commercially available and was purchased from a gasoline pump at a typical refuel station. To prepare the diesel contaminated soil samples, the soil was at first dried and then spiked with diesel fuel. One kilogram of dry soil was mixed with about 100 mL of diesel fuel. Then the sample was stirred with stainless steel spoons in a glass beaker, to ensure that the contaminants were evenly distributed through the soil. After mixing, the sample was allowed to evaporate for about two weeks. Before the tests, the spiked samples were saturated with demineralized water and allowed to evaporate overnight at room temperature before being inserted in the experimental setup.

Two parameters were used to consider the contaminant content in the soil samples: TPH (total petroleum hydrocarbons), which refers to a family of many petroleum-based hydrocarbons, and TOC (total organic carbon), which represents the whole content of organic substances in the soil samples.

During the second part of the research, the effectiveness of the electrochemical remediation was evaluated for old date PAH-contaminated sediments. The contaminated sediments of concern were collected in a canal in Trento, Italy, which for several decades had experienced industrial wastewater pollution by organic and inorganic compounds, deriving from a coal tar production site (Ferrarese et al., 2007). Several samples (total weight about 10 kg) of fine-grain silty sediments were collected from the first 30-40 cm layer at the bottom of the canal; these samples were then mixed together and mechanically stirred to produce an homogeneous sample.

At first, the collected sediments were characterized and analyzed for BTEX (i.e. aromatic hydrocarbons: benzene, toluene, ethylbenzene, xilene), PAHs, pH, and total organic matter, represented by the value of TOC. Both organic pollutants and natural organic matter occurred in the sediment samples, which proved to be contaminated by PAHs, but not by BTEX, whose presence was detected just in traces. The initial total PAH concentration in sediment samples was about 1090 mg/kg$_{SS}$ (light PAHs about 731 mg/kg$_{SS}$, heavy PAHs about 359 mg/kg$_{SS}$) and a 90% degradation was required to meet the remediation goals. The initial PAH concentrations in the samples may vary because the pollutant content of the sediments was not homogeneous. The TOC content was about 99 g/kg$_{SS}$ and the sediment pH was about 7.8. The sediments also showed a significant metal content, with a total iron concentration about 30621 mg/KgSS and a manganese content about 614 mg/kgSS.

2.2 Experimental Apparatus and Procedure

In order to conduct the experimental investigation, a one-dimensional experimental setup for bench scale testing was developed and several laboratory tests were performed.

The setup (Figure 1) consisted in a rectangular reactor (10 cm wide, 10 cm high and 50 cm long, made up of 10 mm thick transparent PVC), a pair of electrodes, a stabilized DC power supply (Mitek MICP 3005S-2, providing up to 60 V and up to 5 A), and tanks for the pore fluid collection at both electrode compartments. In this system, the soil specimen was 10 cm wide, 10 cm high and its length could be varied from 2 cm to 50 cm by changing the position of the electrodes. The electrodes were rectangular plates (10 cm by 10 cm) made up of stainless steel with holes to allow the pore fluid to flow across them. After positioning the electrodes in the

setup, the space between them was filled with the contaminated soil. The soil was compacted to achieve the same density of natural soils (about 2 kg/L) and trying to avoid leaving cavities in the specimen. Filter papers were inserted between the electrodes and the soil. The setup was also equipped with a digital multimeter (ISO-Tech IDM 207, with the data logging software ISO-Tech 300 Virtual DMM) for continuous current monitoring, a scale (Sartorius GW6206 Gold Scale) which allowed the monitoring of the electroosmotic flux and a pc for data logging.

A list of the tests performed during the experimental investigation is given in Table 2. During each experiment, a soil sample was placed in the experimental setup, and a constant electric potential was applied across it for a fixed period of time. At the end of the trial, the soil specimen was removed from the test setup and transversally sliced into five segments. Each segment was analyzed for soil moisture content, pH and contaminant concentrations, in order to assess the extent of electrochemical reactions at different distances from the electrodes and the eventual contribution of electromigration. Equal parts of these segments were mixed together to produce a final homogeneous sample, representing the whole specimen. The setup also allowed us to open the reaction cell to measure soil pH and to collect samples while the tests were in progress: during all tests except for test 5, samples were collected once a week from the upper part of the soil specimen, to assess the extent of the oxidation process. During each test, other physical parameters were recorded, including the electroosmotic flux, voltage, and current.

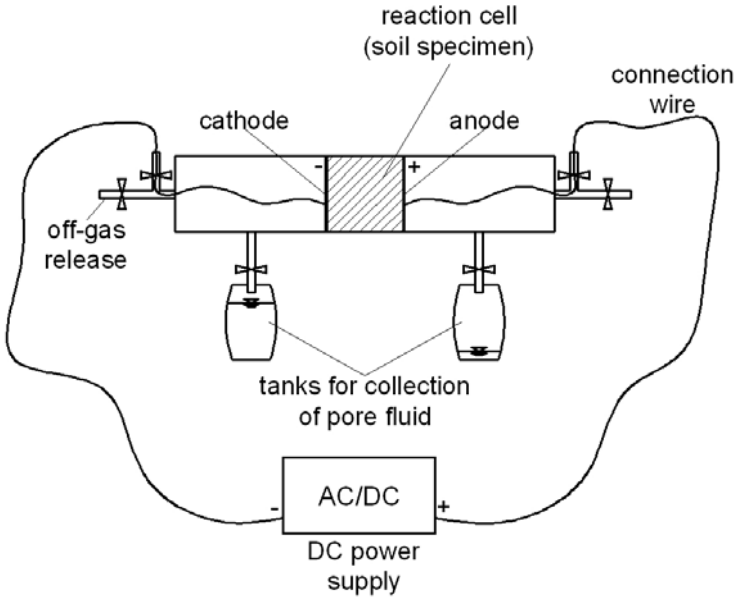

Figure 1. Scheme of the test setup used in the experimental investigation.

Table 2. List of the laboratory tests performed.

Test	Matrix	Contaminant	Sample lenght [cm]	Applied voltage [V]	Specfic voltage [V/cm]	Duration [d]
1	kaolin	diesel fuel	10	5	0.5	28
2	kaolin	diesel fuel	10	10	1	28
3	kaolin	diesel fuel	10	30	3	28
4	kaolin	diesel fuel	10	60	6	28
5	kaolin	diesel fuel	50	50	1	28
6	montmorilonite	diesel fuel	10	5	0.5	28
7	montmorilonite	diesel fuel	10	10	1	28
8	sediments	PAHs	10	15	1.5	14
9	sediments	PAHs	10	10	1	28
10	sediments	PAHs	10	20	2	28

All the tests were performed at room temperature and were unenhanced, i.e. no conditioning fluid was dosed at the electrode compartments to improve the soil conductivity, to adjust the soil pH or to promote contaminant migration. Moreover, no hydraulic gradient was applied across the electrodes.

Four trials (tests 1, 2, 3 and 4) were performed on contaminated kaolin samples (the specimens being 2 kg ,10 cm long, 10 cm high and 10 cm wide), with test duration of 4 weeks (28 days), and constant voltages of 5, 10, 30 and 60 V respectively (specific voltages 0.5, 1, 3 and 6 V/cm). The recorded initial current densities were about 0.1-1 mA/cm^2 and the flowing current tended to decrease with time after an initial increase. Another test (test 5) was performed on contaminated kaolin to assess the treatment efficiency in case of larger soil specimen. In this test, the soil specimen had a length of 50 cm, with a cross section of 100 cm^2 (10 cm by 10 cm), and it was tested under a constant voltage gradient of 50 V (1 V/cm) for 4 weeks.

Two tests were performed on diesel contaminated montmorillonite (tests 6 and 7), each one on a soil specimen having dimensions of 10 cm x 10 cm x 10 cm. Both tests lasted for 4 weeks and the voltages applied were 5 and 10 V respectively (0.5 and 1 V/cm).

During tests 1, 2, 3, 6 and 7, samples were also collected from the soil specimen at different times (7, 14 and 21 days after the beginning of the trial) during the test, so as to assess the extent of the electrochemical reactions with time.

The tests on PAH-contaminated sediments (tests 8, 9 and 10) were performed on specimens having dimensions of 10 cm in length, 10 cm in height and 10 cm in width, with a mass of about 2 kg. The sediment samples were saturated with demineralized water and carefully stirred before being inserted in the electrochemical cell. During test 8, a sample of sediments was tested under a constant voltage of 15 V (specific voltage 1.5 V/cm) for 14 days. In tests 9 (1 V/cm) and 10 (2 V/cm) samples were tested for 4 weeks. The PAH volatilization was evaluated during test 8, while ecotoxicity tests were carried out on the sediment samples before and after tests 9 and 10.

3. ANALYSIS

The TOC content was determined by IR analysis of thermal induced carbon dioxide with a TOC Analyzer Shimadzu TOC-V CSH, after heating the sample at 900°C with a Shimadzu Solid Sample Module.

The TPH content was determined by gravimetric method after pollutant extraction by sonication and solvent addition. To perform the analysis, a soil sample (mass about 5 g) was carefully weighted and mixed with anhydrous sodium sulfate to eliminate soil humidity. The sample was extracted by sonication for 15 min, then 10 mL of solvent (HPLC grade n-esane) were added to it. About 5 mL of the obtained solvent were collected and cleaned-up on a Florisil tube. The solvent sample was transferred into a pre-weighted vial, it was allowed to evaporate and the vial was weighted. The TPH content was determined from the difference between the initial and final weight of the vial.

As for PAH detection in sediment samples, in order to achieve a good resolution both for light and for heavy PAH species, light PAH concentrations in sediments samples were determined with analysis by gas chromatography (GC) and heavy PAH concentrations were detected by high performance liquid chromatography (HPLC).

As for light PAH detection by GC, the pollutants were at first extracted by sonication and solvent addition (HPLC grade acetonitrile), then a sample of solvent was injected into the gas-chromatograph and analyzed using a Varian 4000 GC/MS. As for heavy PAH detection, the samples were at first extracted by solvent addition (HPLC grade dichloromethane) and filtered on a 0.45 μm filter. The solvent was allowed to evaporate; then an acetonitrile solution (70% HPLC grade acetonitrile and 30% water) was added to the sample. A sample of the obtained solution was injected into the HPLC and analyzed. The HPLC included: auto-sampler Gilson ASPEC XL (solid base extraction), Dionex P680 HPLC Pump, Dionex STH 585 Column Oven, HPLC detector Dionex UVD 340U (diode array). A Supelco-SIL LC-PAH column (520 mm × 4.6 mm i.d., 5 μm particle size) was used for PAH detection. The setups were tested before analyzing the samples; external standards were used for HPLC calibration, while internal standards were used for GC calibration. The extraction efficiencies were about 85% both for HPLC and for GC.

BTEX concentrations were determined through purge and trap extraction followed by gas chromatographic analysis with VARIAN 4000 GC/MS.

To detect the contaminant content in the samples, the solid and liquid phases were extracted together, so as to take into account all pollutants in the samples.

Metal (iron and manganese) contents were determined by inductively coupled plasma (ICP): the samples were at first mineralized according to method EPA 3051: a sample of soil having a mass about 1 g (carefully weighted) was mixed with 10 mL of demineralized water and 8 mL of nitric acid in a closed teflon bottle. The sample was then mineralized in a microwave oven at 180°C for 20 minutes and allowed to cool. A certain volume of demineralized water was added so as the final sample volume was exactly 100 mL and the sample was passed thought a 0.45 μm filter. Then the sample was analyzed according to the method APAT IRSA-CNR 3020 using a

VARIAN ICP-OES VISTA. Before the analysis, the setup was calibrated using five external standards and one internal standard.

The ecotoxicity tests on PAH-contaminated sediment samples were performed according to the international standard methods ISO 113348-3:1998(E) "Water quality – determination of the inhibitory effect of water samples on the light emission of Vibrio fischeri (Luminescent bacteria test)", using a Microbics Mictrotox 500. Each test was conducted on a soil sample having a mass of 7 g diluted with 35 mL of demineralized water; after stirring the sample for 10 minutes, sub-samples were collected to evaluate the sediment toxicity at different dilution rates.

The pH was taken in a soil/water suspension using a pH-meter, the HI 99121 by Hanna Instruments, with HI 1292D electrode for soil pH measurement. The same instrument was also used to measure soil and water temperature.

4. RESULTS AND DISCUSSION

The results of the tests performed are presented as follows. For the diesel contaminated soils (kaolin and montmorillonite), the influence of electric current, electroosmotic flow, soil pH and moisture content are also discussed.

4.1 Electric Current Densities

The electric current was monitored at regular time intervals during the tests. As shown in Figure 2, in all tests the current started to decrease rapidly after the application of the voltage gradient and reached a steady state value a few days after the beginning of the tests. In the experiments performed with diesel contaminated kaolin (tests 1-4), the initial values of the electric current ranged from 16 mA to 150 mA, while at the steady state the current was about 1-9 mA. During test 5, which was performed on a 50 cm-long kaolin specimen, the maximum current value, about 17 mA, was achieved after a one-day test, then the current gradually decreased and at the steady state it was lower than 0.01 mA. When the montmorillonite was tested (trails 6 and 7), the values of the electric current were much lower than those registered with kaolin, the initial values ranging from 3 mA to 6 mA, with steady state values about 0.05-0.6 mA.

Commonly in electrochemical and electrokinetic tests the current is found to be decreasing with time. In fact, the capacitive current decreases to zero at the steady state. Moreover, the metal oxide and hydroxide precipitation reduces the number of ions and of microconductors available to carry the charge and increases the soil electric resistance (Rahner et al., 2002; Röhrs et al., 2002; Lynch et al., 2007). Current densities can also be affected by changes in soil pH, which influence chemical precipitations and dissolutions, so that unless conditioning agents are used to adjust soil pH to low values and to provide new ions as charge carriers, the soil resistivity increases and the current decreases with time (Reddy et al., 2006). In the tests performed the measured electric currents are thought to be so low because the tests were unenhanced, i.e. no

buffer solution was added to increase the ion concentration. It is expected that if a ion solution had been added to the system, the current would have increased (Isosaari et al., 2007).

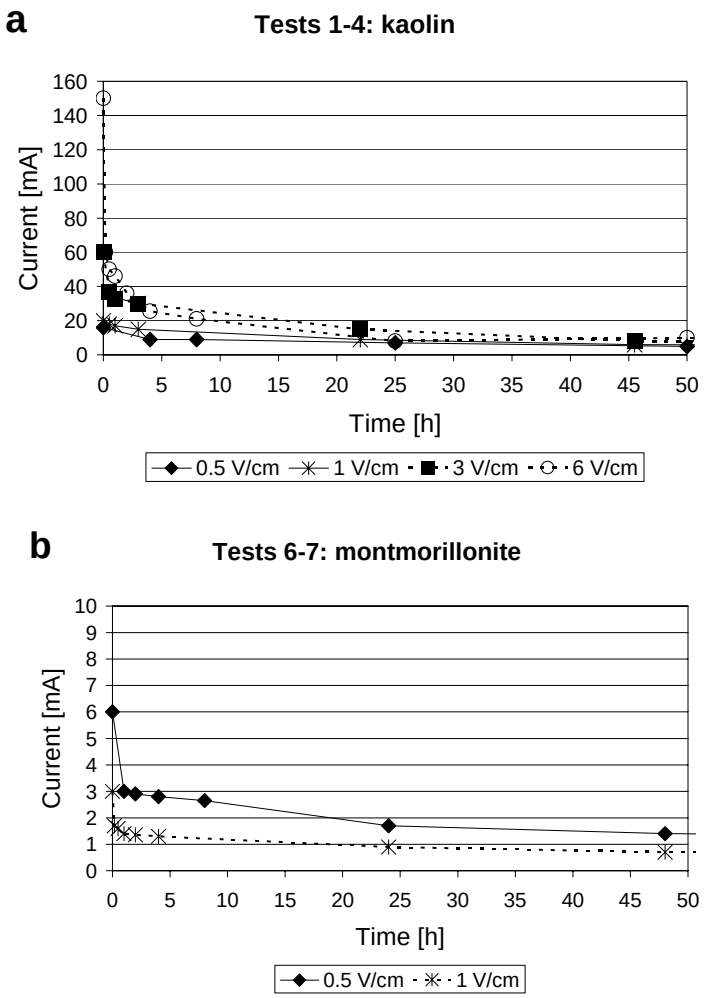

Figure 2. Current densities measured during the first hours in the tests with diesel contaminated kaolin (a) and montmorillonite (b).

From the values of voltage and current, it was possible to make an approximate estimation of the energy consumption required for a remediation action. To calculate the energy expenditure, the current was modeled as an exponential function of time with a constant component at the steady state. The following function was used to model the current:

$$i = (i_0 - i_{ss}) \cdot \exp(-t/\tau) + i_{ss} \quad (3)$$

where i_0 is the initial current, i_{ss} is the current at the steady state, t is time and τ is a time constant. For kaolin tests (the soil samples having a volume of about 1 L and a mass about 2 kg) the estimated energy expenditure increased with the applied voltage, ranging from 17 kJ (test 1)

to 1933 kJ (test 4), while the maximum applied power (corresponding to the maximum current) was about 0.08-9.0 W.

For montmorillonite, the energy expenses were lower since the applied currents were lower than for kaolin: in these cases the energy expenditure was about 3.5-7.6 kJ, with maximum required powers of 0.015-0.6 W.

Thus, according to the results achieved, the process seems to require a low energy expenditure, being the current densities applied very low (< 0.01-1 mA/cm^2).

4.2 Electroosmotic Flux

During the experiments performed with kaolin, an electroosmotic flux occurred when the intensity of the electric current was appreciable (e.g. for current of the order of magnitude of 10 mA or above). As during the tests the electric current showed to start to decrease a few hours after the beginning of the tests, the electroosmotic flux, when occurring, was appreciable only in the first days of treatment, and became negligible afterwards. The electroosmotic flow has already been reported to decrease rapidly with time, especially when no ionic solution is added to the soil and the resulting current is weak (Reddy et al., 2006; Isosaari et al., 2007).

When kaolin was tested, the volume of the pore fluid collected at cathode compartment was limited, about 7 mL, 42 mL, 22 mL, 13 mL and 11 mL for tests 1, 2, 3, 4 and 5 respectively, with no clear dependence on the applied voltage. In both the tests performed with montmorillonite, the electroosmotic flux was negligible, as the current densities were lower than for kaolin, being about 3-6 mA at the beginning of the trials and lower than 2 mA after a one-day treatment. However, since a good contaminant removal was achieved during the tests (see section 3.4), the occurrence of the electroosmotic flux does not seem to be necessary to achieve a significant mineralization of the organic pollutants, although the electroosmotic flux was previously considered necessary to provide fresh water for electrolysis and for further redox reactions (Röhrs et al., 2002).

4.3 Soil pH Profiles and Soil Moisture

During the tests performed, the soil pH tended to increase at the cathode and to decrease at the anode (Figure 3) as a result of water hydrolysis, which leads to the production of an acid front moving from the anode toward the cathode and a base front moving from the cathode toward the anode. This effect was particularly evident in the tests performed with kaolin, for which the initial pH (about 6) gradually changed to about 3-4 nearby the anode and to about 8-10 near the cathode a few days after the beginning of the tests. For longer test duration (e.g. 2-4 weeks), all the soil volume tended to be acidified, because of the acid front moving across the soil form the anode towards the cathode. This evidence was stronger for high specific voltages (i.e. 3-6 V/cm) rather than lower voltages (0.5-1 V/cm). When the electroosmotic flow occurred, the fluid collected at cathode compartment was slightly acidic, with pH ranging from 6.2 to 6.7.

As for montmorillonite (initial pH about 10), the pH variations were very limited, because of the high buffer capacity of this type of soil.

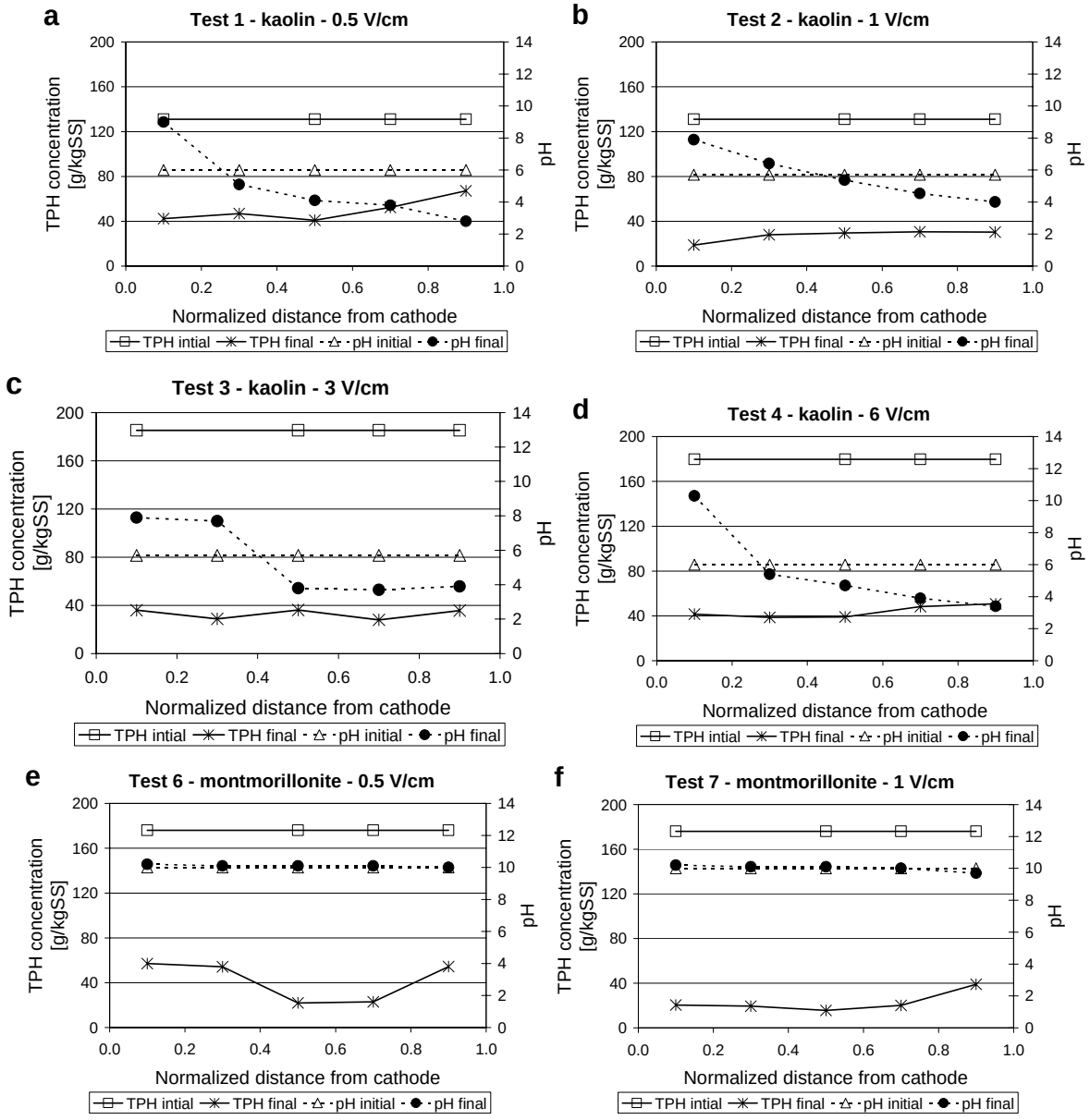

Figure 3. Results of the tests performed on diesel-contaminated soils: pH and TPH concentration at different distances from the electrodes at the beginning and at the end (4 weeks) of the tests performed on kaolin (a, b, c and d) and montmorillonite (e and f).

The soil humidity at the beginning of the tests was about 37% for kaolin and 38% for montmorillonite. Despite the fact that no fluid was provided at the electrodes, the soil did not dry out. The final water content near the anode ranged from 33% to 34% for kaolin, from 37% to

38%, and for montmorillonite, with even slightly higher moisture contents in other sections. On the whole, the soil moisture content remained fairly constant and comparable to the initial water content.

Occasional monitoring of soil temperature did not show any changes, which were however not expected, since an increase in soil temperature have been reported to occur as a consequence of electric processes only when higher currents are flowing (Isosaari et al., 2007).

The soil slightly compacted near the anode at the end of the tests. This effect has already been observed in previous studies (Isosaari et al., 2007). Moreover, a change in the oxidation state of iron and probably other metals was observed near the anode, so that after a few weeks from the beginning of the test, some clogging proved to occur near this electrode. The soil also changed to a yellow-orange color, probably because of the formation of iron hydroxides from the soil natural iron content; a further iron supply deriving form the anode corrosion is also possible (Röhrs et al., 2002). The formation of iron oxides or oxohydrates has already been reported to occur and to be able to block the electrode surface, resulting in a decrease of the flowing current (Rahner et al., 2002). Sometimes complexing or conditioning agents are used to retard the electrode fouling and to increase the current flow.

4.4 Diesel Fuel Remediation

The main results of the tests performed on diesel-contaminated kaolin are reported in Table 3 and in Figure 4. As can be seen from the data shown, the TPH removal after 28 days of treatment increased significantly as the applied voltage increased form 0.5 V/cm to 1 V/cm, ranging from 66% in test 1 to 80% in test 2. As the voltage increased to 3 V/cm (test 3), the TPH removal slightly increased to 85%. During test 4 (6 V/cm) the removal efficiency was even lower than for tests 2 and 3: this is thought to be due to sample heterogeneity, and the result achieved in test 4 with 6 V/cm can be considered of the same order of magnitude of the results of tests 2 and 3. During these tests, the TOC removal also increased from 46% to 54% as the specific voltage increase form 0.5 V/cm to 1 V/cm, but it remained almost constant afterwards.

The fact that the removal efficiency of TOC was always lower than the TPH removal is due to the fact that TOC represents all the organic matter in a soil sample; therefore, it accounts also for the presence of by-products that derive from the degradation of petroleum hydrocarbons, which on the opposite do not appear in the TPH content.

During tests 1, 2 and 3, the increase of the contaminant removal efficiency with time was monitored. As seen in Figure 4, both the TOC and the TPH removal significantly increased with time during the first weeks of treatment. The time dependency was, however, different for different voltages. In fact, when the lowest voltage was applied (i.e. 0.5 V/cm), the contaminant removal gradually increased, so that more than 20 days of treatment were required to achieve a good contaminant removal efficiency (e.g. more than 40% TOC removal and 60% TPH removal). When higher voltages were applied, these remediation performances could be achieved in shorter times, i.e. about 15 days for 1 V/cm and less than 10 days for 3 V/cm. An increase in the applied voltage therefore allowed to achieve a good contaminant removal in shorter times than lower voltages, but this advantage is counterbalanced by the fact that higher

specific voltages (e.g. 3 V/cm or more) result in higher energy expenditure and require more complicated setups for real scale applications.

One additional test (test 5) was performed on diesel-contaminated kaolin to assess treatment efficiencies in case of larger soil specimen. In this test, the soil specimen had a length of 50 cm, with the usual cross section of 100 cm^2 (10 cm by 10 cm). As in test 2, a specific voltage gradient of 1 V/cm was applied for 4 weeks. This test resulted in 49% TOC removal and 89% TPH removal, thus confirming, despite some variability due to sample heterogeneity, the results achieved with the same specific voltage on a smaller soil specimen during test 2.

One test was performed on diesel contaminated kaolin without the applications of electric current, as a reference test to assess any loss of contaminants due to volatilization or other chemical, physical or biological phenomena not linked with the electrochemical processes. The test was performed with the same setup used for the other experiments and lasted for four weeks. At the end of the trial, the soil sample showed a TOC content about 209.7 g/kg_{SS} and a TPH content about 144.5 g/kg_{SS}. The test was conducted in parallel with test 3; therefore, the loss of contaminants during the trail was about 5% for TOC and 22% for TPH, significantly lower than the removal achieved with the electrochemical method (about 54% and 85% respectively).

Table 3. Results of the tests performed on diesel contaminated kaolin: TOC and TOH removals.

Test	**Elapsed time [d]**	**TOC [g/kg_{SS}]**	**TPH [g/kg_{SS}]**	**TOC Removal**	**TPH Removal**
Test 1 - 0.5 V/cm	0	208,1	131,0	-	-
	7	189,9	93,8	9%	28%
	14	183,1	83,7	12%	36%
	21	126,0	70,3	39%	46%
	28	112,3	45,2	46%	66%
Test 2 - 1 V/cm	0	208,1	131,0	-	-
	7	113,6	65,0	45%	50%
	14	109,2	60,3	48%	54%
	21	107,8	30,9	48%	76%
	28	95,5	26,6	54%	80%
Test 3 - 3 V/cm	0	221,1	185,3	-	-
	7	128,9	49,9	42%	-
	14	121,7	43,6	45%	76%
	21	112,1	33,8	49%	82%
	28	101,3	27,4	54%	85%
Test 4 - 6 V/cm	0	185,0	179,8	-	-
	28	84,0	40,3	55%	78%
Test 5 - 1 V/cm	0	133,6	37,4	-	-
	28	94,4	19,2	49%	89%

Two tests were performed on diesel-contaminated montmorillonite (tests 6 and 7): the results achieved are shown in Table 4 and Figure 5.

Since the results obtained with kaolin had showed that good results could be achieved with specific voltages as low as 1 V/cm, only two voltages (5 and 10 V, i.e. 0.5 and 1 V/cm) were tested with diesel-contaminated montmorillonite. The results proved the electrochemical method to be very effective for the remediation of this type of soil. In fact test 6, characterized by a specific voltage of 0.5 V/cm, resulted in 60% TOC removal and 73% TPH removal after a 4 week treatment, while test 7 (1 V/cm) showed even higher performances, with 69% TOC removal and 87% TPH removal after 4 weeks. Similarly to kaolin, the contaminant removal proved to increase significantly with time, and more than two weeks were required to achieve a TOC and TPH removal higher than 50%.

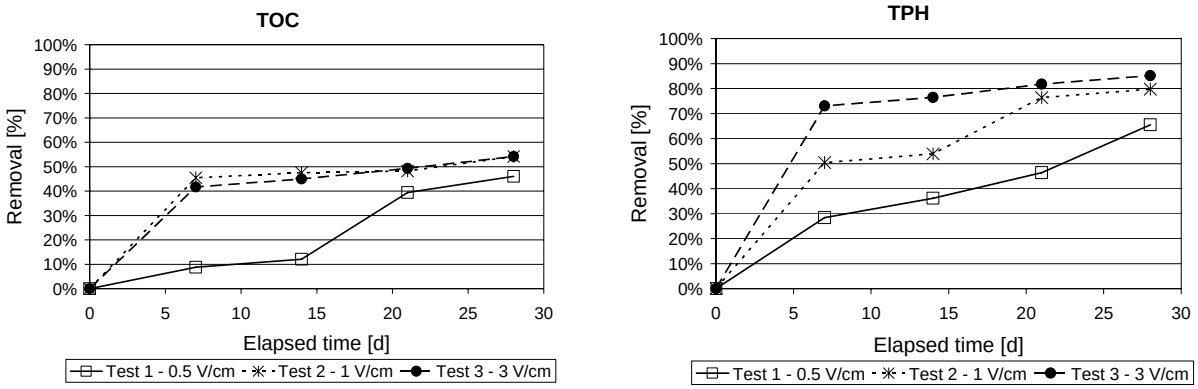

Figure 4. Results of the tests performed on diesel-contaminated kaolin: comparison of the TOC and TPH removal efficiencies achieved during tests 1, 2 and 3.

As can be seen from the data shown in Table 3 and Table 4, the removal efficiencies achieved with montmorillonite were much higher than for kaolin. This difference is not due to a higher conductivity of montmorillonite, which on the opposite showed lower current densities (i.e. a higher electric resistivity) than kaolin. Therefore, these results are thought to be due to the different mineralogy of the two soils considered in this study, and in particular by the higher iron content of montmorillonite than kaolin, which is supposed to have enhanced both the production of H_2O_2 (microconductor effect) and the Fenton-like reactions that lead to the production of hydroxyl radicals, responsible of the oxidation processes.

Table 4. Results of the tests performed on diesel contaminated montmorillonite: TOC and TOH removals.

Test	Elapsed time [d]	TOC [g/kg$_{SS}$]	TPH [g/kg$_{SS}$]	TOC Removal	TPH Removal
Test 6 - 0.5 V/cm	0	264.8	176.0	-	-
	7	-	-	-	-
	14	131.6	102.2	50%	42%
	21	113.4	72.8	57%	59%
	28	107.0	47.0	60%	73%
Test 7 - 1 V/cm	0	264.8	176.0	-	-
	7	184.2	77.0	30%	56%
	14	127.4	71.4	52%	59%
	21	95.5	55.0	64%	69%
	28	81.6	23.0	69%	87%

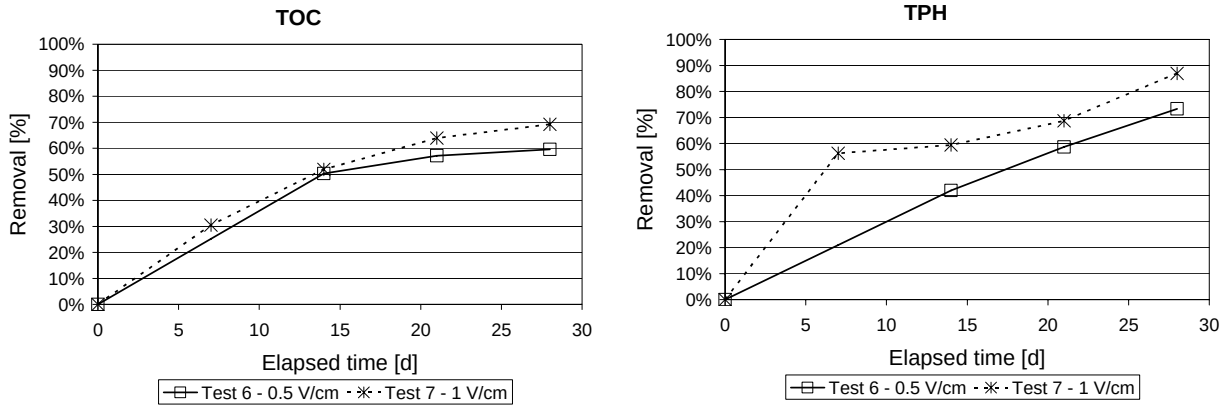

Figure 5. Results of the tests performed on diesel-contaminated montmorillonite: comparison of the TOC and TPH removal efficiencies achieved during tests 6 and 7.

On the whole, the results of the tests performed indicated that a significant oxidation of organic pollutants can be achieved with electrochemical methods. For example, after a 28 day treatment about 50% TOC removal and 60% TPH removal were encountered for kaolin (Table 3), and about 70% TOC removal and 85% TPH removal were reached for montmorillonite (Table 4).

Major conclusions can be drawn from the results achieved. An increase in the applied voltage proved to cause a limited contaminant removal increase, a good removal being encountered for specific voltages as low as 1 V/cm. On the opposite, the contaminant removal seems to increase significantly with process duration. For example, the application of a constant voltage of 1 V/cm to a montmorillonite sample led to 30% TOC decrease after 7 days, but the TOC removal increased to about 70% after 28 days of treatment (Table 4).

The final contaminant concentrations were found to be evenly distributed across the treated sample, as shown in Figure 3. This suggests that the oxidation reactions take place within all the treated volume and not only nearby the electrodes. Moreover the results indicate that the pollutants electromigration during the test performed, which were unenhanced, can be considered negligible.

The pH changes were expected to influence the system efficiency, since a low pH can enhance the Fenton-like reactions, which lead to the production of hydroxyl radicals. However, the mineralization process did not seem to be influenced by pH changes, the contaminant removal being of the same order of magnitude both in areas with low and high pH (Figure 5). On the opposite, the soil mineralogy, and in particular the iron content, seems to affect significantly the treatment results. In fact, the removal efficiency achieved for montmorillonite (iron content about 2794 mg/kg$_{SS}$ and manganese content about 34 mg/kg$_{SS}$) were much higher than for

kaolin, which was characterized by a lower metal content (iron content about 10180 mg/kg_{SS}, manganese content about 44 mg/kg_{SS}), despite the fact that the two soils showed similar current densities, which were even lower for the montmorillonite than for the kaolin. Even if the addition of ferrous ions has been reported not to have any influence on the electric conductivity of the soil, the large reservoir of iron that is present in natural occurring iron-containing minerals is supposed to act as a microconductor source, promoting redox reactions and the formation of H_2O_2 and to enhance the Fenton-like reactions that promote the oxidation processes (Rahner et al., 2002; Isosaari et al., 2007).

4.5 PAH Remediation

This part of the study aimed at investigating the feasibility of using electrochemical oxidation for the remediation of river sediments contaminated by PAHs, in case of old date pollution.

Three tests (tests 8, 9 and 10) were performed to assess the applicability of the electrochemical methods to the contamination of concern and the results achieved are presented in Table 5. To assess the efficiency of the tested treatments, the removal percentages were calculated for single PAH species and of PAH summation, as well as for TOC, which stands for the total amount of the organic matter in the sample, both from natural and anthropogenic origin. The results were also correlated with PAH octanol-water partition coefficient Kow, which represents the lipophilicity of a certain chemical and indicates the tendency of that compound to be sorbed onto organic matter or to dissolve in water.

The first laboratory test performed on PAH-contaminated sediments (test 8) was conducted to assess the effectiveness of electrooxidation in removing the addressed contaminants. During the trial a constant specific voltage of 1.5 V/cm was applied for 14 days. An initial current of 50 mA and a final current of 4 mA were recorded. At the end of the test an 85% total PAH removal was encountered (light PAH removal 90%, heavy PAHs removal 75%), with a final total PAH concentration in the treated sample about 162.8 mg/kg_{SS}. The TOC removal was about 14%. In this case the low values of TOC removal can be considered due to the very high natural organic matter content in the sediment samples. At the end of the test, a part of the soil specimen was transversally sliced into five segments and each segment was analyzed for pH and contaminant concentrations, in order to assess the extent of electrochemical reactions at different distances from the electrodes and the eventual contribution of electromigration.

The values of soil pH and contaminant concentration across the specimen are presented in Figure 6. Despite some variability due to sample heterogeneity, which can be considered a typical feature of PAH contamination, final pollutant concentrations were found to be evenly distributed across the treated sample, both for PAHs and for TOC, without any trend towards the electrodes. The same result had been found for diesel fuel contamination. Other Authors who studied the PAH removal via electrochemical processes reported that PAHs can be transported towards the cathode zone and also be partially removed from soil with the catholyte solution if the occurrence of a sufficient electroosmotic flow is enhanced by the application of sufficient voltages and hydraulic gradients (Chung and Kamon, 2005; Isosaari et al., 2007); however, in this case this effect was not expected because the electroosmotic flux was very limited. In fact, at the end of the trial, 103 mL of pore fluid were found to be accumulated in the tank at the cathode

compartment as a result of the electroosmotic flux. The water collected showed a strongly basic pH (about 9.3), while the TOC content was 525 mg/L. All PAH species were below the detection limit (<0.1 mg/L), showing that no significant transport effect occurred as a result of the electroosmotic flux for the addresses contaminants, which are, indeed, very hydrophobic organic species, with very little water solubilities (Table 1).

As already observed for diesel fuel contaminated soils, during the tests the soil pH tended to increase at the cathode and to decrease at the anode (Figure 6). However, the mineralization process did not seem to be influenced by pH changes, the contaminant removal being evenly distributed both in areas with low and high pH.

During tests 8 the PAH volatilization was estimated. The reactor was kept closed while the test was in progress to avoid vapors diffusing into external air. At the end of the trial, before opening the reactor, the air was sampled onto an ORBO Tube for collecting airborne PAHs. An ORBO-43 (Supelco, Bellefonte, PA) was used for the air sampling and a vacuum pump was used to induce the air flow across the tube (200 mL/min). The ORBO tube was then analyzed by GC to determine the PAH content. The analysis showed that the PAH content in the tube was less than 0.1 mg, so it can be concluded that no significant contaminant loss due to volatilization occurred during the test.

Other two laboratory tests (tests 9 and 10) were performed to assess the influence of the applied voltage (1-2 V/cm) and treatment duration (7, 14, 21, 28 days) on PAH removal efficiency, in order to optimize the remediation conditions. During these tests the initial current values were about 6.5 mA (test 9) and 50 mA (test 10), while at the end of both trials the electric current was below 1 mA. The results achieved are presented in Figure 7.

During test 9, a 72% total PAH removal was encountered 7 days after the beginning of the trial; as the treatment proceeded, the total PAH removal gradually increased to 74% (14 days), 81% (21 days) and 91% at the end of the test, after a 28-day treatment. In the meanwhile, the TOC removal increased from about 2% (7 days) to 8% (14 days), 17% (21 days) and 25% (28 days).

Higher removal efficiencies were encountered during test 10, when a higher specific voltage (2 V/cm) was applied. In this case the total PAH removal efficiency was about 33% after 7 days after the beginning of the treatment, but it rapidly increased to 85% after 14 days, 93% after 21 days and 96% after 28 days. The results achieved in these two latter tests are consistent with the removal efficiencies measured at the end of test 8, with a total PAH removal efficiency about 74-85% after a two-week treatment.

In all the tests performed with PAH-contaminated sediments, the removal efficiency for light PAHs was found to be higher than for the heavy PAHs. This can be considered as a typical behavior of PAHs, whose lighter species are generally more available to reactants than heavy species, which are more hydrophobic and more sorbed onto sediments (Ferrarese et al., 2007; Zheng et al., 2007). For traditional chemical oxidation, the PAH contaminant availability has been well reported to influence the treatment efficiency, the less sorbed pollutants (i.e. the species that are less hydrophobic) being more available for mineralization, while the more hydrophobic and more sorbed molecules proved to be more resistant to oxidation than

Table 5. Results of the tests performed on PAH-contaminated river sediments.

Test		**Test 8 - 1.5 V/cm**		**Test 9 - 1 V/cm**					**Test 10 - 2 V/cm**				
Elapsed time [d]		**0**	**14**	**0**	**7**	**14**	**21**	**28**	**0**	**7**	**14**	**21**	**28**
1 naphthalene	[mg/kg$_{SS}$]	54.1	1.6	55.2	6.2	6.8	4.9	1.3	99.5	36.0	3.9	0.7	<0.1
2 acenaphtylene	[mg/kg$_{SS}$]	1.5	0.2	0.7	0.3	0.1	0.3	0.2	0.6	<0.1	<0.1	<0.1	<0.1
3 acenaftene	[mg/kg$_{SS}$]	101.7	7.2	162.6	29.1	24.8	18.2	6.3	242.2	154.7	22.8	6.3	0.4
4 fluorene	[mg/kg$_{SS}$]	65.4	3.9	78.2	16.6	14.6	10.6	3.9	123.5	92.5	13.8	5.1	3.5
5 phenantrene	[mg/kg$_{SS}$]	278.9	21.5	273.7	72.3	61.7	43.8	19.5	415.8	288.1	56.6	18.0	7.7
6 anthracene	[mg/kg$_{SS}$]	55.7	3.6	47.7	15.1	12.8	8.6	3.8	77.2	49.4	9.8	3.3	0.4
7 fluoranthene	[mg/kg$_{SS}$]	173.4	34.9	275.3	90.9	82.4	63.7	30.2	407.8	303.8	69.6	29.8	7.6
8 pyrene	[mg/kg$_{SS}$]	116.2	21.3	46.4	16.3	17.3	13.5	8.5	52.1	29.2	12.4	9.7	11.8
9 chrysene	[mg/kg$_{SS}$]	45.9	9.9	19.5	7.4	8.0	6.2	3.9	21.8	13.8	5.2	4.5	5.2
10 benzo(a)anthracene	[mg/kg$_{SS}$]	30.0	7.6	16.2	6.0	7.6	4.9	3.0	18.4	13.8	4.4	3.7	4.5
11 benzo(b)fluoranthene	[mg/kg$_{SS}$]	56.8	16.0	19.7	9.3	9.6	8.7	5.4	23.1	14.9	7.4	7.4	7.9
12 benzo(k)fluoranthene	[mg/kg$_{SS}$]	21.2	5.5	7.5	3.3	3.6	2.9	1.8	8.5	5.8	2.5	2.4	2.7
13 benzo(a)pyrene	[mg/kg$_{SS}$]	41.5	11.3	13.4	6.2	7.0	5.7	3.9	16.1	12.3	6.2	5.6	6.0
14 dibenzo(a,h)antracene	[mg/kg$_{SS}$]	3.4	1.0	1.6	0.9	0.8	0.9	0.4	1.7	1.0	0.6	0.5	0.6
15 benzo(g,h,i)perylene	[mg/kg$_{SS}$]	20.7	7.7	7.2	3.9	4.3	4.0	2.6	7.4	4.3	3.4	3.7	3.6
16 indeno(1,2,3-cd)pyrene	[mg/kg$_{SS}$]	22.9	9.6	7.9	4.3	4.2	4.1	2.3	7.3	3.5	3.0	2.9	2.7
Total light PAHs (1-7)	[mg/kg$_{SS}$]	730.7	72.8	893.4	230.6	203.2	150.1	65.1	1366.5	924.5	176.5	63.1	19.5
Total heavy PAHs (8-16)	[mg/kg$_{SS}$]	358.6	89.9	139.4	57.6	62.4	50.8	31.8	156.4	98.6	45.1	40.4	45.0
Total PAHs	[mg/kg$_{SS}$]	1089.3	162.8	1032.8	288.2	265.5	200.9	96.9	1522.9	1023.1	221.5	103.5	64.5
TOC	[g/kg$_{SS}$]	99.0	85.6	88.5	87.1	81.2	73.3	66.2	90.6	78.8	75.1	74.8	70.5
Total light PAH removal	[%]	-	90%	-	74%	77%	83%	93%	-	32%	87%	95%	99%
Total heavy PAH removal	[%]	-	75%	-	59%	55%	64%	77%	-	37%	71%	74%	71%
Total PAH removal	[%]	-	85%	-	72%	74%	81%	91%	-	33%	85%	93%	96%
TOC removal	[%]	-	14%	-	2%	8%	17%	25%	-	13%	17%	17%	22%

contaminants in solution; this difference in the removal efficiency can be overcome by using vigorous oxidation conditions, such as high oxidant dosages (Kakarla et al., 2002; Watts et al., 2002; Bogan and Trbovic, 2003; ITRC, 2005; Watts et al., 2005; Ferrarese et al., 2007).

To highlight this effect, the removal efficiency of different PAH species achieved in tests 9 and 10 was compared to the octanol-water partition coefficient (K_{ow}) (Figure 8). As the K_{ow} coefficient represents the lipophilicity of a certain chemical, it indicates the tendency of that compound to be sorbed onto organic matter or to dissolve in water. The higher the K_{ow} coefficient is, the more the PAHs tend to be sorbed onto organic matter. As shown in Figure 8, the PAH removal efficiency tended to decrease as the value of $Log(K_{ow})$ increases, thus indicating that the removal efficiencies are always higher for light PAH species than for heavy PAHs. This effect has already been observed in previous studies for the electrochemical treatment of PAH-contaminated soils (Isosaari et al., 2007; Zheng et al., 2007). Figure 8 also indicates that as the treatment duration increases, the pollutant removal increases, both for light and heavy PAH species, rising up to 90-99% for light PAHs and about 70-80% for heavy PAHs after a four week treatment.

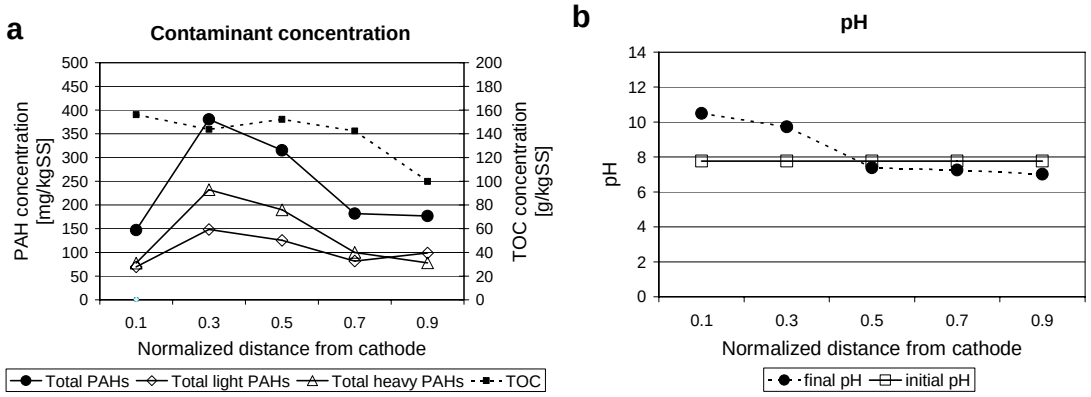

Figure 6. Results of test 8: contaminant concentrations (a) and pH (b) at different distances from the electrodes.

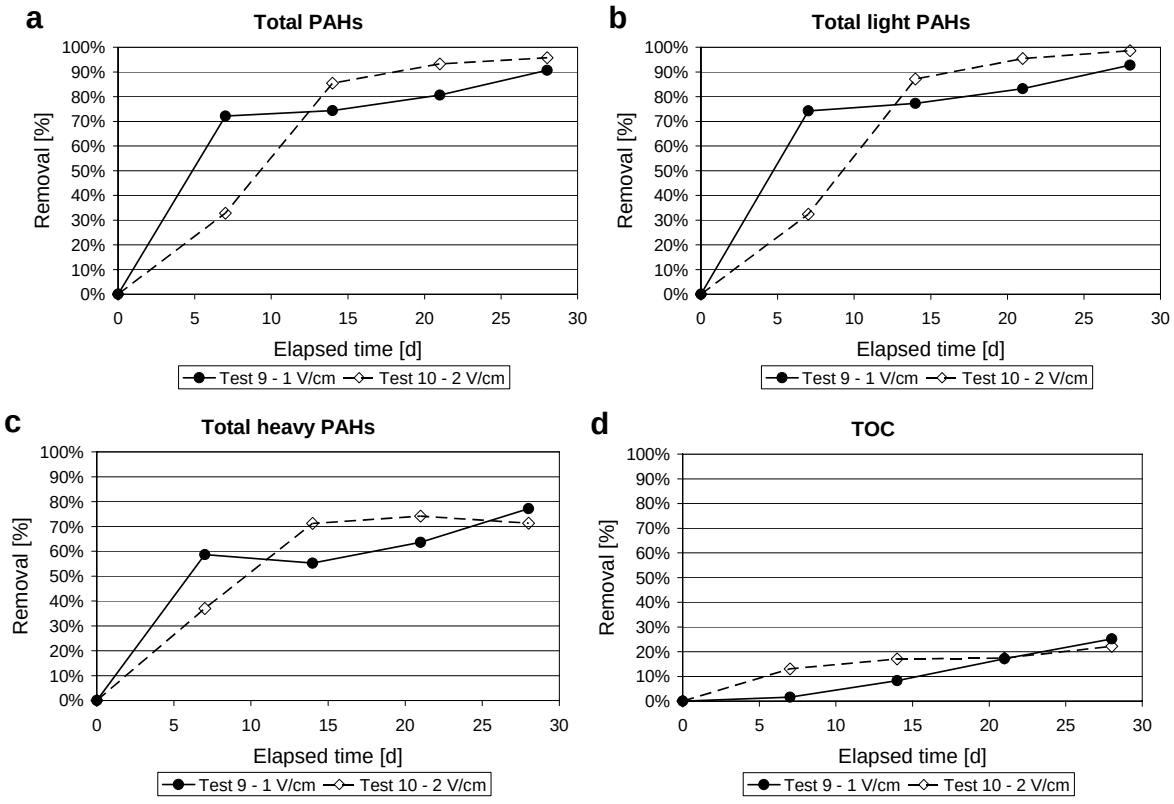

F*igure 7.* Results of tests 9 and 10 performed on PAH-contaminated sediments: comparison of the removal efficiencies achieved for total PAHs, light PAHs, heavy PAHs and TOC.

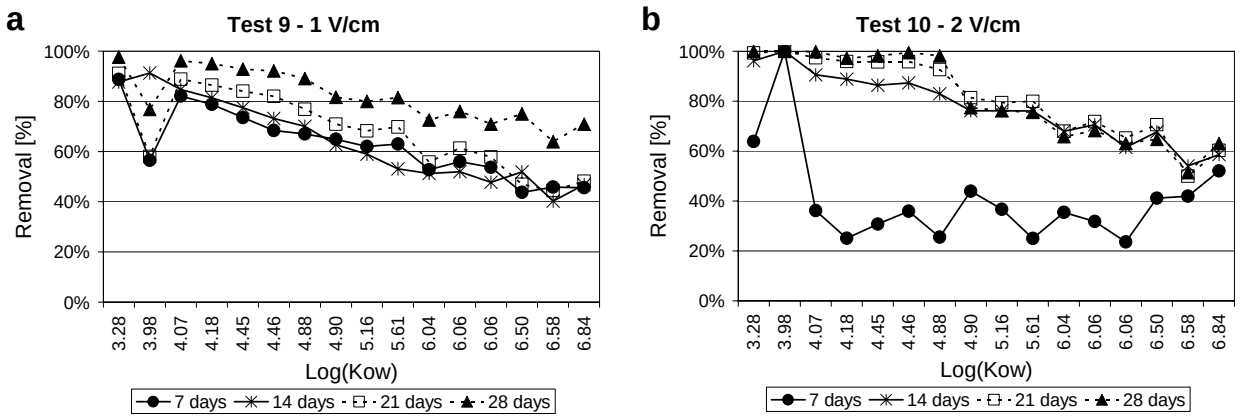

Figure 8. Results of tests 8 and 9: removal efficiencies achieved as a function of PAH ocatnol-water partition coefficient (Kow). Since benzo(a)pyrene and benzo(k)fluoranthene are characterized by the same value of Kow, as weel as phenentrene and anthracene, in the plots only the results for benzo(a)pyrene and for phenantrene are presented.

A problem that may arise during the oxidation of PAH contaminated soils is the risk of incomplete mineralization and the consequent production of degradation by-products, which may be of concern because of the high toxicity of certain species. PAHs are known to create a certain number of degradation intermediates, which commonly include aldehydes, ketones, and quinones as main oxidation by-products (oxy-PAHs) (Watts et al., 2002; Brown et al., 2003; Flotron et al., 2005; Lundstedt et al., 2006; Perraudin et al., 2007). Despite the fact that many compounds are known as single PAH derivatives, a complete identification of all PAH by products has not been achieved yet.

Most of PAH derivatives are known to have polar functional groups, which are likely to enhance not only higher aqueous solubility but also availability for natural biodegradation more than the parental compounds (Brown et al., 2003; Kulik et al., 2006). On the other hand, the fact that in natural soils PAHs are commonly strongly sorbed and incorporated into organic matter is also thought to act as a sort of detoxification process, by reducing their bioavailability and their mass transfer, thus decreasing their toxic effect towards natural microbial community (Richnow et al., 1995; Sun and Yan, 2007). On the other hand this effect is absent in desorbed PAH and PAH derivatives, which may be therefore characterized by a stronger toxic effect than the parental compounds. As a consequence, a remediation action that results in the desorption of PAH molecules without achieving a complete mineralization can even lead to an increase in the toxic effect towards the natural biota, rather than reducing it.

In this study, the identity of the oxidation reaction by-products has not been determined, but the ecotoxicity of the original and final samples has been evaluated in the last experiments (tests 9 and 10), to assess any change in the toxic effect of the sediments toward the local biota. The original untreated sample showed a toxic effect of 0.23 TU50, while the toxic effect in both the treated samples was below the detection limit. These results indicate that the toxic effect of the original sediments was not very high; this is attributed to the fact that PAHs are strongly sorbed onto sediments and do not tend to solubilize in water (Ferrarese et al., 2007). This limits their

mass transfer and their bioavailability, also preventing them to have a strong toxic effect (Luthy et al., 1994; Taylor and Jones, 2001). Since the toxic effect became negligible after the tests, the electrochemical treatment does not seem to enhance the sole desorption of the addressed pollutants, promoting their mineralization in the sorbed form or oxidizing them as soon as they are desorbed. This result was confirmed by the fact that the PAH concentration in the pore fluid collected at cathode compartment during tests 8 was below the detection limit (<0.1 mg/L).

In sum, based on the results of this study, electrochemical oxidation proved to be an effective remediation technology for the sediments of concern, amenably applicable both for in situ or ex situ remediation actions.

5. CONCLUSIONS

The tests performed allowed to evaluate the feasibility of using electrochemical oxidation for the remediation of different organic contaminants (diesel fuel and PAHs from two types of fine grain soils (kaolin and montmorillonite) and freshwater sediments.

According to the results achieved, electrochemical oxidation proved to be effective for the remediation of fine-grain soils contaminated by various types of hydrocarbons. A good removal was achieved both for PAHs and diesel fuel: about 90% contaminant removal was achieved for PAH-contaminated sediments after a four week treatment, while the diesel fuel contaminated soils resulted in about 50% TOC removal and 60% TPH removal for kaolin, and about 70% TOC removal and 85% TPH removal for montmorillonite.

As for the most important design parameters, the applied voltage seems to have a limited influence on the efficiency of the remediation action, good results being achieved with specific voltages as low as 1 V/cm, with low energy expenditures. On the opposite, the remediation efficiency proved to increase significantly with process duration. For example, the application of a constant voltage of 1 V/cm to a montmorillonite sample led to 30% TOC removal after 7 days, but the TOC removal increased to about 70% after 28 days of treatment. The effectiveness of the process seems also to be affected by soil mineralogy, and primarily by the soil iron content, so that significant iron content in the treated soil is thought to be able to improve the applicability of this remediation method. The final contaminant concentrations were found to be evenly distributed across the treated sample. This suggests that the oxidation reactions take place within all the treated volume and not only nearby the electrodes; moreover, the results indicate that the pollutants' electromigration during the test performed, which was unenhanced, can be considered negligible. The buffer capacity of the soil can affect soil pH changes, by determining the tendency of the treated medium towards acidification or basification, but the remediation efficiency does not seem to be influenced by changes in soil pH, nor by the occurrence of the electroosmotic flux, which does not seem to be necessary to achieve a significant mineralization of the organic pollutants.

On the whole, electrochemical oxidation seems to be effectively and amenably applicable for the mineralization of many organics with low energy expenditure, especially in finest soils like clays, with significant iron content.

6. REFERENCES

Acar, Y.B., Gale, R.J., Alshawabkeh, A.N., Marks, R.E., Puppala, S., Bricka, M., Parker, R. 1995. Electrokinetic remediation: basics and technology status. J. Hazard. Mater. 40, 117-137.

Alshawabkeh A.N. 2001. Basics and Applications of Electrokinetic Remediation. Handouts Prepared for a Short Course. Federal University of Rio de Janeiro, Rio de Janeiro, Brazil, 19-20 November 2001.

Alshawabkeh A.N., Sheahan T.C., Wu X. 2004. Coupling of electrochemical and mechanical processes in soils under DC fields. Mech. Mater. 36, 453-465.

Antizar-Ladislao B., Lopez-Real J., Beck A.J. 2005. Laboratory studies of the remediation of polycyclic aromatic hyrocarbon contaminated soil by in-vessel composting. Waste Manage. 25, 281-289.

Bissey, L.L., Smith, J.L.; Watts, R.J. 2006. Soil organic matter–hydrogen peroxide dynamics in the treatment of contaminated soils and groundwater using catalyzed H2O2 propagations (modified Fenton's reagent). Water Res. 40, 2477-2484.

Borgan, B.W., Trbovic, V. 2003. Effect of sequestration on PAH degradability with Fenton's reagent: roles of total organic carbon, humin, and soil porosity. J. Hazard. Mater. 100, 285-300.

Brown G.S., Barton L.L., Thomson B.M. 2003. Permanganate oxidation of sorbed polycyclic aromatic hydrocarbons. Waste Manage. 23, 737-740.

BSI (British Standards Institute). 1999. Code of practice for site investigations. BS 5930. British Standards Institution Standard Sales, London (GB).

Chung H.I., Kamon M. 2005. Ultrasonically enhanced electrokinetic remediation for removal of Pb and phenanthrene in contaminated soils. Eng. Geol. 77, 233-242.

Curtis F., Lammey J. 1998. Intrinsic remediation of a diesel fuel plume in Goose Bay, Labrador, Canada. Environmen. Pollut. 103, 1998, 203-210.

Cuypers M.P:, Grotenhius T.C., Rulkens W.H. 1998. Characterization of PAH contaminated sediments in a remediation perspective. Water Sci. Technol. 37, 157-164.

Da Pozzo A., Merli C., Sirés I., Garrido J.A., Rodriguez R.M., Brillas E. 2005. Removal of the herbicide amitrole from water by anodic oxidation and electro-Fenton. Environ. Chem. Lett. 3, 7-11.

ECP (Electrochemical Processess). 2003. White paper: Electrochemical GeoOxidation (ECGO) – a Synthesis. Septemper 18, 2003. http://www.ecp-int.com.

Ferrarese E., Andreottola G., Oprea I.A. 2007. Remediation of PAH-contaminated sediments by chemical oxidation, J. Hazard. Mater. 2007, doi:10.1016/j.jhazmat.2007.06.080.

Flotron V., Delteil C., Padellec Y., Camel V. 2005. Removal of sorbed polycyclic aromatic hydrocarbons from soil, sludge and sediments samples using the Fenton's reagent process. Chemosphere 59, 1427-1437.

Haapea, P., Tuhkanen, T. 2006. Integrated treatment of PAH contaminated soil by soil washing, ozonation and biological treatment. J. Hazard. Mater. 136, 244-250.

Harvey, R.G. 1997. Polycyclic Aromatic Hydrocarbons. New York, Wiley-VCH Publishers.

Henner, P., Schiavon, M., Morel, J.L., Lichtfouse, E. 1997. Polycyclic aromatic hydrocarbon (PAH) occurrence and remediation methods. Analusis 25, M56-M59.

Höhener P., Hunkeler D., Hess A., Bregnard T., Zeyer J. 1998. Methodology for the evaluation of engineered in situ bioremediation: lessons from a case study. J. Microbiol. Meth. 32, 1998, 179-192.

Hunkeler D., Jörger D., Häberli K., Höhener P., Zeyer J. 1998. Petroleum hydrocarbon mineralization in anaerobic laboratory aquifer columns. J. Contam. Hydrol. 32, 41-61.

IARC (International Agency for Research on Cancer). 1983. Polynuclear Aromatic Compounds, Part 1: Chemical, Environmental and Experimental Data. IARC Monographs on the Evaluation of Carcinogenic Risks to Humans, Volume 32. World Heath Organization, Lyons, France.

IARC (International Agency for Research on Cancer). 1984. Polynuclear Aromatic Compounds, Part 2: Carbon Blacks, Mineral Oils (Lubricant Base Oils and Derived Products) and Some Nitroarenes. IARC Monographs on the Evaluation of Carcinogenic Risks to Humans, Volume 33. World Heath Organization, Lyons, France.

Isosaari P., Piskonen R., Ojala P., Voipio S., Eilola K., Lehmus E., Itävaara M. 2007. Integration of electrokinetics and chemical oxidation for the remediation of creosote-contaminated clay. J. Hazard. Mater. 144, 538-548.

ITRC (Interstate Technology Regulatory Council). 2005. Technical and Regulatory Guidance for In Situ Chemical Oxidation of Contaminated Soil and Groundwater, 2nd Edition. ITRC, ISCO Team, Washington D.C.

Iturbe R., Flores C., Flores R.M., Torres L.G. 2005. Subsoil TPH and other petroleum fractions-contamination levels in an oil storage and distribution station in north-central Mexico. Chemosphere 61, 1618-1631.

Kakarla P.K., Andrews T., Greenberg R.S., Zervas D. 2002. Modified Fenton's Processes for Effective In-Situ Chemical Oxidation – Laboratory and Field Evaluation. Remed. J. 12, 23-36.

Kim J.-H., Han S-.J. Kim S.-S., Yang J.-W. 2006. Effect of soil chemical properties on the remediation of phenanthrene-contaminated soil by electrokinetic-Fenton process. Chemosphere 63, 1667-1676.

Kim S.-S., Kim J.-H., Han S-.J. 2005. Application of the electrokinetic-Fenton process for the remediation of kaolinite contaminated with phenanthrene. . J. Hazard. Mater. B118, 121-131

Kong, S., Watts, R.J.,; Choi, J. 1998. Treatment of Petroleum-Contaminated Soils Using Iron Mineral Catalyzed Hydrogen Peroxide. Chemosphere 37, 1473-1482.

Kulik N., Goia A., Trapidoa M., Tuhkanenb T. 2006. Degradation of polycyclic aromatic hydrocarbons by combined chemical pre-oxidation and bioremediation in creosote contaminated soil. J. Environ. Manageme. 78, 382-391.

Laine D.F., Cheng I.F. 2007. The destruction of organic pollutants under mild reaction conditions: a review. Microchem. J. 85, 183-193

Lundstedt S., Persson Y., Oberg L. 2006. Transformation of PAHs during ethanol-Fenton treatment of an aged gasworks' soil. Chemosphere 65, 1288-1294.

Luthy R.G., Dzombak D.A., Peters C.A., Roy S.B., Ramaswami A., Nakles D.V., Nott B.R. 1994. Remediating tar-contaminated soils at manufactured gas plant sites. Environ. Sci. Technol. 28, 266A–276A.

Lynch R.J., Muntoni A., Ruggeri R., Winfield K.C. 2007. Preliminary tests of an electrokinetic barrier to prevent heavy metal pollution of soils. Electrochim. Acta 52, 3432-3440.

Masten, S.J., Davies, S.H.R. 1997. Efficacy of in-situ ozonation for the remediation of PAH contaminated soils. J. Contam. Hydrol. 28, 327-335.

Meinero S., Zerbinati O. 2006. Oxidative and energetic efficiency of different electrochemical oxidation processes for chloroanilines abatement in aqueous medium. Chemosphere 64, 386-392.

Muller P. 2002. Potential For Occupational and Environmental Exposure to Ten Carcinogens in Toronto. Tox Probe Inc., March 2002.

Namkoong W., Hwang E.Y., Park J.S., Choi J.Y. 2002. Bioremediation of diesel-contaminated soil with composting. Environ.Pollution, 119, 2002, 23-31.

O'Mahony M.M., Dobson A.D.W., Barnes J.D., Singleton I. 2006. The use of ozone in the remediation of polycyclic aromatic hydrocarbon contaminated soil. Chemosphere 63, 307-314.

Park J.-Y., Kim S.-J., Lee Y.-J., Baek K., Yang J.-W. 2005. EK-Fenton process for removal of phenanthrene in a two-dimensional soil system. Eng. Geol. 77, 217-224.

Perraudin E., Budzinski H., Villenave E. 2007. Identification and quantification of ozonation products of anthracene and phenantrene adsorbed on silica particles. Atmos. Environ. 41, 6005-6017.

Powell S.M., Harvey P.M., Stark J.S., Snape I., Riddle M.J. 2007. Biodegradation of petroleum products in experimental plots in Antarctic marine sediments is location dependent. Mar. Pollut. Bull. 54, 434-440.

Puppala S.K., Alshawabkeh A.N., Acar Y.B., Gale R.J., Bricka M. 1997. Enhanced electrokinetic remediation of high sorption capacity soil. J. Hazard. Mater. 55, 203-220.

Rahner D., Ludwig G., Röhrs J. 2002. Electrochemically induced reactions in soils—a new approach to the in-situ remediation of contaminated soils? Part 1: The microconductor principle. Electrochim. Acta 47, 1395-1403.

Reddy K.R., Ala P.R., Sharma S., Kumar S.N. 2006. Enhanced electrokinetic remediation of contaminated maufactured gas plant soil. Eng. Geol. 85, 132-146.

Ribeiro A.B., RodrIguez-Maroto J.M., Mateus E.P., Gomes H. 2005. Removal of organic contaminants from soils by an electrokinetic process: the case of atrazine. Experimental and modeling. Chemosphere 59, 1229-1239.

Richnow H.H., Seifert R., Kastner M., Mahro B., Horsfield B., Tiedgen U., Bohm S., Michaelis W. 1995. Rapid screening of PAH-residues in bioremediated soils. Chemospehere 31, 3991–3999.

Rivas, F.J. 2006. Polycyclic aromatic hydrocarbons sorbed on soils: A short review of chemical oxidation based treatments. J. Hazard. Mater. 138, 234-251.

Rivera-Espinoza Y., Dendooven L. 2004. Dynamics of carbon, nitrogen and hydrocarbons in diesel-contaminated soil amended with biosolids and maize. Chemosphere 54, 379-386.

Röhrs J., Ludwig G., Rahner D. 2002. Electrochemically induced reactions in soils—a new approach to the in-situ remediation of contaminated soils? Part 2: remediation experiments with a natural soil containing highly chlorinated hydrocarbons. Electrochim. Acta 47, 1405-1414.

Saner M., Bollier D., Schneider K., Bachofen R. 1996. Mass transfer improvement of contaminants and nutrients in soil in a new type of closed soil bioreactor. J. Biotechnol. 48, 1996, 25-35.

Sarkar D., Ferguson M., Datta R., Birnbaum S. 2006. Bioremediation of petroleum hydrocarbons in contaminated soils: Comparison of biosolids addition, carbon supplementation, and monitored natural attenuation. Environ. Pollut. 136, 187-195.

Silva A., Delerue-Matos C., Fiuza A. 2005. Use of solvent extraction to remediate soils contaminated with hydrocarbons. J. Hazard. Mater. B124, 224-229.

Sun H.-W., Yan Q.-S. 2007. Influence of Fenton oxidation on soil organic matter and its sorption and desorption of pyrene. J. Hazard. Mater. 144, 164–170.

Szpyrkowicz L., Radaelli M., Bertini S., Daniele S., Casarin F. 2007. Simultaneous removal of metals and organic compounds from a heavily polluted soil. Electrochim. Acta 52, 3386-3392.

Taylor L.T., Jones D.M. 2001. Bioremediation of coal tar PAH in soils using Biodiesel. Chemosphere 44, 1131–1136.

USAEC (U.S. Army Environmental Center). 2000. In-situ electrokinetic remediation of metal contaminated soils – Technology Status Report. U.S. Army Environmental Center. Report Number: SFIM-AEC-ET-CR-99022. July 2000.

USEPA (U.S. Environmental Protection Agency). 2002. Electrochemical Remediation Technologies Remove Mercury in Soil. Technology News and Trends. National Service for Environmental Publications, Cincinnati, OH 45242. EPA 542-N-02-004. Issue 2, September 2002.

USEPA (U.S. Environmental Protection Agency). 2004. Electrochemical remediation technologies (ECRTs) - Demonstration Bulletin. National Risck Management Research Laboratory, Cincinnati, OH 45268. EPA/540/MR-04/507. October 2004.

Van Cauwenberghe L. 1997. Electrokinetics. Technology Overview Report, GWRTAC (Ground-Water Remediation Technologies Analysis Center), Pittsburgh, PA. TO 97-03. July 1997.

Watts R.J., Dilly S.E. 1996. Evaluation of iron catalysts for the Fenton-like remediation of diesel-contaminated soils. J. Hazard. Mater. 51, 209-224.

Watts, R.J.; Stanton, P.C.; Howsawkeng, J., Teel, A.L. 2002. Mineralization of a sorbed polycyclic aromatic hydrocarbon in two soils using catalyzed hydrogen peroxide. Water Res. 36, 4283-4292.

Watts R.J., Asce M., Teel A.L. 2005. Chemistry of Modified Fenton's Reagent (Catalyzed H2O2 Propagations – CHP) for In Situ Soil and Groundwater Remediation. J. Environ Eng. 131, 612-622.

Wild S.R., Jones K.C. 1995. Polynuclear Aromatic Hydrocarbons in the United Kingdom Environment: a Preliminary Source Inventory and Budget. Environ. Pollut. 88, 91-108.

Yang G.C.C., Liu C.-Y. 2001. Remediation of TCE contaminated soils by in situ EK-Fenton process. J. Hazard. Mater. B85, 317-331.

Zheng X.-J., Blais J.-F., Mercier G., Bergeron M., Drogui P. 2007. PAH removal from spiked municipal wastewater sewage sludge using biological, chemical and electrochemical treatments. Chemosphere 68, 1143-1152.

Zhou D.-M.,Deng C.-F., Alshawabkeh A.N., Cang L. 2005. Effects of catholyte conditioning on electrokinetic extraction of copper from mine tailings. Environ. Int. 31, 885-890.

Chapter 26

PILOT EXPERIMENT OF IMMOBILIZATION OF CONTAMINANTS IN-SITU

Jiří Mužák[§], Ludvík Kašpar and Vladimír Beneš
DIAMO, s. p., o. z. TUU, Machova 201, 471 27 Straz pod Ralskem, Czech Republic

ABSTRACT

At the end of 2006 the project of pilot experiment of immobilization of contaminants in-situ was prepared in DIAMO, s. p., o. z. TUU. Realisation of the experiment is planned for years 2007 and 2008.

The principle of immobilization of contaminants in-situ is to develop special conditions in water bearing sandstone sediments when transformation of contaminants from mobile form to immobile form can happen. Under the conditions of remediation after chemical mining (using sulphuric acid) of uranium on the deposit Straz it means injecting suitable alkaline medium and its spreading in contaminated sandstone aquifer. It will lead to decreasing of acidity of contaminated groundwater and precipitating of contaminants (SO_4^{2-}, Al, Fe) in pores. This process is followed by co-precipitation and sorption of other toxic contaminants as As and Be.

The results of the pilot experiment will be used for design of application of method of immobilization in-situ in the frame of remediation after chemical mining of uranium on the deposit Straz with the aim to decrease time and costs of the whole remediation process.

Keywords: Immobilization of Contaminants; Uranium Mining; Remediation

1. INTRODUCTION

Uranium mining using in-situ acidic leaching method was performed from 1967 to 1995 on the uranium deposit Straz located in North Bohemian cretaceous table in Czech Republic. During this period an enormous amount (almost 5 mil. tons) of chemicals, mostly sulfuric acid as the leaching medium, was injected into the ground. The products of leaching and the rest of injected chemicals cumulated in the groundwater of the Cenomanian horizon. The influenced volume of groundwater is more than 300 millions m^3 in the area of 27 km^2.

[§] Corresponding Author: Jiří Mužák, DIAMO, s. p., o. z. TUU, Machova 201, 471 27 Straz pod Ralskem, Czech Republic, Tel: +420 487 894 324, muzak@diamo.cz

In 1996 the injecting of sulfuric acid was finished and then the remediation of contaminated groundwater started. The groundwater is cleaning using classical pump and treat technology. The contaminants are abstracted from groundwater in surface technologies, and then they are reprocessed into industrially usable products (alum, aluminum sulfate, ammonium sulfate) or deposited in tailings pond of former chemical treatment plant. The part of cleaned water is discharged in the river and the rest is injected back in the ground.

In original remediation conception the use of the method of in-situ immobilization of contaminants was planned for the last years of a remediation process when concentration of contaminants in groundwater will sufficiently decrease.

The updated remediation conception assumes more extended use of neutralization cleaning technologies to accelerate contaminants' abstraction from groundwater. It seems to be optimal to take advantage of the basicity of solutions after neutralization and to inject these solutions into the ground to neutralize less acidic groundwater (see scheme on Fig. 1) before it was originally planned. It means not only at the end of the remediation process but also during the remediation.

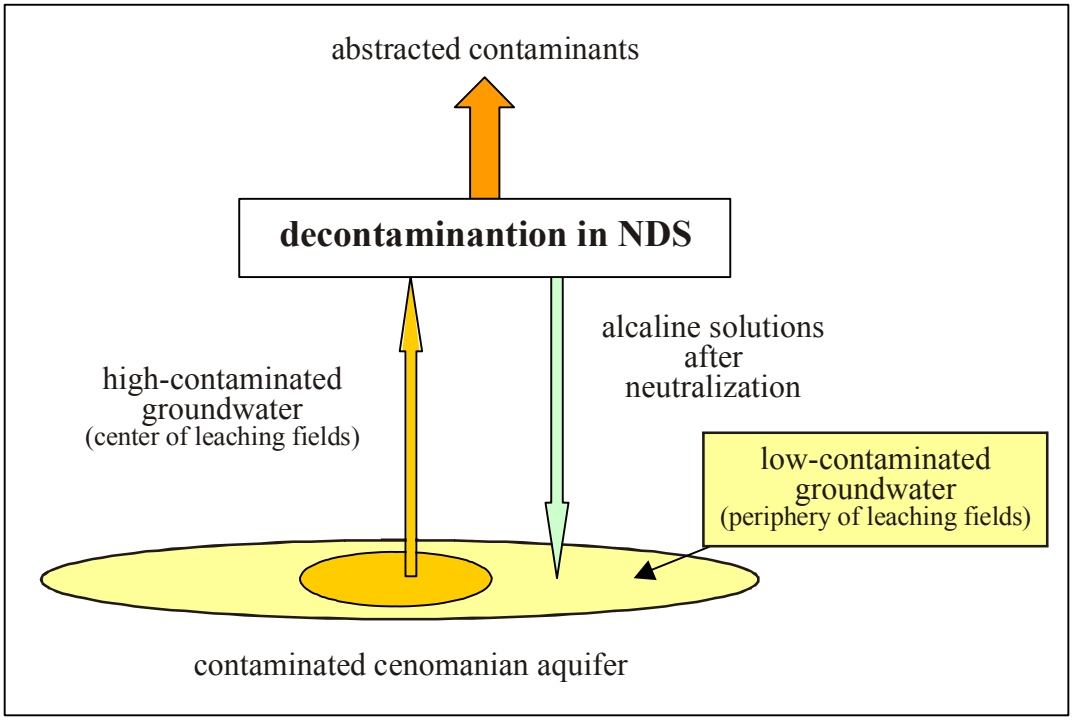

Figure 1. Scheme of injection of alkaline solutions after neutralization (decontamination)

2. PRINCIPLE OF IMMOBILIZATION

The principle of immobilization of contaminants in-situ is to develop special conditions in water bearing sandstone sediments when transformation of contaminants from mobile form to

immobile form can happen. Under the conditions of remediation after chemical mining (using sulphuric acid) of uranium on the deposit Straz, it means injecting a suitable alkaline medium and its spreading in contaminated sandstone aquifer. It will lead to decreasing of acidity of contaminated groundwater and precipitating of contaminants (SO42-, Al, Fe) in pores. This process is followed by co precipitation and sorption of other toxic contaminants as As and Be.

Since 1996 when remediation process began, the evaluation of changes in rock environment on the former deposit Straz have been continuously performed. The results of the evaluation have formed a view on target and effect of immobilization. In the beginning of the remediation process the massive decrease in porosity and permeability was considered as the main effect of immobilization. Now we see the effect in following:

- neutralization of acidic contaminated groundwater;
- decreasing of salinity of groundwater in consequence of transformation of contaminants into the form of insoluble precipitate;
- creating an environment suitable for long-lasting positive chemical changes in groundwater;
- liquidation of contaminants from inactive pores and sediments with low permeability;
- creating protective and reactive barriers and isolating of rest contamination in small volume of groundwater in central part of leaching fields;
- creating of conditions suitable for natural attenuation.

Since it is possible to use immobilization from the beginning of remediation, we expect a shortening of the complete remediation process. We also expect a decrease in total remediation costs.

The solutions after neutralization will be available during the whole remediation process in sufficient volume. There will be no need to use any other medium for immobilization which preparation is much more expensive.

Performed static and dynamic laboratory experiments and chemical processes simulation calculations have brought important knowledge which helps to forecast (using numerical modeling) expected hydrogeological and geochemical trends. Unfortunately they cannot fully answer questions connected to large scale immobilization applications. To obtain such answers we prepared at the end of 2006 the project of pilot experiment of immobilization (DIAMO, 2006).

3. DESCRIPTION OF PILOT EXPERIMENT

The pilot experiment of immobilization will be realized in south-eastern part of leaching field VP 8C (see Fig. 2). This area has suitable geographic position, geological, hydrogeological and hydrochemical conditions.

It was designed using numerical models to use currently operating well network in chosen locality and to add five new wells (see Fig. 3). Four of five new wells together with six to eight wells from the currently operating well network will be used for monitoring of pilot experiment.

The fifth new well will be used for injecting of immobilization medium (solution after neutralization). The depth of wells is approx. 200 m.

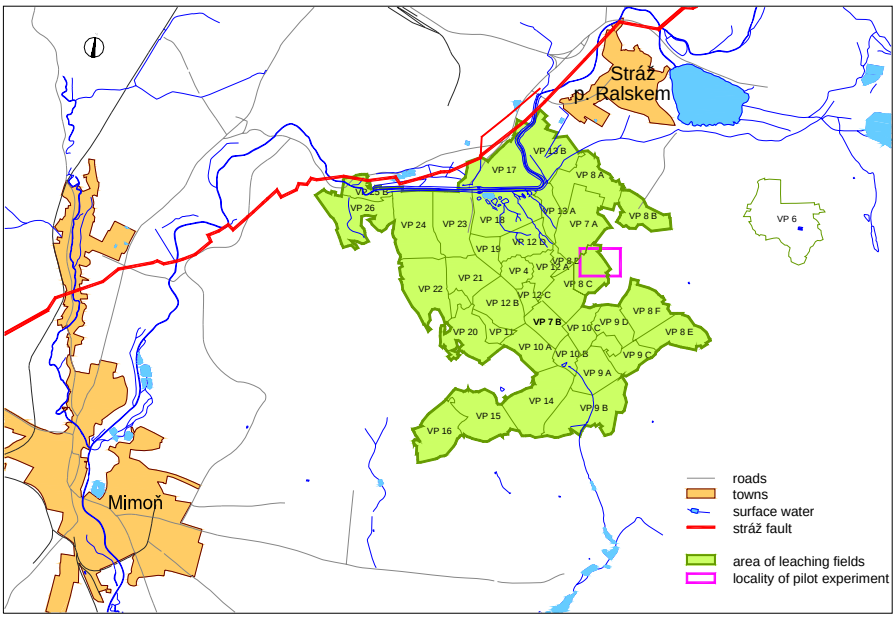

Figure 2. Locality for realization of pilot experiment of immobilization

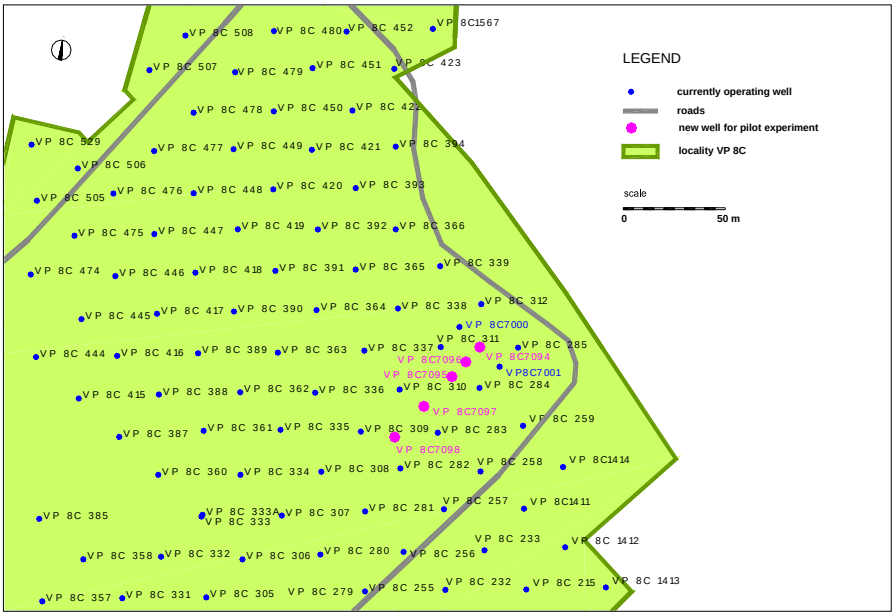

Figure 3. Location of five new wells for pilot experiment

As the immobilization medium, the filtrated solution after neutralization on decontamination station NDS 6 was chosen. The solution will lead from separation tank on NDS 6 to pilot experiment locality on VP 8C by 2500 m long pipeline.

The chemical composition of alkaline solution after neutralization and quality of groundwater influenced by chemical mining of uranium on locality VP 8C are documented in the following table, Table 1.

Table 1. Chemical composition of immobilization medium and quality of groundwater on locality VP 8C

	unit	**immobilization medium**	**VP 8C groundwater**
pH (20 °C)		11,5 – 12	2,0 – 2,1
Eh (abs) (20 °C)	[mV]	240	~ 800
Spec. conductivity (20 °C)	[$mS.m^{-1}$]	415	1 400 – 1500
Density	[$g.cm^{-3}$]	1,002	~ 1,016
RL	[$mg.l^{-1}$]	2 000 – 2 100	20 000 – 25 000
NH_4^+	[$mg.l^{-1}$]	80 – 100	300 – 400
Na	[$mg.l^{-1}$]	140	10 – 15
K	[$mg.l^{-1}$]	30	20 – 25
Mg	[$mg.l^{-1}$]	1,5	25 – 35
Ca	[$mg.l^{-1}$]	600 – 650	150 – 200
Fe	[$mg.l^{-1}$]	< 0,05	500 – 550
Al	[$mg.l^{-1}$]	< 0,5	1 800 – 2 400
NO_3^-	[$mg.l^{-1}$]	50 – 60	230 – 280
F^-	[$mg.l^{-1}$]	1,0	60 – 100
Cl^-	[$mg.l^{-1}$]	20	~ 5
SO_4^{2-}	[$mg.l^{-1}$]	100 – 1 100	15 000 – 20 000

The preparation and realization of the pilot experiment of immobilization will last two years (2007-2008). The whole experiment is divided into two phases – phase of preparation and phase of realization.

Phase of preparation will include:

- the building of a pipeline from NDS 6 to VP 8C locality and building of technological equipment;
- check of current status of existing wells;
- cleaning of wells;
- drilling of five new wells (one for injecting of immobilization medium, one core well for monitoring using special zonal sampling method and three wells for classical hydrogeological monitoring);

- logging, groundwater quality sampling, piezometric head measuring, chemical analyzing;
- numerical modeling.

Realization phase will include:

- injecting of the immobilization medium for at least 150 days in the volume rate of 200 $l.min^{-1}$ (52.8 gal. per minute);
- logging, groundwater quality sampling, piezometric head measuring, chemical analyzing.

Care will be given also to long term monitoring of groundwater quality evolution in pilot experiment locality. It will mainly include:

- monitoring of time behaviour of chemical equilibrium setting in groundwater in the all influenced area using sampling and logging;
- monitoring of hydraulic parameters change using pumping tests;
- monitoring of vertical distribution of chemical composition of groundwater;
- drilling of control core well, core sampling and analyzing.

The results obtained during and after the pilot experiment will be evaluated continuously from the finishing of the injection until a steady state in the Cenomanian aquifer will be reached.

After finishing the pilot experiment the following activities will be performed:

- evaluation of chemical composition of groundwater;
- evaluation of retardation of monitored components;
- evaluation of permeability changes;
- evaluation of stability of immobilization effect;
- evaluation of diffusion intrusion of immobilization medium into low permeable sediments;
- evaluation of the practical realization of in-situ immobilization in large scale;
- risk identification with the view to large scale application of in-situ immobilization as the part of complex remediation process.

The specialized numerical model based on FEM for simulation of groundwater flow and contaminant transport was developed at DIAMO for evaluation of pilot experiment of in-situ immobilization results. It follows from testing calculations that the model is fully usable for pilot experiment simulation. During the preparation phase many numerical tests will be performed. They will help to predict expected rates of change of monitored parameters to set frequency of piezometric head measurements and frequency of groundwater sampling and analyzing. The calculations will not be performed only using the above mentioned numerical model, but we will use MODFLOW™ in parallel.

4. CONCLUSION

Results of the long term monitoring of stability of geochemical equilibrium setting in the ground will be the base knowledge for prediction of possibility of targeted influencing the quality of cenomanian groundwater. They would also help to determine the parameters of future planned large scale in-situ immobilization; for example, the quality of groundwater into which

the alkaline solutions can be injected, the volume of immobilization medium needed to inject in particular parts of deposit, final quality of groundwater after injection of alkaline solutions (pH, Eh, concentration of SO_4^{2-}, U, Al, Fe, …), vertical distribution of chemical composition of groundwater caused by gravity effect or by diffusion effect on the contact areas of sediments with extremely different permeability and many others.

During the pilot experiment of in-situ immobilization together with commonly used methods of monitoring the special method of zonal groundwater sampling from several vertically separated profiles will be tested.

The results and evaluation of the pilot experiment will be used as a source for future design of large scale applications of in-situ immobilization method. It will be possible to determine:

- number of wells for injection of needed volume of alkaline solutions;
- location and dimension of feeding pipelines;
- process control and monitoring system;
- optimal timing and aerial distribution of injection (using numerical models);
- prediction of total cost of remediation with use of in-situ immobilization method in combination with pump and treat technology;
- expected risks of large scale immobilization method application.

5. REFERENCES

DIAMO, 2006. Project of Pilot Experiment of Immobilization of Contaminants In-situ. DIAMO, s. p., o. z. TUU, Straz pod Ralskem, 471 27, Czech Republic. Project proposal, November 2006. In Czech.

Chapter 27

ATRAZINE BIODEGRADATION AS RELATED TO THE PHYSIOCHEMICAL PROPERTIES OF A CISNE SOIL FROM A MAJOR ATRAZINE SPILL SITE: ATRAZINE BIODEGRADATION IN A CISNE SOIL EXPOSED TO A MAJOR SPILL

Elizabeth Shaffer[1§], Malcolm Pirnie[1], Gerald Sims[2], Alison M. Cupples[3], Charles Smyth[4], Joanne Chee-Sanford[2]

[1]1300 E 8th Ave Suite F100, Tampa, FL 33067 [2]USDA-ARS, 1102 S. Goodwin Ave, Urbana, IL, 61801-0000, [3]A129 Research Engineering Complex, Department of Civil and Environmental Engineering, Michigan State University, East Lansing, MI 48842,[§ 4]Crop Sciences, 1102 S. Goodwin Ave, Urbana, IL, 61801-0000

ABSTRACT

Conventional soil tests, culture-based microbial methods, and the novel method of ^{15}N-DNA stable isotope probing (SIP) were employed to illustrate atrazine biodegradation as related to the physiochemical properties of an atrazine-exposed Cisne soil. This soil exhibited enhanced atrazine degradation. Mineralization underestimated the rate of atrazine dissipation demonstrated by the accumulation of several metabolites. The soil showed high ambient concentrations of NO_3^-; however, NO_3^- did not suppress atrazine degradation. Atrazine natural attenuation was limited by incomplete distribution through the unsaturated soil matrix. Direct plating experiments from the Cisne soil isolated an atrazine-degrading microorganism, ES-1. Analysis of the 16S rRNA gene sequences from the isolate confirmed that ES-1 is closely related (99%) to *Arthrobacter* sp. In pure culture, the isolate rapidly converted atrazine to cyanuric acid. Accumulation of this product was consistent with metabolites in the Cisne soil, suggesting that isolate ES-1 influenced in-situ remediation of atrazine. ^{15}N- SIP experiments were conducted using ^{15}N-*ethylamino*-atrazine. The results of these experiments failed to establish a causal relationship between in-situ atrazine-degradation and ES-1 enrichment; however, these results are likely due to isotopic dilution. Further experiments using ^{13}C-ethyl/isoproylamino-atrazine may yet verify a link between ES-1 and the enhanced natural attenuation exhibited in the Cisne soil.

Keywords: Cisne, Atrazine, stable isotope probing, natural attenuation

1. INTRODUCTION

Atrazine and other s-triazine herbicides have been used for over 50 years for the control of a variety of weeds in agricultural crops, most notably maize (U.S. Department of Agriculture,

§ Corresponding Author: Elizabeth Shaffer, 1300 E 8th Ave Suite F100, Tampa, FL 33067, Phone: 813-242-7236, Email: eshaffer@pirnie.com

2004). These chemicals are moderately persistent, but also sufficiently water-soluble as to create contamination problems in surface and groundwater (Solomon et al., 1996, Tasli et al., 1996).

Atrazine contamination of water resources is a concern because the compound is a suspected endocrine-disruptor (Hayes et al., 2002, Hayes, 2004). Widespread use of these herbicides has influenced the microbial ecology of agricultural soils world-wide.

The following experiments characterize a Cisne-Darmstadt intergrade (Cisne) soil exposed to high levels of atrazine through a single chemical spill. Large atrazine releases are not uncommon during peak application periods and there is no way to know how many spills go unreported. Therefore, it is important to examine the factors that influence the potential for natural attenuation in soils.

2. MATERIALS AND METHODS

2.1 Chemicals and Materials

Unlabeled atrazine (98%) was purchased from ChemService (West Chester, PA). Uniformly ^{14}C-ring-labeled-atrazine (9.3 mCi per mmol, radiochemical purity ≥95%) was purchased from Sigma-Aldrich (St. Louis, MO). Atrazine-ethylamino-^{15}N (99 atom % ^{15}N) was purchased from Isotec (Miamisburg, OH). Uniformly ^{15}N-ring-labeled atrazine was synthesized from ^{15}N-urea according to the method described in (Bichat et al. 1999). Atrazine metabolite standards: deethylatrazine (2-amino-4-chloro-6-isopropylamino-s-triazine) (98%), deisopropylatrazine (2-amino-4-chloro-6-ehtylamino-s-triazine)(99%), hydroxyatrazine (2-hydroxy-4ethylamino-6-isopropylamino-s-triazine)(99%), deethylhydroxyatrazine (2-hydroxy-4-amino-6-isopropylamino-s-triazine)(98%), and deethyldeisopropylatrazine (2-chloro-4,6-diamino-s-triazine)(99%), were a gift of W. Roy (United States Geological Survey, Champaign, IL). Cyanuric acid (99%) was purchased from Alfa Aesar (Ward Hill, MA). Organic solvents were Optima grade (Fisher Scientific, Pittsburg, PA).

2.2 Enrichment, Isolation, Characterization, and Maintenance of Atrazine-Degrading Microorganisms

Previously researched atrazine-degrading isolates of Pseudomonas sp. Strain ADP and Pseudaminobacter sp. Strain C147 were generously donated by Drs. Larry Wackett and Edward Topp respectively. Atrazine degrading cultures in this study were grown on atrazine mineral salts (AMS) media previously described (Topp et al., 2000a), modified with the addition of 1ml MR2A trace element solution (Atlas, 1997). Post autoclaving, the medium was supplemented with 1ml of a filter-sterilized (0.22 μm, polyethersulfone, Millex-GP,) vitamin solution (Yang and McCarty, 1998) modified with the addition of 0.005 g of thiamine hydrochloride and 0.005 g of nicotinamide L-1, and 1ml of filter sterilized iron stock solution (5g Fe $SO_4 \cdot 7H_2O$ L-1). Solid media preparations consisted of the mineral salts media modified with the substitution of 0.5 g L-1 atrazine instead of 0.025 g L-1 of atrazine (delivered in 1ml of methanol) and supplemented with 15g of Noble agar (Difco, Sparks, MD). Carbon and nitrogen supplied by the vitamin solution were negligible, thus atrazine represented the sole source of those elements.

The concentration of atrazine in the solid media preparations exceeded the solubility limit resulting in a chalky suspension (Mandelbaum et al., 1995). Colonies that developed zones of clearing on the opaque surface of the plates, considered putative atrazine-degraders, were purified by streak plating, and maintained on this medium. Isolates were stored at -80°C in a 15% glycerol solution.

2.3 Properties and Preparation of Soils

The atrazine-contaminated soil, a Cisne-Darmstadt intergrade (Cisne), consisted of surface material excavated five months prior to this investigation from a spill in Patoka, IL. The initial atrazine burden for the Cisne soil is unknown, but exposure was assumed to be significant owing to near complete release of the contents of an applicator truck at the site. The source contamination came from an herbicide tank mix consisting of metolachlor and atrazine. The site had been excavated to a depth of two meters and the contaminated soil was stored under a tarp for approximately six months prior to land application. To obtain soil with the greatest atrazine exposure, the darkest material, presumed to be from the surface horizon, was used for these studies. Reference soils, taken from agricultural production sites throughout Illinois with a known history of atrazine use, were collected from a depth of 0-15cm. These soils included: material from a former pesticide mixing-loading facility (Drummer-chemical loading) and the alfalfa field adjacent to the mixing-loading facility (Drummer-field), two manure-amended agricultural production areas (Thorp and Clarksdale), and the zero nitrogen treatment from the University of Illinois Morrow plots long-term fertility experiment (Flanagan) shown previously to exhibit rapid atrazine mineralization (Sims, 2006). Each of the soils was thoroughly homogenized, sieved to through a 2mm screen, and stored at 4°C. Atrazine histories and taxonomic information for the soils used in this study are described in Table 1. A more detailed account of the Cisne soil properties is listed in Table 2.

Table 1. Physical characteristics, soil taxonomy, and atrazine exposure history for the soils used in this experiment

Soil Name	Abbreviation	Soil Series	Taxonomy	Atrazine History
Cisne	PET	Cisne-Darmstadt intergrade	Fine, smectitic, mesic Mollic Albaqualfs / Fine-silty, mixed, superactive, mesic Aquic Natrudalfs	extensive recent exposure
Drummer-field	GCA	Drummer	Fine-silty, mixed, superactive, mesic Typic Endoaquolls	unknown
Drummer-chemical loading	GCC	Drummer	Fine-silty, mixed, superactive, mesic Typic Endoaquolls	exposure 10 years prior
Flanagan	MP	Flanagan	Fine, smectitic, mesic Aquic Argiudolls	continous exposure for >10 years
Thorp	CHN18	Thorp	Fine-silty, mixed, superactive, mesic Argiaquic Argialbolls	ammended with manure and exposed to glyphosate and atrazine
Clarksdale	BGWF1	Clarksdale	Fine, smectitic, mesic Udollic Endoaqualfs	ammended with manure and exposed to glyphosate and atrazine

Table 2. Physical and chemical properties of the Cisne soil

Cisne Soil Properties								
%Organic Carbon	Soil pH	Buffer pH	CEC meq/100g	NO3 ppm	NH4 ppm	% Sand	% Silt	% Clay
2.8	6.7	6.9	18.9	161	3	43	44	13

2.4 Determining Atrazine Mineralization Rates of Various Soils

The atrazine mineralization rate for the contaminated Cisne soil was compared to reference soils using laboratory incubations. Owing to the potential for inorganic N sources to suppress atrazine degradation, and a very high residual nitrate concentration in the Cisne soil, a leaching treatment was included to remove excess nitrogen (Mulvaney et al., 2001) from the study soils. Unleached controls were also included for Cisne, Drummer-field, and Drummer-chemical loading. Mineralization of ^{14}C-ring-labeled-atrazine was monitored over a period of 84 days for soils incubated in 473-mL Mason jar microcosms (Mervosh, 1995) at 19°C. Each replicate (three per treatment) received field moist soil (3.5 g on a dry weight basis), which was adjusted to 40% water-filled pore space using an aqueous solution containing uniformly ^{14}C-ring-labeled-atrazine and unlabeled atrazine to deliver a concentration of 30 µg atrazine and 300 Bq ^{14}C / gram soil (dry weight basis). Physical mixing of the treatment solution in the soil was avoided to prevent the collapse of the relatively weak Cisne soil structure and ensure proper aeration at the relatively high water content. Instead, atrazine was allowed to disperse through the soil via advection. Microcosms also contained a 1-mL 0.2M NaOH trap and a 90mm qualitative filter wetted with 0.5 ml buffer (0.575mM KH_2PO_4) to maintain the proper headspace humidity. At 3-7 day intervals the microcosms were aerated and the evolved [^{14}C] CO_2 in the NaOH trap was measured in a 2-mL aliquot using liquid scintillation spectrometry (LSS) in a Packard model 1600TR-Tri-Carb instrument (Packard Instruments, France).

2.5 Soil Incubations with Uniformly ^{15}N/^{14}C Ring-Labeled-Atrazine

Control and treatment samples of the Cisne soil (5 replicates/treatment) were amended twice (Day 0 and 26) with either ^{14}C-ring-UL- atrazine (1110 Bq) and unlabeled atrazine (30µg g-1), or ^{14}C-ring-UL- atrazine (1110 Bq) and uniformly ring labeled 15N atrazine (99 atom%, 30µg g-1). This was accomplished by delivering atrazine to empty scintillation vials in ethyl acetate, which was then allowed to evaporate. Sufficient deionized water was added to dissolve the atrazine and bring the soil to 40% water-filled pore space. Finally, 4 grams (dry weight basis) of the study soil were added to each vial, the vials were placed in sealed microcosms containing a 10-ml 0.1M NaOH trap, and a 90mm qualitative filter wetted with 0.5 ml (0.575 mM) KH_2PO_4 was added to maintain proper humidity. The microcosms were stored at 19°C in the dark. Soils (unlabeled and labeled with 15N-atrazine) were destructively sampled on days: 5, 10, 15, and 41. The procedure described above was used to respike the samples on day 26; however the samples were transferred to new scintillation vials. Between days 15 and 41 the microcosms were opened at 3-4 day intervals and the NaOH trap was sampled for analysis and replaced. The evolved [^{14}C] CO_2 was measured using LSS.

2.6 Atrazine Extraction and HPLC Analysis

On days 5, 10, 15, and 41 soil samples (1 gram dry weight equivalent for each replicate) were removed for DNA extraction using the Powersoil kit (Mobio Laboratories, Carlsbad, CA) according the manufacturer's instructions. The remaining 3 grams of soil were stored at -20°C for chemical analysis. Soil samples (2.5 gram) were transferred to 50–ml Teflon centrifuge tubes and extracting solutions were introduced sequentially to recover atrazine in pools assumed to represent decreasing degrees of microbial bioavailability. Soils were initially extracted with 0.01M $CaCl_2$ (4ml), followed by two methanol extractions (4ml each). Extractions in 0.01M $CaCl_2$ were mixed for 1.5 hours and methanol extractions were mixed for 2 hours on a horizontal shaker and then centrifuged at 17,200g for 15min. Four milliliters of the supernatant were removed from the 0.01M $CaCl_2$ extraction and 1ml was filtered (PTFE, Alltech Associates, Deerfield, IL) prior to reverse phase high performance liquid chromatography (HPLC, Hewlett Packard Series 1050, San Fernando, CA) analyses to measure reversibly-sorbed, bioavailable atrazine. A similar procedure was followed for the first methanol extraction with the exception that only 3.8mls of the supernatant was removed for analysis of the irreversibly-sorbed, potentially bioavailable atrazine. Prior to bound residue analysis, the second methanol extraction was used to remove residual extracting solution (containing atrazine) that remained trapped in the interstitial pore space. This extract was discarded. HPLC conditions were: injector volume, 100µl; mobile phase flow rate, 1.0mL min-1; UV detector wavelength 215 nm; reverse phase C18 column (150mm × 4.6mm, Alltima column, Alltech Associates, Deerfield, IL) and an isocratic mobile phase (methanol:water, 65:35). An apparent Kd value was determined for atrazine and each of the detected metabolites from the ratio of potentially bioavailable (sorbed) to bioavailable (solution) phase material. After the extraction procedure the soil samples were air dried and combusted according to the method described in.Cupples et al. (2000). Finally, to account for any residual radioactivity due to precipitated atrazine, the incubation containers were washed with 1ml of MeOH and the radioactivity in the liquid was measured using LSS.

2.7 Isolation of Atrazine-Degrading Bacteria

Atrazine-degrading bacteria were isolated by selective enrichment. Soil suspensions were directly plated onto semi-selective solid media using the method described in (Weaver et al., 1994). Briefly, 1g soil samples were added to 9.5mls of PBS solution (pH = 8.0) and 0.5g (approximately 15) 3mm autoclaved glass beads in sterile polypropylene 50mL conical tubes (Corning Inc. Corning, NY). Samples were shaken by hand for 1 minute to ensure dispersion of the soil, and then placed on a horizontal shaker for 10min at 160 oscillations per minute. After allowing 30 seconds for the samples to settle, a 1-mL aliquot of the soil suspension from the middle of the tube was used as an innoculum for a dilution series. Samples were diluted in ten-fold serial transfers and 100 µL aliquots from the 10-3 to 10-7 dilutions were spread onto AMS plates. The plates were incubated at 19°C for approximately four weeks. Colonies that developed zones of clearing on the AMS medium were purified by successive streak plating and maintained on the same medium.

2.8 Kinetics of Atrazine Degradation in Pure Culture

The colony producing the largest clearing zone was denoted isolate ES-1 and isolated for further study. A loopful of cells from a purified culture of this isolate was inoculated into culture

flasks containing 2mls LB (Fisher Chemicals) and 3mls AMS. Cells were grown overnight on a rotary shaker at room temperature. The contents of the flasks were pelleted at 3000g and washed once in PBS solution. A single pellet was re-suspended in 40mL liquid AMS supplemented with uniformly ^{14}C ring-labeled-atrazine (650 Bq). The same medium was used for uninoculated controls to confirm the biological basis of atrazine degradation. Atrazine and potential metabolites were determined by reverse phase HPLC using the conditions described earlier. Control and treatment samples were measured after 0, 1, 3, 6, 12, and 24 hours of incubation.

2.9 PCR Amplification of 16S rRNA gene of ES-1

Whole cells from isolate ES-1 and DNA from the Cisne soil were used as template for the amplification of the following genes using the referenced primers: 16S rRNA gene (Liu et al., 1997), atzA, atzB, atzC (Costa et al., 2000), atzD, atzE, atzF (Piutti et al., 2003), trzD (Rousseaux et al., 2001), and trzN (Mulbry et al., 2002). PCR conditions for atrazine-degrading genes were as follows: 94°C (10 min); 94°C, 58°C for atzA, atzD, and trzN / 68°C for atzB / 62°C for atzC, atzD, atzE, atzF, and trzD, 72°C (1 min) (30 cycles); 72°C (10min). PCR conditions for amplifying the 16S rRNA genes were as follows: 94°C (10 min); 94°C (1.5 min), 55°C (1.5 min), 72°C (1.75 min) (25 cycles); 72°C (10min). 25µl PCR reactions were performed according the manufacturer's protocol. PCR products were cloned into Escherichia coli TOP10 using a TOPO TA cloning kit (Invitrogen Corporation, Calsburg, CA). Plasmids were extracted from the cloned cells with a QIAprep miniprep system (Qiagen, Inc., Valencia, CA), and the insertions were sequenced at the W.M. Keck Center for Functional Genomics (Keck Center), UIUC, Urbana, IL.

2.10 Terminal Restriction Fragment (TRF) Profiles

Whole cells from isolate ES-1 were also analyzed to determine its TRF patterns of the 16S rRNA gene patterns obtained after digestion using three restriction endonucleases. The TRF patterns were determined using the standard procedures as outlined in (Liu et al. 1997). PCR primers (Operon Biotechnologies) used were 27F-FAM (5' AGAGTTTGATCMTGGCTCAG, 5' end-labeled with carboxyfluorescein) and 1492R (5' GGTTACCTTGTTACGACTT). PCR mixtures (100µl) included the TaKaRa Ex Taq mixture (Takara Bio), primers (45 pmol each), and 1µl whole cell suspension. The PCR conditions were: 94°C (10 min); 94°C (1.5 min), 55°C (1.5 min), 72°C (1.75 min) (25 cycles); 72°C (10min). PCR products were purified using the QIAquick® PCR purification kit (Qiagen Inc.), according to the manufacturer's instructions. The purified PCR products were separately digested using the restriction endonucleases: HaeIII, RsaI, and MspI according to the recommended protocol (New England Biolabs, Beverly, MA). DNA fragments were separated by capillary electrophoresis (model 3730xl Genetic Analyzer, Applied Biosystems, Foster City, CA) at the Keck Center. The ROX 1000 (Applied Biosystems) internal standard was used to size terminal restriction fragment (TRF) lengths. Data were analyzed with GeneMapper V3.7 software (Applied Biosystems). A separate profile was generated from each sample and restriction endonuclease combination.

2.11 ^{15}N-DNA-SIP of Pure Cultures of Atrazine-Degraders

2.11.1 Bacterial Strains and Culture Conditions

Experiments were performed to determine the feasibility of using ^{15}N-SIP to identify atrazine-degrading organisms in environmental samples. Two isotopically labeled forms of atrazine were used in pure culture experiments with bacterial isolates known to utilize all of the N atoms in the atrazine molecule. Using atrazine-ethylamino-^{15}N as a treatment, two cultures of Pseudaminobacter strain sp. C147 were grown (rotating at 25°C) on AMS media (5mL) supplied with either ^{15}N- or unlabeled atrazine (25mg/L) and then transferred (5% v/v) to media of the same type. To explore the use of uniformly ^{15}N ring-labeled-atrazine as a treatment, cultures of Pseudaminobacter strain sp. C147 and cultures of Pseudomonas strain sp. ADP were grown under the conditions described above on AMS media supplied with either ^{15}N- or unlabeled atrazine. Following growth, cells were harvested from the culture suspension in late exponential growth stage by centrifugation (3000g) and the cell pellets were frozen at -20°C for subsequent DNA extraction.

2.11.2 DNA Extraction and CsCl Density Gradient Ultracentrifugation

DNA from cell pellets was extracted using the DNeasy tissue system (Qiagen, Inc., Valencia, CA) following the manufacturer's instructions for Gram-negative bacteria. DNA was added to a solution of CsCl and Tris-EDTA (TE, pH 8.0). The CsCl/TE starting BD was adjusted to approximately 1.71 g/mL. Ultracentrifugation of samples was performed in Quick-Seal polyallomer tubes (13 X 51 mm, 5.1 ml, Beckman Coulter) in an Optima LE-80K Preparative Ultracentrifuge (Beckman Instruments) outfitted with a VTi 65.2 vertical tube rotor for 48 h, 184 000g (20°C). Buoyant densities (BD) were measured with a model AR200 digital hand-held refractometer (Leica Microsystems Inc. Depew, NY). Following ultracentrifugation, water was injected with a precision pump (model PHD 2000, Harvard Apparatus, Holliston, MA) into the headspace of the centrifuge tube and fractions (75µl) were collected at the bottom as previously described (Cupples et al., 2006, Cupples and Sims, 2007, Lueders et al., 2004). After fractionation, DNA was dialyzed using a 0.025-µm Millipore mixed cellulose ester dialysis filter (Bedford, MA) as previously described (Gallagher et al., 2005). Fractions and purified DNA were stored at -20°C.

2.11.3 Detection of Changes in DNA Buoyant Density

Purified DNA from the atrazine-ethylamino-^{15}N experiment was used as template for PCR amplification of the 16S rRNA gene using the conditions described above. PCR products from labeled and unlabeled incubations were paired according to buoyant density of the template, and separated by electrophoresis on a 1% agarose gel. The effect of the treatment on template buoyant density was determined by comparing the buoyant densities of the heaviest fractions that produced a PCR product. DNA collected in the experiments using uniformly ^{15}N ring-labeled atrazine as a treatment was fluorometrically quantified using the PicoGreen nucleic acid quantification dye (Molecular Probes, Invitrogen, Carlsbad, CA) according to the manufacturer's instructions. Fluorometry was performed on an Opticon 2 Real Time Thermal Cycler (MJ Research, Bio-Rad Laboratories, Hercules, CA) as previously described (Cupples et al., 2006,

Tian and Edenberg, 2004). The effect of the treatment on template buoyant density was determined by comparing the buoyant densities of the first significant fluorometric peak.

2.12 Environmental ^{15}N-SIP

2.12.1 Incubations with Uniformly ring labeled ^{15}N Atrazine

Incubation and DNA extraction procedures are described earlier. DNA samples taken from the replicates on day 41 were individually separated by ultracentrifugation and purified as described above.

2.12.2 Atrazine-ethylamino-15N incubations

Samples (3 replicates/treatment) were amended once (Day 0) with the following forms of atrazine introduced at 30µg atrazine g-1 soil: unlabeled atrazine (control), atrazine-ethylamino-^{15}N (treatment), or uniformly ring-labeled ^{14}C-atrazine (53 Bq g-1 soil), the latter treatment was included to facilitate radiochemical analysis of atrazine fate. Atrazine solutions were prepared in methanol (3.2-3.5 µg atrazine/µl methanol) and added to the volume of water necessary to bring the water-filled pore space of the soil to 40%. The atrazine/water solutions were deposited onto the bottom of aluminum weigh boats (57mm, Life Science Products, Fredrick, CO) and six grams of the study soil were placed on top of the solution allowing the solution to diffuse through the soil pore space. The weigh boats were placed in sealed microcosms containing a 90mm qualitative filter paper wetted with 0.575mM KH_2PO_4 and a 10ml 0.1M NaOH trap in the radioactive monitoring samples. The microcosms were stored at 19°C in the dark. One gram of soil was removed from each replicate on days 5, 10, 15, 21, 26 and sacrificed for DNA extraction using the Powersoil kit (Mobio Laboratories, Carlsbad, CA) according the manufacturer's instructions. NaOH samples were also collected, as previously described, from the ^{14}C-atrazine treatments on these dates to estimate the percent of compound mineralized in the control and treatment samples. DNA samples from each replicate taken on day 15 were individually separated by ultracentrifugation and purified as described above.

2.12.3 TRF Analysis of Environmental Samples

After fractionation and recovery of DNA, TRF profiles were generated from the 12 heaviest fractions of each sample tube using the primers and PCR conditions described above for the amplification of the 16S rRNA gene. PCR products were purified using the AMPure PCR purification system (Agencourt Bioscience Corp., Beverly, MA) according to the manufacturer's instructions. Purified PCR products were quantified using a UV spectrophotometer (NanoDrop Technologies, Wilmington, DE). Approximately 150ng of the purified PCR products were separately digested using the restriction endonucleases: HaeIII, RsaI, and MspI (New England Biolabs, Ipswich, MA) and the subsequent TRF profiles were generated as described above. Each TRF had a unique fragment length, and a reported peak area of fluorescently labeled product, in arbitrary fluorescence units (FU). Percent abundance of each TRF was determined by dividing the FU under each TRF by the total FU under all the TRFs in the profile as described previously (Abdo et al., 2006, Yu and Chu, 2005). Values given for the percent abundance of

each FU are reported as relative fluorescence units (RFUs). Data sets were constructed of TRFs that were between 50bp and 1000bp in length and greater than 50 FU in height. Each TRF was identified with a sample name, isotopic treatment, buoyant density (determined during fractionation), and RFU value.

2.13 Statistical Analyses

Statistical analyses were developed with the assistance of Charles Smyth, department of Crop Sciences. Analyses were performed using the statistical functions in Excel (Microsoft Corp, Seattle, WA) and SAS (SAS Institute Inc, Cary, NC). The continuous and quantifiable nature of the CsCl density gradient necessitated the use of a covariance model for detecting upward shifts in TRF buoyant density due to isotopic treatment. If the buoyant densities of individual fractions were the same across test tubes then an Analysis of Variance would be appropriate. However, since they are not, it was necessary to include TRF buoyant density as a continuous parameter in the model. An Analysis of Covariance using SAS Proc Mixed was performed on the TRF data generated from the day 15 atrazine-ethylamino-15N incubations and the day 41 uniformly ring labeled 15N atrazine incubations. Analysis was performed using the model:

Yijkl = Isotope i + Test tube (Isotope) j(i) + Densityl + Error k(ijl)

Error = Sample (test tube, isotope, density)

Sample information was entered in the following categories: tube (enzyme), fraction, isotope, density, peak, and RFU. Results were considered significant if the analysis of the effect of isotope produced F values correlating to an α error rate less than 0.25. This error rate is fairly liberal and allows for the detection of TRF buoyant density shifts that may not be due to isotopic treatment; however this liberal error rate allows for the screening and detection of possibly enriched TRFs. TRFs that have been identified as possibly enriched require further analysis using the remaining two enzymes. TRFs with the same relative abundance in TRFLP profiles generated with the remaining enzymes must be examined using the same method. TRFs that comprise similar relative abundances and show similar shifts in buoyant density would be considered enriched. This process could be accelerated through the use of Multivariate Analysis of Covariance to detect concurrent buoyant shifts using all three enzymes simultaneously.

3. RESULTS AND DISCUSSION

3.1 Atrazine Mineralization Kinetics

Atrazine mineralization kinetics for the six soils are given in Figure 1. When compared to five reference soils in our laboratory as well as previous reports in the literature, the Cisne soil appeared to exhibit enhanced atrazine degradation. Leaching did not significantly increase mineralization rates for the Cisne soil, indicating inorganic N concentration was not likely rate limiting. The unleached Cisne soil exhibited the most rapid initial degradation rate (1.822x10-5 mmoles atrazine mineralized day-1) and cumulatively mineralized >82% of the atrazine applied, apparently meeting criteria for enhanced degradation (Zablotowicz et al., 2006). Mineralization

kinetics for the Cisne soil appeared sigmoidal, indicating decreased microbial growth rates with time as local atrazine solution concentration decreased and population numbers increased (Alexander and Scow, 1989). The kinetics of atrazine degradation indicated that degradation was not due to abiotic processes; thus the soil was a good candidate for examination of natural attenuation.

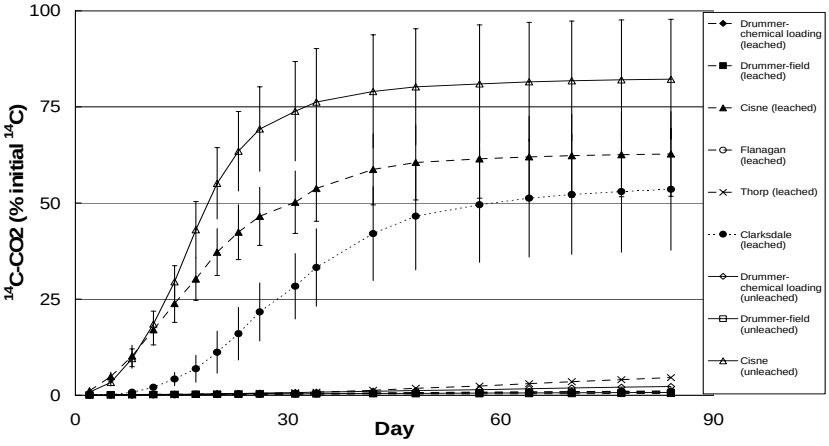

Figure 1. Representative atrazine mineralization in six Illinois soils previously exposed to atrazine. Samples included leached treatments and unleached controls.

To provide a broader context for the Cisne soil findings, mineralization rates were compared to those reported by Zablotowicz et.al (2006) for 7 agricultural soils varying in atrazine exposure history (Figure 2). The Cisne soil exhibited mineralization rates comparable to soils described in the paper as enhanced, likely due to the unusually large exposure to atrazine from the spill. These findings are consistent with atrazine mineralization potential observed for other soils with prior exposure to atrazine (Pussemier et al., 1997, Barriuso and Houot, 1996, Martin-Laurent et al., 2004, Yassir et al., 1999, Vanderheyden et al., 1997). A significant portion of the atrazine applied to the Cisne soil (18%) was not mineralized, and may have been present in the soil as atrazine, metabolites, or bound residues. Incomplete degradation of herbicides has been attributed largely to bioavailability limitations resulting from sorption (Sims and Cupples, 1999) or diffusion limitation through tortuous paths in unsaturated soils (Johnson et al., 1998). Owing to the relatively high carbon content (2.8 %) in the Cisne soil, both of these mechanisms are likely. Mineralization studies were thus followed with more detailed degradation studies in which a mass balance was performed on the C and N added as atrazine to provide a better understanding of material flow in the Cisne soil.

3.2 Soil Incubations with Uniformly $^{15}N/^{14}C$ Ring-Labeled-Atrazine

A mass balance of applied atrazine C and N was obtained by incubating the Cisne soil with uniformly ring-labeled $^{15}N/^{14}C$ atrazine as described in earlier. ^{14}C-mineralization kinetics were calculated as described above, and the distribution of radioactivity among mineralized, bioavailable ($CaCl_2$ extractable), potentially bioavailable (MeOH extractable), and non-extractable fractions was determined at the end of the incubations. After 26 days, the rate of atrazine mineralization in this second incubation was approximately 61% of that observed in the first incubation, likely due to limited bioavailability of solid phase atrazine (Figure 3). Data in

Figure 3 shows no significant label effect on atrazine mineralization. Mineralization had reached a plateau by day 25, thus, though much of the atrazine had not been degraded.

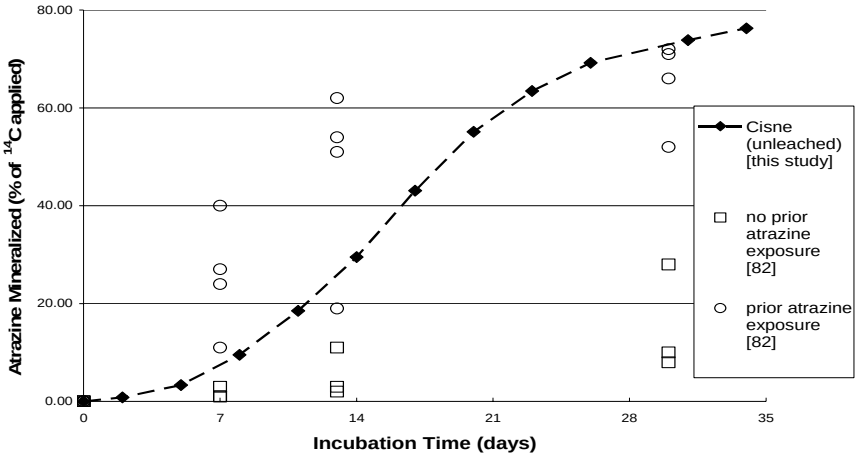

Figure 2. Kinetics of atrazine mineralization in the Cisne soil collected in this study compared to several enhanced (prior exposure) and unenhanced (no prior exposure) soils examined by Zablotowicz et al.

Additional atrazine and water (as described above) were introduced on day 26 (re-spike) to promote degradation. A sharp increase in $^{14}CO_2$ evolution detected on day 26 indicates a response to the re-spike, and suggests that much of the atrazine present at day 25 was no longer bioavailable. The concentration of atrazine used exceeded the solubility limit in this study. Soil moisture content prior to the re-spike was maintained at or below 40% water-filled pore space to ensure proper aeration, and was increased to 50% water-filled pore space during the re-spike process. Thus it is likely that atrazine availability was increased as a consequence of a higher water content and more complete redistribution of the compound through the soil matrix to the active atrazine-degraders. This hypothesis is supported by several observations. Both the bioavailable (aqueous extractable) and potentially bioavailable (methanol extractable) atrazine pools were preferentially depleted to a relatively constant value in the first ten days of incubation with a corresponding release of radiocarbon as CO_2 (Figure 4). A resurgence of mineralization was observed at 41 days (after the 26-day re-spike), even though a considerable amount of atrazine remained present in the system. This increase in mineralization coincided with a decrease in precipitated atrazine, presumably as a result of improved dissipation and redistribution of the chemical due to the additional water added with the re-spike. These findings are consistent with previous work showing increased utilization of an aromatic substrate present in soil solution as water content reached a threshold expected to result in greater continuity of pore space (Johnson et al., 1998). Based on that work, also performed with a Cisne soil, a significant portion of the atrazine present in a bioavailable form would be expected to reside in discontinuous pore space at the lower water content initially used.

When combined, the two extractable fractions accounted for 6.5-18.2% of the initial 14C-atrazine, whereas the non-extractable bound residues only accounted for 2-3% of the initially applied atrazine. The relatively little bound residue detected in the extracted soil is consistent with the unavailability of atrazine ring carbon for incorporation into biomass (Bichat et al., 1999), which would be expected to appear as bound residue in the analysis scheme used here. In a similar study by Houot et al.(2000), soils showing accelerated degradation tended to equally partition residual radioactivity between the extractable and non-extractable fractions, which

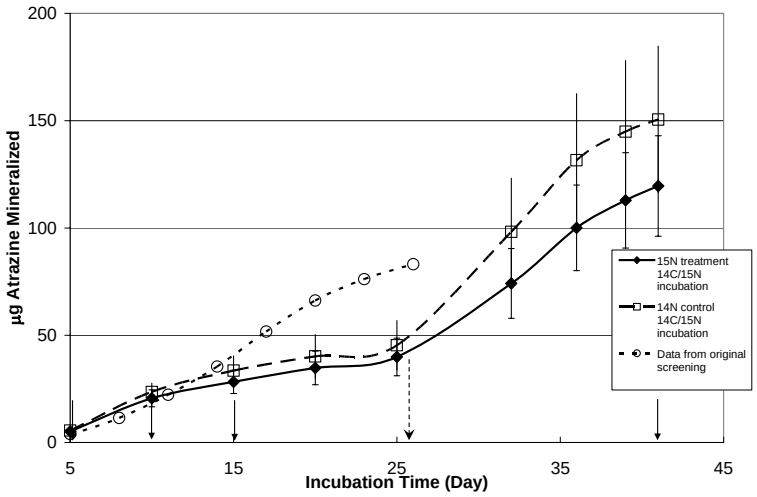

Figure 3. Atrazine mineralization in the Cisne soil incubated with uniformly ring labeled $^{14}C/^{15}N$ atrazine and data from its initial screening . ^{15}N Series includes treatment replicates. Unlabeled series includes control replicates. Solid arrows indicate destructive sampling points for DNA extraction and HPLC analyses. The broken arrow indicates the respike of 30µg atrazine g-1 soil on day 26.

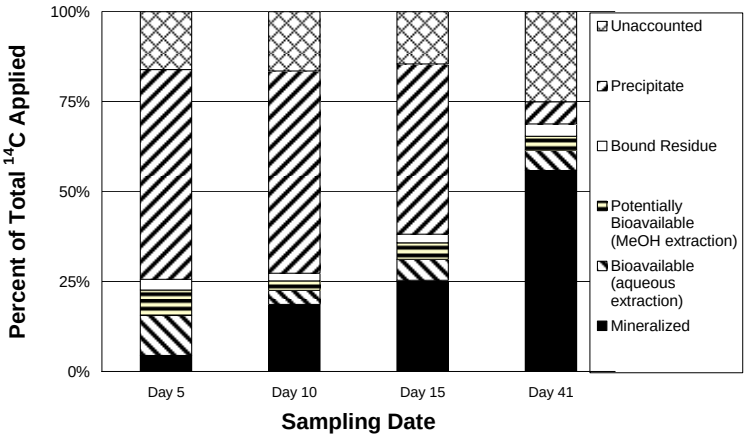

Figure 4. Mass balance of atrazine in the experimental system. Represented as the mean percentage of the total amount of ^{14}C atrazine applied (10 replicates). No distinction is made between control and treatments samples, as the trends were consistent for both groups.

combined to equal 5-10% of the initial atrazine application. The same study showed that in soils showing minimal atrazine degradation, approximately 50% of the initial radioactivity remained extractable and 30% remained as non-extractable bound residues. The fractioning of radioactivity in the Cisne soil more closely resembled the pattern displayed in soils with accelerated degradation than the non-degrading soils described in the Houot study.

Mineralization kinetics in the Cisne soil underestimated the rate of atrazine dissipation demonstrated by the accumulation of several metabolites. In addition to atrazine, three metabolite peaks were detected in the fractions extracted from the Cisne soil. These metabolite peaks corresponded to the retention times for hydroxyatrazine (3.8-4.0min), deethylatrazine and deethylhydroxy atrazine (3.3 min), and the unresolvable peaks of deethyldeisopropylatrazine,

deethyldeisopropylatrazine, and cyanuric acid (2.3-2.5 min), however, these identities have not been confirmed. The metabolites represent approximately 50% of the extracted radioactivity in the bioavailable fraction, but only 20-40% of the extracted radioactivity in the potentially bioavailable fraction (Figure 5), likely owing to the more polar nature of the metabolites.

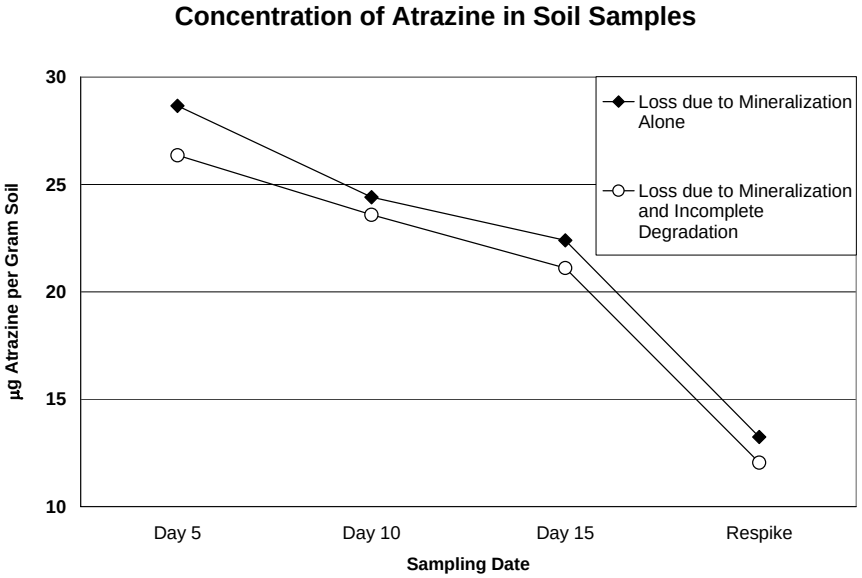

Figure 5. Change in atrazine concentration over time. Mineralization kinetics alone in the Cisne soil underestimate the rate of atrazine degradation .Mean values are presented without standard error bars. Treatment and control replicates exhibited similar results and were grouped together (10 replicates).

3.3 Isolation and Characterization of an Atrazine-Degrading Isolate

The results of metabolite analysis supported the presence of an active population of atrazine-degraders in the Cisne soil comparable to other sites from which such organisms have been successfully isolated (Mandelbaum et al., 1995, Topp et al., 2000a, Topp et al., 2000b Aislabie et al., 2005). Direct soil plating experiments were performed to elucidate some of the microbial interactions taking place in the Cisne soil. Initially, several bacterial colonies showed faint signs of clearing on agar plates that were supersaturated with atrazine. One colony demonstrated distinct removal of particulate atrazine from the medium. This isolate, ES-1, was selected for further study. The atrazine-degrading bacterium formed rounded, shiny white colonies on solid media. Examination of cultures in the exponential growth phase indicated cells were long, slender, Gram-positive rods; however, examination of late-stage cultures indicated cells were Gram-negative cocci.

Analysis of the 16S rRNA gene confirmed the organism to belong the Gram-positive genus Arthrobacter. Isolate ES-1 was identified by comparison of the partial 16S rRNA sequences with bacterial accessions in GenBank using a megablast search (Zhang et al., 2000) and confirming the results using the bl2seq function (Tatusova and Madden, 1999) (open gap penalty=5, extension gap penalty=2). The isolate showed 99% identity with Arthrobacter sp. AD12 (Gen Bank accession AY628690.1) and 97% identity with Arthrobacter aurescens (Gen Bank accession AJ871298) (Table 3).

Table 3. BLAST comparison of sequence identities for 16S rRNA gene and atrazine-degradation genes amplified using isolate ES-1 whole cells as template

Source	Strain	Target Gene	Closest identity in BLAST accession number	Similarity (%)	# Bases used for search	% similarity to corresponding genes encoded by P. ADP catabolic plasmid (U66917.2)
Cisne Soil	ES-1	16S	AY628690.1 16S r RNA from *Arthrobacter* sp. AD12	99	1490	n/a
Cisne Soil	ES-1	*trz* N	AY456696.1 *trzN* from *Arthrobacter aurescens* strain TC1	99	432	n/a
Cisne Soil	ES-1	*atz* B	AY456696.1 *atzB* from *Arthrobacter aurescens* strain TC1	100	523	100
Cisne Soil	ES-1	*atz* C	AY456696.1 *atzC* from *Arthrobacter aurescens* strain TC1	99	626	99

3.4 Kinetics of Atrazine Degradation in Pure Culture

Pure culture experiments in uniformly ^{14}C ring-labeled-atrazine AMS media were conducted to determine the atrazine-degrading capabilities of ES-1. Mass balance of the culture media indicated no loss of radioactivity, though growth response of the organism was linked to the presence of atrazine in the medium. Analysis of the CO_2 traps suspended in the culture flasks revealed no mineralization, suggesting that the organism degraded atrazine incompletely.

Further time-course kinetic experiments using isolate ES-1 demonstrated rapid dechlorination and dealkylation of atrazine. Results from this kinetic study show that 100% of the atrazine initially added to the culture medium was converted into metabolites. The bulk (>90%) of the atrazine was converted to a polar metabolite with a retention time of approximately 2.3 minutes that co-eluted with authentic cyanuric acid. Approximately 10% of the atrazine in solution was converted to a metabolite that co-eluted with a hydroxyatrazine standard at approximately 4 minutes. The latter compound was detected earlier in the growth medium, suggesting it was a precursor of the terminal product. A number of Gram-positive, atrazine-degrading organisms have been isolated in pure culture including members of the genera: Arthrobacter, Clavibacter, Nocardiodies, and Rhodococcus (Piutti et al.2003, Rousseaux et al., 2001, Topp et al., 2000b, Aislabie et al., 2004, Behki and Khan, 1994, DeSouza et al. 1998, Strong et al., 2002). To date, members of the Arthrobacter genus have demonstrated the most complete degradation of atrazine of all gram positive organisms—metabolizing atrazine to cyanuric acid (Rousseaux et al., 2001, Aislabie et al., 2005, Cai et al., 2003, Strong et al., 2002). These organisms have also shown degradative capacities for a variety of other xenobiotic compounds including pesticides such as: pyridines (O'Loughlin et al., 1999), PCP, phenoxyacetate herbicides, organochlorines, triazones, N-methylcarbonates, N-phenylcarbamates, organophosphates, and glyphosate (De Schrijver and De Mot, 1999).

3.5 Amplification of 16S rRNA Gene Sequence and Atrazine Degrading Genes atzA, atzB, atzC, trzD, and trzN

Isolate ES-1 was identified by comparison of the partial 16S rRNA sequences with bacterial accessions in GenBank using a megablast search (Zhang et al., 2000) and confirming the results using the bl2seq function [105] (open gap penalty=5, extension gap penalty=2). The isolate showed 99% identity with Arthrobacter sp. AD12 (Gen Bank accession AY628690.1) and 97% identity with Arthrobacter aurescens (Gen Bank accession AJ871298) (Table 3).

Genes encoding enzymes involved in atrazine degradation have been characterized including atzABCDEF from Pseudomonas sp. strain ADP (de Souza, M.L., et al. 1998, Piutti et al., 2003, Sadowsky et al., 1998), trzN in Nocardioides strain C190 (Mulbry et al., 2002), and trzD from various gram negative bacteria (Rousseaux et al., 2001). PCR amplification of these atrazine degrading genes in isolate ES-1 using aforementioned primers resulted in an approximately 400bp amplicon for trzN, a 500bp amplicon for atzB, and a 600bp amplicon for atzC. No PCR products were formed using primers specific to atzA or trzD (Table 3). PCR amplification of environmental DNA extracted from the Cisne soil produced amplicons of the expected size for reactions specific to atzABC and trzDN (Table 4); suggesting the presence of other atrazine-degrading organisms besides ES-1. No detectable PCR products resulted from using atzDEF primers when either isolate ES-1 cells or environmental DNA was used as template. Nucleotide sequencing analysis of the cloned genes confirmed that the PCR products were sufficiently homologous to the targeted sequences.

Table 4. BLAST comparison of sequence identities for atrazine-degradation genes amplified using Cisne DNA as template

Source	Strain	Target Gene	Closest identity in BLAST accession number	Similarity (%)	# Bases used for search	% similarity to corresponding genes encoded by P. ADP catabolic plasmid (U66917.2)
Cisne Soil	predominant soil clone	*atzA*	DQ089655.2 *atzA* from *Herbaspirillum* sp. B601 (smzA) gene	99	531	99
Cisne Soil	predominant soil clone	*atz* B	AY456696.1 *atzB* from *Arthrobacter aurescens* strain TC1	100	523	100
Cisne Soil	predominant soil clone	*atz* C	AY456696.1 *atzC* from *Arthrobacter aurescens* strain TC1	99	628	99
Cisne Soil	predominant soil clone	*trz* D	AF086815 from *trzD Acidovorax avenae* subsp. citrulli	100	854	n/a
Cisne Soil	predominant soil clone	*trz* N	AY456696.1 *trzN* from *Arthrobacter aurescens* strain TC1	99	237	n/a

Since the isolate was cultivated from the Cisne soil it is reasonable to expect that atrazine-degrading genes present in ES-1 would comprise a subset of the atrazine-degrading genes residing in the soil metagenome. The presence of putative genes not found in the isolate indicates that other atrazine-degrading organisms are present in the soil. Environmental sequences homologous to atzA support the idea that two competing chlorohydrolases (and populations of atrazine degrading organisms) are present in the same niche environment. The

presence of homologous sequences to the trzD genes indicates organisms other than isolate ES-1 were responsible for the relatively high rate of atrazine mineralization in the Cisne soil. However, microbial degradation of cyanuric acid is relatively common in soil (Cook, 1987, Karns, 1999, Cook et al., 1985) and there may be other cyanuric acid-metabolizing organisms that were not detected with the primers used in this study. The presence of competing chlorohydrolase and aminohydrolase enzymes plus the genetic diversity in the atzBC sequences indicate that multiple and unique atrazine degrading consortia may have been functional in the Cisne soil. Isolate ES-1 was isolated and cultured without enrichment techniques indicating that it may have been one of the more dominant atrazine-degrading microorganisms in the soil, however the genetic diversity exhibited in the soil precludes the possibility that it is the only organism responsible for atrazine degradation.

The detection and isolation of isolate ES-1 helps to explain how atrazine was rapidly degraded in the contaminated soil. The broad substrate range of Arthrobacter species makes them well-suited as agents of bioremediation, especially at sites with multiple contaminants as is often the case with agrochemical contamination. Arthrobacter aurescens strain TC1, also isolated from a highly contaminated soil, has an extremely diverse substrate range and is capable of degrading more s-triazine compounds than any bacterium previously characterized (Strong et al., 2002).

3.6 TRF Analysis of Isolate ES-1

TRFLP analysis of isolate ES-1 pure cultures showed the following TRFs: HaeIII 229bp; MspI 229bp; RsaI 465bp. Each TRFLP profile showed one major peak. These peaks were present in the whole soil TRFLPs, and as noted below, were also detected in soil DNA during the SIP experiments.

3.7 Pure culture ^{15}N-DNA-SIP

DNA based SIP is a relatively new microbial tool used to examine microbial interactions in the environment. Previous research in our lab demonstrated that ^{15}N enriched compounds can be used as substrates for SIP (Cupples et al., 2006, Cupples and Sims, 2007). Experiments were conducted to examine if two different forms of ^{15}N-labeled atrazine, atrazine-ethylamino-^{15}N and uniformly ^{15}N ring-labeled atrazine, could also serve as suitable substrates for SIP-based investigations. Fine fractions were collected and sensitive DNA detection methods were employed to detect small changes in buoyant density. Results from the atrazine-ethylamino-^{15}N experiment indicated that the buoyant density of Pseudaminobacter strain C147 DNA increased from approximately 1.733220 g/ml to 1.736735 g/ml, an increase of 0.003515 g/ml (Figure 6). Results from the uniformly ^{15}N ring-labeled atrazine experiment indicated that the buoyant density increase of Pseudomonas strain ADP DNA was 0.007040 g/ml and the average buoyant density increase of Pseudaminobacter strain C147 DNA was 0.006143 g/ml +/- 0.001663 g/ml. Figure 7 shows how the results of these experiments compare with the buoyant density increases demonstrated in Cupples et al. (2006) and Meselson and Stahl (1958). The buoyant density shifts found in these previous investigations were reported for substrates that were enriched to 100 atom% ^{15}N. The buoyant density increase published in Meselson and Stahl (0.014 g/ml) was used to calculate the theoretical buoyant density increases expected at other enrichment levels. The two N-labeled forms of atrazine used herein were selectively labeled at 100 atom %

^{15}N at the label positions. Incorporation of all five N atoms from atrazine would thus result in enrichment of DNA equivalent to 20 atom % ^{15}N for the ethylamino-labeled atrazine and 60 atom % ^{15}N for the ring labeled material. Based on that assumption, the data from our experiments closely follows the trend projected by the Meselson and Stahl data. Our results demonstrate that addition of substrates with known enrichment levels of ^{15}N will result in reliable increases in DNA buoyant density.

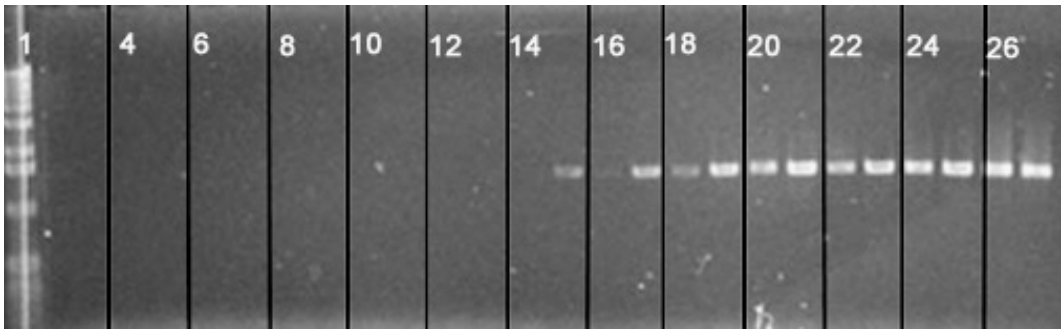

Figure 6. Detection of *Psuedaminobacter* sp. C147 in fractions from a buoyant density gradient using 16S rRNA gene PCR products. Even lanes contain PCR products using template from cells grown on unlabeled atrazine and odd lanes contain PCR products using template from cells grown on ^{15}N-labeled atrazine. Lanes are paired according to closest buoyant density fractions. Lane 1- 1kb ladder. Lane 15- first PCR product detected using ^{15}N enriched *Pseudaminobacter* sp C147 DNA as a template (BD= 1.736735 g/mL), Lane 18- first PCR product detected using , unenriched *Pseudaminobacter* sp C147 DNA as a template (BD = 1.733220).

The consistent relationship between substrate enrichment and increases in DNA buoyant density makes it possible to anticipate the amount of substrate incorporation necessary to result in a detectable increase in buoyant density. In our experiments, the decrease in buoyant density from one fraction to the next is approximately 0.00136 +/- 2.074 E^{-4} g/ml. Using this data, it is possible to extrapolate that at least 13.6% of the nitrogen atoms in the target organism's nucleic acids must be labeled with the ^{15}N isotope in order for the separation of light and heavy DNA to be observed. Nucleic acid enrichment levels below this threshold will not be detectable in our study system.

3.8 ^{15}N-SIP of Environmental Microbial Communities

Most practitioners of stable isotope probing rely on the visible separation of "heavy" and "light" nucleic acids. As our lab demonstrated earlier, enrichment with ^{15}N does not result in a sufficient buoyant density increase to visually resolve enriched and un-enriched nucleic acids from one another (Cupples et al., 2006). In such instances, fine fractionation of the buoyant density gradient must be collected and compared to control samples using quantitative PCR or TRF profiles. Comparison of control and treatment TRFs can be tedious if the effect of the treatment is not pronounced. In such instances, a sensitive detection method is needed. To our knowledge, we have developed the first statistical model capable of distinguishing enriched and un-enriched TRF profiles from one another.

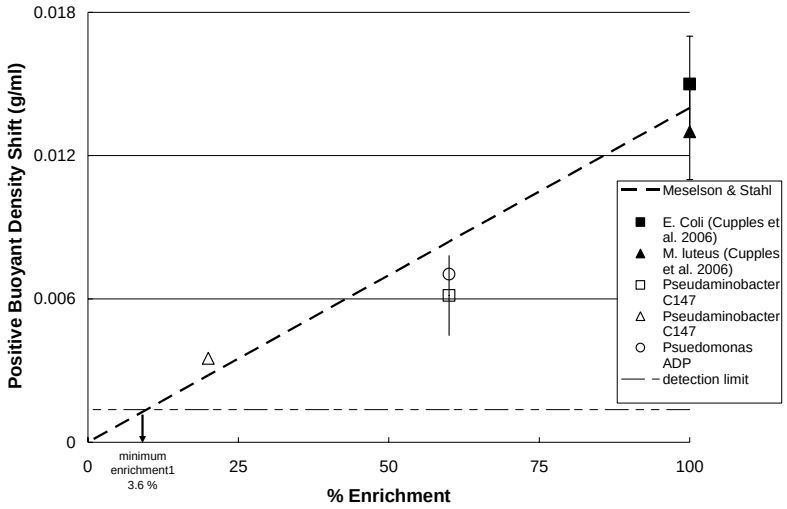

Figure 7. Effect of enrichment with ^{15}N on DNA buoyant density. Closed data symbols show effect of enrichment observed by Cupples et al. [61], and Meselson and Stahl [113]. Open symbols report buoyant density increases demonstrated in the current study. The buoyant density increase published in Meselson and Stahl (0.014 g/ml) for 100% ^{15}N enrichment was used to calculate a theoretical relationship between buoyant density and enrichment indicated by the dashed line.

TRF profiles from soil SIP studies were examined for the three fragments characteristic of isolate ES-1 to determine if the addition of ^{15}N-labeled atrazine resulted in an increase in the organism's DNA buoyant density. As tables 5 and 6 indicate, DNA from isolate ES-1 was not enriched in either the uniformly ring-labeled ^{15}N atrazine incubations or the atrazine-ethylamino-15N incubations

It is expected that treatments of uniformly ring-labeled ^{15}N atrazine would not produce enrichment of DNA in the target organism, since the results of the PCR screening for atrazine degrading genes and kinetic study indicate that isolate ES-1 lacks the genes necessary for ring cleavage. Any incorporation atrazine ring ^{15}N into ES-1 biomass would have been the result of cross-feeding on NH_4^+ (or other products) produced by an organism capable of ring fission. However, this isolate is capable of utilizing the nitrogen present in the alkylamine side chains; therefore, treatments with atrazine-ethylamino- ^{15}N could have produced an effect.

Table 5. Statistical analyses of the TRFLP profiles associated with Isolate ES-1 in the atrazine-ethylamino-^{15}N SIP experiments. Results indicate probability of BD increase due to treatment. Analyses were conducted using 72 observations.

Atrazine-ethylamino-^{15}N SIP							
			mean relative fluorescence of trf				
restriction endo-nuclease	terminal fragment length (trf)	◊ level associated with isotope effect	control	standard error	treatment	standard error	treatment mean signficantly > control
HaeIII	229	0.7575	5.51E-04	3.49E-04	7.19E-04	3.49E-04	no
RsaI	465	0.356	4.60E-05	8.20E-05	1.70E-04	8.10E-05	no
MspI	229	0.5288	4.72E-04	7.00E-05	4.01E-04	7.00E-05	no

Table 6. Statistical analyses of the TRFLP profiles associated with Isolate ES-1 in the uniformly ring-labeled ^{15}N atrazine SIP experiments. Results indicate probability of BD increase due to treatment. Analyses were conducted using 120 observations.

Uniformly ring-labeled ^{15}N atrazine SIP							
			mean relative fluorescence of trf				
restriction endo-nuclease	terminal fragment length (trf)	≅ level associated with isotope effect	control	standard error	treatment	standard error	treatment mean signficantly > control
HaeIII	229	0.3317	6.32E-03	2.68E-03	1.02E-02	2.68E-03	no
RsaI	465	0.1107	2.38E-03	6.79E-04	6.57E-04	6.79E-04	no
MspI	229	0.9543	3.66E-03	2.14E-03	3.49E-03	2.14E-03	no

It is likely that the failure to produce a significant treatment effect in the atrazine-ethylamino-^{15}N incubations is a result of insufficient enrichment of the target nucleic acids. To avoid enrichment-bias atrazine was added to the microcosms at 30µg g-1soil. This is an environmentally relevant concentration of atrazine comparable to the concentrations seen in some agricultural surface soils. As demonstrated in the pure culture SIP experiments, target organisms must utilize the substrate in sufficient quantities to ensure that at least 13.6% of the nitrogen atoms in nucleic acids are ^{15}N -labeled. In pure culture experiments, this parameter is easily controlled; however, in the soil environment there are many competing sources of nitrogen.

The Cisne soil contained excess nitrate either from excess fertilization or mineralization of atrazine N; however, the presence of NO_3- did not suppress atrazine degradation. The study soil contained more than 161 mg/kg NO_3-N; unfertilized Cisne soils typically contain one-tenth this amount of nitrate (Mulvaney et al., 2006). The high nitrate load in the Cisne soil could have competed with atrazine resulting in a dilution of the treatment and a decreased likelihood of detection in SIP. It is possible that the high concentrations of nitrate are the result of the degradation of the initial atrazine and metolochlor spill. The final degradation of atrazine compounds results in the release of NH_4 which in soil is then converted to NO_3^-. Since the soil was stored under a tarp for a number of months before it was remediated the NO_3^- generated from atrazine degradation would not have been leached away. If the high nitrate concentration is due to atrazine degradation, then it is likely that the organisms have a preference for atrazine-N over NO_3^-N, otherwise an accumulation of NO_3^- would not occur. The high nitrate conditions of our study soil create bias for the detection of organisms that prefer atrazine-N over NO_3^-N in the ^{15}N -DNA-SIP experiments.

Despite the high concentrations of NO_3^-N in the study soil it is reasonable to expect some organisms could incorporate significant amounts of ^{15}N into biomass. In the atrazine-ethylamino-^{15}N incubations 180µg of atrazine were added to each sample equaling approximately 12.5µg ^{15}N sample-1. Organisms that only incorporated N from the side chain moieties of atrazine would have accumulated equal amounts of ^{14}N and ^{15}N from the herbicide. The chemical analysis of the Cisne soil (Table 2) indicates that the soil contained 18µg of NH_4^-N and 966µg of NO_3^-N per 6 gram sample. No information is available on the amount of nitrogen contributed by organic matter. If we assume that all identified forms of nitrogen are equally incorporated into biomass then the ratio of ^{15}N:^{14}N is 1:80. However, since the incorporation of NO_3 into biomass requires the input of energy to convert it to NH_4 many microorganisms may prefer less energetically costly forms of nitrogen under aerobic conditions. It is unlikely that

there were substantial anaerobic microenvironments in the atrazine-ethylamino-^{15}N incubations since aggregates greater than 2mm in diameter were removed and research has shown anaerobic microenvironments are unlikely to form in aggregates smaller than 1cm in diameter (Sexstone et al., 1985). Care was taken to avoid disrupting the soil structure and only 40% of the pore space was filled with water. Furthermore, removing excess NO_3 from the Cisne soil through leaching did not show an increase in atrazine mineralization. This may suggest that atrazine-N was preferred over NO_3^-N. Therefore, we will make the assumption that the microorganisms preferentially utilized the atrazine and NH_4^- N before utilizing NO_3^-N for biomass. Under that assumption, the ratio of ^{15}N:^{14}N in the sample is 1:2.4. To achieve a 13.6% ^{15}N enrichment in DNA approximately 1 in 8 N atoms in DNA must be labeled with 15N. The ratio of 1 ^{15}N atom to 2.4 ^{14}N atoms in the readily assimilable nitrogen pool is within the requirements for ^{15}N SIP.

There are several possible reasons why we did not see an increase in the buoyant density of the ES-1 TRFs. Only about 55% of the atrazine added in the ethylamino- ^{15}N incubations was mineralized and metabolite analysis of the uniformly-ring-labeled incubation indicates that approximately 7% of the atrazine applied was incompletely degraded; therefore a conservative estimate would indicate that approximately 62% of the atrazine applied could have been degraded and used for biosynthesis. Using this estimate, the effective ratio of ^{15}N:^{14}N in the sample is reduced to 1:4 assuming only native soil NH_4 competed as an N source for biosynethesis. This ratio is still within the requirement for effective isotopic encorporation, however these estimates assume that all the available ^{15}N was utilized by a single group of atrazine degrading organisms. It is more likely that the ^{15}N label was distributed among several taxa preventing the ES-1 from assimilating enough ^{15}N to significantly increase its BD. Although the ratio of enriched to unenriched readily assimilable nitrogen was favorable, the presence of many atrazine-degrading bacteria would have diluted the treatment effect. This explanation is supported by the presence of atrazine-degrading genes not found in the isolate. If the atzA and trz D genes detected in the Cisne soil code for functional enzymes, then there are several populations of atrazine-degrading bacteria thereby minimizing the incorporation of ^{15}N into the DNA of one organism.

As a member of the Arthrobacter genus, isolate ES-1 probably has a G+C content ranging from 50-70% (Stackebrandt et al., 1983) giving it a relatively high unenriched BD. Our analysis of BD fractions was limited to the 12 heaviest fractions, which included the BD range of ES-1, and favored the detection of organisms with high G+C contents. That isolate ES-1 did not show any enrichment, even though the sampling technique and study design favored its detection, further supports the theory that the effect of the treatment isotope was diluted by multiple atrazine-degrading species and/or incorporation of nitrogen from other sources.

In future experiments these problems can be ameliorated with use of dual-labeled treatments. Experiments by Cupples and coworkers demonstrated that the use of ^{13}C and ^{15}N -dual labeled substrates produced a buoyant density increase of 0.045g/ml when supplied as the sole sources of carbon and nitrogen (2006). A buoyant density increase of that magnitude would simplify detection visually or by comparison of TRFLP profiles. The use of dual-labeled substrates in environmental samples would greatly improve the probability of detection when the treatment is applied at low concentrations.

4. CONCLUSION

Mineralization kinetics appeared to be a conservative estimate of atrazine degradation rates for determining the suitability of this soil for natural attenuation. Natural attenuation of atrazine appeared to be primarily limited by incomplete distribution of the compound through the unsaturated soil matrix, as has been reported for other aromatic compounds under similar conditions. Mineralization kinetics underestimated the rate of atrazine dissipation owing to the accumulation of several metabolites. Additional study soils did not mineralize a significant mass of atrazine, indicating that while natural attenuation was rapid in the Cisne soil, not all soils are suitable for natural attenuation. The Arthrobacter isolate, ES-1, obtained from the Cisne soil without enrichment degraded at an unusually rapid rate, and the termination of the degradative pathway at cyanuric acid was precedented by the atrazine degradative genes detected in the organism. The accumulation of this product was consistent with observations of metabolite accumulation in the soil.

TRFLP analysis revealed fragments consistent with the Arthrobacter sp. in the Cisne soil, though no enrichment of these fragments was observed when the soil was supplied with atrazine labeled with ethylamino- ^{15}N. Results from pure-culture studies with atrazine-degrading organisms indicate that under the right conditions stable-isotope probing SIP may be a useful tool in identifying populations responsible for natural attenuation. The use of fine fractions and statistical analysis coupled with traditional SIP techniques will hopefully allow for the detection of microorganisms responsible for the degradation of nitrogen-containing compounds such as herbicides and explosives. The results of these experiments suggest that this site is a good candidate for remediation by natural attenuation, however stable isotope probing is not a suitable method to elucidate the microbial interactions governing natural attenuation.

5. REFERENCES

U.S.Department.of Agriculture. 2004. Agricultural Chemical Usage: 2003 Field Crops Summary.

Solomon, K.R., et al. 1996. Ecological risk assessment of atrazine in North American surface waters. Environmental Toxicology and Chemistry. 15(1): p. 31-74.

Tasli, S., et al. 1996. Persistence and leaching of atrazine in corn culture in the experimental site of La Cote Saint Andre (Isere, France). Archives of Environmental Contamination and Toxicology. 30(2): p. 203-212.

Hayes, T.B., et al. 2002. Hermaphroditic, demasculinized frogs after exposure to the herbicide atrazine at low ecologically relevant doses. Proceedings of the National Academy of Sciences of the United States of America. 99(8): p. 5476-5480.

Hayes, T.B. 2004. There is no denying this: Defusing the confusion about atrazine. Bioscience. 54(12): p. 1138-1149.

Pussemier, L., et al. 1997. Rapid dissipation of atrazine in soils taken from various maize fields. Weed Research. 37(3): p. 171-179.

Costa, R.M., N.D. Camper, and M.B. Riley. 2000. Atrazine degradation in a containerized rhizosphere system. Journal of Environmental Science and Health Part B-Pesticides Food Contaminants and Agricultural Wastes. 35(6): p. 677-687.

de Souza, M.L., et al. 1998. The atrazine catabolism genes atzABC are widespread and highly conserved. Journal of Bacteriology. 180(7): p. 1951-1954.

Piutti, S., et al.2003. Isolation and characterisation of Nocardioides sp SP12, an atrazine-degrading bacterial strain possessing the gene trzN from bulk- and maize rhizosphere soil. Fems Microbiology Letters. 221(1): p. 111-117.

Rousseaux et al.. 2001. Isolation and characterisation of new Gram-negative and Gram-positive atrazine degrading bacteria from different French soils. Fems Microbiology Ecology. 36(2-3): p. 211-222.

Topp, E., et al. 2000a. Characterization of an Atrazine-Degrading Pseudaminobacter sp. Isolated from Canadian and French Agricultural Soils. Applied and Environmental Microbiology. 66(7): p. 2773-2782.

Topp, E., et al. 2000b. Characterization of S-triazine herbicide metabolism by a Nocardioides sp isolated from agricultural soils. Applied and Environmental Microbiology. 66(8): p. 3134-3141.

Aislabie, J., et al. 2005. Characterization of Arthrobacter nicotinovorans HIM, an atrazine-degrading bacterium, from agricultural soil New Zealand. Fems Microbiology Ecology. 52(2): p. 279-286.

Mulbry, W.W., et al. 2002. The triazine hydrolase gene trzN from Nocardioides sp strain C190: Cloning and construction of gene-specific primers. Fems Microbiology Letters. 206(1): p. 75-79.

Sadowsky, M.J., et al. 1998. AtzC is a new member of the amidohydrolase protein superfamily and is homologous to other atrazine-metabolizing enzymes. Journal of Bacteriology. 180(1): p. 152-158.

Cai, B., et al. 2003. Isolation and characterization of an atrazine-degrading bacterium from industrial wastewater in China. Letters in Applied Microbiology. 36(5): p. 272-276.

Cupples, A.M., et al. 2006. DNA buoyant density shifts during 15N-DNA stable isotope probing. Microbiological Research. In Press, Corrected Proof.

Bichat, F., G.K. Sims, and R.L. Mulvaney. 1999. Microbial Utilization of Heterocyclic Nitrogen from Atrazine. Soil Sci. Soc. Am. J., 63: p. 100-110.

Atlas, R.M. 1997. Handbook of Microbiological Media. 2nd ed, ed. L.C. Parks. University of Louisville, KY: CRC-Press. 1712 pages.

Yang, Y.R. and P.L. McCarty. 1998. Competition for hydrogen within a chlorinated solvent dehalogenating anaerobic mixed culture. Environmental Science & Technology,. 32(22): p. 3591-3597.

Sims, G.K. 2006. Nitrogen starvation promotes biodegradation of N-heterocyclic compounds in soil. Soil Biology & Biochemistry. 38(8): p. 2478-2480.

Mulvaney, R.L., et al. 2001. A soil organic nitrogen fraction that reduces the need for nitrogen fertilization. Soil Sci. Soc. Am. J. 65: p. 1164-1172.

Mervosh, T.L., G.K. Sims, and E.W. Stoller. 1995. Clomazone Fate in Soil as Affected by Microbial Activity, Temperature, and Soil-Moisture. Journal of Agricultural and Food Chemistry. 43(2): p. 537-543.

Cupples, A.M., et al. 2000. Effect of Soil Conditions on the Degradation of Cloransulam-Methyl. J. Environ. Qual. 29: p. 786-794.

Weaver, R.W., et al. 1994. Part 2. Microbiological and Biochemical Properties (#5). Methods of Soil Analysis, ed. S.H. Mickelson and J.M. Bigham. Vol. 5. 1994, Madison, WI: Soil Science Society of America. 1121.

Liu, W.-T., et al.1997. Characterization of Microbial Diversity by Determining Terminal Restriction Fragment Length Polymorphisms of Genes Encoding 16S rRNA. Applied and Environmental Microbiology. 63(11): p. 4516-4522.

Cupples, A.M. and G.K. Sims. 2007. Identification of In Situ 2,4 Dichlorophenoxyacetic Acid-Degrading Soil Microorganisms using DNA-Stable Isotope Probing. Soil Biology & Biochemistry, 39:232-238.

Lueders, T., M. Manefield, and M.W. Friedrich. 2004. Enhanced sensitivity of DNA- and rRNA-based stable isotope probing by fractionation and quantitative analysis of isopycnic centrifugation gradients. Environmental Microbiology. 6(1): p. 73-78.

Gallagher, E., et al. 2005. 13C-carrier DNA shortens the incubation time needed to detect benzoate-utilizing denitrifying bacteria by stable-isotope probing. Applied and Environmental Microbiology. 71(9): p. 5192-5196.

Tian, H.J. and H.J. Edenberg. 2004. High-throughput quantitation of double-stranded DNA using the ABI Prism 7700 sequence detection system. Analytical Biochemistry. 326(2): p. 287-288.

Abdo, Z., et al. 2006. Statistical methods for characterizing diversity of microbial communities by analysis of terminal restriction fragment length polymorphisms of 16S rRNA genes. Environmental Microbiology. 8(5): p. 929-938.

Yu, C.P. and K.H. Chu. 2005. A quantitative assay for linking microbial community function and structure of a naphthalene-degrading microbial consortium. Environmental Science & Technology. 39(24): p. 9611-9619.

Osborne, C.A., et al., New Threshold and Confidence Estimates for Terminal Restriction Fragment Length Polymorphism Analysis of Complex Bacterial Communities. Appl. Environ. Microbiol., 2006. 72(2): p. 1270-1278.

Zablotowicz, R.M., M.A. Weaver, and M.A. Locke. 2006. Microbial adaptation for accelerated atrazine mineralization/degradation in Mississippi Delta soils. Weed Science. 54(3): p. 538-547.

Alexander, M. and K.M. Scow. 1989. Kinetics of Biodegradation in Soil. In: Reactions and Movement of Organic Chemicals in Soils. 1989, Soil Science Society of America and American Society of Agronomy: Madison, WI. p. 243-269.

Barriuso, E. and S. Houot. 1996. Rapid mineralization of the s-triazine ring of atrazine in soils in relation to soil management. Soil Biology & Biochemistry. 28: p. 1341-1348.

Martin-Laurent, F., et al. 2004. Estimation of atrazine-degrading genetic potential and activity in three French agricultural soils. Fems Microbiology Ecology. 48(3): p. 425-435.

Yassir, A., et al. 1999. Microbial aspects of atrazine biodegradation in relation to history of soil treatment. Pesticide Science. 55(8): p. 799-809.

Vanderheyden, V., P. Debongnie, and L. Pussemier. 1997. Accelerated degradation and mineralization of atrazine in surface and subsurface soil materials. Pesticide Science. 49(3): p. 237-242.

Sims, G.K. and A.M. Cupples. 1999. Factors controlling degradation of pesticides in soil. Pesticide Science. 55: p. 598-601.

Johnson, T.A., et al. 1998. Effects of moisture and sorption on bioavailability of p-hydroxy-benozoic acid to Arthrobacter sp. in soil. Microbiological Research. 153: p. 349-353.

Houot, S., et al. 2000. Dependence of accelerated degradation of atrazine on soil pH in French and Canadian soils. Soil Biology & Biochemistry. 32(5): p. 615-625.

Mervosh, T.L., et al., Clomazone Sorption in Soil - Incubation-Time, Temperature, and Soil-Moisture Effects. Journal of Agricultural and Food Chemistry, 1995. 43(8): p. 2295-2300.

Aislabie, J., et al. 2004. Atrazine mineralisation rates in New Zealand soils are affected by time since atrazine exposure. Australian Journal of Soil Research. 42(7): p. 783-792.

Behki, R.M. and S.U. Khan. 1994. Degradation of Atrazine, Propazine, and Simazine by Rhodococcus Strain B-30. Journal of Agricultural and Food Chemistry. 42(5): p. 1237-1241.

De Souza, M.L., et al. 1998. Molecular basis of a bacterial consortium: Interspecies catabolism of atrazine. Applied and Environmental Microbiology. 64(1): p. 178-184.

Strong, L.C., et al. 2002. Arthrobacter aurescens TC1 metabolizes diverse s-triazine ring compounds. Applied and Environmental Microbiology. 68(12): p. 5973-5980.

102. O'Loughlin, E.J., G.K. Sims, and S.J. Traina. 1999. Biodegradation of 2-methyl, 2-ethyl, and 2-hydroxypyridine by an Arthrobacter sp isolated from subsurface sediment. Biodegradation. 10(2): p. 93-104.

De Schrijver, A. and R. De Mot. 1999. Degradation of pesticides by actinomycetes. Critical Reviews in Microbiology. 25(2): p. 85-119.

Zhang, Z., et al., 2000. A greedy algorithm for aligning DNA sequences. Journal of Computational Biology. 7(1-2): p. 203-214.

Tatusova, T.A. and T.L. Madden. 1999. BLAST 2 SEQUENCES, a new tool for comparing protein and nucleotide sequences (vol 174, pg 247, 1999). Fems Microbiology Letters. 177(1): p. 187-188.

Cook, A.M. 1987. Biodegradation of s-triazine xenobiotics. Fems Microbiology Reviews. 46(2): p. 93-116.

Karns, J.S. 1999. Gene sequence and properties of an s-triazine ring-cleavage enzyme from Pseudomonas sp strain NRRLB-12227. Applied and Environmental Microbiology. 65(8): p. 3512-3517.

Cook, A.M., et al. 1985. Ring Cleavage and Degradative Pathway of Cyanuric Acid in Bacteria. Biochemical Journal. 231(1): p. 25-30.

Shapir, N., et al., Substrate specificity and colorimetric assay for recombinant TrzN derived from Arthrobacter aurescens TC1. Applied and Environmental Microbiology, 2005. 71(5): p. 2214-2220.

Meselson, M. and F.W. Stahl. 1958. The Replication of DNA in Escherichia coli. Proceedings of the National Academy of Sciences of the United States of America. 44(7): p. 671-682.

Mulvaney et al. 2006. Need for a Soil-Based Approach in Managing Nitrogen Fertilizers
for Profitable Corn Production. Soil Sci. Soc. Am. J. 70: p.172–182 .

Pinar, G. and J.L. Ramos, A strain of Arthrobacter that tolerates high concentrations of nitrate. Biodegradation, 1998. 8(6): p. 393-399.

Eschbach, M., et al., Members of the genus Arthrobacter grow anaerobically using nitrate ammonification and fermentative processes: anaerobic adaptation of aerobic bacteria abundant in soil. Fems Microbiology Letters, 2003. 223(2): p. 227-230.

Sexstone, A.J., et al. 1985. Direct Measurement of Oxygen Profiles and Denitrification Rates in Soil Aggregates. Soil Science Society of America Journal. 49(3): p. 645-651.

Stackebrandt, E., et al. 1983. Taxonomic Studies on Arthrobacter-Nicotianae and Related Taxa - Description of Arthrobacter-Uratoxydans Sp-Nov and Arthrobacter-Sulfureus Sp-Nov and Reclassification of Brevibacterium-Protophormiae as Arthrobacter-Protophormiae Comb Nov. Systematic and Applied Microbiology. 4(4): p. 470-486.

CHAPTER 28

EFFECTS OF SOIL MATRIX AND AGING ON THE DERMAL BIOAVAILABILITY OF HYDROCARBONS AND METALS IN THE SOIL: DERMAL BIOAVAILABILITY OF SOIL CONTAMINANTS

Mohamed S. Abdel-Rahman[1], Rita M. Turkall[1,2 §], and Gloria A. Skowronski[1]

University of Medicine and Dentistry of New Jersey, [1]Pharmacology and Physiology Department, New Jersey Medical School, and [2]Clinical Laboratory Sciences Department, School of Health Related Professions, Newark, New Jersey

ABSTRACT

The potential health risk from exposure to chemically contaminated soil can be assessed from bioavailability studies. The aims of this research were: (a) to determine the dermal bioavailability of contaminants in soil for representatives of hydrocarbon classes of chemicals, namely, volatiles (toluene) and polycyclic aromatic hydrocarbons [benzo(a)pyrene] as well as for heavy metals (arsenic, mercury, and nickel, respectively, as arsenic acid, mercuric chloride, and nickel chloride); and (b) to examine the effects of soil matrix and chemical sequestration in soil with time ("aging") on their bioavailability. In vitro flow-through diffusion cell studies were performed utilizing dermatomed male pig skin and radioactive chemicals to measure dermal penetration. The volatility of toluene reduced the amount of the chemical available for dermal penetration. With soil contact, the penetration of toluene was 16-fold to 21-fold less than toluene without soil. Benzo(a)pyrene penetration was decreased faster in soil with a higher clay content than one with more organic carbon. The soil matrix as well as aging in soil lowered the dermal penetration of the metal compounds by 95-98%. This study provided evidence that the bioavailability from dermal exposure to the chemicals examined can be significantly reduced by soil matrix and aging in soil.

Keywords: soil contaminants, dermal exposure, bioavailability effects

1. INTRODUCTION

The potential health risk from exposure to chemically contaminated soil is related to the amount of chemical that desorbs from soil and which is subsequently absorbed by the body, i.e.

§ Corresponding Author: Rita M. Turkall, Ph.D., Clinical Laboratory Sciences Dept., UMDNJ, School of Health Related Professions, 65 Bergen Street, Newark, NJ, 07107 Tel: (407)568-5122 Email: turkalrm@umdnj.edu

bioavailability. Soil properties such as organic carbon content, clay content, particle size, and pH affect chemical sorption and desorption processes, and thus may have significant impacts on the bioavailability of chemicals from soils (NEPI, 2000a; Pu et al., 2004). Another major determinant of bioavailability is chemical aging in soil (Alexander, 2000). Chemical aging in soil is the movement of chemicals from the surface of soil particles into less accessible sites with time (Linz and Nakles, 1997; Reid et al., 2000). The mechanisms for chemical aging are not fully understood, however, it has been proposed that hydrophobic chemicals can partition into the solid phase of soil organic matter as well as become entrapped within soil nanopores where they may be retained and become less accessible (Steinberg et al., 1987; Brusseau et al., 1991; Pignatello and Xing, 1996).

Most of the emphasis on chemical aging has been on organic chemicals in soil (Steinberg et al., 1987; Scribner et al., 1992; Hatzinger and Alexander, 1995; Kelsey et al., 1997; Roy and Singh, 2001; Abdel-Rahman et al., 2006). However, metals also age in soil (Lock and Janssen, 2003; Turpeinen et al., 2003). The interaction of metals with soil is more complex than organic chemicals with soil. Metals may be associated with many components of soil in various ways (ion exchange, adsorption, precipitation, complexation) or be present in the structure of minerals (Balasoiu et al., 2001). The mechanism for the aging of metals in soil may be different than for organic compounds (Alexander, 2000). Proposed mechanisms include penetration into the mineral lattice of soil and diffusion through intraparticle pores (Yin et al., 1997). Intraparticle diffusion may lead to the sequestration of metals within microporous solids, such as hydrous iron, aluminum, and manganese oxides, and some types of organic matter (Axe and Trivedi, 2002).

Compared to other routes of exposure to soil contaminants (oral, inhalation), the dermal route may not always be the most important route, but it can contribute significantly to total exposure. Because human skin comprises more than 10% of total body mass and 1.8 m2 of body surface (Roberts and Walters, 1998; USEPA, 2001), it has the potential to absorb significant quantities of chemicals into the body during daily activities. A chemical that cannot penetrate skin may be limited to local toxic effects on the skin but if it readily penetrates skin and enters the circulation, it may have systemic effects. Therefore, it is necessary to know the capacity of a chemical for dermal absorption in order to assess its overall potential risk (Mattie et al., 1994).

The studies reported in this paper were conducted to assess the dermal bioavailability of contaminants in soil for representatives of hydrocarbon classes of chemicals, namely, volatiles (toluene) and polycyclic aromatic hydrocarbons [benzo(a)pyrene] as well as for heavy metals (arsenic, mercury, and nickel, respectively, as arsenic acid, mercuric chloride, and nickel chloride). Toluene is a very common contaminant of soil in the vicinity of hazardous waste sites. The chemical has been identified in 84% of the soil samples collected from National Priorities List (NPL) hazardous waste sites where it was detected in environmental media (ATSDR, 2000a,b). Toluene is not usually found in high concentrations in surface soils due to loss through volatilization, but it remains in subsurface soils (NEPI, 2000a). Dermal contact with toluene can remove protective epidermal lipids from skin. The defatting action of the chemical alters the barrier properties of skin (Boman and Maibach, 2000) and can cause irritation and cell damage (Shibata et al., 1994; USEPA, 1983).

PAHs are ubiquitous contaminants of soil and are derived from the incomplete combustion of organic materials (ATSDR, 1995; Loehr and Webster, 1997). New Jersey has the most sites with PAH contamination. Soil concentrations of benzo(a)pyrene (BaP) in NPL sites in the state range between 1.1 and 8,100 mg/kg (ATSDR, 1995; ATSDR, 1999a). BaP has been classified as a probable carcinogen in humans. Dermal exposure to BaP can cause skin irritation with rash and/or burning sensations. Repeated exposure can produce skin changes such as thickening and darkening (NJDHSS, 1998).

Natural levels of arsenic in soil usually range from 1 to 40 mg/kg, although much higher levels may be found in mining areas, at waste sites, near high geological deposits of arsenic-rich minerals, or from pesticide applications (ATSDR, 2000c). In soil, arsenic can occur as arsenates (AsO4-3) or arsenites (AsO2-), with trivalent arsenites being more toxic than the pentavalent arsenates. At high redox potential and acidic pH, the arsenate species predominates in soil. However, at low redox potential and alkaline pH, the arsenite species is more significant (Masscheleyn et al., 1991; Peters et al., 1996; Balasoiu et al., 2001). Direct dermal contact with inorganic arsenicals may cause skin irritation and contact dermatitis. Usually the effects are erythema and swelling which may progress to papules, vesicles, or necrotic lesions in extreme cases (Holmqvist, 1951; ATSDR, 2000c).

Most of the mercury in soil is generally present as the divalent species. Compounds such as HgCl2 and Hg (OH)2 as well as inorganic Hg (II) compounds complexed with organic anions can be formed in soil (Andersson, 1979). Levels of Hg (II) as high as 123,000 mg/kg have been detected in heavily contaminated sites such as Berry's Creek in New Jersey (Lipsky et al., 1981; Yin et al., 1997). However, from 0.2 to 19,500 mg/kg of mercury (species not specified) have also been found in urban NPL sites in New Jersey (ATSDR, 1999b). Contact with skin of all species of mercury can result in systemic toxicity (Hostynek et al., 1998). The predominant skin reaction to mercury is erythematous and pruritic skin rashes (ATSDR, 1999b).

Analytical methods for nickel usually do not distinguish the form of nickel in soil. Therefore, the total amount of nickel is reported but the nature of the nickel compounds is often not known. Nickel or nickel compounds have been detected in soils near NPL sites at concentrations ranging from 2 to 10,522 μg/kg. Soil concentrations of nickel up to 9,000 mg/kg have also been found near industries that extract nickel from ore (ATSDR, 2005). Allergic contact dermatitis is the most common adverse health effect of nickel in humans. Approximately 10-20% of the population is sensitive to nickel and once an individual is sensitized, even minimal contact with the metal may cause a reaction in some sensitive individuals (ATSDR, 2005).

The relative contribution of the soil matrix and chemical aging in soil on the dermal bioavailability of the representative chemicals were determined so that the impact of the results on health risk could be evaluated. Bioavailability was assessed by measuring dermal penetration. Specifically: (a) the dermal penetration of each of the chemicals aged in soil was compared to the respective pure chemicals (without soil) and to the chemicals added freshly to soil; (b) the effects of soil composition (percent sand, clay, organic matter) on dermal penetration were examined.

2. MATERIALS AND METHODS

2.1 Chemicals

[Ring-U-^{14}C] toluene, with a specific activity of 16.4 mCi/mmol and radiochemical purity of 95%, was purchased from Amersham Corp., Arlington Heights, IL. Prior to use, the radioisotope was diluted with non-radioactive toluene (HPLC grade, Aldrich Chemical Co., Milwaukee, WI). Benzo(a)pyrene, generally labeled with tritium [^{3}H(G)], having a specific activity of 50 Ci/mmol and radiochemical purity of 99%, was obtained from American Radiolabeled Chemicals, Inc., St. Louis, MO. Arsenic in the form of arsenic acid ($H_3AsO_{4)}$ (Sigma/Aldrich Chemical Co., St. Louis, MO) was used as a carrier and labeled with arsenic-73 (Los Alamos National Laboratory, Los Alamos, NM). Mercury-203 as mercuric chloride (3.1 mCi/mg specific activity, radiochemical purity > 99%) was a product of Amersham Pharmacia Biotech, Inc., Piscataway, NJ. Nickel-63 as nickel chloride (12.6 mCi/mg specific activity, 99.9% radiochemical purity) was obtained from New England Nuclear Life Science Products, Boston, MA.

2.2 Soils

Studies were conducted on two different soils that are representative of soil types widely distributed in the United States (USDA, 1972; 1977). The Atsion soil consists of 90% sand, 8% silt, 2% clay, 4.4% organic matter; has a pH of 4.2; and was collected from the Cohansey sand formation near Chatsworth in south central New Jersey. The Keyport soil contains 50% sand, 28% silt, 22% clay, 1.6% organic matter; has a pH of 5; and was collected from the Woodbury formation near Moorestown in southwestern New Jersey. Soil particle size distribution was as follows: Atsion soil = 50-100 μm (22.2%), 100-250 μm (76.3%), > 250 μm (1.5%); Keyport soil = 50-100 μm (17%), 100-250 μm (65.3%), 250-500 μm (13.6%), > 500 μm (4.1%). Soil analyses were performed by the Soil Testing Laboratory at Rutgers Cooperative Extension Resource Center, Rutgers University, New Brunswick, NJ. Organic matter content was measured by a modified Walkley and Black (1934) dichromate oxidation method.

2.3 Chemical Aging in Soil

Individual chemicals were added to each of the soils that were previously autoclaved and hydrated to 11% (w/w) with sterile distilled-deionized water. This is the maximum amount of water that could be used to lightly moisten the soils without there being an excess of water when each chemical was added to the soils. Toluene was added to soil at a concentration of 72 mg chemical/g soil (sum of labeled and unlabeled toluene). The final concentration of ^{3}H-BaP tracer (400 ng/g soil) together with unlabeled BaP was 1.67 mg/g soil. For the metal compounds, there were 83, 5.4, and 2.4 μg/g soil, respectively, for arsenic acid, mercuric chloride, and nickel chloride. After each chemical was mixed thoroughly with the soils to ensure uniform distribution of chemical, treated soils were added to Teflon-sealed vials and aged in the dark at room temperature for three months.

2.4 Animal Model

Whole pig skin was obtained from the costo-abdominal areas of euthanized (40-60 lb) male Yorkshire pigs (Cook College Farm, Rutgers University, New Brunswick, NJ). The pig has been widely accepted as an animal model for studying human percutaneous absorption of a large variety of chemicals under various experimental conditions (Bartek et al., 1972; Reifenrath and Hawkins, 1986) because of the well documented histological (Monteiro-Riviere and Stromberg, 1985), physiological, biochemical, and pharmacological similarities between pig skin and human skin (Qiao and Riviere, 2000). Skin was transported to the laboratory in ice-cold HEPES buffered (25 mM) Hank's balanced salt solution (HHBSS), pH 7.4, containing gentamycin sulfate (50 mg/l) (Collier et al., 1989) after which it was immediately prepared for diffusion cells according to Bronaugh and Stewart (1985).

2.5 In Vitro Dermal Penetration Studies

Excised skin was cut to a thickness of 200 μm with a dermatome (Padgett Electro-Dermatome Model B, Padgett Instruments Inc., Kansas City, MO) and circular pieces were mounted into Teflon flow-through diffusion cells (Crown Bio Scientific, Inc., Somerville, NJ). The exposed skin surface area (0.64 cm2) was maintained at a temperature of 32oC. The dermal side of each skin sample was perfused with HHBSS containing 10% fetal bovine serum (Sigma/Aldrich) at a flow rate of 3 ml/h and aerated continuously with oxygen (Collier et al., 1989). Each chemical was applied separately to the stratum corneum surface of the skin either alone in 5 μl of vehicle (acetone for BaP, ethanol for the metals), immediately after the addition of 30 mg of soil, or after aging in 30 mg of each of the two soils. The chemical doses/cm2 of skin surface area were: BaP (78 μg), arsenic acid (3.9 μg), mercuric chloride (253 ng), and nickel chloride (112.5 ng). After skin was treated and diffusion cells were capped, charcoal tubes (SKC Inc., Eighty-Four, PA) attached to the upper chambers of the diffusion cells, trapped any toluene volatilizing from the skin surface. Volatilization of toluene that occurred during soil treatment, during the aging process, and skin treatment, decreased the amount of the toluene dose that was available for dermal penetration. Toluene losses were detected by measuring radioactivity in glacial acetic extracts of charcoal as well as non-aged and aged chemical in soil. Volatilization losses of the toluene dose were very high and varied between the treatment groups (90% for pure toluene, 64–66% for freshly spiked soils, and 94–95% for aged soils). The maximum amount of toluene that was available for dermal penetration in each treatment was the fraction of the initial dose that remained after volatilization. Therefore, the available toluene doses were 337 $\mu g/cm^2$ of skin for pure toluene; 1210 and 1159 $\mu g/cm^2$, respectively, in freshly spiked Atsion and Keyport soils; and 180 and 218 $\mu g/cm^2$, respectively, for toluene in aged soils.

Receptor fluid (perfusate) was collected in scintillation vials containing 10 ml of Formula-989 liquid scintillation cocktail (Packard Instruments Co., Inc., Meriden, CT) up to 16 h postdosing. After 16 h of exposure to chemical alone or in soil, loosely adsorbed chemical was washed from the surface of the skin with soap and water (once with 1 ml of a 1% aqueous soap solution and twice with 1 ml of distilled-deionized water). Skin samples were completely solubilized in Solvable (Packard) for 8 h at 50oC to determine the amount of radioactivity remaining in skin. Radioactivity in all samples was counted by liquid scintillation spectrometry

(LS 7500, Beckman Instruments, Inc., Fullerton, CA). Sample quench was corrected by using the H-ratio method.

2.6 Statistical Analysis

All data were reported as the mean + standard error of the mean (SEM). Statistical differences between treatment groups were determined by one-way analysis of variance (ANOVA) with Scheffe's test except for differences between the soils which were determined by Student's independent t-test. The level of significance was $p < 0.05$.

3. RESULTS

The dermal penetrations of the chemicals are reported in Tables 1 and 2 as total penetrations. Total penetration represents the sum of chemical penetrating into receptor fluid and the amount in skin that potentially can penetrate into receptor fluid with time (Chu et al., 1996). Percent total penetration equals: (the amount of the initial dose that penetrated skin divided by the amount of the initial dose applied to skin) X 100 for all chemicals except for toluene. For toluene, the percent total penetration equals: (the amount of the available dose that penetrated skin divided by the amount of the available dose applied to skin) X 100. Tables 1 and 2 show that contact with either Atsion or Keyport soils for a short time (16 h) significantly decreased the total penetration of each chemical versus their pure counterparts.

Table 1. Effects of Time in Atsion Soil on the Dermal Penetration of Hydrocarbon or Heavy Metal Compounds

Chemicals	Pure	Freshly Spiked	Aged
Toluene	92.8 ± 4.5 [a]	5.9 ± 0.8 [b]	3.9 ± 0.5 [b]
Benzo(a)pyrene	76.0 ± 3.2	8.5 ± 0.9 [b]	3.7 ± 0.5 [b]
Arsenic	44.6 ± 2.8	10.0 ± 1.6 [b]	1.5 ± 0.3 [b,c]
Mercury	66.3 ± 4.2	37.8 ± 3.6 [b]	3.3 ± 0.9 [b,c]
Nickel	57.9 ± 2.2	11.5 ± 1.0 [b]	2.8 ± 0.3 [b,c]

[a] Percent total penetration (mean ± SEM) = (amount of available dose that penetrated skin divided by amount of available dose applied to skin) X 100 for toluene. For the other chemicals, available dose is replaced by initial dose. For each chemical, n = 8-14 replicates per treatment from three pigs.
[b] Significantly different from pure chemical ($p < 0.05$, ANOVA)
[c] Significantly different from chemical in freshly spiked Atsion soil ($p < 0.05$, ANOVA)

Although the available dose of toluene in the freshly spiked soils was higher than for pure toluene, the total penetration of non-aged toluene in Atsion and Keyport soils was only 5.9% and 4.5%, respectively. Three months aging in the soils further reduced the total penetration of each chemical compared to chemical in freshly spiked soil, however, the difference was only significant for the three metals. In spite of the fact that the dose was lower for toluene aged in the two soils than in the freshly spiked soils, aging did not significantly reduce the total penetration of toluene relative to the total penetration of toluene in the freshly spiked soils.

Table 2. Effects of Time in Keyport Soil on the Dermal Penetration of Hydrocarbon or Heavy Metal Compounds

Chemicals	Pure	Freshly Spiked	Aged
Toluene	92.8 ± 4.5 [a]	4.5 ± 0.6 [b]	2.6 ± 0.4 [b]
Benzo(a)pyrene	76.0 ± 3.2	3.5 ± 0.5 [b]	1.8 ± 0.2 [b]
Arsenic	44.6 ± 2.8	6.0 ± 0.8 [b]	0.8 ± 0.1 [b,c]
Mercury	66.3 ± 4.2	39.8 ± 4.2 [b]	2.5 ± 0.2 [b,c]
Nickel	57.9 ± 2.2	12.4 ± 2.0 [b]	1.8 ± 0.5 [b,c]

[a] Percent total penetration (mean ± SEM) = (amount of available dose that penetrated skin divided by amount of available dose applied to skin) X 100 for toluene. For the other chemicals, available dose is replaced by initial dose. For each chemical, n = 8-14 replicates per treatment from three pigs.
[b] Significantly different from pure chemical ($p < 0.05$, ANOVA)
[c] Significantly different from chemical in freshly spiked Keyport soil ($p < 0.05$, ANOVA)

Although the individual data for the receptor fluid and skin are not presented in the tables, it should be noted that very small quantities of each chemical (< 0.5% of the initial/available dose) penetrated into the receptor fluid for all BaP and metal treatments as well as for toluene aged in both soils. For pure toluene, 11.1% of the available dose was detected in the receptor fluid. This amount decreased significantly to 2.8% and 2%, respectively, in the freshly spiked Atsion and Keyport soils. From 92% to greater than 99% of the total penetration of the chemicals was due to the amount of chemical found in skin except for the following treatments: pure toluene (88%), toluene in freshly spiked Atsion (52%) and Keyport (56%) soils, and arsenic aged in Keyport soil (75%). The remainder of the initial/available dose that did not penetrate skin for each treatment was found in the skin wash (data not shown). From 7–57% of the initial/available dose was detected in the skin wash for the pure chemicals. As less soil-sorbed chemical penetrated skin than pure chemical, quantities of chemical in the skin wash increased to 59–99% of the initial/available dose.

When comparisons of the total penetration were made between the soils for each chemical (Table 3), it was determined that total penetration was significantly lower in the Keyport than in the Atsion soil for freshly spiked BaP and arsenic as well as for aged BaP, arsenic, and nickel.

Table 3. Impact of Soil Type on the Dermal Penetration of Hydrocarbon or Heavy Metal Compounds

Chemicals	Fresh Atsion	Fresh Keyport	Aged Atsion	Aged Keyport
Toluene	5.9 ± 0.8 [a]	4.5 ± 0.6	3.9 ± 0.5	2.6 ± 0.4
Benzo(a)pyrene	8.5 ± 0.9	3.5 ± 0.5 [b]	3.7 ± 0.5	1.8 ± 0.2 [c]
Arsenic	10.0 ± 1.6	6.0 ± 0.8 [b]	1.5 ± 0.3	0.8 ± 0.1 [c]
Mercury	37.8 ± 3.6	39.8 ± 4.2	3.3 ± 0.9	2.5 ± 0.2
Nickel	11.5 ± 1.0	12.4 ± 2.0	2.8 ± 0.3	1.8 ± 0.5 [c]

[a] Percent total penetration (mean ± SEM) = (amount of available dose that penetrated skin divided by amount of available dose applied to skin) X 100 for toluene. For the other chemicals, available dose is replaced by initial dose. For each chemical, n = 8-14 replicates per treatment from three pigs
[b] Significantly different from chemical in freshly spiked Atsion soil ($p < 0.05$, Student's independent t-test)
[c] Significantly different from chemical aged in Atsion soil ($p < 0.05$, Student's independent t-test)

4. DISCUSSION

Both soils were equally effective in decreasing the dermal penetration of toluene regardless of the time that the chemical was in the soils. Batch equilibrium experiments performed by Tell

and Uchrin (1991) to determine the sorption of toluene in the organic components of the Atsion soil identified humic acid as the prime organic sorption component. Since the Atsion soil contained three times more organic matter than the Keyport soil, it was expected that the total penetration of toluene would have been significantly lower in the Atsion soil than in the Keyport soil. However, toluene that is released to soil tends to volatilize quickly. Although the rate of volatilization from soil depends on temperature, humidity, and soil type, under typical conditions, more than 90% of the toluene in the upper soil layer volatilizes to air within 24 h (Thibodeaux and Hwang, 1982; Balfour et al., 1984). Volatilization losses as high as 95% for toluene decreased the amount of chemical that was available for dermal penetration in this study, indicating that the volatility of toluene was the predominant factor in reducing the dermal penetration of the chemical. With soil contact, the dermal penetration of toluene was 16-fold to 21-fold less than toluene without soil.

Lipophilic compounds such as BaP have a tendency to form reservoirs of the chemical in skin (Chu et al., 1996) as was observed in the present study. The formation of a dermal reservoir of BaP is important because of the ability of skin enzymes to biotransform BaP to a carcinogenic metabolite (Scribner, 1985; Ng et al., 1992). While most of the applied BaP dose was detected in skin, only 0.2% of the initial dose was found in receptor fluid after pure treatment; decreasing to 0.1% after chemical aging in either soil. Roy and Singh (2001) showed that as a result of 110 days of chemical aging in a coal tar contaminated field soil, 50% less coal tar BaP penetrated human abdominal skin sections into receptor fluid compared to freshly spiked 3H-BaP. Yang et al. (1989) and Wester et al. (1990) also reported significant reductions in dermal bioavailability when BaP was sorbed to soil but their studies did not include chemical aging. In general, it is difficult to make direct comparisons between present and previous dermal penetration studies because of differences in experimental conditions (e.g., source of skin, soil composition, receptor fluid, chemical concentration).

For BaP, surface adsorption was faster in the Keyport soil than in the Atsion soil. The adsorption of BaP onto the Atsion soil was evidenced by the 89% decrease in total penetration for freshly spiked BaP. Then, sequestration of BaP in the Atsion soil occurred with time ("aging"). This was reflected in the further reduction in total penetration (95%) after aging in the Atsion soil. In contrast, surface adsorption was greater in the Keyport soil since the decrease in the total penetration of BaP in freshly spiked Keyport soil was equal to that after aging in the Atsion soil. Furthermore, the total penetration of BaP in the Keyport soil (freshly spiked or after aging) was significantly lower than in freshly spiked Atsion soil and after aging in the Atsion soil. Most likely this was due to the 10-fold higher percentage of clay in the Keyport soil than in the Atsion soil. Clays, which typically have high surface areas, can enhance sorption through weak physical interactions and can impede chemical mass transfer due to clay aggregation and clay interlayers (Ake et al., 2001; Pu et al., 2004). Although organic matter acts primarily as a partition medium, mineral matter acts as an adsorbent for organic chemicals in soil (Karickhoff et al., 1979; Gschwend and Wu, 1985; Haderlein and Schwarzenbach, 1993; Chiou et al., 2000). Therefore, with increasing organic matter content and sometimes clay content, retention of an organic chemical increases and the rate of release decreases, potentially decreasing overall chemical availability (Pu et al., 2004).

Skin is a critical organ of arsenic toxicity. Because of the affinity of arsenic for sulfhydryl groups, it can accumulate in skin (Hostynek et al., 1993) and penetrate slowly into the systemic

circulation after exposure ends (Dutkiewicz, 1977). In the present study, soil decreased the total penetration of arsenic (mainly due to the amount of chemical in the skin reservoir). Iron, manganese, and aluminum oxides; clay content; and organic matter content are soil constituents that are strongly related to arsenic sorption (Galba and Polacek, 1973; Thanabalasingam and Pickering, 1986; Yan-Chu, 1994; Balasoiu et al., 2001). However, soils with a higher clay content have been shown to retain more arsenic than soils with a lower clay content (Woolson and Kearney, 1973; Elkhatib et al., 1984). This was evidenced in the current study where the total penetration of arsenic in freshly spiked soil and after aging were lower in the Keyport soil than in the Atsion soil.

The decrease in the total penetration of mercury was similar in the two soils. Yin et al. (1997) showed that organic matter was the principal component of soil that was responsible for the resistance of divalent mercury to desorption from soil in their studies on three sandy loams and a stony loam. From the investigations by Andersson (1979), it was concluded that the only effective sorbent for inorganic mercury in acidic soils (pH < 4.5-5) is the organic material, but iron oxides and clay minerals may become more effective in neutral soils (pH > 5.5-6). Since both soils in the present study are acidic (pH 4.2 and 5), it is suggested from Andersson (1979) that even a small amount of organic matter (1.6% in the case of the Keyport soil) is very effective in sorbing significant quantities of mercury.

Soil pH is an important property of soil in the sorption of nickel. When King (1988) examined the ability of 13 soils (pH range 3.9-6.5) to retain metals, he determined that with increasing pH (differences as little as 0.2 units), nickel retention increased substantially in their study. Soil pH and to a lesser extent, clay content and the amount of hydrous iron and manganese oxides, most influenced nickel sorption in batch adsorption experiments by Anderson and Christensen (1988) on 38 different agricultural soils. In the nickel study reported here, the higher pH as well as the clay content of the Keyport soil most likely were factors in decreasing the total penetration of nickel in that soil compared to the Atsion soil.

The soil load (47 mg/cm2) that was used in these studies was based on soil adherence values reported in the literature (10-3 to 102 mg/cm2) which depended on soil properties, occupational and recreational activities, and different parts of the body (Kissel et al., 1996, 1998; Holmes et al., 1999). However, Yang et al. (l989), Duff and Kissel (l996), and Roy and Singh (2001) showed that only chemical in the monolayer of soil that is in direct contact with the skin surface is likely to be absorbed by skin. Monolayers of 3-9 mg/cm2 were reported by those investigators and their studies showed that increasing the soil load decreased the percent of the applied dose of chemical absorbed. However, the soil loading that will achieve a monolayer is dependent on the particle size distribution of the soil being tested (Driver et al., 1989; NEPI, 2000b). For example, a soil load of 40 mg/cm2 was used in Wester et al.'s (1993) studies on sodium arsenate in soil. Their studies showed a total penetration of 0.8% from soil on human cadaver skin and a dermal bioavailability of 3.2-4.5% in monkeys. Because the soil particle sizes were very large (180-300 μm) in their studies, the soil loading was only slightly higher than a monolayer (Duff and Kissel, 1996) Particles less than 150 μm in diameter have been shown to have greater adherence to skin than larger size fractions (Driver et al., 1989; NEPI, 2000b). For the two soils used in the studies reported here, only 17-22% of the soil particles have an arithmetic mean particle size diameter less than 150 μm. This suggests that monolayer coverage was slightly exceeded. With a lower soil load, the dermal penetration of the studied chemicals may be a little higher.

Another factor that must be considered in addition to the soil load is the amount of chemical applied per unit area of skin. Although there were no significant differences in the percutaneous absorption of arsenic between a trace dose of arsenic in soil (4 X 10-5 µg/cm2) and a higher dose (0.6 µg/cm2) in Wester et al.'s (1993) study in monkeys, the penetration rate of pure mercuric chloride through human skin in vitro was shown by Wahlberg (1965) to be concentration dependent.

5. CONCLUSIONS

Health risk assessments are often based on exposure to the total concentration of a chemical in a contaminated site. The total concentration is usually determined by rigorous extraction procedures such as acid digestion, sonication, or Soxhlet extraction to remove the chemicals from soil (USEPA, 1986, 1992; Tang et al., 1999). This approach can result in an overestimation of risk because when humans are exposed to contaminated soil, only a fraction of the total concentration (the bioavailable fraction) may be absorbed into the systemic circulation. The data presented in this paper highlight the need to incorporate bioavailability data into the health risk assessment of exposure to contaminated soils. The overall conclusion from this study is that soil decreased the dermal bioavailability of the organic chemicals and heavy metal compounds examined. Moreover, differences in soil composition and residence time in soil produced significant quantitative differences in bioavailability. However, further experiments should be performed at lower soil loads and additional concentrations to determine the effects of the soil layer thickness and the amount of chemical per unit area of skin on dermal penetration.

6. REFERENCES

Abdel-Rahman, M.S., Skowronski, G.A., and Turkall, R.M. 2006. Impact of aging time on the dermal penetration of phenol in soil. Soil and Sediment Contam. 15, 47-60.

Ake, C.L., Mayura, K., Huebner, H. et al. 2001. Development of porous clay-based composites for sorption of lead from water. J. Toxicol. Environ. Health, Part A. 63, 459-475.

Alexander, M. 2000. Aging, bioavailability, and overestimation of risk from environmental pollutants. Environ. Sci. Technol. 34, 4259-4265 .

Anderson, P.R. and Christensen, T.H. 1988. Distribution coefficients of Cd, Co, and Zn in soils. J. Soil Sci. 35, 15-22.

Andersson, A. 1979. Mercury in soils. In: The Biogeochemistry of Mercury in the Environment, pp. 79-112. (Nriagu, J.O., Ed.). Amsterdam, Elsevier/North-Holland.\

ATSDR (Agency for Toxic Substances and Disease Registry). 1995. Toxicological Profile for Polycyclic Aromatic Hydrocarbons (PAHs), pp. 1-11, 235, 261. U.S. Department of Health and Human Services, Public Health Service, Atlanta, GA.

ATSDR (Agency for Toxic Substances and Disease Registry). 1999a. HazDat (Hazardous Substances Database). U.S. Department of Health and Human Services, Public Health Service, Atlanta, GA.

ATSDR (Agency for Toxic Substances and Disease Registry). 1999b. Toxicological Profile for Mercury, pp. 1-28, 396. U.S. Department of Health and Human Services, Public Health Service, Atlanta, GA.

ATSDR (Agency for Toxic Substances and Disease Registry). 2000a. Toxicological Profile for Toluene, pp. 1-3, 64, 89, 98, 171, 179-206. U.S. Department of Health and Human Services, Public Health Service, Atlanta, GA.

ATSDR (Agency for Toxic Substances and Disease Registry). 2000b. HazDat (Hazardous Substances Database). U.S. Department of Health and Human Services, Public Health Service, Atlanta, GA.

ATSDR (Agency for Toxic Substances and Disease Registry). 2000c. Toxicological Profile for Arsenic, pp. 15-132, 172, 243-299. U.S. Department of Health and Human Services, Public Health Service, Atlanta, GA.

ATSDR (Agency for Toxic Substances and Disease Registry). 2005. Toxicological Profile for Nickel, pp. 1-10, 167,

205-263. U.S. Department of Health and Human Services, Public Health Service, Atlanta, GA.
Axe, L. and Trivedi, P. 2002. Intraparticle surface diffusion of metal contaminants and their attenuation in microporous amorphous Al, Fe, and Mn oxides. J. Colloid Interface Sci. 247, 259-265.
Balasoiu, C.F., Zagury, G.J., and Deschênes, L. 2001. Partitioning and speciation of chromium, copper, and arsenic in CCA-contaminated soils: Influence of soil composition. Sci. Total Environ. 280, 239-255.
Balfour, W.D., Wetherold, R.G., and Lewis, D.L. 1984. Evaluation of Air Emissions from Hazardous Waste Treatment, Storage and Disposal Facilities. U.S. Environmental Protection Agency, Land Pollution Control Division, Hazardous Waste Engineering Research Laboratory, Office of Research and Development, Cincinnati, OH.
Bartek, M.J., LaBudde, J.A., and Maibach, H.I. 1972. Skin permeability in vivo: Comparison in rat, rabbit, pig, and man. J. Invest. Dermatol. 58, 114-123.
Boman, A. and Maibach, H.I. 2000. Influence of evaporation and solvent mixtures on the absorption of toluene and n-butanol in human skin in vitro. Ann. Occup. Hyg. 44, 125-135.
Bronaugh, R.L. and Stewart, R.F. 1985. Methods for in vitro percutaneous absorption studies. IV. The flow-through diffusion cell. J. Pharm. Sci. 74, 64-67.
Brusseau, M.L., Jessup, R.E., and Rao, P.S.C. 1991. Nonequilibrium sorption of organic chemicals: elucidation of rate-limiting processes. Environ. Sci. Technol. 25, 134-142.
Chiou, C.T., Kile, D.E., Rutherford, D.W. et al. 2000. Sorption of selected organic compounds from water to a peat soil and its humic-acid and humin fractions: Potential sources of the sorption nonlinearity. Environ. Sci. Technol. 34, 1254- 1258.
Chu, I., Dick, D., Bronaugh, R. et al. 1996. Skin reservoir formation and bioavailability of dermally administered chemicals in hairless guinea pigs. Food Chem. Toxicol. 34, 267-276.
Collier, S.W., Sheikh, N.M., Sakr, A. et al. 1989. Maintenance of skin viability during in vitro percutaneous absorption/metabolism studies. Toxicol. Appl. Pharmacol. 99, 522-533.
Driver, J.H., Konz, J.J., and Whitmyre, G.K. 1989. Soil adherence to human skin. Bull. Environ. Contam. Toxicol. 43, 814-820.
Duff, R.M. and Kissel, J.C. 1996. Effect of soil loading on dermal absorption efficiency from contaminated soils. J. Toxicol. Environ. Health. 48, 93-106.
Dutkiewicz, T. 1977. Experimental studies on arsenic absorption routes in rats. Environ. Health Pespect. 19, 173-176.
Elkhatib, E.A., Bennet, O.L., and Wright, R.J. 1984. Arsenite sorption and desorption in soils. Soil Sci. Soc. Am. J. 48, 1025-1029.
Galba, J. and Polacek, S. 1973. Sorption of arsenates under kinetic conditions in selected soil types. Acta Fytotech. 28, 187-197.
Gschwend, P.M. and Wu, S.C. 1985. On the constancy of sediment-water partition coefficients of hydrophobic organic pollutants. Environ. Sci. Technol. 19, 90-96.
Haderlein, S.B. and Schwarzenbach, R.P. 1993. Adsorption of substituted nitrobenzenes and nitrophenols to mineral surfaces. Environ. Sci. Technol. 27, 316-326.
Hatzinger, P.B. and Alexander, M. 1995. Effect of aging of chemicals in soil on their biodegradability and extractability. Environ. Sci. Technol. 29, 537-545.
Holmes, K.K., Jr., Shirai, J.H., Richter, K.Y. et al. 1999. Field measurement of dermal soil loadings in occupational and recreational activities. Environ. Res. A 80, 148-157.
Holmqvist, I. 1951. Occupational contact dermatitis: A study among employees at a copper ore smelting work including investigations of skin reactions to contact with arsenic compounds. Acta Derm. Venerol. 31 (Supp. 26), 26-29, 44-45, 110-112, 195-204.
Hostynek, J.J., Hinz, R.S., Lorence, C.R. et al. 1993. Metals and the skin. Crit. Rev. Toxicol. 23, 171-235.
Hostynek, J.J., Hinz, R.S., Lorence, C.R. et al. 1998. Human skin penetration by metal compounds. In: Dermal Absorption and Toxicity Assessment, pp. 647- 668. (Roberts, M.S. and Walters, K.A., Eds.). New York, Marcel Dekker.
Karickhoff, S.W., Brown, D.S, and Scott, T.A. 1979. Sorption of hydrophobic pollutants on natural sediments. Water Res. 13, 241-248.
Kelsey, J.W., Kottler, B.D., and Alexander, M. 1997. Selective chemical extractants to predict bioavailability of soil-aged organic chemicals. Environ. Sci. Technol. 31, 214-217.
King, L.D. 1988. Retention of metals by several soils of the southeastern United States. J. Environ. Qual. 17, 239-246.
Kissel, J.C., Richter, K.Y., and Fenske, R.A. 1996. Field measurement of soil load attributable to various activities. Implications for exposure assessment. Risk Anal. 16, 115-125.
Kissel, J.C., Shirai, J.H., Richter, K.Y. et al. 1998. Investigation of dermal contact with soil in controlled trials. J. Soil Contam. 7, 737-752.
Linz, D.G. and Nakles, D.V. 1997. Executive Summary. In: Environmentally Acceptable Endpoints in Soil, pp. 22-40. (Linz, D.G. and Nakles, D.V., Eds.). Annapolis, Maryland, American Academy of Environmental Engineers.
Lipsky, D., Reed, R.J., and Harkov, R. 1981. Mercury Levels in Berry's Creek. Newark, New Jersey, Department of Environmental Protection.

Lock, K. and Janssen, C.R. 2003. Influence of aging on metal availability in soils. Rev. Environ. Contam. Toxicol. 178, 1-21.

Loehr, R.C. and Webster, M.T. 1997. Effect of treatment on contaminant availability, mobility, and toxicity. In: Environmentally Acceptable Endpoints in Soil, pp. 137-386. (Linz, D.G. and Nakles, D.V., Eds.). Annapolis, Maryland, American Academy of Environmental Engineers.

Masscheleyn, P.H., Delaune, R.D., and Patrick, W.H., Jr. 1991. Effect of redox potential and pH on arsenic speciation and solubility in a contaminated soil. Environ. Sci. Technol. 25, 1414-1419.

Mattie, D.R., Grabau, J.H., and McDougal, J.N. 1994. Significance of the dermal route of exposure to risk assessment. Risk Anal. 14, 277-284.

Monteiro-Riviere, N. and Stromberg, M. 1985. Ultrastructure of the integument of the domestic pig (Sus scrofa) from one through fourteen weeks of age. Anat. Histol. Embryol. 14, 97-115.

NEPI (National Environmental Policy Institute). 2000a. Assessing the Bioavailability of Organic Chemicals in Soil for Use in Human Health Risk Assessments. Washington, DC.

NEPI (National Environmental Policy Institute). 2000b. Assessing the Bioavailability of Metals in Soil for Use in Human Health Risk Assessments. Washington, DC.

NJDHSS (New Jersey Department of Health and Senior Services). 1998. Hazardous Substance Fact Sheet: Benzo(a)pyrene.

Ng, K.M.E., Chu, I., Bronaugh, R.L. et al. 1992. Percutaneous absorption and metabolism of pyrene, benzo(a)pyrene, and di(2-ethyl-hexyl)phthalate: Comparison of in vitro and in vivo results in the hairless guinea pig. Toxicol. Appl. Pharmacol. 115, 216-223.

Peters, G.R., McCurdy, R.F., and Hindmarsh, J.T. 1996. Environmental aspects of arsenic toxicity. Crit. Rev. Clin. Lab. Sci. 33, 457-493.

Pignatello, J.J. and Xing, B. 1996. Mechanisms of slow sorption of organic chemicals to natural particles. Environ. Sci. Technol. 30, 1-10.

Pu, X., Lee, L.S., Galinsky, R.E. et al. 2004. Evaluation of a rat model versus a physiologically based extraction test for assessing phenanthrene bioavailability from soils. Toxicol. Sci. 79, 10-17.

Qiao, G. and Riviere, J.E. 2000. Dermal absorption and tissue distribution of 3,3', 4,4'-tetrachlorobiphenyl (TCB) in an ex-vivo pig model: assessing the impact of dermal exposure variables. Int. J. Occup. Environ. Health, 6, 127-137.

Reid, B.J., Jones, K.C., and Semple, K.T. 2000. Bioavailability of persistent organic pollutants in soils and sediments – a perspective on mechanisms, consequences, and assessment. Environ. Pollut. 108, 103-112.

Reifenrath, W. and Hawkins, G. 1986. The weanling Yorkshire pig as an animal model for measuring percutaneous penetration. In: Swine in Biomedical Research, pp. 673-680. (Tumbelson, M.E., Ed.). New York, Plenum.

Roberts, M.S. and Walters, K.A. 1998. The relationship between structure and barrier function of skin. In: Dermal Absorption and Toxicity Assessment, pp. 1-42. (Roberts, M.S. and Walters, K.A., Eds.). New York, Marcel Dekker.

Roy, T.A. and Singh, R. 2001. Effect of soil loading and soil sequestration on dermal bioavailability of polynuclear aromatic hydrocarbons. Bull. Environ. Contam. Toxicol. 67, 324-331.

Scribner, J.D. 1985. Chemical carcinogenesis. In: Environmental Pathology, pp.17-55. (Mottet, N., Ed.). New York, Oxford University Press.

Scribner, S.L., Benzing, T.R., Sun, S. et al. 1992. Desorption and bioavailability of aged simazine residues in soil from a continuous corn field. J. Environ. Qual. 21, 115-120.

Shibata, K., Yoshita, Y., and Matsumoto, H. 1994. Extensive chemical burns from toluene. Am. J. Emerg. Med., 12, 353-355.

Steinberg, S.M., Pignatello, J.J., and Sawhney, B.L. 1987. Persistence of 1,2- dibromoethane in soils: Entrapment in intraparticle micropores. Environ. Sci. Technnol. 21, 1201-1208.

Tang, J., Robertson, B.K., and Alexander, M. 1999. Chemical-extraction methods to estimate bioavailability of DDT, DDE, and DDD in soil. Environ. Sci. Technol. 33, 4346-4351.

Tell, J.G. and Uchrin, C.G. 1991. Relative contributions of soil humic acid and humin to the adsorption of toluene onto aquifer solid. Bull. Environ. Contam. Toxicol. 47, 547-554.

Thanabalasingam, P. and Pickering, W.F. 1986. Arsenic sorption by humic acids. Environ. Pollut. 12, 233-246.

Thibodeaux, L.J. and Hwang, S.T. 1982. Landfarming of petroleum wastes – modeling the air emission problem. Environ. Progress. 1, 42-46.

Turpeinen, R., Virta, M., and Häggblom, M.M. 2003. Analysis of arsenic bioavailability in contaminated soils. Environ. Toxicol. Chem. 22, 1-6.

USDA (U.S. Department of Agriculture). 1972. National Cooperative Soil Survey: Official Series Description, Keyport Series, Soil Conservation Service, Washington, DC.

USDA (U.S. Department of Agriculture). 1977. National Cooperative Soil Survey: Official Series Description, Atsion Series, Soil Conversation Service, Washington, DC.

USEPA (United States Environmental Protection Agency). 1983. Health Assessment Document for Toluene. Office of

Health and Environmental Assessment, Washington, DC. EPA-600/8-82-008F.
USEPA (United States Environmental Protection Agency). 1986. Test Methods for Evaluating Solid Wastes. Office of Solid Wastes, Washington, DC. SW-846.
USEPA (United States Environmental Protection Agency). 1992. Framework for Ecological Risk Assessment. Risk Assessment Forum, Washington, DC. EPA/630/R92/001.
USEPA (United States Environmental Protection Agency). 2001. Risk Assessment Guidance for Superfund (RAGS),
Volume 1: Human Health Evaluation Manual (Part E, Supplemental Guidance for Dermal Risk Assessment), Interim Guidance. Office of Emergency and Remedial Response, Washington DC, EPA/540/R- 99/005.
Wahlberg, J.E. 1965. Percutaneous absorption of sodium chromate (^{51}Cr), cobaltous (^{58}Co), and mercuric (^{203}Hg) chlorides through excised human and guinea pig skin. Acta Dermato-Venereol. 45, 415-426.
Walkley, A. and Black, I.A. 1934. An examination of Degtjareff method for determining soil organic matter and a proposed modification of the chromic acid titration method. Soil Sci. 37, 29-37.
Wester, R.C., Maibach, H.I., Bucks, D.A.W. et al. 1990. Percutaneous absorption of [^{14}C] DDT and [^{14}C] benzo(a)pyrene from soil. Fund. Appl. Toxicol. 15, 510-516.
Wester, R.C., Maibach, H.I., Sedik, L. et al. 1993. In vivo and in vitro percutaneous absorption and skin decontamination of arsenic from water and soil. Fund. Appl. Toxicol. 20, 336-340.
Woolson, E.A. and Kearney, P.C. 1973. Persistence and reactions of ^{14}C-cacodylic acid in soils. Environ. Sci. Technol. 7, 47-50.
Yan-Chu, H. 1994. Arsenic distribution in soils. Adv. Environ. Sci. Technol.: Arsenic in the Environ. 26, 17-49.
Yang, J.J., Roy, T.A., Krueger, A.J. et al. 1989. In vitro and in vivo percutaneous absorption of benzo(a)pyrene from petroleum crude-fortified soil in the rat. Bull. Environ. Contam. Toxicol. 43, 207-214.
Yin, Y., Allen, H.E., Huang, C.P. et al. 1997. Kinetics of mercury (II) adsorption and desorption in soil. Environ. Sci.

Chapter 29

ASSESSING THE PUBLIC HEALTH SIGNIFICANCE OF SUBSURFACE-CONTAMINANT VAPORS INTRUDING INTO INDOOR AIR

By Henry J. Schuver[§]
USEPA, OSW, Ariel Rios Bldg (MC-5303W), 1200 Pennsylvania Ave. NW, Washington, DC 20460

ABSTRACT

To assess the public health significance of exposures via the vapor intrusion pathway for exposure a risk assessment was conducted for a common VOC trichloroethylene (TCE) in an unbiased sample of all the contaminated sites within a large geographic setting (northern New Jersey). Probabilistic methods were used to minimize the impact of single point-estimate input values and to help assess the impact of variability and uncertainty in input parameters. Central-tendency probabilistic methods were used to provide an estimate of the most likely exposure point concentrations. The exposure assessment involved 709 TCE-contaminated groundwater sites with 29,856 groundwater samples from 11,210 monitor wells in the state's Hazsite database. The groundwater mapping component focused on the 78 sites with one or more TCE-contaminated wells located on land classified as residential. The extent of groundwater contamination beyond the monitor well locations was estimated (mapped) using generic GIS-based Inverse Distance Weighted methods on a natural-log scale and additional hypothetical 'clean wells.' The risk assessment focused on the 38 sites with one or more hypothetical residences overlying groundwater with a house-plot averaged concentration greater than 2.7 ug/L. The attenuation of vapors generated from the upper-most groundwater was estimated for the 883 hypothetical overlying residential structures using the USEPA's national empirical database of vapor attenuation factors. Receptor characteristics based on county-level statistics are used to estimate adult individual and childhood age-specific exposures using probabilistic "age at move in" techniques and with possible in-utero and lactation exposures. The exposure estimates are combined with central-tendency probabilistic estimates of toxicity (primarily based on NYDOH, 2006a) to estimate central-tendency risks for the cancer and non-cancer outcomes under study (Non-Hodgkin's Lymphoma and Central Nervous System effects). In general the

[§] Corresponding Author: Henry J. Schuver, U.S. EPA – OSW, Ariel Rios Bldg (MC-5303W), 1200 Pennsylvania Ave. NW, Washington, DC 20460, Email: 703-308-8656, Fax: 703-308-8609

*This is a personal perspective and does not represent Agency policies or positions.

risks are low and highly skewed. Only those few individuals at the highest level of exposure are estimated to be subject to risks of typical concern. However, the methods used include limitations and these results are not likely to be representative of some other areas of the country. Sensitivity and two-dimensional analyses indicate the inputs for vapor attenuation and groundwater concentration dominate the risk estimates.

1. INTRODUCTION

The recent legislative proposal ("TCE Reduction Act of 2007") reported that "exposures to volatile organic compound vapors from migration to indoor air have become a concern throughout the United States." However, the threat to public health from vapor intrusion remains largely unknown because no study has summarized the frequency and magnitude of vapor intrusion exposures and risks across a broad spectrum of contaminated sites over a large geographic area.

This study conducted an assessment of the risks possible due to vapor intrusion in a full and unbiased sample of all the contaminated sites within a large geographic area. Vapor intrusion exposures have been assessed in an increasing number of contaminated-site investigations, however, typically only at sites suspected to have a high potential for vapor intrusion. Because these 'high potential' sites investigated for vapor intrusion to date are not likely representative of all contaminated sites, the possible impact of vapor intrusion exposures on public health has not been fully assessed. The purpose of the risk assessment, to assess the public health significance of exposures via the vapor intrusion pathway, necessitated a scope broad enough to include a sufficient number of sites potentially affected by vapor intrusion from a full and unbiased sample of all the contaminated sites within a large geographic setting.

2. METHODS

This risk assessment is based on current risk literature and U.S. EPA risk assessment guidance (e.g., USEPA, 1989; 2005a; 2005b), including EPA guidance on probabilistic risk assessments (USEPA, 2001a). However, differing from the EPA's typical methods for estimating upper-bound risks, the method used here was designed to produce typically expected (i.e., central tendency) results (as has been recommended by the Office of Management and Budget (OMB, 2002, 2007)). This risk assessment uses probabilistic ('Monte Carlo') techniques (Cullen and Frey, 1999) for randomly selecting individual point-estimate input values from distributions of input values in each of multiple model iterations to obtain a distribution of individual risks. Distributions are used for both the exposure and the dose-response inputs. Models are presented describing the expected distribution for dose-response relationships and the distribution of exposures for the exposed population. These distributions are integrated into risk estimates in the probabilistic risk model using Crystal Ball software, version 7.2.1 (Decision Engineering, 2006). Probabilistic methods are used to help minimize the impact of single point-estimate input values where there are high levels of variability and uncertainty (USEPA, 2001a).

Probabilistic methods are also used to assess the impact of variability and uncertainty in risk input values on the resulting risk estimates.

This risk assessment uses the environmental evidence from groundwater investigations of contaminated sites in the state of New Jersey (NJ) that was available in electronic formats as of June 2004 (estimated to be approximately 2/3 of groundwater samples collected (Defina, 2004)).

The study area is defined by the political and hydrologic boundaries of the nine watershed management areas (WMA 01 to 09) making up the northern portion of the state of New Jersey. To focus the risk assessment and normalize the dose-response component, a single indicator compound of vapor-forming chemicals was selected (Trichloroethylene (TCE)). In summary, this quantitative risk assessment estimates typical population-wide vapor intrusion exposures and risks for a selected indicator VOC (Trichloroethylene (TCE)), which is present as a contaminant in groundwater beneath residents of northern New Jersey.

2.1 Hazard Assessment

Trichloroethylene or TCE (Cl2C=CHCl; CASRN 79-01-6) is a once widely used chlorinated-solvent VOC (USEPA, 2001b) that has a long history of animal and human studies indicating an association with various health outcomes. These outcomes include non-cancer effects to the central nervous system, liver, and kidney, as well as reproductive and developmental effects, and several cancers such as liver, kidney, lung, and testicular, as well as lymphoma and leukemia (Schiotz, 1938; Waters 1977; and NRC, 2006). The historical industrial use of TCE was substantial (e.g., 145,000,000 kg in 1994 (USEPA, 2001b)), and releases to the subsurface have resulted in TCE being the fourth most commonly detected contaminant in the nation's groundwater (Zogorski et al., 2006) as well as the substance with the most commonly completed exposure pathways at Superfund sites (45% of 1,356) (Johnson, 2002; NRC, 2006). TCE is one of a class of contaminants (chlorinated solvents) that are relatively resistant to bio-degradation and persistent in the subsurface and thus are more likely to be present through a complete vapor migration pathway into indoor air. In summary, trichloroethylene is a generally recognized hazard for its potential to increase the risk for cancer and other adverse health effects and can present a hazard via the vapor intrusion exposure pathway.

2.2 Exposure Assessment

The exposure assessment consisted of five major elements: 1) the preparation of the groundwater contaminant data, 2) the prediction of groundwater concentrations underlying specific residences, 3) the prediction of indoor air concentrations, 4) the descriptions of receptors, and 5) the calculation of average daily exposures. For this study the TCE-contaminated groundwater is the source of the TCE vapors potentially intruding into the indoor air of overlying residences and this study used analytical results (concentrations) from groundwater samples (and 26 associated parameters) that were made available in an electronic format from the state of New Jersey's Department of Environmental Protection (NJDEP) Site Remediation Program's Hazsite Database Submittal System (HDSS) (NJDEP 1999a; 1999b). The data used in this risk assessment was from groundwater samples collected over an approximately 10-year period between October 1993 and April 2003, but the majority of the

samples were collected between 2000 and 2003. The data was reviewed and preliminarily prepared for use in the risk assessment. The preparation included the removal of inappropriate or inconsistent data and the addition of fields for units-corrected result concentration values and adjusted estimates for the depths to water. The data used from Watershed Management Areas 01 to 09 for the risk assessment included 29,856 groundwater samples analyzed for TCE from 11,210 monitoring wells at 709 contaminated sites (see Figure 1).

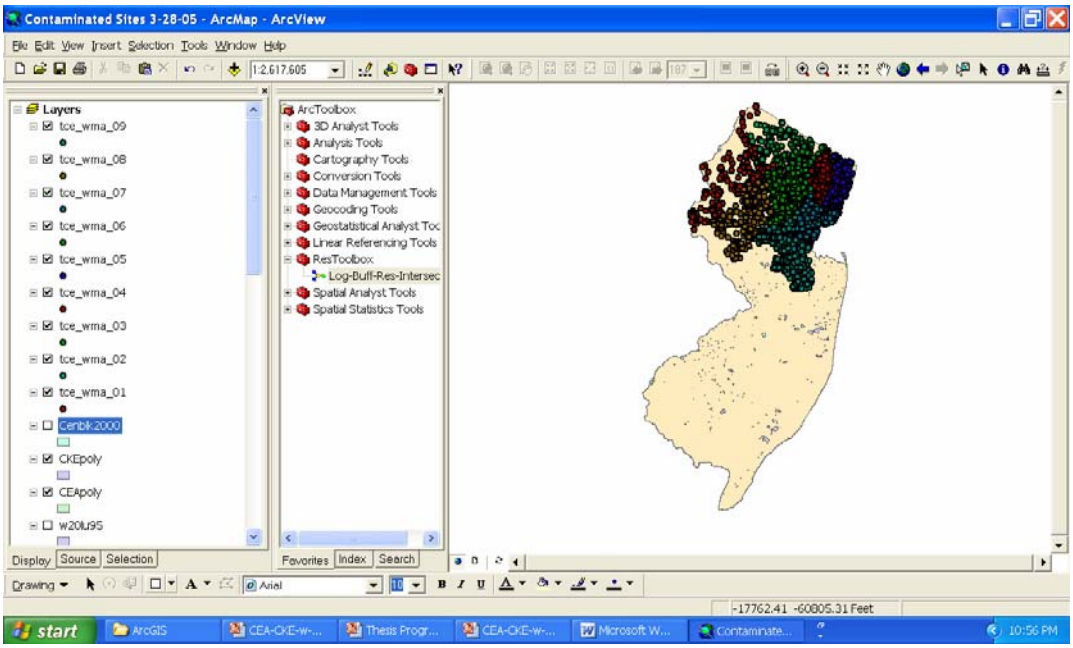

Figure 1. Map of New Jersey showing available groundwater samples indicating the location of study area (Watershed Management Areas 01 to 09)

Spatial modeling (mapping) of the groundwater concentrations was performed to estimate the concentration of TCE in the upper-most groundwater under individual hypothetical residential structures. This was completed using a GIS mapping software, specifically ArcInfo version 9.1 (ESRI, 2006). Preliminary GIS analysis identified those projects that had one or more TCE-contaminated wells located on land that was observed to be residential (NJDEP 2007a) and contained a mean concentration of TCE greater than the lower limit of concern for this study (2 ug/L). Only 78 of 709 contaminated site projects (11 %) were carried forward for prediction of the groundwater plume extent.

The spatial models used to predict of the extent and concentrations of groundwater plumes involved a number of techniques intended to provide a reasonably confident estimate of the concentration under any specific residential location, given the available information. The low number of monitor wells located on residential properties and the lack of critical site-specific parameters, such as the groundwater gradient, hydraulic conductivity, and aquifer thickness, prevented the use of more complex (site-specific) groundwater plume fate and transport models. In general, it was assumed that the contaminated groundwater plume extent was largely defined

by the existing monitor wells. However, none of these wells were expected to be located immediately beneath residential structures and thus it was necessary to estimate the concentrations and extent of contamination between and beyond the monitor wells. The concentrations of TCE in the groundwater beyond the monitor wells were estimated using a generic (non-site specific) assumption that the concentrations decreased in all directions on a log scale away from locations with documented concentrations (monitor wells). The approach used Inverse Distance Weighted (IDW) techniques (ESRI, Geostatistical Analyst) with concentrations expressed in natural-log units. Additional hypothetical 'clean wells' (with assumed zero concentration of TCE) were added to the spatial models to further bound the concentrations in the estimated up- and cross-groundwater gradient directions.

It was assumed that the general direction of groundwater flow could be approximated by the surface topography (USGS, 1983). More specifically, it was assumed that the groundwater flow direction can be approximated using the surface topography from a NJDEP produced Digital Elevation Model (DEM) with a 10 meter cell size that was based on a United States Geological Survey (USGS) data (NJDEP, 2007b). The mapping technique developed to estimate the groundwater flow direction involved the use of the "Least-Cost" raster path (aka "Rain Drop") tool (within the Spatial Analyst program, ESRI 2006) to approximate the down-gradient groundwater 'flow line' direction based on expected surface run-off. An assumed 300 ft buffer was then added to both sides of this central down-gradient flow line and hypothetical clean (0 ug/L TCE concentration) wells were added at 50 ft intervals along the 300 ft buffer lines to bound the contamination in the up- and cross-groundwater gradient directions (see Figure 2).

The approach developed to determine 'shallow' samples (which can generate vapors for possible vapor intrusion) used the minimum "START_DEPTH" (NJDEP, 1999a; 1999b) value from any sample in the entire site (or adjacent sites with wells within the area) and then added 10 feet (one typical monitor well screen-length interval) to that value to arrive at a preliminary 'shallow' limit value for the site. Histograms (Geostatistical Analyst, Data Explorer, ESRI, 2006) of both the minimum and the mean sample START_DEPTH values per well were then inspected to assess whether this preliminary 'shallow' limit value captured the population of samples most likely intended to represent the upper-most waters and also to be distinct (e.g., via an expected clean break) from samples intended to represent deeper portions of the aquifer.

In general, the shallowest histogram category (calculated using 'natural breaks' statistics (ESRI, 2006)) that included the preliminary 'shallow' limit value was used as the final 'shallow' limit value for the site. This analysis involved some hydro-geologic interpretations, particularly when there was substantial topographic relief within the area of the site's wells, included or excluded specific samples to ensure the sample population represented the quality of the upper-most water. In general, only samples with START_DEPTH values less than the final 'shallow' limit value were used to represent the upper-most groundwater (i.e., only the acceptably shallow data were exported as "shallow" files for mapping the distributions of contaminant concentrations, and depth to water).

Finally, the hypothetical homes were assumed to be located at the centroid of regularly spaced average lot-sized areas for the specific land-use density classification, as documented in the NJDEP's 1995/97 Landuse/Landcover files (NJDEP 2007a). Further, it was assumed that the

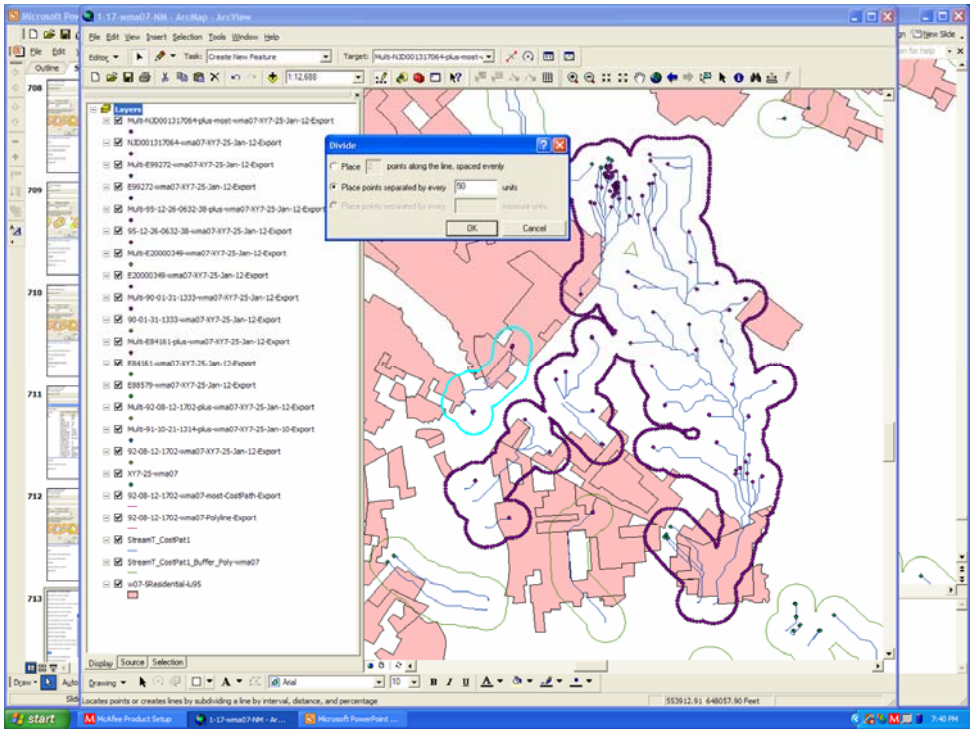

Figure 2. Hypothetical clean wells being added at 50 ft intervals along the 300 ft buffer lines surrounding monitor wells and flow lines (multiple site's wells shown here). Note buffer lines highlighted in light blue tone indicates a monitor well that is located on residential land.

groundwater concentration representing the vapor source for an overlying building could be estimated by using the mean groundwater concentration for the estimated 30 x 30 ft footprint of the home. Only projects with one or more hypothetical residential structures located at the centroid of their lot sizes that had 30 x 30 ft house plot area averaged estimated groundwater concentrations greater than one natural log unit (2.7 ug/L) (see Figure 3 below) were considered further in the risk assessment (38 of the 78 mapped projects).

The prediction of indoor air concentrations in the hypothetical residential structures overlying TCE-contaminated groundwater was based on the estimated residence-specific groundwater concentrations, the vapor partitioning coefficient (Henry's Law), the resulting estimated soil-gas concentration expected to be present immediately above the groundwater table, and a national empirical vapor attenuation data set.

Prior to being used as input into the risk calculation models, the individual predicted hypothetical residence-specific shallow groundwater concentrations (derived by the mapping above) were first depth-adjusted. Predicted residence-specific groundwater concentrations where the depths to water were estimated to be < 5 ft below ground surface (bgs) were adjusted to account for the lower attenuation expected due to the shorter distance for attenuation and likelihood that the contaminated groundwater could be in direct contact with building materials ('wet basement' scenario; USEPA, 2002a). Approximately 40% of the building-specific

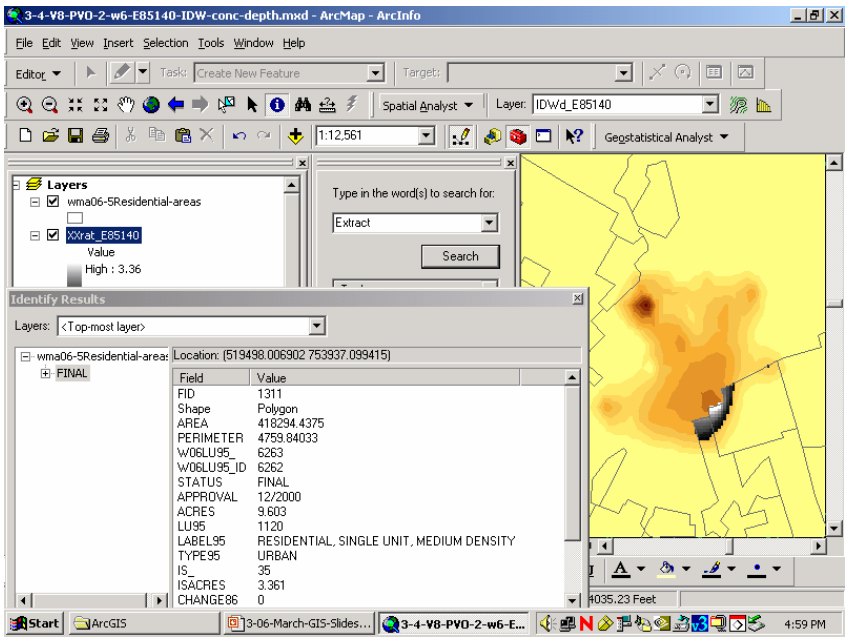

Figure 3a. Predicted groundwater concentrations and impacted residential land (showing concentrations for all 30 x 30 ft potential building plots (concentrations up to 3.36 ln)).

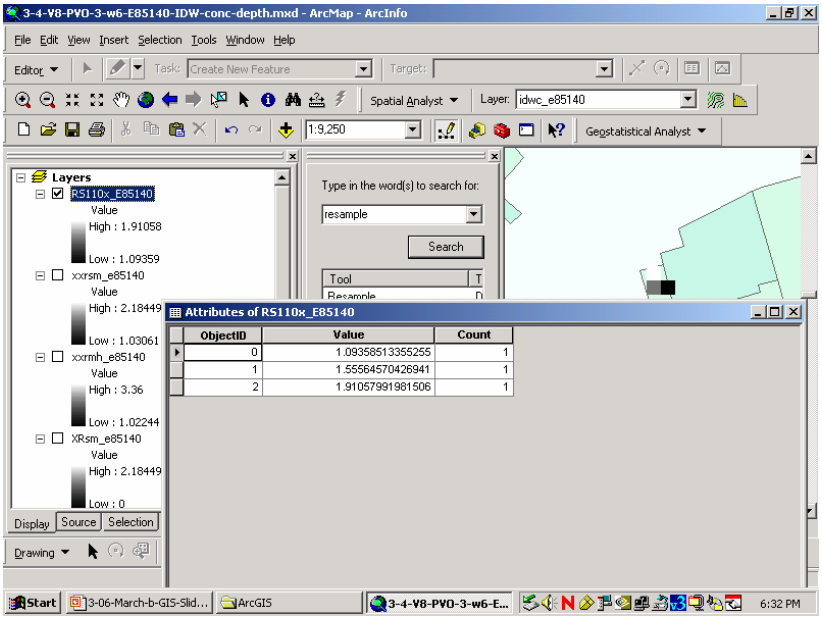

Figure 3b. Re-sampling of all potential building plots resulted in three lots with residential building-specific shallow groundwater concentrations greater than one log resulting from the placement of the (30 x 30 ft) building sites at the centroid of the applicable lot size (here 110 ft by 110 ft).

groundwater estimates were found to be shallow (i.e., <5 ft bgs) and their concentrations were multiplied by a factor of 3.3x, and the 13% of the building-specific groundwater estimates that

were found to be very shallow (<3.3 ft bgs) and were multiplied by an additional 3.0x factor. This approach provided location-specific adjustments for the expected reduction in attenuation from shallow sources where direct contact with building materials is possible.

The distribution of predicted groundwater concentrations, including the values that were depth-adjusted, were then fit to a continuous distribution using Crystal Ball software with Chi-Square fitting criteria. Randomly selected values from the best-fit distribution of (depth-adjusted) groundwater concentrations were the initial and primary input into the calculation of probabilistic estimates of the indoor air concentration of TCE due to vapor intrusion.

The concentration of TCE in the soil-gas immediately above the contaminated groundwater (vapor source) was estimated using a unit-less Henry's Law partitioning coefficient for an average shallow groundwater temperature for northern New Jersey of approximately 52 degrees F (11.1 degrees Celsius) (USEPA, 2004a). The unit-less Henry's Law partitioning coefficient for this temperature has a value of 0.216 using the Office of Solid Waste and Emergency Response (OSWER) method (USEPA, 2004a). TCE dissolved in the upper-most portions of the groundwater was assumed to fully partition at the predicted Henry's Law equilibrium level (as is needed to be consistent with the practice used in calculating the empirical attenuation factors) and has been observed in the field (Wertz, 2006; MADEP, 2000). Each hypothetical residence-specific groundwater concentration estimate was multiplied by the Henry's Law partitioning coefficient for TCE (and a unit conversion of 1000 liters/m^3) to estimate the concentration TCE vapors (in ug/m^3) immediately above the upper-most groundwater underlying each residential structure.

The reduction (attenuation) of vapor concentrations between the vapor source (e. g., concentration in soil gas immediately above the groundwater) and the indoor air has been described by an attenuation "factor" (Johnson and Ettinger, 1991) which is defined as the ratio of concentrations in indoor air to the subsurface vapor source (immediately above the groundwater). For ease of communication, and to allow whole numbers to be entered in the risk software, for this study an attenuation 'value' was defined as the ratio of the subsurface vapor source concentration divided by the indoor air concentration (i.e., 1/attenuation factor). This nomenclature allows high amounts of attenuation to be represented by high attenuation 'values' and low amounts of attenuation to be represented by low numerical attenuation 'values.' This terminology is similar to the "dilution factor" term used by others (ITRC, 2007).

The distribution of expected groundwater to indoor air attenuation values is based on empirical data collated by the USEPA. Over the last six years the USEPA has been building a national database of paired data including measured groundwater concentrations and measured indoor air concentrations that were collected under the authority of various federal and state regulatory authorities (Dawson, Hers, and Truesdale, 2007). While many variables can influence the attenuation values observed for an individual building and paired data set, the overall distribution of observed attenuation values from groundwater has remained somewhat stable over the last few years with a median groundwater attenuation 'value' of approximately 10,000 (attenuation factor of 1/10,000). For this study the distribution of national empirical attenuation values was filtered to include only those attenuation values where the vapor source (soil-gas) concentration term was greater than 100 times the 90th percentile of recent literature indoor air "background" values (i.e., 0.5 ug/m^3; Dawson, 2007). This distribution was assumed to

approximately represent the range and distribution of possible attenuation of intruding vapors that could be expected in northern New Jersey. A best-fit curve for the distribution of observed attenuation factors in the USEPA vapor intrusion database (from 1,020 sample pairs) was used in the Crystal Ball models. The curve representing the distribution of observed attenuation values was log-normal with a mean value of 51,648, a minimum attenuation value of 23.5, and a maximum attenuation of 2,080,000. In summary, the calculation divided the vapor concentration at the source (i.e., in the soil-gas immediately above the groundwater table) by the randomly selected attenuation 'value' to estimate the indoor air concentration.

The population occupying the residential structures overlying the TCE contaminated groundwater plumes was expected to be similar to the rest of the population of these counties and of New Jersey. Current statistics for populations in the northern counties of New Jersey, and state-wide, show approximately 2.7 persons per household (US Census, 2004). For the purpose of this risk assessment there was expected to be one adult male and one adult female occupant and 0.7 children (under 18) per household/residence. Given the exposure assessment identified 883 hypothetical residences expected to overlie shallow TCE-contaminated groundwater and the average occupancy rate (2.7 persons / residence), the population of potential receptors would be approximately 2,384 persons at a given point in time.

Given that people move in and out of homes with a median of every nine years (USEPA, 1997) and the 30 year period of this study (1985-2015), it can be expected that approximately 3.3 (30/9) different families/groups would occupy each of the homes over the 30 year period of this study. The total potential receptor population could be expected to be approximately 7,867 (3.3 x 2,384) persons.

State-wide and northern-county New Jersey statistics show approximately 75% (approximately 2/2.7) of the population is over age 18, and 25% (approximately 0.7/2.7) is under 18 (US Census, 2004). Thus, of the 7867 expected occupants over the 30 year period, approximately 5900 are adults and approximately 2000 are children. Given the northern-county approximate average of 14 live births per 1000 population per year (over the period from 1982-2002; NJDHSS, 2002) it can be estimated that approximately 1000 children would be born to residents in these homes over the 30 year study period (14 live births/1000/yr x 2,384 residents at any year = 33 births/yr x 30 yrs = approximately 1000 births from parents in residences over plumes). Assuming that approximately one-half of the children expected to be born in these residences are not already included in the population estimates, it is possible that another 500 children could be born and raised (for some period of time) in these residences (for a possible total of approximately 2500 children residents over the 30 year period of the study).

The calculation of average daily exposures for occupants of the hypothetical residential structures overlying TCE-contaminated groundwater was based on the estimated indoor air concentrations due to vapor intrusion, the exposure duration, exposure frequency, and exposure time, as well as the appropriate averaging time for the potential outcomes. The calculation of average daily exposure was performed similarly in each of the two adult risk models: adult-cancer, and adult-non-cancer (see Appendix 1 and 2). The calculations for the child-cancer and child-non-cancer models were somewhat different to account for child-specific factors and the age-specific time of exposure (see Appendix 3 and 4). The calculations for adults will be discussed first.

The general equation for characterizing inhalation exposure, when using either units of Reference Concentrations (RfC) for non-cancer risks or Inhalation Unit Risks (IUR) for cancer risks, is presented below, as modified after USEPA (1994):

$$I = \frac{C_{vi} \times EF \times ED}{AT}$$

Where:

I = effective long-term avg. daily exposure (ug/m^3)

C_{vi} = concentration of contaminant in indoor air due to VI (ug/m^3)

EF = exposure frequency (in 24hr-days/yr) spent inside residence

ED = exposure duration (yrs) residing at that location

AT = averaging time (days)

The predicted concentration of TCE contaminants in residential indoor air from vapor intrusion (C_{vi}) is derived from procedures described above (and shown in Appendix 1 and 2 on row 6).

For this probabilistic assessment the exposure frequency (EF) normally expressed in terms of days/yr spent at residence, and exposure times (ET) normally expressed in hrs/day actually spent in the residential structure, were combined and expressed as a single population of exposure frequency (EF in 24-hr-days/yr). This is equivalent to the number of full 24-hr-days actually spent inside the residence per year. This was done to improve the accuracy of the probabilistic calculations using distributions of exposures.

The distribution of 24-hr-day exposure frequencies for adults was modeled with a triangular distribution with 240 24-hr-days/yr as the most likely value. This 24-hr-days/yr value represents mean residential indoor air exposures of 948 minutes (15.8 hrs) per day (USEPA, 1997) for 365 days per year. The distribution's minimum exposure frequency value was from the fifth percentile of time in residence (equivalent to 137 24-hr-days/yr) and the maximum value for all adult age groups (>18 years old) was equivalent to 365 24-hr-days/yr) from EPA (USEPA, 1997).

The distribution of exposure duration (ED) values for the duration of time (years) that adults would reside in a specific residence overlying the contaminated groundwater (ED in years are based on USEPA guidance (1997) and literature values. The distribution of Exposure Durations (residence times) was modeled with a triangular distribution having nine (9) years as the most likely value and an assumed practical minimum (adult) value of one year in residence and maximum of 40 years.

The exposure averaging times (AT in years) for cancer effects in adults were presented as single point estimates for this risk assessment (70 years; USEPA, 1997). The averaging time for non-cancer effects in adults is based on the individual's (randomly selected) exposure duration.

For children, the derivation of exposure durations and frequencies were similar but more complicated than for adults (see Appendix 3 and 4). The exposure duration values used for children (ED in years) were similar to those for adults; however, they included a possible shorter minimum period (min. 0.1 years) as these short exposures may still be relevant for children, and the child's distribution was capped at maximum of 18 years (USEPA, 2002a). Additionally, because children could be of any age at the time the family moves into the home, could be born any time within the family residence duration and/or could attain the age of 18 (i.e., no longer be expected to be at home) prior to the family moving out, the models needed to account for the actual age of the child at 'move in' and the time of birth within the family residence duration. The child's age at 'move in' was designed to be randomly selected from a uniform distribution with ranges up to 18 years at the time of family 'move in' and to be as young as being born up to 10 years after the family 'moves in' (see Appendix 3 and 4, rows 8 to 11). The calculations in Appendix 3 and 4, rows 9 to 11, calculate the total child residence duration. The calculations in rows 12 and 13 provide the individual child's exposure durations within the specific 0-2 years of age, and 2-18 years of age, periods. In summary, the individual children's exposure durations, including that of newborn infants, were modeled using a probabilistic structure so that children could be born up to 10 years after family move-in.

For children, the USEPA reports the central tendency estimate (median) of exposure time (in hours per day) spent in the residential structure is 21 hours per day for ages 0-4 (years) and approximately 16.4 hours per day (approximately the same as adults) for aged 5-17 (EPA, 2002a, Table 9-41; and 1997, Table. 15-131). For this assessment, children 0-2 yrs of age were estimated to have a central tendency exposure time of 21 hours per day which relates to an approximate central tendency exposure frequency of 300 24-hr-days per year. The distribution of exposure frequencies for children aged 0-2 was assumed to be triangular with a minimum of 150, a most likely value of 300, and a maximum of 365 24hr-days per year.

For children aged 3-18 the exposure times for children ages 0-4 (21 hr/day) and ages 4-18 (16.4 hrs/day) are combined with the exposure frequency value for children aged years 7-18 of 240 24-hr-days/yr (i.e., the same as adults). This resulted in a combined estimate of 268 24hr-days per year for children of ages 3-18 years. The distribution of exposure frequencies for children was modeled with a triangular distribution having 268 24-hr-days/yr as the most likely value and the minimum value of the fifth percentile of time in residence (148 24-hr-days/yr) and maximum of the 95% for all age groups <18 years old (365 24-hr-days/yr) as the minimum and maximum values (EPA, 2002a; Table 9-41).

For children the exposure averaging times for cancer effects (during childhood) were presented as single point estimates for the entire childhood of 18 years (Appendix 3, row 35). The averaging time for non-cancer effects in children is equal to the individual's (randomly selected) exposure duration (Appendix 3, row 31).

In summary, the exposure calculations for each of these receptors and appropriate exposure factors are performed within the probabilistic Crystal Ball risk calculator software. The model structures and formula are described above, shown in detail in Appendices 3 and 4.

Several versions of childhood age-adjusted exposures were also calculated based on the growing volume of research on and evidence for the potential heightened effects for exposure

during critical periods of growth and development (e.g., USEPA, 2005b, 2006; Barton, et al., 2005). The age-period-specific adjustments to exposure are used as surrogates for possible differential response (toxico-kinetic and -dynamic effects) due to exposures during critical periods of a child's development.

For cancer risks to children, the use of the single point estimate exposure averaging period of 18 years, discussed above, established an effective minimum age-adjustment factor of approximately 3.3 (18/70) relative to adult cancer risks for all cancer risks to children (i.e., ages $\leq$ 18 yrs). This is generally consistent with EPA guidance for exposures to children up to 16 years of age, for exposures to chemicals acting through a mutagenic mode of action (USEPA, 2005b). Note, while TCE is not commonly considered to act through a mutagenic mode of action, the USEPA has only recently proposed a definition of what is meant by a mutagenic mode of action (USEPA, 2007), and TCE is known to have multiple complex and not fully defined modes of action (Chiu et al., 2006) particularly for NHL (NYSDOH, 2006a). Additionally, recent evidence indicates cancers (particularly childhood cancers) may be influenced by the interaction of genetic and epigenetic processes such as "alterations in gene expression, DNA repair, cell cycle control, genome stability and genome reprogramming" (Preston, 2006). Barton et al. (2005) report a "reasonable expectation that children are more susceptible to some carcinogenic agents than adults" and a geometric mean ratio of early-life to adult cancer potencies of 3.4 for lifetime exposures for six chemicals known to act through a non-mutagenic mode of action. There have been some observed associations that indicate a heightened cancer response in children can occur for exposures to chemicals outside of those typically considered to have a mutagenic mode of action, e.g., for VOCs such as TCE (e.g., Cohn et al. 1994; Costas, Knorr, and Condon, 2002; Infante-Rivard et al. 2005) as well as a still incomplete, but suggestive, study (ATSDR, 2003) where additional and possibly continuing exposures due to vapor intrusion have only recently recognized (ATSDR, 2007). Additionally, this 3.3x factor can be considered to compensate for the use of the IUR as the toxicity metric, because the IUR values do not consider the body weight or breathing rate of children. Recent studies have indicated an approximate two-fold higher dose for Category 3 gases in the pulmonary region for children (Ginsberg, Foos, and Firestone, 2005), and the "peak concentration of an inhaled VOC depends greatly on cardiac output and ventilation rate" (Bushnell et al., 2005). Finally, this 18 yr averaging-period approach helps avoids the discontinuities possible when randomly selected exposure durations of < 10% of 70 yrs (e.g., 6 yrs) would otherwise indicate the use of sub-chronic exposure assessment techniques for those individuals.

For cancer effects in children four versions of age adjustments for exposures for children aged 0-2 yrs were calculated. The risk without additional age adjustment (i.e., assuming no more heightened risk than was already included in the 18 yr averaging time (a 3.3x factor)) was considered the baseline. In addition, three types of adjustments to the exposures during the first two years of life were made. The first version of age-adjusted exposure, termed "1x+," adds a distribution around the most likely value of 1.0. The distribution has a minimum of 0.9, a maximum of 3.0 and a most likely value of 1.0. The second version of age-adjusted exposure, termed "3.0x," uses a single point estimate multiplier of 3.0 for all exposures in the 0-2 age period (a value that is consistent with USEPA's (2005b) total 10x adjustment). The third version of age-adjustment for child cancer, termed "3.0+x," uses the same 3.0 point estimate multiplier for exposures during the 0-2 age period, but also adds the possibility of additional exposures bio-

transferred from the mother, if she was exposed more than one year prior to birth and she breast-fed the child (Appendix 3 and 4, rows 24-25).

Unlike cancer risks, for non-cancer risks to children no inherent child age-adjustment factor was included in the baseline case. However, a variety of non-cancer effects, including neurological, have been found to be elevated or unique to children such as *in utero* exposures and should be considered when using typical adult-animal or adult-human based toxicological reference concentrations values (e.g., ATSDR, 1999; White et al., 1997). Thus, in addition to the baseline model without any age adjustment (i.e., assuming no heightened risk), four additional types of adjustments to the exposures during childhood were made. A quantitatively-minor multiplicative age adjustment (i.e., 1.25) was assumed possible for children 2-18 yrs (versus exposures to adults), a higher adjustment (i.e., 1.5) was assumed appropriate for exposures in the 0-2 age period, and an even higher adjustment (i.e., 1.75) was assumed to be appropriate for exposure during the *in utero* period (age -3/4 to 0 yrs). Finally, exposures possibly bio-transferred from the mother, if she was exposed more than 1 year prior to birth and she breast-fed the child, was assumed to be an additional factor of 1.5 times (Appendix 3 and 4, rows 17-19).

In summary, a variety of age-adjustment factors were explored in this risk assessment. These ranged from the typically assumed default value of 1 (i.e., assuming no effect due to age at exposure) to various distributions of values at different ages as well as the possibility of pre-natal exposures and the bio-transfer of contaminants in mother's milk.

2.3 Dose-Response Assessment

Over the last 40+ years there has been a substantial amount of research on the dose-response relationships for cancer and non-cancer effects associated with TCE exposures. Much of this work has been summarized and reviewed since 2000, including a 'state of the science' TCE-dedicated issue of *Environmental Health Perspectives* in 2000 (Scott and Cogliano, 2000), a draft TCE risk assessment by the USEPA (2001c), a review by the USEPA's Science Advisory Board (USEPA, 2002c), a summary of the recent evidence by the USEPA (2004a, 2005c), a TCE-dedicated mini-monograph (Chiu et al., 2006), a review of the critical issues by the National Academy of Sciences (NRC, 2006), and updated toxicity values by NYSDOH (2006a), as well as a number of other newly published studies, summary reviews, and meta-analyses.

This quantitative risk assessment focused on two specific health outcomes: those believed to have a sufficient number of consistent observations of an association with TCE inhalation exposures and those where low-level environmental exposures may be relevant to the public's health. This risk assessment considered one cancer, Non-Hodgkin's Lymphoma (NHL), and one non-cancer, Central Nervous System (CNS), health outcome.

The results of the dose-response assessment are represented as distributions in the probabilistic models. For both cancer and non-cancer effects this relationship is represented in the probabilistic model using a triangular frequency distribution with the central tendency risk as the most likely value, the lower-bound confidence interval (CI) values as the estimated 2.5 percentile or minimum response value, and the upper CI as the estimated 97.5 percentile value or maximum response value.

For non-cancer effects, TCE has been long recognized to interrupt the transmission of nerve/pain signals in the human central nervous system, and TCE was introduced as a narcotic in 1911 and was being widely used for surgical anesthesia by the 1950s (Waters, Gerstner, and Huff, 1977). While the exact mechanisms of action were not fully understood, TCE was used an anesthetic until as recently as the 1970s, when awareness of some of the undesirable side effects of these very high-level TCE exposures (approximately 2,000 ppm) grew (Waters, Gerstner, and Huff, 1977).

TCE is also recognized for central nervous system (CNS) effects in humans at much lower concentrations than used for anesthesia, albeit typically with longer exposure durations. The ATSDR (1997) has summarized the observations of a variety of CNS effects in humans associated with occupational-level TCE exposures (e.g., low 100s ppm), including headaches, drowsiness, confusion, dizziness, nausea, loss of facial sensation, nerve damage, and reduced scores on a variety of neurological function tests. A number of community-based studies have also documented some associations with CNS effects in environmental TCE-exposed populations (ATSDR, 1999, White et al., 1997). Research on possible impacts of low concentrations on public health continues (Barton and Clewell, 2000) and has focused on bio-chemical markers of neurotoxicity (Bushnell, et al., 2005).

This dose-response assessment has focused on two well-conducted studies of animals exposed to low levels of TCE in air showing a variety of CNS effects that, while subtle, may also be important for public health. First, Arito, et al. (1994) reported statistically significant associations for decreased wakefulness and heart rate. Using continuous polygraph recordings, Arito, et al. (1994) found that "exposure to all levels of TCE resulted in a statistically significant, dose-related decrease in the amount of time spent in wakefulness ($p<0.01$) during the 8-hour exposure period. Rats exposed to 50 ppm or higher [i.e., all doses] also had statistically significant decreases in time averaged heart rates during stages of wakefulness ($p<0.05$), slow wave sleep ($p<0.01$) and paradoxical sleep ($p<0.01$) during the 22-hour post exposure period" (NYDOH, 2006a). The NYDOH suggested that this could be due to "TCE-induced disruption of wakefulness and its circadian rhythm" (NYDOH 2006a). Arito et al. (1994) also observed at higher doses spontaneous bradyarrhythmia epidsodes in older (20-26 months) rats. Second, Briving et al. (1986) observed statistically significant associations for biochemical changes in the brains of gerbils (as did Haglid et al. (1981) and Kyrklund et al. (1984)). Specifically, Briving et al. (1986) documented significant changes in the amounts of brain proteins (glutamate and GABA [*gamma*-amino butyric acid], as well as GSH [Growth Stimulating Hormone] at higher doses) that are believed to be indicators of neuronal damage.

The NYSDOH (2006a) has provided the most recent quantitative analysis of both animal and worker evidence for CNS effects associated with TCE inhalation exposures. After consideration of a wide variety of both animal and human evidence, the NYSDOH considered a human-based occupational study (Rasmussen, Arlien-Soborg, and Sabroe, 1993) to best represent the high toxicity end of the TCE exposure to CNS response relationship for humans. In summary, Rasmussen, Arlien-Soborg, and Sabroe, (1993) found 33/99 (33%) metal degreasers primarily using TCE having at least one abnormal motor coordination score and the mean number of abnormal coordination tests (six tests) illustrating a dose-related trend. Clinical evidence of cranial nerve dysfunction was also found in the more highly exposed workers of that study. The abnormal motor coordination tests from that study and the physiologically-based pharmo-kinetic

(PBPK) model derived Human Equivalent Concentrations (HEC) calculated by NY State (NYSDOH, 2006a) were used to develop NYDOH's high-toxicity low-response percentile (RfC) value of 11 ug/m^3.

For non-cancer effects this assessment used a Reference Concentration (RfC) metric (risk per ug/m^3 of TCE in air) and assumed a triangular distribution for frequency of risks with an estimated upper-bound risk (minimum RfC concentration level) of 11 ug/m^3 as the point estimate for subtle CNS effects in a low percent of the general population resulting from inhalation exposures to TCE (NYSDOH, 2006a). The estimated central tendency RfC value, general residential population was estimated to be 74 ug/m^3 and the maximum RfC value estimated to produce perhaps subtle, but nonetheless observable, CNS effects in a majority of the general population was estimated to be 110 ug/m^3.

For cancer effects, and in contrast to the long history of non-cancer effects, the data base of observations for TCE exposures and lymphoid cancers (such as NHL, Hodgkin's disease, multiple myeloma, and leukemia) has begun relatively recently, has been increasing rapidly, and some of the highest quality human observations have been completed only very recently. Observations for NHL were addressed in recent quantitative analyses and/or summary reviews by Wartenberg, Reyner, and Scott (2000), USEPA (2001c), USEPA's Science Advisory Board (2002b), Hansen, et al. (2001), Raaschou-Nielsen et al., 2003, Kelsh, et al. (2005), USEPA(2005c), Chiu et al., (2006), Scott and Chiu (2006), Mandel et al. (2006), and NYSDOH (2006a), but was not addressed by the NRC (2006).

In the most recently released quantitative toxicity value assessment of available occupational epidemiology studies, the State of New York's Dept. of Health chose to use the upper 95% confidence interval for NHL risk from the Hansen et al., (2001) study, with support from the exposure data from the Raaschou-Nielsen et al., (2002) study, to develop a potential lifetime air concentration criterion for NHL (NYSDOH, 2006a; Table 5-18). The lifetime air concentration value correlating to a 10^{-6} risk for upper-bound risks was reported to be 0.29 ug/m^3, which relates to an Inhalation Unit Risk (IUR) value of 3.5 x 10^{-6} risk per ug/m^3 (NYSDOH, 2006a, Table 5-18). The NYDOH reported a central estimate for the IUR of 1.3 x 10^{-6} based on mean risks for the middle category of exposure durations in the Hansen et al. (1980) study.

After a review of available animal and human studies, the State of New York's Dept. of Health chose to use the upper 95% confidence interval of a statistically significantly elevated risk of malignant lymphoma from a mouse inhalation study (Henschler et al. 1980) to develop its final air criteria for Non-Hodgkin's Lymphoma (NHL) (NYSDOH, 2006a; Table 5-39). The (non-age adjusted) Lifetime Average Daily Exposure (LADE) air concentration correlating to a 1.0 x 10^{-6} lifetime incremental increase in cancer risk for humans was reported as 0.3 ug/m^3 (NYSDOH, 2006a, Table 5-38) which relates to an Inhalation Unit Risk (IUR) value of approximately 3.5 x 10^{-6} risk per ug/m^3 of TCE. Note that this result is nearly identical to the value derived from the human-based studies discussed above.

This risk assessment used an Inhalation Unit Risk (IUR) metric (risk per ug/m^3 of TCE in air) with an assumed triangular distribution for the frequency of risks with an upper-bound value of 3.5 x 10^{-6} and the central tendency value of 1.3 x 10^{-6} developed by the State of New York based on human evidence (NYDOH, 2006a). A linear extrapolation from the NYDOH central

tendency risk estimate (1.3×10^{-6}) was made to estimate an approximate lower bound risk level of 4.7×10^{-7} per ug/m^3 of TCE.

2.4 Risk Characterization

The adult cancer calculations (model) will be described as an example. Appendix 1 illustrates the structure, example central tendency input values, and formula for calculating the adult cancer risks. The calculations for adult cancer risk begins with the lifetime average concentration, as described above, which is then multiplied by the randomly selected IUR value to produce the incremental lifetime cancer risk due to the vapor intrusion of TCE for the hypothetical individual person represented by the individual trial run. This process is repeated for a total of 5,900 times to produce a distribution of individual risks to the population of adult residents of buildings overlying these groundwater plumes. The model for adult non-cancer (CNS) risk is similar (Appendix 2), except that the average daily exposures are divided by a randomly selected Reference Concentration (RfC) value and the randomly selected exposure-averaging period. The children's risk models are similar to the adult models in that they use an average daily exposure level, although they also included, as described above, child-specific exposure durations in the home and a variety of age-adjustment factors (see Appendices 3 and 4).

3. RESULTS

The results of the GIS-based mapping of the estimated extent and concentrations of TCE-contaminated groundwater indicate that approximately one-half (38/78) of the 78 mapped sites, with one or more TCE-contaminated wells located on land that was classified as residential, have predicted concentrations of concern (> 2.7 ug/L) located under one or more of the hypothetical residential structures. Only these 38 sites were considered further in this risk assessment. The total area of mapped contaminated groundwater plumes (with concentrations > 2.7 ug/L) from these 38 sites was estimated to underlie 883 hypothetical residential structures. The groundwater concentrations estimated to underlie the 883 individual hypothetical residential structures (including depth-adjustments) were generally relatively low (median of 5.9 and a mean of 19.5 ug/L (ppb)). These concentrations were represented in the models by a highly skewed best-fit log-normal distribution with a mean of 19.5 and a standard deviation of 61.09.

The mean predicted indoor air concentrations of TCE due to vapor intrusion (Cvi) in the four primary models (adult and child cancer and non-cancer) ranged from 1.62 to 1.75 ug/m^3, and the median values for all models are 0.13 ug/m^3. The estimated average daily exposures for the receptor populations are presented as separate distributions for adults and children and for cancer and non-cancer outcomes and are summarized in Table 1 below.

In summary, these results show the adult and child average daily exposures are generally low and highly skewed, with a few individuals with higher levels of exposure. Additionally, in general, the average daily exposures for non-cancer effects are two to four times higher than

those for cancer effects which is expected to be largely due to the differences in the averaging periods (which included only the actual exposure period for non-cancer effects).

Table 1. Average Daily Exposures (ug/m^3)

Receptor	Cancer		Non-Cancer	
	Mean	Median	Mean	Median
Adult	0.28	0.02	1.15	0.08
Child	0.56	0.04	1.35	0.09
Child age-adj.	0.69	0.04	2.76	0.18

3.1 Cancer risk

Probabilistic estimates of the risks for NHL for the estimated 5900 adult residents of the 883 hypothetical residences overlying TCE-contaminated waters over the 30 years of this study are presented in Table 2 below. In general, the risks are low and highly skewed. The median risk is approximately 3 x 10-8, and the mean risk is approximately 5 x 10-7. The maximum individual risk was estimated to be approximately 1 x 10-4 risk. Only individuals at the highest percentiles of exposure (>90%) are subject to risks in the vicinity of levels of typical concern (i.e., at least 10-6 levels).

Table 2. Cancer Risk

Receptor	Median risk	Mean risk	Max. risk
Adult	3×10^{-8}	5×10^{-7}	1×10^{-4}
Child 1.0x	6.3×10^{-8}	1×10^{-6}	2.1×10^{-4}
Child 1+x	6.5×10^{-8}	1.1×10^{-6}	2.1×10^{-4}
Child 3.0x	7.3×10^{-8}	1.2×10^{-6}	2.2×10^{-4}
Child 3.0x+	7.5×10^{-8}	1.3×10^{-6}	2.2×10^{-4}

Probabilistic estimates of the risks for NHL for the estimated 2500 child residents of the 883 hypothetical residences overlying TCE-contaminated waters over the 30 years of this study for various age-adjustment scenarios are also presented in Table 2 above. Figure 2 shows the results for both Adults and Children (under the four age-adjustment scenarios).

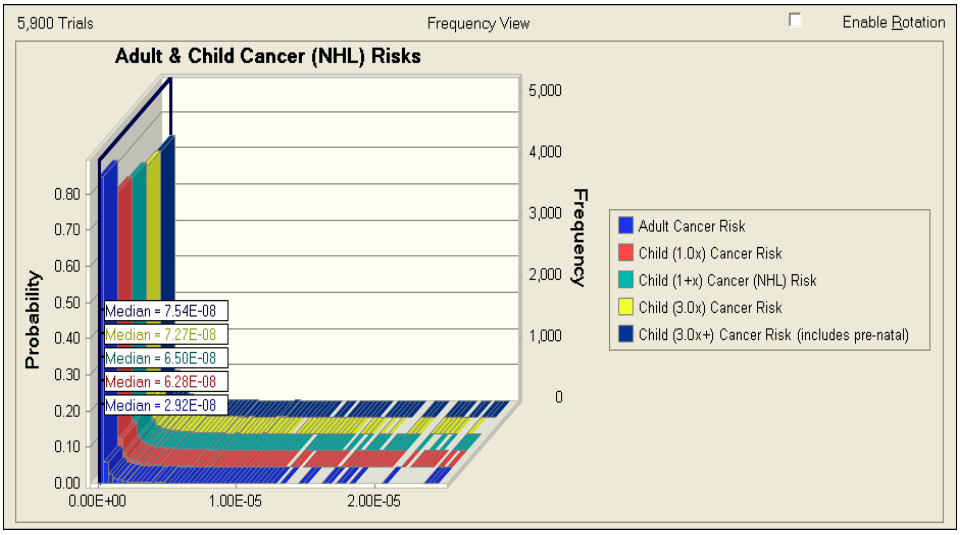

Figure 3. Overlay (frequency) chart for Adult and Child age-adjusted Cancer (NHL) risks.

3.2 Non-Cancer risk

Probabilistic estimates of the risks for CNS effects for the estimated 5900 adult residents of the 883 hypothetical residences overlying TCE-contaminated waters over the 30 years of this study are presented in Table 3 below. The non-cancer risks have a median value of approximately 0.001 and a mean risk of approximately 0.02. The maximum individual risk modeled has a Hazard Quotient (HQ) of 7.4. These non-cancer risks, which are typically compared to a HQ of 1.0, are mostly very low. Only adult residents at the highest percentiles of exposure (e.g., >>90%) are subject to risks above levels of concern (i.e., HQ > 1.0).

Table 3. Non-Cancer Risk

Receptor	Median risk	Mean risk	Max. risk
Adult	0.0013	0.02	7.4
Child (un-adj.)	0.0015	0.022	6.6
Child (age-adj.)	0.0028	0.052	30.8

Probabilistic estimates of the risks for CNS effects in the estimated 2500 child residents of the 883 hypothetical residences over the 30 years of this study are also presented in Table 3 above. When no age adjustments are considered, i.e., assuming that exposures during childhood (age period) had no higher effect on children than on adults, the median risk is approximately 0.0015, and the mean risk is 0.022. Only child residents at the highest percentiles of exposure

(i.e., >>90%) are subject to risks near levels of concern (e.g., 90% risks have a HQ of 0.03) and the maximum modeled risk has an HQ of 6.6.

The non-cancer risks to children when the age of exposures (age adjustment) is taken into account are presented in Table 3 above. The risks, considering various childhood periods (see Table 3), have a median value of approximately 0.003, and the mean risk is approximately 0.05. Only children residents at the higher percentiles of exposure (i.e., >>90%) are subject to risks in the vicinity of levels of concern (90% exposures have an HQ of only approximately 0.07), and the maximum risk has an HQ of approximately 31.0.

To compare the frequency and distribution of non-cancer (CNS) risks for both adults and children (under the two versions of childhood age adjustment), these risks are presented together in Figure 4. From this figure it is possible to see the gradual transition to slightly higher risks (and lower bar height for near-zero risks) beginning with adults and then for children without, and with, age adjustment. The median non-cancer risks (HQ) for all three receptors are in the low 10^{-3} range. In summary, the non-cancer risks to both adult and child receptors are generally low and highly skewed. Only individuals at the highest percentiles of exposure (>90%) are subject to risks above levels of typical concern (i.e., hazard indices of >1.0).

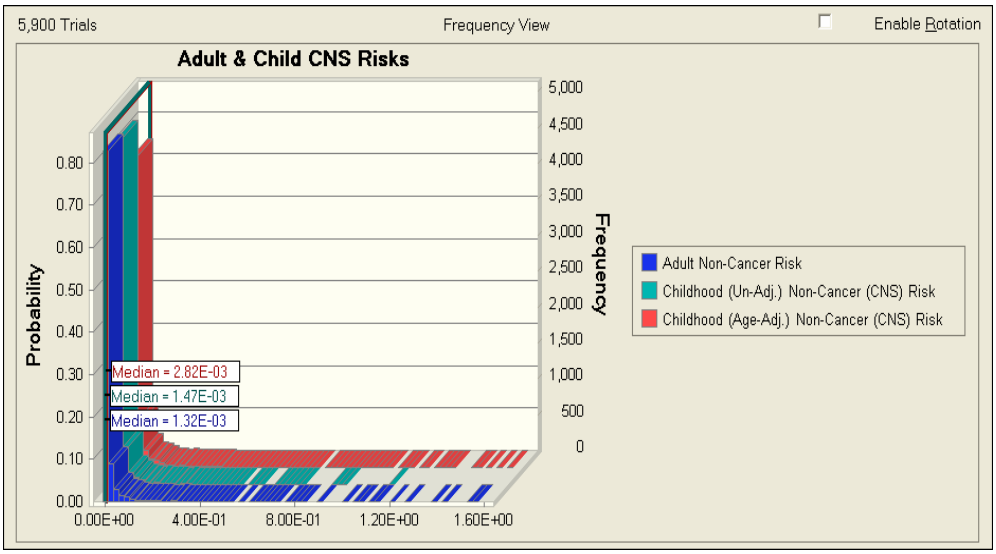

Figure 4. Overlay (frequency) chart for Adult and Child age-adjusted Non-Cancer (CNS) risks.

3.3 Secondary Analyses

Further analysis of the role of the inputs (assumptions) on the results was performed to better understand the leading causes of these risks and their distributions. These secondary analyses included sensitivity analyses and two-dimensional analyses.

Sensitivity analyses assess the impact of the input variables in the context of the sensitivity of the specific model structure and for the range of inputs tested. The “Sensitivity” analysis for

cancer (NHL) risks to adults shows that when all the inputs are allowed to vary, the risks are dominated by only two input variables: the attenuation of vapors value (-54% of the variance in risks) and the concentration of contaminant in water (36% of the variance in risks). These inputs are followed by the much smaller effects of the exposure duration (7%), the Inhalation Unit Risk (IUR) toxicity factor (2.5%), and the exposure frequency (0.5%). These values are summarized in Table 4 below. The results from another form of sensitivity analysis (one-at-a-time) also shows a very similar rank order and magnitude of effects of these same inputs (i.e., with attenuation and concentration having the most influence) for both adult and child cancer risks.

Table 4. Sensitivity of Cancer Risks

Input variable	Adult Cancer Contribution to Variance (%)	Child Cancer (3.0x) Contribution to Variance (%)
Attenuation	-54	-53
Concentration	36	35
Duration	7	0.6
Age at move in	-	-7.4
Toxicity	2.5	2.8
Frequency	0.5	0.5

The sensitivity analyses for non-cancer risks to both adults and children show results that are very similar to those for cancer risks, discussed above. As shown in Table 5 below, when all the inputs are allowed to vary, the risks are dominated by only two input variables: the attenuation of vapors value (-55 to -59% of the variance in risks) and the concentration of contaminant in water (38% of the variance in risks). These inputs are followed by the much smaller effects of the inhalation Reference Concentration (RfC) toxicity factor (-2.1%), the exposure frequency (1.2%), and the exposure duration (0.1%). The results from another (one-at-a-time) sensitivity analysis also shows a very similar rank order and magnitude of effects of these same inputs (i.e., with attenuation and concentration having the most influence) for both adult and child non-cancer risks.

Table 5. Sensitivity of Non-Cancer Risks

Input variable	Adult Contribution to Variance (%)	Child – age adjusted Contribution to Variance (%)
Attenuation	-59	-55
Concentration	38	38
Age at move in	-	4.4
Toxicity	2.1	3.1
Frequency	1.2	0.1
Duration	0.1	0.0

In summary, the results of the several forms of sensitivity analyses all suggest that the risks are largely influenced by the attenuation value and concentration of contaminant in groundwater input values. Furthermore, as modeled here, the risks are not significantly modified other variables such as age adjustments for exposures in early age or exposures prior to birth.

An additional form of sensitivity analyses ('Spider Charts') also indicate that these two inputs (attenuation and concentration) are most influential in the lower and upper ends of their distribution ranges (for all four models, adult example shown in Figure 5). The other inputs have nearly linear, lower-level influences across their ranges (with the only exception being the 'age at move in' input variable in the child models since it limits the duration of exposure possible during childhood (i.e., $\leq$ 18 yrs of age)).

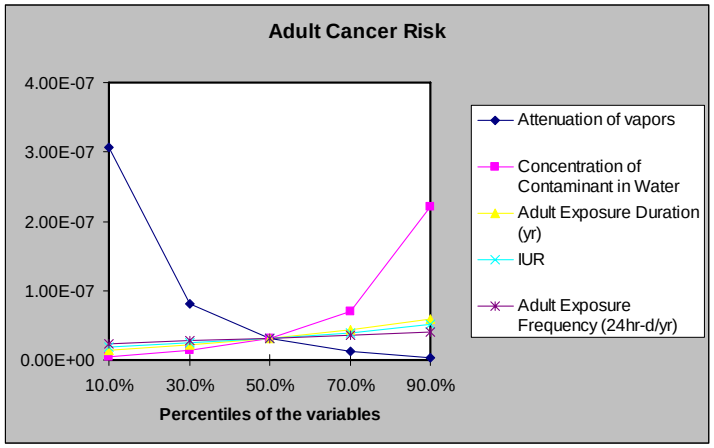

Figure 5. One-at-a-time sensitivity 'Spider Chart' (by percentiles) for Cancer - Adult

The risk estimates in this risk assessment included elements of both variability and uncertainty. That is to say the inputs to the models varied both due to recognized variability that occurs within a known range of values and also due to uncertainties (lack of knowledge) where, for example, both the range and the value of inputs can be unknown. Making a distinction between variability and uncertainty can be very important in part because uncertainty can, in theory, be reduced through research, whereas variability will remain as a natural feature of the problem. Furthermore, understanding the sources of uncertainty can help target research efforts towards reducing the most important uncertainties. Probabilistic methods allow analyses that can help to separate the impacts of input variability and uncertainty on risk predictions. The primary techniques are two-dimensional simulations that are comprised of a set of nested models that can help illustrate and differentiate between the influences of inputs that are primarily defined by uncertainty and those primarily defined by well-understood variability.

3.4 Two Dimensional Analyses

The two dimensional (2-D) methods used involve the random selection of a set of ten possible values for those input parameter(s) that are primarily defined by uncertainty. Each of these possible values (for the uncertain parameter(s)) is held fixed at the randomly selected value while a full model is run with all the other inputs; e.g., those primarily characterized by variability are allowed to vary across their expected distributions. Thus, for a 2-D simulation 10 full models (of 5900 iterations each) are run. One model is run for each of the ten randomly selected values of the uncertain parameter(s) that are held constant.

For this study the input values for attenuation, concentration, and toxicity (IUR or RfC) were considered to have the highest amount of uncertainty, and all the other input values (e.g., exposure duration, frequency, etc.) were allowed to vary across their expected (better understood, but variable) distributions. In a sense, this 2-D analysis is the opposite of the one-at-a-time sensitivity analyses discussed above because this 2-D approach fixes one (or more 'uncertain' inputs) and varies all others, whereas the one-at-a-time sensitivity approach discussed earlier fixed all but one parameter that was allowed to vary.

A number of 2-D simulations (each composed of 10 full model runs) were conducted with various combinations of inputs being considered to represent those with the most uncertainty. For each of the primary risk models (cancer and non-cancer, in adults and children), four versions of 2-D simulations were completed where the inputs that were considered to primarily represent uncertainty were 1) attenuation, 2) concentration, 3) attenuation and concentration, and 4) attenuation, concentration, and toxicity. This approach of running various combinations of fixed and varying inputs was used to provide insight into the effect of these inputs on risks. Thus, this approach could be considered a form of 'probabilistic sensitivity analysis' (Cullen and Frey, 1999). Two examples of the results from 2-D simulations for adult cancer are shown in Figure 6 below.

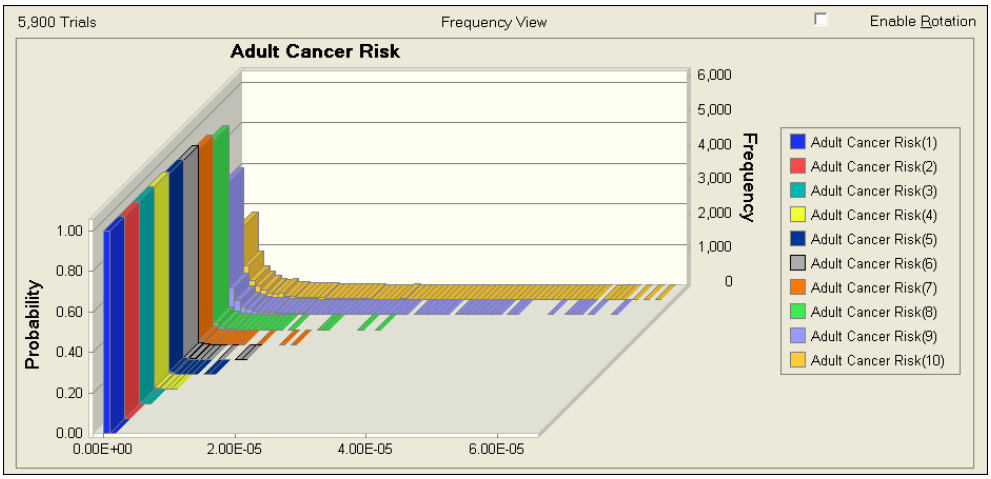

Figure 6a. 2-D Overlay-Frequency chart - Adult Cancer – Uncertainty = Attenuation

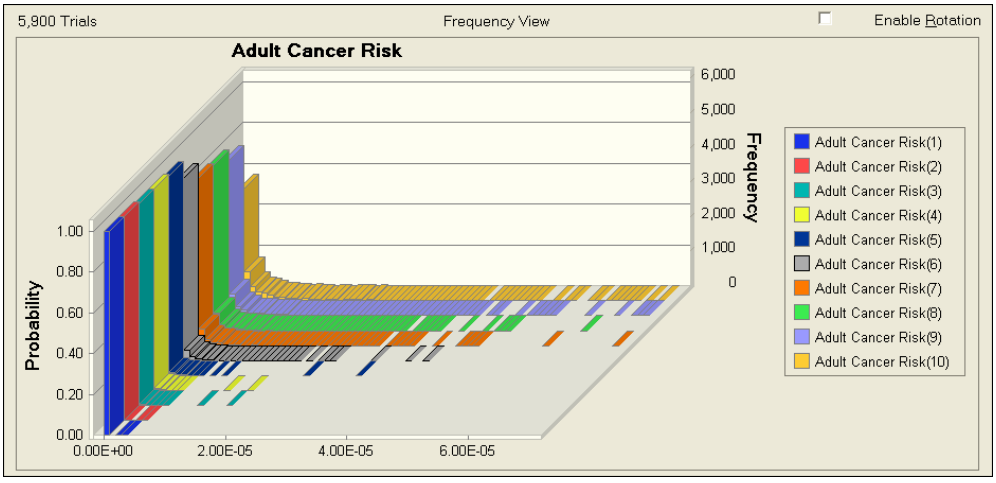

Figure 6b. 2-D Overlay-Frequency chart - Adult Cancer – Uncertainty = Concentration

In summary, the results of all the 2-D analyses, which involved 16 simulations (160 individual model runs), reconfirm the earlier observations that, across receptors (adults and children) and across outcomes (cancer and non-cancer), the risks 1) have central tendency values that are quite low; 2) have very few individual risks high enough to be within the range of typical concerns (i.e., cancer risks > 1 x 10^{-6} or hazards indices > 1.0); 3) are primarily influenced by the attenuation value and the concentration of the contaminant in groundwater (i.e., the vapor source term), particularly at the extremes of their input ranges.

4. DISCUSSION

The results of this assessment suggest that significant risks due to vapor intrusion of TCE in northern New Jersey are limited to a few individuals. There are, however, numerous limitations to the data and assumptions bridging data gaps in the methods used. For example, the electronic data set used was estimated to only represent 2/3 of the groundwater data collected in the study area and it was assumed this fairly represents all contamination in the study area. The generic (non-site-specific) groundwater plume mapping methods estimated the median shallow groundwater concentration (with depth adjustments) under the 883 residential structures was relatively low, i.e., only 5.9 ug/L (using the available evidence and the methods described above). Furthermore, the resulting risks presented here are central tendency probabilistic risks and these may be more comparable to other risks, e.g., groundwater-ingestion risks, if those risks were also calculated using central-tendency probabilistic methods (which is not commonly done).

Also note however, that several adverse health outcomes have been statistically associated with relatively low concentrations of TCE in groundwater that was used for tap-water (e.g., Cohn et al., 1994, where the maximum concentration category was only > 5 ug/L) and in some other cases reviewed by Bove et al., (1995) and Bove, Shim, and Zeitz (2002). Additionally, some associations have been observed in cases where vapor intrusion could be expected to be a contributing or primary exposure pathway. For example, observations of statistically significant associations with plausible outcomes in children and adults, with relatively low TCE vapor intrusion exposures have been found (e.g., NYSDOH, 2006b), and it is possible vapor intrusion may have played some contributory role in the proximity-based observations by Gerschwind, et al. (1992) which involved multiple sites across the state of New York. To improve their health studies' statistical power, and perhaps due to their experiences and informal observations at vapor intrusion sites, the New York State Dept. of Health has recently recommended a formal study of health associations at multiple sites with similar vapor intrusion exposures (NYSDOH, 2007). While it is likely that these NY sites could have somewhat higher exposures than the results of this study they could still have relatively 'low' central tendency probabilistic risks (compared to typical regulatory point-estimate reference values) and yet these exposures appear potentially relevant to public health.

5. CONCLUSIONS

Consideration of the methods and results of this risk assessment, as well as the inputs and secondary (sensitivity and two-dimensional) analyses, suggest that, while there are numerous limitations to the data and methods used, some observations can be made:

Significant risks due to vapor intrusion of TCE in northern NJ appear to be limited to a few individuals.

The data used indicate the most influential uncertain variable was the attenuation of the vapors between the subsurface vapor source and the indoor air.

The apparent second-most influential uncertain variable was the concentration of TCE in the groundwater actually beneath the home being assessed.

All other input variables had significantly less influence on the risks predicted.

There may be some concern that the monitor well data used in this study (reported only 2/3 of all data collected) may not be fully representative of the true groundwater vapor source-term concentrations in all residential areas of northern NJ. There may also be some concern that this study's generic groundwater modeling (IDW) methods may have underestimated the predicted groundwater vapor-source concentrations actually beneath some occupied residences. Nevertheless, the predicted population risks are so low that it appears unlikely that "the quality of the data or assessment methods is sufficiently poor that the true exposures might" miss significant population risks (Wilson and Crouch, 2001) in this portion of New Jersey.

However, New Jersey may not be representative of many states (e.g., its groundwater standard and screening criteria for vapor intrusion of TCE is the lowest in the nation (1 ug/L; NJDEP, 2007; Eklund et al., 2006), and other states have residential vapor intrusion screening criteria for groundwater up to 15,000 times higher (MIDEQ, 2006). That is to say, other states may have significantly more poorly assessed, or unknown, potential for vapor intrusion exposures and health risks.

6. REFERENCES

2007. TCE Reduction Act of 2007. U.S. Senate Bill S.1911, Proposed by Senators Clinton, Dole, Boxer, Lautenberg, and Kerry. Aug. 1. Available at: http://www.capitolpub.com/images/newsletters/clintontces1911.pdf

ATSDR (Agency for Toxic Substances and Disease Registry). 1997. Toxicological Profile for Trichloroethylene (update Sept. 1997). U.S. Department of Health and Human Services, Public Health Service, Atlanta, GA. see: http://www.atsdr.cdc.gov/toxprofiles/tp19.html

ATSDR (Agency for Toxic Substances and Disease Registry). 1999. National Exposure Registry, Trichloroethylene (TCE) Subregistry. Available at www.**atsdr**.cdc.gov/NER/index.html

ATSDR (Agency for Toxic Substances and Disease Registry). 2003. Progress Report: Survey of Specific Childhood Cancers and Birth Defects Among Children Whose Mothers Were Pregnant While Living at U.S. Marine Corps Base Camp Lejeune, North Carolina, 1968-1985. Division of Health Studies, Atlanta, Georgia 30333. July 2003 [online]. Available: http://www.atsdr.cdc.gov/sites/lejeune/survey_full.html

ATSDR (Agency for Toxic Substances and Disease Registry). 2007. Analyses of Groundwater Flow, Contaminant Fate and Transport, and Distribution of Drinking Water at Tarawa Terrace and Vicinity, U.S. Marine Corps Base Camp Lejeune, North Carolina: Historical Reconstruction and Present-Day Conditions - Chapter A: Summary of Findings. ATSDR, Atlanta, Georgia. July 2007.

Arito, H., Takahashi, M., and Ishikawa, T. 1994. Effects of subchronic inhalation exposure to low-level trichloroetheylene on heart rate and wakefulness-sleep in freely moving rats. Jpn J Ind Health. 36:1-8.

Barton, H.A., and Clewell, H.J. 2000. Evaluating noncancer effects of trichloroethene: Dosimetry, mode of action and risk assessment. Environ Health Perspect. 108(Suppl 2):323-334.

Barton, H.A., Cogliano, V.J., Flowers, L., Valcovic, L., Setzer, R.W., Woodruff, T.J. 2005. Assessing Susceptibility from Early-Life Exposure to Carcinogens. Environ Health Perspect. 113:1125-1133 (2005). [online]. doi:10.1289/ehp.7667 (available at http://dx.doi.org/)

Bove, F., Shim, Y., Zeitz, P. 2002. Drinking water contaminants and adverse pregnancy outcomes: A review. Environ Health Perspect. 110(Suppl. 1):61-74.

Bove, F.J., Fulcomer, M.C., Klotz, J., Esmart, J., Dufficy, E.M., Savrin, J.E. 1995. Public Drinking Water Contamination and Birth Outcomes; Am. J. Epidemiol. 141(9):850-862.

Briving, C., Jacobson, I., Hamberger, A., Kjellstrand, P., Haglid, H.G., and Rosenren, L.E. 1986. Chonic effects of perchloroethylene and trichloroethylene on the gerbil brain amino acids and glutathione. Neurotoxicology 7(1):101-108.

Bushnell, P.J., Shafer, T.J., Bale, A.S., Boyes, W.K., Simmons, J.E., Eklund, C., and Jackson, T.L. 2005. Developing an exposure-dose-response model for the acute neurotoxicity of organic solvents: an overview and progress on in vitro models and dosimetry. Environ Tox Pharma 19 (2005) 607-614.

Chiu, W. A., Caldwell, J.C., Keshava, N., and Scott, C.S. 2006. Key Scientific Issues in the Health Risk Assessment of Trichloroethylene. Environ Health Perspect. 114:1445-1449 (2006). EHP On-line, doi:10.1289/ehp.8690 (Trichloroethylene Monograph).

Cohn, P., Klotz, J., Berkowitz, M., and Fagliano, J. 1994. Drinking water contamination and the incidence of leukemia and Non-Hodgkin's lymphoma. Environ Health Perspect. 102(6-7):556-561.

Costas, K., Knorr, R.S., and Condon, S.K., 2002. A case-control study of childhood leukemia in Woburn, Massachusetts: The relationship between leukemia incidence and exposure to public drinking water; Sci Total Environ. 300(1-3): 23-35.

Cullen, A.C., and Frey, H.C., 1999. Probabilistic Techniques in Exposure Assessment (A Handbook for Dealing with Variability and Uncertainty in Models and Inputs), Society for Risk Analysis, Plenum Press, New York 335 pp.

Dawson, H., 2007. Personal communication, USEPA Region VIII Hydrogeologist, October 3.

Dawson, H., Hers, I., and Truesdale, R., 2007. Analysis of Empirical Attenuation Factors in EPA's Expanded Vapor Intrusion Database. Proceedings from Vapor Intrusion: Learning from the Challenges. Sept. 26-28, 2007 in Providence RI, p. 5-17. (AWMA) Air and Waste Management Association, Pittsburgh, PA.

Decision Engineering, 2006. Crystal Ball 2000 v. 7.2.1. Software, Denver, Colorado.

Defina, J. 2004. Personal communication, NJDEP GIS Coordinator, November 9.

ESRI (Environmental Systems Research Institute). 2006. ArcInfo version 9.1 Geographic Information System (GIS) mapping software, Redding, CA.

Eklund, B., D. Folkes, J. Kabel, and R. Farnum. An Overview of State Approaches to Vapor Intrusion. Environmental Manager. Air & Waste Management Association. February 2007.

Ginsberg, G.L., Foos, B.P., and Firestone, M.P. 2005. Review and analysis of inhalation dosimetry methods for application to children's risk assessment. J. Toxicol. Environ. Health A. 2005 Apr 23;68(8):573-615.

Gerschwind, S., Stolwijk, J., Bracken, M., Fitzgerald, E., Stark, A., Olsen, C., and Melius, J., Risk of Congenital Malformations Associated with Proximity to Hazardous Waste Sites. Am J Epidemiol. 1992: 135:1197-1207.

Haglid K.G., Briving, C., Hansson, H.A., Rosengren, L., Kjellstrand, P., Stavron, D., Swedin, U., Wronski, A. 1981. Trichloroethylene: Long-lasting changes in the brain after rehabilitation. Neurotoxicology. 2(4):659-673.

Hansen, J., Raaschou-Nielsen, O., Christensen, J.M., Johansen, I., McLaughlin, J.K., Lipworth, L., Blot, W.J., and Olsen, J.H. 2001. Cancer incidence among Danish workers exposed to trichloroethylene. J. Occup. Environ. Med. 43(2):133-139.

Henschler, D., Elsasser, H., Romen, H., and Eder, E. 1980. Carcinogenicity study of trichloroethylene by long-term inhalation in three animal species. Arch Toxicol. 43:237–248.

Infante-Rivard, C., Siemiatycki, J., Lakhani, R., and Nadon, L. 2005. Maternal exposure to occupational solvents and childhood leukemia. Environ. Health Perspect. 113(6):787-792.

ITRC (Interstate Technology and Regulatory Council). 2007. Vapor Intrusion Pathway: A Practical Guide. Technical and Regulatory Guidance, available at: http://www.itrcweb.org/gd_VI.asp

Johnson, B.L., 2002. Hazardous Waste: Human Health Effects. In: Advances in Modern Environmental Toxicology, Vol. 26, Impacts of Hazardous Chemicals on Public Health, Policy, and Service. (De Rosa, C.T., Holler, J.S., and Mehlman, M.A. Eds.). Agency for Toxic Substances and Disease Registry**.** Atlanta, GA.

Johnson, P.C., and Ettinger, R.A., 1991. Heuristic Model for Predicting the Intrusion Rate of Contaminant Vapors into Buildings. Environ Sci & Tech. 25(8):1445-1452.

Kelsh, M.A., Weingart, M., Mandel, J. Mink, P., Alexander, P. Basu, R. Kalmes, R., and Goodman, M. 2005. A Meta-Analysis of Epidemiology Studies of Occupational TCE Exposure and Selected Cancers. Presentation by M.A. Kelsh at the Third [USEPA] Meeting on Assessing Human Health Risks of Trichloroethylene, June 9, 2005, Irvine, CA.

Kyrklund, T., Goracci, G., Haglid, K.G., Rosengren, L., Porcellait, G., and Kjellstrand, P. 1984. Chronic effects of trichloroethylene upon S-100 protein content and lipid composition in the gerbil cerebellum. Scand J Work Environ Health. 10(2):89-93.

MADEP (Mass. Dept. Environ. Protection). 2000. What we've learned. A handout from Nancy Fitzpatrick to the USEPA's RCRA CA EI Vapor Summit Jan. 2000, Wash. DC.

Mandel, J.H., Kelsh, M.A., Mink, P.J., Alexander, D.D., Kalmes, R.M., Weingart, M., Yost, L., Goodman, M. 2006. Occupational trichloroethylene exposure and non-Hodgkin's lymphoma: a meta-analysis and review. Occup Environ Med. Sept. 2006; 63(9):597-607. Epub 2006 Apr 27.

MIDEQ (Michigan Dept. of Environmental Quality). 2006. Table 1. Groundwater: Residential and Industrial-Commercial Part 201 Generic Cleanup Criteria and Screening Levels; Part 213 Tier 1 Risk-Based Screening Levels (RBSLs). (Jan. 23, 2006). Accessed Oct. 4, 2007.
http://www.deq.state.mi.us/documents/deq-rrd-OpMemo_1-Attachment1Table1GW.pdf

NJDEP (New Jersey Dept. of Environmental Protection). 1999a. Site Remediation Program Electronic Data Interchange Manual. Site Remediation Program, Trenton, NJ (April, 1999). see www.state.nj.us/dep/srp/hazsite/about/site_map.htm

NJDEP (New Jersey Dept. of Environmental Protection). 1999b. Electronic Data Submittal Application (EDSA) User's Manual. Site Remediation Program, Trenton, NJ. July, 1999.

NJDEP (New Jersey Dept. of Environmental Protection). 2007, NJDEP Vapor Intrusion Guidance (updated March 2007) available at:

http://www.state.nj.us/dep/srp/guidance/vaporintrusion/vig.htm

http://www.state.nj.us/dep/srp/guidance/vaporintrusion/vig_tables.pdf

NJDEP (New Jersey Dept. of Environmental Protection). 2007a. 1995/97 Landuse/Landcover files (available at: http://www.state.nj.us/dep/gis/digidownload/zips/lulc95/w01lu95.zip

NJDEP (New Jersey Dept. of Environmental Protection). 2007b. Digital Elevation Models (DEM) for State of New Jersey (available at: http://www.state.nj.us/dep/gis/digidownload/zips/statewide/nj100mlat.zip

NJDHSS, (New Jersey Dept. of Health and Senior Services). 2002. New Jersey Health Statistics 2002. New Jersey Department of Health and Senior Services, Trenton, NJ. Available at: http://www.state.nj.us/health/chs/stats02/natality.htm (accessed March 16, 2007)

NRC (National Research Council). 2006. Assessing the Human Health Risks of Trichloroethylene: Key Scientific Issues. Washington, DC., National Academy Press.

NYSDOH (New York State Dept. of Health). 2006a. Trichloroethene Air Criteria Document. New York State Department of Health, Center for Environmental Health, Bureau of Toxic Substances Assessment, Final Report, October 2006. http://www.health.state.ny.us/environmental/chemicals/trichloroethene/docs/cd_tce.pdf

NYSDOH (New York State Dept. of Health). 2006b. Health Consultation, Endicott Area Investigation, Health Statistics Review: Cancer and Birth Outcome Analysis, Endicott Area, Town of Union, Broome County, New York. May 26, 2006, available at: www.health.state.ny.us/nysdoh/environ/broome/hsr_health_consultation.htm

NYSDOH (New York State Dept. of Health). 2007. Public Comment Draft: Public Health Consultation: Endicott Area Investigation Health Statistics Review Follow-up. (March 26, 2007).

http://www.health.state.ny.us/environmental/investigations/broome/hsr_public_comment_draft.htm#8

OMB (Office of Management and Budget). 2002. Guidelines for Ensuring and Maximizing the Quality, Objectivity, Utility, and Integrity of Information Disseminated by Federal Agencies (2002) 67 Fed. Reg. 8452 (Feb. 22, 2002). Office of Management and Budget, Executive Office of the President. Washington, DC. Available at:

http://www.whitehouse.gov/omb/fedreg/reproducible2.pdf

OMB (Office of Management and Budget). 2007. Memorandum for the Heads of Executive Departments and Agencies (M-07-24). Re: Updated Principles for Risk Analysis. (Sept. 19, 2007). Office of Management and Budget, Executive Office of the President. Washington, DC.

Available at:http://www.whitehouse.gov/omb/memoranda/fy2007/m07-24.pdf

Preston, J.R. 2007. Epigenetic processes and cancer risk assessment. Mutat Res. 2007 Mar 1;616(1-2):7-10. Epub 2006 Dec 4.

Raaschou-Nielsen, O., Hansen, J., Thomsen, B.L., Johansen, I., Lipworth, L., McLaughlin, J.K., and Olsen, J.H. 2002. Exposure of Danish workers to trichloroethylene, 1947-1989. Appl. Occup. Environ. Hyg. 17(10):693-703.

Raaschou-Nielsen, O., Hansen, J., McLaughlin, J.K., Kolstad, H., Christensen, J.M., Tarone, R.E., and Olsen, J.H. 2003. Cancer risk among workers at Danish companies using trichloroethylene: A cohort study. Am. J. Epidemiol. 158(12):1182-1192.

Rasmussen, K., Arlien-Soborg, and Sabroe, S. 1993. Clinical neurological findings among metal degreasers exposed to chlorinated solvents. Acta Neurol Scand. 87(3):200-204.

Rodenbeck, S.E., Sanderson, L.M., Rene, A. 2000. Maternal exposure to trichloroethyelene in drinking water and birth-weight outcomes. Arch Environ Health. 55(3):188-194.

Schiotz, E.H., 1938. Trichloroethylene poisoning with particular reference to chemical cleaning. Nord Med Tidskr. 15:808-813.

Scott, C. S., and Chiu, W. (2006). Trichloroethylene cancer epidemiology: a consideration of selected issues. Environ Health Perspect. 114:1471-1478 (2006). EHP On-line, doi:10.1289/ehp.8949 (Trichloroethylene Monograph).

Scott, C. S., and Cogliano, V.J. 2000. Introduction: trichloroethylene health risks – state of the science." Environ. Health Perspect. 108(Suppl 2):159-160.

US Census. 2004. Quickfacts. U.S. Dept. of Census. Washington, DC. Available at: http://quickfacts.census.gov/qfd/states/34/34039.html. Accessed March 16, 2007.

USEPA (U.S. Environmental Protection Agency). 1989. Risk Assessment Guidance for Superfund, Volume I: Human Health Evaluation Manual (Part A), Interim Final. Office of Emergency and Remedial Response, Washington, DC. EPA/540/1-89/002. Available at:

http://www.epa.gov/oswer/riskassessment/ragsa/index.htm

USEPA (U.S. Environmental Protection Agency). 1994. Methods of Derivation of Inhalation Reference Concentrations and Application of Inhalation Dosimetry. Office of Research and Development, Research Triangle Park, NC. EPA/600/8-90/066F.

USEPA (U.S. Environmental Protection Agency). 1997. Exposure Factors Handbook. National Center for Environmental Assessment, Washington, DC, EPA600-P-95-002Fa-c. http://cfpub.epa.gov/ncea/cfm/recordisplay.cfm?deid=12464

USEPA (U.S. Environmental Protection Agency). 2001a. Risk Assessment Guidance for Superfund (RAGS) Vol. 3, Process for Conducting Probabilistic Risk Assessments (Part A), EPA 540-R-02-002, OSWER 9285.7-45 PB2002 963302, December, 2001.

www.epa.gov/superfund/programs/risk/tooltrad.htm

USEPA (U.S. Environmental Protection Agency). 2001b. Sources, Emission and Exposure to Trichloroethylene (TCE) and Related Chemicals. Office of Research and Development, National Center for Environmental Assessment (NCEA). Washington DC.

USEPA (U.S. Environmental Protection Agency). 2001c. Trichloroethylene Health Risk Assessment: Synthesis and Characterization (External Review Draft). Office of Research and Development, National Center for Environmental Assessment (NCEA). Washington DC. Washington, D.C.

USEPA (U.S. Environmental Protection Agency). 2002a. OSWER Draft Guidance for Evaluating the Vapor Intrusion to Indoor Air Pathway from Groundwater and Soils. Subsurface Vapor Intrusion Guidance. OSWER. EPA530-D-02-004, Nov. 2002, Wash. DC.

USEPA (U.S. Environmental Protection Agency). 2002b. Child-Specific Exposure Factors Handbook. Office of Research and Development, National Center for Environmental Assessment (NCEA). Washington, DC. EPA 600-CP-00-002B.

http://cfpub.epa.gov/ncea/cfm/recordisplay.cfm?deid=55145

USEPA (U.S. Environmental Protection Agency). 2002c. Review of Draft Trichloroethylene Health Risk Assessment: Synthesis and Characterization: An EPA Science Advisory Board Report, A Review by the TCE Review Panel of the Environmental Health Committee of the US EPA Science Advisory Board (SAB), EPA-SAB-EHC-03-002, Dec. 2002, www.epa.gov/sab.

USEPA (U.S. Environmental Protection Agency). 2004a. Symposium on New Scientific Research Related to the Health Effects of Trichloroethylene, National Center for Environmental Assessment, U.S. Environmental Protection Agency. Washington DC.

Available: http://cfpub.epa.gov/ncea/cfm/recordisplay.cfm?deid=795934

USEPA (U.S. Environmental Protection Agency). 2004b. User's Guide for Evaluating Subsurface Vapor Intrusion into Buildings. Revised. Office of Emergency and Remedial Response.

(www.epa.gov/oswer/riskassessment/airmodel/pdf/2004_0222_3phase_users_guide.pdf)

USEPA (U.S. Environmental Protection Agency). 2005a. Guidelines for Carcinogen Risk Assessment, Risk Assessment Forum, Washington, D.C. EPA/630/P-03/001F. http://cfpub.epa.gov/ncea/cfm/recordisplay.cfm?deid=116283

USEPA (U.S. Environmental Protection Agency). 2005b. Supplemental Guidance for Assessing Cancer Susceptibility from Early-Life Exposure to Carcinogens. Risk Assessment Forum, Washington, DC. EPA/630/R-30/003F. http://cfpub.epa.gov/ncea/cfm/recordisplay.cfm?deid=116283

USEPA (U.S. Environmental Protection Agency). 2005c. Trichloroethylene (TCE) Issue Papers. EPA/600/R-05/022, 2005.

http://cfpub.epa.gov/ncea/cfm/recordisplay.cfm?deid=117502

USEPA (U.S. Environmental Protection Agency). 2006. A Framework for Assessing Health Risks of Environmental Exposures to Children. External Review Draft. EPA/600R-05/093A. Washington DC: National Center for Environmental Assessment. http://cfpub.epa.gov/ncea/cfm/recordisplay.cfm?deid=158363

USEPA (U.S. Environmental Protection Agency). 2007. Framework for Determining a Mutagenic Mode of Action for Carcinogenicity. External Peer Review Draft, September, 2007. EPA 120/R-07/002-A. Risk Assessment Forum, Washington, DC.

http://www.epa.gov/osa/mmoaframework/pdfs/MMOA-ERD-FINAL-83007.pdf

USGS (U.S. Geological Survey) 1983. Basic Ground-Water Hydrology, Water Supply Paper 2220, US Gov. Printing Off., Washington DC.

Wartenberg, D., Reyner, D., and Scott, C.S. 2000. Trichloroethylene and cancer: Epidemiologic evidence. Environ. Health Perspect. 108(Suppl 2):161-176.

Waters, E.M., Gerstner, H.B., and Huff, J.E., 1977. Trichloroethylene. I. An Overview. Jour Tox Environ Health. 2:671-707.

Wertz, W. 2006. Near-Building and Subslab Sampling at the Endicott (NY) Site, Implications for Site Screening Approaches. Slide 16 of 22 in a presentation at the EPA's - A Summary Workshop in the Context of EPA's VI Guidance Revisions held at the AEHS West Coast Conference, 16 March 2006, San Diego, CA. http://iavi.rti.org/attachments/WorkshopsAndConferences/PART_I_-_1940_-_Wertz.pdf

Wertz, W. 2007. Unpublished data from vapor intrusion exposures at a former typewriter site in Endicott, NY.

White, R.F., Feldman, R.G., Eviator, I.I., Jabre, J.F., and Niles, C.A. 1997. Hazardous waste and neurobehavioral effects: A developmental perspective. Environ Res. 73(1-2):113-124.

Wilson, R., and Crouch, E.A.C. 2001. Risk Benefit Analysis, Center for Risk Analysis, Harvard Univ. Press, Cambridge, MA.

Zogorski, J. S., Carter, J.M., Ivanhnenko, Tamara, Lapham, W.W., Moran, M.J., Rowe, B.L., Squillace, P.J., and Toccalino, P.L. (2006). Volatile organic compounds in the Nation's ground water and drinking-water supply wells. The quality our Nation's waters series -Washington DC, U.S. Geological Survey**:** 101.

APPENDIX 1: ADULT – NHL MODEL STRUCTURE AND FORMULA

1a) Model Structure - Row# H

3	Conc(depth-adj) TCE in GWater	19.50	micrograms per liter (ug/liter)
4	Soil-gas Conc.@ Source	4212.00	micrograms per cubic meter (ug/m^3)
5	1/Attenuation Factor (GW-IAQ)	2280.82	unit-less
6	Indoor Air Conc. of TCE	1.85	micrograms per cubic meter (ug/m^3)
7	Exposure Frequency (adults)	240	days (full 24-hr) per year (24hr-day/yr)
8	Exposure Duration (adults)	9	duration of residence over plume (yrs)
9	Total Exposure	2160	days (full 24-hr) (24hr-day)
10	Background environ. exposures	0	Sharing metabolic pathways & mode of action
11	Background occupat. exposures	0	
12	Averaging Time (days)	25550	days in 70 yr lifetime (d)
13	Lifetime Average Conc.	0.156120746	micrograms per cubic meter (ug/m^3)
14	Inhalation Unit Risk - NHL	1.3E-06	Inhalation Unit (cancer) Risk per ug/m^3
Adult Cancer Risk		2.03E-07	unitless

1b) Model Formula - Row# H

3	Conc(depth-adj) TCE in GWater	19.5
4	Soil-gas Conc.@ Source	=Concentration*0.216*1000
5	1/Attenuation Factor (GW-IAQ)	2280.81779072092
6	Indoor Air Conc. of TCE	=H4/H5
7	Exposure Frequency (adults)	240
8	Exposure Duration (adults)	9
9	Total Exposure	=H8*H7
10	Background environ. exposures	0
11	Background occupat. exposures	0
12	Averaging Time (days)	25550
13	Lifetime Average Conc.	=(H6*H7*H8)/H12
14	Inhalation Unit Risk - NHL	0.0000013
Adult Cancer Risk		=H13*H14

APPENDIX 2: ADULT – CNS MODEL STRUCTURE AND FORMULA

2a) Model Structure - Row#	H	
3 Conc(depth-adj) TCE in GWater	19.50	micrograms per liter (ug/liter)
4 Soil-gas Conc.@ Source	4212.00	micrograms per cubic meter (ug/m^3)
5 1/Attenuation Factor (GW-IAQ)	2280.82	unitless
6 Indoor Air Conc. of TCE	1.85	micrograms per cubic meter (ug/m3)
7 Exposure Frequency (adults)	240	days (full 24-hr) per year (24hr-day/yr)
8 Exposure Duration (adults)	9	duration of residence over plume (yrs)
9 Total Exposure	2160	24 hr-days
10 Background environ. exposures	0	Sharing metabolic pathways & mode of action
11 Background occupat. exposures	0	
12 Averaging Time (days)	3285	Total duration of exposure in days (d)
13 Average Daily Exposure Conc.	0.156120746	micrograms per cubic meter (ug/m3)
14 Reference Conc. - CNS	7.4E+01	Inhalation RfC (non-cancer) Risk in ug/m^3
Adult Non-Cancer Risk (HQ)	2.11E-03	Unitless

2b) Model Formula - Row#	H
3 Conc(depth-adj) TCE in GWater	19.5
4 Soil-gas Conc.@ Source	=Concentration*0.216*1000
5 1/Attenuation Factor (GW-IAQ)	2280.81779072092
6 Indoor Air Conc. of TCE	=H4/H5
7 Exposure Frequency (adults)	240
8 Exposure Duration (adults)	9
9 Total Exposure	=H8*H7
10 Background environmental Exposures	0
11 Background occupational Exposures	0
12 Averaging Time (days)	=H8*365
13 Average Daily Exposure Conc.	=H6*(H9/H12)
14 Reference Conc. – CNS	74
Adult Non-Cancer Risk (HQ)	=H13/H14

APPENDIX 3: CHILD – CNS MODEL STRUCTURE AND FORMULA (W/ & W/O AGE-ADJUSTMENTS)

3a) Model Structure - Row#	H	
3 Conc(depth-adj) TCE in GWater	21.94	micrograms per liter (ug/liter)
4 Soil-gas Conc.@ Source	4738.67	micrograms per cubic meter (ug/m^3)
5 1/Attenuation Factor (GW-IAQ)	2280.82	unitless
6 Indoor Air Conc. of TCE	2.08	micrograms per cubic meter (ug/m^3)
7 Family Residence Duration	9	years (yrs)
8 Theoretical Child age at move in	0	constant distribution in years of age (-10 to 18)
9 Actual Child Age at move in	0	years
10 Child age at move out	9	years (max. age 18 at move out)
11 Tot. child residence duration	9	years
12 Child residence at 0-2 yr ages	2	years
13 Child residence at 2-18 yr ages	7	years
14 Exposure Frequency (0-2 yrs)	300	days (full 24-hr) per year (24hr-day/yr)
15 Exposure Frequency (2-20 yrs)	268	days (full 24-hr) per year (24hr-day/yr)
16 Total Childhood Exposure	2476	24 hr-days
17 Age >2 Period Adjustment Factor	1.25	Assumed 25% adj for higher response due to exposure in critical period
18 Age 0 to 2 Period Adj Factor	1.5	Assumed 50% adj for higher response due to exposure in critical period
19 Age -3/4 to 0 Period Adj Factor	1.75	Assumed 75% adj for higher response due to exposure in critical period
20 Breast feeding	1	Yes (1) - No (0) (unitless)
21 Age <-1 Period Adj. Factor	1.5	Assumed 50% (0-2 yrs) adj for bio-transfer from mother, if breast fed
22 Tot. Adjust. move in Age >2	1.25	
23 Tot. Adjust. move in Age 0 to 2	1.875	
24 Tot. Adjust. move in Age -3/4 to 0	3.28125	
25 Tot. Adjust. move in Age < -1	4.78125	
26 Individual move in Age Adj Factor	3.28125	Affects full exposure duration - to account for observed effects for longer durations
27 Tot. Adjusted Childhood Exposure	8124.375	24 hr-days
28 Background Exposures	0	Sharing metabolic pathways and mode of action

29 Maternal Exposure Adj Factor	0	
30 Paternal Exposure Adj Factor	0	
31 Averaging Time (days)	3285	total # days with possible exposure in childhood (d)
32 Childhood Avg. Conc. (Un-Adj.)	1.565962258	micrograms per cubic meter (ug/m^3)
33 Childhood Avg. Conc. (Age-Adj.)	5.13831366	micrograms per cubic meter (ug/m^3)
34 Inhalation RfC Non-Cancer Risk	7.4E+01	Non-Cancer reference concentration in ug/m^3
Childhood Unadj. Non-Cancer Risk	2.12E-02	Unitless
Childhood Age-adj. Non-Cancer Risk	6.94E-02	Unitless

3b) Model Formula - Row#	H
3 Conc(depth-adj) TCE in GWater	21.9382946446673
4 Soil-gas Conc.@ Source	=Concentration*0.216*1000
5 1/Attenuation Factor (GW-IAQ)	2280.81779072092
6 Indoor Air Conc. of TCE	=H4/H5
7 Family Residence Duration	9
8 Theoretical Child age at move in	0
9 Actual Child Age at move in	=IF(H8<0,0,H8)
10 Child age at move out	=IF(H9+H7>18,18,H9+H7)
11 Tot. child residence duration	=H10-H9
12 Child residence at 0-2 yr ages	=IF(H9<2,2-H9,0)
13 Child residence at 2-18 yr ages	=IF(H9>2,H11,H11-(2-H9))
14 Exposure Frequency (0-2 yrs)	300
15 Exposure Frequency (2-20 yrs)	268
16 Total Childhood Exposure	=(H12*H14)+(H13*H15)
17 Age >2 Period Adjustment Factor	1.25
18 Age 0 to 2 Period Adj Factor	1.5
19 Age -3/4 to 0 Period Adj Factor	1.75
20 Breast feeding	1
21 Age <-1 Period Adj. Factor	=1.5
22 Tot. Adjust. move in Age >2	=H17
23 Tot. Adjust. move in Age 0 to 2	=H18*H17
24 Tot. Adjust. move in Age -3/4 to 0	=H19*H18*H17
25 Tot. Adjust. move in Age < -1	=(H21*H20)+H24
26 Individual move in Age Adj Factor	=IF(H8>2,H22,IF(H8<-1,(H25),IF(H8>0,H23,H24)))
27 Tot. Adjusted Childhood Exposure	=H16*H26
28 Background Exposures	0
29 Maternal Exposure Adj Factor	0
30 Paternal Exposure Adj Factor	0
31 Averaging Time (days)	=H11*365
32 Childhood Avg. Conc. (Un-Adj.)	=H6*(H16/H31)
33 Childhood Avg. Conc. (Age-Adj.)	=H6*(H27/H31)
34 Inhalation RfC Non-Cancer Risk	74

Childhood Unadj. Non-Cancer Risk	=H32/H34
Childhood Age-adj. Non-Cancer Risk	=H33/H34

APPENDIX 4: STRUCTURE AND FORMULA FOR CHILD NHL MODEL (W/ & W/O AGE-ADJUSTMENTS)

4a) Model Structure - Row#	H	
3 Conc. (depth-adj) TCE in GWater	21.94	micrograms per liter (ug/liter)
4 Soil-gas Conc.@ Source	4738.67	micrograms per cubic meter (ug/m^3)
5 1/Attenuation Factor (GW-IAQ)	2280.82	Unitless
6 Indoor Air Conc. of TCE	2.08	micrograms per cubic meter (ug/m^3)
7 Family Residence Duration	9	years (yrs)
8 Theoretical Child Age at move in	-1.5	proportional distribution in years of age (-10 to 18)
9 Actual Child Age at move in	0	(w/o negatives)
10 Child Age at move out	9	years (up to max. age 18 at move out)
11 Tot. Child Residence Duration	9	Years
12 Child Residence at 0-2 yr Ages	2	Years
13 Child Residence at 2-18 yr Ages	7	Years
14 Exposure Frequency (0-2 yrs)	300	days (full 24-hr) per year (24hr-day/yr)
15 Exposure Frequency (2-18 yrs)	268	days (full 24-hr) per year (24hr-day/yr)
16 Total Childhood Exposure	2476	days (full 24-hr) (24hr-days)
17 0 to 2 Age Adj Factor (1.0x)	1	Assumes no higher response due to age
18 0 to 2 Age Adj Factor (1+x)	1	Adds variability for possible higher response for age
19 0 to 2 Age Adj Factor (3.0x)	3	Assumes 3.0x higher response due to age
20 Tot. Post-Natal Exposure (1.0x)	2476	days (full 24-hr) (24hr-days)
21 Tot. Adj. post-natal Exposure (1+x)	2476	days (full 24-hr) (24hr-days)
22 Tot. Adj. post-natal Exposure (3.0x)	3676	days (full 24-hr) (24hr-days)
23 Considering Pre-Natal Exposures?	1	Yes (1) - No (0) (unitless)
24 Age -3/4 to 0 Pre-Natal Adj Factor	1	Adds & adjusts for higher response due to age
25 Breast Feeding?	1	Yes (1) - No (0) (unitless)
26 Age < -3/4 Pre-natal Adj Factor	1	Adds & adjusts bio-transfer from mother, if breast fed
27 Total Possible Pre-natal Exposures	300	days (full 24-hr) (24hr-day/yr)
28 Total Childhood Exposure (1.0x)	2476	24 hr-days
29 Tot. Adj. Childhood Exposure (1+x)	2476	24 hr-days
30 Tot. Adj. Childhood Exposure	3676	24 hr-days

(3.0x)		
31 Tot. Adj. Childhood Exposure (3.0x+)	3976	24 hr-days - includes pre-natal exposures
32 Background Exposures	0	If sharing metabolic pathways or mode of action
33 Maternal Exposure Adj Factor	0	
34 Paternal Exposure Adj Factor	0	
35 Averaging Time (days)	6570	total # days in 18 yr childhood (d)
36 Childhood Average Conc. (1.0x)	0.782981129	micrograms per cubic meter (ug/m^3)
37 Childhood Average Conc. (1+x)	0.782981129	micrograms per cubic meter (ug/m^3)
38 Childhood Average Conc. (3.0x)	1.16245502	micrograms per cubic meter (ug/m^3)
39 Childhood Average Conc. (3.0x+)	1.257323493	ug/m3, "+" = includes pre-natal exposures
40 Inhalation Unit Risk (IUR)	1.3E-06	Cancer risk per ug/m^3
Child (1.0x) Cancer Risk	1.02E-06	Risk – Unitless
Child (1+x) Cancer Risk	1.02E-06	Risk – Unitless
Child (3.0x) Cancer Risk	1.51E-06	Risk – Unitless
Child (3.0x+) Cancer Risk	1.63E-06	Risk - Unitless ("+" includes pre-natal exposures)

4b) Model Formula - Row#	H
3 Conc. (depth-adj) TCE in GWater	21.9382946446673
4 Soil-gas Conc.@ Source	=Concentration*0.216*1000
5 1/Attenuation Factor (GW-IAQ)	2280.81779072092
6 Indoor Air Conc. of TCE	=H4/H5
7 Family Residence Duration	9
8 Theoretical Child Age at move in	-1.5
9 Actual Child Age at move in	=IF(H8<0,0,H8)
10 Child Age at move out	=IF(H9+H7>18,18,H9+H7)
11 Tot. Child Residence Duration	=H10-H9
12 Child Residence at 0-2 yr Ages	=IF(H9<2,2-H9,0)
13 Child Residence at 2-18 yr Ages	=IF(H9>2,H11,H11-(2-H9))
14 Exposure Frequency (0-2 yrs)	300
15 Exposure Frequency (2-18 yrs)	268
16 Total Childhood Exposure	=(H12*H14)+(H13*H15)
17 0 to 2 Age Adj Factor (1.0x)	1
18 0 to 2 Age Adj Factor (1+x)	1
19 0 to 2 Age Adj Factor (3.0x)	3
20 Tot. Post-Natal Exposure (1.0x)	=(H12*H14*H17)+(H13*H15)
21 Tot. Adj. post-natal Exposure (1+x)	=(H12*H14*H18)+(H13*H15)
22 Tot. Adj. post-natal Exposure (3.0x)	=(H12*H14*H19)+(H13*H15)
23 Considering Pre-Natal Exposures?	1
24 Age -3/4 to 0 Pre-Natal Adj Factor	1
25 Breast Feeding?	1
26 Age < -3/4 Pre-natal Adj Factor	1
27 Total Possible Pre-natal Exposures	=IF(H8<-

	1,(0.75*H14*H24)+(0.25*H14*H26*H25),0)
28 Total Childhood Exposure (1.0x)	=(H12*H14*H17)+(H13*H15)
29 Tot. Adj. Childhood Exposure (1+x)	=(H12*H14*H18)+(H13*H15)
30 Tot. Adj. Childhood Exposure (3.0x)	=(H12*H14*H19)+(H13*H15)
31 Tot. Adj. Childhood Exposure (3.0x+)	=(H12*H14*H19)+(H13*H15)+(H27*H23)
32 Background Exposures	0
33 Maternal Exposure Adj Factor	0
34 Paternal Exposure Adj Factor	0
35 Averaging Time (days)	=18*365
36 Childhood Average Conc. (1.0x)	=H6*(H28/H35)
37 Childhood Average Conc. (1+x)	=H6*(H29/H35)
38 Childhood Average Conc. (3.0x)	=H6*(H30/H35)
39 Childhood Average Conc. (3.0x+)	=H6*(H31/H35)
40 Inhalation Unit Risk (IUR)	0.0000013
Child (1.0x) Cancer Risk	=H36*H40
Child (1+x) Cancer Risk	=H37*H40
Child (3.0x) Cancer Risk	=H38*H40
Child (3.0x+) Cancer Risk	=H39*H40

Chapter 30

CONSTRUCTION OF BIOLOGICALLY PRODUCTIVE ARTIFICIAL TIDAL FLATS WITH SOLIDIFIED SEA BOTTOM SEDIMENTS

Daizo Imai,[1,2,§] Satoshi Kaneco,[2] Ahmed H. A. Dabwan,[3] Hideyuki Katsumata,[2] Tohru Suzuki,[4] Tadaya Kato[1], and Kiyohisa Ohta[2]

[1] Mie Industry and Enterprise Support Center, Core Lab., Shimashi, Agocho, Ugata, 3098-9, Mie 517-0501, Japan [2] Department of Chemistry for Materials, Graduate School of Engineering, Mie University, Tsu, Mie 514-8507, Japan [3] Anotsu Research Institute for Environmental Restoration, Tsu, Ano, Ano 2630-1, Mie 514-2302, Japan [4] Environmental Preservation Center, Mie University, Tsu, Mie 514-8507, Japan

ABSTRACT

Ago Bay is a typical enclosed coastal sea that is connected to the Pacific Ocean via a very narrow and shallow entrance. The bay has been contaminated by the practice of culturing pearls, which has been occurring for the past 110 years. To address this problem, a new technology — the Hi-Biah-System (HBS) — was introduced in 2005. This product of this system, which dewaters muddy dredged sediments and reduces them to their raw materials, was used to construct a tidal flat. The purpose of this study was to evaluate the environmental conditions of the constructed tidal flat 2 years after it was built. We monitored the physico-chemical (oxidation–reduction potential, acid volatile sulphide, loss on ignition, water content, total organic carbon, total nitrogen, chlorophyll a, and particle size) and biological characteristics of five constructed tidal flats and a natural tidal flat. At the same tidal level, the physico-chemical parameters were similar among the five constructed tidal flats and the natural one. However, the biomass and macrobenthic population were higher in the constructed flat compared to the natural one. We suggest that the muddy dredged sediments generated by the HBS could provide useful materials for enhancing the productivity of the tidal coastal environment.

Keywords: Muddy dredged sediments; Constructed tidal flat; macrobenthos; Total organic carbon; Ago Bay; Japan

[§] Corresponding Author: Daizo Imai, Mie Industry and Enterprise Support Center, Core Lab., Shimashi, Agocho, Ugata, 3098-9, Mie 517-0501, Japan. Tel.: +81-599-44-1017; fax: +81-599-43-1172. *E-mail address:* d-imai@miesc.or.jp (D. Imai).

1. INTRODUCTION

Ago Bay is a typical enclosed coastal sea that is connected to the Pacific Ocean via a very narrow and shallow entrance. The bay, which is world-famous for its cultured pearls, lies in the Mie Prefecture, Japan. Over the past 110 years, the practice of culturing pearls in the bay has led to contamination. The expansion of human populations and anthropogenic impacts on sensitive natural systems, such as shallow areas, sea grass beds, and tidal flats, have further increased the input of contaminated materials into Ago Bay, leading to the accumulation of organically enriched sediments on the sea bottom.

In 2000, dredging of the contaminated sea floor sediments was initiated in an attempt to restore the sea environment to a healthier condition and to prevent deterioration resulting from the pearl industry. However, because dredged sea floor sediments tend to emit a horrible smell, finding areas for disposal has become a serious problem. Moreover, the large water content of sediments makes their transport and disposal extremely difficult. The technical feasibility of dredging and disposal, economic and environmental issues, and possibilities for reuse of sediments have not yet been resolved. Thus, the development of an alternative system to treat dredged sea bottom sediments is needed.

The Corps of Engineers manual on beneficial uses of dredged material (USACE, 1987) lists ten broad categories of use: habitat restoration; beach nourishment; aquaculture; recreation; agriculture; land reclamation and landfill cover; shoreline erosion control; industrial use; material transfer for dikes, levees, parking lots, highways; and multiple purposes. Graalum et al. (1999) suggested that dredged material might be useful for manufacturing topsoil, which would help reduce and recycle waste soil and provide an additional alternative for the long-term management of dredge disposal sites by reducing the amount of land needed for disposal facilities.

Using dredged sediment to construct tidal flats is another alternative use of dredge materials. Many tidal flats have been lost as a result of industrial, agricultural, and urban development of coastal areas. According to the Ministry of the Environment, Japan, the total area of natural tidal flats was about 826 km^2 in the 1940s; by the 1980s, approximately 40% of these natural flats were lost (Kikuchi, 1993; Kimura, 1994; Takahashi, 1994). To date, about 70% of the natural tidal flats that existed in Ago Bay in the 1940s have been lost (Kokubu et al., 2004). Tidal flats perform many environmental functions, such as providing a habitat for benthic organisms and playing a role in water purification and biological productivity. Currently, a number of projects are under way to protect and maintain natural tidal flats and wetland ecosystems in Ago Bay. Furthermore, efforts are being made to restore damaged tidal flats and to create constructed tidal flats to mitigate those that have been lost (Miyoshi et al., 1990; Cofer and Niering, 1992; Ogura and Imamura, 1995; Lee et al., 1998).

In the inner area of Ago Bay, large amount of organic matter have accumulated on the sea bed due to eutrophication, which has resulted in the occurrence of oxygen-deficient water from the bottom to the middle layer of water during the summer. This phenomenon has occurred in many enclosed coastal seas, such as Tokyo Bay, Osaka Bay, and Ise Bay (Suzuki and Matsukawa, 1987; Joh, 1989; Omori, et al., 1994), as well as in aquaculture areas (Hirata et al., 1994; Tsutsumi, 1995). The hypoxic (or anoxic) water can lead to environmental impacts, such

as blue tide (Aoshio) and red tide (Akashio) (Kakino et al., 1987; Takeda et al., 1991). Shallow-water regions such as tidal flats can mitigate these problems; sea grass and seaweed beds act as water purifiers and they play an important role in preventing habitat deterioration and in promoting fish nursery grounds in the inner-bay environment (Takeda et al., 2007).

The Environmental Restoration Project on Enclosed Coastal Seas in Ago Bay — also called the Ago Bay Project — began in 2004 to deal with efforts to restore the environmental conditions in the bay under the Collaboration of Regional Entities for the Advancement of Technological Excellence (CREATE) program of the Japan Science and Technology Agency (JST). The goal of the project was to improve the natural self-cleaning capability of the bay by forming constructed tidal flats, shallow-water areas, and sea algae and/or sea grass beds inside the bay.In 2005, up-to-date technology for a new in situ solidification system for treating muddy sea bottom sediments (the Hi-Biah-System (HBS)) was developed (Imai el al., 2007; Dabwan et al., 2007). The product of the process — solidified sediments — contain a great deal of mud. This mud was used to construct tidal flats in Ago Bay. To our knowledge, few experimental and monitoring data exist concerning these muddy, enriched, constructed tidal flats. In this study, we continuously monitored the ecosystem and environmental conditions in a constructed tidal flat and compared it to data from a natural tidal flat.

2. MATERIALS AND METHODS

2.1 Study site

The study site is located in Ise-Shima National Park, a semi-enclosed area around the Shima peninsula that is connected to the Pacific Ocean via a very narrow (the width is 1.5 km) and shallow (the water depth is 25 m) entrance called the Fukaya Channel (Fig. 1a). The interior part of the bay is complexly divided into many branch bays. The pearl culture industry uses the whole interior area of the bay and the cultivation rafts are spread out like the reticulation; thus, a large-scale dredger cannot enter these inner parts of the bay.

The natural tidal flat analyzed in our study lies in the inner part of a branch bay in the Tategami area in Ago bay. The amplitude of the flat varies from 0.5 to 3.0 m and its inclination is 1/10 (Fig. 1b). The constructed tidal flat was built in the same area.

2.2 Solidification method for disposal of sediments

Figure 2 shows the in situ solidification system. The detailed information has been described previously (Imai at al., 2007; Dabwan et al., 2007). The HBS consists of a main stock tank of sediments, a coagulant chamber, reactors 1 and 2, and a dewatering section. The treatment capacity was approximately 1~2 m^3/hour. The water content of the dredged sediments was 90% by weight. After treatment with HBS, the content was lowered to 60 wt%.

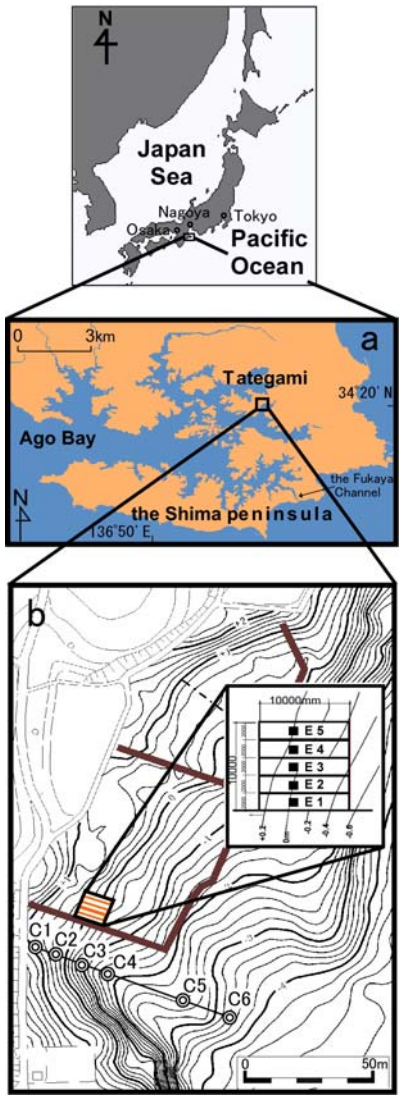

Figure 1. Location of Ago Bay in Mie prefecture, Japan. The stations indicate the artificial tidal flats (E1 to E5) and the natural tidal flats (C1 to C6).

2.3 Building the constructed tidal flat

The constructed tidal flat was settled from February to March 2005 in Tategami, Ago Bay as shown in Figure 1b. It was then divided into 5 sections (E1 to E5), each with an area of 10 m length × 2 m width × 0.5 m depth.

For section E1, the coagulant in the HBS consisted of 1.5 wt% of soil conditioner made of paper sludge ash exhausted from the pulp and paper industry. The chemical components of the soil conditioner were 44.2% CaO, 26.9% SiO_2, 12.7% Al_2O_3, and 12.2 % SO_3. After the water

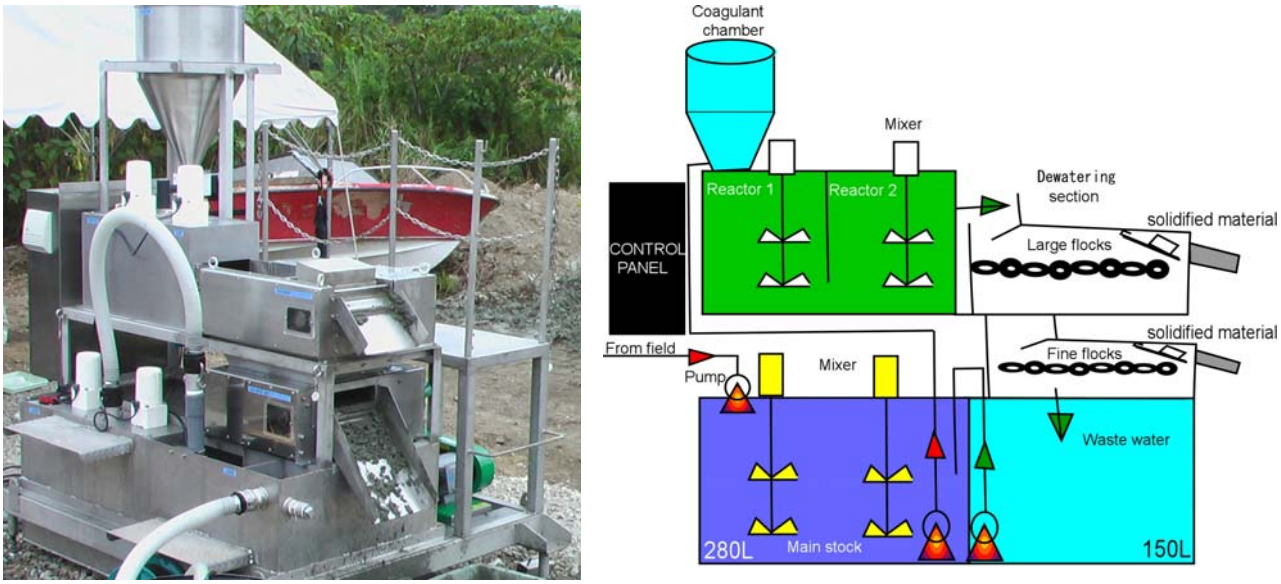

Figure 2. The solidification machine (Hi-Biah-System) developed for treatment of bottom sediments.

content of the sediments was reduced to 60 wt%, they were mixed with sand obtained from Ago Bay at a ratio of 3:7, and then an area of the constructed tidal flat was created from these materials.

For section E2, solidified materials with 60 wt% water content were produced in a similar way: After adding 20 wt% of the same soil conditioner, a pellet was formed with a pelletizer, as illustrated in Figure 3. The shape of the pellet was a column with a diameter of 8 mm and length of 20 mm. The E2 section of the constructed tidal flat was then produced from the pellets mixed with sand (weight ratio 3:7).

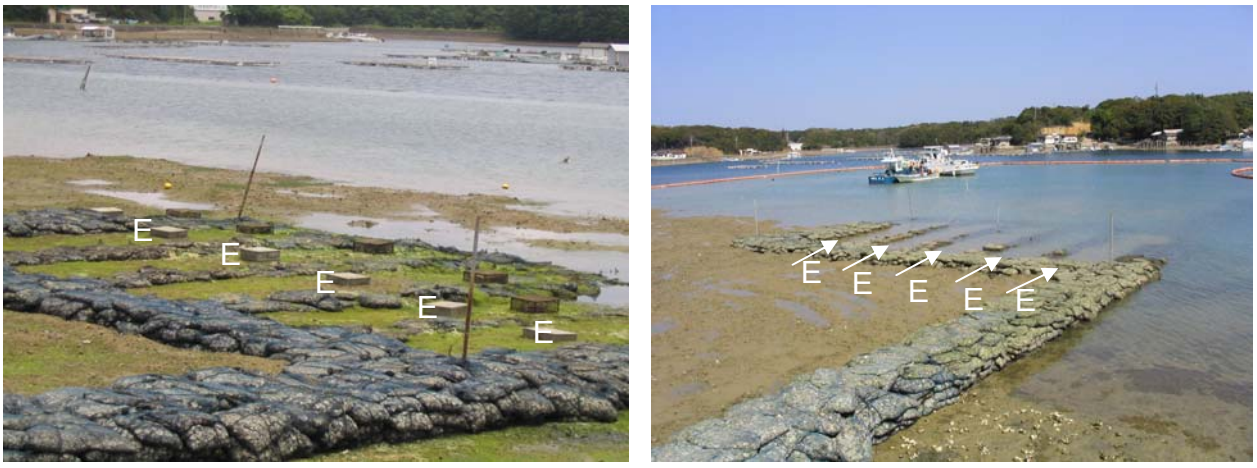

Figure 3. The sections of the artificial tidal flat.

The E3 section of the flat was constructed from sand obtained in Ago Bay. For the E4 section, 5 wt% of coagulant consisting of gypsum was used in the HBS solidification treatment. After dewatering, the sediment water content was reduced to 60 wt%, then the solidified materials were mixed with sand (weight ratio 3:7), and an area of the tidal flat constructed.

For section E5, approximately 2 wt% of poly aluminum chloride (PAC) was added as the inorganic polymer coagulant. After dewatering, the water content of the solidified materials was reduced to 40 wt% and the solidified sediments were mixed with solidification agents consisting of waste steel slag (20% by weight) and then with sand (weight ratio 3:7). The resulting materials were used to construct the E5 area of the tidal flat.

2.4 Monitoring of environmental conditions in the constructed tidal flat

We monitored the physico-chemical parameters and biological characteristics of the natural and constructed tidal flats every 4 months from 28 May 2005 to 20 June 2007. The parameters examined were water content, WC (JIS, 2000a); loss on ignition, LOI (JIS, 2000b); total organic carbon, TOC (Vario MAX CHS, Elementar Analysensysteme GmbH); chemical oxygen demand, COD (JIS, 1998); chlorophyll a (N,N-Dimethylformamide extraction method); acid volatile sulphide, AVS (Gas detector tube, GASTEC); and particle size (JIS, 1999). These physico-chemical parameters were evaluated using soil materials core-sampled from the surface to 12 cm depth. The amount of chlorophyll a was measured in soil materials from the surface to a depth of 1 cm. Particle size was measured at 3 and 16 months in the natural tidal flat and every 4 months in the artificial tidal flat. To evaluate biomass and a population density of macrobenthos, soil samples were collected within quadrats (25 cm x 25 cm x 25 cm). Subsequently, the samples were sieved through a mesh size of 1 mm and the organisms on the sieve were fixed in 10 vol% formaldehyde. Organisms then were sorted, identified, counted, and weighed.

3. RESULTS AND DISCUSSION

3.1 Physico-chemical parameters on the constructed tidal flat

We monitored the physico-chemical environmental conditions on the constructed tidal flat every 4 months for 20 months. Tables 1 and 2 summarize the results of the particle size analysis of the natural tidal flat and the artificial tidal flat, respectively. In the natural tidal flat, the percentage (abundance ratio) of particles with a diameter < 75 μm increased with depth from C1 to C6. At stations C3 to C6 the median particle size was < 75 μm, which illustrates that the natural tidal flat in this study area is a muddy tidal flat. In contrast, only 20–45% of the particles from the artificial tidal flat (not including E3) were < 75 μm. These values were similar to those from stations C1 and C2, but lower than the value from adjacent station C3, which sits at a water depth similar to that of the artificial tidal flat.

Table 1. Particle size analysis of the natural tidal flat.

Time passed[#] (months)		C1	C2	C3	C4	C5	C6
3	< 75 μm[a]	42.1%	48.2%	64.1%	72.9%	83.1%	56.2%
	median[b]	96 μm	83 μm	41 μm	23 μm	4 μm	43 μm
16	< 75 μm	35.7%	47.7%	67.3%	81.4%	69.0%	75.7%
	median	120 μm	80 μm	31 μm	6 μm	10 μm	6 μm

[#] In 2005, monitoring was performed in Apr. (1 month), Jul. (3 months), and Oct. (6 months); in 2006 in Jan. (9 months), Jun. (13 months), Sep. (16 months), and Nov. (18 months); and in Jan. 2007 (20 months).
[a] Percentage of particles with a diameter < 75 μm
[b] Median particle size

No remarkable temporal differences in the muddy fraction percentage in the artificial tidal flat were observed during the 20 months of monitoring. Previous research has documented the movement of fine particles on tidal flats (Yang, 1999; Osborne, 2005; Chang, 2007). Although the effusion of muddy fraction (small particle size fraction) was expected in the artificial tidal flat , these results that no remarkable change in the particles of less than 75 μm were observed may support that this phenomenon was not occurred.

In the estuaries that lie at the interface between freshwater and marine systems, organic matter mineralization processes occur (Middelburg at al., 1996). Thus, when constructing man-made artificial tidal flats, evaluating these processes over time is important. Figures 4 and 5 depict the seasonal variations in each of the examined parameters. The WC (a), LOI (b), TOC (c), and COD (d) were almost constant among the monitoring periods. However, the values of these parameters were lower at stations C1 and C2 in the natural tidal flat and at station E3 in the artificial tidal flat, compared to the other stations of both tidal flats. The value of chlorophyll a increased over time on the artificial tidal flat. This phenomenon also was observed on the natural tidal flat on the deeper side that sat at the same level as the artificial tidal flat.

3.2 Monitoring of macrobenthos on the constructed tidal flat

Evaluating the benthic fauna's response to the constructed tidal flat requires analysis of both abundance changes that occur over space and time (Beukema, 1976; Koh and Shin, 1988; Castel et al., 1989). Figures 6 and 7 depict the population density and biomass of macrobenthos in the natural (a) and constructed (b) tidal flats over time. On the constructed flat, the population density and biomass were close to zero after 1 month, but after 3 months the population density increased relative to that observed in the natural tidal flat (especially at the same depth level station (C3), as shown by the arrows). On the other hand, the biomass of macrobenthos reached a level similar to that of the natural tidal flat after 6 months. After 20 months of monitoring,

Table 2. Particle size analysis of the materials used to construct each section of the artificial tidal flat.

Time passed[#] (months)		E1	E2	E3	E4	E5
1	< 75 μm[a]	35.6%	28.0%	16.9%	36.1%	25.7%
	median[b]	271 μm	292 μm	861 μm	245 μm	636 μm
3	< 75 μm	45.1%	22.6%	28.8%	26.3%	19.3%
	median	111 μm	986 μm	286 μm	529 μm	1963 μm
6	< 75 μm	33.3%	20.0%	15.2%	23.4%	20.3%
	median	210 μm	1504 μm	666 μm	480 μm	631 μm
9	< 75 μm	43.6%	43.3%	29.1%	45.8%	26.0%
	median	107 μm	115 μm	207 μm	109 μm	346 μm
13	< 75 μm	28.0%	36.0%	21.1%	32.5%	26.0%
	median	310 μm	220 μm	340 μm	240 μm	360 μm
16	< 75 μm	33.9%	25.7%	18.3%	31.7%	25.9%
	median	230 μm	330 μm	370 μm	250 μm	340 μm
18	< 75 μm	36.6%	27.5%	20.1%	29.2%	26.0%
	median	210 μm	280 μm	350 μm	240 μm	320 μm
20	< 75 μm	31.2%	31.3%	19.0%	26.0%	22.9%
	Median	240 μm	230 μm	320 μm	260 μm	390 μm

[#] In 2005, monitoring was performed in Apr. (1 month), Jul. (3 months), and Oct. (6 months); in 2006 in Jan. (9 months), Jun. (13 months), Sep. (16 months), and Nov. (18 months); and in Jan. 2007 (20 months).
[a] Percentage of particles with a diameter < 75 μm
[b] Median particle size

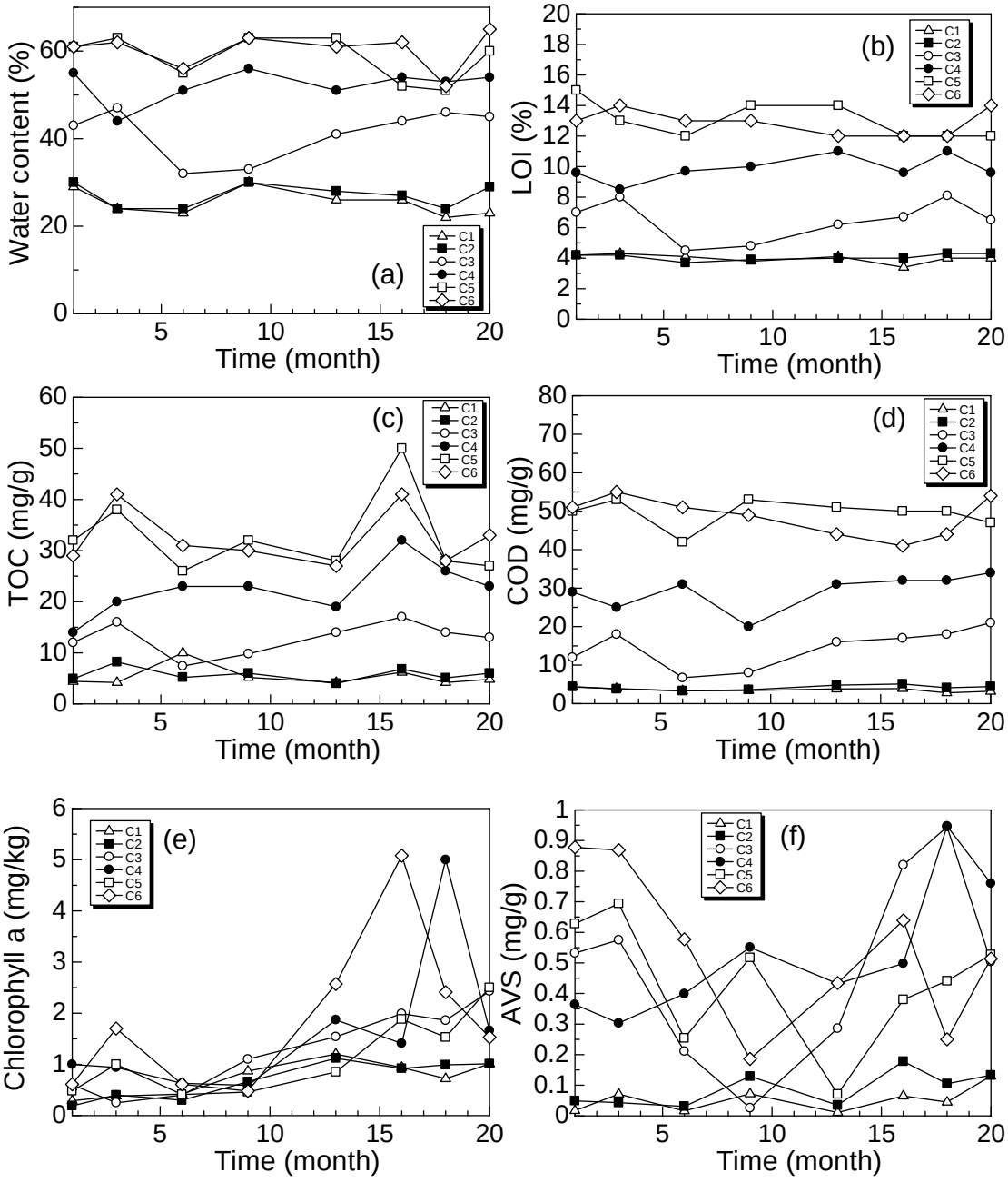

Figure 4. Chemical parameters of the natural tidal flat. See Table 1 for monitoring dates. (a) WC: water content, (b) LOI: loss on ignition, (c) TOC: total organic carbon, (d) COD: chemical oxygen demand, (e) Chlorophyll a, (f) AVS: acid volatile sulphide.

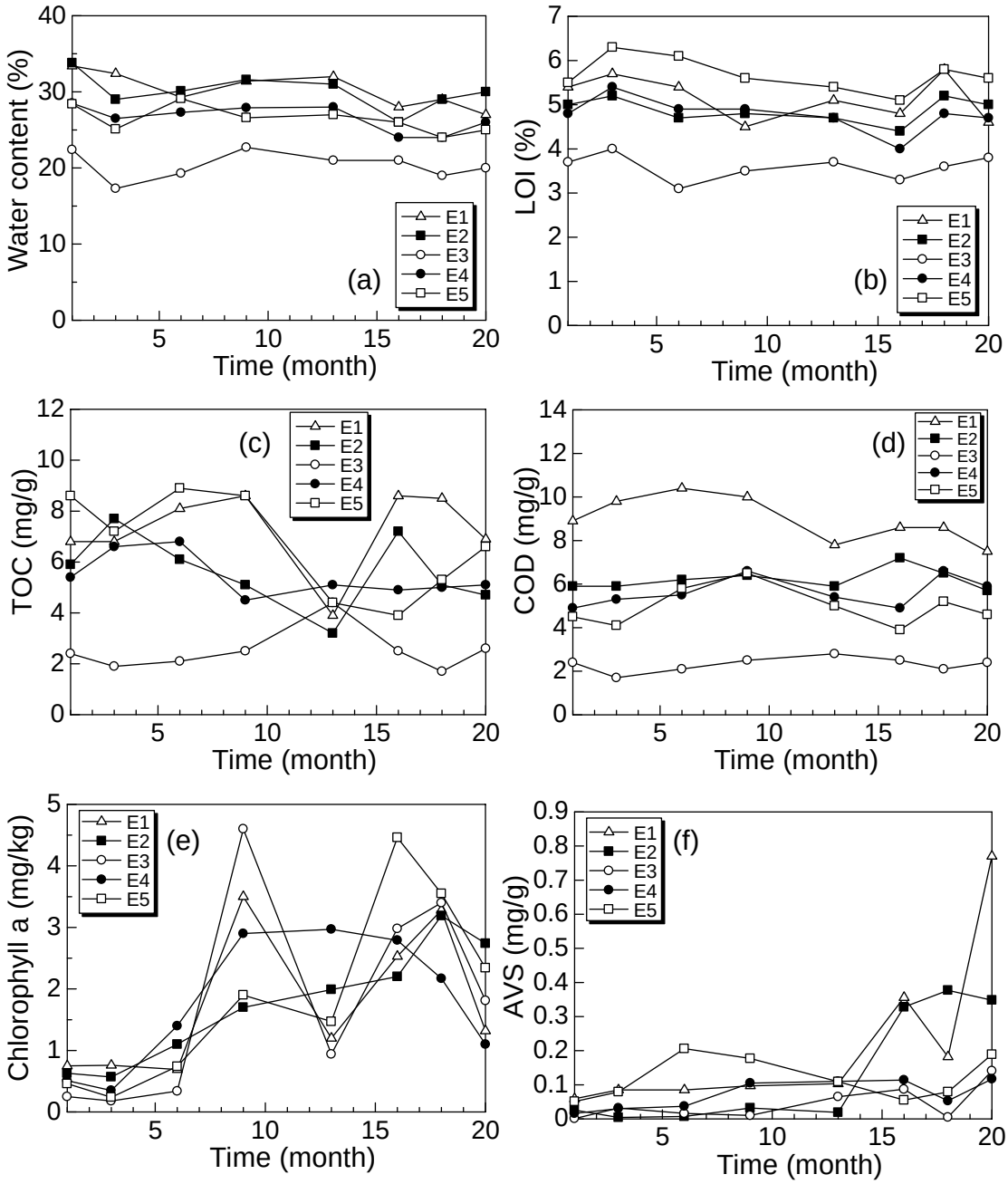

Figure 5. Chemical parameters of the artificial tidal flat. See Table 1 for monitoring dates. (a) WC: water content, (b) LOI: loss on ignition, (c) TOC: total organic carbon, (d) COD: chemical oxygen demand, (e) Chlorophyll a, (f) AVS: acid volatile sulphide.

despite the appearance of increases and decreases, the population density and biomass of macrobenthos in the constructed tidal flat increased relative to that of the natural tidal one. The predominant macrobenthic species in the constructed tidal flat were polychaetes and molluscs. At the deeper stations of the natural tidal flat, the predominant species were bivalves, but the species observed were similar at both tidal flats and the species composition of the two types of flat were not significantly different. These results were similar to data reported previously (Havens et al., 1995; French et al., 2004). These observations for better population and biomass of macrobenthos may be due to the minerals supplied by the solidified sea bottom sediments, which would generate good ecological conditions for benthic animals. However, Herman et al. (2001) reported that the abundance of microalgae is much lower at muddy than at sandy sites, and they hypothesized that high mud content decreases the availability of benthic microalgae. Likewise, Billerbeck et al. (2007) pointed out that benthic photosynthesis was greater in the submerged inner bay with sandy substrate than in the muddy area.

Long-term monitoring is needed to better understand the effects of using these muddy solidified sea bottom sediments to construct tidal flats. To our knowledge, few long-term investigations have been undertaken in the artificial tidal flats (Cammen et al., 1974; Seneca et al., 1976), but the little data available suggest that the habitat functions (e.g., primary production, organic carbon content) on a constructed tidal marsh would be similar to those of a natural tidal one after several years.

Lee et al. (1988) investigated the physico-chemical and biological characteristics of several natural tidal flats and constructed tidal flats with various types of sandy and muddy conditions on the in the semi-closed sea environment. They found no remarkable differences in the population density and biomass of macrobenthos. In contrast, bacterial populations of the sandy constructed tidal flats were remarkably lower than those in the natural flats. However, the population density of samples collected from the constructed tidal flat with high silt content was similar to that of the natural tidal flat. These results indicate that silt particles play an important role in providing habitats for benthic bacteria and biologically productive environments for tidal flats. Ueda (2000) reported that on tidal flats, the sediments were kept oxygenated and accessible to benthic animals throughout the year and the dominant benthic fauna were larger than those found in adjacent inner bay bed.

In the natural tidal flats (Fig. 6a and Fig. 7a), the water depth increased from C1 to C6 and station C3 was at almost the same depth as the constructed flat (E1 to E5). The macrobenthic population density at stations C1 and C2 was lower than at stations C3 to C6 (Fig. 1). C1 and C2 also had lower water content and organic matter content (LOI, TOC, and COD; Fig. 5) than did the other natural stations. These values were lower than those obtained in the constructed tidal flat (not including E3), although the high silt contents was observed in natural tidal flat rather than the artificial tidal flats. These results suggest that it is important to construct artificial tidal flats by considering not only organic matter content but also water depth.

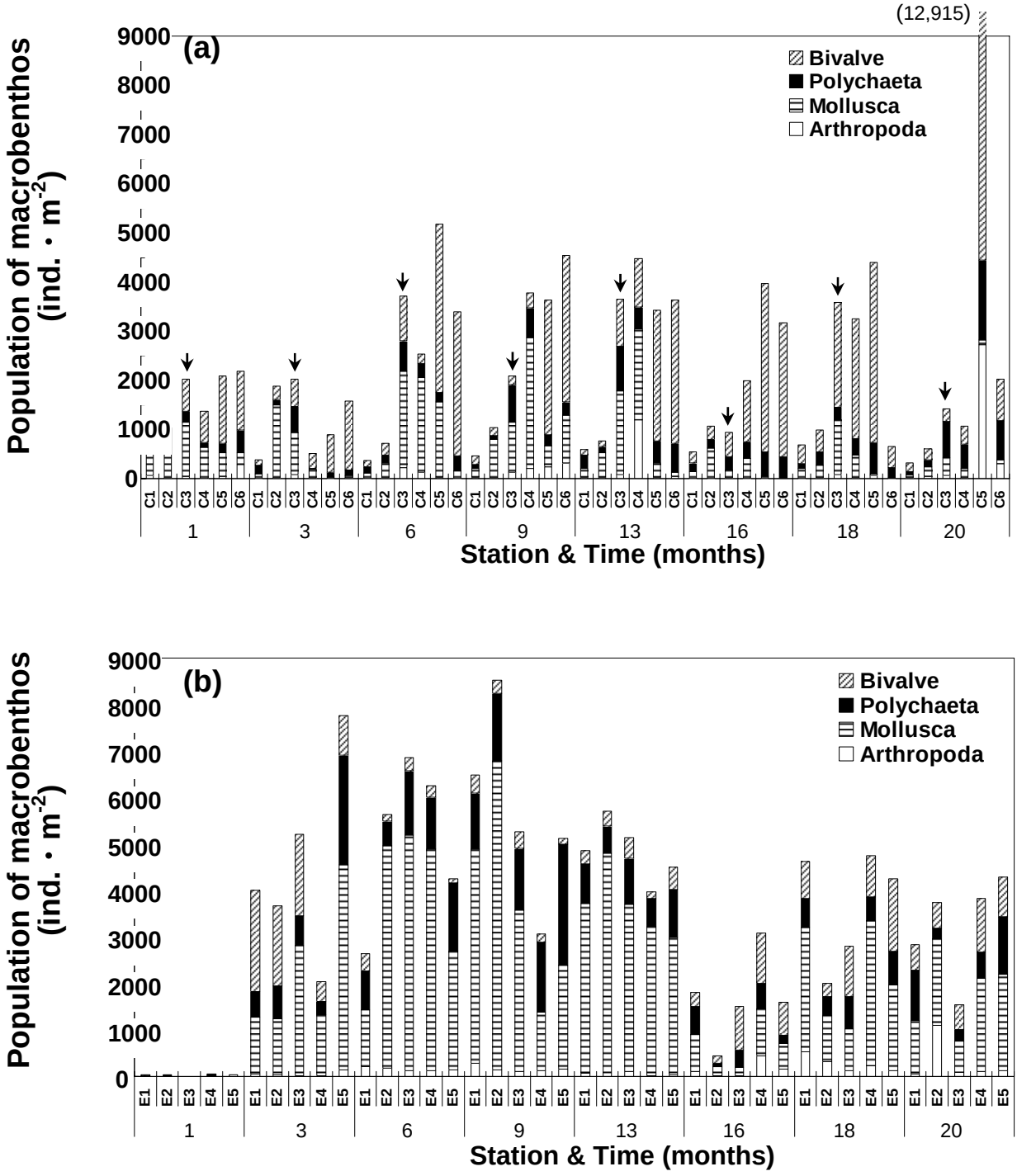

Figure 6. Population of macrobenthos in the natural tidal flat (a) and the artificial tidal flat (b). See Table 1 for monitoring dates. C1 to C6: the natural tidal flat.

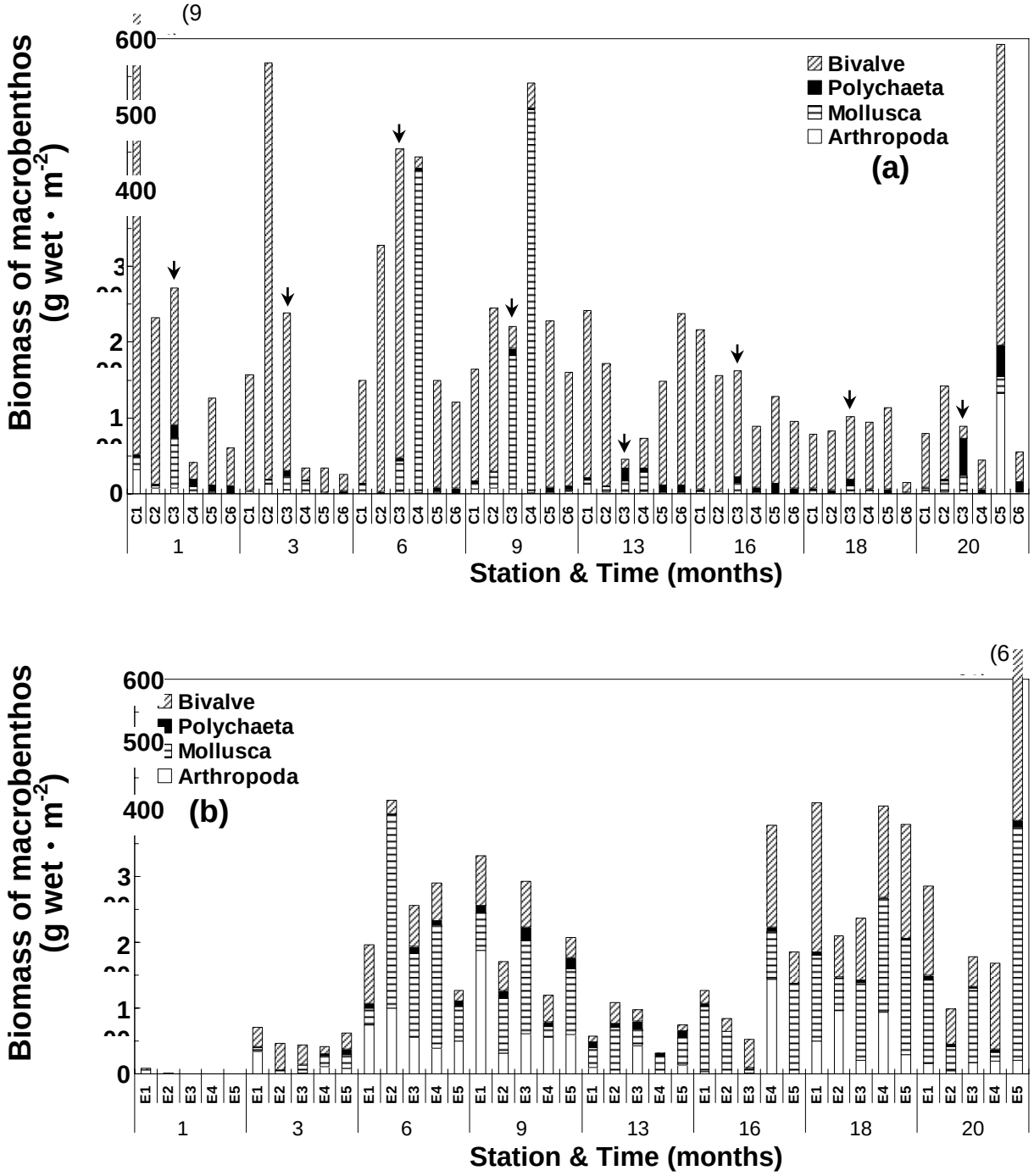

Figure 7. Biomass of macrobenthos in the natural tidal flat (a) and the artificial tidal flat (b). See Table 1 for monitoring dates. C1 to C6: the natural tidal flat.

4. CONCLUSIONS

We developed an in situ solidification system for treatment of sea bottom sediments (the Hi-Biah-System (HBS)). These solidified sea bottom sediments were then used to construct an artificial tidal flat in Ago Bay. The ecosystem and environmental conditions of the constructed tidal flat, which were monitored and compared to a natural tidal flat over the course of 2 years, were found to be very similar and/or superior to those of the adjacent natural tidal flat.

5. ACKNOWLEDGMENTS

This research was partly supported by the Ministry of Education, Culture, Sports, Science, and Technology of Japan. The present work was performed as part of the joint collaboration of research projects titled "Environmental Restoration Project on the Enclosed Coastal Seas, Ago Bay," supported by the CREATE (Collaboration of Regional Entities for the Advancement Technological Excellence) activity program organized by the Japan Science and Technology (JST) Agency. Any opinions, findings, conclusions, or recommendations expressed in this paper are those of the authors and do not necessarily reflect the view of the supporting organizations.

6. REFERENCES

Beukema, J.J. 1976. Biomass and species richness of the macro-benthic animals living on the tidal flats of the Dutch Wadden Sea. Netherlands Journal of Sea Res. 10, 236–261.

Billerbeck, M., Roy, H., Bosselmann, K., and Huettel, M. 2007. Benthic photosynthesis in submerged Wadden Sea intertidal flats. Estuarine Coastal Shelf Sci. 71, 704–716.

Cammen, L.M., Seneca, E.D., and Copeland, B.J. 1974. Animal colonization of salt marshes artificially established on dredge spoil. University of North Carolina Sea Grant Program Publ. UNC-SG-74-15, Chapel Hill, NC, 67 pp.

Castel, J., Labourg, P-J., Escaravage, V., Auby, I., and Garcia, M.E. 1989. Influence of seagrass beds and oyster parks on the abundance and biomass patterns of meio- and macrobenthos in tidal flats. Estuarine Coastal Shelf Sci. 28, 71–85.

Chang, T.S., Flemming, B.W., and Bartholoma, A. 2007. Distinction between sortable silts and aggregated particles in muddy intertidal sediments of the East Frisian Wadden Sea, southern North Sea. Sedimentary Geol. Doi:10.1016/j.sedgeo.2007.03.009.

Cofer, S.R., and Niering, W.A. 1992. Comparison of created and natural freshwater emergent wetland in Connecticut (U.S.A.). Wetlands Ecol. Manage. 2(3), 143–56.

Dabwan, A.H.A., Imai, D., Kato, T., Kaneco, S., Suzuki, T., Katumata, H., and Ohta, K. 2007. Use of solidified sea bottom sediments as soil parent material for the germination/growth of seagrass. OCÉANIS submitted for publication.

French, K., Robertson, S., and O'Donnell, M.A. 2004. Differences in invertebrate infaunal assemblages of constructed and natural tidal flats in New South Wales, Australia. Estuarine Coastal Shelf Sci. 61, 173–183.

Graalum, S.J., Randall, R.E., and Edge, B.L. 1999. Methodology for manufacturing topsoil using sediment dredged from the Texas Gulf Intracoastal Waterway. J. Mari. Environ. Eng. 5, 121–158.

Havens, K.J., Varnell, L.M., and Bradshaw, J.G. 1995. An assessment of ecological conditions in a constructed tidal marsh and two natural reference tidal marshes in coastal Virginia. Ecol. Eng. 4, 117–141.

Herman, P.M.J., Middelburg, J.J., and Heip, C.H.R. 2001. Benthic community structure and sediment processes on an intertidal flat: results from the ECOFLAT project. Continental Shelf Res. 21, 2055–2071.

Hirata, H., Kadowaki, S., and Ishida, S. 1994. Evaluation of water quality by observation of dissolved oxygen content in mariculture farms. Bull. Natl. Res. Inst. Aquacult. (Suppl. 1), 61–65.

Imai, D., Dabwan, A.H.A., Kato, T., Kaneco, S., Suzuki, T., Katumata, H., and Ohta, K. 2007. Construction and Environmental Condition Monitoring of Artificial Tidal Flat with Solidified Sea Bottom Sediments. OCÉANIS in press.

JIS (Japanese Industrial Standards). 1998. Test method for chemical oxygen demand of soils and water, K0102:1998, Japanese Standards Association.

JIS (Japanese Industrial Standards). 1999. Test method for water content of soils, A 1203:1999, Japanese Standards Association.
JIS (Japanese Industrial Standards). 2000a. Test method for ignition loss of soils, A 1226:2000, Japanese Standards Association.
JIS (Japanese Industrial Standards). 2000b. Test method for particle size distribution of soils, A 1204:2000, Japanese Standards Association.
Joh, H. 1989. Oxygen-deficient water in Osaka Bay. Bull. Coastal oceanography. 26, 87–98.
Kakino, J., Matsumura, S., Sato, Y., and Kase, N. 1987. Relationship between aoshio, blue-green water, and wind-driven current. Nippon Suisan Gakkaishi 53, 1475–1481.
Kikuchi, T. 1993. Ecological characteristics of the tidal flat ecosystem and importance of its conservation. Japanese J. Ecol. 43, 223–235.
Kimura, K. 1994. The function of water purification in constructed tidal flat. Jpn. Bottom Sediment Management Assoc. 60, 50–81.
Koh, C.H., and Shin, H.C. 1988. Environmental characteristics and distribution of macrobenthos in a mudflat of the west coast of Korea (Yellow Sea). Netherlands Journal of Sea Res. 22, 279–290.
Kokubu, H., Okumura, H., Ueno S., Takayama, S., and Yuasa, S., 2004. The optimal condition of tidal flat sediment obtained from field study of a tidal flat using muddy dredged sediment (in Japanese). J. Costal Eng. 51, 1191–1195.
Lee, J.G., Nishijima, W., Mukai, T., Takimoto, K., Seiki, T., Hiraoka, K., and Okada, M. 1998. Factors to determine the functions and structures in natural and constructed tidal flats. Wat. Res. 32(9), 2601–2606.
Middelburg, J. J., Klaver, G., Nieuwenhuize, J., Wielemaker, A., Haas, W., Vlug, T., and Van der Nat, J.F.W.A. 1996. Organic matter mineralization in intertidal sediments along an estuarine gradient. Mar. Ecol. Prog. Ser. 132, 157–168.
Miyoshi, K., Shimati, T., and Kimura, K. 1990. A capacity of purification at constructed tidal flat. Tokyo Metropolitan Research Institute of Environ. Sci. An Annual Report 120–125.
Ogura, O., and Imamura, H. 1995. Creative technique for constructed tidal flat. Jpn. Bottom Sediment Management Assoc. 64, 61–78.
Omori, K., Hirano, T., and Takeoka, H. 1994. The limitations to organic loading on a bottom of a coastal ecosystem. Mar. Poll. Bull. 28, 73–80.
Osborne, P.D. 2005. Transport of gravel and cobble on a mixed-sediment inner bank shoreline of a large inlet, Grays Harbor, Washington. Mar. Geol. 224, 145–156.
Seneca, E.D., Broome, S.W., Woodhouse, W.W., Cammen, L.M., and Lyon, J.T. 1976. Establishing *Spartina alterniflora* marsh in North Carolina. Environ. Conserv. 3, 185–188.
Suzuki, T., and Matsukawa, Y. 1987. Hydrography and budget of dissolved total nitrogen and dissolved oxygen in the stratified season in Mikawa Bay, Japan. J. Oceanographical Society Japan 43, 37–48.
Takahashi, M. 1994. Ocean, living being and man □7, bays and inland seas and their current conditions. Aquabiology 16, 2–5.
Takeda, K., Ishida, M., Ieda, K., Ishida, T., Kuwae, T., and Suzuki, T. 2007. Biological production and water purification functions of mega-infaunal community at an artificial tidal flat. Fisheries Eng. 44, 11–19 (in Japanese with English abstract).
Takeda, S., Nimura, Y., and Hirano, R. 1991. Optical, biological, and chemical properties of Aoshio, hypoxic milky blue-green water, observed at the head of Tokyo Bay. J. Oceanographical Society Japan 47, 126–137.
Tsutsumi, H. 1995. Impact of fish net pen culture on the benthic environment of a cove in south Japan. Estuaries 18, 108–115.
Ueda N., Tsutsumi H., Yamada M., Hanamoto K., and Montani, S. 2000. Impacts of Oxygen-deficient water on the macrobenthic fauna of Dokai Bay and on adjacent intertidal flats, in Kitakyushu, Japan. Mar. Poll. Bull. 40, 906–913.
USACE (U.S. Army Corps of Engineers). 1987b. Beneficial Uses of Dredged Material. Engineer Manual EM-1110-2-5026.
Volkman, J.K., Rohjans D., Rullkotter, J., Scholz-Bottcher, B.M., and Liebezeit, G. 2000. Sources and diagenesis of organic matter in tidal flat sediments from the German Wadden Sea. Continental Shelf Res. 20, 1139–1158.
Yang, S.L. 1999. Sedimentation on a growing intertidal island in the Yangtze River Mouth. Estuarine Coastal Shelf Sci. 49, 401–410.

Chapter 31

ENCLOSING DIOXINS CONTAMINATED SEDIMENTS BY GEOTEXTILE TUBES

Yugo Masuya[1§], Hitoshi Taninaka[1], Isamu Takahashi[1], and Hidetoshi Kohashi[1]
Public Works Research Institute, Japan, 1-6 Minamihara, Tsukuba city, Ibaraki, Japan

ABSTRACT

In 2002, Japan enacted environmental standards for dioxins contaminated sediment. A nationwide sediment dioxins survey of public waters found sediment exceeding environmental standards in some rivers: a problem requiring countermeasures. The Eco-tube is a permeable geotextile container with soft and high water content sediment deposited in rivers, lakes, and marshes. It promotes dewatering of the sediment, and the filtering function of the tubes c[§]an purify the drain and enclose toxic substances such as dioxins. After dewatering, they are used to build embankments by taking advantage of their tensile strength. This report describes a trial execution of Eco-tubes that enclose dioxins contaminated sediment. The trial followed preliminary testing: measuring the quantity and turbidity of the drain by pressurized filtering test to examine the geotextile's filtering performance and select the coagulant. Next, 0.2m^3 tubes of the selected material were filled with sediment and used for laboratory experiments based on the actual execution, confirming the dewatering speed and filtering effectiveness of the method. The trial applied 2 patterns (5 cases) based on the test results.

(1) Filling high density tubes with sediment already containing coagulant. (2 cases) (2) Filling tubes with sediment and adding coagulant into drain. (3 cases) Results: (1) Drain of 130pg-TEQ/g dioxins contaminated sediment becomes 2.4pg-TEQ/l. (2) Drain including the 960pg-TEQ/l dioxins went down 0.42pg-TEQ/l by adding coagulant. Pattern (2) was much easier to execute, and more effectively reduced turbidity of the water. The tube height fell to 1/2 to 1/7 of maximum height in about 5 months. These findings confirmed that Eco-tube enclose dioxins contaminated sediment and reduce the volume of sediment by dewatering.

Keywords: geotextile, dioxins, contaminated soil

§ Corresponding Author: Yugo Masuya, Public Works Research Institute, Japan, 1-6 Minamihara, Tsukuba city, Ibaraki, Japan, Tel: +81-29-879-6767, Fax: +81-29-879-6798, Email: masuya@pwri.go.jp

1. INTRODUCTION

In Japan, several dioxins contaminated sites have drawn. The proper disposal of dioxins contaminated sediments and soil have become a major problem in recent years. Considering these conditions, the Japanese government made a law called the Law Concerning Special Measures against Dioxins. The Eco-Tube that has been developed jointly by the Public Works Research Institute and private companies as a measure to enclose dioxins contaminated sediments. This method was used to promote dewatering and lower the volume of dioxins contaminated sediments. This report presents the results of field executions and various laboratory experiments.

1.1 The Eco-Tube

The Eco-Tube involves packing a water-permeable geotextile tube with soft and high water content soil such as dredged sediments from rivers, lakes, and marshes (Mori et al. 2002a). Fig. 1 shows the configuration of the Eco-Tube. The Tube after dewatering can also be used as embankments using reinforcement of the geotextile. The water drained from the tubes has low turbidity, because soil particles are retained inside the tubes thanks to the filtration function of the permeable material used to make the tubes. Mori et al. (2002b, 2002c) suggested the utilizing a geotextile tube to trap toxic substances such as dioxins and heavy metals. And also Lawson (2006) given an Example of enclosing contaminated sediment by geotextile tube.

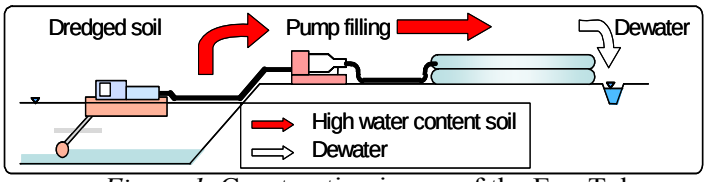

Figure 1. Construction image of the Eco-Tube

Nowadays there are 3 methods adopted for preventing the spread of contamination and each has some problems.

The following are problems of concern regarding past technologies adopted as methods of preventing the spread of contamination by bottom sediments polluted with dioxins. 1) Sand covering method and in-situ stabilization: Increase in the volume is accompanied. And because they are not purification technologies that make the dioxins harmless, contaminated soil may be exposed by construction work. 2) Dredging removal with sediment purification: Soil burning methods, chemical methods, etc. are used, but these are all expensive and time-consuming. 3) Dredging removal with stabilization: Because dredging removal produces a large quantity of surplus water, when the environmental standard is exceeded, purifying the drainage may become very expensive. And the stabilized soil has increased volume, so ensuring a site for disposal of the treated soil is a problem.

The Eco-Tube promotes the dewatering and the lower the volume of contaminated sediments. Therefore it can be used as a low cost method of prevent pollution diffusion.

2. LABORATORY EXPERIMENTS

2.1 Purpose of the Experiments

It is preferable that the water drained from the tubes satisfy wastewater standards (dioxin concentration: 10pg-TEQ/1) without further treatment. Laboratory experiments were done in order to select tube material and coagulant that can satisfy wastewater standards. Advance experiments confirmed that if the turbidity was 20NTU or less, the dioxin concentration was below the wastewater standard, so the turbidity was used as an indicator of the wastewater standard.

2.2 Experiment Samples

Table 1 shows the results of the physical and chemical properties of the experiment specimens. Dioxin concentration was 130pg-TEQ/g that was below the bottom sediment environmental standard (150pg-TEQ/g).

Table 1. Properties of Bottom Sediment

Density of soil particles ρ_s(g/cm^3)		2.533
Water content w(%)		156
Grain size distribution	Gravel (%)	0
	Sand (%)	22
	Silt (%)	51
	Clay (%)	27
	Maximum grain size (mm)	2
Consistency	Liquid limit w_L(%)	78
	Plastic limit w_P(%)	45.9
	Plastic index I_P	32.1
Classification of geomaterials for Engineering purposes		Sandy silt (High liquid limit)
pH		6.67
Ignition loss L_i(%)		8.9
Dioxins (pg-TEQ/g)		130

2.3 The Pressure Filtration Test

2.3.1 Purpose of the Test

It is important that tubes used to enclose contaminated soil reduce the turbidity of water drained from the tubes at the same time as they do not break, discharging the enclosed material. The pressure filtration test was done as an experiment intended to select the tube materials that can be applied to this experiment, because the tube material varies in filtration

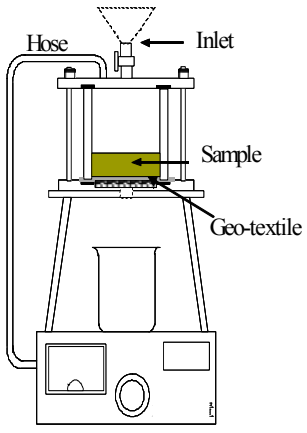

Figure 2. Pressure Filtration Tester

performance and strength according to its standard and its maker. Figure 2 shows the pressure filtration test equipment.

2.3.2 Test Conditions

Table 2 shows the specifications of the tube materials used for the tests and Table 3 shows the test conditions. Tube material was selected considering safety (turbidity capture performance, strength) and cost, and with ① coefficient of permeability in a range of 10^{-2} to 10^{-4}, ② aperture diameter of the tube material within 0.2mm, and ③ elongation of the tube material within 40% (in order to prevent the decline of filtration performance by expansion of the apertures by tension). And the cover factor is an index of the percentage of the tube material surface that is fiber surface: a value dependent on the fiber density and fiber thickness.

Table 2. Tube Material Specifications

Geo-textile	Type A	Type B	Type C
Mass［g/m^2］	210	260	530
Thickness［mm］	0.35	0.37	0.69
Tensile strength［N/cm］	720,720	500,450	740,1470
Elongation［%］	13,13	40,25	17,13
Ripping Strength［N］	640,640	150,150	920,1090
Hydraulic conductivity［cm/s］	1.5×10^{-3}	1.2×10^{-3}	2.6×10^{-4}
Cover factor	1644	2314	2033

※Strength values ; vertical, lateral

Table 3. Pressure Filtration Test Cases

Case	Geo-textile	Flocculant	Water content (%)
1	Type A	-	500
2		PAC	500
3		Anion	500
4		Cation	500
5		PAC + Cation	500
6		Low cation	500
7	Type B	-	300
8			500
9			700
10	Type C	-	300
11			500
12			700

2.3.3 Experimental Results

2.3.3.1 Comparison of Turbidity of Water Drained from the Tube Material

The turbidity of the drainage was compared under conditions such that the water content of the specimen is 500% and coagulant is not added. Figure 3 shows the results. It shows that the turbidity varies by tube material: B < A < C. Beginning thirty minutes after the start of the test, the turbidity in all experimental cases had fallen below 20NTU that is the drainage standard index.

2.3.3.2 Comparison of Coagulants

It confirmed the results for each type of coagulant using tube material A and 500% water content specimen. Figure 4 shows the results. The drainage turbidity fell according to the coagulant, in the order low cation type > PAC + cation type > cation type > PAC > anion type.

2.3.3.3 Comparison of Water Content

Tube materials B and C were used to study the impact of varying the water content between 300%, 500%, and 700%. The results are shown in Figure 5. It confirms that as the water content rose, more water was drained and its turbidity was lower.

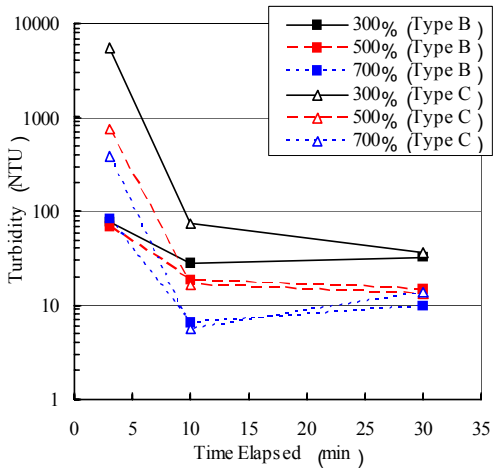

Figure 3. Comparison of Tube Materials

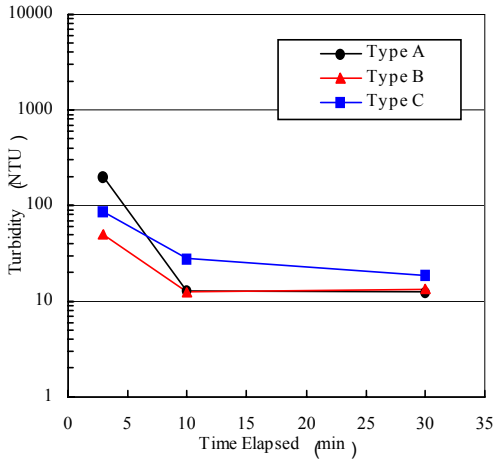

Figure 4. Comparison of Coagulants

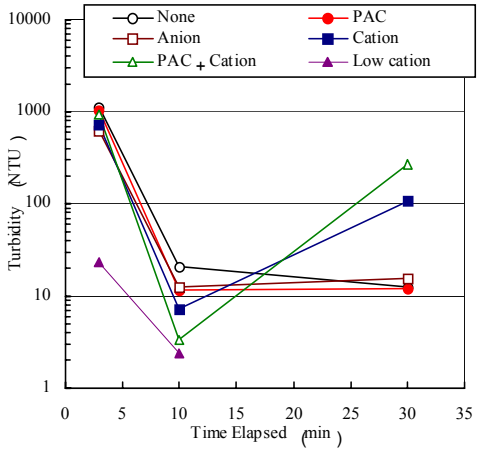

Figure 5. Comparison of Water Contents

2.4 Two-hundred Liter Tube Filling Experiment

2.4.1 Purpose of the Experiment

Two-hundred liter tubes were used for filling experiments to confirm the turbidity capture capacity during actual execution.

2.4.2 Experiment Method

An electric pump was used to fill tubes with specimen with its water content adjusted to 500%. Water drained from the tubes was sampled at periodically to measure the quantity of drainage and its pH. The drainage was collected in 5 liter batches and the turbidity was measured. Table 4 shows the experiment conditions.

Table 4. Experimental case

Case	Geo-textile	Flocculant	Water content (%)
1	A	-	500
2		PAC	
3		PAC + Cation	
4		Low cation	
5	B	PAC	
6		Low cation	
7	C	PAC	

2.4.3 Experiment Results

2.4.3.1 Comparison of Turbidity of Water Drained from the Tubes

A specimen prepared by mixing PAC as the coagulant with bottom sediment was used to fill the tubes and the turbidity of drainage form the tubes was measured. The results are shown in Figure 6. They reveal that the turbidity fell in the sequence: tube material B>C>A. This result differs from the results of the pressure filtration test described in the previous part of this report, but they show that the larger the cover factor, the lower the turbidity.

2.4.3.2 Comparison of Coagulants

Specimens prepared by adding and mixing low cation type, PAC, and PAC + cation type as the coagulant with bottom sediments were used to fill tubes. The tubes used were made of tube material A. Figure 7 shows the results. The turbidity of the drainage fell in the sequence: low cation type > PAC + cation type > PAC > no coagulant. But although the turbidity was low immediately after drain, when it had been left alone for a few hours, all drainage was colored yellow. This is assumed to be an effect of oxidation of iron that was leached out. Figure 8 shows the relationship of the quantity of drainage with the time. From the result of Figure 7 and 8, no clear relationship of the drain speed and turbidity was observed.

2.4.3.3 Adding Coagulant to the Drainage

A tube made of tube material C was filled with bottom sediment (without the addition of coagulant), and then PAC and low cation type coagulants were added to the drainage. Figure 9 shows the results. The turbidity rose in the sequence PAC < low cation type < no coagulant. Looking at the quantity of coagulant that was added, in the case of PAC, up to 10mg/l, the more that was added, the lower the turbidity, but above that level, very little change was seen. With the low cation type, clear characteristics were not confirmed. And unlike the case where the tube was filled with bottom sediment after coagulants were added to it (2), the drained wastewater was not colored even when the drainage was left standing for several days.

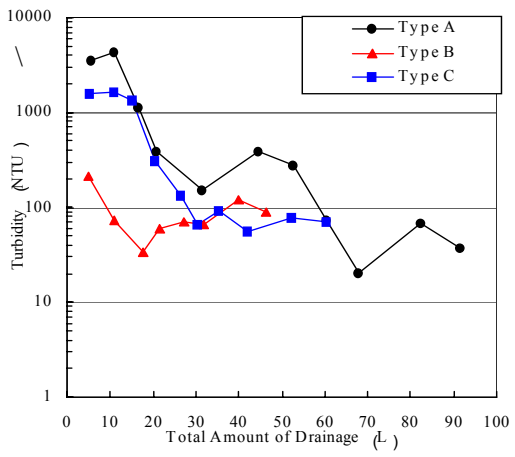

Figure 6. Comparison of Tube Materials

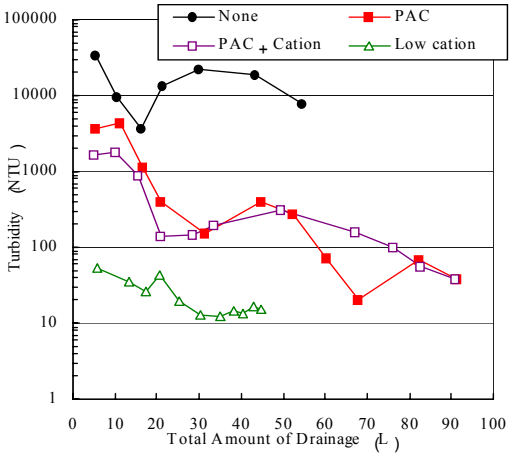

Figure 7. Comparison of Coagulants

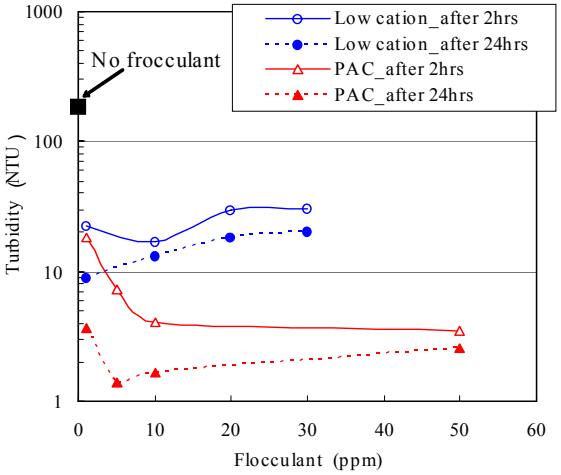

Figure 8. Drain Speed

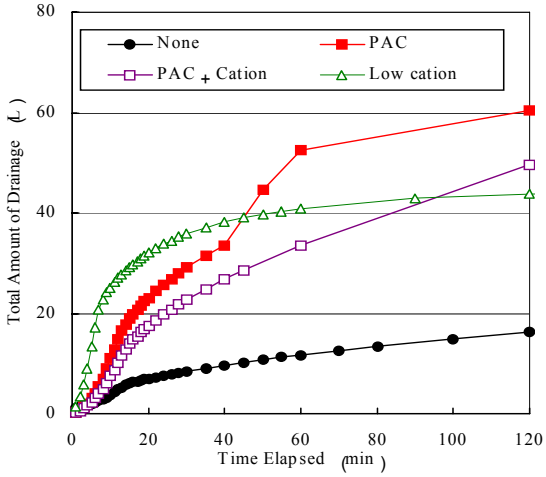

Figure 9. Quantity of Coagulant Added

2.5 Summary of the Laboratory Experiments

The results of the pressure filtration experiments and the 200 liter tube filling experiment show that when the coagulant was directly mixed with the bottom sediment and when it was mixed with the drainage, the turbidity was most effectively lowered by the low cation coagulant and the PAC respectively. And mixing the coagulant with the drainage was easier than mixing the coagulant uniformly with the bottom sediment. The results of the pressure filtration experiment and the 200 liter tube filling experiment differed partially depending on the tube material. So it is vital to select the tube material not only by performing a pressure filtration experiment before the actual execution; but by also performing a filling experiment using a smaller tube such as a 200 liter tube.

3. ONSITE EXECUTION

3.1 Outline of the Execution

The Eco-Tube was applied to approximately 15m^3 of dredged bottom sediment. The execution was performed by applying two patterns with differing coagulant addition methods based on the results of the laboratory experiments. Figure 10 is a flow chart of the execution. The water drained from the tubes was stored temporarily in a tank where its dioxins concentration was measured, and if it was confirmed that it satisfied the wastewater standard (10pg-TEQ/1), it was released. Photo 1 shows a view of the execution and Figure 11 shows a section of the tube installation. The tube material was tube material B in Case 1 and tube material C in Case 2. In Case 2, the bottom sediment was filled in the tube by the pattern shown in Table 5 in order to confirm the impact of differences in the quantity filled and the water contents of the specimen.

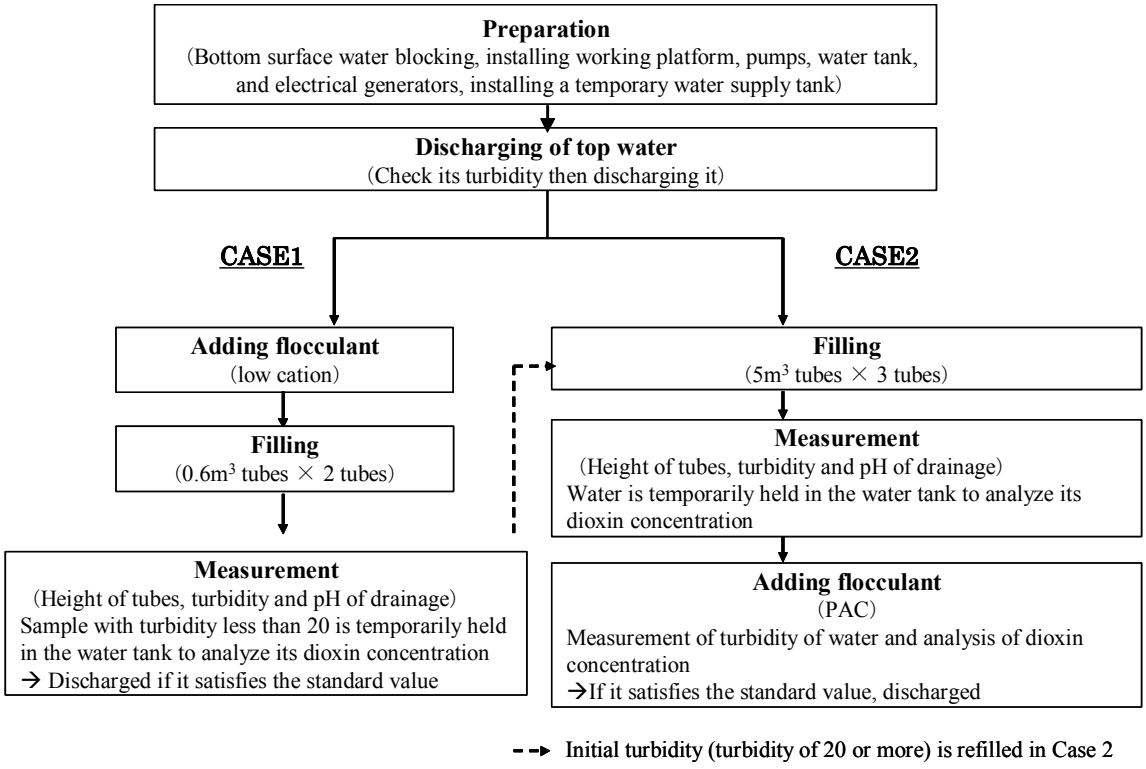

Figure 10. Execution Flow Chart

Table 5. Case 2 Experiment Pattern

CASE	Height of Tubes / Quantity filled	Water content condition
CASE2-1	70cm / 5.0m^3	High
CASE2-2	60cm / 4.3m^3	High
CASE2-3	48cm / 3.7m^3	Low

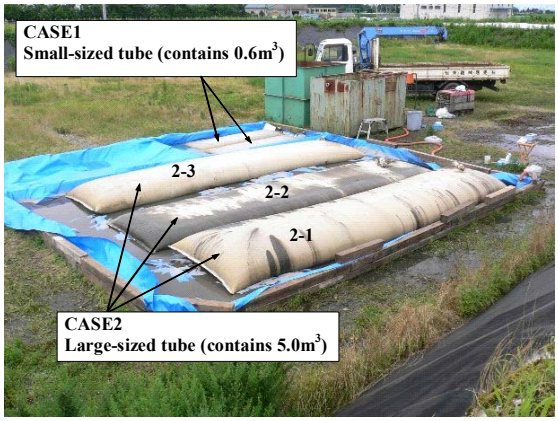

Photo 1. View After Execution

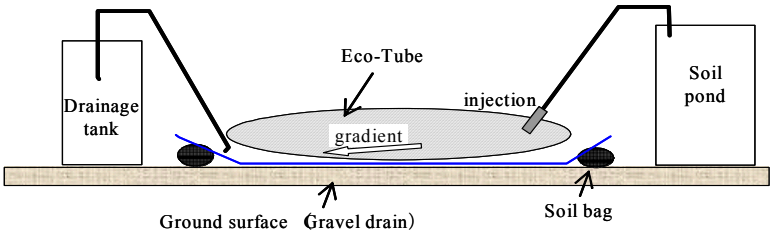

Figure 11. Cross Section of Tube Installation

3.2 Items Measured and Measurement Results

The turbidity and pH of the water drained from the tubes and the height of the tubes were measured from the start of execution. The height and water content of the tubes, and the cone penetration resistance were surveyed continually in order to confirm the way the bottom sediment changed after it was placed in a tube.

3.2.1 Turbidity of the drainage

Figure 12 shows the results of the measurements of the turbidity of the drainage. In Case 1, the turbidity fell below 20NTU that is the control standard at about 60 minutes after the start of filling (about 30 minutes after the pump stopped operating). And the dioxins concentration of the drainage stored in the water tank was 2.4pg-TEQ/l (SS: 13mg/l). It was, therefore, the drainage standard is satisfied confirmed except the initial turbidity that occurred until the mud membrane is formed in a tube and filtration function became effective (here, this refers to drainage with turbidity of 20NTU or more) is removed.

In Case 2, as shown by Photo 1, the turbidity remained almost unchanged without any decline in Case 2-2. And in Case 2-1 where the conditions of the specimen filled was almost the

same, the turbidity fell to about 20NTU that is the control standard as shown in Figure 12. This difference is assumed to be based on the quantity filled. In Case 2-2, it was confirmed that air was trapped at a location far from the inlet, and water with high turbidity continued to be drained from this part. As a result of collecting drainage in Case 2 in a water tank, adding PAC as the coagulant, letting it settle, then measuring the dioxins concentration, drainage that was 960pg-TEQ/l (SS: 2020mg/l) before addition of the coagulant fell to about 0.42pg-TEQ/l (SS: mg/l).

3.2.2 Tube Height

Figure 13 shows change of tube height over time. In all cases, the tube height fell as dehydration reduced its quantity. In Case 1, it fell to about 1/3 in both cases. And in Case 2-1, Case 2-2, and Case 2-3, it fell to about 1/7, 1/6, and 1/2 respectively.

3.2.3 Water Content

Specimens inside the tubes were sampled and their water content measured at about 40 days after filling and at about 150 days after filling. Figure 14 shows the results. In all cases, no significant change was found between 40 days and 150 days after filling. The water content of the specimens of soil that filled the tubes was wide, ranging from 100% to 400%, but 150 days later it ranged from 50% to 90% in all cases. For this reason, it was confirmed that the water content declined to a stipulated level regardless of the water content conditions of the filled specimens.

3.2.4 Cone Penetration Resistance

Like the measurements of the water content of the specimens, the cone penetration tests were done at 40 days and at 150 days after filling. Figure 15 shows the results. At 150 days after filling, in almost all cases, strength became more than 200kN/m2. In Case 2-2 and Case 2-3, the strength after 150 days was lower than it was after 40 days. This is assumed to be an impact of differences between test locations.

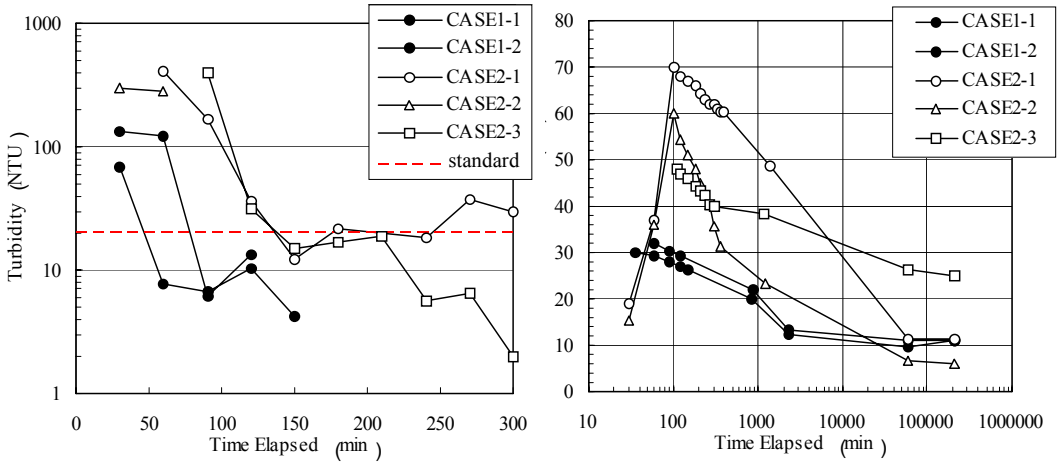

Figure 12. Turbidity of drainage

Figure 13. Tube Height

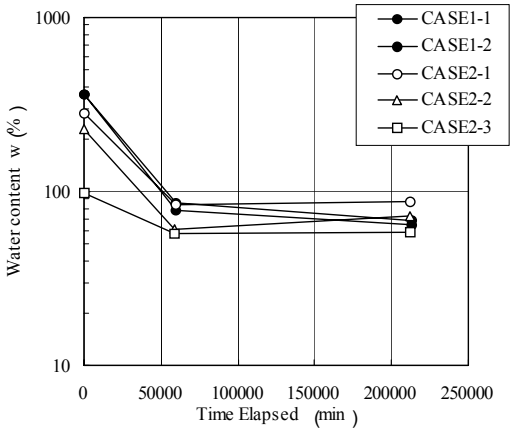

Figure 14. Water Content

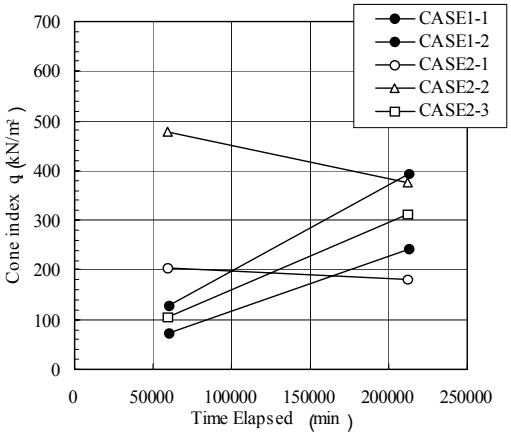

Figure 15. Cone Insertion Resistance

3.3 Summary of the Onsite Execution

The results of the execution reveal that there are cases where the mud membrane that was expected to form on the interior of the tube during the early stage of dehydration cannot form and the filtration function cannot be fully performed, because of differences in the quantity of bottom sediment and its water content. In this way, in cases where the water drained from the tube does not satisfy the control standards, coagulant should be added to the water that is drained from the tube to remove turbidity from the drainage.

4. CONCLUSIONS

The results of the laboratory experiments and the onsite executions have confirmed that the Eco-Tube encloses dioxin contaminated sediment and dehydrates bottom sediment reducing its quantity, and have also confirmed that it is effective as a contamination spread prevention method that will cover the shortcomings of the sand covering method, the stabilization method, and the dredging removal methods that are the conventional ways of preventing the spread of contaminants from bottom sediment that has been contaminated by dioxins.

5. REFERENCES

Mori, H., Tsuneoka, N. Miki, H., Dobashi, K. and Takahashi, I. 2002a. Swamp Restoration Using the Geo-Tube Method, Dredging02, the 3rd International conference on dredging technology.

Mori, H., Miki, H. and Tsuneoka, N. 2002b. The geo-tube method for dioxin-contaminated soil, the special edition of Geotextiles and Geomembrans, pp 281-288

Mori, H., Miki, H. and Tsuneoka, N. 2002c. The use of geo-tube method to retard the mifration of contaminants in dredged soil, Proceedings of the 7th International Conference on Geosynthetics, Vol. 3, pp 1017-1020.

Lawson, C.R. 2006. Geotextile containment for hydraulic and environmental engineering, Proceedings of the 8th International Conference on Geosynthetics, Vol. 1, pp 41-44.

Index